HENYEY

SCEC Southern California Earthquake Center

Science Director
K. Aki
Executive Director
T. Henyey
Southern California
Earthquake Center
University of
Southern California
Los Angeles, CA
90089

Institutional
Representatives
R. Clayton
Seismological
Laboratory
California Institute
of Technology
Pasadena, CA
91125

D. Jackson
Department of
Earth and
Space Sciences
UCLA
Los Angeles, CA
90024

R. Archuleta
Department of
Geological Sciences
UCSB
Santa Barbara, CA
93106

K. McNally
Earth Sciences
Board of Studies
UCSC
Santa Cruz, CA
95064

B. Minster
Scripps Institution
of Oceanography
UCSD
La Jolla, CA
92093

L. Seeber
Lamont-Doherty
Geological Obs.
Columbia University
Palisades, NY
10964

T. Heaton
USGS - OEVE
525 S. Wilson Ave.
Pasadena, CA
91106

Southern California Earthquake Center

1992 Report

prepared for the

SCEC Annual Meeting
October 6-8, 1992

NSF/USGS Site Review
SCEC Advisory Council Meeting
October 8-9, 1992

University Hilton Hotel
Los Angeles, California

Telephone (213) 740-5843 FAX (213) 740-0011

Table of Contents

1992 SCEC ANNUAL MEETING AGENDA

TUESDAY, OCTOBER 6

1:30 p.m. to 6:00 p.m.

Plenary Session: Joshua Tree-Landers-Big Bear Earthquakes

1:30	Welcome and Introduction	Tom Henyey
1:40	Social Impact and Emergency Response	Paul Flores
2:00	Damage to Structures and Lifelines	Le Val Lund
2:20	Crustal Stress Changes	Ruth Harris
2:50	Ground Rupture	Kerry Sieh
3:20	Coffee Break	
3:40	Mainshock Rupture Process	Hiroo Kanamori
4:10	Strong Ground Shaking	Ralph Archuleta
4:40	Aftershocks	Egill Hauksson
5:10	Geodetic Measurements and Strain	Dave Jackson
5:40	Impact on the Master Model	Kei Aki

Posters for Landers earthquake sequence will be up on Tuesday afternoon and Wednesday.

6:30 to 8:00 p.m. SCEC Barbecue at USC

1992 LANDERS EARTHQUAKE POSTER SESSION

Rachel Abercrombie, USC, "Near field observations of the onset of the 28 June 1992 Landers earthquake"

Donna Eberhart-Phillips, Lorraine Hwang and Rufus Catchings, USGS, "Seismic calibration experiment along the Landers rupture"

Saskia Goes and Steven Ward, USCS, "Synthetic seismicity for the San Andreas and probabilities after the Landers earthquake"

J. Gonzalez, L. Mendez, A. Hinojosa, L. Inzunza, F. Farfan, L. Orozco, A. Vidal, O. Galvez and J. Frez, CICESE, "Resnor: The digital telemetry seismic array south of the scarlet"

S.E. Hough, J. Mori, L. Hwang, E. Sembera, C. Mueller, L. Werneberg, G. Glassmoyer and S. Lydeen, USGS, "Analysis of GEOS recordings of the Landers earthquake sequence"

C. Lazarte and R. Lemmer, Leighton and Assoc., "Preliminary site assessment of the effects of ground displacement from the Landers earthquake"

Jonathan Lees and Craig Nicholson, UCSB, "3-D tomographic velocity inversion of the 1992 Landers-Big Bear-Joshua Tree sequence"

T. Levshina and I. Vorobieva, UCLA, "Application of the algorithm for prediction of a strong second aftershock to the Joshua Tree and the Landers earthquakes' aftershock sequence"

Y.G. Li, K. Aki, D. Adams and A. Hasemi, USC, "Seismic trapped waves and attenuation along the fault zone of the Landers earthquakes"

Anne Lilje, Caltech, "An ARC/INFO database of the Landers surface rupture: Design and content"

Scott Lindvall and Tom Rockwell, Lindvall Richter Benuska Assoc. and SDSU, "Paleoseismic studies along the Landers rupture"

M. Mahdyiar, K. Aki, B.H. Chin and S. Park, Leighton and Assoc., USC and UCR, "Strong motion prediction for the Landers earthquake and a magnitude 7.8 earthquake on the southern segments of the San Andreas fault"

Sally McGill and Charlie Rubin, Cal State San Bernardino and Central Washington University, "Displacement along the southern Emerson fault during the Landers earthquake"

Bernard Minster and Nadya Williams, UCSD, "The M8 intermediate-term earthquake prediction algorithm: An independent assessment with focus on the Loma Prieta and Landers events"

Jim Mori and Lucy Jones, USGS, "Spatial clustering of foreshocks to the Landers earthquake"

Craig Nicholson, Aaron Martin, Frank Vernon, Adam Edelman, Egill Hauksson, David Johnson, Yong-gang Li, Michelle Robertson, Stephen Day and Harold Magistrale, UCSB, UCSD, Caltech, USC and SDSU, "SCEC portable instrument deployment for the 1992 Landers-Big Bear-Joshua Tree earthquake sequence"

M.C. Robertson and C.G. Sammis, USC, "A 3-D fractal analysis of hypocentral locations for the Joshua Tree/Landers/Big Bear aftershock sequences"

James Spotila and Kerry Sieh, Caltech, "Thrust faulting across the Homestead Valley fault"

R. Stein, G. King and J. Lin, USGS and WHOI, "Stress change on the San Andreas fault and surrounding faults caused by the M7.4 Landers earthquake"

Dave Wald, Doug Dreger and Don Helmberger, Caltech, "Preliminary results on modeling the Landers earthquake"

F. Wyatt, D. Agnew and H. Johnson, UCSD, "Deformation from the Landers earthquake sequence recorded at Pinon Flat Observatory"

Judith Zachariasen and Kerry Sieh, Caltech, "The transfer zone between the Homestead Valley and Emerson faults"

Dapeng Zhao and Hiroo Kanamori, Caltech, "Landers earthquake sequence: Joint inversion for 3-D velocity structure and hypocentral locations"

WEDNESDAY, OCTOBER 7

8:30 to 9:00 a.m. (Plenary Session)	Charge to Product Discussion Groups (PDG): Kei Aki/Tom Henyey
9:00 to 10:00 a.m.	PDG 6: Products from real-time seismology/Egill Hauksson
	PDG 2: Fault-slip maps for southern California/Steve Wesnousky
	PDG 7: Intermediate-term earthquake prediction/Bernard Minster
10:00 to 11:00 a.m.	PDG 3: Plausible earthquakes in southern California/Kerry Sieh
	PDG 1: Probabilistic seismic hazard analysis/Allin Cornell
	PDG 9: Tectonic framework/Rob Clayton
11:00 to noon	PDG 4: Ground motion prediction for plausible earthquakes/Steve Day
	PDG 5: Seismicity Simulation/Leon Knopoff
	PDG 8: Fault zone structure/Leon Teng
12:00 to 1:00 p.m.	**Lunch at hotel**
1:00 to 2:30 p.m. (Plenary Session)	PDG Reports and Charge to Working Groups

Working Groups (WG)

2:30 to 4:00 p.m.	WG B & H: Archuleta/Martin WG C: Sieh
4:00 to 5:30 p.m.	WG D: Clayton WG E: Jackson Outreach: McNally
5:30 to 7:00 p.m.	WG F: Hauksson WG G: Knopoff
7:30 to 9:00 p.m.	WG A: Aki

THURSDAY, OCTOBER 8

9:00 a.m. to 12:30 p.m.
(Plenary Session) Reports on future plans from WG leaders

SCEC Administrative Report	Tom Henyey
Education and Outreach/SCEPP	Karen McNally
WG G (Earthquake Physics)	Leon Knopoff
WG F (Regional Seismicity)	Egill Hauksson
WG E (Crustal Deformation)	Dave Jackson
WG D (Subsurface Imaging)	Rob Clayton
WG C (Earthquake Geology)	Kerry Sieh
WG H (Engineering Applications)	Geoff Martin
WG B (Strong Motion)	Ralph Archuleta
WG A (Master Model)	Kei Aki

End of SCEC Meeting

12:30 to 1:30 p.m.

Lunch meeting of SCEC Directors/Advisory Council/NSF-USGS Site Team

1:30 to 3:00 p.m.

Advisory Council and NSF-USGS Site Review Teams meet to review meeting

3:00 to 6:30 p.m.

Advisory Council and NSF-USGS Site Review Team meet with members of SCEC Steering Committee

7:00 p.m.

Dinner with Steering Committee, Advisory Council, and Site Review Team

FRIDAY, OCTOBER 9

8:30 a.m. to noon

Aki and Henyey meet with Advisory Council and NSF/USGS Site-Review Team

Noon to 1:00 p.m.

Lunch for Advisory Council and NSF/USGS Site-Review team

1:00 to ? Site teams complete reports

Academic Co-Investigators (1992)

CORE INSTITUTIONS

University of Southern California: (Coordinating Institution)	Keiiti Aki Thomas Henyey M. Dravinski Simeon Katz Yong-Gang Li Vincent Lee	Geoff Martin David Okaya Charles Sammis Ta-liang Teng M. Trifunac
California Institute of Technology:	Robert Clayton James Dolan John Hall Egill Hauksson Donald Helmberger	Kenneth Hudnut Hiroo Kanamori Ron Scott Kerry Sieh
Columbia University:	John Beavan Leonardo Seeber	Lynn Sykes Christopher Scholz
University of California, Los Angeles:	Paul Davis David Jackson Yan Kagan	Leon Knopoff M. Vucetic
University of California, San Diego:	Duncan Agnew Yehuda Bock	Bernard Minster Frank Vernon
University of California, Santa Barbara:	Ralph Archuleta Bruce Shaw	Craig Nicholson Sandra Seale
University of California, Santa Cruz:	Thorne Lay Karen McNally	John Vidale Steven Ward

PARTICIPATING INSTITUTIONS

University of California, Riverside:	Stephen Park	
University of Nevada, Reno:	John Anderson	Steven Wesnousky
San Diego State University:	Steven Day	Thomas Rockwell
Harvard University:	James Rice	
Stanford University:	Allin Cornell	
Massachusetts Institute of Technology:	Bradford Hager	
Princeton University:	John Suppe	
Oregon State University:	Robert Yeats	
Central Washington University:	Charles Rubin	

California State, San Bernadino:	Sally McGill	
Woods Hole Oceanographic Inst.:	Jian Lin	

INDUSTRY PARTICIPANTS

ACTA, Inc.:	Mark Legg	
Davis and Namson, Consulting Geologists:	Thom Davis	Jay Namson
Leighton and Associates, Inc.:	Eldon Gath	M. Mahdyiar
Lindvall, Richter, Benuska, Assoc.:	Scott Lindvall	

DIRECTOR'S OVERVIEW, 1992

Introduction

The past year has been quite eventful for SCEC. The M6.1 Joshua Tree earthquake occurred just before the second meeting of the Advisory Council on April 23-24, 1992. This meeting was held in conjunction with the April monthly SCEC workshop which focused on master model products. If we had scheduled it a week later, we would have been in the midst of the Los Angeles riots. The Landers-Big Bear earthquakes occurred on the Sunday following the June monthly workshop on real-time seismology.

The fundamental recommendations of the Advisory Council to SCEC were to (a) identify the objectives and products of the master model, (b) for each disciplinary group to outline its particular goals, priorities for funding, and timetable for milestones or products, and (c) to lay out an approach for assembling individual components into the final product. The Council noted several areas of significant progress such as in geology, geodesy, master model concept, the data center, and GIS availability to Center scientists, but expressed concern about the relevance of the physics group and the level of funding in certain areas such as seismicity.

Procedure for Funding

The funding of current (year-2) SCEC projects was decided by the following procedure. First, discussions by individual working groups of the year-2 science plan took place during the first annual SCEC meeting, October 29-November 1, 1991. Next, summaries of working groups' objectives, written by the group leaders, were included in the call for proposals. Then in mid-December, 1991, the Science Director received copies of all year-2 research proposals submitted to SCEC. Proposal copies were also sent to the appropriate working group leaders. A list of PI's, proposal titles and requested funds of all submitted proposals were also delivered to each group leader. Copies of actual proposals from all of the groups were available to each of the group leaders upon request.

In late January, 1992, SCEC was informed of its 1992 funding from the NSF and USGS -- a total of $2.754M ($1.62M from NSF and $1.134M from USGS). A new increment of $125K was also received from FEMA for support of education and outreach. $181K was carried forward from 1991, since the cost of equipment for the data center was less than anticipated. This carryover meant that $3.060M was available for 1992 research and infrastructure. With this budget, the Science Director, after consulting with the Executive Director and Assistant Director for Administration, proposed a preliminary plan to the SCEC Board of Directors on February 6, 1992.

Requests for support under infrastructure totaled $2.428M. At the meeting on February 6, support of $1.555M was approved unanimously by the Board for various elements of the infrastructure.

In approving the infrastructure plan, the following items were taken into consideration:

1. The need for additional funding for workshops and AdvisoryCouncil meetings.
2. Expenses of the Visitor's Program should be spread over 1992 and 1993. $150K was authorized for '92 and $110K for '93.

3. All GIS service activities were to be put under the supervision of one scientist (Steve Park of UCR). Putting the GIS center at Riverside complements the USGS operation of Doug Morton, also at Riverside.
4. SCEC had a mandate to begin an education and outreach program.
5. The Director and Board felt it was imperative to support data transfer from Pinon Flat to the data center in real time and to support the new TERRAscope network being established by Caltech.

In proposing a science plan to the Board, the Director used the following general criteria:

1. Quality of science in the proposed research.
2. Relevance to the master model construction.
3. Prospect for immediate products.
4. Achievement in year-1 work (for those funded in 1991).
5. Participation in SCEC activities.

The above five criteria were used with approximately equal weight. In distributing the research funds among proposals, the current status and future direction of individual groups were taken into consideration. This was done through discussions between the group leaders and the Science Director who visited all the group leaders individually in January, 1992.

During the week of February 10, a final plan for each group was agreed upon by the group leaders and the Science Director. The plan went to the Board for approval on February 14. The plan was approved by the Board on February 19. Requests for research support totaled $2.97M for 94 projects. Fifty-one projects were supported for a total science funding of $1.38M

Discipline-Task Matrix

In order to begin responding to the product or task oriented recommendation of the Advisory Council, it is useful to show the distribution of current science funding in matrix form, in which the disciplinary working group defines the column, and the task defines the row. The tasks as currently defined are as follows:

Task 1: real-time earthquake information, including technical and software support for TERRAscope. The currently funded PI's are Hauksson, Helmberger, Lay, Agnew and Aki.

Task 2: velocity and Q models for propagation path effects. The PI's are Clayton, Davis, Helmberger, Zhao and Aki.

Task 3: earthquake source characterization including investigation of active faults, crustal deformation, and models of earthquake recurrence and rupture. The PI's are Sieh, Dolan, Gath, Lin, Lindvall, McGill, Namson, Rockwell, Rubin, Suppe, Ward, Yeats, Ghisetti, Gratier, Legg, Okaya, Agnew, Hager, Hudnut, Jackson, Humphreys, Snay, Harris, Rice, Wesnousky, and Cornell.

Task 4: mapping the local site effects on ground motion. The PI's are Archuleta, Anderson, Aki, Dravinski, Seal, Vidale, and Kanamori.

Discipline - Task Matrix

No.		Master Model Seismic Hazard	Strong Ground Motion	Earthquake Geology	Subsurface Imaging	Crustal Deformation	Seismicity and Source Process	Physics of Earthquake Sources	Infrastructure	SUM
		A	B	C	D	E	F	G		
1	Real Time Earthquake Information					20 K	90 K		60 K	**170 K**
2	Seismic Structure and Propagation Path Effects		20 K		100 K					**120 K**
3	Earthquake Source Characterization	121 K		400 K		113 K				**634 K**
4	Local Site Effects	49 K	129 K				10 K			**188 K**
5	Synthesis of Source, Path and Site Effects into GIS Based Seismic Hazard Map	66 K							100 K	**166 K**
6	Structure and Physical Processes in Fault Zones				70 K		50 K	15 K		**135 K**
7	Observational and Physical Bases for Intermediate-Term Earthquake Prediction	38 K						109 K		**147 K**
	SUM	**274 K**	**149 K**	**400 K**	**170 K**	**133 K**	**150 K**	**124 K**	**160 K**	**1,560 K**

Task 5: synthesis of source, path and site effects into GIS-based probabilistic seismic hazard maps. The PI's are Aki, Sykes, Petersen, Mahdyiar, Archuleta, and Park.

Task 6: investigation of structure and physical process in the fault zones. The PI's are Seeber, Sammis, Okaya, Li, Teng, Henyey.

Task 7: observational and physical bases for intermediate-term earthquake prediction. The PI's are Keilis-Borok, Katz, Minster, Kagan, Knopoff, and Shaw.

Although some of the projects may not exactly match the task definition, it is clear from the matrix that SCEC is currently putting the greatest emphasis on the task of earthquake source characterization (Task 3).

In order to define the tasks more tangibly in terms of products, the morning of October 7 of the annual meeting will be devoted to the discussion of the following products:

1. Methodology for probabilistic seismic hazard analysis
2. Fault slip maps for southern California
3. Plausible large earthquakes in southern California
4. Ground motion prediction for plausible earthquakes
5. Seismicity simulation
6. Products from real-time seismology
7. Intermediate-term earthquake prediction
8. Fault zone structure
9. Tectonic framework

In these meetings, we hope to decide what the actual products to be produced by SCEC by May 1, 1993 (for the new SCEC five-year plan due July 1) will be, how the work will be done, and who will participate in completing identified products. In the afternoon of October 7, the disciplinary groups will meet to discuss how to address the tasks and develop their programs for 1993. We hope that this matrix approach will enable us to effectively respond to recommendations by the Advisory Council.

Impact of the Landers-Big Bear Earthquake

The Landers-Big Bear earthquake on June 28, 1992 resulted in SCEC developing definite deadlines for producing master model products precisely along the lines of the primary goal of SCEC. A one-day workshop was held at USC two weeks after the earthquake to discuss the implications of the event and SCEC's response. The workshop participants were: Agnew, Aki, Dieterich, Ellsworth, Harris, Heaton, Jackson, Jin, Jones, Kagan, Katz, Lindh, McEvilly, Minster, Reasenberg, Rubin, Simpson, Stein, Sykes and Williams.

The workshop started with Aki's introduction to the historical background of earthquake probability assessment beginning with a working group report (U.S.G.S. Open-File Report 88-398) on major California earthquakes published in 1988. About a year ago, SCEC was asked by the chairman of NEPEC to reassess the probabilities for southern California estimated by the 1988 working group. At that time, SCEC's response was to postpone the reassessment in order to include a probabilistic analysis of ground motion hazard. The recent Landers-Big Bear earthquakes, however, demanded an immediate reassessment.

Such a reassessment was made for large earthquakes in the San Francisco Bay region after the Loma Prieta earthquake by another working group (U.S.G.S. Circular 1053) in 1990. Working group 90 followed the basic model used by working group 88, and re-evaluated the segmentation and recurrence time for faults in the Bay region using new data. In addition, the group attempted to include the effect of the Loma Prieta earthquake by estimating the change in the earthquake recurrence time for a particular fault segment due to the change in stress on that segment. It also introduced the logic tree approach to reflect the diversity of expert opinions.

Working group 90 did not include so called "intermediate-term precursors" such as the seismicity pattern, in the revision of probabilities, although the increased seismicity level was used to support the revised probability estimates.

The above introduction was followed by presentations on the seismicity (Jones), distant earthquakes triggering (Reasenberg, Ellsworth), stress redistribution (Stein, Sykes, Simpson, Harris), GPS and strain measurements (Jackson, Agnew), and intermediate-term precursors (Minster, Jin, Katz). These presentations convinced participants of the urgent need for producing a public document on the implications of the Landers-Big Bear sequence on seismic hazards in southern California.

The workshop concluded with a unanimous decision to produce two documents. The first document (Phase I) should be written by Sept. 1, 1992, in a form to be reviewed by NEPEC and CEPEC. It would address (1) recent seismicity in southern California, (2) effects of the Landers-Big Bear sequence on nearby faults, and (3) the potential for future ground shaking in southern California. The second (Phase II) document should address issues which cannot be resolved in the short Phase I timeframe, and consider the seismic hazard broadly over the whole of southern California. The second document should be completed July 1, 1993.

Another workshop was held at USC on July 27, 1992 to follow up on the consensus developed in the July 13 workshop. The workshop participants were: Adams, Agnew, Aki, Cornell, Davis, Harris, Henyey, Jackson, Jones, Jin, Kagan, King, McNally, Minster, Sieh, Schwartz, Teng, Weldon and Wesnousky.

In this meeting, Agnew and Jackson agreed to take responsibilities for assembling contributions from SCEC scientists to the Phase I report which will form the technical basis for a document to be prepared by a joint NEPEC/CEPEC/SCEC ad-hoc working group. Final review, organization and editing of the report was done by Aki and Henyey, and the report has been submitted to NEPEC and CEPEC.

Recurrence Models with Interacting Fault Segments

In the course of preparing the Phase I report, several fundamental issues which are directly relevant to the goals of SCEC have been brought up. A primary issue is the need for a recurrence model that allows for interaction between fault segments. This issue was brought up for several reasons. First, paleoseismic data for the southern San Andreas fault suggest that adjacent segments can break separately or simultaneously. Second, it is not clear how the recurrence model based on the assumption of non-interacting segments (e.g. the 1988 Working Group) can incorporate the effect of stress redistribution due to a nearby earthquake. The 1990 Working Group included such an effect by "clock-advancing" based on the assumption of a time-predictable model. The procedure taken by the 1990 Working Group, however, produces no effect due to stress redistribution if the distribution of recurrence time intervals is Poissonian. Then, if failure of San Andreas fault is always triggered by adjacent events like the Landers earthquake, and if the latter follows a

Poissonian process, the estimate of the probability increase based on the clock-advance approach will underestimate the real probability of the failure of San Andreas fault.

Another possibility is that the occurrence of Landers-like earthquakes in the vicinity of the San Andreas fault and the resultant stress redistribution may be a part of the process which is already accounted for in the distribution of recurrence time intervals used in the 1988 Working Group probability estimation. Then, we should not introduce any additional probability increase by the stress redistribution, but consider that it is simply confirming the high estimated conditional probability due to the proximity to failure.

In order to deal with the problem properly, we need to investigate the recurrence statistics of a system composed of interacting fault segments. Such investigations have already been undertaken by SCEC researchers using various approaches (Ward, Barrientos, Cornell, Wu, Rice, Ben-Zion). We need to develop a versatile recurrence model of fault segments with well defined mechanical interactions.

In the past, when considering interactions among fault segments, the effect of the loading boundary condition has been usually neglected. For example, if the Landers earthquake is caused by a loading from slip in the ductile part of lithosphere immediately below the fault, the stress redistribution may be restricted near epicentral area. If, on the other hand, it is caused by a distant pull from the moving Pacific plate exerted on the boundary of the western strong lithosphere, including Sierra Nevada, and the eastern weak lithosphere of the Basin and Range, the stress relaxation in the epicentral area of the Landers earthquake may facilitate the motion of the Pacific plate and increase the loading on the rest of the boundary, explaining the observed triggering of distant earthquakes by the Landers earthquake along the above boundary as far north as Mt. Shasta. In any case, the change in loading boundary condition needs to be included in the recurrence model of interacting fault segments.

Ground Motion Simulation for the Landers Earthquake and the Anticipated Failure of the southern San Andreas Fault Segments

The Landers earthquake offered an excellent opportunity to test the methodology for predicting strong ground motion for the anticipated failure of southern San Andreas fault segments (the so called "Big One") based on existing information on the earthquake source, propagation path effects, and geologic site conditions. At SCEC, we now have three such methods for ground motion simulation.

Agnew uses the method of Evernden et al (1981) for calculating seismic intensity. It includes the effect of local geology as mapped by Evernden, although resampled to a 1.5 mile grid. The advantage of this method is that it has been validated by observed intensities for many earthquakes, and used in the past by the State of California as the basis for emergency preparedness planning.

Wesnousky's method is based on the empirical attenuation relation of Joyner and Boore (1988), combined with the results of Petersen on local site effects using data from the 1972 San Fernando earthquake (amplification factors at period of 3 seconds being 1.0, 2.0 and 3.0 for hard rock (crystalline), soft rock (Tertiary sediment) and alluvium, respectively). He also uses the digitized geology (0.5 minute mesh) of southern California supplied by Agnew.

The third method being developed by Mahdyiar et al takes advantage of maps of frequency dependent site amplification factor in the linear regime obtained by Aki et al (1992) which combine site geologic ages and empirical factors measured at regional

network seismograph sites. They use the w-squared model of Hanks and McGuire (1981), and Boore (1983) to represent the subevent of the specific barrier model of Papageorgiou and Aki (1983) for which a systematic relation between the model parameters and magnitude is known for past major California earthquakes (Chin and Aki,1991). The propagation path effect is approximated by a 1/R geometrical spreading law and frequency dependent Q.

The above combination of source, path and site effect modeling was tested using strong motion data from the Loma Prieta earthquake (Chin and Aki, 1991). The test showed the validity of the model for rock sites at all levels of acceleration, and for soil sites beyond about 50 km from the hypocenter. At shorter distances, however, the predicted motion overestimated the observed at soil sites; the discrepancy can be explained by non-linear amplification effects known from laboratory experiments on soil.

As an initial attempt to include non-linear effects in ground motion calculations, Mahdyiar et al use the following rule for alluvium sites when the calculated acceleration exceededs 0.1 g. They assume that a common curve applies to the relation between peak acceleration at the surface of an alluvium site and peak acceleration at the top of basement beneath the site. The curve is non-linear and approaches 0.4 g when the basement acceleration becomes large. They further assume that the damping is independent of frequency, and the attenuation factor may be expressed in the form, e^{-af}, where f is frequency and a is a constant. a is determined at each alluvium site iteratively so that the resultant peak acceleration falls on the assumed common curve.

This method can predict the time history of acceleration from which various useful ground motion parameters, such as peak ground acceleration, response spectra and duration can be calculated by the random vibration technique.

The above three methods, each with distinct advantages and disadvantages are currently tested against the observed strong ground motion data from the Landers-Big Bear earthquakes.

Conclusion

In response to the recommendation of the SCEC Advisory Council, we have tried to reorganize science projects according to well defined tasks. We still recognize the importance of the disciplinary working group structure, but plan to accomplish the goals of SCEC using a discipline-task matrix approach.

The Landers-Big Bear earthquake sequence on June 28, 1992 provided SCEC an opportunity to develop our first iteration of the master model. Toward this end considerable effort has been given in the past several months to construct an acceptable recurrence model with interacting fault segments and to simulate ground motion based on the existing information on the earthquake source, propagation path effects, and geologic site conditions.

SOUTHERN CALIFORNIA EARTHQUAKE CENTER
HIGHLIGHTS -- YEAR 2

- Preparation of Landers earthquake Phase I report and submittal to NEPEC and CEPEC (Agnew, Jackson, and SCEC scientists)
  - Foreshocks and aftershocks
  - Distant triggered events
  - Changes in failure stress on adjacent faults
  - Plausible future large earthquakes as a result of Landers
  - Probable ground shaking for future earthquakes
  - Intermediate-term probability estimates

- Post-earthquake studies of the Joshua Tree/Landers/Big Bear sequence (SCEC scientists)
  - Deployment and operation of 20 element arrays of Refteks (Nicholson, Vernon, Li, Hauksson)
  - Association and archiving of data at SCEC data center (Vernon)
  - Fault rupture mapping and slip measurement (Sieh, Dolan Hudnut, Rubin)
  - Observed displacement from Landers earthquake at over 50 sites and documented post-seismic displacement up to 2 mm/day following the earthquake (Jackson and GPS group)

- Unequivocal evidence for fault zone trapped waves (Li and Aki)
  - Fault zone structure at depth
  - Relation to segmentation and rupture dynamics

- Development of map of linear amplification factors in the frequency range, 1.5 to 12 Hz for the whole of southern California (Aki and Park)
  - GIS-based
  - Combines empirically determined amplification factors from coda waves with the surface geology

- Synthesis of existing information on the earthquake source, propagation path effects, and geologic site conditions for strong ground motion simulation in southern California (Mahdyiar and Aki)
  - Uses random vibration technique
  - Can supply most ground motion parameters useful for engineering applications

- Field investigation and compilation of long-period ($0.5<T<10$ sec) amplification factors (Dravinsky)
  - Uses microtremor analysis
  - 148 sites in the Los Angeles basin
  - Pipes Canyon near Landers epicenter
  - Done in cooperation with Japanese researchers from Hokkaido University

- First observation of post-seismic extensional strain at Pinon Flat (Agnew)
  - Amounted to 3% of coseismic strain on the NW-SE component over the 8 days following the Landers event

- Determined deformation velocity at 50 points spanning 400 km across the San Andreas fault (Jackson and GPS group)

- Introduction of the concept of characteristic cell size of geometric disorder within a fault zone (Rice)
  - If the cell size is greater than the nucleation size determined from the parameters of the friction law, spatio-temporal complexity of slip results
  - If the cell size is smaller than the nucleation size, simple cyclic large earthquakes occur
  - It has been suggested that Parkfield-like events will have highly variable moment release and recurrence intervals

- Update and synthesis of slip rates and paleoseismic data for all known southern California faults and seismogenic structures (Wesnousky)
  - Can be readily input into any GIS data base

- Expanded fault zone geology of the Los Angeles basin
  - Evidence from the Wilshire arch for buried thrusting and complexity of the Elysian Park/Hollywood Hills anticlinorium (Yeats)
  - Evidence for Holocene scarps atop the Wilshire arch northwest of downtown Los Angeles (Dolan and Sieh)
  - Excavations across a Holocene scarp on Santa Monica fault suggest earthquake recurrence intervals of several thousand years, but events are large (Dolan)
  - Trenching on the Whittier fault suggests that recurrence intervals are also on the order of thousands of years and are large -- M≥6.5 (Rockwell)
  - Growth wedges on the western flank of the L.A. basin are interpreted to be the result of slip on a NW-dipping blind thrust capable of M≥6.6 earthquakes (Suppe)
  - Dextral slip on the Newport-Inglewood fault at Signal Hill estimated to be 0.035 mm/yr (Suppe)
  - Models of deformation of terraces on the Palos Verdes Peninsula suggest that dextral/reverse slip on the Palos Verdes fault is about 3 mm/yr (Ward and Valensise)

- Improved P-wave tomographic imaging of the crust and uppermost mantle in southern California (Zhao)
  - Used 131,372 P-wave arrival times from 6,437 local and regional earthquakes recorded on the Southern California Seismic Network over the past 12 years

- Improved P-wave velocity structure of the Los Angeles basin (Clayton and Hauksson)
  - Inverted arrival time data from 530 earthquakes and 2 blasts
  - Model consisted of 2048 grid nodes with 6 km horizontal spacing

SOUTHERN CALIFORNIA EARTHQUAKE CENTER (SCEC)

- **A consortium** of seven core academic institutions in partnership with the U.S. Geological Survey.

- **Coordinating Institution:** University of Southern California

- **Goal:** To integrate research findings from different disciplines in earthquake science in order to develop a prototype probabilistic seismic hazard model (master model) for southern California.

- **Funding:**

	Year 1	Year 2
National Science Foundation	$1.400M	$1.620M
U.S. Geological Survey	$1.850M	$1.134M
F.E.M.A.	$0.000M	$0.125M
TOTAL	$3.250M	$2.879M

- **Expenditures:**

Management	$0.240M	$0.225M*
Infrastructure	$1.680M	$1.274M
Project Science	$1.330M	$1.380M
TOTAL	$3.250M	$2.879M

Note: NSB recommended funding for SCEC = $13.4M for 5 yrs.

* Does not include institutional participation.

SOUTHERN CALIFORNIA EARTHQUAKE CENTER
BUDGET

	Year 1	Year 2
● Infrastructure		
Management	$240K	$225K
Workshops/Meetings	$ 45K	$ 90K
Visitors Program	$290K	$150K
Education and Outreach	$ 30K	$225K
Data Center	$470K	$ 27K
Seismic Instrumentation	$290K	$192K
GPS Data Acquisition	$475K	$410K
GIS Development	$ 80K	$ 70K
Data Basing	$ 0K	$ 50K
TERRAscope	$ 0K	$ 60K
Subtotal	$1,920K*	$1,499K
● Project Science		
Master Model Construction	$150K	$274K
Strong Motion Studies	$200K	$149K
Earthquake Geology	$200K	$400K
Subsurface Imaging	$275K	$170K
Geodesy	$160K	$113K
Seismology	$145K	$150K
Earthquake Physics	$200K	$124K
Subtotal	$1,330K	$1,380K
Grand Total	**$3,250K**	**$2,879K**

* $181K carried forward due to savings in equipment purchases; $173K designated for data center at Caltech and $8K to instrument center at UCSB.

NSF/USGS SITE VISIT OF THE SCEC
October 8-9, 1992

NSF Visitors

James H. Whitcomb - NSF Coordinator for the SCEC, Program Director, Geophysics
Tel (202)357-7356, FAX (202)357-0364

James F. Hays - Director, Earth Sciences Division
Tel (202)357-7958, FAX (202)357-0364

Shih-Chi Liu - Program Director, Earthquake Hazard Mitigation
Tel (202)357-9780, FAX (202)357-9803

USGS Visitors

Elaine Padavani - USGS Coordinator for the SCEC, Deputy Chief for External Research
Tel (703)648-6722, FAX (703)648-6717

Robert L. Wesson - Office Head, USGS Office of Earthquakes, Volcanos and Engineering
Tel (703)648-6714, FAX (703)648-6717

Wayne R. Thatcher - Geophysicist, Menlo Park Office
Tel (415)329-4810, FAX (415)329-5163

Outside Visitors

Charles A. Langston
Department of Geosciences
Deike Building
Pennsylvania State University
University Park, PA 16802
Tel (814)865-0083
FAX (814)863-7823

Susan L. Beck
Geoscience Department
Gould Simpson Building
University of Arizona
Tucson, AZ 85721
Tel (602)621-8628
FAX (602)621-2672

John L. Aho
General Engineering Manager
CH2M Hill
2550 Denali St., 8th Floor
Anchorage, AK 99503
Tel (907)278-2551
FAX (907)277-9736

NATIONAL SCIENCE FOUNDATION
1800 G STREET, N.W.
WASHINGTON, D.C. 20550

March 5, 1992

Prof. Keiiti Aki
Prof. Tom Henyey
Southern California
Earthquake Center
University of Southern California
Los Angeles, CA 90089

Dear Kei and Tom:

Enclosed is a copy of the Site Visit Report for the November 1, 1991, site visit to the SCEC.

Everyone is excited about the progress made in the first year and the considerable potential in the future for the center concept applied to regional earthquake hazards. I believe, as do you, that this will be a model that will be applicable to seismically active regions throughout the U.S. and the world.

Please give my thanks on behalf of the site visit team to all of the participants for their considerable effort.

Sincerely yours,

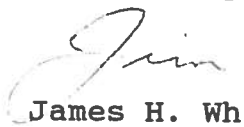

James H. Whitcomb
Program Director
for Geophysics
(202)357-7356
(202)357-0364 FAX
jwhitcom@nsf.gov

cc: Wesson/USGS/OEVE
Sperlich/NSF/STC
Corell/NSF/GEO
Hays/NSF/EAR
Site Visit Team

SOUTHERN CALIFORNIA EARTHQUAKE CENTER
NSF/USGS ANNUAL SITE VISIT; NOVEMBER 1, 1991

The first annual site visit to the Southern California Earthquake Center (SCEC) was done November 1, 1991, by a team of NSF, USGS, academic, and industry personnel. The SCEC is supported under a cooperative agreement by the NSF and USGS and is an NSF Science and Technology Center (STC). The site review team members were James H. Whitcomb, team leader and NSF coordinator for the Center, Elaine Padavani, USGS coordinator for the Center, John L. Aho, CH2M Hill Co., Susan L. Beck, Univ. of Arizona, James F. Hays, NSF, Charles A. Langston, Pennsylvania State Univ., Wayne R. Thatcher, USGS, and Robert L. Wesson, USGS.

This annual site visit occurred when the SCEC was just eight months old and was coincident with SCEC's first annual meeting and the first meeting of its Advisory Council.

Intrinsic Merit of the STC Research

The site visit team felt that the synergy of the research participants is the greatest strength of the SCEC. This synergy has brought world-class scientists from different fields to focus on a single problem, earthquake hazard reduction, in a natural laboratory of high seismic hazard, southern California.

The ultimate aim of the SCEC is the development of a formal framework, called the master model. The master model is vague in the minds of many outside the Center and needs better definition. Through the model, SCEC will apply research results to seismic hazard estimation; the transfer of the results to the user community in an effective way is a major outreach goal. A sampling of research accomplishments in the brief time since the birth of the SCEC include:

- Inauguration of monthly, topic-specific workshops that have attracted national/international interest;
- Development of a seismic-hazard data base and retrieval system;
- Development of interaction between seismologists and geotechnical engineers that has identified a key need for further research: non-linear soil amplification;
- Discovery of a young east-west trending fold south of the Hollywood Hills and mapping of youthful traces of faults; these discoveries have revised thinking about tectonics and seismic hazard in the Los Angeles basin area;
- Generation of a daily probability map that a given location will experience an earthquake acceleration greater than 0.1 g; this is the first of the master model's outreach products.

These results are changing seismic hazards thinking in southern California and are a direct result of the Center environment.

Research plans for the next year's operations are developed in detail by each of the seven research working groups with guidance on focus from the SCEC Steering Committee. Next year, SCEC will:

- Intensify the effort to delineate seismogenic structures in the Los Angeles basin;
- Study site amplification effects and non-linearity of earthquake strong motions;
- Study the role of fault interactions, segmentation, bends and branching in estimation of earthquake potential;
- Enhance the master model of seismic hazards and its transfer of technology to the user community.

Institutional resources are significantly enhanced by the fact that the core institutes of the Center have a history of research activity in seismic hazards. In addition to utilizing existing academic staff and students, the SCEC is using the data base capabilities of the Caltech/USGS installation in Pasadena, a continuously-recording GPS network installed with the support of NASA, and the broad-band seismic network TERRAscope installed by Caltech using private support.

Educational and Training Component, Including Outreach

The primary contribution of SCEC to education and training is through graduate and post-doctoral research support. Currently, 28 graduate students and 14 post-doctoral fellows are being supported with SCEC funds.

Significant expansion of outreach activities has occurred with the development of a memorandum of understanding with the Southern California Earthquake Emergency Preparedness Project (SCEPP) of the Governor's Office of Emergency Services. This is an ideal collaboration that will take advantage of SCEPP's experience in outreach with education, business, and local governments. SCEPP will in turn benefit from closer ties to the research community through an in-house SCEC liason. Support from FEMA and from NSF's Education and Human Resources Directorate will be sought to expand the joint effort.

Linkages to Other Sectors (Academic, Federal, State, & Local Government, National Laboratories, Industry) and Knowledge Transfer

Links to other sectors is one of the strengths of the SCEC. Seven universities and the USGS form the core. The NSF, USGS, and FEMA fund the Center. State and local governments participate directly through the new SCEPP association and an engineering applications project being formulated between the SCEC and Caltrans, County of Los Angeles, and the City of Los Angeles. Industry participates directly in the research and will have an important role in coming technology transfer stages.

Management and Leadership

The management structure of Aki as Science Director and Henyey as Executive Director is very effective in the judgement of the visiting team. A high degree of participation has been fostered that has resulted in a new level of integration of quality scientists from varied disciplines focused on an important problem.

Possible weaknesses were perceived in the funding of individual research projects. The philosophy for future allocation of funds needs a clearer statement. The funding decision process also is not clear, especially at the working group level. Although large numbers of funded participants might be desirable in the initial data gathering and synthesis stages of the Center, concern was expressed that future resources of the Center might be spread too thinly if the same philosophy holds.

Support was expressed by the site-visit team for a more formal long-range plan with products and milestones.

Institutional and Other Sector Support for the STC

The SCEC has been very aggressive in efforts to broaden its support. In addition to the base support provided by the NSF and USGS, SCEC initiatives are in the advanced stage for FEMA support in the SCEPP cooperation, and for state, county and city support for the engineering applications effort. Proposals are underway also for undergraduate and pre-college outreach programs.

Budget Analysis

The site visit team felt that the SCEC is getting a lot of mileage out of the funding provided. The SCEC participants themselves are concerned about the NSF/USGS funding level being inadequate for the planned scope of the Center. After first-year funding, some modest increases in NSF funding are expected but USGS funding has been reduced, giving a net reduction for the second year. These realities require a reevaluation of the scope of the SCEC to match actual funding levels.

Summary and Recommendations

Strengths. A summary of strengths of the Center is highlighted by the high quality, diversity and number of scientists participating in Center activities. The integration and group focus on the problem of earthquake hazard reduction in a specific high-hazard region is unique, and would not be likely under any but a center structure.

The next-highest-ranked strength category is the outreach effort. This includes the nascent relationship with SCEPP, which is a ready-made outreach to business, government, and educational groups. Also important is the unified science front presented by SCEP to the southern California community where damaging earthquakes have been occurring at an unusually high rate during the last 20 years.

Other highly rated strengths include progress on the seismic hazards data center and the new discoveries leading to a revision of thinking about the neotectonics of the Los Angeles basin. Progress in the latter justifies an increase in support of earthquake geology. In general, it was felt that substantial progress has been made on limited resources.

Weaknesses. Leading the list of weaknesses is a perceived general uncertainty about how funds are allocated among component projects. This process should be clearly spelled out to potential grantees as to the influence of the goals of the Center, executive committee, steering committee, subgroup chairman, subgroup, and outside reviewers. The most important of these should be relevance to the immediate goals of the Center for which the SCEC Directors have ultimate responsibility. This is the main factor that distinguishes the Center grants from general NSF and USGS research grants.

The SCEC has initially sought a broad initial participation so as to facilitate effective gathering of the existing seismic hazard data sets for incorporation into the data center. This has been successful. However, the extension of this philosophy into the future presents the danger of spreading the available support too thinly to adequately accomplish the goals of the Center. The number of projects should be reduced in order to concentrate support on the highest priorities.

The site visit team felt that a more formalized long-range plan with intermediate products and milestones is now needed.

Southern California Earthquake Center

ADVISORY COUNCIL

Report on the First Meeting of the Advisory Council to the Southern California Earthquake Center October 31-November 1, 1991 University Hilton, Los Angeles, California.

The first meeting of the SCEC Advisory Council occurred in conjunction with the SCEC's first annual meeting. It began with a "get acquainted" executive meeting on the afternoon of October 31, followed by a whole day of presentations and discussions, some of which were shared with the NSF/USGS site review panel. The following is the report of the Advisory Council to the Center, which represents the essence of the discussion held in the executive session at the end of the day on November 1. Attached is the full list of names and addresses of the Council members. Present at the meeting were Drs. J. Davis, J. Dieterich, I. M. Idriss, T. Jordan, D. Miletti, W. Petak, B. Romanowicz and R. Smith.

The council is impressed by the level of synergy that has been developed over the short time of existence of the Center, the eagerness of the participants to reach across their disciplinary boundaries and work towards the common goal. Seeing the progress accomplished over the past 8 months, it is clear that the Center's structure has provided the ingredients for a type of interaction, at both the individual and institutional level, that would not have otherwise occurred.

We particularly wish to commend the Scientific Director, Dr. Kei Aki and Executive Director, Dr. Tom Henyey, for their leadership, the quality of their management and administration, which have been critical at this first stage of implementation of the Center.

The Center has had a good start, has brought together in the first year the appropriate scientific community and has established a good balance of investments between infrastructure and research projects. The question which needs to be addressed now is whether the mechanisms for moving forward towards the long term goal are appropriately designed and fully thought out.

The Advisory Council sees an urgent need for an overall strategic plan for the Center, comprising two major components: a Science Plan and a Plan for Outreach and Technology Transfer.

Science Plan.

A more specific plan should be developed and made available to the community. It should be continuously updated as the Center moves along in its progress towards the Master Model. It should present the rationale for how funding is being distributed among the different working groups, so that there is a sense among the participants that the process is not arbitrary, but fair and in accordance with an overall strategy. We endorse the short term plan followed for proposal handling in the first year, and recommend that the small grants program be kept at its current level, reserving additional funding, as it becomes available, to special target projects.

While we do not intend to enter a too detailed discussion of the Center's scientific activities, here are some of the issues that we would like to see addressed in the Science Plan:

- How does the theoretical modelling group contribute to the development of the Master Model?

- Does the attribution of several permanent positions to UCLA for GPS activities not represent an over commitment to GPS, given the rapid evolution of the technology, and will this not impair the flexibility of center planning?

- What is the role of continuously recording, high-resolution strainmeters in monitoring pre-, co-, and postseismic phenomena in Southern California? How do these measurements relate to continuously recorded GPS measurements?

- How is the shift of focus of the Center activities from the potentially hazardous San Andreas fault system to the Los Angeles Basin justified? The Center should make sure that the risk is its primary focus and that it is not driven purely by scientifically interesting problems.

- What is the rationale for the large refraction experiment proposed across the LA Basin? What is the relevance and cost effectiveness of this project? How will the information gathered help the Master Model? Southern California has been the site of numerous refraction and reflection experiments in

the past 10-20 years, and it is not clear how much new information on crustal structure would come from the planned experiments. In particular, have the large reflection datasets collected by the oil industry, for the L.A. basin and surrounding areas been sought and exploited?

- What are the mechanisms by which the Center will bring in outside investigators and topics, given the focus that it creates of so much of our communities limited resources?

Outreach Plan.

The Advisory Council feels that the way to communicate the final product of the Center is talk about it **NOW.** It therefore recommends that appropriate strategic thinking be devoted to putting out a product based on presently available information as soon as possible and that mechanisms be developed for updating it periodically. This should serve to build up confidence of the public and provide the necessary visibility to the Center.

We endorse the on-going effort at developing the SCEC/SCEPP relationship, and encourage the Center to also investigate new ideas and new ways of reaching the users. Initiatives at reaching large communities, through presentations in front of large groups, for a charge, should be developed. These could take the form of public seminars, society sponsored workshops (such as the ASCE, SME, etc.), state and local government workshops, etc. At the same time, the example of the successful recent Gamble House workshop should be followed in order to establish communication with other communities, among them at least structural engineers and planners. Such workshops should be repeated at least every two years. Outreach activities that extend beyond workshops should also be explored.

Some process needs to be established to secure the two way flow of information with the users even as the Center's scientists progress towards the Master Model. We feel that a special group responsible to the Steering Committee should be formed to deal with these issues within the Center.

The Center should put together a formal outreach plan. It should solicit input from risk communication specialists in the development of this outreach plan. As currently structured, the

Center is not able to take advantage of this area of knowledge given its own membership or through its affiliation with SCEPP.

Finally, the Advisory Council, in its enthusiastic support to the Center, wishes to be able to meet twice a year, in order to be able to more actively follow the Center's progress, and provide input into it. The next meeting has been scheduled to occur in early Spring 1992, in conjunction with one of the monthly Center seminars, in order, in particular, to discuss and review the Center Plan before its distribution. At that time it will be practical to also give further consideration to the performance measures in the context of the Science and Outreach plans. The Council endorses the desire of some Center members to try and shorten the length of their Annual Meeting, and, at the same time, expresses interest in attending a larger part of the meeting, for better exposure to the Center activities, progress, and plans.

In the name of the Advisory Council members,

Barbara Romanowicz
Chair
Berkeley, November 22, 1991

Report on the
2nd meeting of the Advisory Council
to the Southern California Earthquake Center
April 23-24,1992,
University of Southern California.

The SCEC Advisory Council met for the second time in conjunction with the April monthly SCEC workshop on April 23rd. On April 24rd, the council met with individual Center Directors and representatives of core institutions before holding an executive session and reporting to the Center's scientific and executive directors. The following is the report of the Advisory Council to the Center, which represents the essence of the discussions held on April 24th, and concluded in executive session at 3pm on that day. Present at the meeting were Drs J. Davis, J. Dieterich, P. Flores, I. Idriss, T. Jordan, D. Mileti, W. Petak, B. Romanowicz (chair), J. Rundle, and R. Smith.

The advisory council wishes to express its wholehearted support for the activities and progress of the SCEC, and, once again, commend its scientific Director, Professor Kei Aki, and its executive Director, Professor Tom Henyey, for their superb leadership.
The overall impression of the council is very positive. We have found it very useful to meet individually with the Center's Directors. We feel we have thus obtained a very complete picture of the Center's healthy dynamics and some understanding of a few emerging problems, that need to be dealt with. We note several areas in which the progress has been strongest: geology, geodesy, concept of the Master Model, Data Center and GIS availability to Center scientists.

The first question that naturally comes up is that of the reduced funding of the Center with respect to original recommendations and plans, as well as concerns for future funding. Given the achievements and success of SCEC in its first 2 years, we encourage the Center to take a positive attitude towards consolidation of its funding. Since the Center's program is "product" oriented, it should be able to attract industrial sponsorship. Also, the Center should be in a position to defend its current level of funding and, in any case, survive in the event of further budget cuts. We feel that this can best be achieved by laying out a strategic/science plan that would serve several important purposes:

1) to serve as the reference document to be used when approaching other agencies/foundations for complementary funding
2) to clarify the goals, priorities and choices of the Center for the benefit of both the Center community and the rest of the seismological community.
3) to serve as reference in the event that future budget cuts make it necessary to enforce priorities.

This plan, as already recommended in our previous report, should be constructed by first identifying the objectives and products of the master model, e.g., predicted ground motion maps, probability of earthquakes on given faults, site motion vectors and so forth. The specific constributions to each of these goals by the various disciplinary groups should be identified, so that the purpose of each group and the interactions between them can be more clearly understood. Moreover, a series of benchmarks and timetables should be constructed to enable an assesment to be made of how efficiently and effectively the Center is approaching its goals.

Particularly important points that have emerged, after our meeting with Center actors, in addition, or in reinforcement of the points already brought up in November 1991 are:

- The plan should spell out the rationale for change of focus of the Center towards the L.A. Basin. How is it justified, what impact does it have on the different groups?

- The plan should have an outline by each individual group of its particular goals, priorities for funding, approach towards reaching the goals, timetable for realization.

It should describe how the individual components will be assembled to build the final product. It should clearly lay out considerations of the relative importance of infrastructure versus research funding among the different groups, and the prioritization of the different groups with respect to the goals.

It should state the intents of the Director(s) in setting up certains features and mechanisms of the Center: e.g., the role of the Physics group, the funding of Scientific Director's projects across all the groups. It should spell out the relative importance of R&D with respect to practical efforts towards the final product.

-The plan should distinguish between two types of products: policy/public products and science products. These need not require the same level of effort before being made accessible to their respective users. For example, assembled "raw" datasets can be directly useful to the scientific community, while their interpretation is part of an evolving product for the public, which needs to be constantly updated as new information and understanding is gained.

Also, we commend the Center on their efforts to build outreach activities: the conclusion of an agreement with SCEPP, the initiative towards hiring an assistant director for Engineering and one for Outreach. However, we reiterate the need for an Outreach Plan, which would, in particular, define what the Center proposes to do for outreach, and the urgent need to actively establish two-way communication between the Center and the users. SCEC

should begin dissemination of available outreach products now. We refer to our previous report (November'91) for details on how we view this Outreach Plan. An obvious observation is that very few engineers attended the April 23 Center workshop which contained much potentially important information for them.

Finally, we feel that several specific issues should be addressed, preferably within the Science Plan:

- clarify perception by the outside community on the level of funding in certain areas - e.g. seismicity.
- The relevance of the Physics Group to SCec goals appears to be poorly understood by other SCEC groups. The relationship of the Physics Group to other groups and to the master model should be attended to and developed. While recognizing the value of theoretical investigations of unpredicatble outcome we further recommend that the Physics Group focus on some specific issues of near-term interest to the master model.
- Review the current organisation of monthly workshops and other meetings optimize the balance between dynamics (served by frequent workshops) efficiency for individual participants (disserved by frequent commuting).
- Find a way to provide a forum for debate on some key issues such as linear/non-linear site response, the relative importance of path effects versus site effects etc..

Berkeley, May 20 , 1992
Barbara Romanowicz, Chairman

SOUTHERN CALIFORNIA EARTHQUAKE CENTER (SCEC) EVALUATION CRITERIA

I. Goal of the Center

The Southern California Earthquake Center (SCEC) is composed of scientists from seven core institutions and a number of participating institutions, in partnership with the United States Geological Survey's Office of Earthquakes, Volcanoes, and Engineering (USGS). The goal of the Center is to integrate research findings from the various disciplines in earthquake-related science in order to develop a prototype probabilistic seismic hazard model (master model) for southern California. The master model will represent a distillation of Center thinking which is developed through various meetings and workshops, and updated on a regular basis as new research results become available. This distillation may be stated in terms of a consensus on some issues, while on other issues it may be represented in terms of two or more differing opinions.

II. Research and Research Performance

A. Research Directions and Objectives

Master Model Construction

The master model is a framework in which geologic, geodetic, geophysical, and seismological information pertinent to earthquakes will be integrated for the purpose of developing a prototype probabilistic seismic hazard analysis of southern California. SCEC will develop, refine and apply (i.e. transfer to the user community) the master model on one hand, and acquire and integrate the pertinent data for model improvement on the other. Its substance will be debated in regularly scheduled workshops, and developed into forms applicable to earthquake hazard mitigation in the public and private sectors.

THE MASTER MODEL

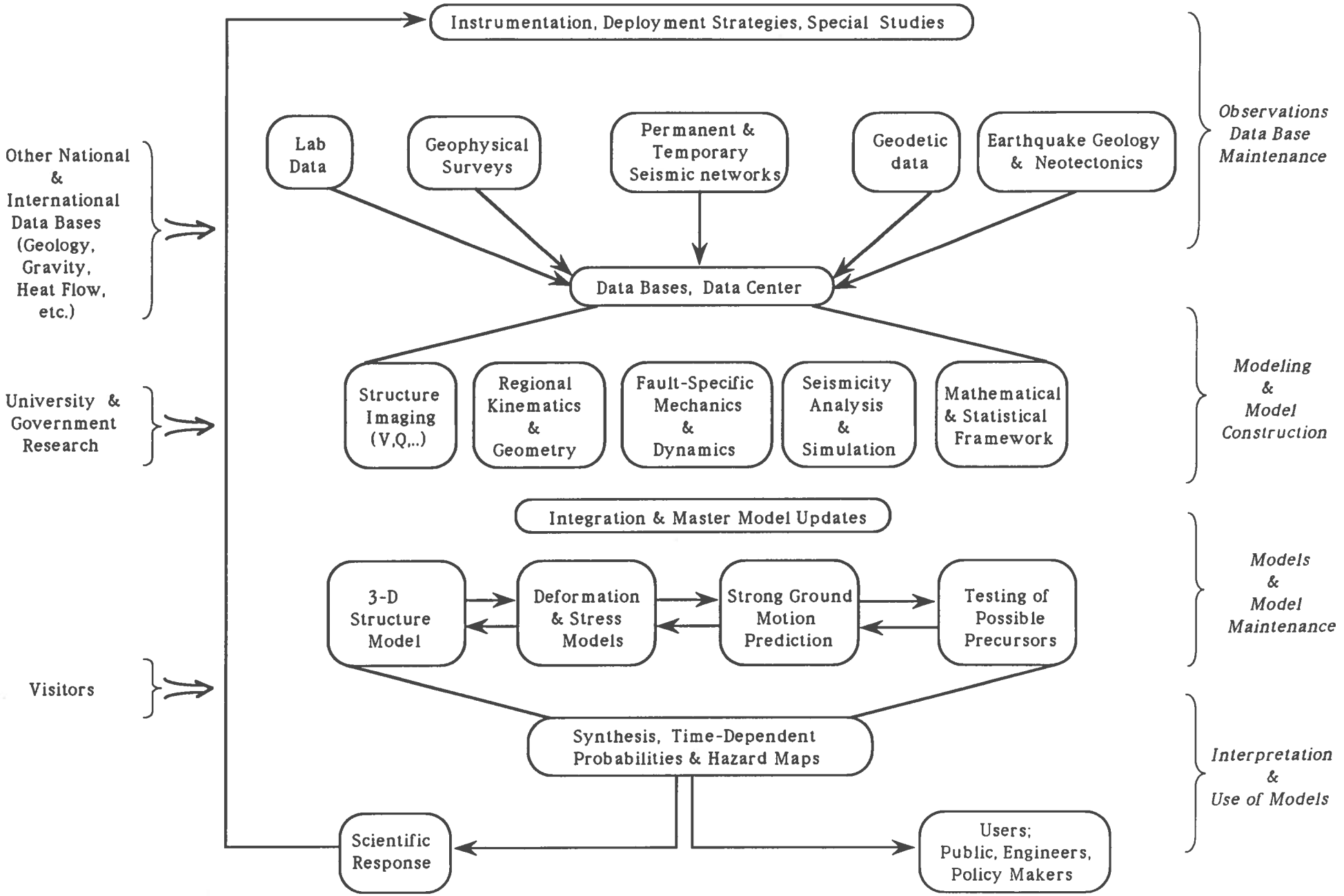

Master Model Improvement and Maintenance

The requirements of the master model will guide data acquisition and interpretation through the processes of interaction and feedback. As such, the master model will be constantly improved and updated as new research results become available. To facilitate master model improvement and define its research directions and objectives, the Center has been configured into eight disciplinary working groups as follows:

A) Seismic Hazard Analysis and Master Model Construction
B) Strong Ground Motion Prediction
C) Fault Zone Geology
D) Subsurface Seismic Imaging
E) Crustal Deformation
F) Regional Seismicity
G) Physics of Earthquake Sources
H) Engineering Applications

The research results of working groups B to F will provide input to the master model, and when fully integrated by working group A, will be the best representation of the earthquake process. Group A will maintain the master model in its most current form. The master model will be maintained as a data base, a set of model parameters, and a set of products (principally digital maps) at the SCEC data center in Pasadena. Working group H will provide for engineering applications of the master model.

Master Model Output

The products derived from SCEC research will consist largely of maps and data bases related to probabilistic estimates of earthquake occurrence and strong ground motion. Estimates of strong ground motion depend on a knowledge of fault failure as well as propagation path and local site conditions, particularly since the population distribution in southern California is concentrated away from the main San Andreas fault.

The Center will undertake the hazard analysis in two steps. The first step, which will be completed in two years, will involve updating the geologic data on faults (mainly from trenching), and determining the propagation and site effects to construct maps of exceedance probabilities for strong ground motion parameters in southern California. The second step, which will be completed in five years, will involve adding to our hazard analysis the new geodetic data, particularly those data relevant to blind thrusts. In its product, the Center will combine all pertinent information on earthquake hazards using a Bayesian approach.

B. Measures of Research Performance

- *Publication*
  - What is the scientific and/or technical impact of research results in guiding other research and in improving probabilistic hazard analyses?
  - Are papers published in peer-reviewed scientific journals?
  - Is there timely dissemination of information regarding center workshops to the scientific community and publication of technical reports detailing various elements of the master model?
  - Are information circulars published from time to time, for example, after major earthquakes or to assist in classroom instruction?

- *Interaction*
  - Is the Center, through its working group structure and its focus on the master model, and through workshops, monthly meetings, special symposia, and joint publications effective in facilitating scientific interaction?
  - Does the Center facilitate interaction between the various earth science disciplines involved in earthquake studies and seismic hazard analysis?
  - Does the Center facilitate interactions between scientists at the participating institutions and the USGS?
  - Does the Center facilitate interactions between earth scientists and engineers?

- *Master Model Impact*
  - What is the impact of the master model on the earth sciences and on earthquake hazard reduction methodologies?
  - Do the scientific and earthquake hazard mitigation communities accept the master model as a useful way of both structuring scientific research programs on earthquakes and developing probabilistic earthquake forecasting and strong ground motion prediction strategies?
  - Is the master model significantly improved from year to year beyond relatively elementary models?

- *Data and Ideas*
  - Is the Center assuming the role of a clearinghouse for data and ideas pertaining to earthquake research and hazard mitigation?

- Is the Center effective in assimilating data and ideas not only from its own participants, but also from other researchers world-wide who are funded from other sources?
- What is the level of use by both Center and non-Center scientists and accessibility of the SCEC data center in Pasadena, as well as its compatibility with other data centers such as those operated by IRIS, the USGS, and UC Berkeley?
- What is the quality and quantity of new data (seismic, GPS, strong ground motion, fault zone geology, etc.) generated by SCEC, and the timeliness with which those data are archived by the data center for general use?
- Is the southern California earthquake catalog being properly maintained and updated?

- *Post-Earthquake Information*
  - Does the Center assume a responsibility for timely and accurate dissemination of data and other information to scientists, public officials, and the press following a damaging earthquake in southern California?
  - Does the Center develop effective communication and coordination of function with other organizations such as the USGS, SCEPP (Southern California Earthquake Preparedness Project), CDMG (California Division of Mines and Geology), CEPEC (California Earthquake Prediction Evaluation Council, and NEPEC (National Earthquake Prediction Evaluation Council) following a damaging earthquake?
  - Does the Center assume an effective role in the coordination of post-earthquake scientific investigations?

- *Other Funding*
  - Is the Center effective in its ability to leverage funding from other sources such as FEMA, foundations, business, and state and local government?

III. Education and Outreach

A. Objectives

The Center has a primary role in the education of individuals who will assume future leadership roles in earthquake research and hazard

reduction. To this end it desires to train graduate students and post-doctoral fellows, and to invite interaction with visiting scientists from elsewhere in the U.S. and the world. The Center must also reach out to undergraduates and high school students in the southern California area as a means of encouraging careers in earth sciences, specifically, and science, in general. It must also be sensitive to the need to bring more women and minorities into the scientific mainstream, particularly given the present and projected population demographics of the southern California region. Finally, given the societal importance of earthquakes and earthquake hazard reduction in southern California, the Center has a responsibility to increase earthquake awareness among public officials, the media, the business community and the public at large, and to communicate with these groups, in understandable format, the Center's research findings.

B. Measures of Performance

- *Students, Post-docs, and Visitors*
  - What is the quality of graduate students, post-doctoral fellows, and visitors attracted to the Center?
  - Where do students and post-docs end up after their tenure with the Center? Are they in demand? Do they assume leadership roles?
  - What is the quality of the experience for visitors and hosting scientists under the visitors program?
  - Has the Center developed an effective program of outreach to high school students and teachers, perhaps in conjunction with SCEPP?
  - Has the Center provided an opportunity for college undergraduates to make meaningful contact with Center scientists and/or projects at the various core and participating institutions?

- *Women and Minorities*
  - Does the Center include participation by women and minorities?
  - What efforts are being made to recruit and/or interest such persons in the activities of the Center?
  - Are such persons involved in decision making?

- *Special Interest Groups*
  - Is there effective communication with groups such as emergency preparedness and response officials, corporate disaster planning coordinators, insurance underwriters, realtors, newswriters and newscasters, etc. who are concerned with earthquake awareness?
  - Do SCEC, SCEPP, and the USGS develop an effective working relationship in reaching out to the above groups?

IV. Technology Transfer

A. Objectives

The master model is the product of the Center. Its essence must be transferred to other scientists, earthquake engineers, emergency preparedness and response personnel, government officials and policy makers, the business community, the media, and the general public. SCEC will make use of workshops, technical reports, special publications, maps, and data bases to transfer the master model to the users. Forms of information transfer will necessarily be different for the different user groups. Newsletters and master model updates will issued on a regular basis. SCEC will team up with SCEPP in the transfer of information to the less technical user community. It will cooperate with the USGS and CDMG (California Division of Mines and Geology) in the transfer of more technical information.

B. Measure of Performance

- Are workshops held for the user groups? How effective are they?
- Are the publications which are required for technology transfer being produced by the Center?
- Are the master model products accepted and/or used by other scientists, engineers, private consultants, public officials, and the public at large?
- How universally applicable is the master model concept?
- Is the Center effective in increasing earthquake awareness in southern California and the rest of the nation?
- Does the Center have an impact on seismic policy in California and the nation as a whole?
  - Is it being used as a consultative body on matters pertaining to the study of earthquakes and how to use the results of such studies for earthquake hazard mitigation?
  - Does it help facilitate the implementation of federal and state programs in earthquake research?

VI. Institutional Support and Management

- Institutional Support
  - What is the level of institutional support at the core and participating institutions?

- Management
  - How effective is the management in keeping the Center focused, interactive and generally productive?
  - Are the scientific participants and officials at the participating institutions satisfied with the managers and management structure?
  - How is the Center management perceived by NSF, the USGS, and other outside organizations with which SCEC has relationships?

- Governing Boards
  - How effective are the Center Board of Directors, the Steering Committee, Group Leaders, and Advisory Council in providing guidance and oversight? Do these groups show a genuine interest in making the Center viable and productive?

- Research Groups
  - Are the research groups and group leaders effective in planning, organizing, carrying out, summarizing, and integrating the research activities and results?

- Funding
  - Have objective procedures been devised for distributing research funds to the various principal investigators, including the development of an overall scientific plan, and accounting for their expenditure vis-a-vis research productivity and scientific quality?

1992 SCEC INFRASTRUCTURE

Administration:

Education and Outreach/GIS Coordination:

GPS Operations:

Data Center/Database Operations:

Facilities Support:

SCEC ORGANIZATION

Management

Science Director:	Keiiti Aki University of Southern California
Executive Director:	Thomas Henyey University of Southern California
Assistant Director for Engineering Applications:	Geoffrey Martin University of Southern California
Assistant Director for Education and Outreach:	To Be Named
Assistant Director for Administration:	John McRaney University of Southern California
Administrative Assistant:	Denise Steiner University of Southern California

Board of Directors

Chair:	Keiiti Aki University of Southern California
Vice-Chair:	David Jackson University of Southern California
Members:	Robert Clayton California Institute of Technology
	Ralph Archuleta University of California, Santa Barbara
	Karen McNally University of California, Santa Cruz
	Bernard Minster University of California, San Diego
	Leonardo Seeber Columbia University
	Thomas Heaton United States Geological Survey
Ex-officio:	Thomas Henyey University of Southern California

Group Leaders

A: Master Model	Keiiti Aki University of Southern California
B: Strong Motion	Ralph Archuleta University of California, Santa Barbara
C: Earthquake Geology	Kerry Sieh California Institute of Technology
D: Subsurface Imaging	Robert Clayton California Institute of Technology
E: Crustal Deformation	David Jackson University of California, Los Angeles
F: Seismicity and Source Parameters:	Egill Hauksson California Institute of Technology
G: Earthquake Source Physics:	Leon Knopoff University of California, Los Angeles
H: Engineering Applications:	Geoffrey Martin University of Southern California

SOUTHERN CALIFORNIA EARTHQUAKE CENTER (SCEC) ORGANIZATION

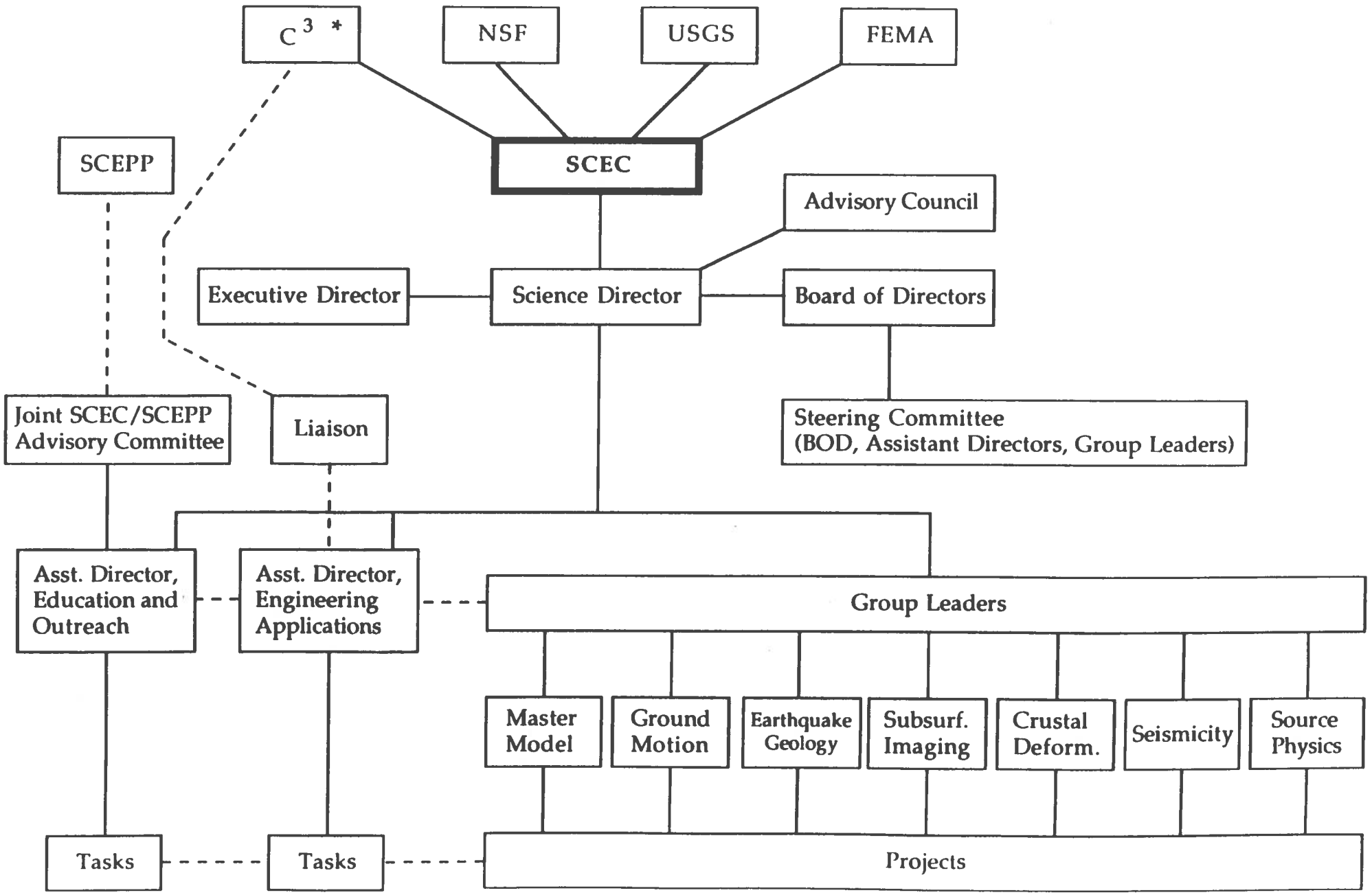

* Caltrans, County of Los Angeles, City of Los Angeles

1992 Workshops and Meetings

During 1992, SCEC is co-sponsoring the following workshops:

1. Electrical Precursors to Earthquakes - Lake Arrowhead, CA, June, 1992
   Convenor: Steve Park, UC-Riverside

2. Non-Equilibrium Systems - Santa Barbara, CA, July, 1992
   Convenors: Jim Langer and Jean Carlson, UC-Santa Barbara

3. Synthesis of Geological, Geophysical, and Geodetic Framework for Seismicity in Southern California - not yet scheduled
   Convenors: Lee Silver, Caltech and Tom Henyey, USC

The following monthly meetings have been held in 1992:

1.	January:	Tectonics of the Los Angeles Basin
	Host:	USC/Tom Henyey and Craig Nicholson
2.	February:	Prediction of Strong Ground Motion
	Host:	UCSB/Ralph Archuleta
3.	March:	Earthquake Prediction
	Host:	UCLA/Leon Knopoff
4.	March:	SCEC Visitors Seminar
	Host:	USC/Kei Aki
5.	April:	Master Model
	Host:	USC/Kei Aki
6.	May:	Basement Tectonics of Southern California
	Host:	Caltech/Lee Silver, Rob Clayton, and Tom Henyey
7.	June:	Real-Time Seismology
	Host:	Caltech/Egill Hauksson
8.	August:	Landers Earthquakes
	Host:	USC/Kei Aki

Southern California Earthquake Center

1992-93 Visitors and Post-doctoral Fellows

Visitor	Host Institution	Research Project
Francesca Ghisetti (Italy)	Lamont/UCSB	Parametric Growth Laws for the San Andreas Fault
Jean-Pierre Gratier (Grenoble)	UCSB/USC	Strain Partitioning Compatibility between Faults, Creep, and Folds
Ruth Harris (NRC/USGS)	USGS (Stein)	3-D Dynamic Modeling Effects of Fault Geometry on Earthquake Ruptures in Southern California
Eugene Humphreys (Oregon State)	Caltech (Clayton)	Numeric Kinematic and Dynamic Modeling of Southern California Deformation
Mark Peterson (Post-doctoral Fellow)	Reno (Wesnousky)	Seismic Hazards Assessment, Southern California
Richard Snay (NOAA/Maryland)	UCLA (Jackson)	Comparing Geodetic Models for Horizontal Deformation in California
Dapeng Zhao (Post-doctoral Fellow)	Caltech (Kanamori)	3-D Seismic Velocity Model of the Crust and Upper Mantle beneath Southern California

Infrastructure: Center for GIS Applications in SCEC
P.I: Stephen K. Park
Institution: University of California, Riverside
Date: September 21, 1992

This center is now a reality with facilities and full-time personnel this year. A SPARC2 color workstation was purchased early this year with funds from SCEC and UCR, and the Department of Earth Sciences obligated a room for the center. Most significantly, SCEC hired Eric Lehmer as a full-time research assistant in August. His responsibilities include assisting other SCEC scientists with GIS applications in research and advising other SCEC institutions in the purchase of ARC/INFO and workstations. Currently, he is working on a fault database which incorporates Wesnousky's compilation of slip rates and recurrence intervals. Digital fault data are being obtained from counties or by digitizing the Alquist-Priolo fault maps from the state, and these data should be available by December.

We have also negotiated an interagency agreement between UCR and CDMG to install a second workstation in the GIS Center and provide network connections and a phone. We are currently awaiting final approval from CDMG.

We have also provided support to other institutions in the past year, and most of this is detailed in our final report. That section is reproduced below:

The 1:750000 geologic map of southern California has been supplied to users at Leighton and Associates and at USC for predictions of ground amplification factors and response maps. Additionally, we assisted scientists at USC in designing and producing map of amplification factors (see Aki and Chin's work in this report), and have developed displays for Mahdyiar's site response maps. Wesnousky's slip data is now in the database and we are currently acquiring the Alquist-Priolo fault maps in digital form from the various counties. The updated faults should be ready by December, 1992, and we will then be able to implement Wesnousky's probability maps in ARC/INFO. We hired Eric Lehmer as a research assistant in August, his time will be dedicated to compiling this database. Geologic data from ARC/INFO have been provided to both the San Bernardino Planning Department and the Sheriff's Department.

Project: Digital Geologic Map Database for Southern California
P.I: Stephen K. Park
Institution: University of California, Riverside
Date: September 14, 1992

Results from this project fall into two categories: service to SCEC; and specific results for the San Bernardino basin.

Service: (Most of our efforts this year have been in this category, with the research in the San Bernardino basin given a lower priority because of lack of personnel. Now that SCEC has hired a research assistant to handle the service component, my technician can resume work on San Bernardino.) The 1:750000 geologic map of southern California has been supplied to users at Leighton and Associates and at USC for predictions of ground amplification factors and response maps. Additionally, we assisted scientists at USC in designing and producing map of amplification factors (see Aki and Chin's work in this report), and have developed displays for Mahdyiar's site response maps. Wesnousky's slip data is now in the database and we are currently acquiring the Alquist-Priolo fault maps in digital form from the various counties. The updated faults should be ready by December, 1992, and we will then be able to implement Wesnousky's probability maps in ARC/INFO. We hired Eric Lehmer as a research assistant in August, his time will be dedicated to compiling this database. Geologic data from ARC/INFO have been provided to both the San Bernardino Planning Department and the Sheriff's Department. On a more mundane level, ARC/INFO is now installed on a SPARC2 workstation dedicated to SCEC operations and we have arranged for an interagency agreement with CDMG to install a second workstation and provide some support at SCEC's Digital Geologic Map Center at UC Riverside.

San Bernardino Basin: The goal in this project is to examine the ground shaking and liquefaction potential of the region between the San Andreas and the San Jacinto fault zone. Previous studies [Matti and Carson, 1986; Tinsley and Fumal, 1985; Fumal and Tinsley, 1985] have examined these factors in this region, but only for specific earthquake scenarios. Ground shaking and liquefaction potential will depend on distance to the rupture zone, attenuation of the seismic wave, magnitude and duration of the earthquake, and site specific factors such as degree of consolidation, thickness of sediments, and depth to water table. Our project is an attempt to set up a database of relevant geotechnical, geologic and structural data which will allow a user to specify a particular earthquake and then assess its effect on the San Bernardino basin. The geology of the San Bernardino basin is now compiled at a scale of 1:24000 and is reconciled between the different quadrangles (Figure 1). We chose to divide the alluvium into three distinguishable units based on expected ground response behavior: younger Holocene alluvium; older Holocene alluvium; and Pleistocene alluvium. The younger Holocene alluvium consists primarily of unconsolidated sediments in active channels, while the older Holocene alluvium is more consolidated and found on inactive drainages. The Pleistocene alluvium is the most consolidated. Note that over 25 Quaternary units were mapped on the six quadrangles, and consistent unit designations were not used between quadrangles. Studies of liquefaction and ground

shaking will require the lithology of the unit, thickness of the sediments, material properties of the units, and the depth to the water table. We have compiled both the estimated shear wave velocities for the basin and the geotechnical data (SPT) in order to estimate liquefaction potential. Additionally, Hwong [1987] developed a 3-D model of groundwater in the basin which matches the fluctuations at observation wells from 1971 to 1983. We will initially include the map for 1983 (Figure 2) in the database, but predictions through the year 2000 under various recharge conditions can also be incorporated. Thus, predictive maps of liquefaction under various groundwater management schemes can be studied.

References

Fumal, T.E., and J.C. Tinsley, Mapping shear-wave velocities of near-surface geologic materials, in Ziony, J.I, ed., Evaluating earthquake hazards in the Los Angeles Region - an earth-science perspective, U.S. Geol. Surv. Prof. Pap., 1360, 127-160, 1985.

Hwong, T.J., 3D modeling of groundwater in the San Bernardino valley, southern California, M.S. Thesis, University of California at Riverside, 1987.

Matti, J.C., and S.E. Carson, Liquefaction susceptibility in the San Bernardino Valley and vicinity, southern California- a regional evaluation, U.S. Geol. Surv. Bull., 1898, 53 p., 1986.

Tinsley, J.C., and T.E. Fumal, Mapping Quaternary sedimentary deposits for areal variations in shaking response, in Ziony, J.I, ed., Evaluating earthquake hazards in the Los Angeles Region - an earth-science perspective, U.S. Geol. Surv. Prof. Pap., 1360, 101-126, 1985.

Figure Captions

Figure 1 - Geologic map compiled from published and unpublished sources for the San Bernardino Basin.

Figure 2 - Elevation of water table predicted from history matching data from 18 observation wells with 3-D groundwater model of San Bernardino basin (from Hwong [1987]).

Figure 1

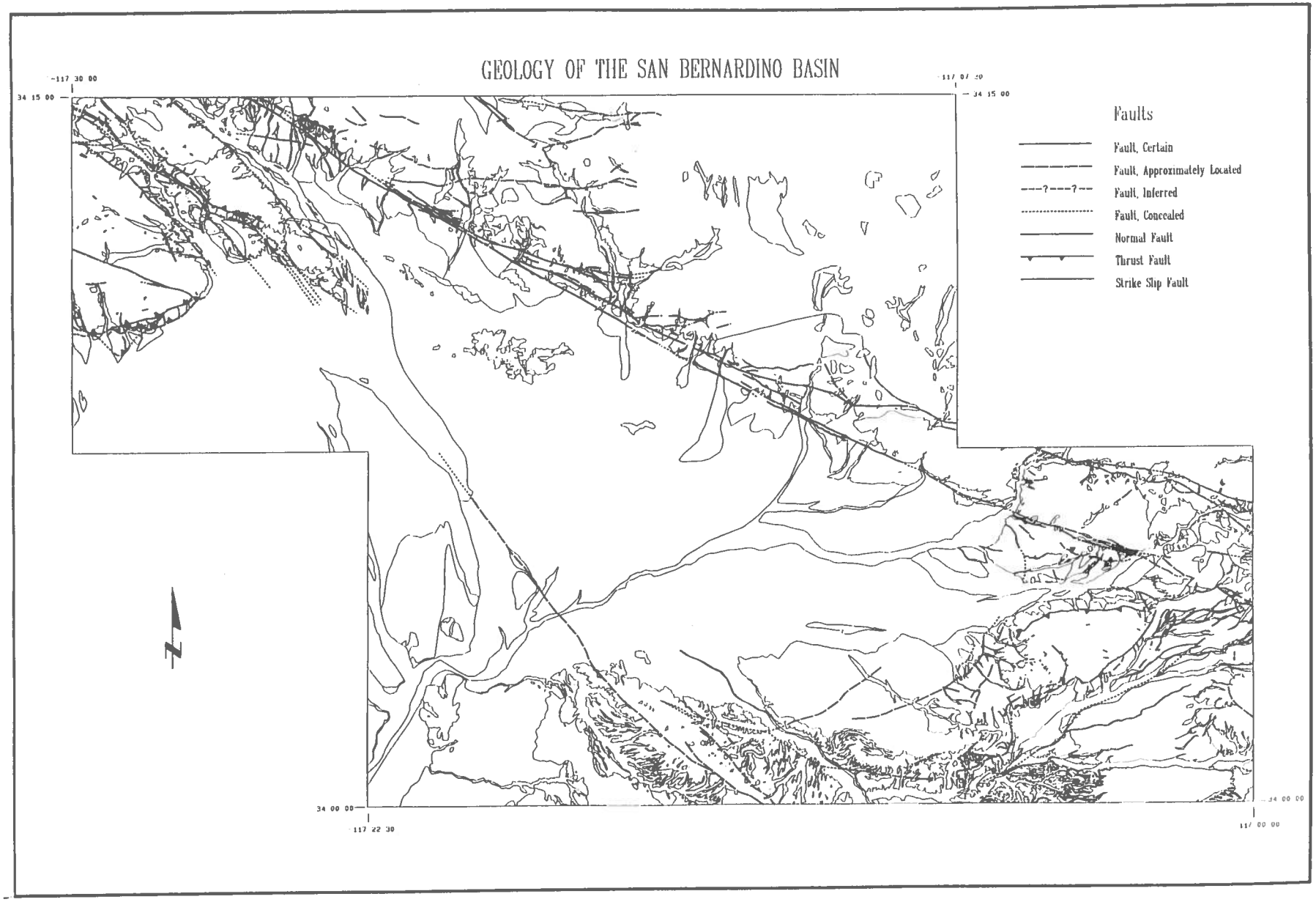
GEOLOGY OF THE SAN BERNARDINO BASIN
-117 30 00
34 15 00
-117 07 30
34 15 00
Faults
Fault, Certain
Fault, Approximately Located
Fault, Inferred
Fault, Concealed
Normal Fault
Thrust Fault
Strike Slip Fault
34 00 00
-117 22 30
34 00 00
-117 00 00

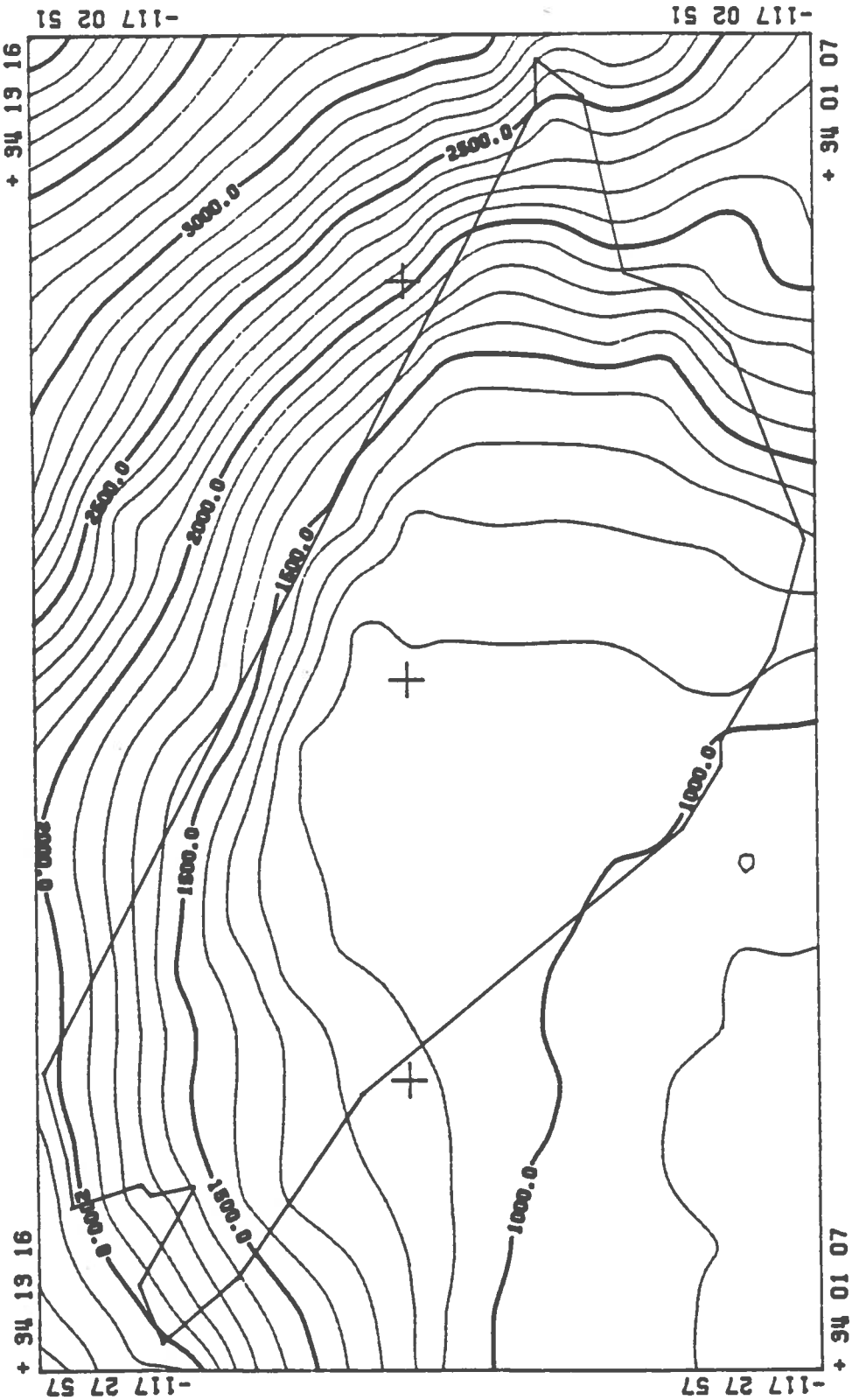
-117 02 51
-117 02 51
+ 34 19 16
+ 34 01 07
3000.0
2500.0
2500.0
2000.0
1500.0
1000.0
1000.0
1000.0
1500.0
1500.0
+ 34 19 16
+ 34 01 07
-117 27 57
-117 27 57

Figure 2

NEW EXHIBITS FOR THE EARTHQUAKE EXHIBIT AT THE CALIFORNIA STATE MUSEUM OF SCIENCE AND TECHNOLOGY

Charles G. Sammis
Department of Geological Sciences
University of Southern California
Los Angeles, CA 90089-0740

The earthquake exhibit at the California state museum is one of their most popular attractions for both adults and the thousands of field-tripping school children who visit each year. I have been collaborating over the past few months with the museum curator, Eugene Gendel, to upgrade the exhibits to more accurately reflect the current state of earthquake science.

Although there are many good exhibits, the information content is very low. For example, the mathematics exhibit at the museum is much more sophisticated, and I believe should serve as a model toward which the earthquake exhibit should be aimed. In addition to the action displays for the younger children, the walls of the math exhibit are covered with tidbits to read - contributions of famous mathematicians, interesting bits about symmetry, and fractals, and so on. A more interested visitor can actually spend hours in the math exhibit. The curator has told me that several professional mathematicians have said that their interest in mathematics started as school children in that exhibit.

Toward this goal of increasing the information content of the earthquake exhibit, we have made the following progress:

1) A paleoseismicity display.

We have obtained permission to use a large-format color photo of Kerry Seih's trench wall taken several years ago by a free-lance photographer for the LA.. Times color section. A 3 by 4 foot light box has been constructed to back-light this image. The exhibit has been designed to include:

a) Information about the site, sag pond, and peat formation.
b) Information about radiocarbon age dating.
c) Identification of the events which can be seen in the photo.
d) A time line showing past events with a discussion of the problems involved in predicting the next big one.

We hope to have this exhibit finished by the SCEC annual meeting in October.

2) A computer display of world seismicity through time.

We are using a program developed at SUNY Buffalo which plots earthquake epicenters through time on a world map. Each earthquake appears initially as a bright yellow spot which fades to red with time. As the program runs the plate boundaries are clearly outlined in red. This computer display will be supplemented with text about the different types of earthquakes at the different types of plate boundary. Also we will point out and explain first-order observations such as the arcuate shape and greater width of earthquake belts in subduction zones as compared with midocean belts.

This program can also be run in a mode in which it plots seismicity through time on a California map. Text accompanying this display will emphasize the point that the San Andreas fault system is not the plate boundary, but that deformation associated with the relative plate motion is spread across the entire state. We are currently finalizing the programming required to allow the visitor to chose between the world and California display.

3) A P-wave and S-wave display.

The current seismic wave display is based on the torsion of a rod. There is little or no informative text. We are designing a new display which uses slinkys to display both compressional and shear waves. Besides allowing small children to bash away at the handles attached to an end of the slinkys, this display will also allow a discussion comparing (1) the sense of motion in the two waves, (2) the different velocities, and (3) why shear waves don't propagate in liquids or gasses.

4) The CUBE display

We are currently negotiating with CalTech to install a CUBE (CalTech-USGS Broadcast of Earthquakes) display at the museum, thus allowing visitors to see the most recent seismic activity in Southern California in something approaching real time.

5) A 3-D display of faults and seismicity in the LA basin.

We originally proposed to build a four foot square 3-D display of basin seismicity by laminating Plexiglas sheets. We since have decided to use mylar sheets for the various layers to avoid refraction problems. We have constructed a small scale mock-up and are experimenting with fluorescent paints and black light to get the best visual display. The museum technical staff are designing frames to stretch and hold the stack of mylar sheets.

We have discussed with SCEPP the possibility of providing more information about the exhibit in the form of han-outs to visitors which they can take home. We will continue to pursue this possibility through the new outreach coordinator.

PERMANENT GPS GEODETIC ARRAY OPERATIONS AT SIO (1992 SCEC ANNUAL REPORT)

Yehuda Bock, Principal Investigator
Scripps Institution of Oceanography, IGPP 0225, UCSD
9500 Gilman Drive, La Jolla, CA 92093-0225
Office phone: (619) 534-5292, Fax: (619) 534-5332
E-mail: BOCK@BULL.UCSD.EDU

1. Introduction

The Permanent GPS Geodetic Array (PGGA) has been operated in California since the spring of 1990 by SIO and JPL with assistance from Caltech, MIT and UCLA. Funding for the maintenance of the network is provided by NASA, NSF and USGS. The goals of the PGGA are to monitor crustal deformation related to the earthquake cycle in California, continuously, in near real-time and with millimeter accuracy, using a fully automated and economically viable system. The roles of the PGGA also include providing reference sites and precise GPS orbital and earth rotation information to support detailed GPS geophysical surveys in California. We have collected and analyzed an uninterrupted time series of data since 14 August, 1991. The Landers earthquake sequence generated the first real geophysical signals that were detected by PGGA. Data collected around the period of the Landers earthquake have been studied extensively for coseismic and postseismic deformation.

2. Accomplishments

c) We detected coseismic deformation caused by the Landers earthquake sequence at four of the PGGA stations with the largest signal at PFO which is situated about 80-90 km from the rupture zone. We submitted a paper to Nature (Bock et al., 1992) in which we reported on this analysis. After a rough correction for the effects of crustal layering, comparison with a fault dislocation model derived from seismic data indicates good agreement with the coseismic GPS measurements (Figures 1,2) and implies a combined moment for the two earthquakes of 0.9×10^{20} N-m. We have also detected an apparent postseismic signal on the PFO to Goldstone baseline (Figure 3) of about 1.3±0.4 mm/day for about a 15 day period after the Landers and Big Bear earthquakes (Wdowinski et al., 1992).

a) We have developed an automated system to collect, analyze and archive data from the PGGA sites at JPL, Piñon Flat Observatory (PFO), SIO, Goldstone and Vandenberg Air Force Base, and from a globally distributed set of about 30 GPS tracking stations. We monitor data at a 30 second sampling rate to all visible satellites, 24 hours a day, 7 days a week. All raw data in the SIO archive are translated into the Receiver Independent Exchange (RINEX) format for GPS data. These are archived on an optical storage device, the Epoch-1 Infinite Storage Server. All data collected to data are on-line and accessible via anonymous ftp. We have also archived the Caltrans California High Precision Network data collected from April to August 1991, the San Diego County High Precision Network collected in April 1991, the GIG '91 data collected in January to February 1991, and the International GPS Service (IGS) '92 data collected in June to September, 1992. We are serving as a global archive and data processing facility during the IGS campaign.

b) Since August 1991, we have been generating precise satellite ephemerides and improved earth orientation parameters (polar motion) in support of GPS surveys in southern California. These products are available within 5-7 days of collection.

(d) We have upgraded our computing facilities to streamline our automatic operations.

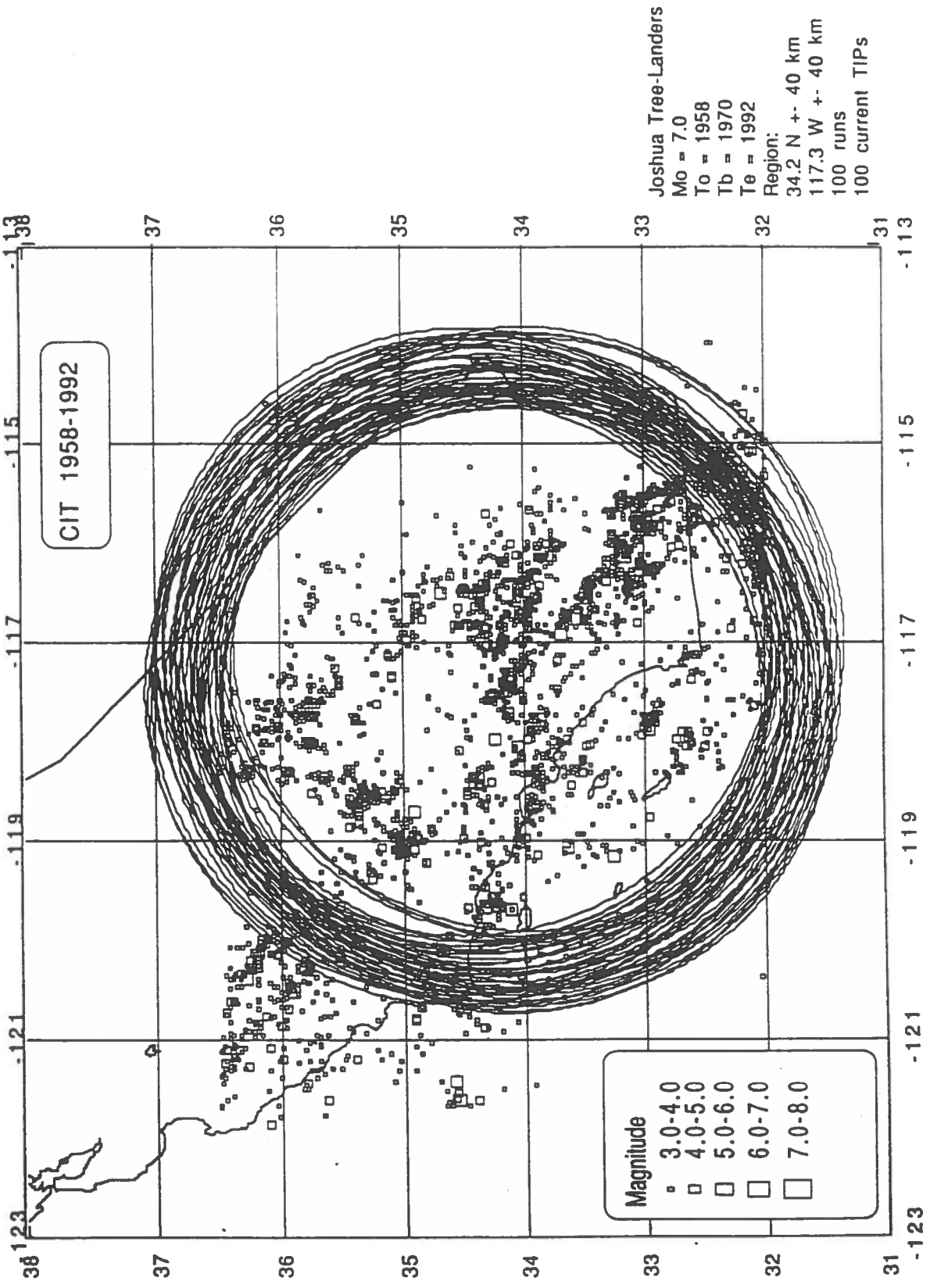

Figure 1: Circles for the M8 runs described in Case No. 1, Table 1. All these circles lead to a current TIP at the end of 1991, apparently because they include seismicity to the north and west of the region of the Joshua-Tree Landers sequence.

(e) We have made significant improvements to the GAMIT GPS software package in collaboration with MIT. This software is used by several SCEC investigators.
(h) A highly stable monument has been built at Vandenberg Air Force Base with funding from MIT and an Ashtech P-12 receiver has been deployed there since May, 1992. We have signed an agreement with Riverside County Flood Control that will result in an additional site at Lake Mathews, we are working with MIT to add a site at China Lake, and we plan through SCEC to deploy a site at Yucaipa.

References

Bock, Y., D.C. Agnew, P. Fang, J.F. Genrich, B.H. Hager, T.A. Herring, R.W. King, S. Larsen, J.B. Minster, K. Stark, S. Wdowinski and F.K. Wyatt, Detection of coseismic deformation in southern California using continuous Global Positioning System measurements, submitted to Nature, August, 1992.

Wdowinski S., Y. Bock, P. Fang, J.F. Genrich, D.C. Agnew and F.K. Wyatt, The 1992 Landers Earthquake Sequence: Detection of Coseismic and Postseismic Surface Deformation, AGU abstract, 1992 Fall meeting.

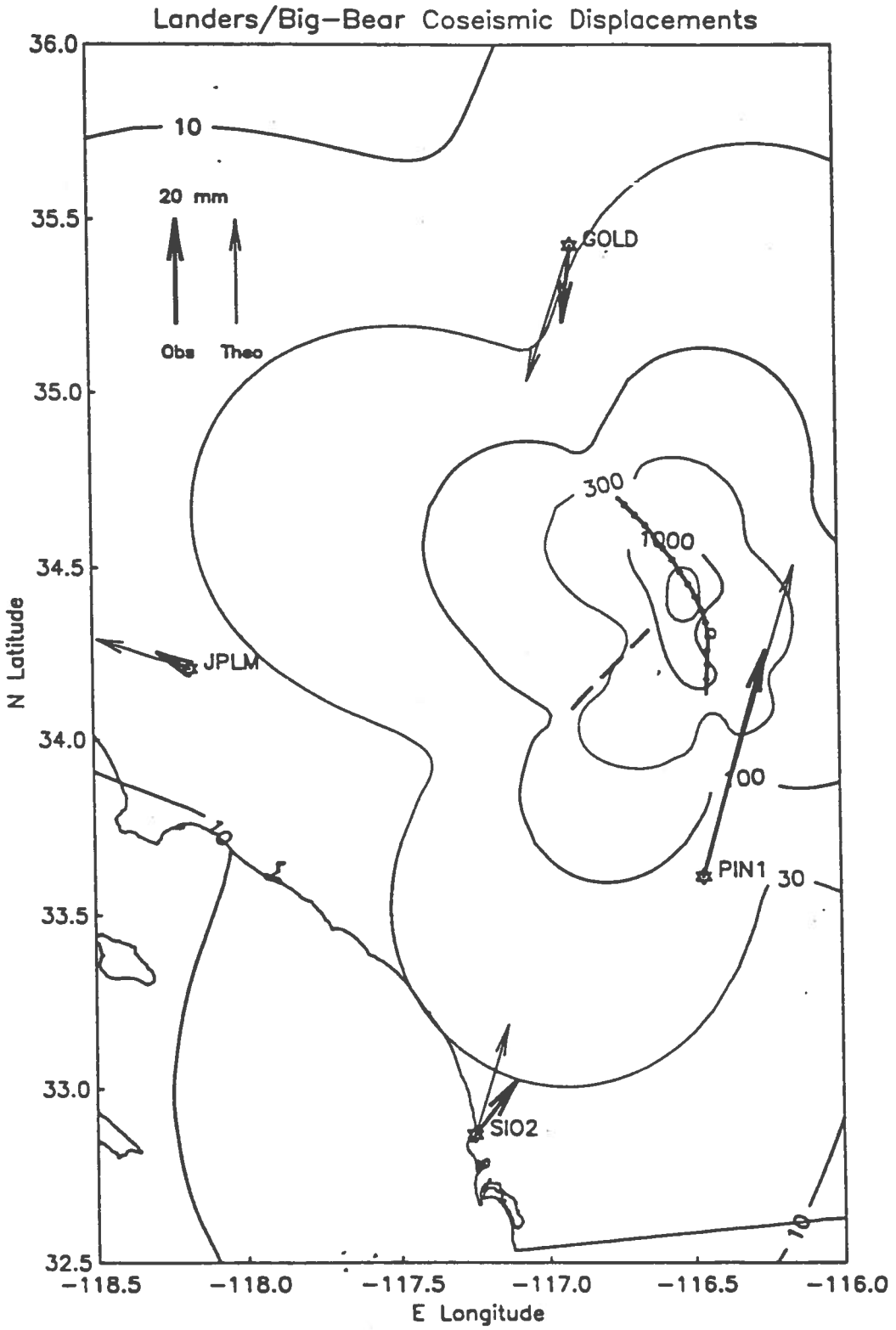

Figure 1: Plot showing the observed (solid arrowheads) and computed (open arrowheads) displacements at the PGGA stations. The contours (displacement magnitude), and the computed displacements are for an elastic halfspace (all units mm). The 2000 mm contour rupture is shown but not labeled. The fault segments used for the Landers earthquake are shown by the heavy hatched line; the segment edges are at 34.133 -116.442, 34.292 -116.433, 34.350 -116.442, 34.433 -116.483, 34.525 -116.550, 34.617 -116.633, 34.700 -116.733; the magnitudes of slip are 3.3, 0.5, 5.3, 6.3, 2.3, and 1.3 m right lateral respectively, with all segments from 0 to 15 km depth. The dashed line shows the dislocation assumed for the Big Bear earthquake, with 1 m of left-lateral slip on a segment from 3 to 18 km, and end-points 34.091 -116.899, 34.317 -116.634.

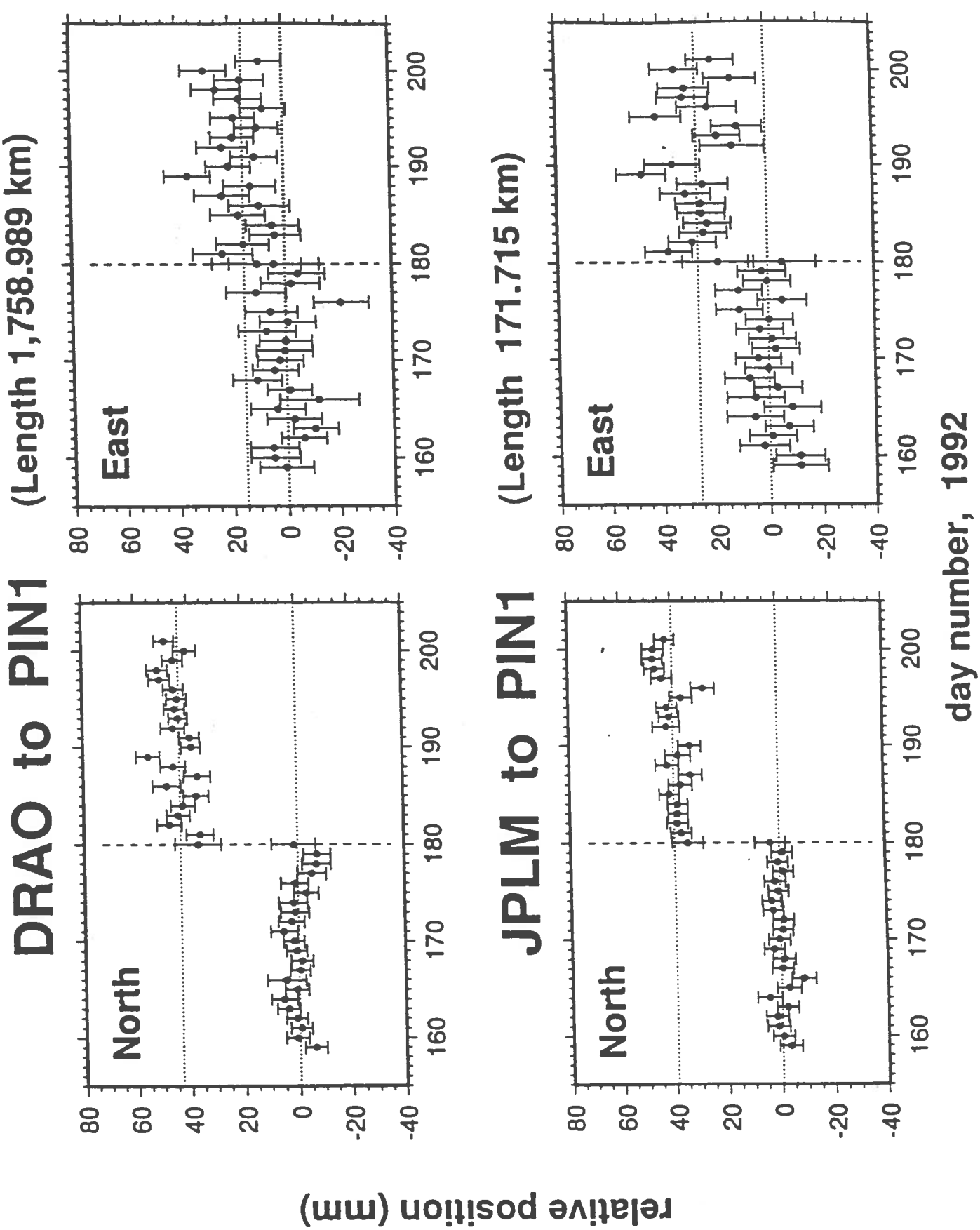

Figure 2: Time series of daily horizontal relative positions over a six week period centered on the day of the earthquakes (day 180, 28 June 1992) for the DRAO to PIN1 and JPLM to PIN1 baselines. The dotted horizontal lines are determined from the weighted means of the data points for the three week period before and after the earthquakes, and indicate the coseismic signature. The error bars are one-sigma standard deviations.

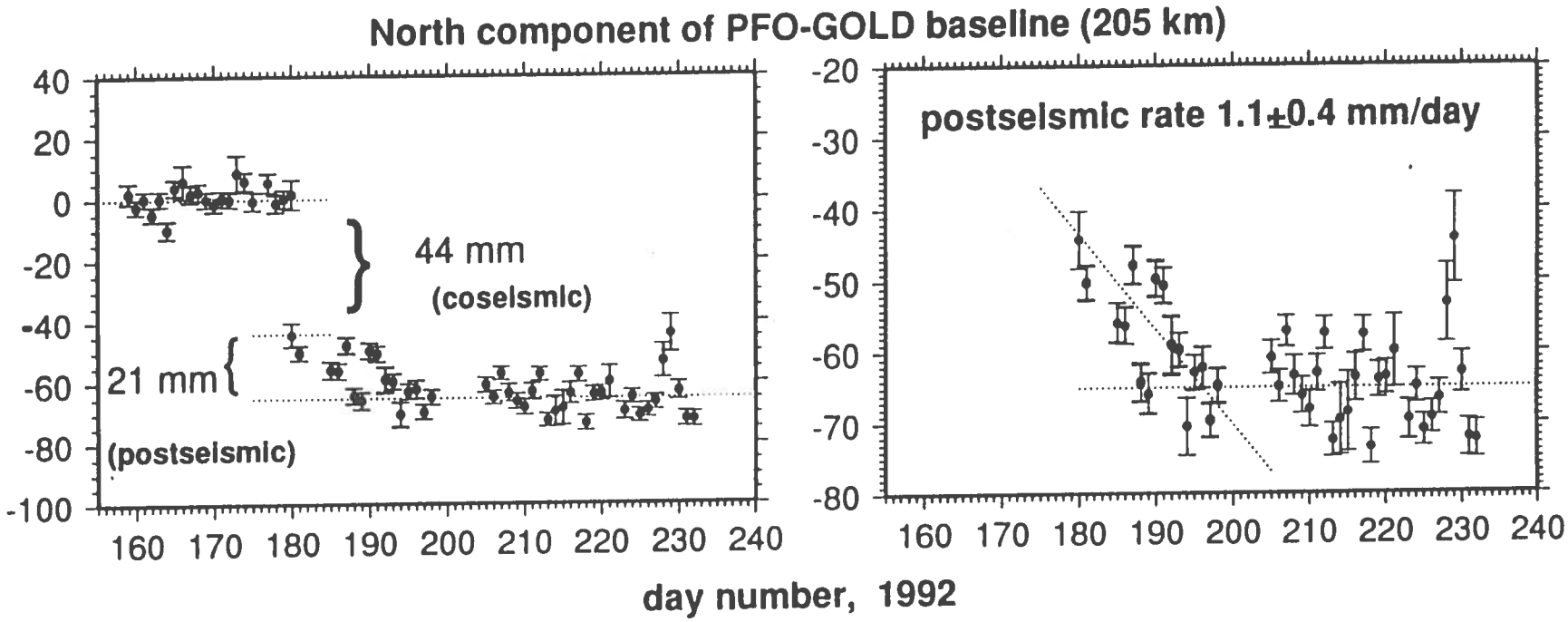

Figure 3: North component of the time series of daily position determinations on the north trending baseline between the PGGA stations at Piñon Flat Observatory (PFO) and Goldstone. We compute a coseismic displacement of 44±3 mm and an apparent postseismic displacement of 21 mm over a 15 day period. As a first approximation we compute a postseismic rate of 1.1±0.4 mm/day which is consistent with near-field GPS measurements (Shen et al.).

SOUTHERN CALIFORNIA EARTHQUAKE CENTER

GEODESY INFRASTRUCTURE

Progress Report Oct 1, 1991-Sep 30, 1992

David D. Jackson
Department of Earth & Space Sciences
UCLA

Data processing: We have processed (and in some cases reprocessed) over 1000 station-days of data to determine locations of the sites to within 3-10 mm. A large part of the effort is in editing and cleaning the data files; we have saved and archived the clean files to facilitate later refinements to the data processing. We have completed processing of all data collected by SCEC through Sep 1, 1992.

Archiving: We have acquired and organized all of the data from the Transverse Ranges Experiment conducted by UCLA, UCSD, MIT, and Caltech from 1986-1992; UCLA data for southern California collected from 1987 to present; Inter-county campaign data for 1991 and 1992; and Riverside County and San Bernardino County data for 1991 and 1992 in the region near the Landers Earthquake. We have reformatted and copied these data onto erasable optical disk, and transfered most of these data to the SCEC data archive at Pasadena. We have made a complete index of all of the files in our possession, and written computer programs for sorting, finding, and copying records.

We have made an index of all sites known to have high quality GPS data in southern California, and cataloged paper copies of site descriptions.

The index of GPS data files and the index of GPS sites is available by FTP from the SCEC data center at Pasadena, or or on floppy disk.

GPS data collection: We have acquired new GPS data for about 150 sites in southern Calfornia, mostly in the Los Angeles Basin, Mojave Desert, and Parkfield-Cholame areas. A map of these sites is enclosed as Figure 1. Data collection can be divided into three time intervals. Before the Joshua Tree Earthquake in April, our primary focus was on the Los Angeles Basin, as we had decided at the 1991 SCEC Annual meeting. Following the Joshua Tree earthquake, we surveyed eight sites near the epicenter for about one week each, to search for time-dependent postseismic relaxation, and to assure good coverage in the event that further earthquakes might occur. After the Landers earthquake in June, near the site of the Joshua Tree event, we reocuppied the same sites,

and another ten sites that we had not previously occupied. We continue to measure at these sites for about three weeks, again with the objective of observing any postseismic relaxation, and monitoring changes on the San Andreas Fault that might presage a future earthquake.

We have begun a cooperative project with the National Geodetic Survey to observe a network of 50 sites in the Gorman area (the "big bend" of the San Andreas Fault) to be completed by November 1992. An additonal project currently being negotioted with NGS will focus on the intersection of the San Andreas Fault and the San Jacinto fault. Caltrans, Riverside County, and San Bernardino County will also participate in this project.

Permanent GPS array in southern California: We have collaborated with UCSD, Caltech, and MIT to install sites for permanent GPS stations at Vandenberg AFB and at Palos Verdes. Vandenberg is now in operation, and Palos Verdes should be operating about October 15, 1992. We have selected a site for a permanent receiver near Gorman, and begun negotiations for a site near Yucaipa. We have purchased receivers, or arranged for indefinite use of receivers, for the sites at Palos Verdes, and Yucaipa, and we hpe to obtain support from Caltrans for the receiver at Gorman.. We have processed some data from existing sites at Scripps, Pinyon Flat, and JPL to determine rates of baseline change.

Coordinating City, County, State, and Federal GPS projects: We have helped to coordinate efforts of various governmental groups with GPS surveying programs to encourage high accuracy surveying and to promote free exchange and archiving of data. NSF, USGS, Caltrans, LA City, LA County, Riverside County, and San Bernardino County have all agreed to contribute data to our project. Caltrans has agreed to consider geophysical objectives in establishing new survey monuments when it can do so without compromising its other objectives.

Figure Caption: Sites at which SCEC personnel help to collect or coordinate collection of GPS data in 1992. Additional data were collected by USGS and other agencies in the Landers earthquake region, and SCEC will observe about 50 additional sites in the Gorman area during 1992.

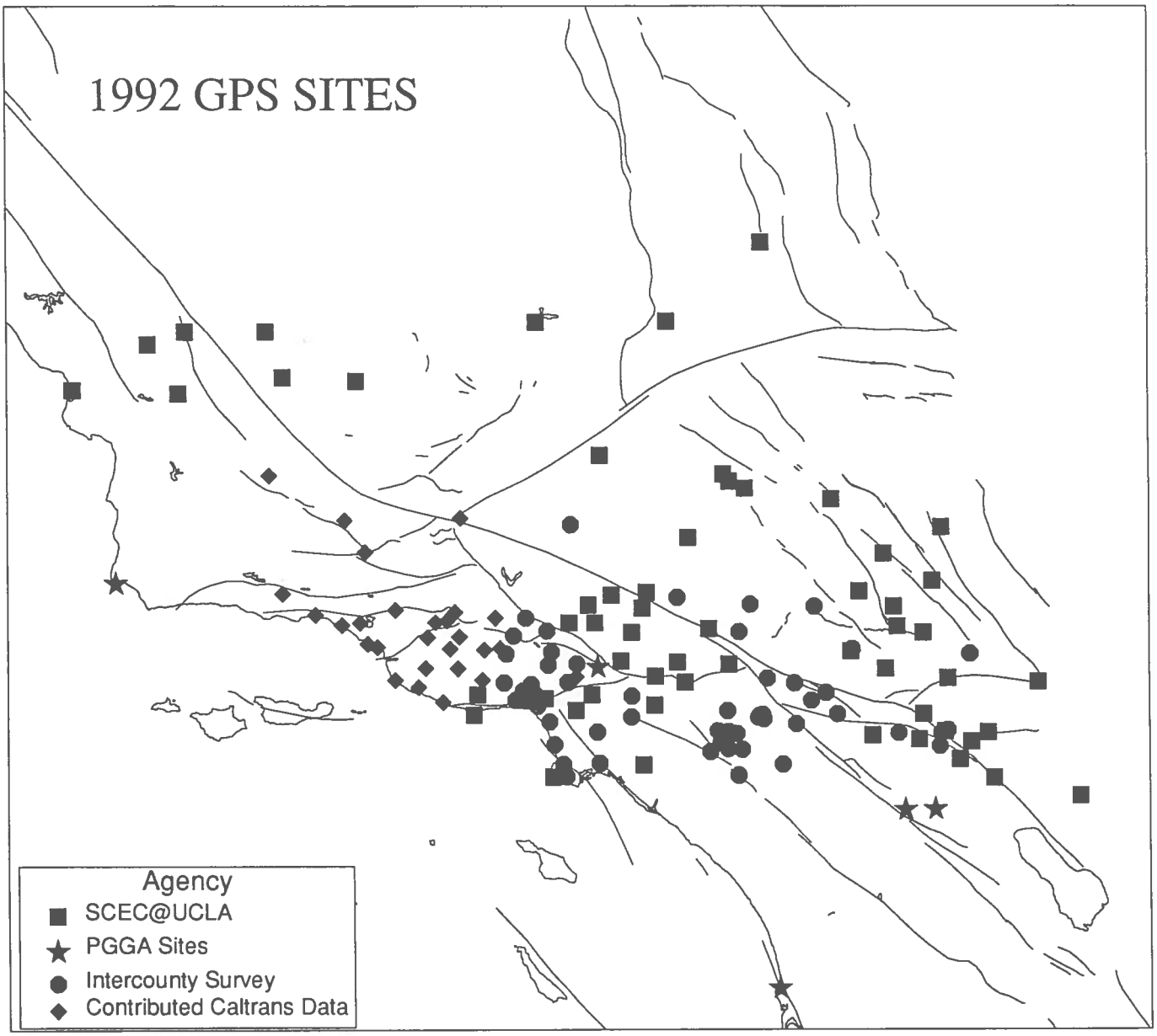
1992 GPS SITES
Agency
SCEC@UCLA
PGGA Sites
Intercounty Survey
Contributed Caltrans Data

Status of the SCEC Data Center

Rob Clayton

The Southern California Earthquake Center Data Center (SCEC-DC) currently has the following types of data:

1) SCSN EARTHQUAKE CATALOG LISTINGS - 1931 to present

2) ASCII DATA FILES - contain event information associated with each digital seismogram; among other things, these files contain phase, epicentral location, magnitude, and coda decay information.

3) CUSP digital seismograms.

Approximately 99% of all of the short period digital seismograms recorded by the Southern California Seismic Network during the time periods of July, 1981 - October 1982 and July, 1983 - June 28, 1992 are currently online.

The SCEC-DC has been working with its counterparts at USGS/Menlo Park and UCB to create a common format for archiving the seismic data. To date, a format for the ascii version of CUSP/mem files has been agreed upon.

An abstract of the status of the SCEC-DC has been submitted for the fall 1992 AGU meeting.

Joshua Tree-Landers-Big Bear (JT-Landers-BB) Data

As of October 1, ascii files and seismograms are available for the following events in the JT-Landers-BB earthquake sequence:

1) JOSHUA TREE EARTHQUAKE - all events except for those recorded ~2 hours after the time of the mainshock.

2) LANDERS-BIG BEAR SEQUENCE: Approximately 5400 events (about 22% of all the events recorded since June 28) as follows:

   events> M=2.5 recorded since August 1
   events> M=4.0 (but including smaller events) recorded since June 28.

The SCEC-DC plans to have all JT-Landers-BB events of M>2.5 available online by December 1.

The SCEC-DC has also recently received time corrected, portable seismometer data recorded by UCSD between July 1 and July 19. This data, consisting of ~9,100 events (~5000 mb) is currently stored on data and exabyte tapes. The SCEC-DC's immediate plans consist of associating the portable data with events recorded by the SCSN, and transferring the associated events from the tapes to a magnetic disk on the data center. In addition, to the above data, GPS RINEX data, recorded between July 1 and 16, are currently being transferred from UCLA to the data center.

STATUS OF SCSN DATA PROCESSING
(Figure 1)

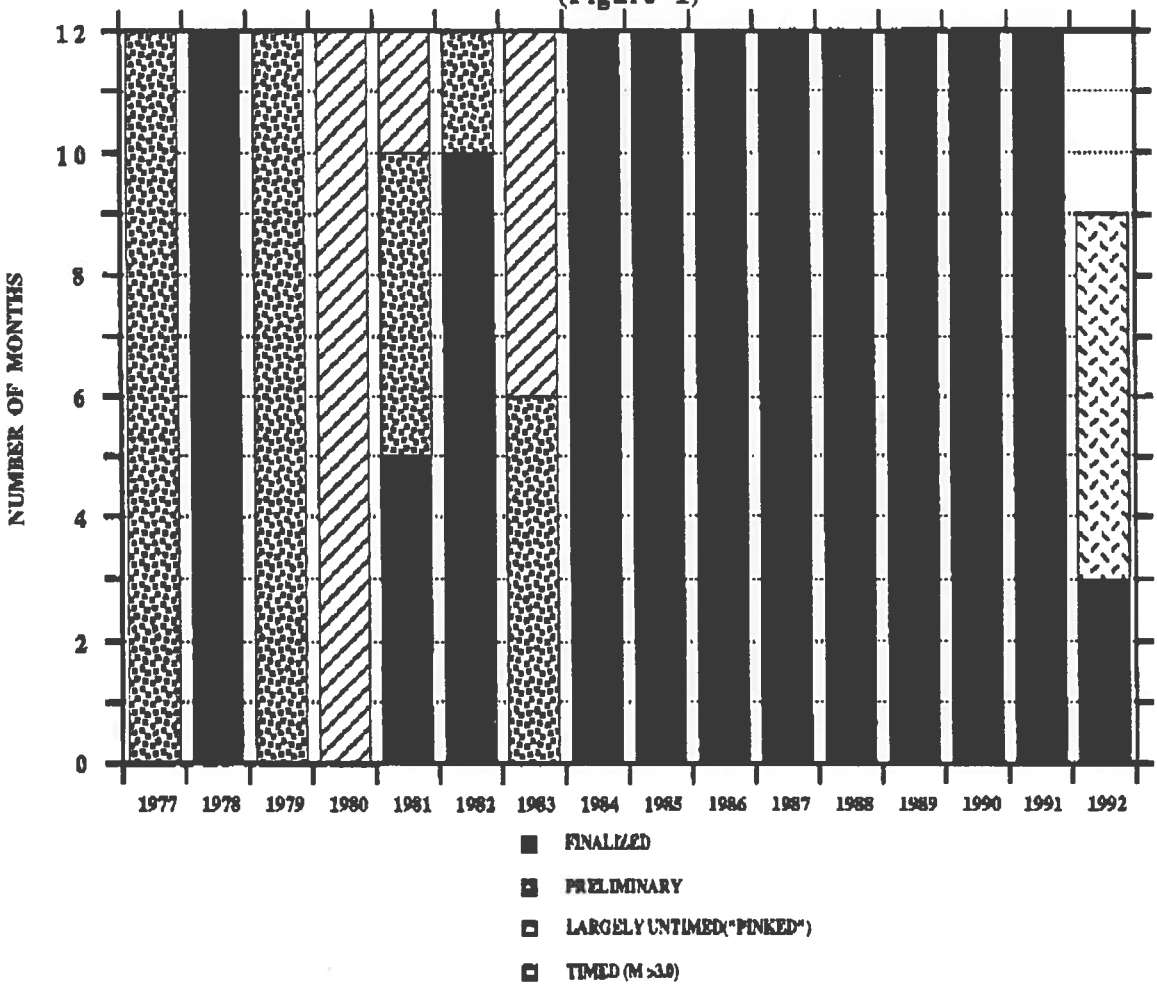

STATUS OF LANDERS - BIG BEAR AFTERSHOCK PROCESSING
(Figure 2)

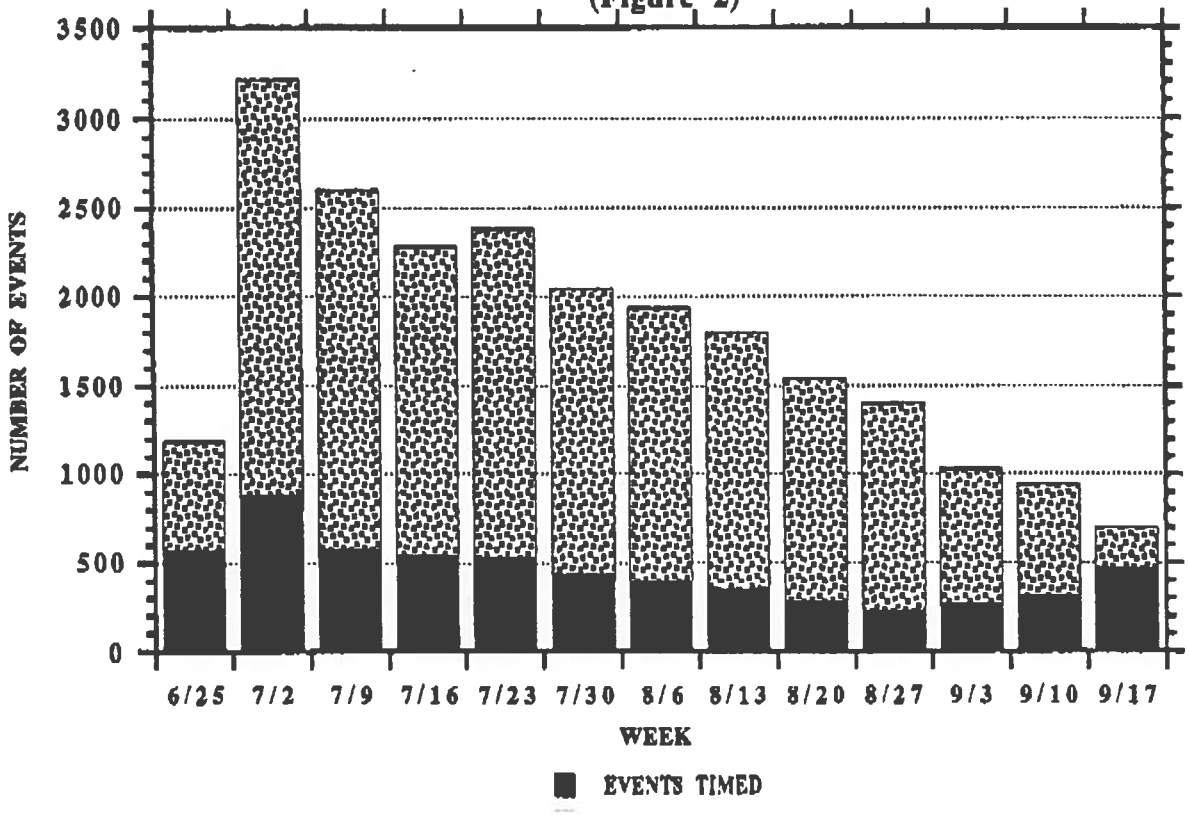

SCEC Progress Report:

Strong-Motion Database for Southern California

P.I.:

Ralph J. Archuleta
Institute for Crustal Studies,
University of California, Santa Barbara

The purpose of this report is to describe a new database SMDB being developed to provide a fast and easy access to the strong-motion data for Southern California.

The database now contains the data on Southern California earthquakes through 1986 obtained from the USGS CD-ROM optical disk with all available ground-level evenly spaced uncorrected digital strong-motion records. By the end of the first year of funding we plan to add data from 1987 Whittier Narrows and Superstition Hills earthquakes. Our future goals are to include also 1990 Upland and 1991 Sierra Madre earthquakes and all available strong-motion data for the 1992 earthquake sequences as well as for the major Nothern California earthquakes.

SMDB is a network database designed using the db_VISTA Database Management System (by Raima Corporation). It consists of three record types related to:

- events (earthquakes) for which strong-motion data was recorded;
- stations which recorded this data;
- parameters of strong-motion time-series.

These records, respectively named EVENT, STATION and TRACE, are interconnected through sets which define a one-to-many relationship between two record types. Thus, unlike a relational database (NCEER, for example), record types are related and accessed directly without requiring duplicate fields and index file. The benefits of this approach are better performance, reduced storage requirements and greater assurance of data integrity.

The major possibilities of the SMDB include:

- performing different types of queries;
- viewing and processing time-series by means of SAC;
- obtaining maps of stations and events.

Developing the SMDB query system we were trying to make it as simple as possible but powerful enough to let a user make various data selections. It incorporates a few easy-to-use macrocommands that allow conditional selection of records and their fields and output of selected data to an ascii file. For the list of database commands see Fig. 1 which also contains a sample selection of records with the peak acceleration exceeding 1500 cm/sec^2.

Time-series are maintained in a SAC (Seismic Analysis Code by Lawrence Livermore National Laboratory) format, so that being inside the database one can work in SAC environment as well (Fig. 1). The time-series files are not stored directly within the database. Each TRACE record contains only a description of these data and a pointer to their location (i.e. a full filename). The time-series files can be copied into a user-defined directory.

SMDB also includes commands for plotting a map of selected events and/or stations and making a hard copy of this map if needed (see Fig. 2, showing the 1986 North Palm Springs earthquake epicenter and all the stations which recorded this event).

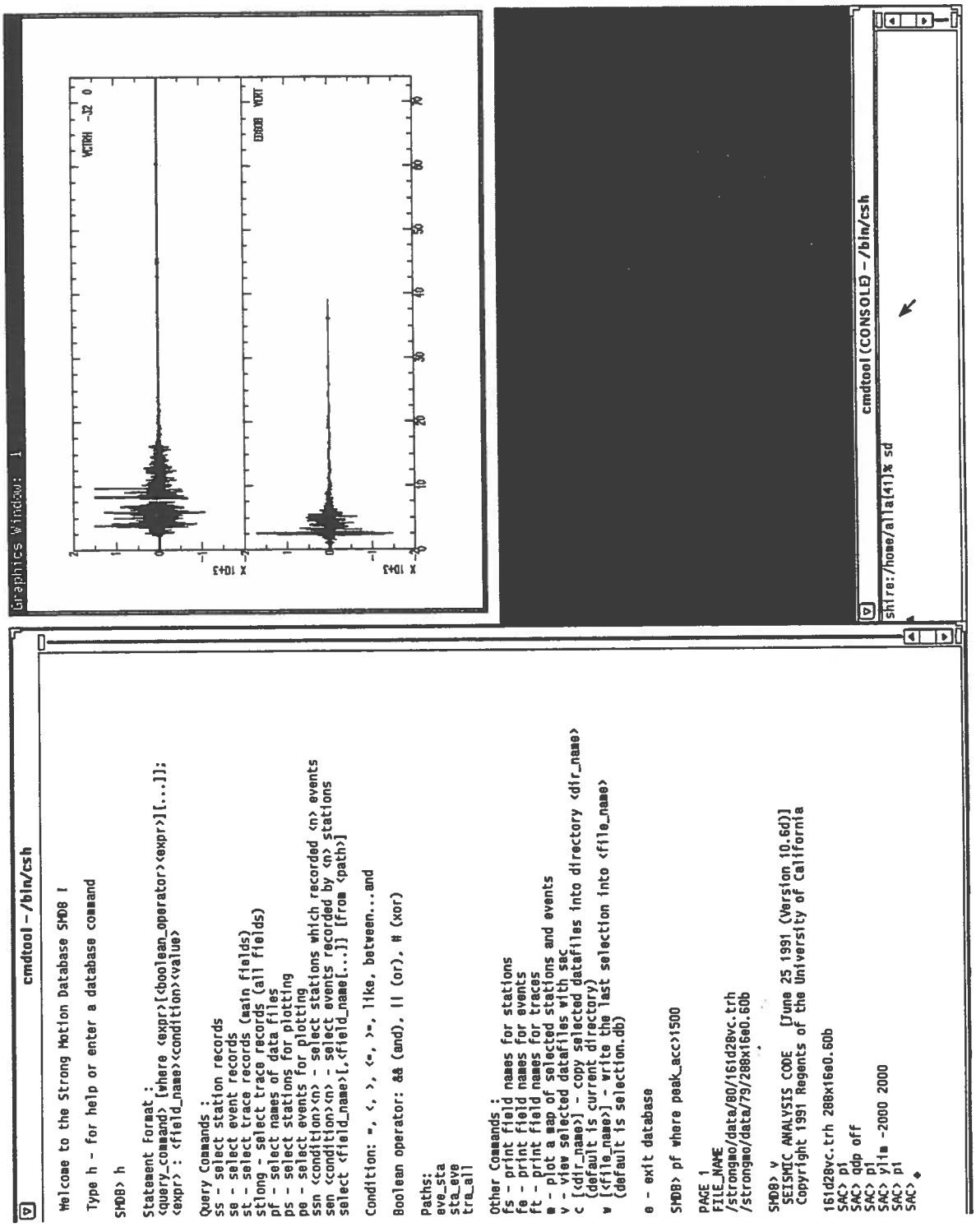
cmdtool - /bin/csh
Welcome to the Strong Motion Database SMDB !
Type h - for help or enter a database command
SMDB> h
Statement Format :
<query_command> [where <expr>[<boolean_operator><expr>][...]];
<expr> : <field_name><condition><value>
Query Commands :
ss - select station records
se - select event records
sr - select trace records (main fields)
stlong - select trace records (all fields)
pf - select names of data files
ps - select stations for plotting
pe - select events for plotting
ssn <condition><n> - select stations which recorded <n> events
sen <condition><n> - select events recorded by <n> stations
select <field_name>[,<field_name[...]] [from <path>]
Condition: =, <, >, <=, >=, like, between...and
Boolean operator: && (and), || (or), # (xor)
Paths:
eve_sta
sta_eve
tra_all
Other Commands :
fs - print field names for stations
fe - print field names for events
ft - print field names for traces
m - plot a map of selected stations and events
v - view selected datafiles with sac
c [<dir_name>] - copy selected datafiles into directory <dir_name>
(default is current directory)
w [<file_name>] - write the last selection into <file_name>
(default is selection.db)
e - exit database
SMDB> pf where peak_acc>1500
PAGE 1
FILE_NAME
/strongmo/data/80/161d28vc.trh
/strongmo/data/79/288x16e0.60b
SMDB> v
SEISMIC ANALYSIS CODE [June 25 1991 (Version 10.6d)]
Copyright 1991 Regents of the University of California
161d28vc.trh 288x16e0.60b
SAC> p1
SAC> qdp off
SAC> p1
SAC> y1m -2000 2000
SAC> p1
SAC>
Graphics Window: 1
cmdtool (CONSOLE) - /bin/csh
shire:/home/a1a[41]% sd

Figure 1.

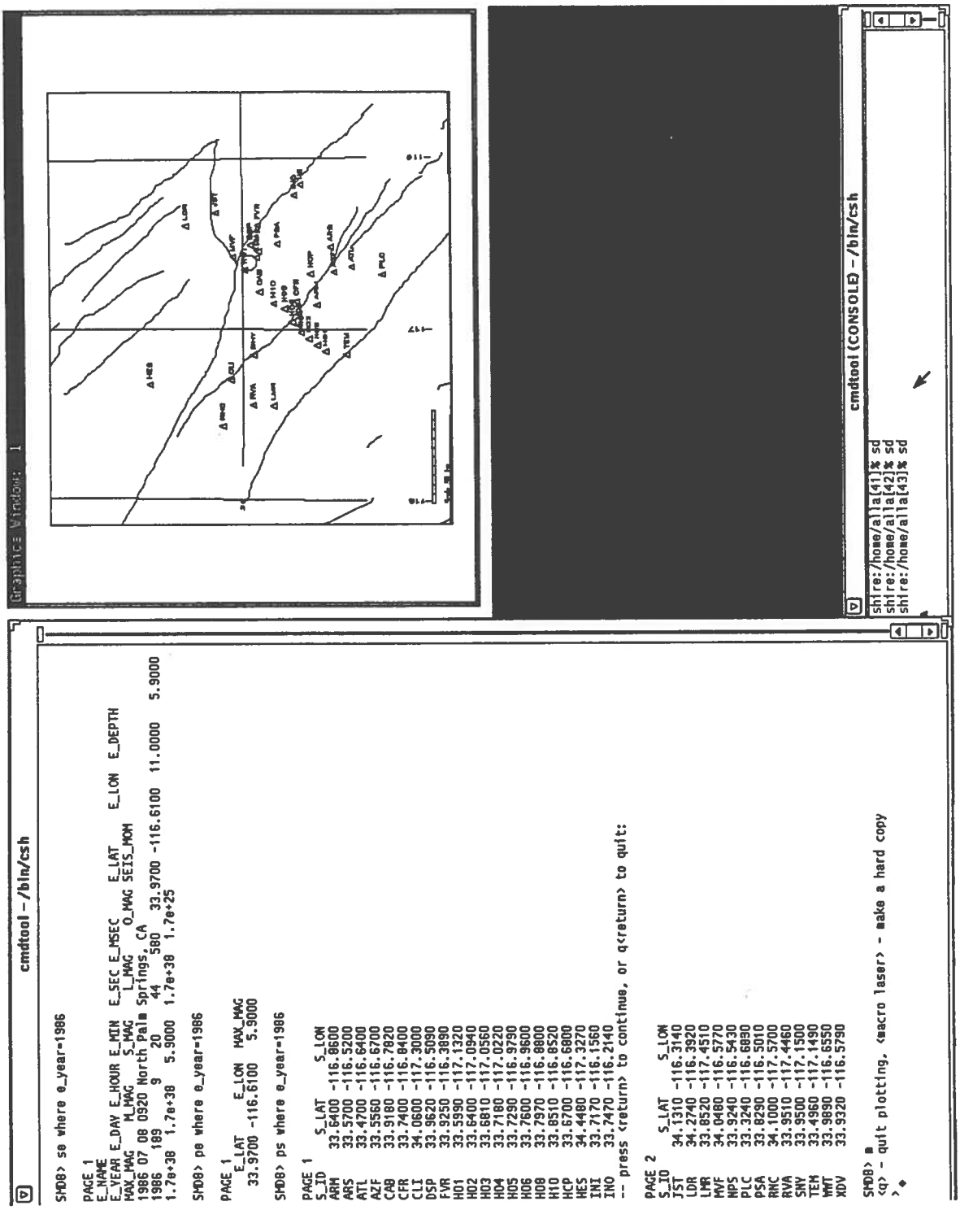
Graphics Window: 1
cmdtool (CONSOLE) - /bin/csh
shire:/home/alla[41]% sd
shire:/home/alla[42]% sd
shire:/home/alla[43]% sd
cmdtool - /bin/csh
SMDB> se where e_year=1986
PAGE 1
E_NAME
E_YEAR E_DAY E_HOUR E_MIN E_SEC E_MSEC E_LAT E_LON E_DEPTH
MAX_MAG M_MAG S_MAG L_MAG O_MAG SEIS_MOM
1986 07 08 0920 North Palm Springs, CA
1986 189 9 20 44 580 33.9700 -116.6100 11.0000 5.9000
1.7e+38 1.7e+38 5.9000 1.7e+38 1.7e+25
SMDB> pe where e_year=1986
PAGE 1
E_LAT E_LON MAX_MAG
33.9700 -116.6100 5.9000
SMDB> ps where e_year=1986
PAGE 1
S_ID S_LAT S_LON
ARM 33.6400 -116.8600
ARS 33.5700 -116.5200
ATL 33.4700 -116.6400
AZF 33.5560 -116.6700
CAB 33.9180 -116.7820
CFR 33.7400 -116.8400
CLI 34.0600 -117.3000
DSP 33.9620 -116.5090
FVR 33.9250 -116.3890
H01 33.5990 -117.1320
H02 33.6400 -117.0940
H03 33.6810 -117.0560
H04 33.7180 -117.0220
H05 33.7290 -116.9790
H06 33.7600 -116.9600
H08 33.7970 -116.8800
H10 33.8510 -116.8520
HCP 33.6700 -116.6800
HES 34.4480 -117.3270
INI 33.7170 -116.1560
INO 33.7470 -116.2140
-- press <return> to continue, or q<return> to quit:
PAGE 2
S_ID S_LAT S_LON
JST 34.1310 -116.3140
LDR 34.2740 -116.3920
LMR 33.8520 -117.4510
MVF 34.0480 -116.5770
NPS 33.9240 -116.5430
PLC 33.3240 -116.6880
PSA 33.8290 -116.5010
RMC 34.1000 -117.5700
RVA 33.9510 -117.4460
SNY 33.9500 -117.1500
TEM 33.4980 -117.1490
WMT 33.9890 -116.6550
XDV 33.9320 -116.5790
SMDB>
<q> - quit plotting, <macro laser> - make a hard copy
>

Figure 2.

PROJECT REPORT: **Near Real-Time Data Transmission from and a Geodetic Test-Range at Piñon Flat Observatory**

PROJECT PERIOD: February 1, 1992 — January 31, 1993

SUBMISSION DATE: September 24, 1992

PRINCIPAL INVESTIGATOR: Duncan Carr Agnew, Professor, Geophysics - (619) 534-2590

ASSOCIATE INVESTIGATOR: Frank K. Wyatt, Senior Development Engineer - (619) 534-2411

Institute of Geophysics and Planetary Physics
Scripps Institution of Oceanography, MC 0225
University of California, San Diego
La Jolla CA 92093-0225

The Southern California Earthquake Center supports two infrastructure activities at Piñon Flat Observatory: a long-term program to make the precise strain data collected at PFO more readily available, and development of a "test range" for GPS measurements, using the existing two-color EDM network measured by the USGS at Pinyon Flat. Both activities played important roles in monitoring and interpreting the 1992 Landers earthquake sequence.

DATA ACCESS: Partly because of the data-recording systems (which are largely onsite), but also because considerable post-processing is needed to produce the best results, the data from many of the better instruments at PFO have not been generally available until days to weeks after they were recorded. We are taking steps to make the raw data more easily accessible on our local computer via *ftp*, and hope to begin routinely depositing fully-processed data in the SCEC database before the end of this grant. Our goal is to make much of the raw data accessible within a day, with as much automatic processing as possible done soon after. In June 1992 we installed a dedicated data-line from the observatory to our lab, to allow real-time inspection of the more critical data.

GPS TEST RANGE: As modes of reducing GPS data proliferate and new observation methods develop (e.g., rapid-static positioning or photogrammetry), we will need to evaluate their quality: this led us to propose a highly accurate "GPS test range", on which such techniques could be tried. Part of this would be based on the continuous GPS measurements that are being made at both ends of a 14-km line from the observatory to a point due west. The scatter in these data is 3-5 mm in the horizontal for daily solutions, meaning that with enough averaging we can reach mm-level precision. In May 1992 we made GPS observations at the monuments of the 4-5 km, 2-color EDM network established by Dr. J. Langbein, USGS. The combination of GPS and 2-color data provide an absolute measure of positions good at the submillimeter level. A paper describing the comparison of results from the two systems is currently in preparation, and shows that even out to distances of 4 km GPS appears to be capable of 1-2 mm accuracy.

LANDERS EARTHQUAKE SEQUENCE: The Landers/Big Bear earthquakes of June 1992 provided us with startling signals; in studying these we benefited considerably from our SCEC support. The improvements in data transmission we had made allowed us to identify, within a day, a 400-fold increase in the secular strain-rate at the observatory, commencing with the Landers shock. (Figure 1 presents the NW-SE laser strain record, both as recorded and with earth tides removed.) We were able to report this to the emergency meeting of CEPEC on June 29, along with the advice that what we were seeing was consistent with ongoing deformation in the epicentral region and so was probably not cause for alarm—simply very interesting new science. Since then the strain-rates have diminished, with the total cumulative postseismic deformation amounting to about 7% of the coseismic.

The measurements of the GPS test range, while now obsolete for their original purpose, are very valuable for seeing the coseismic effects of the earthquakes. A two-color survey was conducted shortly after the event, and gives a preliminary estimate of coseismic strain, but another GPS survey (planned for this fall) will be needed to restore the test range and refine our estimates of strain at Pinyon Flat.

Several abstracts submitted for the upcoming AGU meeting discuss results from the Landers earthquake and our GPS/two-color EDM studies.

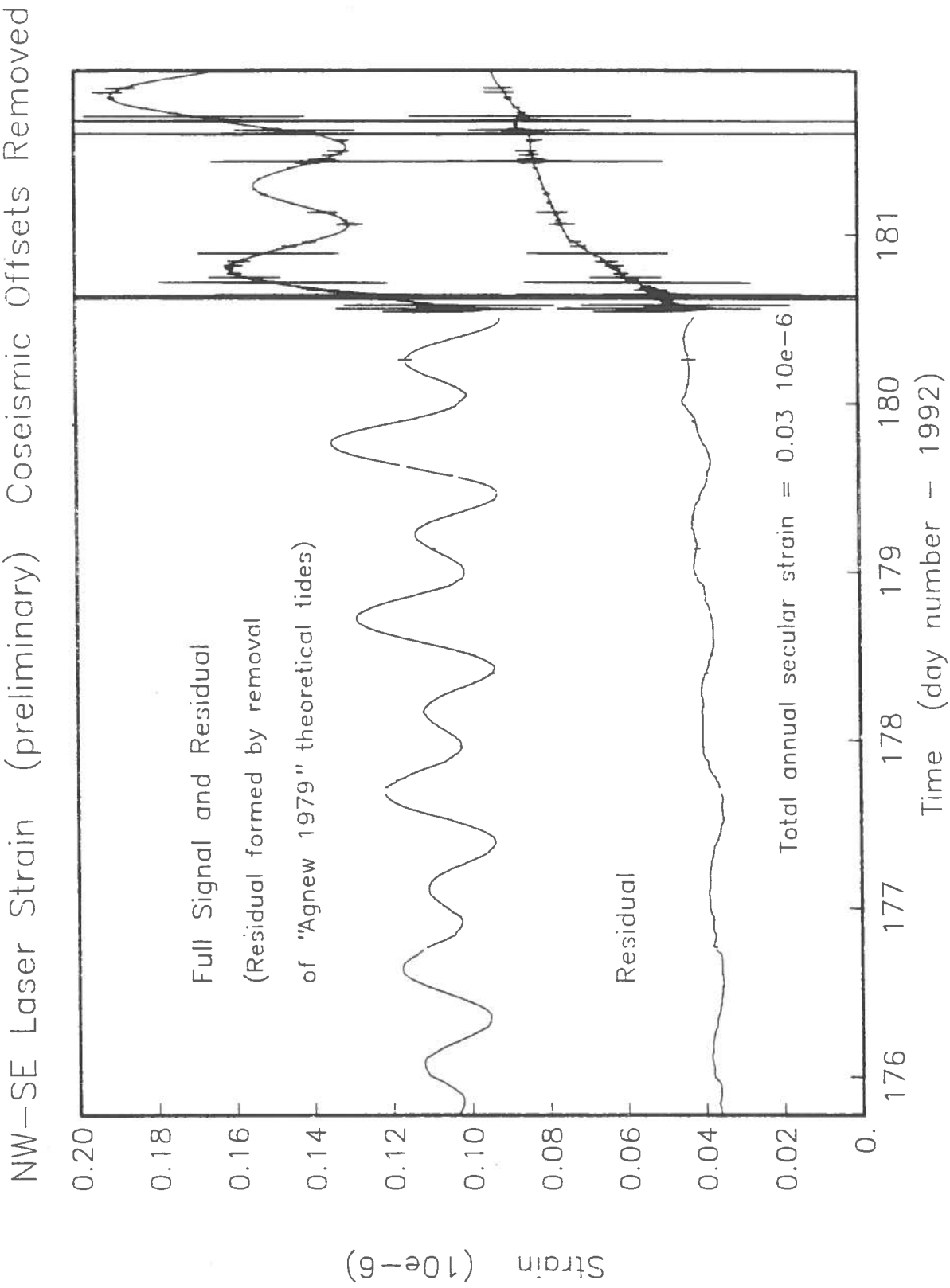
29-Jun-92
(7:15 PM PDT)
NW-SE Laser Strain (preliminary) Coseismic Offsets Removed
Full Signal and Residual
(Residual formed by removal
of "Agnew 1979" theoretical tides)
Residual
Total annual secular strain = 0.03 10e-6
Strain (10e-6)
Time (day number - 1992)
0.20
0.18
0.16
0.14
0.12
0.10
0.08
0.06
0.04
0.02
0.
176
177
178
179
180
181

SCEC 1992 Progress Report

SCEC Portable Broadband Instrument Center (PBIC)

PI: Ralph J. Archuleta
Institute for Crustal Studies
University of California, Santa Barbara

PBIC recorders and sensors were deployed for the three principal earthquakes to strike southern California in 1992: 22 April Joshua Tree, 28 June Landers and 28 June Big Bear. In addition to these earthquakes the recorders/sensors were used by other SCEC investigators for ongoing SCEC experiments.

Five PBIC DAS's were initially deployed within 6.5 hours of the April 22 M6.1 Joshua Tree mainshock. The PBIC assisted in the deployment and maintenance of these sites. Six PASSCAL DAS's were added to the deployment in the following days. The array was maintained until early June and collected about 5-6 Gb of raw data. The PBIC is working on the timing corrections and event association of the 3-4 Gb of data remaining after reduction.

The Joshua Tree earthquake and subsequent data processing was overshadowed by the June 28 M_S 7.4 Landers and M_L 6.6 Big Bear earthquakes. Eight of the PBIC DAS's were deployed for this aftershock sequence, the ninth SCEC DAS being left deployed at the Cajon Pass Deep borehole. PASSCAL supplemented the SCEC array with 10 DAS's in the days following the mainshock. SCEC member institutions worked together to deploy and maintain the array which, once fully deployed, consisted of 18 sites (see figure 1) including 3 STS-2 and 2 CMG-3 broadband sensors. The 18-station array was maintained for about 3 weeks when it was reduced to 6 sites. The remainder of the array was pulled at the beginning of September. A prototype field computer was configured for the aftershock deployment. The computer was used to perform initial field quality control of the data and to make timing corrections necessary for later processing.

In addition to the field deployments the PBIC has continued to improve the use of the DAS systems. These improvements include:

- The PBIC has developed worksheets and forms to assist users during field deployments. The worksheets/forms are a direct result of the PBIC's experiences during the two aftershock deployments.
- The PBIC has examine the compatibility of the DAS characteristics with that of available sensors. This is shown in Figure 2 which shows the relationship between the dynamic range of sensors and the input characteristics of 16 and 24 bit Reftek DAS's. The figure is useful in illustrating the usable magnitude range of each of the sensors at different gains and suggest the limitations of different sensor/DAS combinations.
- The PBIC DAS's have been upgraded to version 2.47 of Refraction Technology's operating system. This upgrade corrects several timing problems from earlier versions and adds some new capabilities, such as detriggering, to the DAS's.

- The PBIC has provided SCEC member institutions with assistance in deployment planning, field data collection, software usage and data salvage.
- Reftek was able to diagnose and find a solution to the low level spiking problem discovered by the PBIC last year. All PBIC DAS's have been upgraded to correct the problem. One omega board has failed and is in for evaluation. The vertical component of one of the L4C-3D's failed and has been repaired. Two disks that failed during the Joshua Tree deployment are being repaired or replaced.

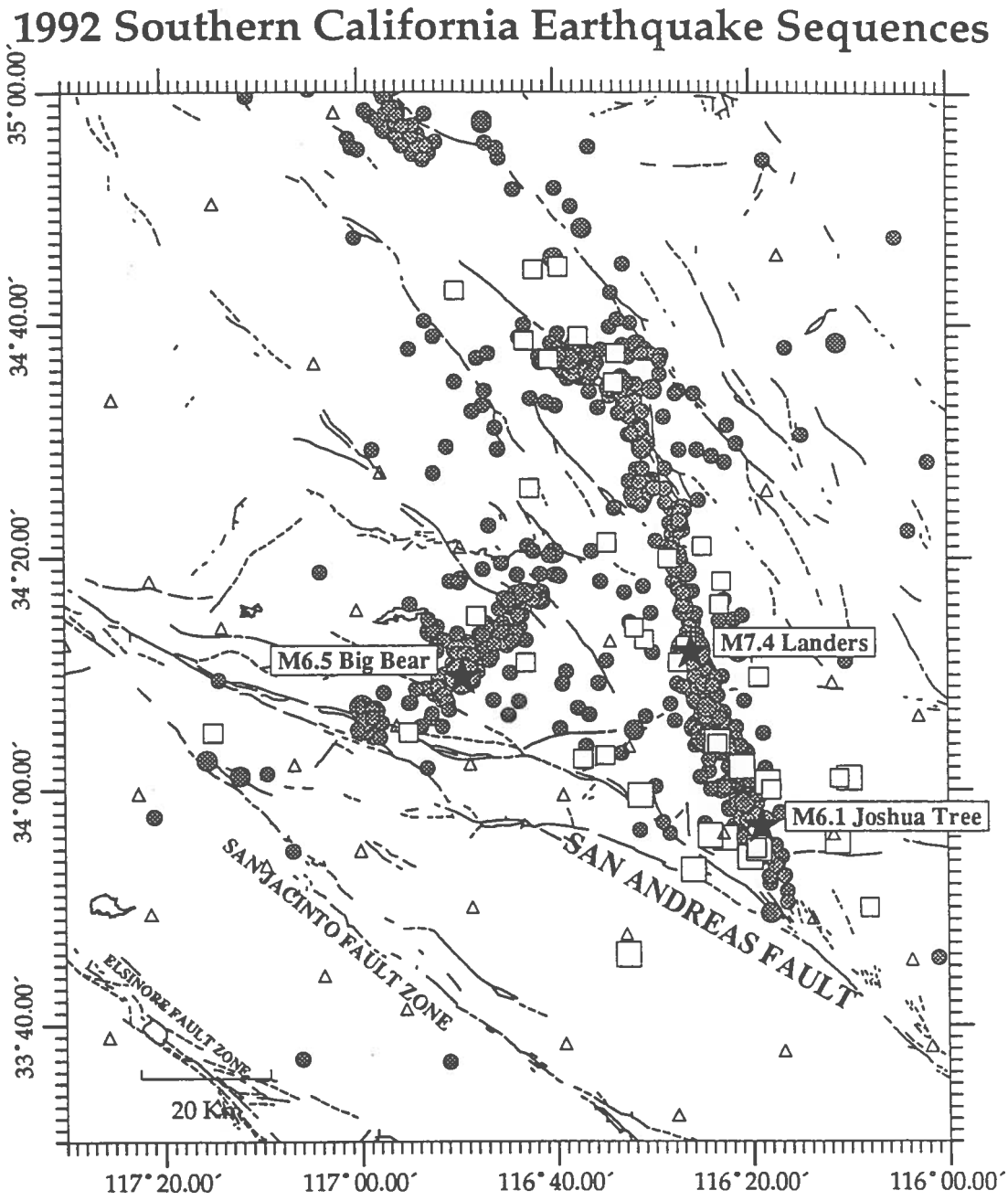

Figure 1. Epicenters (circles) of aftershocks (M≥2.0) of the June 1992 M7.4 Landers and M6.5 Big Bear earthquakes (stars). Squares are portable stations deployed by the Southern California Earthquake Center (SCEC); large squares are SCEC stations deployed following the April 1992 M6.1 Joshua Tree event (star). Triangles are permanent stations.

Sensor and DAS ranges

All calculations in max 0-peak g's @ 1Hz
Note: 0-peak = 3 X rms for FBA-23 in 1/2 octave bandwidth

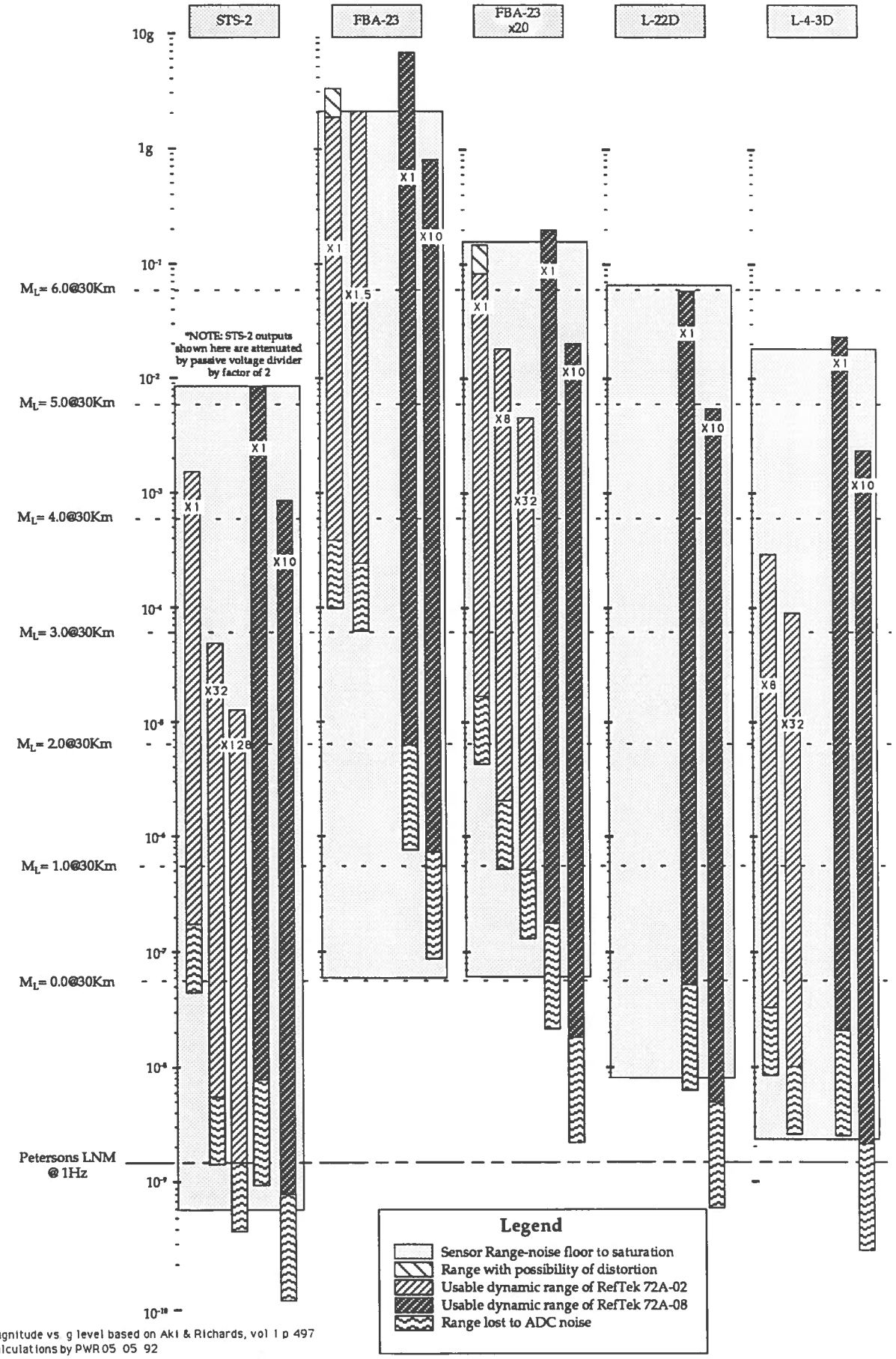

Magnitude vs g level based on Aki & Richards, vol I p 497
Calculations by PWR 05 05 92
Drafted by AJM 05 05 92

A SCEC Project: Progress Report, 24 Sept. 1992

PIs: Egill Hauksson and Hiroo Kanamori
Institution: California Institute of Technology
Title: Enhancement of TERRAscope

INVESTIGATIONS

This project provides support for the installation and operation of the TERRAscope broad-band seismic network. Earthquake data from TERRAscope contribute to the goals of the master model and the seismicity and source processes groups.

RESULTS

We report the following accomplishments:

In 1992-1993 we plan to install 10 new TERRAscope stations (Figure 1). Assembly work has been underway since May 1992. The first station BAR will be installed in early October 1992. The next three stations LVA, USC and RPV will be installed in late October or early November. In December we plan to install the station GLA.

The major job responsibilities of the new field technician are assembly, installation, and field maintenance of broad-band stations in southern California. Most of the hardware for the TERRAscope stations is purchased as independent modules from outside vendors. Under the direction of Wayne Miller, our senior electronics engineer at Caltech, we assemble the different modules and build our own power supplies, including backup power. We also put a large effort into lightning protection. About one month of field technician time is needed to prepare equipment in the laboratory before field installation of each station. After field installation we find that we need to visit each site on the average about 5 to 10 times until all the problems with telephone lines, extraneous noise sources, and computer crashes are sorted out. Support from SCEC for a field technician has ensured rapid deployment of new stations and continuity of high quality data.

We have ordered the real-time data acquisition software from Adebahr Systemtechnik. We plan to telemeter data from at least 6 TERRAscope stations real-time to Pasadena. We plan to hire a computer programmer because we need software support to merge these data real-time with the short-period network data for immediate analysis. We also need software support for implementing new waveform based analysis techniques which take advantage of the dynamic range of the data.

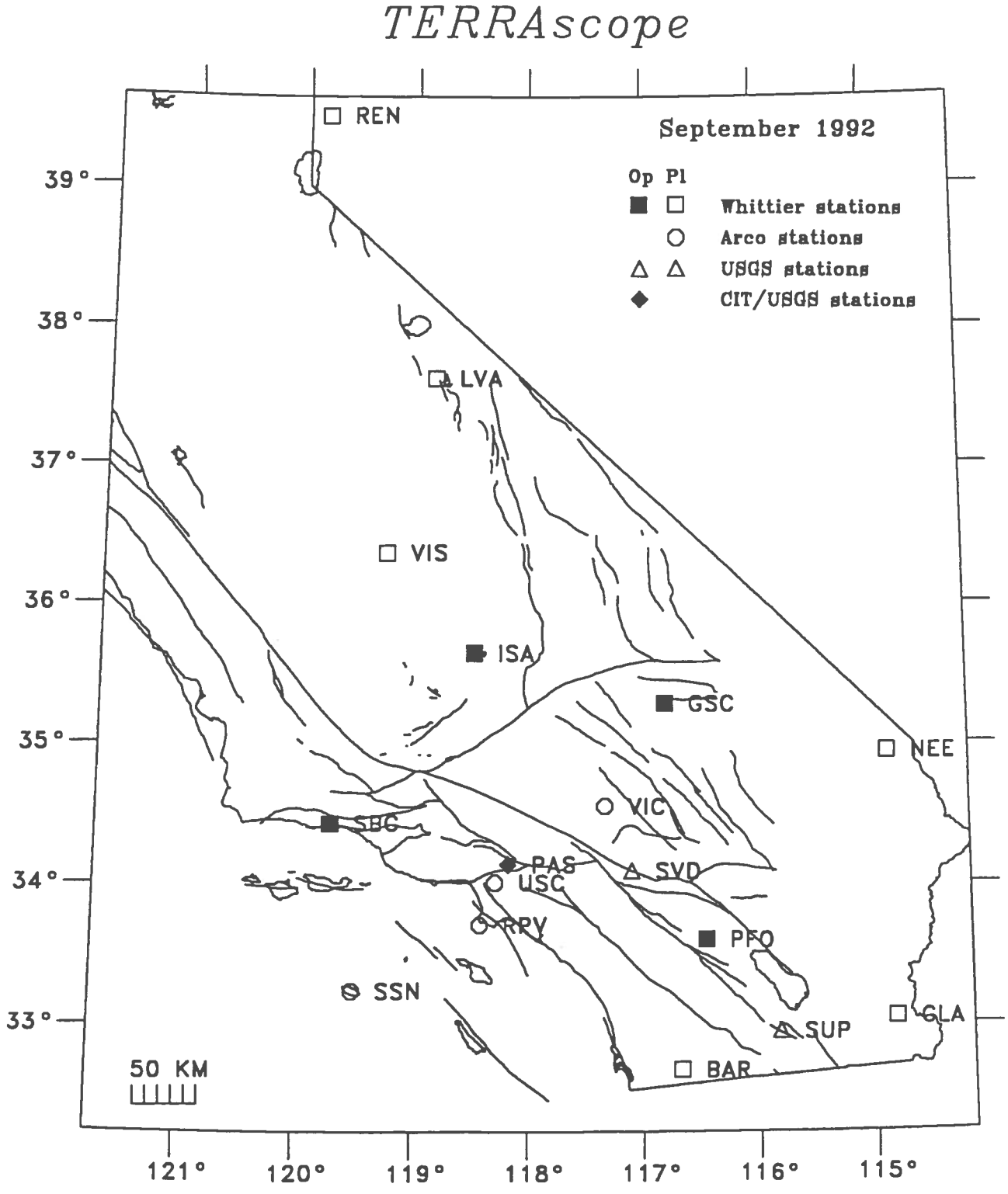
TERRAscope
September 1992
Op Pl
Whittier stations
Arco stations
USGS stations
CIT/USGS stations
REN
LVA
VIS
ISA
GSC
NEE
VIC
SBC
PAS
USC
SVD
RPV
PFO
SSN
SUP
GLA
BAR
50 KM
39°
38°
37°
36°
35°
34°
33°
121°
120°
119°
118°
117°
116°
115°

Figure 1.

EDUCATION AND OUTREACH ACTIVITIES

I. SCEC/SCEPP MOU and Work Plan

SCEC education and outreach activities began this fiscal year (beginning Feb. 1, 1992) with the drawing up of a memorandum of understanding (MOU) between SCEC and the Southern California Earthquake Preparedness Project (SCEPP; Appendix 1). A SCEC/SCEPP steering committee was established to develop a work plan for the next year (Appendix 2). Initiation of activities per the work plan was (a) first held in abeyance until an Assistant Director search and selection process was completed, and (b) preempted by the April 22 Joshua Tree earthquake and subsequent June 28 Landers and Big Bear events. In effect, personnel time and resources in both SCEC and SCEPP that would have been available for education and outreach activities were instead channeled to post-earthquake scientific studies (SCEC) and emergency response (SCEPP). This included the establishment of an earthquake safety information center and 1-800 hotline to address concerns of the southern California populace. In addition, SCEPP personnel and resources were severely impacted by the Los Angeles riots which also preempted personnel and resources.

At this time both the earthquake and riot-related activities are winding down. However, within the last month, the California Office of Emergency Services (OES) has been restructured under its new director -- Richard Andrews -- and both SCEPP and the San Francisco Bay Area equivalent (BAREPP) have been disbanded and absorbed into the overall OES structure. Information that we have indicates that in the future, OES will be more interested in response and recovery rather than preparedness. As such, it will be necessary to review the MOU with OES and perhaps restructure the work plan. This will be done when the reorganization at OES has been completed.

II. Assistant Director for Education and Outreach

As of May 1, 1992, SCEC advertised nationally for a position of Assistant Director for Education and Outreach (Appendix 3). Approximately 30 candidates were encouraged to apply. A selection committee composed of members from both SCEC and SCEPP invited 6 applicants to Los Angeles for interviews, from which 3 finalists were selected. We are currently negotiating with our top candidate.

III. Joshua Tree and Landers/Big Bear Earthquakes

Many SCEC scientists were called upon to provide information to the public and to the media following the Joshua Tree and Landers/Big Bear earthquakes. This included a town-hall meeting convened by Congressman George Brown in San Bernardino.

However, no central SCEC information clearinghouse was established. Most SCEC scientists headed for the field. In retrospect, a SCEC information center would have been desirable and plans will be developed to do this in the future; planning will be one of the first tasks of our new Assistant Director for Education and Outreach. It is anticipated that SCEC can provide background technical information during the first few hours to days after an earthquake, to be coordinated with Caltech's firsthand reporting of mainshock and aftershock parameters and daily news releases. SCEC can also provide data bases and general earthquake information on a longer time scale from its base at USC.

IV. Implications of the Landers Earthquake Sequence

As part of its outreach effort, SCEC has provided working papers on the implications of the Landers earthquake sequence for future seismic hazards in southern California to an *ad hoc* working group composed of members from NEPEC, CEPEC, and SCEC. These working papers are being organized into a semi-technical report for general consumption. Distribution of the report is currently restricted while under review by NEPEC and CEPEC. The title page and preface to the document are given in Appendix 4. It is anticipated that the report will be issued in late October. A second, Phase II, report dealing more broadly with earthquake hazard in southern California is planned for completion on the anniversary of the Landers earthquake.

V. Los Angeles County Museum of Natural History Exhibit

The earthquake exhibit at the California state museum is one of their most popular attractions. SCEC (C. Sammis) has been collaborating with the museum curator, Eugene Gendel, to upgrade the exhibits to more accurately reflect the current state of earthquake science. Toward this goal of increasing the information content of the earthquake exhibit, we are developing the following items:

1) A paleoseismicity display. We have obtained permission to use a large-format color photo of Kerry Sieh's trench wall taken several years ago by a free-lance photographer for the L.A. Times. A 3 by 4 foot light box has been constructed to back-light this image. The exhibit has been designed to include:

a) Information about the site, sag pond, and peat formation.
b) Information about radiocarbon age dating.
c) Identification of the events which can be seen in the photo.
d) A time line showing past events with a discussion of the problems involved in predicting the next big one.

2) A computer display of world seismicity through time. We are using a program developed at SUNY Binghamton which plots earthquake epicenters through time on a world map. This computer display will be supplemented with text about the different types of earthquakes at the different types of plate boundaries. This program can also be run in a mode which plots seismicity through time on a California map.

3) A P-wave and S-wave display. We are designing a display which uses slinkys to display both compressional and shear waves. Besides allowing children to bash away at the handles attached to an end of the slinkys, this display will also allow a discussion comparing (a) the sense of motion in the two waves, (b) the different velocities, and (c) why shear waves don't propagate in liquids or gasses.

4) A 3-D display of faults and seismicity in the L.A. basin. We originally proposed to build a four foot square 3-D display of basin seismicity by laminating Plexiglas sheets. We have since decided to use mylar sheets for the various layers to avoid refraction problems. We have constructed a small scale mock-up and are experimenting with fluorescent paints and black light to get the best visual display. The museum technical staff are designing frames to stretch and hold the stack of mylar sheets.

5) The CUBE display. We are currently negotiating with Caltech to install a CUBE (Caltech- USGS Broadcast of Earthquakes) display at the museum.

VI. GIS Development

In August after a national search, SCEC hired a GIS specialist, Eric Lehmer, to assist the center in the development and research use of GIS data bases, and to begin producing GIS maps and data bases in the form of SCEC products (see report by S. Park in Infrastructure).

VII. "Earthquakes 101"

SCEC has been asked by FEMA/OES to give a short course on earthquakes and seismology to the media at two venues -- one in the Los Angeles area and one in the San Bernardino area. This will be done by Tom Henyey, Lucy Jones, and Karen McNally. The proposed dates are October 23 and 30, and the proposed subject matter is given in Appendix 5.

VIII. CUBE

SCEC has entered into discussions with Caltech and the USGS about the use of CUBE in the public sector. SCEC wishes to make CUBE available to the L.A. County Museum and to several schools in the greater Los Angeles area. We are planning to set aside funds in next year's budget for this purpose. The level of effort needs to be decided, and this will be one of the tasks for our new Assistant Director for Education and Outreach.

IX. Documentary on Landers Earthquake

SCEC is working with the Seismological Society of America and the local PBS television station in Los Angeles (KCET-Channel 28) to produce a documentary on the Landers earthquake (Appendix 6).

X. Earthquake Bulletins

SCEC in cooperation with SCEPP -- as part of the work plan discussed in Section I above (Appendix 2) -- generated the first earthquake bulletin following the June 28, 1991 M5.8 Sierra Madre earthquake. It was sent to all parties on the SCEPP mailing list. A second bulletin covering the April 22, 1992 M6.1 Joshua Tree earthquake was in the final stages of preparation when the June 28, 1992 M7.5 Landers and M6.5 Big Bear earthquakes occurred. The decision was made to combine these three events into a single bulletin which has not yet been completed due to the heavy post-earthquake and post-riot workloads of both SCEC and SCEPP. It is planned to finish this document in November. Material assembled for the Landers report and for the special Landers session at the SCEC annual meeting will form a good basis.

XI. Los Angeles City Emergency Preparedness

SCEC scientists participated in the City of Los Angeles Emergency Operation Workshop (September 29-October 2, 1992) held at Lake Arrowhead, CA. This workshop began the effort to develop a new 5-year strategic emergency preparedness plan for the city. SCEC scientists have been asked to contribute to this effort on an ongoing basis, particularly with respect to intermediate-term forecasts.

XII. SCEC/NCEER Memorandum of Cooperative Agreement

SCEC and the National Center for Earthquake Engineering Research signed a memorandum of cooperative agreement (Appendix 7) for collaborative development and research efforts in: (a) ground motion and seismic hazard study, (b) geotechnical research, and (c) integrated seismic hazard data development. It is also proposed to hold joint meetings to share progress on the cooperative efforts.

APPENDIX 1

MEMORANDUM OF UNDERSTANDING
Between
Southern California Earthquake Center (SCEC)
and
Southern California Earthquake Preparedness Project (SCEPP)
Governor's Office of Emergency Services

I. PURPOSE AND SCOPE

The organizations: The parties to this Memorandum of Understanding are the Southern California Earthquake Center (SCEC) and the Southern California Earthquake Preparedness Project (SCEPP).

Based at the University of Southern California, SCEC was established in 1991 to coordinate the earthquake science research efforts of various university and USGS groups and to make such work accessible to a wide range of public and private organizations. Core institutions include USC, Caltech, UCLA, UC Santa Barbara, UC Santa Cruz, UC San Diego (Scripps Institute of Oceanography), Columbia University (Lamont-Doherty Geological Observatory) and the USGS. It is funded by the National Science Foundation, the U.S. Geological Survey and the Federal Emergency Management Agency.

SCEPP's mission is to encourage and maintain the highest levels of earthquake preparedness possible in its 10-county service region. It carries out a comprehensive annual work program consisting of earthquake education, response and recovery planning assistance to schools, business & industry, local governments and local jurisdictions. SCEPP is a project of the Governor's Office of Emergency Services and is funded by the California State Legislature and the Federal Emergency Management Agency.

Activity Areas: SCEC's activity area includes the entire southern California region, with an emphasis on earthquake phenomena impacting the major metropolitan areas. The administrative offices of the Center are located on the campus of USC. Satellite activities are located at some of the core institutions, including a data center at Caltech, an instrument center at UC Santa Barbara, and and a Global Positioning System Center (GPS) at UCLA.

SCEPP's service area includes a 10-county region in southern California. The Project is located in Pasadena, with satellite offices operating in San Diego, and Santa Barbara.

The Joint Mission: SCEPP and SCEC will work in a collaborative and coordinated manner to translate and transfer earth science information to practitioners to enhance awareness, education, planning and policy development. Such practitioners include building design professionals, hazard managers, educators, journalists, risk managers,

policy makers/elected officials and other research scientists. This will make it possible for SCEC to fulfill its responsibility to provide education and outreach while expanding SCEPP's work program by its stronger association with the scientific community and by focusing SCEPP resources on mutually funded tasks.

II. WORK PLANS

The principal mechanism for coordination and cooperation between the two organizations will be a multi-year work plan with a specific statement of work developed for each year in which this MOU operates. The plans will be developed and monitored by a "Joint Advisory Committee" aided by professional staff support from a SCEC-funded and supervised position entitled "Assistant Director for Education and Outreach". The tasks comprising the SCEC/SCEPP annual plan will be compatible with the elements of SCEPP Work Program. Thus, SCEC funds will supplement and enhance SCEPP's planning efforts.

Multi-Year Work Plan: The following general objectives are intended to provide a conceptual framework for a multi-year work plan which will be updated on an annual basis and which is subject to change as mutually agreed upon by the Joint Advisory Committee.

1) To identify, translate and transfer new information on scientific developments and technologies that will contribute to a better definition of seismic risk for users in southern California.

2) To promote the development of earthquake science education and curricula for practitioners and the public (primary and secondary grades, undergraduate and continuing education).

3) Facilitate the development and implementation of a Geographic Information System (GIS) for earthquake preparedness response and recovery planning.

4) To provide special workshops and seminars to translate and transfer scientific information to various organized groups concerned with earthquake preparedness and response.

5) To coordinate and publish periodic newsletters other information and distribute for constituents.

Annual Statement of Work: This plan will include tasks of mutual interest compatible with SCEPP's work plan representing the primary elements of
(1) Resource Development, (2) Research Transfer and Application and (3) Public Information and Outreach.

It is understood that the selected tasks within each element will be compatible with SCEPP's work program.

III. ORGANIZATIONAL RELATIONSHIP:

Advisory Committee

The SCEC/SCEPP joint mission will be guided by a Joint Advisory Committee made up of:

- The Director or Executive Director of SCEC
- The Director of SCEPP
- Selected members of SCEC's Steering Committee.
- The Chairperson and/or Vice-Chairperson and other selected members of SCEPP's Policy Advisory Board

This committee will oversee development and implementation of the multi-year and annual planning process. Staff support to this committee will be provided by the SCEC Assistant Director for Education and Outreach.

In addition, each organization will have full membership and voting rights on the other's advisory body.

Staffing and Funding

SCEC: The position of Assistant Director for Education and Outreach will be funded and supervised by SCEC. This individual will work cooperatively with the Joint Advisory Committee and SCEPP staff on the education and outreach tasks which make up the SCEC/SCEPP annual statement of work. In addition he or she will provide professional management services for the administration of the Center's education and outreach programs.

SCEPP: Program staff assigned to the joint tasks will work in concert with the SCEC staff person as co-lead and program support.

SCEPP and SCEC will each provide physical housing for the Assistant Director, including office space, computer, clerical support, desk & supplies, telephone, FAX, reproduction and related services.

Products and Reports

The SCEC/SCEPP joint mission can be expected to generate products and reports that may have proprietary and/or commercial value. Policies governing the ownership, copy right, etc, of these materials will be established by the Joint Advisory Committee.

Amendments

This Memorandum of Understanding may be amended in writing as may be mutually agreed to by the parties hereto. Any such changes, as mutually agreed, become an operative part of this Memorandum.

Termination of this Memorandum of Understanding

Either party may terminate this Memorandum of Understanding upon thirty (30) days written notice during which time both parties shall continue to perform the responsibilities listed herein and prepare a closing report on work completed to date. Each party to this Memorandum will also release to the other all data, information, papers and other supporting materials needed for the joint work. Any work efforts related to activities must be turned over to the appropriate manager of each organization (Executive Director of SCEC or Director of SCEPP) in such a manner that progress is not negatively impacted.

OES Director	SCEC Director
SCEPP PAB Chair	SCEC Executive Director

APPENDIX 2

SCEC/SCEPP TASKS: 1992-93

GIS Workshop

- Identify locally-based experts in Geographic Information Systems (GIS) and representatives of the user community for participation in a one-day workshop to discuss key GIS issues in the region.

Vulnerability Analysis Workshop

- Convene a one-day workshop to identify the specific needs of local jurisdictions for risk and vulnerability information. Participants in the workshop will be planners and emergency managers as well as technical experts responsible for development of risk information for southern California.

Master Model Workshop

- Convene a one-day workshop to introduce the SCEC Master Model concept and significant developments to members of the SCEPP Policy Advisory Board and selected representatives of local jurisdictions within SCEPP's planning region.

Undergraduate Education Curriculum Workshop

- Convene a one-day workshop to develop a dissemination strategy for the interdisciplinary undergraduate earthquake and public policy curriculum assembled by UC Santa Cruz and SCEPP. Participants should include SCEPP Policy Advisory Board members and selected educators.

Earthquake Bulletins

- Upon the occurrence of a damaging earthquake in southern California or a situation of scientifically substantiated increase in short- or intermediate-term seismic potential, SCEPP and SCEC will jointly publish a bulletin containing analysis and commentary on the scientific and public policy implications of the event.

School-Needs Assessment

- Convene a task force to look into the area of earth science curriculum available for K-12 and community colleges. In the first year, this task force will survey material, identify gaps, interview users of such information and compile a needs assessment which includes recommendations for follow-up and an identification of a strategy for dissemination of a new fault map.

L. A. County Museum Exhibit Brochure

- Provide technical and resource assistance in the development of an information brochure on the L. A. County Museum Earthquake Exhibit. The brochure will serve a dual purpose -- to serve as a detailed tour guide of the exhibit features and a general earth science information piece including preparedness information. This work effort will also include the development of an outreach and dissemination strategy for the brochure.

SCEC Brochure

- Develop a public relations/information brochure for the center which presents the goals, objectives, purpose and mission of the work of the center. This work effort will also include the development of an outreach and dissemination strategy for the center and its affiliated universities, as well as possible briefing to selected constituents of the center.

Southern California Earthquake Magazine

- Reassess the feasibility of producing the Southern California Earthquake Magazine and develop a timetable and work plan for the final development of the southern California publication of "The Next Big One" Magazine.

SCEC/SCEPP Newsletter

- Produce newsletters which present state of the art technology and research findings for the purpose of facilitating application and improving awareness levels of seismic risk. This work effort will include the development of an outreach and dissemination strategy for the newsletter and the compilation of a subscriber membership.

CUBE

- Develop proposed SCEPP/SCEC participation in the CUBE project (Caltech-USGS Broadcast of Earthquakes).

Southern California Earthquake Center

The Southern California Earthquake Center (SCEC) invites applications for the following position:

Assistant Director for Education and Outreach, University of Southern California, Los Angeles, CA. This position involves management responsibilities for formulating and administering SCEC's policies and programs as they relate to education and outreach of earthquake information. The successful candidate should have demonstrated skills in his/her ability to take the initiative, coordinate the activities of others, effectively interface with governmental agencies, civic leaders, and the media, and communicate both verbally and in writing. Minimum qualifications include, but may not be limited to, at least four years performing duties in an interdisciplinary setting involving application of earthquake technical information, implementation of seismic safety information, and/or implementation of earthquake preparedness activities, with at least some time spent in a supervisory capacity. The candidate should have a Bachelor of Arts or Bachelor of Science degree and a Master's degree in one of the following majors or related fields (Bachelor's and Master's degrees do not have to be in same discipline): political science, communication, earth science, geography, engineering, planning, sociology, business administration, public administration, social work, public health, architecture, or environmental studies. The deadline for applications for this position is July 1, 1992.

Southern California Earthquake Center (SCEC)
Assistant Director for
Education and Outreach

SCOPE OF DUTIES

Desired skills and talents:

-Demonstrated ability to coordinate activities of others;
-Liaison experience with governmental and nongovernmental agencies;
-Ability to deal tactfully and effectively with civic leaders and the media;
-Ability to have a broad vision;
-Good interpersonal skills;
-Excellent verbal and written communication skills.

- This position involves management responsibilities for formulating or administering the center's policies and programs as they relate to earthquake education and outreach;

- The position is responsible for overseeing multiprograms of regional impact requiring skills and knowledges at the highest level with responsibility for work of the most critical and/or sensitive nature as it relates to the center's primary mission;

- Direct complex earthquake education and outreach programs and studies that involve expert review;

- Acts as the Center's principal staff person on earthquake education and outreach;

- Primary responsibility in planning or developing policy regarding education and outreach;

- Manages, plans, organizes, and directs the center's work program relative to earthquake education and outreach;

- As appropriate supervises center staff on major projects and coordinates the efforts to accomplish objectives;

- Makes decisions on complex and technical issues and assigns work on a broad range of critical or sensitive governmental and managerial problems that may be interdisciplinary in nature;

- Directs the most highly complex assignments independently to formulate and develop solutions;

- Initiates and directs comprehensive earthquake education projects and development of comprehensive local and regional outreach plans and programs;

- Serve as the Center's liaison in complex and sensitive intergovernmental relations;

- Performs management review of contract and agreements in connection with the development of earthquake education and outreach materials which incorporate state-of-the-art scientific, technical and policy information;

- Consults and confers with public and private sector and educational institutional representatives; performs personnel management duties;

- Consults and confers with working group leaders for purposes of recommending outreach policy.

Southern California Earthquake Center (SCEC)
Assistant Director for
Education and Outreach

Minimum Qualifications

Five years performing duties in an interdisciplinary setting of increasingly responsible professional experience in planning and designing programs involving interpretation and application of earth science information and implementation of earthquake preparedness activities, and the use of this information in policy development, plans, and decision making with two years served as a highly professional program expert in a supervisory capacity; or

Four years performing duties in an interdisciplinary setting of increasingly responsible professional experience in planning and designing programs involving interpretation and application of earth science information and implementation of earthquake preparedness activities, and the use of this information in policy development plans, and decision making; two years must be served as a highly level program expert with supervisory capacity; and

Bachelor of Arts or Bachelor of Science degree in one of the following majors or a related field; political science, communications, geology, geography, engineering, planning, sociology, business administration, public administration, social work, public health architecture, or environmental studies; or

Three years performing duties in an interdisciplinary setting of increasingly responsible professional experience planning processes involving interpretation and implementation of seismic safety information and earthquake preparedness, activities, and the use of this information in policy development, plans, and decision making with two years served as a highly professional program expert in a supervisory capacity; and

Possession of a master's degree in one of the following majors or a related field; political science, communications, geology, geography, engineering, planning, sociology, business administration, public administration, social work, public health, architecture, or environmental studies.

Appendix 4

Draft

The Landers Earthquake Sequence and Future Seismic Hazards in Southern California

NEPEC/CEPEC/SCEC
Ad-hoc Working Group

September 28, 1992

Version 4

PREFACE

This document represents the efforts of a joint *ad hoc* working group composed of individuals from the National Earthquake Prediction Evaluation Council (NEPEC), the California Earthquake Evaluation Council (CEPEC), and the Southern California Earthquake Center (SCEC). It is the Phase I report of a two phase study of the probabilities of future large earthquakes in southern California. The Phase II report is scheduled for completion July 1, 1993.

NEPEC was established in 1979 pursuant to the National Earthquake Hazards Reduction Act of 1977 to advise the director of the United States Geological Survey (USGS) concerning any formal predictions of other information pertinent to the potential for the occurrence of a significant earthquake.

CEPEC was named in 1976 under existing administrative authority as the successor to an advisory group formed in 1974. CEPEC advises the Director of the California Office of Emergency Services on the validity of predictions of earthquakes capable of causing damage in California, including the reliability of the data and scientific validity of the technique used to arrive at a specific prediction.

SCEC was established by the National Science Foundation (NSF) and the USGS to integrate earth sciences research on the processes that cause earthquakes so as to improve forecasts of damaging earthquakes and their effects. A fundamental goal of SCEC is to develop a master model that will provide the basis for a probabilistic seismic hazard analysis of southern California. SCEC is a consortium of seven research institutions in partnership with the USGS. Member institutions include the California Institute of Technology, Columbia University, the Universities of California at Los Angeles, San Diego, Santa Barbara, and Santa Cruz, and the University of Southern California -- SCEC's managing institution.

Following the Landers earthquake, SCEC's Science Director organized a workshop to share the preliminary results of ongoing scientific investigations. The group determined that it would produce a series of documents addressing (a) the implications of the Landers earthquake on future seismic hazards in southern California, and (b) update the probabilities for large earthquakes on the region's active faults. Due to the high level of public concern, the Chairs of NEPEC and CEPEC determined the need for a deliberate evaluation, and a more formal procedure was indicated. On August 5, 1992 NEPEC, CEPEC, and SCEC announced the formation of a joint *ad-hoc* working group composed of 12 scientists from the three organizations to oversee the generation of a report. SCEC scientists were asked to provide the necessary working papers which formed the technical basis for the final document. Following NEPEC and CEPEC approval, the final report was submitted to the Directors of the USGS and California Office of Emergency Services for their approval.

Appendix 5

Earthquakes 101 - Content - - Proposed

Program Orientation:

* Ad Hoc committee report is due at end of October. What it will be about, and what we can expect from it?

* Just what is the Big One? What criteria is used? Does everyone agree on the definition? If not, what are the various definitions that different people use? and so on.

Seismologist(s):

* What an earthquake is, what causes them, and what really happens to the ground when they happen. This will include an overview of the basic structure of our planet.

* P, S, and Surface waves; what they are, how they are felt, and how they are used to both measure a quake's magnitude and pinpoint its location.

* What "earthquake alarms" can and cannot do.

* Tectonic plates, what faults are, how many there are, and how and why earthquakes follow the fault lines and, at times, create new ones.

* What the Richter scale is and how it is different from the Mercalli scale.

* Liquefaction; what it is, what causes it and what it can lead to.

* How earthquakes and volcanoes are related.

* What the differences are between earthquakes, foreshocks and aftershocks.

* Geological time will be examined and discussed, including the fact that seismologists and geologists measure "trends:" and "cycles" in decades, generations and millenniums, not days, weeks, months and years.

* What does it really mean when a scientists talks about "probability."

* How the length of a fault limits the size of an earthquake.

* The differences between tidal waves and tsunamis.

* What scientists can and cannot "predict" -- and why.

OES:

* Hotline

* Preparedness

* How a major earthquake will impact the functions of both print and electronic media during and immediately after a major earthquake; what reporters, photographers, camera crews, etc. need to do personally to adjust their operations; news gathering during seismic activity.

* The impact of "scare stories" and "rumors" on the general public; quoting psychics, reporting pseudo-scientific pronouncements and predictions without checking with the real authorities, etc.

EARTHQUAKE REPORTING: SEISMOLOGY FOR JOURNALISTS

PROGRAM

12:00 noon	Luncheon
1:00 p.m.	Opening remarks by Southern California Edison
1:15 p.m.	Program orientation
1:25 p.m.	Seminar by seismologist(s)
2:15 p.m.	OES remarks
2:30 p.m.	Open Q & A with seismologist(s) and OES
3:00 p.m.	Media facilitated group discussion on how the media covers disasters
3:30 p.m.	Close
3:30 - 5:00 p.m.	Seismologist(s) and OES available for media interviews

A PROPOSAL TO KCET FROM THE SEISMOLOGICAL SOCIETY OF AMERICA (SSA) AND THE SOUTHERN CALIFORNIA EARTHQUAKE CENTER (SCEC) REGARDING PRODUCTION OF A TELEVISION DOCUMENTARY ON THE RECENT LANDERS EARTHQUAKE

I. Background

The recent M=7.5 Landers earthquake was the largest earthquake to strike California in 40 years. This earthquake sequence appears to be one of the most scientifically important seismic events in California's history, with possible implications for future large earthquakes on the San Andreas fault and elsewhere in southern California. The Landers earthquake has yielded a number of surprises which are of great interest to the scientific community, and to the public.

Most of the media coverage of the Landers earthquake has been in the form of 30 to 60 second sound bytes and off-the-top-of-the-head remarks by a variety of scientists. While this approach conveys a certain amount of useful information, the information is often incomplete, disorganized, and confusing. Certain more technical or graphical material requires more explanation than can be easily provided in short sound bytes.

We propose that KCET consider a more extensive presentation of the Landers earthquake and related issues. We feel that Southern Californians would benefit from a deeper exploration of what scientists really know about the recent earthquakes and about the role of seismologists in assessing earthquake hazard.

Although it is not within our expertise to propose to KCET the type of programming format to be used, we would like to suggest that the material be organized under the following three subject areas:

- What actually happened in the Landers and Big Bear areas?
- What do these earthquakes mean for the "seismic climate" of southern California?
- What are scientists doing with their understanding of these events to help public officials prepare for the next big earthquake?

II. What happened?

The Landers earthquake broke and deformed the ground extensively along a 100 km strip in the desert from Yucca Valley northward. Fault scarps and offset roads, fences etc. up to 6 meters can be seen. The rupture in many places is as impressive as that which resulted from the 1906 San Francisco earthquake. Specialized geodetic systems based on global positioning satellites (GPS) are being used by geophysicists to measure the broader-scale deformation in the high desert around the Landers and Big Bear epicenters north of the San Andreas fault.

The number of aftershocks is staggering -- more than 20,000. Their patterns are providing important data on the nature of the very complex rupture which occurred -- a rupture which jumped across six different faults or fault segments. Seismologists have generally believed that massive earthquakes could only be generated on long faults. These results may put to rest the notion that the size of an earthquake can be only as large as the length of the segment of fault on which it nucleates.

The Landers earthquake apparently triggered a number of smaller earthquakes -- many at considerable distance from the epicenter. Distant triggering of earthquakes had not been previously established. The triggering mechanism is not well understood, but a number of interesting hypotheses are emerging.

The Landers earthquake provided a rich new data set on the level of strong ground motions which result from a major earthquake in southern California. The data will permit scientists to develop much improved scenarios as to what we might expect in the event of a

large earthquake on the southern San Andreas fault. The effects in the Los Angeles basin were distinctly different from those in the desert area around Landers.

III. What does all of this mean?

It is important that the Landers and Big Bear earthquakes be put into the context of the historical seismicity and what is known about big earthquakes on the San Andreas fault. Some would suggest that a pattern of earthquake clustering may be emerging in regions to the east of Los Angeles.

Why did the earth rupture in the high desert near Landers rather than, for example, along the San Andreas fault? Is this consistent with what we know about the plate tectonic regime of southern California? What are the implications for the so-called "Eastern Mojave Shear Zone" and major faults in the Owens Valley farther north? Does the suggestion that a "new" San Andreas may be forming have any credibility?

The Landers earthquake seems to have modified the stresses in the vicinity of the southern San Andreas fault, and perhaps along other faults as well. Fault ruptures of this type are surrounded by complex patterns of stress build-up and release. Now, along parts of the San Andreas the "locking" stresses have been reduced and the "driving" stresses increased -- more conducive to future rupture. In other places the reverse has occurred. These results may have important implications for the timing and potential size of the next big earthquake on the southern San Andreas -- an event long forecast by seismologists.

IV. What are we doing about it?

Scientists are trying to assess the rupture information, GPS, and aftershock data, and the calculations pertaining to changes in stress along the San Andreas fault to determine if any patterns are developing which might be suggestive of an impending earthquake on the San Andreas fault. The earth is a very complex system and our data on its behavior are still comparatively limited. Seismologists often must rely on intuitive feelings about the way the earth behaves. It is important that the public understand the speculative nature of earthquake forecasting.

The Southern California Earthquake Center (SCEC) was established to bring together scientists working a seven University research institutions and the U.S. Geological Survey. SCEC is working to develop a probabilistic seismic hazard model ("master model") for forecasting future earthquakes and their associated strong ground motions. This effort is a coordinated activity among more than 40 scientists from the participating research institutions. The goal of the master model is to help emergency preparedness officials, policy makers, and the general public plan for the future.

Emergency officials * need rapid and accurate information on seismic events. New technologies such as the global position satellites, broad-band seismometers (TERRAscope), high speed computers, and mass storage devices are providing better, faster data and are important new tools for earthquake study.

Following the Landers earthquake, a special working group was appointed by the U.S. Geological Survey in consultation with the California Office of Emergency Services to review the implications of the earthquake sequence on future earthquake hazards in southern California. The report of this working group will be issued in mid-October. The findings of the group might form the core of a documentary or in-depth news report.

---

* How mitigation and preparedness officials will use this master model is another interesting story and might be the subject of another focus. We would be happy to refer you to appropriate contacts at the Southern California Earthquake Preparedness Project (SCEPP) which will transfer the model to emergency preparedness officials, policy makers and the general public; and at the California Office of Emergency Services (OES) which is leading an effort to develop a system of advisories, alerts, and warnings.

V. How can SSA and SCEC help KCET?

SSA is a scholarly society devoted to the advancement of earthquake science. Organized in San Francisco after the 1906 earthquake, SSA now has about 2000 members throughout the world, publishes the primary English-language journal of advanced research in seismology, and holds conferences where scientists report on the results of their research.

SCEC, a consortium of seismic research institutions in partnership with the U.S. Geological Survey, was established in 1991 with funding from the National Science Foundation and the U.S. Geological Survey to develop a master model of southern California earthquakes. The coordinating institution for SCEC is the University of Southern California.

As part of their mandates for public education and outreach, SSA and SCEC wish to provide KCET with the necessary expertise to produce a technically sound, interesting, and informative presentation. SCEC scientists will cooperate with KCET personnel as needed, both in the laboratory and in the field. Individual scientists can be made available for interviews, discussions, field excursions, and the like. SSA and SCEC will appoint a seismologist to coordinate and to identify knowledgeable, articulate, and interesting speakers. SCEC scientists will assist KCET in exploring the new technologies both in the laboratory and in the field.

EDUCATION AND OUTREACH ACTIVITIES

I. SCEC/SCEPP MOU and Work Plan

SCEC education and outreach activities began this fiscal year (beginning Feb. 1, 1992) with the drawing up of a memorandum of understanding (MOU) between SCEC and the Southern California Earthquake Preparedness Project (SCEPP; Appendix 1). A SCEC/SCEPP steering committee was established to develop a work plan for the next year (Appendix 2). Initiation of activities per the work plan was (a) first held in abeyance until an Assistant Director search and selection process was completed, and (b) preempted by the April 22 Joshua Tree earthquake and subsequent June 28 Landers and Big Bear events. In effect, personnel time and resources in both SCEC and SCEPP that would have been available for education and outreach activities were instead channeled to post-earthquake scientific studies (SCEC) and emergency response (SCEPP). This included the establishment of an earthquake safety information center and 1-800 hotline to address concerns of the southern California populace. In addition, SCEPP personnel and resources were severely impacted by the Los Angeles riots which also preempted personnel and resources.

At this time both the earthquake and riot-related activities are winding down. However, within the last month, the California Office of Emergency Services (OES) has been restructured under its new director -- Richard Andrews -- and both SCEPP and the San Francisco Bay Area equivalent (BAREPP) have been disbanded and absorbed into the overall OES structure. Information that we have indicates that in the future, OES will be more interested in response and recovery rather than preparedness. As such, it will be necessary to review the MOU with OES and perhaps restructure the work plan. This will be done when the reorganization at OES has been completed.

II. Assistant Director for Education and Outreach

As of May 1, 1992, SCEC advertised nationally for a position of Assistant Director for Education and Outreach (Appendix 3). Approximately 30 candidates were encouraged to apply. A selection committee composed of members from both SCEC and SCEPP invited 6 applicants to Los Angeles for interviews, from which 3 finalists were selected. We are currently negotiating with our top candidate.

III. Joshua Tree and Landers/Big Bear Earthquakes

Many SCEC scientists were called upon to provide information to the public and to the media following the Joshua Tree and Landers/Big Bear earthquakes. This included a town-hall meeting convened by Congressman George Brown in San Bernardino.

However, no central SCEC information clearinghouse was established. Most SCEC scientists headed for the field. In retrospect, a SCEC information center would have been desirable and plans will be developed to do this in the future; planning will be one of the first tasks of our new Assistant Director for Education and Outreach. It is anticipated that SCEC can provide background technical information during the first few hours to days after an earthquake, to be coordinated with Caltech's firsthand reporting of mainshock and aftershock parameters and daily news releases. SCEC can also provide data bases and general earthquake information on a longer time scale from its base at USC.

SCEC Southern California Earthquake Center

Memorandum of Cooperative Agreement between SCEC and NCEER on Earthquake Hazard Mitigation

The National Center for Earthquake Engineering Research (NCEER) and the Southern California Earthquake Center (SCEC) promote and support the study of technical issues related to earthquake hazard mitigation. Their principal aim is to reduce loss of life and property and to minimize economic disruption due to earthquakes. Emphasis is also placed on the development and successful transfer of knowledge to potentional users.

At this time, the primary interests of NCEER's research and implementation program are: (1) Existing and New Structures, (2) Secondary and Protective Systems, (3) Lifelines and Bridges, (4) Disaster Research and Planning, and (5) Education and Technology Transfer. SCEC's primary interest is in the prediction of strong ground motion for Southern California.

Since NCEER and SCEC share elements of current and anticipated research activities, they shall make every effort to jointly develop a effective mechanism to achieve the overall objectives of earthquake hazard mitigation.

This cooperative agreement includes, but is not limited to , the collaborative development of research efforts, sharing of preliminary and final results and mutual consideration of technology transfer and knowledge utilization mechanisms. Primary areas of interest for this cooperative endeavor will focus on:

(a) Ground motion and seismic hazard study
(b) Geotechnical research
(c) Integrated seismic hazard data development

A joint meeting will be held at least twice yearly to share progress on the cooperative effort in those areas of primary interest, and determine future direction of joint efforts, which may include common areas of interest not initially considered.

Signed:

Keiiti Aki 29/6/92
Date

Keiiti Aki
Southern California Earthquake Center

Date

Masanobu Shinozuka
National Center for Earthquake Engineering Research

Group A: Master Model Construction and Seismic Hazard Analysis

Group Leader: Keiiti Aki

GROUP A SUMMARY REPORT: MASTER MODEL CONSTRUCTION AND SEISMIC HAZARD ANALYSIS

by

Keiiti Aki

The goal of SCEC is to integrate all relevant earth science information about earthquakes in southern California into the estimation of time- and space-dependent probabilistic seismic hazard. Group A is responsible for developing the methodology for the integration and producing the seismic hazard estimate. In the past year, we made considerable progress in both methodology development and prototype products. The Landers earthquake helped us to focus our areas of research and to accelerate the work toward our goal.

The Landers earthquake taught us the importance of including the interaction between fault segments. Three projects in Group A are concerned with the consequences of interacting fault segments on seismic hazard estimation. A. Cornell and S. Winterstein completed methodology development for computing the exceedance probability of ground motion at a site near a set of mechanically interacting fault segments. S. Ward, in cooperation with a SCEC visitor, S. Barrientos, calculated synthetic seismicity for the San Andreas fault, and estimated the mean recurrence time and coefficient of aperiodicity (fitting the Weibull distribution) for earthquakes with various magnitudes at each segment. J. Rice, on the other hand, addressed the physical conditions of fault zone for the characteristic earthquake type behavior using the rate- and state-dependent friction law. All these are trying to directly respond to our need for an acceptable recurrence model which allows interaction among fault segments.

An important element of seismic hazard estimation is the effect of local geologic conditions on ground shaking. A preliminary GIS-based map of the amplification factor (linear regime) for the frequency range from 1.5 to 12 Hz was constructed by B. H. Chin and K. Aki, with the help of S. Park. The map combines the empirically determined amplification factors for coda waves measured at stations of the Caltech-USGS regional network with the surface geology of southern California. This map was used to simulate strong ground motion for the Landers earthquake by M. Mahdyiar as mentioned below.

M. Dravinski, G. Ding and T. Zhou, on the other hand, carried out an extensive survey of the site effect for longer periods ($0.5 < T < 10$ sec) using microtremors in cooperation with H. Kagami, S. Okada, S. Sasaki and K. Morohashi from Hokkaido University. They have completed measurements at 147 sites in the Los Angeles Basin.

A major task of Group A is the prediction of strong ground motion based on the existing information about the earthquake source characterization, seismic wave propagation effects and site geologic conditions. Three approaches are taken currently. D. Agnew uses the method of Evernden et al. (1981) for calculating seismic intensity. The advantage of this approach is that the method has been validated by observed intensity for many earthquakes, and used in the past by the State of California as the basis for emergency preparedness planning. Digitized geology used by Agnew for calculating seismic intensity is also being used by S. Wesnousky, who combines his own 1986 programs with the site response estimated by Sykes and Petersen using 1971 San Fernando

earthquake data. M. Mahdyiar, on the other hand, uses the so-called "w-squared" model (Hanks-McGuire, 1981; Boore, 1983) to represent the subevent of the specific barrier model of Papageorgiou and Aki (1983), and incorporates the empirically determined frequency-dependent site amplification factor mentioned above. Mahdyiar introduces a procedure for including the non-linear amplification effect at soil sites.

The above three methods are currently being tested against the strong motion data from the Landers and Big Bear earthquakes.

In addition to his study on the Landers earthquake, S. Wesnousky continues his groundwork for the master model, and completed the update and synthesis of slip rate and paleoearthquake data for all known and remaining southern California faults and seismogenic structures. The compiled data are in a format readily input into any GIS data base.

The validity and reliability of the intermediate-term precursors are important for the time-dependent seismic hazard estimation. Along this line, B. Minster and N. Williams tested the M8 algorithm with a focus on the 1989 Loma Prieta and 1992 Landers earthquakes. S. Katz also continued to test his monthly prediction using Adaptive Neural Network.

PROJECT REPORT: **Short-term Prediction and Intensity Models**

PROJECT PERIOD: February 1, 1992 — January 31, 1993

SUBMISSION DATE: September 24, 1992

PRINCIPAL INVESTIGATOR: Duncan Carr Agnew, Professor, Geophysics - (619) 534-2590
Institute of Geophysics and Planetary Physics
Scripps Institution of Oceanography, MC 0225
University of California, San Diego
La Jolla CA 92093-0225

As with many of the projects covered by SCEC, the work planned on this was somewhat diverted by the occurrence of the Landers earthquake Most of the effort budgeted for has been devoted to the preparation of a working paper on the earthquake for submission to a NEPEC ad-hoc committee to report on the effects of this earthquake on earthquake probabilities in southern California, and on participation in that committee. This work included the prediction of ground motion (intensity of shaking) for the Landers event (see attached figure); a comparison of the predicted and observed intensities, shown in Table 1, indicates that the Evernden algorithm gives reasonably satisfactory results, except for underpredicting the intensity in the Los Angeles area. This may arise from the frequency content: the algorithm was designed to fit historical intensity data, which are dominated by the effects of short-period motions, while (for the downtown Los Angeles area), longer-period motions can cause significantly higher intensities in tall buildings.

Observed and Predicted Landers Intensities

Place	Observed	Predicted
Barstow	VI-VII	VI½
Cherry Valley	VI	VI
Forest Falls	VII	VI½
Joshua Tree	VII-VIII	VIII
Los Angeles	VI	IV½
Morongo Valley	VII	VII½
Palm Springs	VI+	VI½
Pasadena	V-VI	IV½
Redlands	VII	VI
Yucca Valley	VIII	VIII

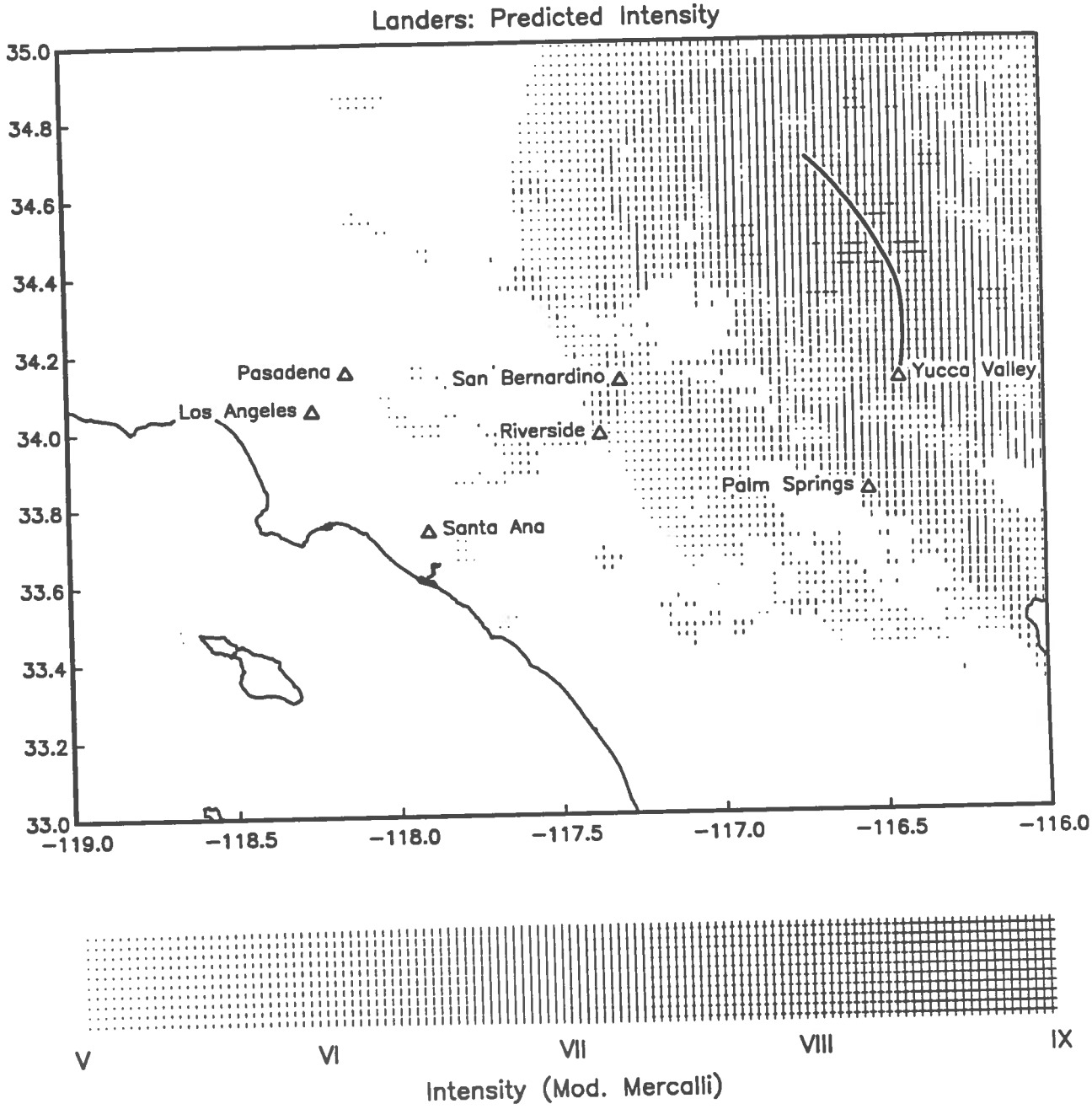
Landers: Predicted Intensity
35.0
34.8
34.6
34.4
34.2
34.0
33.8
33.6
33.4
33.2
33.0
−119.0
−118.5
−118.0
−117.5
−117.0
−116.5
−116.0
Pasadena
San Bernardino
Yucca Valley
Los Angeles
Riverside
Palm Springs
Santa Ana
V
VI
VII
VIII
IX
Intensity (Mod. Mercalli)

The Site Amplification Factor for Weak and Strong Motion in the Los Angeles Basin (Group A report) and The Site Amplification Factor for Weak and Strong Motion in the Imperial Valley Area (Group B report)

by Byau-Heng Chin and Keiiti Aki
Department of Geological Sciences
University of Southern California

A preliminary GIS-based map of weak-motion amplification factor in Southern California is constructed by incorporating the digitized surface geology data provided by Dr. Steve Park of U.C. Riverside. Figure 1 shows the range of inferred amplification factors relative to the homogeneous half-space in natural logarithm $\ln(A/A_g)$ at frequency 1.5 Hz. The smaller or more negative this number (marked as a lighter symbol), the less the amplification. It is found that the amplification factors for the region of Imperial Valley and Central Los Angeles basin are greater than most of Southern California. The value of amplification factor in these two areas decreases with increasing frequency, the range is about 2 to 4 in natural logarithm for 1.5 and 3.0 Hz, about 2 to 3 for 6.0 Hz and about 1 to 2 for 12 Hz. Both the Imperial Valley and Central Los Angeles basin contain great thickness of young, poorly consolidated sedimentary materials.

Recently, the Landers earthquake drew our attention and a detailed strong motion study is in progress. Using the systematic relation of barrier interval and magnitude for the past major California earthquakes (Chin and Aki, 1991), we characterized the fault plane by four subevents separated by 15 km. For each subevent, we use the ω-square model with equal seismic moment 3.5×10^{26} dyne-cm and the stress drop of 100 bars. For the propagation path effect, we used the geometrical spreading 1/R and the attenuation factor $Q(f) = 100f^{0.9}$. The site effect is taken into account from the site amplification factors at various frequencies described above. We, then synthesized the time history of ground acceleration at each strong motion station (OSMS 92-09 reported from CDMG, 1992) by applying Boore's (1983) method.

In order to compare the observed peak acceleration with the predicted, we obtained an average of peak accelerations over 20 realizations of white noise samples. We divided recording sites into two categories, soil and rock. Sites described by such terms as"alluvium," "fill," or "sediment deposit" were assigned to the

soil category, and sites described by such terms as "granite," "limestone," "sandstone," or "Franciscon formation" were assigned to the rock category. There are total 102 sites belong to soil category, and 33 sites are in rock category. The averaged predicted peak acceleration and observed values at each station against hypocentral distances are shown in Figure 2a and 2b for soil and rock site, respectively. The predicted values are designated by solid large symbols and the observed values are marked by small open circles for both rock and soil sites. The shaded area indicates a 84% confidence interval for the predicted peak ground acceleration values and the solid curve represents the least-square fit through the attenuation relation of $\ln \mathrm{PGA} = A_0 - \ln \Delta + A_1 \Delta$, where Δ is the hypocentral distance in km. The results show a fair agreement between the observed and the predicted PGA at all soil and rock site stations within distances 50 km and 150 km from the hypocenter. At distances less than 50 km, the predicted peak acceleration overestimates the observed for soil sites, while the predicted peak acceleration systematically underestimates the observed for the rock sites at distances greater than 150 km. We will examine these disagreements more thoroughly as soon as the digital data become available.

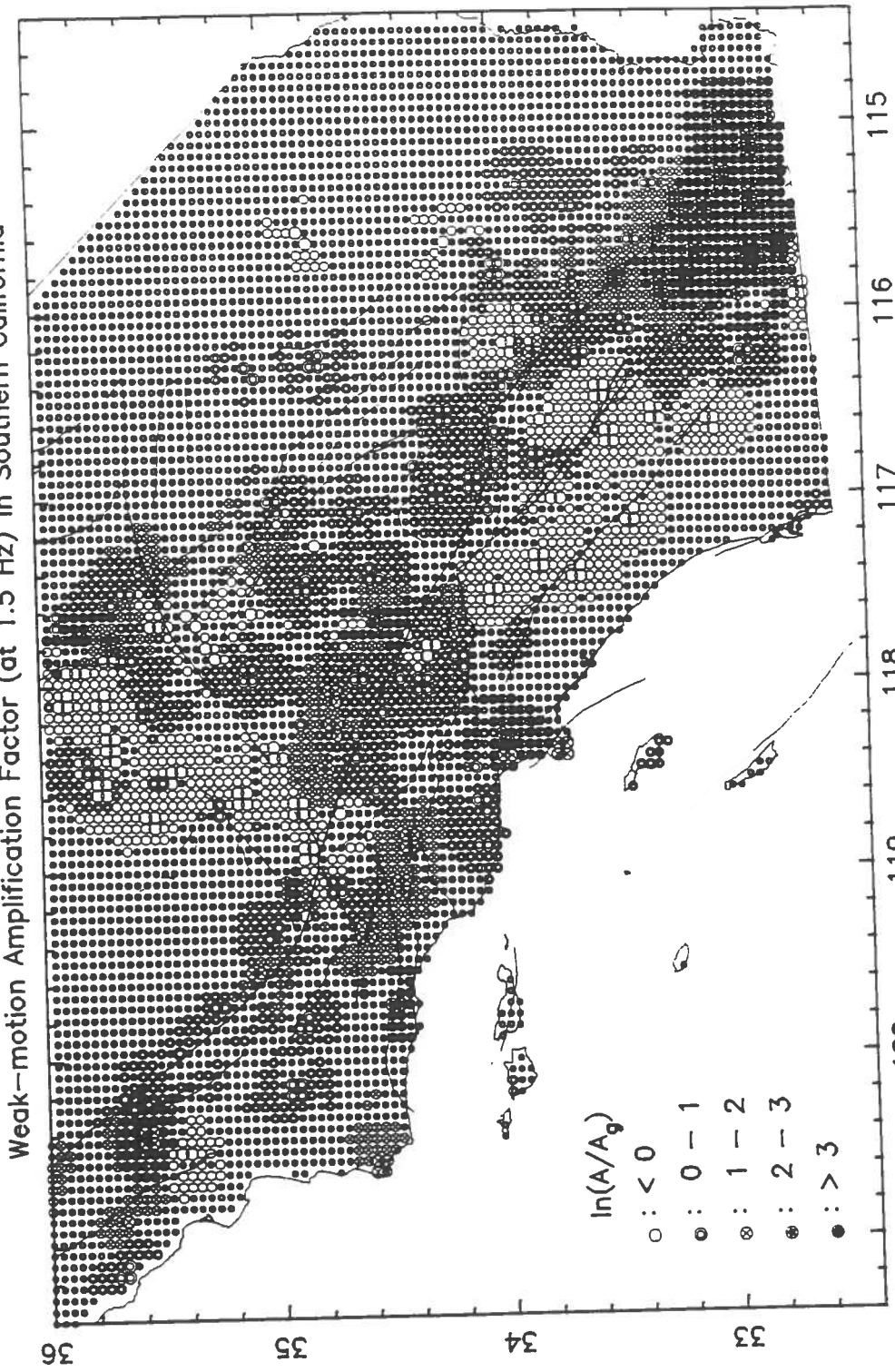

Figure 1 The GIS-based map of weak-motion amplification at frequency 1.5 Hz in Southern California.

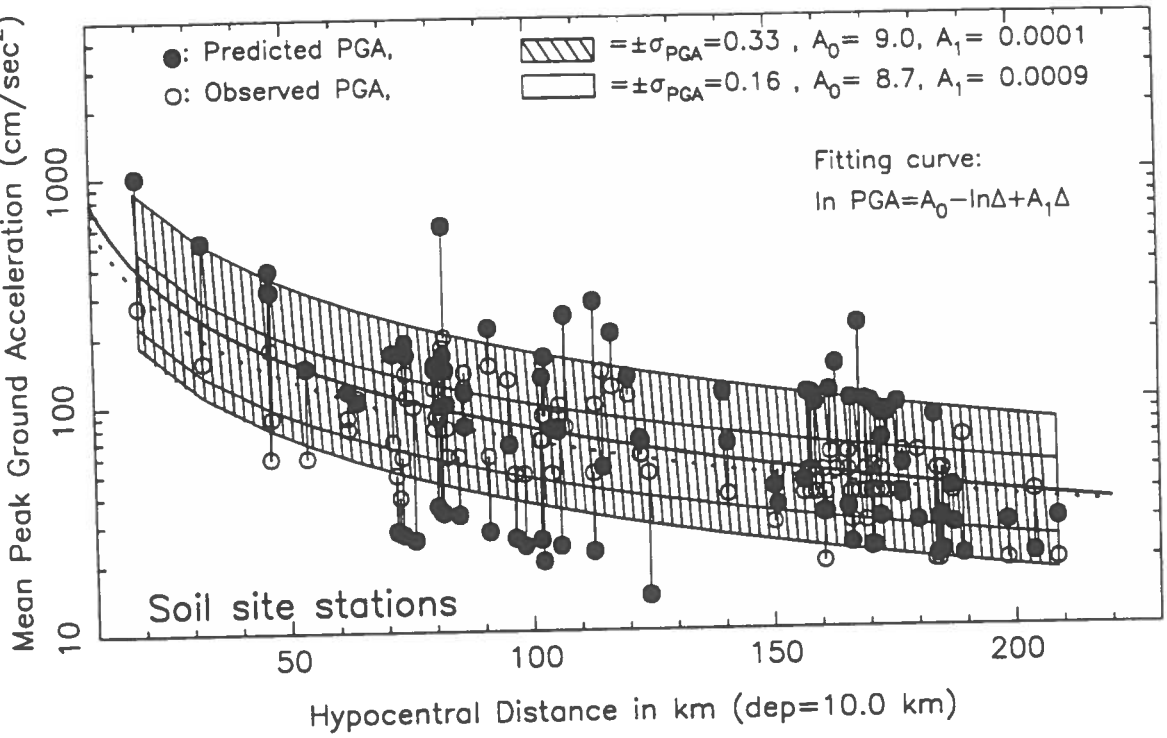

Figure 2a

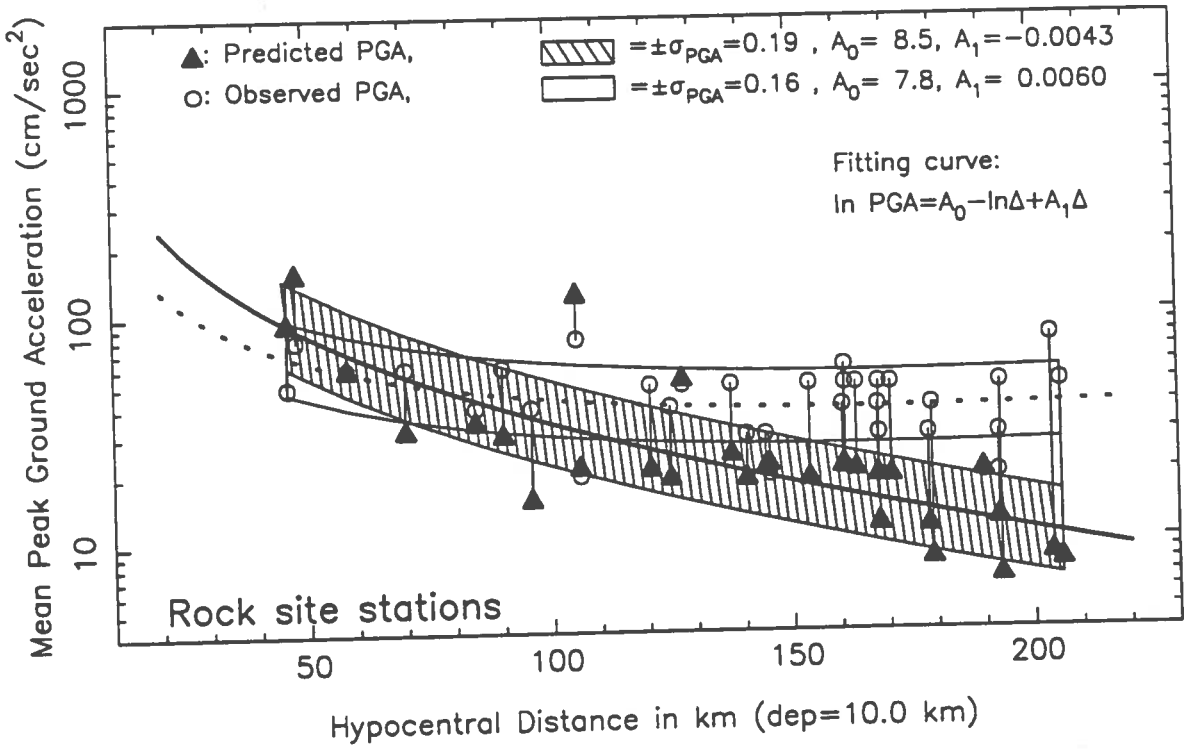

Figure 2b

SCEC
Annual Progress Report
September 15, 1992

Professor C. Allin Cornell
Dr. Steven R. Winterstein
Department of Civil Engineering
Stanford University

Subject: Seismic Hazard Due to Non-Poissonian Interacting Fault Segments

During this year we have completed the primary methodology development for computing seismic hazard (i.e., the annual or n-year probability of exceeding a specified level of ground motion) at a site near a set of mechanically interacting fault segments. The interaction affects the probability distribution of the time between major (characteristic) magnitudes. These events are presumed to follow a renewal process (i.e., to be non-Poissonian). They may "pseudo-cyclic" (coefficient of variation, COV, less than unity) or clustered (COV greater than unity). Other, smaller events are assumed to be Poissonian and exponentially distributed.

This model is of increased recent interest because of the Landers-Big Bear pair of events and their potential effect on stresses on the San Andreas fault segments. Simpson, Harris, Stein, and King have been reporting to SCEC and the NEPEC Working Group their estimates of such effects.

Prior to these earthquakes, we presented to an April, 1992 SCEC meeting our estimates of hazard at a site near San Bernardino based on the elapsed times and on the past and potential interactions among San Andreas and San Jacinto segments, using Working Group 1988 information. The effects were not great. In a similar example for the Bay Area the effects were significant for a site near the Mid-Peninsula segment of the San Andreas.

We have also completed statistical estimation software and example calculations for a variety of California fault segments. The algorithms estimate mean and coefficient of variation of interarrival times of characteristic magnitudes using (1) prior information, such as the typical range of COVs on other fault segments, (2) estimates (and standard errors of estimates) of mean slip rate and mean slip per event, (3) dates and magnitudes of historic events on the segment, (4) estimates of paleoseismic events and their dates, and (5) the elapsed time since the last event.

We have distributed Dr. S. C. Wu's recently completed Ph.D. thesis, including much of this information, as well as two

manuscripts submitted to BSSA this year to interested SCEC investigators. A third and fourth paper are in preparation.

Finally, Professor Cornell has been participating on the new NEPEC Ad Hoc Working Group on Southern California Earthquake Probabilities.

[wplet2\scec.rep]

Site Amplification in Los Angeles Basin Through Measurements of Microseisms

Progress Report for Research on a SCEC Grant
Period February 1992 - September 1992

Marijan Dravinski
Microtremor Laboratory
University of Southern California
Los Angeles, California 90089-1453

Working Group: A
Group Leader: Keiiti Aki

Working Group: B
Group Leader: Ralph Archuleta

September 14, 1992

1 Introduction

This progress report covers research activities supported by the grant for period February 1992 through September 1992. Several large scale microtremor observations were made during that period: (i) Simultaneous long term measurements were made at two sites (USC and La Canada), (ii) Trial measurements along one section of Los Angeles basin, (iii) Large scale measurements in Los Angeles basin, (iv) Measurements at SCEC/UCSB Dense Strong Motion Aftershock Array sites in Pipes Canyon, California, (v) Earthquake simultaneous measurements at two sites (USC and La Canada), and Microtremor measurements in San Fernando Valley. The following personnel was involved in these measurements: M. Dravinski, G. Ding, and T. Zhou of Microtremor Laboratory at USC and H. Kagami, S. Okada, S. Sakai, and K. Morohashi of Hokkaido University.

2 Long Term Measurements: April 13 - April 20, 1992

These measurements were performed in order to study the change with time in fundamental properties of microseisms. Two sites were chosen: USC (sediment) and La Canada (rock) were measurements were performed every two hours for one week. Duration of measurement for each record was 300 sec and the sampling rate was 10 Hz. Eighty four records (EW and NS) were obtained at each site for total of 168 records. So far the following calculations were performed for this data set: (i) Velocity amplitude spectra for each record and (ii) Velocity spectral ratios of the records at sediment vs rock site (for total of 168 ratios) as a function of period. In addition, mean spectral ratios for each component and for each day of measurements were obtained.

These results will provide with variation of predominant period and spectral ratio between the two sites with time. In addition, we plan to compare the records at USC with corresponding strong ground motion records from various earthquakes.

3 Trial Measurements in LA Basin: June 26, 1992

Trial measurements were performed in order to asses the performance of new portable digitizers in the field. The measurements were done at four sediment sites (B3, B4, B5, and B6 of Fig. 1) with simultaneous recordings at a bedrock reference site in La Canada. At the reference site the measurements were done every hour for 300 sec starting at 09h00m and ending at 16h00m with 10Hz sampling rate. The measurements at the sediment sites were done at every full hour in order to coincide with the time of reference measurements. Through these measurements we were able to determine the duration of the power supply which the existing batteries can provide. We found out that in order to perform large scale measurements additional power supplies were needed.

Velocity spectral amplitudes and spectral ratios (sediment vs. bedrock) were calculated from these records.

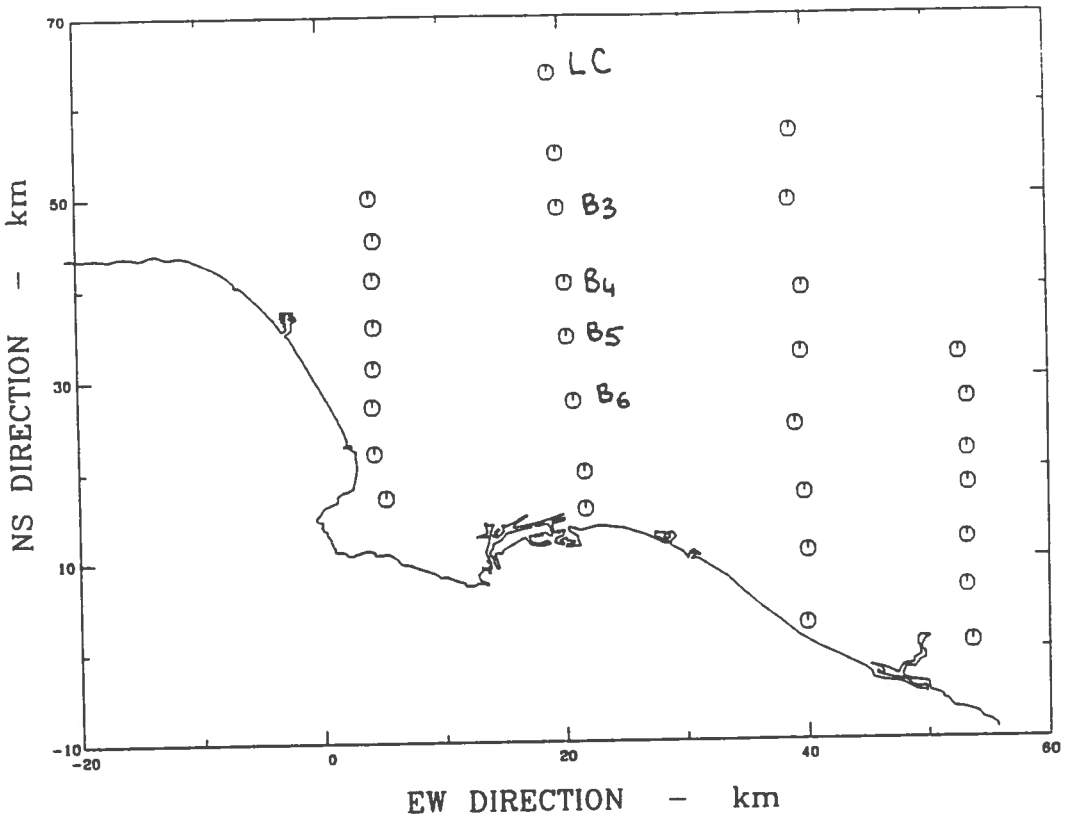

Figure 1: Location of sites for trial measurements on June 26, 1992 in the Los Angeles basin. Reference site: La Canada (LC). Sediment sites: B3, B4, B5, and B6.

4 Measurements in LA Basin: August 4 - August 10, 1992

These large scale measurements were performed at 147 sites (plus a reference site). The site locations are given by Fig. 2. Reference measurements at a bedrock site (La Canada) were performed every hour for 300 sec with sampling rate of 10 Hz. Observations at various sites of the basin were done concurrently with the reference measurements with same sampling rate and duration. Total of 76 records were obtained at the reference site and 147 records at the sediment sites.

So far velocity spectral amplitude for all the records were calculated. In addition spectral ratios for each sediment site relative to the bedrock reference site were calculated for a range of periods ($0.5\ sec < T < 10\ sec$). From these results we shall be able to determine distribution of predominant period throughout the basin and the weak ground motion amplification as well. These will be compared with strong ground motion amplification from recent earthquakes (e.g., Sierra Madre earthquake of 1991).

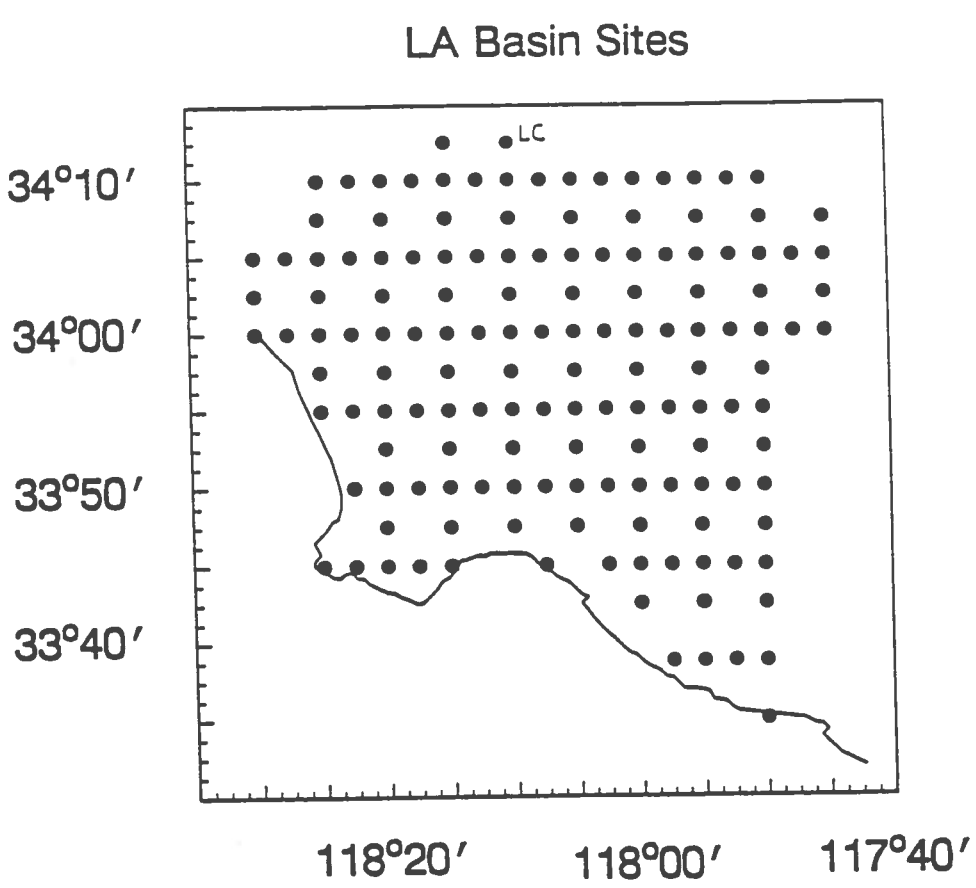

Figure 2: Sites for large scale microtremor measurements in the Los Angeles basin August 4 - 10, 1992. Reference site : La Canada (LC). Total of 147 observation points.

5 Measurements in Pipes Canyon, California: August 11, 1992

These measurements were performed at the sites were SCEC/UCSB Dense Strong Motion Aftershock Array was installed after the Landers earthquake of June 28, 1992. This array recorded several aftershocks following the main event. The array consisted of five rock sites (R0, R1, R2, R3, and R4) and five sediment sites (S0, S1, S2, S3, and S4). We observed simultaneously microseisms at one bedrock site (R4) and all sediment sites. Measurements at the reference site were done for 300 sec every ten minutes (11:00; 11:15; 11:30; 11:45; 12:00; 12:15; 12:30) while the measurements at the sediment site were done every 20 minutes (11:00; 11:30; 12:00; 12:30; 13:00). Sampling rate for all the measurements was 10 Hz.

Microtremor results are to be compared with strong ground motion results for different aftershocks.

6 Earthquake Measurements: August 12 - 19, 1992

During these measurements earthquake monitoring was performed at USC and La Canada sites. The instruments were set in such a way so that an earthquake triggers recorder after a certain threshold motion has been reached. Two small earthquakes were observed at both sites during that period. The events took place on August 14, 1992 at 01h24m PDT and

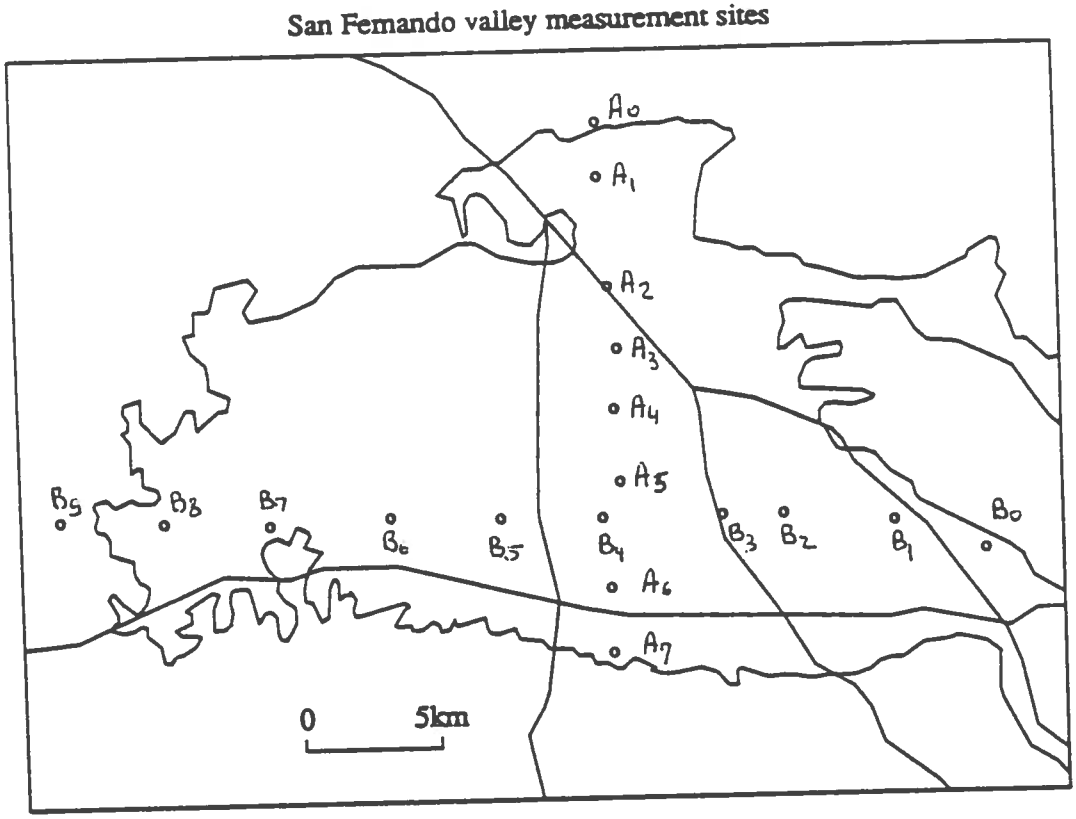

Figure 3: San Fernando Valley observation sites for microtremor measurements of August 13 and 14, 1992. The reference bedrock site is at La Canada (LC).

on August 17, 1992 at 13h42m PDT.

Velocity spectra for these two events have been calculated at both sites. We plan to use the earthquake data at USC and La Canada sites for comparison purposes with microtremor records.

7 San Fernando Valley Measurements: August 13 and 14, 1992

During these measurements microseisms were recorded along two sections (NS and EW) of San Fernando Valley as shown by Fig. 3. The reference bedrock site measurements were performed every 30 minutes for five minutes with sampling rate of 10 Hz. Along the NS section the records were obtained at eight sites (A0 through A7) at times which coincide with the refernce measurements at the bedrock site. Along the EW section microtremors were recorded at ten sites (B0 - B9). These records will be used in resonance study of San Fernando valley which is presently being done.

SCEC Progress Report for 1992

Artificial Earthquake Precursors Generated by Adaptive Neural Network (ANN)

Simeon Katz
University of Southern California

A novel approach to earthquake prediction has been developed and tested on Southern California seismicity catalog data. It is based on the use of three key elements:

(a) It predicts values of the 'Danger Function', which is defined as a maximum magnitude of the earthquakes within a given area calculated in a moving time window. Since the Danger Function is a one dimensional function of time defined on a set of time moments with a fixed time sampling, this essentially simplifies the problem of earthquake prediction.

(b) The prediction methodology is based on the use of a specialized Adaptive Neural Net (ANN) that continuously changes its structure in time. The ANN is constructed in such a way that it is capable of producing stable results even in the case of small training sets. The ability of the ANN to change in time and to work with small training sets allows one to adapt ANN to changing, in time, seismo-tectonic conditions.

(c) The input to the ANN is a multidimensional time series with their time dependent coordinates taken in the form of seismicity attributes, calculated in a moving time window. This makes this earthquake prediction methodology open to inclusion of a number of additional precursory parameters without significant changes in the technique of synthesis of the neural net. ANN methodology based on prediction of the values of the Danger Function allows one to generate alarm signal prior to an incoming earthquake.

We use up to 16 other basis attributes derived from the earthquake catalog. Among these are the following a) the stability of the spatial earthquake distribution calculated in a moving time window, b) the number of earthquakes with a magnitude larger then a given threshold, c) the average and maximum magnitude of earthquakes in a moving time window, d) the differences in percentage of earthquakes or in the number of earthquakes for several magnitude ranges calculated in a moving time window, e) the parametric representation of the depth distribution of the earthquakes in a moving time window, f) fractal parameters relating to the time-space distribution of earthquakes, and g) clustering parameters of spatial distribution of the earthquakes defined as time functions. An additional set of basis attributes was formed as a set of first derivatives of the above attributes. The basis attributes were used to produce a number of complex attributes defined as functions of one or several basis attributes.

The results presented are a continuation of the work that began in 1991. Its aim was development and experimentation with neural net methodology for intermediate-term earthquake prediction in real and reverse time. ANN was trained to predict values of the Danger Function of the form

$$D(t) = \begin{cases} G(t) \; ; \; G(t) > Tr \\ 0 \quad ; \; G(t) \leq Tr \end{cases} \qquad (1)$$

Here $G(t)$ is the maximum magnitude of all the earthquakes recorded within the time-window $(t, t - t_0)$ in the respective area; Tr is a given threshold. Then the ideal precursor is defined to take positive values several months prior to the earthquakes with magnitude larger than the threshold Tr; it is zero otherwise.

Figure 1 shows the Danger Function and the strong alarm signal generated by the neural net in real time 1 month before the June 28 Landers earthquake. In this picture June 1992 is the month with index 138. The alarm signal was generated by the NN in May 1992.

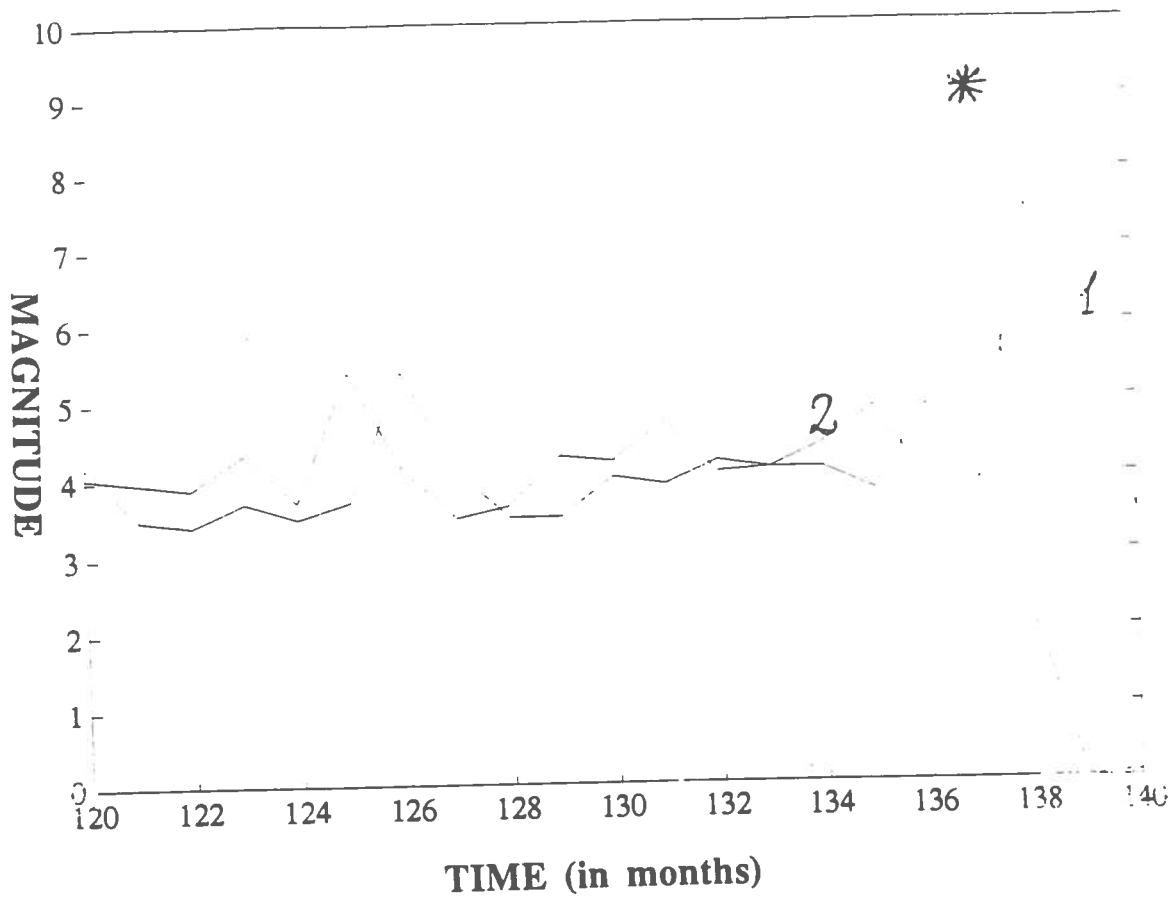

FIGURE 1. ALARM SIGNAL GENERATED 1 MONTH PRIOR TO THE JUNE 28-TH EARTHQUAKE.

1. DANGER FUNCTION
2. OUTPUT OF THE NEURAL NET DURING TRAINING SESSION.
3. * ALARM SIGNAL

Prepare Inner Borderland Fault Maps at a Scale of 1:100,000 for Publication as Geological Society of America Map and Chart Series

Mark R. Legg
ACTA Inc.
23430 Hawthorne Blvd., Suite 300
Torrance, CA 90505

Large-scale maps of late Cenozoic faulting and related geologic structure in the inner California Continental Borderland are being prepared for publication in the GSA Map and Chart Series. These maps include recontoured bathymetry of the offshore region (Fig. 1) from 31° 10' N to 32° 50' N latitude, and faulting associated with four major inner borderland fault zones: 1) San Clemente-San Isidro fault zone; 2) San Diego Trough-Bahía Soledad fault zone; 3) Coronado Bank-Agua Blanca fault zone; 4) Rose Canyon-Descanso-Estero fault zone. In addition, relevant geologic cross-sections and a map of the seafloor geomorphology, representative of late Cenozoic depositional processes and fault geomorphology, is being prepared. A document describing the fault maps, discussing the relevant regional geology and tectonic background, and showing representative high-resolution seismic reflection profiles and interpretations is being written for publication with the map sheets.

To date, two representative cross-sections (Fig. 2) of the regional geologic structure, from seafloor to the upper mantle, have been prepared based upon recently acquired multichannel seismic reflection profiles (USGS cruise L4-90SC) and published interpretations of other geophysical profiles (gravity and geomagnetic) in the region. These profiles show significant differences in the crustal structure between the northern and southern parts of the region. To the south, a partially buried horst and graben basement structure overlies a relatively shallow Moho (about 18 km depth). To the north, more complex, tilted fault block, horst and half-graben structural style is dominant. The block faulted structural style of the inner borderland is remnant from major extensional (transtensional) tectonism during middle to late Miocene time.

The high-resolution seismic reflection profiles show classic examples of well-developed, right-lateral wrench faults that cut the post-Miocene turbidite fill of the inner borderland basins. Some of these major high-angle faults are probably reactivated along older structure associated with the Miocene reorganization of the Pacific-North America tectonic plate boundary; some appear to lie along older structural trends associated with the Mesozoic-Paleogene subduction along the California coast. All show abundant evidence of late Quaternary activity including seafloor scarps and disrupted reflectors in the shallow subbottom sediments of submarine fans, on the basin floor, and the nearshore shelf. Numerous earthquake epicenters crudely aligned along the fault trends attest to the current activity of these fault zones.

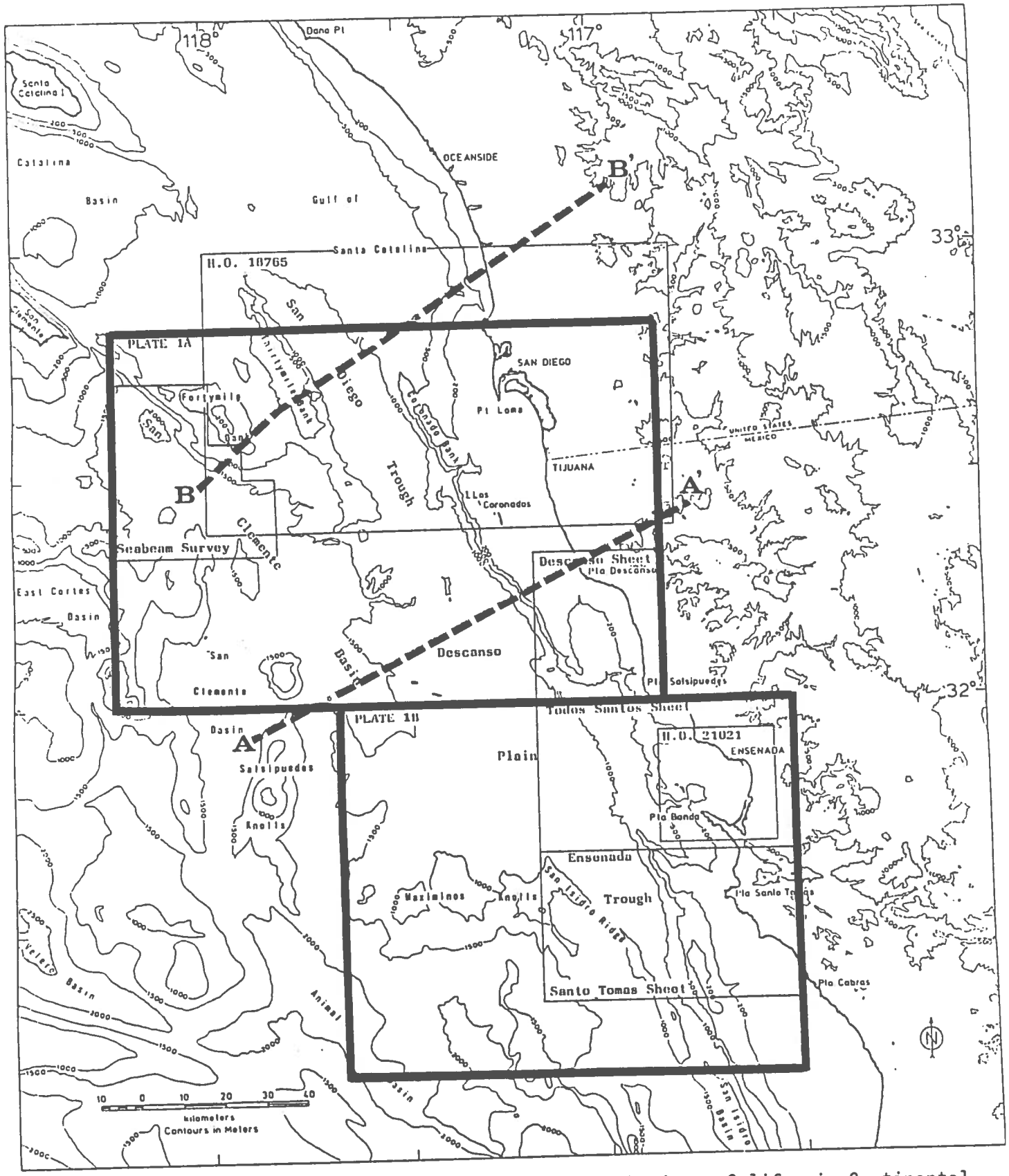

Figure 1. Location of 1:100,000 scale fault maps of the inner California Continental Borderland west of San Diego and northern Baja California, Mexico.

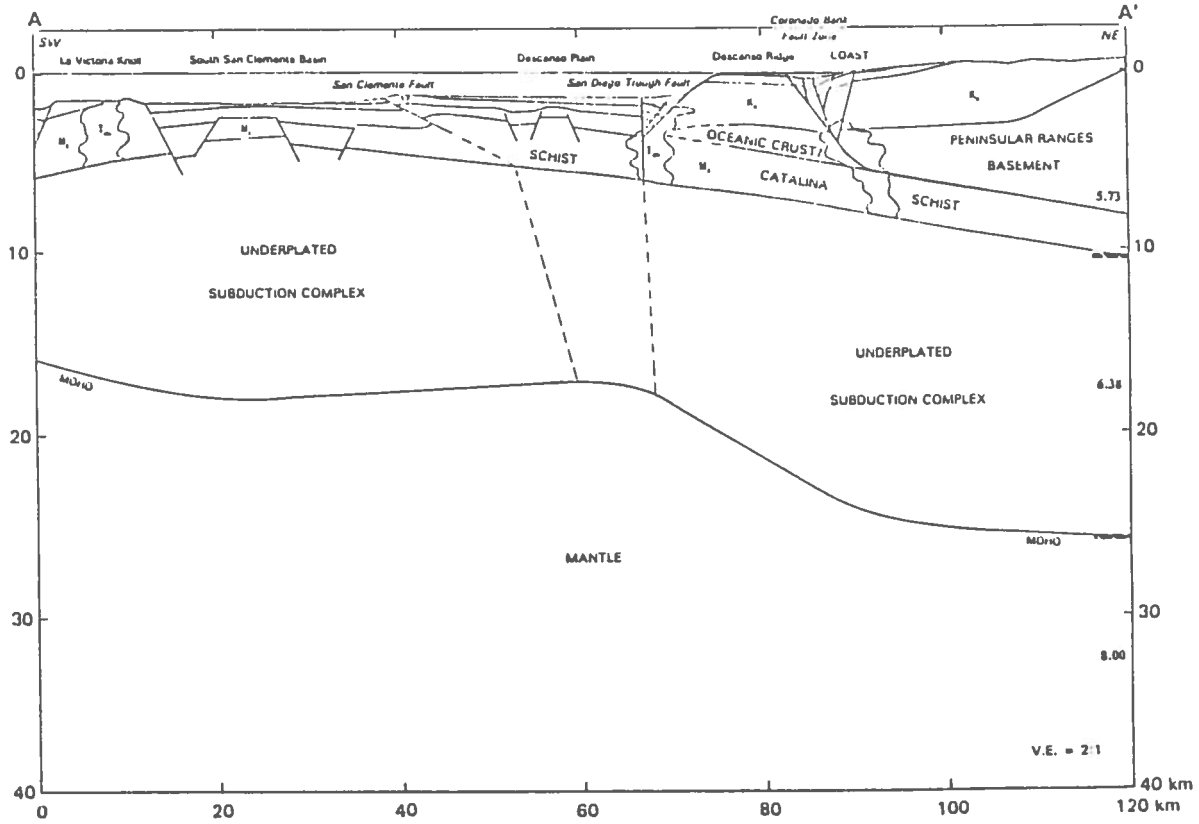

Figure 2. Representative cross-sections of the crustal structure in the Inner California Continental Borderland along the California--Mexico border region. (See Fig. 1 for location of profiles).

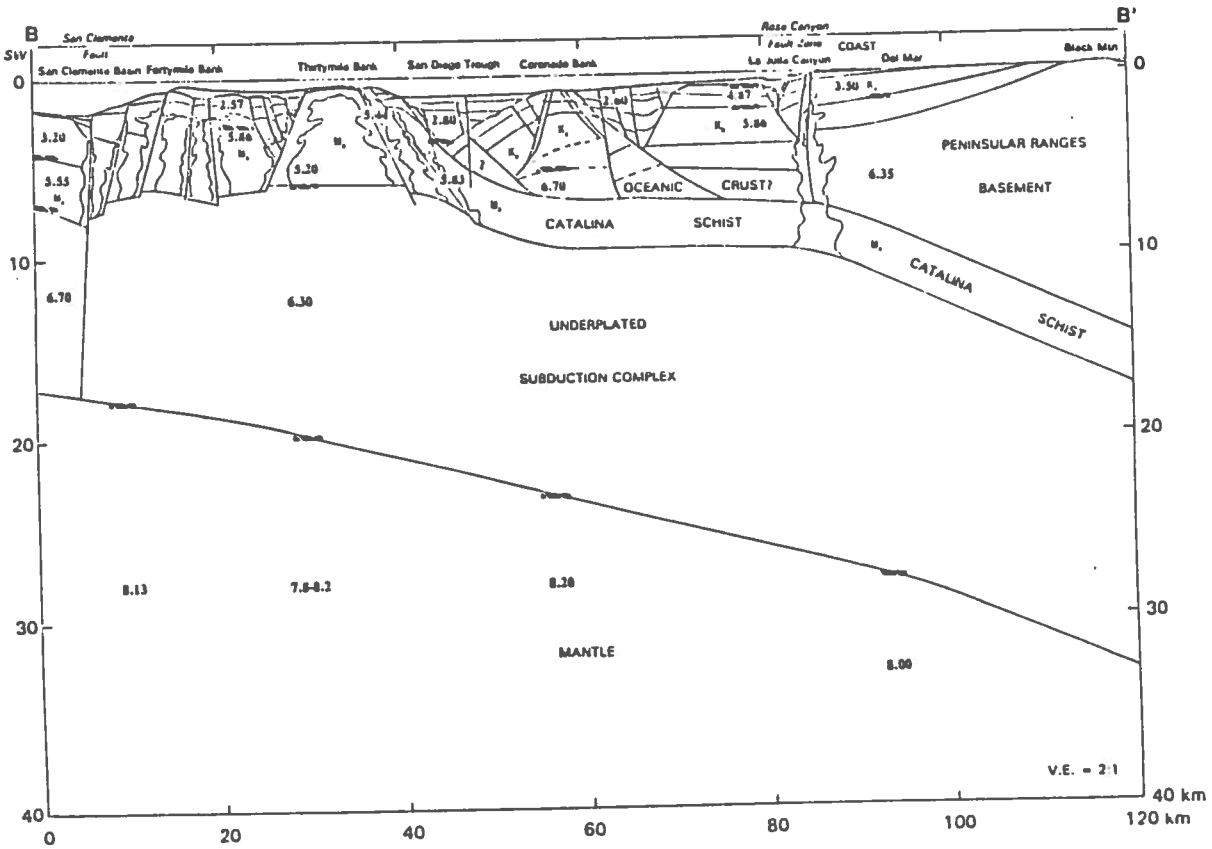

Progress Report
Strong Motion Simulation for the Landers Earthquake and a Magnitude 7.8 Earthquake on the San Andreas Fault

Mehrdad Mahdyiar
Leighton and Associates

Many structural facilities in California are built near major active or potentially active faults. Engineering seismologists, on a routine basis, provide site-specific peak ground motions and response spectra for design or retrofit of these structural facilities. The analysis are mostly based on empirical attenuation equations, which because of the scarcity of the near field data, are not well suited for predicting near field seismic parameters. The strong motion recordings of recent earthquakes in California indicate a rather strong discrepancy between the observed and the predicted peak ground motions even at far distances.

One of the practical technique of simulating ground motions of an earthquake is the empirical Green's function method (EGFM). According to the EGFM, the ground motions of a target earthquake is simulated using the recorded ground motions of smaller events which share the common propagation path as the target earthquake. However, for most site locations and fault systems of interest no strong motion recording is available. To overcome this difficulty, one could take the advantage of the coherent deterministic properties of the long period spectral components of the subevents and treat the high frequency components as the results of a stochastic process. I used the strong motion recordings of the M7.4 Landers (June, 1992) earthquake to examine the predictive capabilities of such a technique.

The rupture area of the Landers earthquake was modeled by four subevents based on the assumption of the Barrier model for the rupture mechanisms and the geometry of the rupture area. The Fourier amplitude spectrum of the target earthquake was obtained using a ω^2 model for the source spectrum of each subevent. The random vibration technique was used to determine the peak ground acceleration and response spectra. Different site conditions were characterized based on the coda waves amplification factors, obtained for southern California. Coda waves amplification factors represent the weak motion amplification. Results of different studies suggest that the peak ground acceleration at soil sites, due to the nonlinear dynamic behavior of the soil materials, will saturate to a level of about 0.4 to 0.5 g. Unfortunately, the information on the velocity-depth structure of the majority of sites in California is not readily available. However, since the parameters of interest are the peak motions including the response spectra, the nonlinear response of the alluvium sites could be approximated by a constant Q model. This is compatible with the equivalent linear representation of the hysteresis model of the material damping properties. The Fourier amplitude spectrum is modified in such a way that the estimated PGA for an alluvium site satisfies a representative nonlinear relationship between the bedrock-alluvium PGA for a typical site in California. It is understood that such a relationship is not universal. For the purpose of this study, it was assumed that the peak ground acceleration of the alluvium sites will saturate to 0.4 g. Figure 1 shows the curve which was used to describe the relationship between PGA on an alluvium site versus the PGA of the underlying bedrock.

The duration of the strong ground motion for each site was calculated as the time between 5% and 95% of the cumulative square of the acceleration amplitudes, which was stochastically simulated for each site.

The results indicate a very good agreement between the recorded and the predicted peak ground accelerations. This method of analysis is a practical way of obtaining seismic parameters for engineering design purposes and earthquake hazard evaluation. Having obtained good results for the Landers earthquake, the method was used to predict peak ground accelerations, duration of shaking, response spectra, and seismic intensity at different locations in southern California for a magnitude 7.8 earthquake on the Coachella and San Bernardino segments of the San Andreas fault.

Figure 2 shows the predicted PGA for the Landers earthquake. The numbers shown on the figure are the peak ground acceleration, in % g, at a number of CDMG and USGS stations. The lower left corner of each number represents the station location. Figure 3 shows the predicted PGA based on the Joyner and Boore (1981) attenuation equation. The Joyner and Boore's (JB) equation over-estimates the PGA of the few stations close to the southern end of the fault. The estimated PGA for these sites based on the RVT technique are in good agreement with the recorded peaks. Figure 4 shows the expected duration from the Landers earthquake at different sites. Figure 5 shows the expected duration from a magnitude 7.8 earthquake on the Coachella and San Bernardino segments of the San Andreas fault. The fault rupture begins at the northern end of the fault.

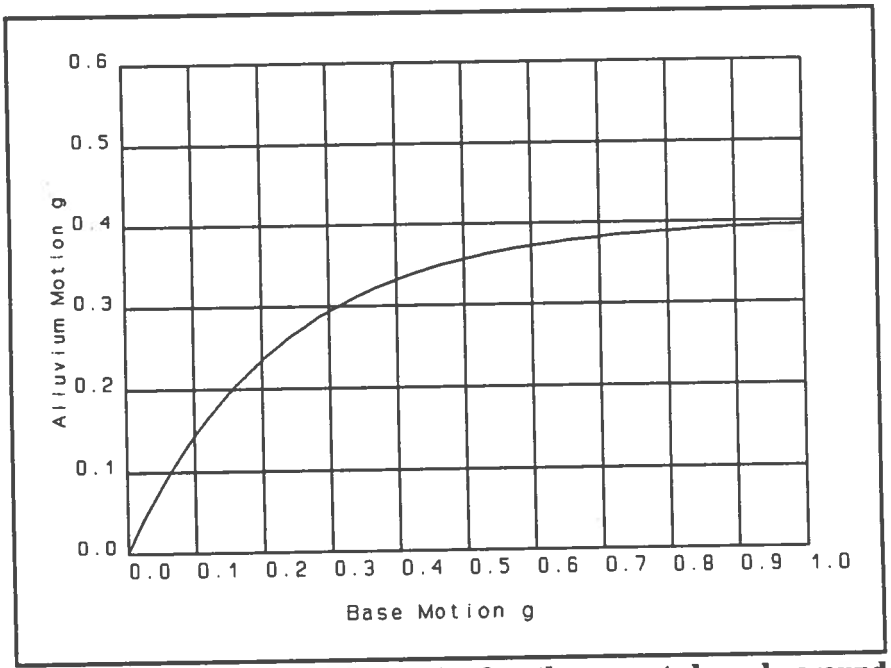

Figure 1. A typical relationship for the expected peak ground acceleration on an alluvium site versus the PGA of the underlying bedrock motion.

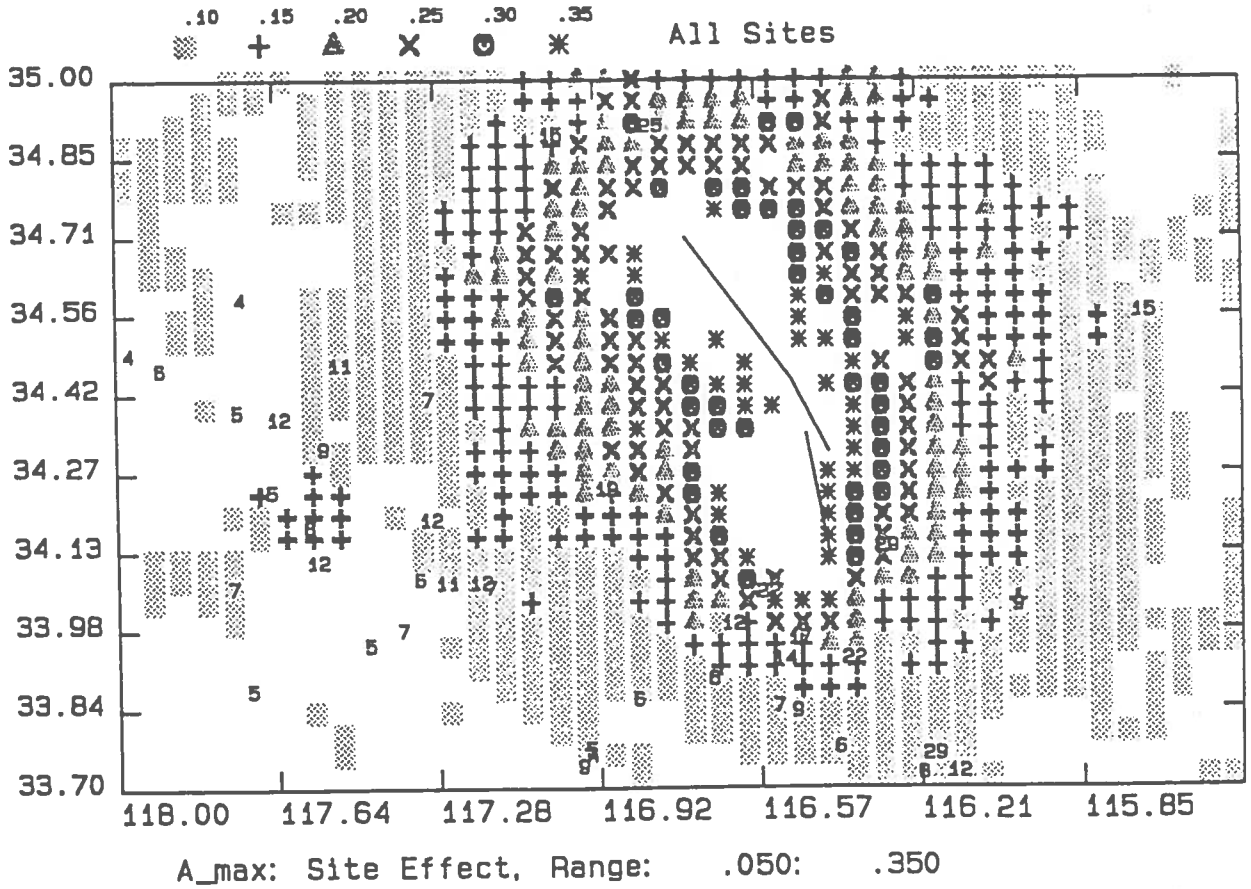

Figure 2.

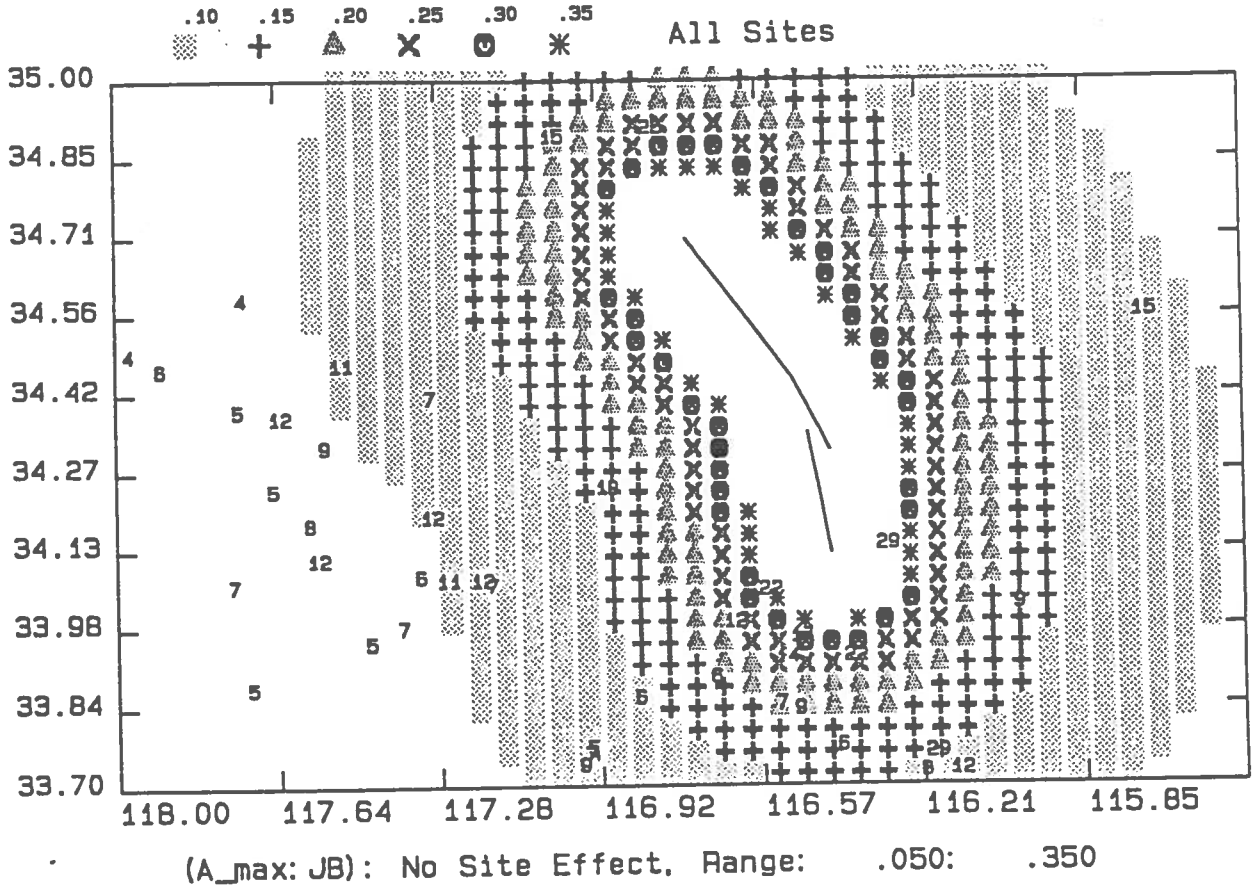

Figure 3.

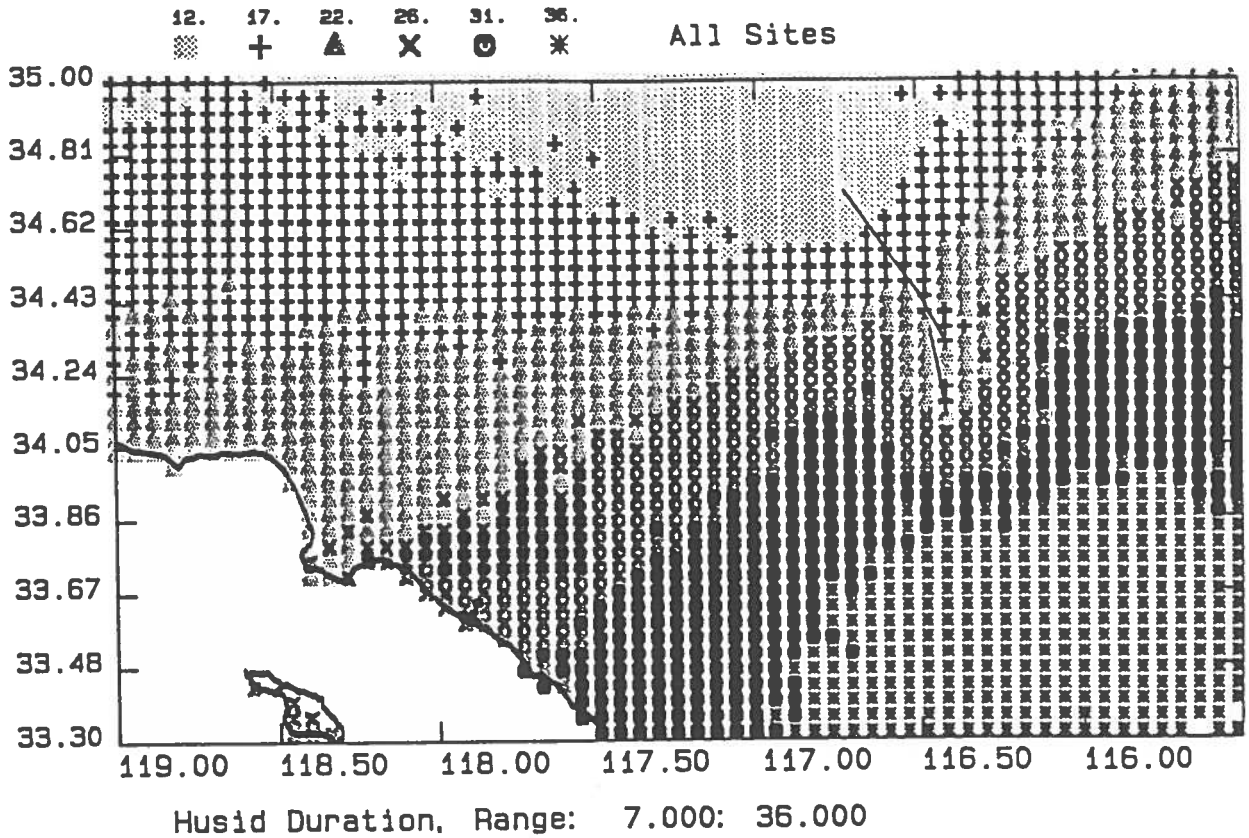

Figure 4.

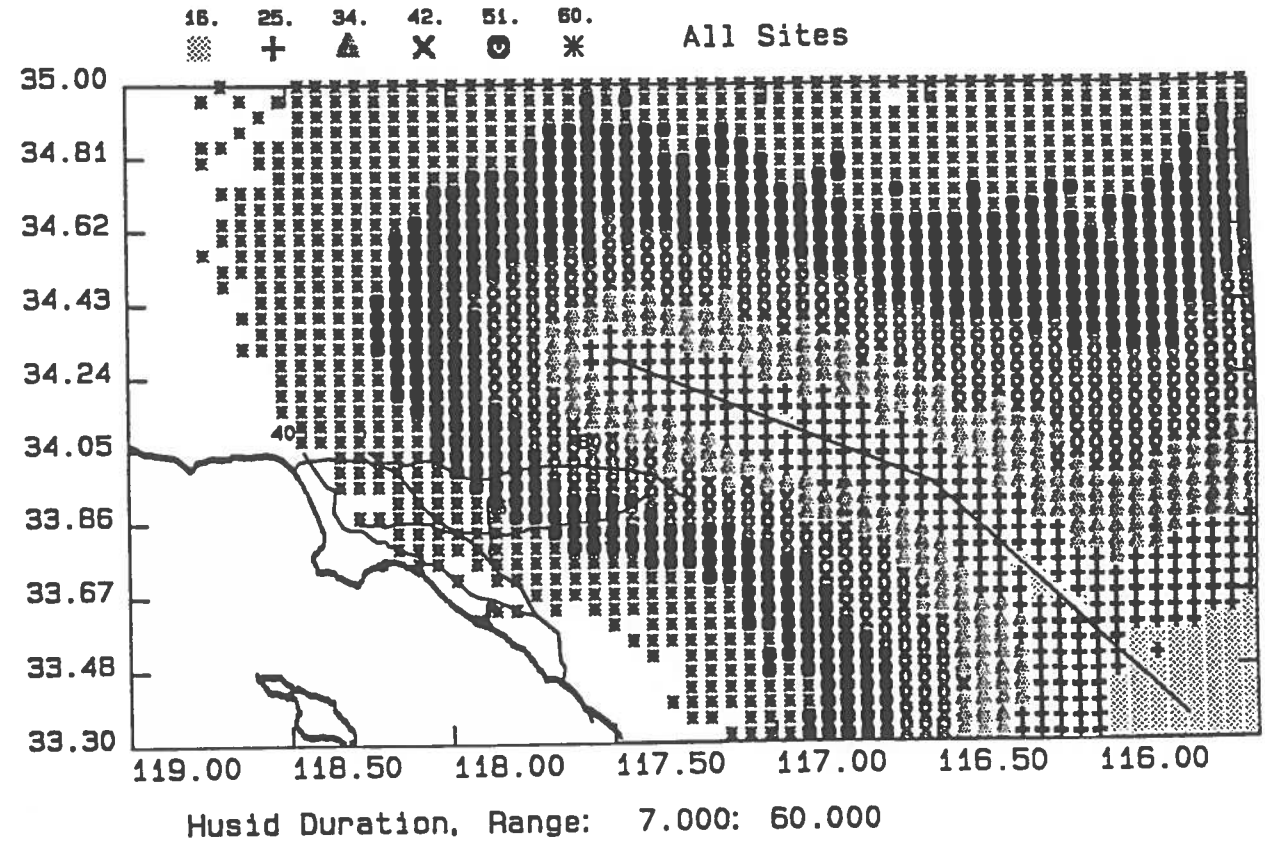

Figure 5.

Southern California Earthquake Center
Activity Report, September, 1992

Jean-Bernard Minster, Principal Investigator
Nadya P. Williams
Institute of Geophysics and Planetary Physics, A-025
Scripps Institution of Oceanography, UCSD,
La Jolla, Ca, 92037-0225

The "M8" Intermediate-term Earthquake Prediction Algorithm: An Independent Assessment focused on the 1989 Loma Prieta and 1992 Landers Earthquakes

The "M8" earthquake prediction algorithm has been proposed by Russian seismologists as a means to achieve intermediate term prediction of large events (e.g. *Gabrielov et al.*, 1986; *Keilis-Borok et al.*, 1990; *Updyke et al.*, 1989; *Healy et. al*, 1992; *Kossobokov et al.*, 1992). The algorithm makes use of a "de-clustered" catalog of mainshocks, from which aftershocks have been removed, to identify large scale seismicity patterns thought to precede large earthquakes in a given region. When such a pattern is detected, a "Time of Increased Probability" (TIP) is declared, for a period of five years.

Under NEHRP and SCEC support, we have undertook an independent assessment of the "M8" algorithm. Our approach has been the following:

1. We collected an unambiguous definition —as much as possible— of the algorithm, from published reports and papers, from a FORTRAN implementation written by Russian seismologists, and from discussions with the developers of the algorithm. Our goal was to obtained an accurate definition of the algorithm at the development stage where it was "frozen". This proved to be rather difficult, and required some reverse-engineering of the Russian code. Although the M8 algorithm involves rather simple manipulations of the catalog, it is complicated to describe. The process of re-coding the algorithm forced us to recognize a number of subtle implementation details which were only accessible through the original FORTRAN code itself, but which do affect the output.

2. We wrote this new implementation, using the C-language, adhering to modern coding standards. This was done, and the product was successfully tested against the original code, in the sense that the same output is produced from the same input, except for minor occasional differences, attributed to different implementation details (e.g. arithmetic precision), all of which we think we understand. The code has been delivered and installed on an SCEC UNIX system at USC, together with on-line documentation, and a PC version was made available to the USGS and to our Russian colleagues. Although the algorithm is "frozen", and could not be modified as part of this assessment, it depends implicitly on a number of user-selectable parameters, such as the time period considered in the analysis or the exact location and size of the target region. Our implementation of "M8" allows us to explore neighborhoods of this parameter space, by repeatedly executing the program after applying random perturbations to nominal parameter selections, in order to ascertain the stability of the results.

3. We then evaluated the algorithm using the 1963-89 NEIC catalog (de-clustered) used by *Keilis-Borok et al.* (1990) to describe a prediction of the 1989 Loma Prieta earthquake, and the Caltech-USGS southern California catalog for the period 1958-

92, to assess the predictability of the 1992 Joshua-Tree—Landers earthquake sequence. In the latter case, we used a computer program kindly provided y Dr. T. Levshina of SCEC to remove aftershock sequences according to the methods of *Gardner and Knopoff* (1974) and *Keilis-Borok et al.* (1980). These methods have recently been reviewed by *Molchan and Dmitrieva* (1992).

In both instances, we find that the algorithm is indeed triggered by large seismicity fluctuations apparent in the catalog. In fact, provided that seismicity in the Coso Range, and/or the Kern County area, and/or the Santa Barbara channel is included, then there is a current TIP at the end of 1991 for many of the circles containing the Landers event. Circles which do not include these critical regions tend not to yield a TIP. However, in our investigation, we have not addressed whether these fluctuations are partially man-made, and not necessarily representative of physical phenomena in the crust. An encouraging result is that randomization of the catalog using a bootstrap technique leads to a dramatic increase of false alarm rate, as illustrated in Tables 1 and 2.

On the other hand, the "M8" algorithm is defined in such a way that its output will be affected by inclusion or exclusion of a single earthquake, and is therefore very sensitive to small perturbations in the time or spatial windows used. This may be ascribed primarily to the use of untapered windows in order to sample a population of discrete points in space and time. As a result, TIPs are often affected by small earthquakes far removed from the target event. This means that attempting to use the algorithm for forward predictions requires specification of additional rules which spell out the strategy adopted for the test. Randomizing input parameters, as we have done, serves to highlight the issue, but does not constitute a satisfactory solution for actual applications. Furthermore, even minor differences in the aftershock identification and removal procedure can lead to rather different TIP distributions, as we have confirmed through minor perturbations to the traditional windowing techniques used to remove aftershocks in "M8" applications to date (see Table 1).

Future work should focus on the definition, identification, and removal of aftershocks, and on mapping the apparent effectiveness of the algorithm as a function of randomization of the catalog.

References

Gabrielov A.M. et al., *Algorithms of long-term earthquake prediction*, Int. School for research oriented to earthquake prediction algorithms, software and data handling, CERESIS, Lima, 1986

Gardner J., and L. Knopoff, Is the sequence of earthquakes in southern California with aftershocks removed Poissonian? Yes, *Bull. Seismol. Soc. Amer.*, **64**, 1363-1367, 1974.

Healy, J.H., V.G. Kossobokov, and J.W. Dewey, *A test to evaluate the earthquake prediction algorithm, M8*, USGS Open-file report, in press, 1992

Keilis-Borok, V.I., L. Knopoff, V.G. Kossobokov, and I.M. Rotvain, Intermediate-term prediction in advance of the Loma Prieta earthquake, *Geophys. Res. Lett.*, **17**, 1461-1464, 1990.

Kossobokov, V.G., J.H. Healy, and V.I. Keilis-Borok, Loma Prieta earthquake prediction by the M8 algorithm, (Preprint) 1992

Keilis-Borok, V.I., L. Knopoff, and I.M. Rotvain, Bursts of aftershocks long term precursors of strong earthquakes, *Nature*, **283**, 259-263, 1980.

Molchan G.M., and O.E. Dmitrieva, Aftershock identification: methods and new approaches, *Geophys. J. Intern.*, **109**, 501-516,1992.

Updyke et al., *Proc. NEPEC June 6-7, 188, Reston VA*, USGS Open-file report 89-144, 1989.

Table 1

Summary of results for runs conducted for the Joshua Tree Landers sequence, using the CIT-USGS southern California earthquake catalog for the 1958-1992 period, for M_0 = 7.0. Aftershock removal was performed using the criteria of *Gardner and Knopoff* (GK) or *Keilis-Borok et al.* (KB). For all runs, the algorithm is assume to start in 1970, with a possible random delay of ΔT_b, and an initialization period starting in 1958. From run to run the center positions and circle radii are perturbed by random amounts within the bounds listed. The key to the TIP summary is as follows: s - successful TIP, fa - false alarm, fp - failure to predict, c - current TIP as of 12/31/1991. Cases 5 and 10 were run on catalogs randomized using a resampling method with granularity of 1 month. Note the dramatic increase in false alarms.

Case	Afer-shocks	number of runs	Nominal Center		Δc	Δr	ΔT_b	TIPs			
			Lat. λ	Lon. ϕ	km	km	yr.	s	fa	fp	c
1	GK	100	34.2	117.3	40	-	-	-	-	-	100
2	GK	100	33.5	116.0	40	-	-	-	-	-	7
3	GK	100	34.0	116.5	40	40	5	-	-	-	54
4	GK	100	34.0	116.5	80	-	-	-	-	-	50
5	GK	200	34.0	116.5	40	40	-	-	59	-	13
6	KB	100	34.2	117.3	40	-	-	-	-	-	100
7	KB	100	33.5	116.0	40	-	-	-	-	-	57
8	KB	100	34.0	116.5	40	40	5	-	-	-	80
9	KB	100	34.0	116.5	80	-	-	-	-	-	88
10	KB	200	34.0	116.5	40	40	-	-	52	-	13

Table 2

Summary of results for runs conducted for the Loma Prieta, using the same catalog (1963-89) as was used by Keilis-Borok et al. for M_0 = 7.0. For all runs, the algorithm is assumed to start in 1975, with a possible random delay of ΔT_b, and an initialization period starting in 1963. From run to run the center positions and circle radii are perturbed by random amounts within the bounds listed. The key to the TIP summary is as follows: s - successful TIP, fa - false alarm, fp - failure to predict, c - current TIP as of 07/31/1989. Cases 1, 3, 5 were run on catalogs randomized using a resampling method with granularity of 1 month. Note the dramatic increase in false alarms.

Case	Afer-shocks	number of runs	Nominal Center		Δc	Δr	ΔT_b	TIPs			
			Lat. λ	Lon. ϕ	km	km	yr.	s	fa	fp	c
1	KB	200	37.5	122.0	40	40	-	-	42	-	39
2	KB	100	37.5	122.0	40	40	2	-	-	-	59
3	KB	200	38.0	119.0	40	40	-	-	65	-	31
4	KB	100	38.0	119.0	40	40	2	-	-	-	88
5	KB	200	36.0	120.0	40	40	-	-	61	-	28
6	KB	100	36.0	120.0	40	40	2	-	-	-	89
7	KB	100	38.0	122.0	40	40	2	-	4	-	56
8	KB	100	37.0	123.0	40	40	2	-	-	-	1

Annual Summary Report, Southern California Earthquake Center, USC P.O. 569928

Rupture Heterogeneity and Evaluation of the Characteristic Earthquake Concept

James R. Rice
Department of Earth and Planetary Sciences and Division of Applied Sciences
Harvard University, Cambridge, MA 02138
September 1992

Studies are underway on identifying possible physical origins of characteristic earthquake response and on examining limitations to the concept, and more generally on modeling the interrelations between fault zone property variations, geometric disorder, and heterogeneity of seismic response. Four projects are described. The 1st and 4th are at a mature stage, whereas work continues actively on the 2nd and 3rd.

(1) Spatio-temporal Complexity of Slip on a Fault

James R. Rice

Three-dimensional analyses are reported of slip on a long vertical strike-slip fault between steadily driven elastic crustal blocks. A rate- and state-dependent friction law governs motion on the fault; the law includes a characteristic slip distance L for evolution of surface state and slip-weakening. Because temperature and normal stress vary with depth, frictional constitutive properties (velocity weakening/strengthening) do also. Those properties are taken either as uniform along-strike at every depth or as perturbed modestly from uniformity. The governing equations of elasticity and frictional slip are solved on a computational grid of cells as a discrete numerical system. The numerical results show richly complex slip when solved for a grid with oversized cells, that is, with cell size h that is too large to validly represent the underlying continuous system of equations. However, in every case for which it has been feasible to do the computations (moderately large L only), that spatio-temporally complex slip disappears in favor of simple limit cycles of periodically repeated large earthquakes with reduction of cell size h. The transition occurs as h is reduced below a theoretically derived nucleation size h* which scales with L but is $2 \cdot 10^4$ to 10^5 larger in cases considered. [It is given as $h^* = 2 L \mu / \pi (B - A)_m$, where μ = shear rigidity and $(B - A)_m$ is the maximum value on the fault of the velocity weakening parameter – $V d\tau_{ss}(V)/dV$.] Cells larger than h* can fail independently of one another whereas those much smaller than h* cannot slip unstably alone, and can do so only as part of a cooperating group of cells. The results contradict an emergent view that spatio-temporal complexity is a generic feature of mechanical fault models. It is pointed out that such generic complexity has so far been found only in models which are inherently discrete in the sense of having no well-defined continuum limit as h diminishes. Those models form a different class of dynamical systems from models like the present one that do have a continuum limit. Strongly oversized cells cause the model developed here to mimic an inherently discrete system. It is suggested that oversized cells, capable of failing independently of one another, may crudely represent geometrically disordered

fault zones, with quasi-independent fault segments that join one another at kinks or jogs. Such geometric disorder, at scales larger than h*, may force a system with a well defined continuum limit to mimic an inherently discrete system and show spatio-temporally complex slip at those larger scales.

Supported by: USGS-14-08-0001-G1788 and SCEC (USC P.O. 569928).

Manuscript completed June 1992; in review for publication in *Journal of Geophysical Research.*

Related oral/poster presentations at Spring 1991 AGU, at June 1991 SCEC/ITP-Santa Barbara Workshop, and at August 1991 IUGG Jeffreys Symp.

(2) Earthquake Failure Sequences Along a Discrete Cellular Fault Model Containing Asperity and Non-asperity Regions in a 3D Elastic Solid: Application to Parkfield

Yehuda Ben-Zion and James R. Rice

Numerical simulations of earthquake failure sequences along a discrete cellular fault zone have been performed in a 3D model intended to approximately represent the central San Andreas Fault system. The model consists of an upper crust overlying a lower crust and mantle region, treated together as an elastic half-space with a vertical half-plane fault. The fault contains a region where slip is calculated on a grid of cells governed by a static/kinetic friction law, and regions where slip is prescribed so as to represent tectonic loading, aseismic fault creep, and adjacent great earthquakes. The computational cell region models a 70 km long and 17.5 km deep section of the San Andreas fault to the NW of the great 1857 rupture zone. Different distributions of stress drops on failing cells are used to model asperity ("Parkfield asperity") and non-asperity fault regions. The model is "inherently discrete", in the terminology of the discussion of spatio-temporal complexity above, and may correspond to a situation in which a characteristic size of geometric disorder within the fault (identified as cell size h, and usually taken as a few hundreds of meters here) is much larger than the "nucleation size" h* based on slip-weakening or state-evolution slip distances.

The computational grid is loaded by a constant plate motion imposed along the lower crust, upper mantle and creeping fault regions, and by a "staircase" slip history imposed on the 1857 and 1906 rupture zones. Stress transfer along and outside the fault due to the imposed loadings and failure episodes within the computational grid are calculated using 3D elastic dislocation theory. The resulting displacement field in the computational region is compatible with geodetic and seismological observations only when the asperity and non-asperity regions are characterized by significantly different average stress drops. The frequency-magnitude (Gutenberg-Richter) statistics of the simulated failure episodes are approximately self similar for small events, with $\log_{10}$ N *versus* $\log_{10}$ (Event cluster areas) showing a b $\approx$ 1, but slightly larger b for $\log_{10}$ N *versus* M [= (2/3) $\log_{10}$ (Potency) + constant; Potency = Moment/Rigidity]. However, the failure episodes are strongly enhanced (with respect to self similarity) for events having cluster area larger than a threshold value related to medium properties and apparently scaling with cell area (it is about 200 h^2 in our cases). This is interpreted as a direct manifestation of our 3D elastic stress transfer

calculations; beyond a certain cluster area (i.e., crack size) and potency release values, the rupture is usually unstoppable. This effect is not accounted for by cellular automata and block-spring models in which the adopted simplified stress transfer laws fail to scale properly with increasing rupture size. A tentative interpretation is that a single scale size of geometric disorder cannot lead to self-similar behavior over a broad range of magnitudes, and geometric disorder over a range of scales may be necessary.

The cases examined in out work cover varying degrees of model heterogeneity. In the least heterogeneous case, the computational grid has uniform properties and model heterogeneity comes only from the assumed loadings. In more heterogeneous cases, the computational grid contains property variations. Our results show spatio-temporal slip complexities for all cases. However, the calculated displacement field is compatible with geodetic and seismological data of the Parkfield region only when strong property variation is assumed along the fault. The results show an irregular sequence of Parkfield-type earthquakes, and a great diversity in the failure mechanism of the model asperity: Some failure events are preceded by a period of accelerated potency release and/or foreshocks, some events resemble slow earthquakes, and other events are abrupt. The results suggest that it is unrealistic to expect a complex crustal system like the SAF to produce periodic earthquakes and/or simple precursory patterns (e.g., accelerated microearthquake slip) repeating from one event to the other, although some form of statistical precursor may exist in terms of evolving seismicity patterns.

Future possible applications of similar model simulations, of the type discussed here, include the San Jacinto and Newport-Inglewood faults in southern CA, and the Hayward and Calaveras faults in northern CA.

Supported by: SCEC (USC P.O. 569928) and NSF-EAR-90-04556.

Manuscript in preparation

Related oral/poster presentations at Fall 1991 AGU, at March 1992 USGS Parkfield Workshop, and scheduled for Fall 1992 AGU.

(3) Characteristic Earthquakes and Variable Earthquake Recurrence Intervals: Rate- and State-Dependent Friction Model with Strong Property Variations Along Strike

James R. Rice

A fault zone with variable properties along strike is modeled by requiring that rate- and state-dependent friction laws be satisfied along the crustal depth range ($\approx$ 24 km) of a vertical half-plane fault in an elastic half-space, with subcrustal portions of the fault slipped steadily at an imposed rate of 35 mm/yr. This is the same model used by Rice (item 1 above) for studies of spatio-temporal complexity of fault slip, but now the depth-variable frictional constitutive properties, based on the Blanpied, Lockner and Byerlee (GRL, '91) data for granite under hydrothermal conditions, are made to vary significantly in amplitude along strike. This variation has been induced in different studies either by varying the degree of pore pressurization along

strike, or by assigning an amplitude factor to multiply some particular depth-variation and letting the amplitude factor vary along strike (this might crudely represent lithological variation). In the case studied most extensively so far, the latter method was used to simulate Parkfield-like conditions, thus producing a creeping zone that is bordered by moderate earthquake zones (like Parkfield and San Juan Bautista) which are, in turn, bordered by zones of infrequent great earthquakes (1857 and 1906 rupture zones). To induce this type of behavior, with characteristic earthquake behavior of different segments, it was necessary to have very strong property variations. E.g., the amplitude factor varied by a factor of 10 between the creep zone and moderate earthquake zones, and by a further factor of 5 between the moderate and great earthquake zones, in the case studied. This may be stronger variation than necessary, although trial runs with weaker variation often show a tendency for phase locking between different zones, which thus lose their characteristic behavior. Presumably, strong geometric barriers at zone ends could induce characteristic-like behavior with weaker variation from zone to zone. The aim in this modeling, unlike in item 2 above, was to not deal with a case dominated by geometric disorder, and thus cell size was kept less than h*; the only way of accomplishing this within practical computational limits was to make the slip weakening distance L vary strongly along strike also. The Parkfield-like events, in versions of the model studied thus far, are found to have highly variable moment release and recurrence intervals. One sequence of five such events, in the time span between adjacent great earthquakes, has a ratio of sample standard deviation to mean of the recurrence intervals of about 0.59, higher than 0.33 for the Bakun and McEvily (JGR, '84) Parkfield catalog.

Supported by: USGS-14-08-0001-G1788 and SCEC (USC P.O. 569928).

Related oral/poster presentation scheduled for Fall 1992 AGU.

(4) Interaction of the San Andreas Fault Creeping Segment With Adjacent Great Rupture Zones, and Earthquake Recurrence at Parkfield

Yehuda Ben-Zion, James R. Rice, and Renata Dmowska

In this purely kinematic study of fault slip effects, 3D finite element calculations were employed to study interactions in space and time between the creeping segment of the San Andreas fault in central California and the adjacent currently locked zones of the 1857 and 1906 great earthquakes. Vertically, the model consists of an elastic upper crust over a Maxwell viscoelastic region, representing the entire lower crust or a narrower horizontal detachment layer, and a stiffer and more viscous upper mantle. The crust has a single vertical fault extending to the top of the mantle at 25 km depth. In zones along strike corresponding to the 1857 and 1906 events, the top 12.5 km of the fault is locked against slip, except in great earthquakes. Below the locked zones and everywhere along the creeping region between them, the fault is freely slipping. The model parameters are compatible with seismological and geological observations, and with a ratio of Maxwell relaxation time to the relaxing layer thickness in the range 1 to 2 yr/km, as established by Li and Rice (1987) and Fares and Rice (1988) based on fits to geodetic data along the San Andreas fault. An imposed constant far field shear motion and periodic 1857- and 1906 type earthquakes generate slip rates along the creeping fault segment that evolve in time throughout the entire earthquake cycle. Shortly after an adjacent great earthquake, slip rates in the creeping zone are

higher than the far field velocity, while later in the cycle they are lower. Hence, time dependency should be accounted for when measurements of fault slip are used to estimate the plate motion. If Parkfield earthquakes are a response to a time dependent loading of the type simulated here, their recurrence interval would tend to lengthen with time since the 1857 event. Thus, the hypothesis of characteristic periodic earthquakes at Parkfield may not provide the best estimate of the occurrence time of the next event. Using, for example, the statistics of past events and assuming that Parkfield earthquakes are a response to a slip deficit near Middle Mountain, and that the elastic crustal layer is 17.5 km thick, we find that the next event is predicted for about 1992 ± 9 yr if the lower crust is a 7.5 km thick layer having a material relaxation time of 15 yr, and 1995 ± 11 yr if the 7.5 km thick lower crust is characterized by a relaxation time of 7.5 yr. These values may be compared to the 1988 ± 7 yr estimate based on periodicity in time. The modeling results also indicate that the interaction between the 1857 and 1906 rupture zones is small. (Analogous broadscale viscoelastic relaxation effects are not included in the models discussed in items 1 to 3 above.)

Supported by: NSF-EAR-90-04556 and SCEC (USC P.O. 569928).

Manuscript completed April 1992; revised version, prepared August 1992, accepted for publication in *Journal of Geophysical Research*; in press.

Related oral/poster presentations at Fall 1991 AGU, at March 1992 USGS Parkfield Workshop, and scheduled for Fall 1992 AGU

PROGRESS REPORT ON SCEC-FUNDED RESEARCH "TIME DEPENDENT SEISMIC HAZARDS ASSESSMENTS, SOUTHERN CALIFORNIA"

Lynn R. Sykes and Mark D. Petersen

During the past year our SCEC-funded research on seismic hazard has resulted in the submission of two papers to the *Bulletin of the Seismological Society of America.*. The first paper "Seismic hazard to the greater Los Angeles region, California, from large earthquakes along the San Andreas and San Jacinto faults from 1992 to 2022" by M.D. Petersen, L.R. Sykes, and K.H. Jacob discusses a probabilistic seismic hazard assessment for strong ground motion within the Los Angeles and San Bernardino regions. The assessment allows for different recurrence models and site responses, and includes error estimates obtained from varying the input parameters. For our seismic input, we use the time-dependent probabilistic estimates of M 7.0 to 8.0 characteristic earthquakes along six segments of the San Andreas and San Jacinto faults for a 30-year time period described by the Working Group on California Earthquake Probabilities (1988). For comparison we also computed the time-independent or Poisson estimates for earthquakes along those segments. Site response at different periods is accounted for in our ground motion estimates by averaging pseudo-velocity response spectra (PSV) obtained from strong-motion accelerograms of the 1971 (Mw = 6.6) San Fernando earthquake recorded on fine to medium grained Holocene alluvium, other Quaternary alluvium, soft rock, and intermediate-to-hard rock. We found that mean PSV amplitudes are about a factor 1.3 higher at 0.3 s PSV, a factor of between 2.0 and 2.5 higher at 1 s, and a factor of between 2.7 and 3.0 higher at 3 s on alluvium than they are on intermediate-to-hard rock sites. We produced seismic ground motion hazard maps that show the probabilities of exceeding various PSV ground motion amplitudes for periods of 0.3, 1, and 3 s (Fig. 1). The hazard estimates, which include site response, indicate that the median 30-year probability of exceeding 30 cm/s PSV at 1 s period for both time-dependent and Poisson recurrence probabilities is greater than 20% for most of the greater Los Angeles region. The 30-year probability of exceeding 30 cm/s PSV is particularly high in the San Bernardino area, exceeding 60% for a time-dependent recurrence and 40% for a Poisson recurrence model. Probabilities near San Bernardino are particularly high because the area is located close to segments of the San Andreas and San

Jacinto faults that have not ruptured in characteristic earthquakes in more than 180 and 100 years, respectively, and because it is located in an alluvial valley that amplifies certain seismic wave motion. We also computed hazard curves with their uncertainties for both rock and alluvial sites in Los Angeles, Ontario, and San Bernardino using both time-dependent and Poisson recurrence models. These hazard curves indicate that the probabilities for the next 30-years of exceeding 20 cm/s PSV at 1 s period for intermediate-to-hard rock sites range from 10% near Los Angeles to 70% near San Bernardino for time-dependent calculations.

Our second paper "Potential Future Large Earthquakes along the San Jacinto Fault Zone and Seismic Hazard to San Bernardino and Riverside, Southern California" by M.D. Petersen and L.R. Sykes discusses the hazard associated with various ruptures along the San Jacinto fault zone. In this paper we present a hazard assessment for the San Bernardino and Riverside areas assuming specified sources of large earthquakes along the northern and central San Jacinto fault zone and including the effects of site amplification. Two earthquake hazard assessments are presented that differ in how the seismic sources are defined. For one assessment we deduce seismic sources from a fault-zone segmentation model that we obtained from an analysis of the seismicity and fault characteristics. We determined a length, down-dip width, and seismic moment for each of these segments. The second assessment is obtained by computing the hazard from earthquake sources of the same dimensions and moment release that are distributed uniformly along the fault zone (Fig. 2). Two portions of the fault that we analyze correspond to the Anza and San Bernardino seismic gaps. These gaps are believed not to have ruptured in over a century and may be capable of rupturing in earthquakes as large as Mw 7.0 to 7.3 if neighboring segments rupture together. Our estimates of maximum size events for those two fault segments are larger than those in most previous studies. Large events along the northern and central segments of the San Jacinto fault can be expected to generate larger seismic moment release per unit length along strike then earthquakes along southern segments since rupture in the former is likely to extend to depths of 18 to 20 km. We find that the expected ground shaking in the San Bernardino-Riverside region from earthquakes along the San Bernardino fault segment is quite high, greater than 100 cm/s PSV and about modified Mercalli intensity IX. The northern 70 km of the fault contributes most to the seismic hazard in San Bernardino and Riverside. A surprising result is that the hazard in that same area from rupture in a similar size event near Anza is only about 20 cm/s PSV, i.e., MMI VI to VII.

Figure 1. 30-year hazard maps of greater Los Angeles region showing probability for exceeding 30 cm/s PSV at 0.3, 1, and 3 s periods using time-dependent and time-independent recurrence models. Probability legend shown at upper right. Lines indicate regional faults and are shown for reference only. This hazard assessment includes only sources along the San Andreas and San Jacinto faults.

Figure 2. Sensitivity study showing the hazard in San Bernardino, Riverside, and Palm Springs for both Holocene alluvium (solid line) and rock sites (dashed line) at periods of 0.3, 1, and 3 s. Plotted are PSV values for which there is a 85% probability of being exceeded given a rupture on each of the fourteen 40-km segments shown at bottom of page.

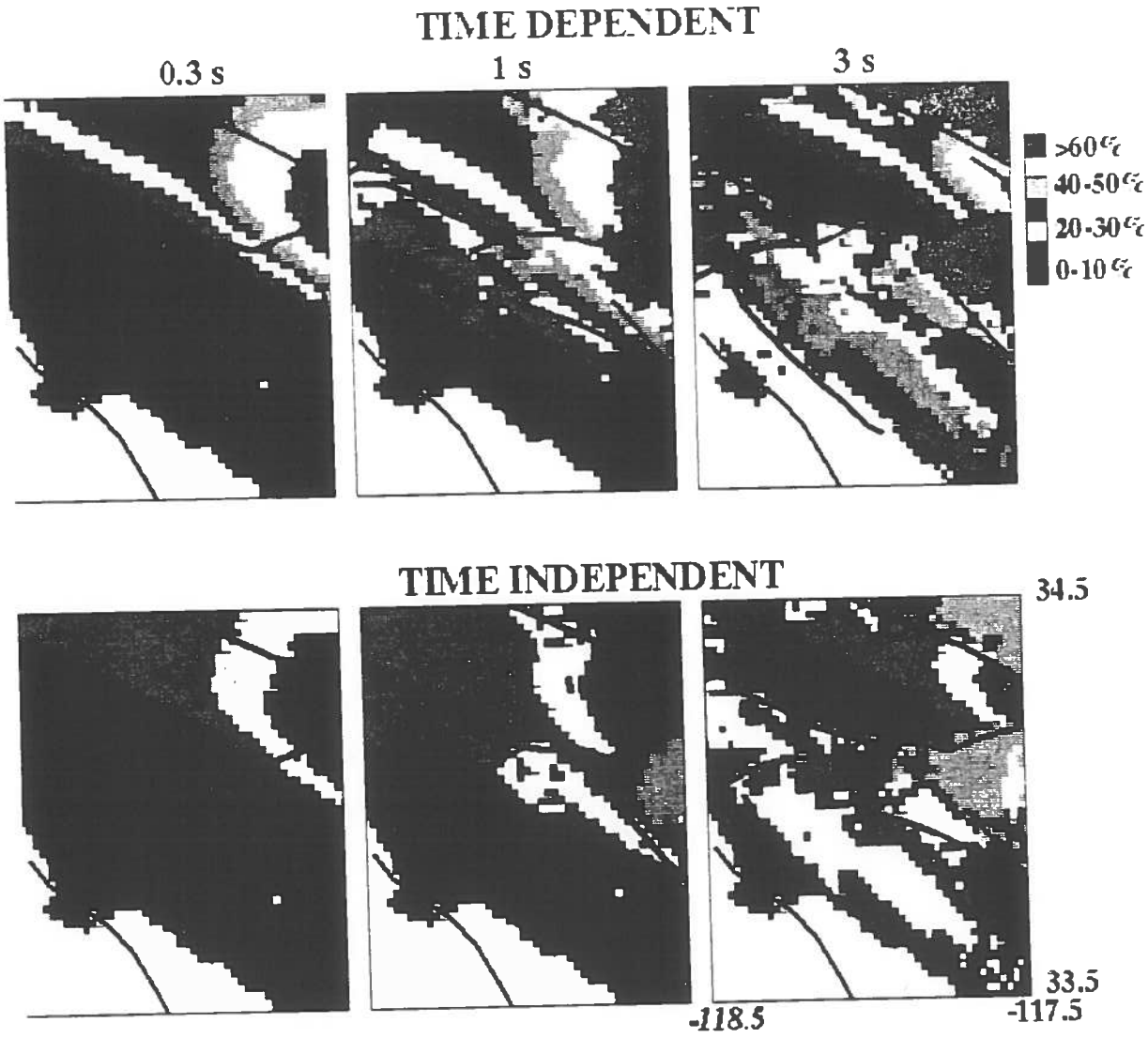
TIME DEPENDENT
0.3 s
1 s
3 s
>60%
40-50%
20-30%
0-10%
TIME INDEPENDENT
34.5
33.5
-118.5
-117.5

Figure

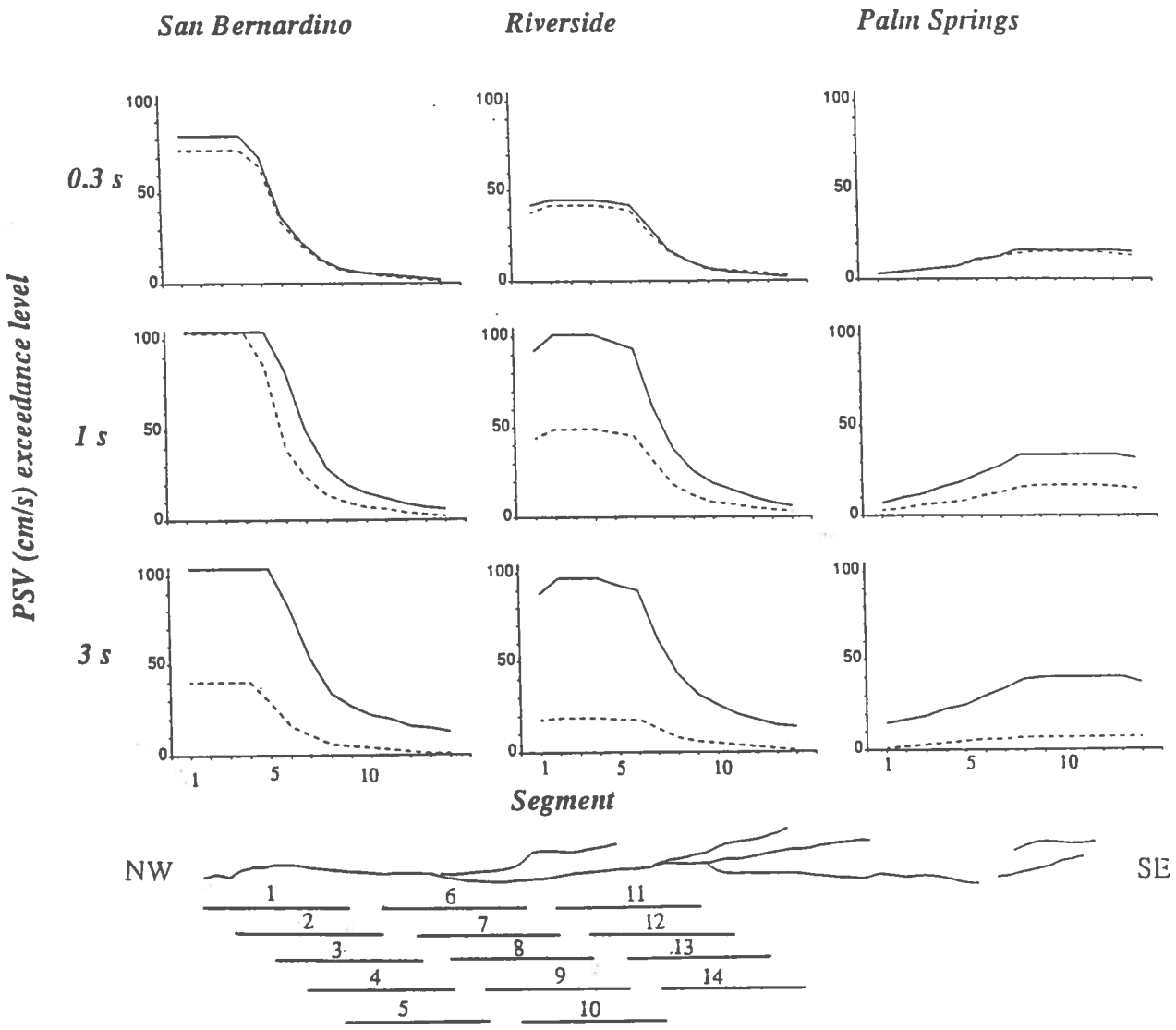
San Bernardino
Riverside
Palm Springs
0.3 s
1 s
3 s
PSV (cm/s) exceedance level
100
50
0
1
5
10
Segment
NW
SE
1
2
3
4
5
6
7
8
9
10
11
12
13
14

Figure 2

SOUTHERN CALIFORNIA EARTHQUAKE CENTER

1. **Name of PI:** Steven N. Ward
2. **Institution:** University of California, Santa Cruz
3. **Title of Project:** Synthetic Seismicity Models of the San Andreas Fault

Progress Report for 1992

We have been attempting to revise the mean repeat time (T_{ave}) and coefficient of aperiodicity (ν) for segments of the San Andreas Fault by using models of synthetic seismicity. Primary inputs into the model are: 1) segment lengths and locations, 2) characteristic earthquake magnitudes, and 3) long-term slip rates. Of all the earthquake information available, these features are probably best constrained.

WGCEP (1990) has presented an eleven segment model for the San Andreas Fault. A slightly adjusted version (Table 1) was employed to address the question: "Can the WGCEP segmentation reproduce observed SAF seismicity? If not, what needs to be done? If so, what can be said about T_{ave} and ν?" Figure 1 shows synthetic seismicity (*top*) and displacement (*bottom*) for the first 1000 years of a 6000 year run of the SAF model. Figure 2 (*stars*) overlays the synthetic seismicity with the observed annual rates (*boxes*) $N_>(M)$ and $N(M)$ of earthquakes within a 40 km wide band centered on the fault. The $N(M)$ plot clearly indicates that the WGCEP segmentation is deficient in magnitude 5.5-6.5 quakes by a factor of three. There are simply not enough small (10-20 km) segments in the WGCEP model to produce the observed number of intermediate strength quakes. Additional generic models suggest that about 50% more segments are required to fill in this hole. Earthquakes greater than $M = 6.5$, on the other hand, are reasonably well reproduced by the WGCEP model, so it is fair to advance some recurrence statistics for the larger events.

Fault Averaged Results. Figure 3 plots cumulative probability of recurrence versus time for $M \geq M_o$ with M_o= 6.0, 6.5, 7.0, 7.5 and 8.0. for the SAF model as a whole. Mean repeat time and spread parameter for a typical large event ($M \geq 7$) is 105 years and 1.0. It is important to recognize however, that both T_{ave} and ν are functions of magnitude; T_{ave} increases with M_o while ν decreases (bottom row, Table 2). Large earthquakes tend to be more periodic than small ones. Small ones tend to cluster early in the cycle. You can see this in the top panel of Figure 3, where the curves crowd to the left. The numerical value of ν bears directly on the concept of seismic gaps. If ν is less than 1.0, gaps behave normally in that the conditional probability of occurrence increases with gap time. If ν is greater than 1.0, the effect is reversed and conditional probability decreases as gap time increases. All of the models run so far show the same tendency; ν decreases from approximately 1.4 at M_o=6 to about 0.7 at M_o=7.75. The cross-over magnitude where gaps become a useful concept occurs around $M = 7$. In all instances the spread parameter is much greater than the 0.21 value used by WGCEP.

Segment Specific Results. Earthquake aperiodicity, while on the average being a decreasing function of characteristic magnitude, is also dependent on the segment's relative location on the fault. Table 2 lists T_{ave} and ν for all of the SAF segments as a function of M_o. In scanning the columns, you can see that certain segments systematically behave more or less periodically than the fault as a whole. Generally, the more isolated a segment, the more periodic are its earthquakes. Note for instance, that the Parkfield segment tends to have a ν less than the fault average. This segment borders the central creeping section to the north which provides a degree of isolation. Although very periodic failures of fault segments may exist, we find it difficult to make any segment conform to a spread value much less than 0.4. Given the information in Table 2 and the date of the last earthquake on a segment, the conditional probability of recurrence can be easily calculated. For

the Parkfield segment [T_{ave}=26.6 and ν=0.95, 1966=previous quake], the conditional probability of recurrence of a $M \geq 6$ quake within the ten year Parkfield Prediction window beginning in 1983 is 32% (versus 95% estimated by Bakun and Lindh, 1985). Probability of recurrence in the 30 year WGCEP window starting in 1988 is 69% (versus > 90% estimated by WGCEP, 1988).

Verification. We have argued previously that unless the earthquake record contains at least ten recurrences, the estimated repeat time and aperiodicity coefficient will almost certainly be too low. Measured against this criteria, there are few data sets with which to compare (and correct) the model. Sieh (1989) reports nine recurrence intervals at Pallet Creek in the Mojave segment. Weibull function fits to these intervals give T_{ave} = 131.8 y and ν=0.84. Because it is not completely certain what magnitude earthquakes the paleoseismic data are detecting, we plot in Figure 4 (*dashed lines*) predictions for recurrence of M_o = 7, 7.25 and 7.5 quakes in the Mojave segment. The model reproduces both T_{ave} and ν quite well. Keep in mind that T_{ave} derives only from the segment length, characteristic magnitude, and slip rate. It is not an input parameter.

Weaknesses. Admittedly, products from synthetic seismicity models are easily attacked as nonunique or parameter dependent. We can't claim the contrary, but given the fact that there is almost a total lack of data on the recurrence statistics of SAF earthquakes, we believe that synthetic seismicity offers two unquestionable advantages over the real thing: 1) Synthetic seismicity can run as long as necessary to get a statistically significant sample. Individual products like "Segment X has a 50% chance of triggering Segment Y" may not agree with our limited historical sample, but at least there is a firm statistical basis for the statement. 2) Synthetic seismicity illuminates connections between physical parameters which otherwise would go unrecognized. Segment length, characteristic magnitude, mean repeat time and aperiodicity are linked; they can not be picked out of a hat. For instance, T_{ave} can not be arbitrarily decreased without cutting the characteristic magnitude or increasing slip rate. Likewise, the characteristic magnitude of a segment can not be reduced without (generally) increasing ν.

We believe that San Andreas earthquake recurrence statistics which derive from synthetic seismicity models such as these are as credible, if not more so, than any other method yet advanced.

Ward, S. N., 1992. An Application of Synthetic Seismicity in Earthquake Statistics: The Middle America Trench, *J. Geophys. Res.*,*97*, 6675-6682.

Segment	Length (km)	Characteristic Magnitude	Slip Rate (mm/y)
Medocino	100	7.0	18
North Coast	240	7.6	18
Mid Peninsula	41	7.0	18
N. Santa Cruz Mts.	20	6.5	18
S. Santa Cruz Mts.	39	6.9	18
Creeping Section	130	aseismic	36
Parkfield	30	6.3	36
Cholame	55	7.0	36
Carrizo	145	7.7	36
Mojave	100	7.4	36
San Bernardino	100	7.25	30
Coachella Valley	100	7.35	30
Imperial Valley	50	6.6	30
Cerro Prieto	50	6.5	30

Table 1. San Andreas Fault segmentation model. Slightly modified after WGCEP.

	$M \geq 6.0$		$M \geq 6.5$		$M \geq 7.0$		$M \geq 7.5$	
Segment	T_{ave} (y)	ν	T_{ave} (y)	ν	T_{ave} (y)	ν	T_{ave} (y)	ν
Medocino	71	1.3	76	1.2	97	1.0	221	0.5
North Coast	67	1.5	89	1.3	103	1.1	205	0.5
Mid Peninsula	59	1.2	69	1.1	99	0.9	324	0.7
N. Santa Cruz Mts.	36	1.2	53	1.1	121	0.8	480	0.9
S. Santa Crua Mts.	51	1.4	62	1.2	163	0.7	688	0.8
Creeping Section								
Parkfield	27	1.0	62	1.0	136	0.8	365	0.3
Cholame	54	1.2	64	1.1	133	0.9	365	0.3
Carrizo	161	1.3	177	1.1	196	1.0	274	0.5
Mojave	92	1.3	108	1.1	114	1.0	232	0.6
San Bernardino	50	1.3	55	1.2	65	1.2	161	0.8
Coachella Valley	61	1.3	64	1.2	77	1.2	193	0.6
Imperial Valley	26	1.0	33	1.0	92	1.0	200	0.6
Cerro Prieto	25	1.0	31	1.0	97	0.9	200	0.6
AVERAGE	46	1.4	59	1.3	105	1.0	247	0.7

Table 2. Predicted earthquake recurrence statistics for the San Andreas Fault segments for magnitudes greater than or equal to 6.0, 6.5, 7.0 and 7.5.

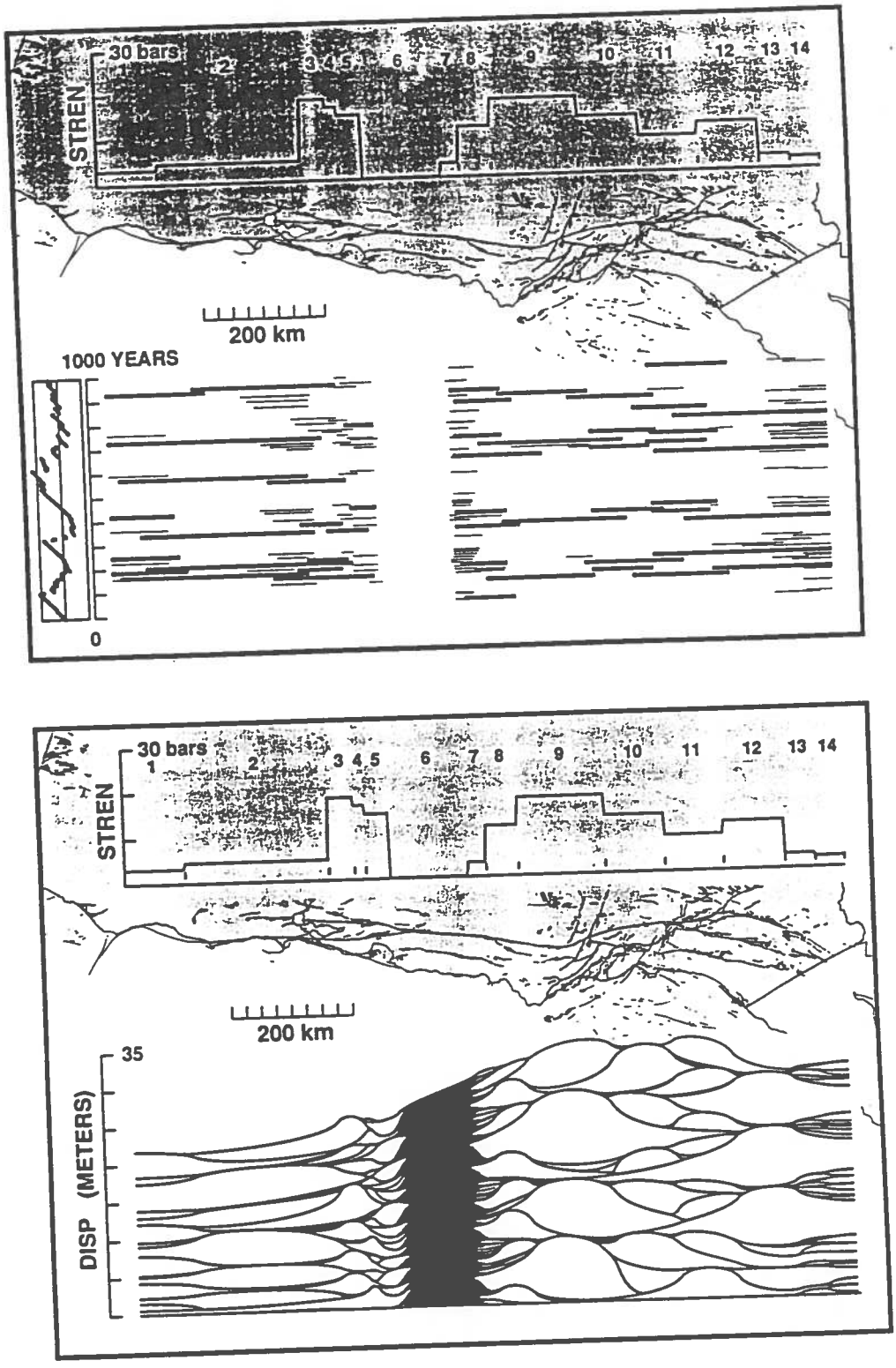

Figure 1. Synthetic seismicity (*top*) and displacement from the initial 1000 years of a 6000 year run of a San Andreas Fault model based closely on the WGCEP segmentation. Length, position and strengths of the 14 segments are drawn along the top. Only events with $M \geq 6$ are shown. Bold line segments are $M \geq 7$ events. The blackened area in the central creeping section is aseismic slip. Note the mixture of characteristic and non-characteristic slip patterns in each segment.

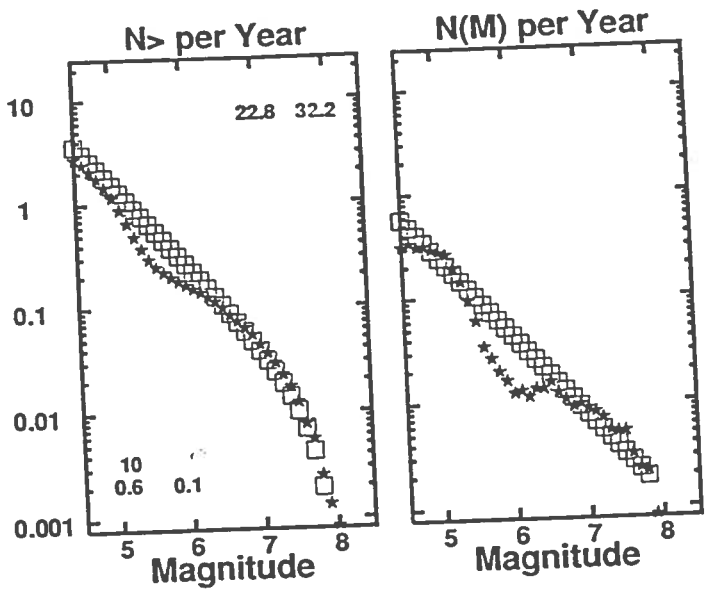

Figure 2. Observed seismicity (*boxes*) and synthetic seismicity (*stars*) from the model of Figure 1. The observed seismicity includes events within a 40 km wide band of the SAF. The WGCEP segmentation produces far too few magnitude 6 earthquakes, but it adequately represents events larger than 6.5.

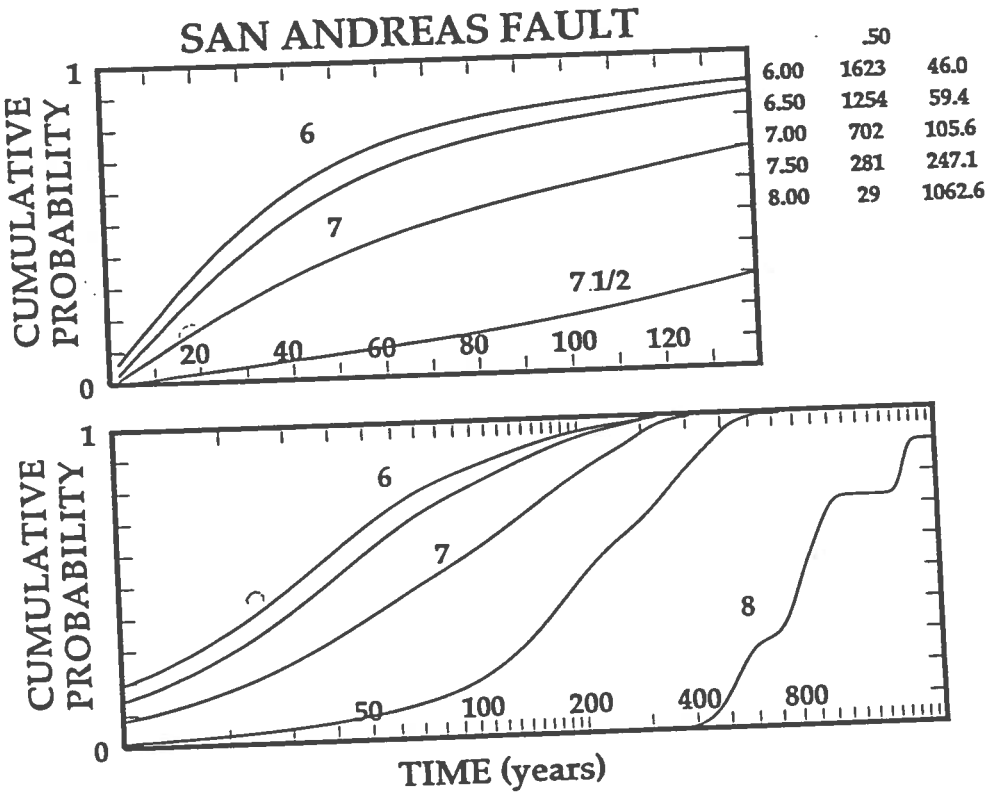

Figure 3. Cumulative probability for the recurrence of a $M \geq M_o$ earthquake within T years of a previous $M \geq M_o$ event. M_o covers the range M_o= 6.0 to 8.0 in 0.5 increments. Curves were tabulated from a 6000 year run of synthetic seismicity for the SAF model. A segment is considered broken if more than 50% of its length slips during an earthquake. Numbers to the upper right give M_o, the number of segment recurrences, and the mean recurrence time. As can be seen in the steepening slopes of the curves, earthquakes tend to become more periodic with increasing magnitude. The concept of seismic gaps is useful for events of magnitude larger than about 7. For smaller quakes, increasing the gap time has little or diminishing effect on conditional probability of recurrence.

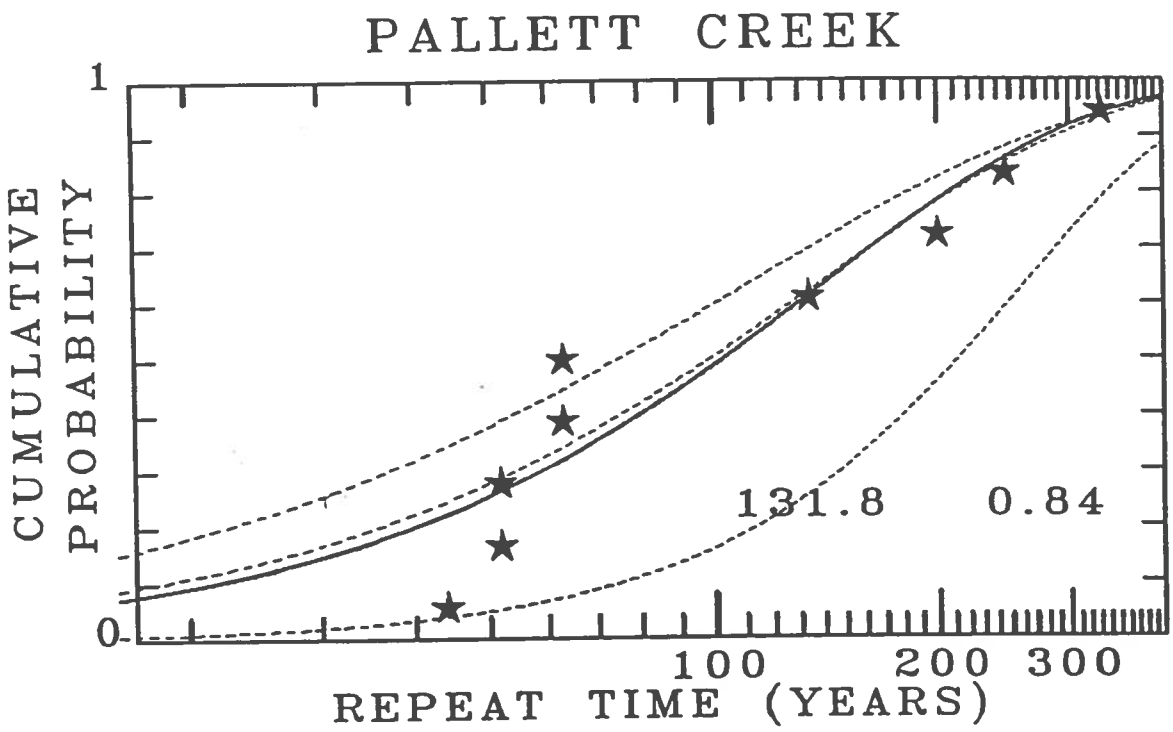

Figure 4. Cumulative probability Weibull fit (*solid line*) to the nine earthquake recurrence times given by Sieh (1989) for the Pallett Creek area of the Mojave segment. Left to right, the dashed lines are the predictions from the synthetic seismicity model for magnitudes greater than or equal to 7.0, 7.25 and 7.5. The predictions for events in the 7.0 to 7.25 range have no argument with the data.

Progress Report for the Southern California Earthquake Center

Project : Groundwork for the Master Model
P.I.: Steven G. Wesnousky

For the year beginning February of 1992, we proposed to

1. Complete the update and synthesis of slip rate and paleoearthquake data for all known and remaining southern California faults and seismogenic structures (e.g. blind thrusts).
2. Place information in tabular format for easy input into a GIS data base.
3. Reevaluate observations bearing on segmentation and recurrence behavior for all faults.
4. Use all of the above to reconstruct hazard maps like those published in Wesnousky (1986), and provide output of hazard calculations to Lucy Jones to establish real-time hazard hazard maps based on estiamtes of probability gain due to possible foreshocks.
5. Incorporate the recurrence rate of lesser-sized, though potentially still damaging events into the construction of the hazard maps and, hence, master model.

I list the progress with respect to each of these tasks below.

1. The synthesis is complete (ignoring any possible findings which have arisen during the last couple of months) for mapped fault traces. Most of this synthesis was provided to SCEC in April of 1992. I have made no headway with the inclusion of possible buried seismogenic structures. I would like to meet with the P.I.'s of the Quaternary Faulting/Structural Geology Task to determine which model and input parameters are most appropriate to consider for buried sources, such as the Whittier thrust, prior to placing this information into a hazard model. I anticipate progress on this latter front subsequent to the annual October SCEC meeting.

2. The slip rate and paleoearthquake data compiled for surface faults is in a format readily input into any GIS data base, as evidenced by the preliminary report turned into the Center during April 1992.

3. Progress on this effort has been delayed because of an increased effort to incorporate site effects into the hazard analysis, which is listed in (4) below. Upon Mark Petersons arrival, we will commence this effort of segmentation. **It is important that the Master Model and Quaternary Fault groups meet to discuss this matter before it is pursued. Before continuing, we would like to understand whether the task of segmentation will be left primarily in out hands, or will it be a group effort.** As well, we will eventually examine the sensitivity of seismic hazard calculations to various scenarios of segmentation.

4. A good deal of effort has been spent in adapting the hazard programs of Wesnousky (1986) to the computer system available at UNR. As well, it has been my sense that it is the incorporation of site amplification effects which will produce the most profound additions to our regional understanding of seismic hazard in Southern California. For that reason, prior to Mark Petersons arrival at UNR, Mark and I have already joined forces toward incorporating his work on site amplification in southern California with my hazard codes and regional data base of active faults. Toward that end (and with the assistance of Duncan Agnew), the digitized geology (at 1/2 minute intervals) of Southern California is now on our computer. The detail availabe is shown at the top of Figure 1 for the San Bernardino $1^{o}x2^{o}$ sheet. The colors red, green and yellow represent intermediate to hard-rock (crystalline), soft rock (Tertiary sediments), and Quaternary alluvium, respectively, for which Mark Pederson's work with the 1972 San Fernando earthquake suggests amplification factors of 1.0, 2.0, and 3.0, respectively, for pseudo-velocity response at 3 seconds. The map at the top of Figure 2 shows the expected pseudo-velocity response at 3 seconds for the Landers earthquake for hard rock sites. The blues represent values of 5 to 30 m/s and the reds range for 60 to 100 m/s. The lower map is for the same Landers earthquake source, but we have included the above site-amplification values. The difference between the upper and lower maps of figure 2 emphasizes the fundamental importance of understanding and incorporating site effects into SCEC's regional seismic hazard maps. The map at the bottom of Figure 1 shows, with the same color scheme, the expected pseudo-velocity response at 3 seconds at the 10% probability level during the next 30 years for all faults in the region, using the updated fault slip rate data set and the same assumptions of segmentation outlined in Wesnousky (1986).

5. The combination of fault slip rate and paleoearthquake information with the instrumental record of the CIT-USGS catalog to determine the shape of the earthquake frequency curve for the southern San Andreas, Garlock, San Jacinto, Elsinore, and Newport-Inglewood faults has been completed. I am now in the process of checking the sensitivity of the results to the size of the box used to define the 'zone' of seismicity along each fault.. The results show that the San Andreas and Garlock show a characteristic-earthquake type recurrence curve whereas the San Jacinto and Newport-Inglewood (less-well constrained) appear to fit the classic Gutenberg-Richter type relationship. The next step is to integrate these empirical curves into the hazard codes.

Figure 1

Figure 2

Group B: STRONG GROUND MOTION PREDICTION

Group Leader: Ralph Archuleta

* This Progress Report under Group A.

1992 SCEC SUMMARY REPORT
SCEC STRONG MOTION WORKING GROUP

Synthesis of progress reports with contributions from Keiiti Aki, John Anderson, Ralph Archuleta, Ornella Bonamassa, Byau-Heng Chin, Steven Day, Marijan Dravinski, Don Helmberger, Hiroo Kanamori, Thorne Lay, Harold Magistrale, Craig Scrivner, Sandra Seale, Raj Siddarthan, Jamison Steidl, M Takeo, Alexei Tumarkin, John Vidale, David Wald and Guang Yu.

The primary emphases within the Strong Motion Working Group (SMWG) has been quantitative analysis of the effect of local site conditions on strong motion and numerical prediction of strong motion by earthquake simulations. The approach has varied from direct measurements to theoretical analysis using nonlinear analysis. Many of the investigators have used the recent earthquakes in southern California (Joshua Tree, Landers and Big Bear) to focus their research.

Dravinsky has been using microtremor recordings to infer long-period spectral characteristics of different regions within southern California. In particular they have recorded microtremors at 148 sites within the Los Angeles basin. All of the basin measurements are then compared to recordings at a reference site. In addition to the LA basin, they have used this approach for the San Fernando Valley and also at Pipes Canyon (Landers epicentral region). The latter experiment will be particularly useful because it is the location of two dense arrays of portable accelerometers: one on rock and the other on soil. This microtremor technique allows for many different sites to be evaluated quickly and in a period range that is critical to long-period structures.

Recording earthquakes in an urban environment using portable recorders/sensor has been the focus of Day and Magistrale. Taking advantage of the Landers earthquake sequence they were able to record some of the larger aftershocks in both the epicentral region and San Diego. Again it is clear from the records that alluvial sites both amplify and prolong the shaking as compared to rock sites.

Predicting strong ground motion from weak motion has always been a major scientific issue. One of the common factors in the analysis of local site effects is that some station or group of stations will serve as the control point from which relative amplification or attenuation can be measured. One of the ideal situations is where the accelerometer on a rock site is in a borehole. This situation exists at Garner Valley where Archuleta, Tumarkin and Steidl have been examining the data from a vertical and horizontal array of accelerometers. Using the data from the Joshua Tree, Landers and Big Bear earthquake sequences they have examined several methods of inferring the ground shaking on alluvium based on a rock record. Using aftershocks of Joshua Tree to predict the amplification of the mainshock they find that the optimum method is based on the gain function (cross-spectrum) rather than the more typical spectral ratio. This method also allows errors to be assigned to predictions of amplification.

The other fundamental question is to what degree, if any, does a alluvial site respond nonlinearly. Basically is the response of the alluvial or soil site dependent on the amplitude of the seismic waves? While there are many laboratory experiments to show this is true for large strains, the seismic observations are more limited. Aki and Chin have been comparing synthetically derived peak accelerations for comparison with Landers records. They see a major difference in their prediction of peak acceleration for soil sites: synthetic values are always greater than recorded values for distances less than 50 km, the region where the largest peak accelerations are recorded. For rock sites they find that there is no systematic difference at distances less than 50 km.

This question of nonlinearity is at the center of Anderson, Yu and Siddharthan's research. Using nonlinear codes for simulating the response of a soil site to different levels of input ground motion they found that the effect of nonlinearity depends on the frequency band which is being examined. The frequency bands are determined by the dominant frequency of the soil column being studied. The low-frequency band is that less than the dominant frequency; the central band is that centered around the dominant frequency and the high-frequency band is that greater than the dominant frequency. The nonlinearity does not affect the lowest frequency band; it decreases the spectral amplitude of the central band at the expense of higher frequency waves; and it increases the spectral amplitudes of the highest frequency band. An interesting result is that if examining the spectrum of a soil that has experienced nonlinear behavior, one would infer a lower linear attenuation. Anderson and others are now examining accelerograms likely to show nonlinear response. As they point out the data are more complicated than theoretical predictions.

The complications of the data are evident in the records being analyzed by Vidale, Lay and Bonamassa. Using recordings of the 1989 Loma Prieta aftershocks they have demonstrated that site effects are spatially varying over distances as small as 25 m. It appears that the site resonances may not only vary spatially but also azimuthally. The cause of these variations are being examined by doing a short-baseline refraction experiment to determine the underlying structure. The time series recorded in the refraction experiment imply a 3-D complexity that is now being examined.

Although the local site effects play a critical role in the observed ground motion, clearly the effects of the source itself cannot be ignored. How the ground motion originates and how it reaches the site are important questions that SMWG has tried to investigate. Takeo and Kanamori have been working on analysis of the 1923 Kanto, Japan, earthquake. The records of the Kanto earthquake are an analogue to the Los Angeles basin in the event of major/great earthquake. They find that the 5% damped velocity response spectrum is 120 cm/s at a period of 13 s and 50 cm/s at 7.5 s. As part of their study they have been able to quantify the effects of key source parameters on the response spectrum as well as the effect of lower-velocity surface

material. For example, the lower velocity surface material can amplify the ground motion by about 1.4 for periods longer than 5 s. The rise time of the slip on the fault can increase the response spectrum by about a factor of 2 at periods less than 10 seconds.

Although the distribution of nearby strong motion accelerometers is sparse for the Landers earthquake, the azimuthal coverage is enhanced by the TERRAscope stations. Seale is using the digital accelerograms from TERRAscope to examine the nature of the rupture of the mainshock. Using the isochron method of Spudich and Frazer (1984) and the slip distribution from the field (Sieh et al., 1992) Seale has made an initial attempt to predict the accelerations at distances of 60-160 km from the earthquake. The isochron method computes only the direct S- and P-wave response. The preliminary results show that surface waves make a major contribution at these distances.

The velocity structure is critical when the waves are travelling large distances and whenever there are major changes in the velocity structure, e.g., waves from Landers into the LA basin. The effects of the LA basin structure on seismograms have been examined by Helmberger, Wald and Scrivner. They find that the basin edges are effective sources for generating complex arrivals in the seismograms. Like others in the SMWG they have examined the strong motion records for Landers. They have constructed a slip model consistent with displacements (doubly integrated accelerations) from five of the closest accelerometers plus the four TERRAscope records.

In summary the SMWG has continued its fundamental research into the two areas that are critical to predicting strong motion: the earthquake source and the local site effects. With the recent earthquakes in southern California the SMWG has been able to not only gather new data but analyze it quickly. Several investigators have already produced slip models consistent with the particle displacement for the Landers event and others are working toward predicting particle accelerations. The recent data has simply reinforced the importance of site effects. Exactly how to extrapolate the results from places where we have direct measurements to a regional scale where data do not exist is being approached from both microtremors and coda measurements. We are now making progress on scaling the weak motion to strong motion including effects of nonlinearity, though nonlinearity may have many faces all of which we have not seen.

Non-Linear Effects on Strong Ground Motion

Southern California Earthquake Center
Annual Summary Report - September, 1992
John G. Anderson[1], Guang Yu[2], Raj Siddharthan[3]

The seismological community has become increasingly interested in non-linear soil response as a part of the effects of complex site response on strong ground motions. During the first year of this project, we initiated a numerical study of non-linear behavior of soils in response to seismic ground motions. Our object was to develop a more thorough understanding of what phenomena seismologists ought to be looking for in ground motions. During the second year, this initial project was completed, and a manuscript was accepted for publication[4].

A numerical code for calculating the time domain response of a non-linear soil to base excitation is used to examine the characteristics of strong motion accelerograms recorded in soil. The results verify several of the effects that are usually cited as evidence of non-linearity: decreased spectral ratios of surface to input motion near the dominant frequency of the soil; decreased statistical uncertainty in prediction of peak acceleration and increased effective period of the surface motion. When examined in the Fourier transform domain, the results show that soil is not effected by the non-linearity. In the central band, the spectral amplitudes are decreased. The increase in the dominant period is caused primarily by a strong decrease in the amplitude of shorter period waves, rather than by amplification of low period motion. Above a cross-over frequency, however, the spectral amplitudes at the free surface are increased relative to linear soil response calculations. This is a consequence of the sudden change in the stiffness of the soil at reversals in the stress-strain curve. This increase in spectral amplitudes at high frequencies causes the spectral decay parameter to decrease for the soil model that was used. The transition frequencies separating these three types of behavior shift to lower frequencies as the thickness of the soil layer is increased.

The experience in these computations provides a basis for investigation of data. For year two, we proposed to complete the above research, and then to carry out a reconnaissance of strong motion data worldwide to identify likely candidates for non-linear behavior, and to investigate whether these none-linear effects are observed. This effort is still underway. At the moment, we are concentrating on a data set from the Acapulco, Mexico region, where several stations on rock and nearby sediments have recorded several moderate and a few strong earthquakes in the past two years. For example, on one station there, we have high quality digital accelerograms with peak accelerations ranging from 18 cm/sec^2 (May 11, 1990, M4.9) to 27 cm/sec^2 (May 31, 1990, M5.9) to 335 cm/sec^2 (April 25, 1989, M6.9) in earthquakes with magnitude 5 to 7. There is the possibility that the larger record shows some signs of non-linearity in terms of a frequency shift of the site response. The spectral decay parameter is the same for both records.

This example also reveals a difficulty of identifying non-linearity when one does not have combination of up-hole and down-hole or rock and adjacent soil sites. The difficulty is in determining a ground motion at the station to use as a reference for what would be expected in the linear case. For example, one approach is to use a simple method of predicting the spectrum on the basis of other stations in the region, and then to look at the residual spectrum of the targeted station from that prediction. Applying this method, the record from the April 25, 1989 earthquake has a much larger positive

residual than the record from the May 31, 1990 earthquake at frequencies near the spectral peak, which is the opposite of what is expected on the basis of the model predictions. At other nearby stations, there is not any significant difference in residuals at the frequencies involved. Other wave propagation phenomena may be involved in this case since the azimuths of the two events differ, complicating the situation, and reducing the confidence in identifying non-linear behavior.

[1, 2] Seismological Laboratory and Department of Geological Sciences, Mackay School of Mines, University of Nevada, Reno, Nevada 89557

[3] Department of Civil Engineering, University of Nevada, Reno.

[4] Guang, Yu, John G. Anderson, and Raj Siddharthan, On the Characteristics of Non-Linear Soil Response, BSSA, in press.

SCEC PROGRESS REPORT: WEAK-TO-STRONG MOTION SCALING

P.I.: RALPH J. ARCHULETA
INSTITUTE FOR CRUSTAL STUDIES, UCSB

What is the optimum method for predicting site response that allows a reliable means of scaling weak motion to strong motion? The commonly used spectral ratio method has an insufficient error analysis and can lead to possible misinterpretations of the site response. The theoretically optimum estimate of the amplification between two sites is the ratio of their cross-spectrum to the power spectrum of the reference site. The coherency between the two sites can be used to assign error to this estimate. A third possibility is the ratio of response spectra. The goal of this study is to determine the advantages and limitations of each method and provide guidelines for their applications in engineering and seismological practice.

Joint analysis of the horizontal motion is used for examining all methods. It treats both horizontal components simultaneously as a complex signal that accounts for the horizontal amplitude and phase. The complex representation considerably enhances all of existing methods for examining site response. The research in progress will lead to a more robust analysis of site response that accounts for the complete horizontal motion and assigns errors to estimates. Its effectiveness will be evaluated using the unique set of downhole and surface strong motion data recorded at sites with different geology.

A unique set of data from the 1992 Southern California Earthquake Sequences provides an opportunity to quantify the strengths and weaknesses of each method. The data include digital accelerograms from SCEC's portable recorders placed in the epicentral regions; from the Garner Valley Downhole Array; as well as the accelerograms from the CSMIP and the USGS permanent accelerographs.

a. Rotary-component method for representation of the horizontal motion.

In order to construct an accurate representation of the horizontal motion we treat both horizontal time histories simultaneously as a two-dimensional signal by forming a complex time-series:

$$A_H(t) = A_X(t) + i \cdot A_Y(t)$$

where,

$$(A_X(t), A_Y(t), A_Z(t))$$

represents the two horizontal (X&Y) and the vertical (Z) components of the record (accelerogram). The amplitude of $A_H(t)$, being the square root of sum of squares of values of both horizontals at the same moment, is exactly the total amplitude of shaking (acceleration) in the horizontal plane. The amplitude spectrum of the complex time-series $A_H(t)$ provides the total amplitude of horizontal motion at a given frequency. By combining the two horizontal components as the real and imaginary parts of the complex time-series our results do not depend on directions of components; we need not consider two spectra individually, rotate the axes or take the RMS of two spectra. An advantage of this approach is that we do not need to revise existing algorithms for processing seismic data. In fact the whole digital spectral analysis is designed for complex signals (e.g., Cooley-Tukey's FFT) treating real signals as complex ones with imaginary part being identically zero [*Marple*, 1987].

b. Spectral estimation.

The standard approach in evaluating the site response at a particular location is to compare the spectral amplitude of the ground motion at the site of interest to the spectral amplitude of a reference site. This is done by first processing the observed site spectra to reduce the effects of noise. The resulting spectral ratio estimate depends on the choice of smoothing technique which obviously affects the amplitudes more significantly than the resonant frequencies [*Safak*, 1991]. We are using other methods of spectral estimation: auto-regressive (Burg's maximum entropy) and Welch's periodogram methods. Thus we have an additional way of controlling the quality of the spectral ratio approach. The comparison of results obtained by these methods is shown in Figure 1a.

c. Optimum estimate of the transfer function.

In order to have more robust estimates of amplification factors (frequency response functions) we use the following expression:

$$H(f) = \frac{S_{12}(f)}{S_{11}(f)} \qquad (1)$$

where H(f) is the frequency response function between the reference Site 1 and Site 2; $S_{12}(f)$ is the cross-spectrum of Site 1 and Site 2 records, $A_1(t)$ and $A_2(t)$; and $S_{11}(f)$ is the power spectrum of $A_1(t)$ [e.g., *Lu et al.*, 1991, 1992; *Safak*, 1991]. H(f) is the optimum estimate of the transfer function between Sites 1 and 2 that minimizes the output noise at each frequency [*Bendat and Piersol*, 1980]. The coherence function:

$$\gamma_{12}^2(f) = \frac{|S_{12}(f)|^2}{S_{11}(f)S_{22}(f)}$$

can be used to evaluate the random error associated with H(f). This error depends in an explicit way on the number of observations. The practical impact is that by using it, we can plan our field experiments for achieving the desired accuracy of estimates of the site amplification. The deviation from unity in the coherence function is either due to noise in the signals or nonlinearity in the system between the input and output.

Figure 1b shows the site response at the GVDA surface instrument, calculated for the Joshua Tree M_L6.1 mainshock using the 220 m downhole instrument as the reference site. This figure shows the utility of our analysis technique by comparing the standard power spectral ratio with the frequency response function (gain) shown in equation (1). The peak in the power spectral ratio at 1.75 Hz is seen as a hole in the gain function. Figure 1c shows the coherence function plotted vs. frequency. At 1.75 Hz there is a hole in the coherence function which corresponds to the peak in the power spectral ratio. This peak is an example of feedback in the system. It is an artifact of the destructive interference between the up-going and down-going waves between the surface and the 220 m downhole instrument. Examination of the standard power spectral ratio alone (or any other spectral ratio estimate, as seen from Figure 1a) would allow one to misinterpret the peak at 1.75 Hz as a site resonance. The cross-spectrum method based on calculating the cross-spectrum does not produce this peak and prevents misinterpretation of the site response.

The coherence function is useful in that it provides a means of examining the error in the gain function. The random error associated with an estimate of the gain factor from n_d measurements is calculated as:

$$\varepsilon_r = \frac{\left(1-\gamma_{12}^2(f)\right)^{1/2}}{|\gamma_{12}(f)|\sqrt{n_d}}. \qquad (2)$$

When the coherence between a site and reference signal is close to unity, the gain function can be evaluated with confidence. Where the coherence drops from unity, the confidence in the gain function is worse. Figure 2a shows the gain function (dashed curve) for the surface instrument at GVDA determined from the downhole and surface recordings of the M_L4.6 Joshua Tree foreshock and two aftershocks (M_L4.5 and M_L4.8). The error envelope (95% confidence) is plotted (dotted curve) along with the gain function. The errors increase at regions where the coherence drops from unity. The error curve represents the limits on the amplification we would expect to observe at this site given an input motion at the downhole sensor. The actual gain function for the M_L6.1 Joshua Tree mainshock is plotted in Figure 2a as well (solid curve). We can see that the observed site response for the mainshock falls within the error bars predicted by the weaker motions. The corresponding estimate of amplification obtained from power-spectral ratios is shown in Figure 2b.

The preliminary analyses suggest that:

1) this new technique for robust estimation of site amplification using the complex representation of horizontal motion provides an improvement over previous methods;

2) the most reliable approach to estimating the site response is based on the joint analysis of results obtained by all three methods (spectral ratios, cross-spectral and response spectral ratios).

Having a means of assigning error to the gain function provides structural engineers with bounds on the site amplification. The use of the coherence function to assign errors demonstrates that the standard approach of using few observations at two instruments separated by distances on the order of several kilometers does not produce very accurate estimates of the site response except at specific frequencies. Using the coherence function allows us to address a practically important problem of knowing the number of observations required to reach a specified accuracy for the site amplification estimate at a given frequency. The comparison of results of different methods allows one to make a more reasonable estimate of what we really know and what we don't know when referring to the site response.

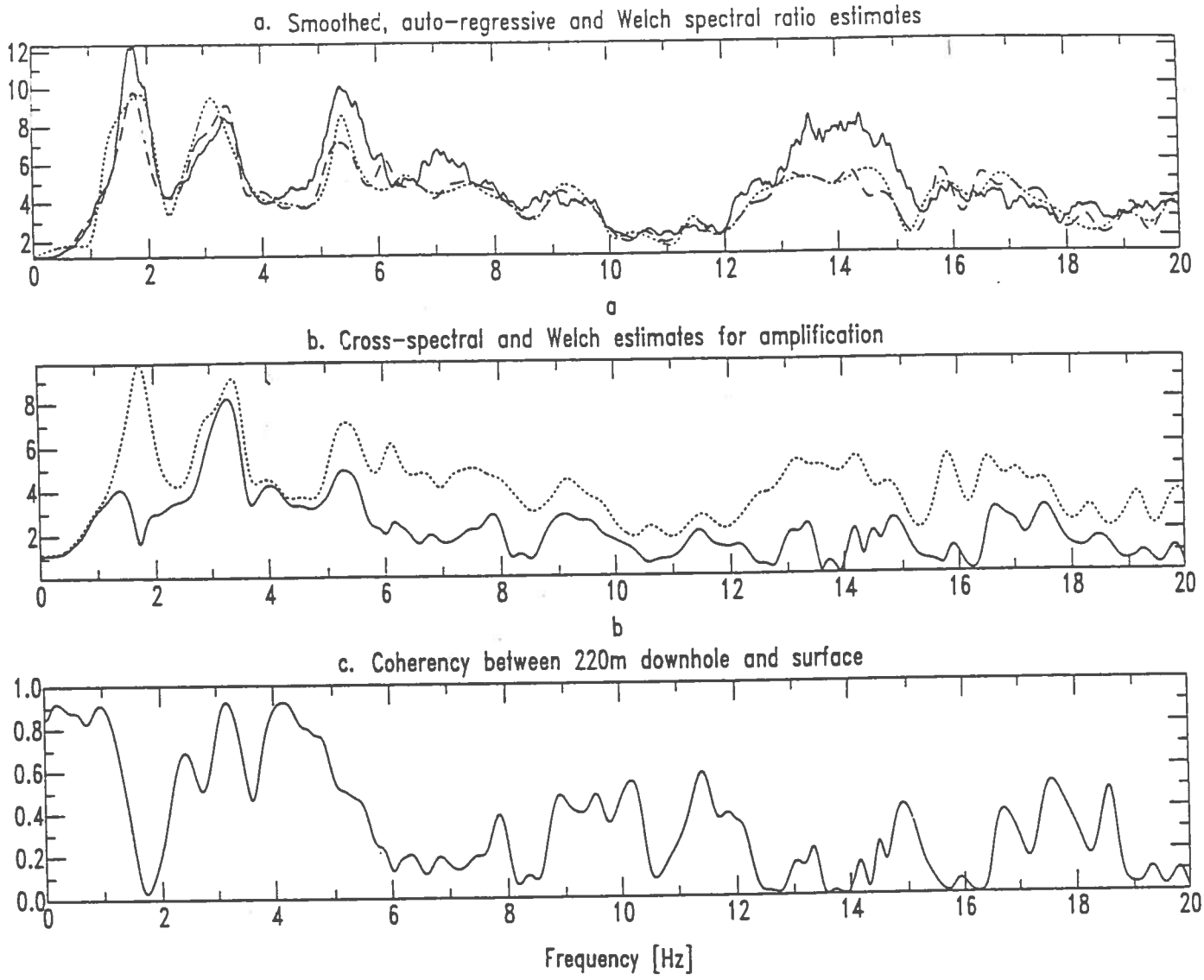

Figure 1. Amplification and coherency between 220 m downhole and surface records at the GVDA for the Joshua Tree mainshock. We use the complex representation of horizontal motion in all methods.

a. Comparison of three spectral estimation methods for site amplification studies: ratio of smoothed spectra (solid), ratio of Burg's auto-regressive fits (dotted), and ratio of square roots of Welch's perodogram estimates (dashed).

b. Comparison of the estimated site amplification using the two techniques: cross-spectral (expression (1)) (solid curve) and spectral ratio (dotted curve). We use Welch's periodogram method for estimating both the cross-spectrum and power spectra.

c. Plot of coherency vs. frequency between 220 m downhole and surface records. The notch in the coherence function around 1.75 Hz indicates that the peak at 1.75 Hz in all spectral ratios is an artifact of the receiver geometry.

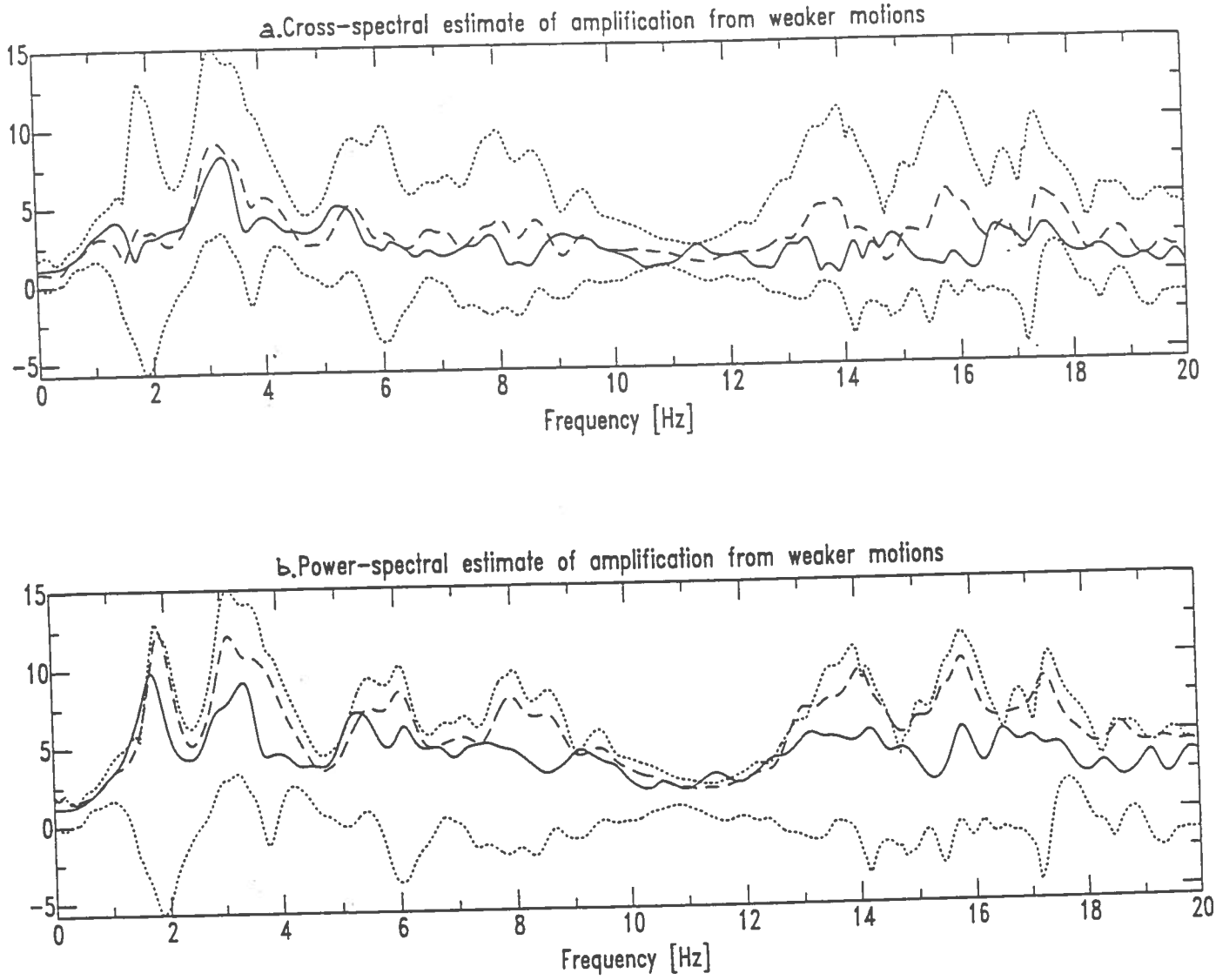

Figure 2. Whole record amplification vs. frequency calculated using the 220 m downhole (reference site) and surface instrument (soil site) recordings at GVDA of the Joshua Tree M4.6 foreshock, M4.8 and M4.5 aftershocks. We use the complex representation of horizontal motion. Calculated error envelope (formula (2)) for this prediction is shown by dotted curves. The amplification determined from the Joshua Tree M6.1 mainshock plots within the error envelope calculated from the prediction using the foreshock and aftershocks.

a. Average gain function for the Joshua Tree M4.6 foreshock, M4.8 and M4.5 aftershocks (dashed curve) and observed gain function for the Joshua Tree M6.1 mainshock (solid curve) .

b. Average spectral ratio (Welch's periodogram method) for the Joshua Tree M4.6 foreshock, M4.8 and M4.5 aftershocks (dashed curve) and observed for the Joshua Tree M6.1 mainshock (solid curve) .

Strong Motion Prediction For Soil Sites

Steven Day and Harold Magistrale, Department of Geological Sciences, San Diego State University, San Diego, CA 92182

Among the primary objectives of the SCEC are development, testing, and application of methodologies for the prediction of strong ground motion. The purpose of our project is to further develop the Green's function summation method for synthesizing site-specific strong ground motion. This includes participation in collaborative deployments of portable instruments to record site responses and empirical Green's function estimates.

It was originally envisioned that SCEC recording experiments would focus on the Los Angeles basin. However, our effort for this year was diverted to a study of aftershocks of the Landers and Big Bear earthquakes of June 28, 1992. In response to these events, we (i) deployed 3 of our portable data loggers, equipped with force balance accelerometers, near the rupture zone of the Landers mainshock, and (ii) deployed 3 data loggers, equipped with velocity sensors, in the San Diego urban area.

The Landers deployment was undertaken in coordination with other SCEC institutions, including UCSD, UCSB, USGS and USC. The instruments were operated in the Landers area from the date of the mainshock, June 28, until August 6. Station locations are given in Table 1. The locations were chosen for azimuthal coverage of the mainshock area and to colocate at sites with permanent, analog accelerometers. During the first 2 weeks of this period, the accelerometers were recorded at low gain, and during the remainder of the deployment, we simultaneously recorded high- and low-gain channels. We also recorded the USGS calibration shots on July 16. Objectives of the Landers recording include: (i) obtain travel time data for tomographic inversion studies and improved aftershock hypocenter locations, (ii) record strong motion from the larger aftershocks, (iii) contribute to source studies of the larger aftershocks, (iv) obtain path and site response information at permanent accelerograph sites that recorded the mainshock. We recorded several hundred events. The Landers data has been forwarded to UCSD to be incorporated with records from other SCEC portable instruments.

The San Diego portion of the study was aimed at recording empirical Green's functions in urban areas. The Landers/Big Bear aftershock sequence provided us an opportunity to record path and site responses appropriate to great earthquakes on the San Bernardino Mountain and Coachella Valley segments of the San Andreas fault. We reoccupied sites previously occupied in San Diego under another project, and added new urban sites, located on Holocene alluvium and on a Plio-Pleistocene sedimentary formation, respectively. The simultaneous recording of prospective empirical Green's functions by the SCEC portable instruments in the epicentral region ensures that the source properties of the events will be well constrained. Figure 1 shows an example of an event which was recorded by both the epicentral portable stations and the San Diego portables. The new Holocene site displays resonances similar to those seen at other San Diego Holocene sites.

Table 1. SDSU Landers recording sites

site	latitude	longitude	elevation (m)
HILL	34 21.72	-116 27.19	920
LADY	34 07.94	-116 08.76	841
RIMR	34 11.18	-116 27.76	1125
FIRE	34 02.88	-116 34.62	792

Figure 1. (next page) Vertical component recordings of a M 5.2 Landers aftershock at 7:40 July 1, 1992 (UTC) near the mainshock location. The top 3 panels are acceleration records from the Landers aftershock zone and the lower 2 panels are velocity records from hard rock (JOHN) and Holocene alluvium (NATC) sites in San Diego.

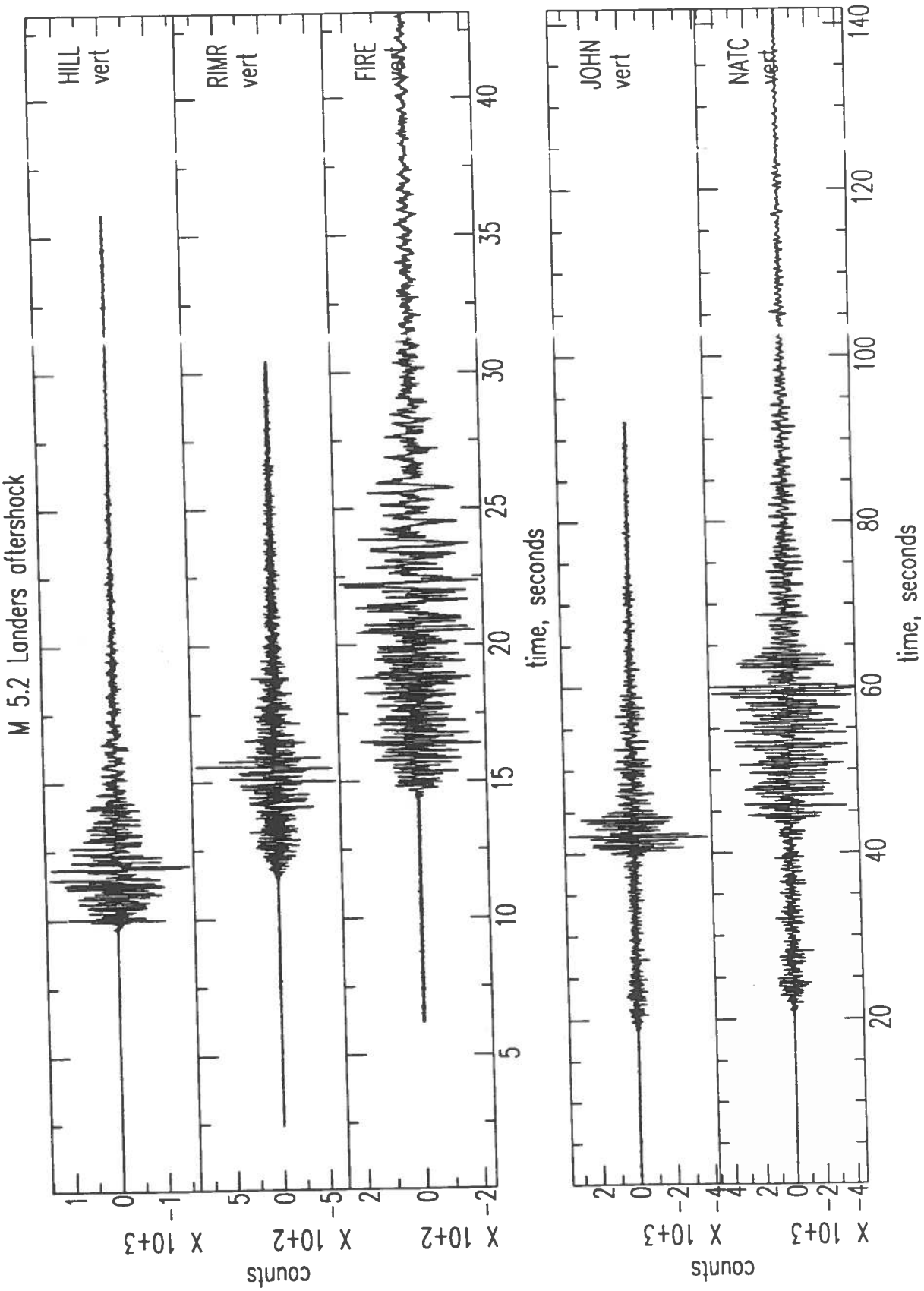
M 5.2 Landers aftershock
HILL vert
RIMR vert
FIRE vert
JOHN vert
NATC vert
counts
X 10+3
X 10+2
time, seconds

Strong-Ground Motions in Los Angeles (continuation)

Don Helmberger, David Wald and Craig Scrivner
California Institute of Technology
Pasadena, California 91125

Summary

Objective: We are analyzing ground motions within the Los Angeles Basin from recordings of earthquakes with well known source parameters, including the October 4, 1987 Whittier Narrows aftershock (ML = 5.3) and the June 28, 1991 Sierra Madre mainshock (ML = 5.8). Forward Waveform modeling of this data allows a more accurate estimate of 2D and 3D velocity structural features that strongly affect ground motion amplitude, duration and frequency content. In turn, these models will provide a clearer picture of the complex basin and ridge structures within the basin as provide increased precision on source locations and fault definition. Additionally, the recent occurrence of the 1992 Landers earthquake (Ms=7.4) has provided a unique opportunity to augment the Los Angeles Basin study with ground motion and source analyses of a large, damaging earthquake within the Southern California region. Hence, we will report on two strong-motion studies, namely 1) two-dimensional modeling of deep sedimentary basin effects and 2) broadband and strong-motion analysis of the 1992 Landers earthquake. The development of an adequate spatial and temporal characterization of slip for the earthquake source is necessary to begin analysis of the effects of propagation and site response on damaging long-period strong-ground motions.

Results: 1) Sedimentary basins are quite effective in trapping and focusing seismic energy. A distinctive feature of ground motion recorded within the Los Angeles Basin is the large amplitude of the first multiple (SS) of the shear waves on the horizontal components. Triple S can also be seen on many records. For the Whittier Narrows aftershock, the waveforms were recorded at stations within 25 km of the epicenter. At such short range, a horizontal seismic velocity gradient is needed to turn rays rapidly enough for large amplitude multiples to form, and this was taken as a primary constraint in the construction of our two dimensional velocity model. A forward modeling approach was employed, using generalized ray techniques and finite difference numerical solutions. A model mimicking a recently constructed geologic cross section across the east edge of the L.A. Basin generates more phases than are seen in the seismic records, and these phases interfere with each other in a complex manner. Simpler models based on dipping sub parallel layers with very low shear velocities in the top few layers fit the data better and the phases are more stable between receivers. The seismic velocity, depth and dip of the layers were varied to fit the timing between the direct SH arrival and the first multiple. When the absolute timing of the direct P and S phases is included as an additional constraint, the data can only be fit by increasing the velocity just above hypocentral depth to values expected 5 to 10

km deeper in the crust, while decreasing the velocity of the shallowest layers in the top few kilometers. The amplitude of the direct and first multiple SH pulses is well modeled, but the phase of the first multiple does not match the data. A steeply dipping edge on the west side of the basin model has little effect on the large amplitude multiples in the synthetics except at distances near that basin edge. The Sierra Madre mainshock occurred about 25 km to the NE of the edge of the L. A. Basin. The model discussed previously was extended this distance; a shallow basin between Whittier and the Sierra Madre hypocenter is included to account for the San Gabriel basin. Phases generated by the edge of the deep basin continue to dominate the synthetics.

2) Preliminary results of ongoing modeling of the Landers earthquake are presented here. Our goal is to determine a source rupture model for the 1992 Landers earthquake consistent with data over a wide frequency range from zero to several Hz. We are developing the ability to model the seismic data (near-field and regional strong motions and broadband teleseismic waveforms) with a variable-slip, multiple-segment, finite-fault model that can also explicitly include constraints from observations of fault surface offset and geodetic displacement. We are particularly interested in determining the temporal and spatial relationship of surface offset with the slip at depth. Our model consists of three fault segments (Figure 1, dashed lines) to accommodate the complex geometry of the mapped surface offset (Figure 1, dark lines).

An initial waveform inversion of a subset of the local strong-motion records (including Amboy, Barstow, Big Bear, Lucerne Valley, Morongo Valley, and Joshua Tree, see Figure 1) combined with near-regional TERRAscope data is presented in Figure 2. We find two main asperities separated by roughly 30 km and a seismic moment of $Mo = 0.8 \times 10^{27}$ dyne-cm. The combined use of near and far-field strong motions is necessary in that the large rupture length (70 km) and sparsity of local accelerograms results in near-in stations with significant distances from some segments of the fault, producing spatial aliasing; yet, the TERRAscope data alone cannot resolve the local slip velocity. We are currently augmenting the waveform inversion analysis to include the observational constraints provided by both the geodetic and surface-offset data.

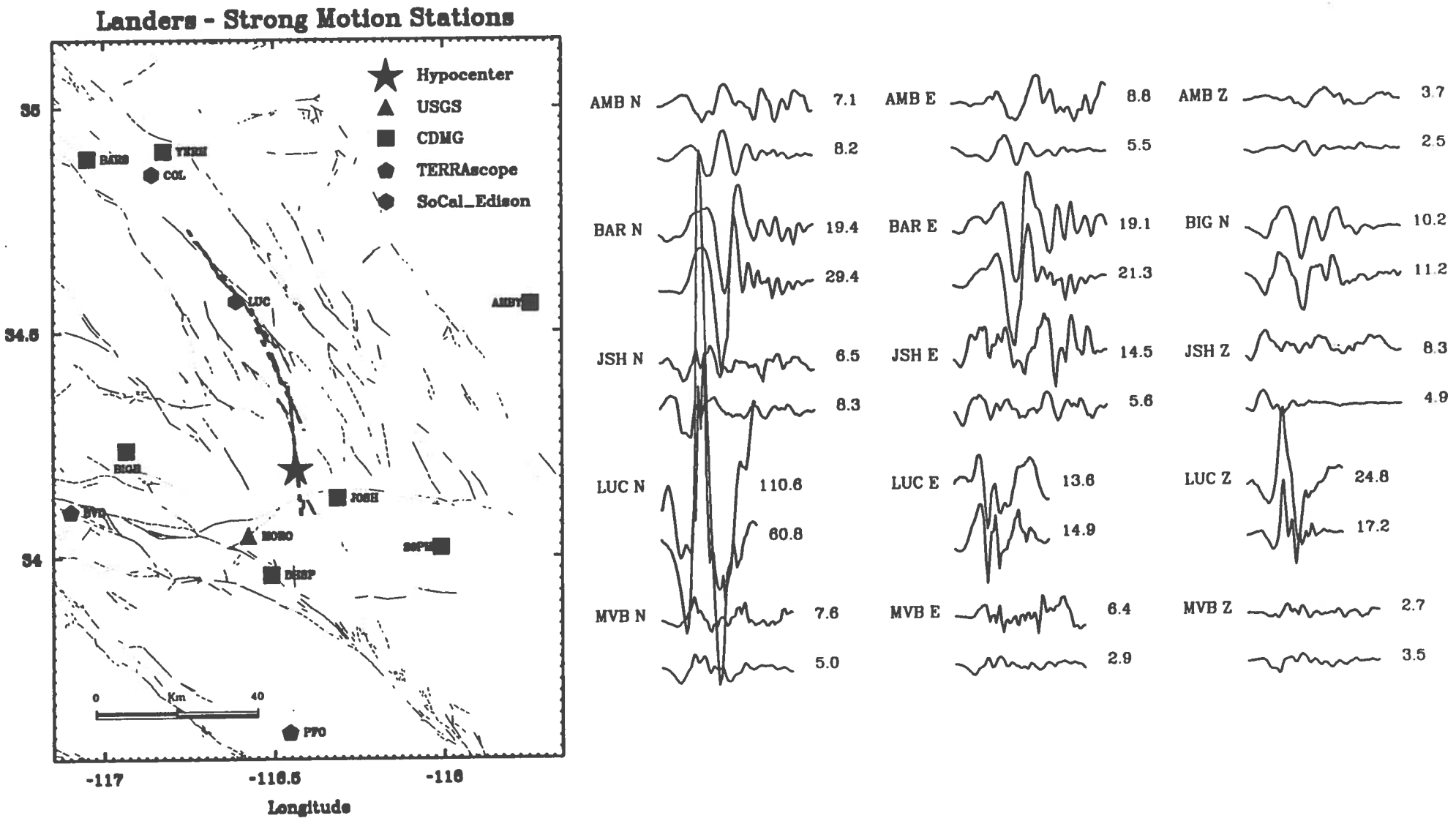

Fig. 1. Location map showing strong motion stations (solid symbols) for the Landers earthquake. The three dashed line segments represent the surface trace of the fault model planes used in this study. Light lines are mapped faults and the thick line indicates surface offset from the Landers event (courtesy of K. Sieh, Caltech). Observed (top) and synthetic (bottom) waveforms are shown for the strong motion stations. Time scale is appoximately 36 sec/in.

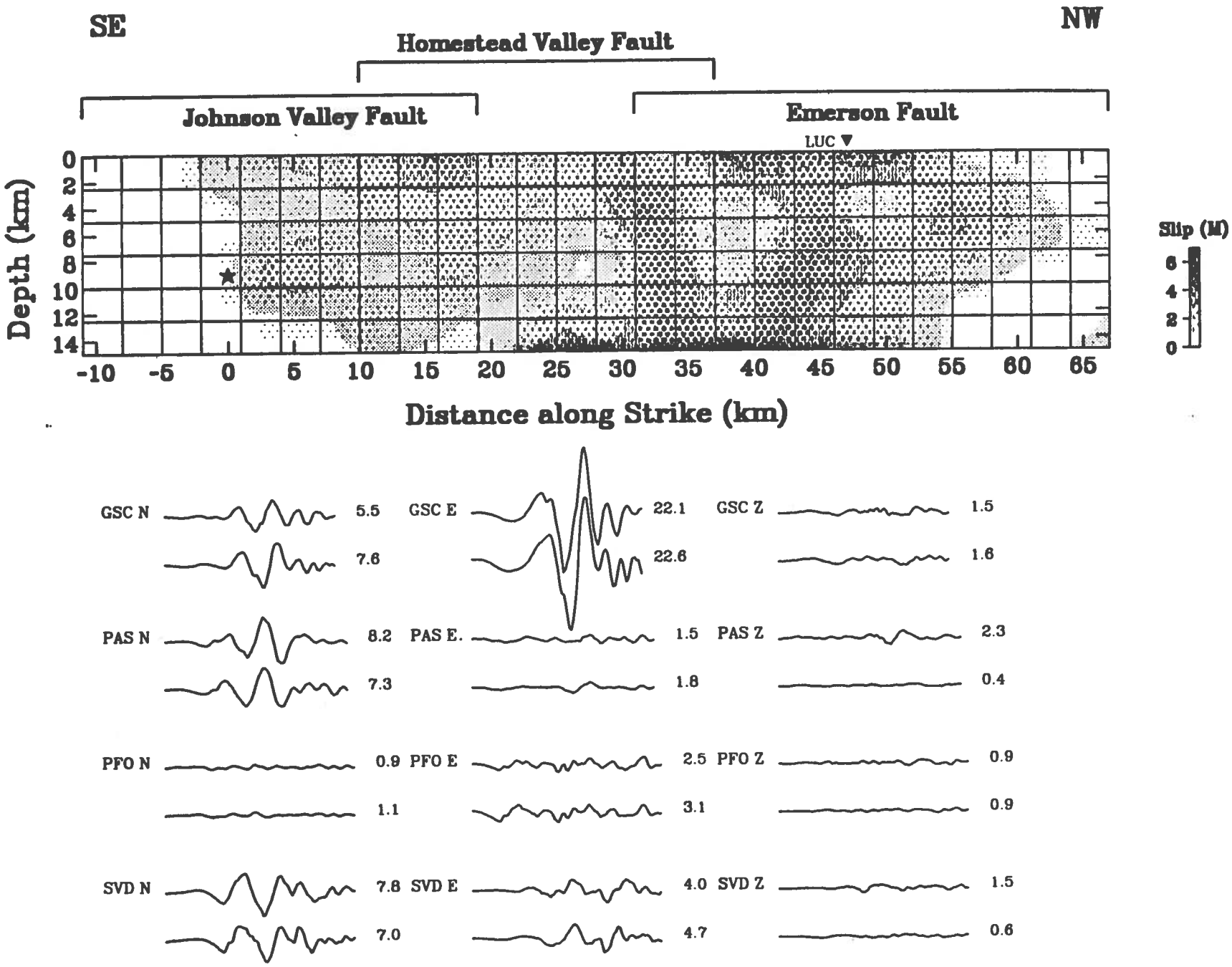

Fig. 2. Preliminary modeling results of the Landers earthquake showing strike-slip distribution. The fault segments overlap as seen in map view in Figure 1. Slip is given in meters. Observed (top) and synthetic (bottom) waveforms are shown for the TERRAscope stations. Time scale is appoximately 36 sec/in.

Progress Report on Broadband Strong-Motion Prediction for the M7.4 Landers, California, Earthquake

Sandra H. Seale, Principal Investigator
Institute for Crustal Studies
University of California
Santa Barbara, CA 93106

The original title of the proposed work was "Broadband Strong-Motion Prediction for San Bernardino". Since the Landers earthquake of 28 June 1992, I have directed my efforts toward the synthesis of strong ground motion from that event. I am applying our technique to the synthesis of ground motion in the frequency band 1 - 10 Hz, which will be validated with data from the Landers event. After the work on Landers is completed, Prof. Ralph Archuleta and I will use this technique to simulate ground motion in the Los Angeles basin from a hypothetical M8 event on the San Andreas fault.

The work on the high-frequency ground motion generated by Landers follows that done in the frequency band 0 - 1.0 Hz by Campillo and Archuleta (1992). Michel Campillo and Ralph Archuleta simulated the Landers rupture on two fault segments and were able to match the dynamic displacements at four TERRAscope stations: GSC, PFO, PAS and SVD.

My model of the Landers rupture has three segments, which are shown in Figure 1. The three segments have strikes of N6°W, N23°W, and N39°W and lengths of 26 km, 14 km and 32 km. The total moment for the event is 1.1 x 10^{27}dynes-cm. The epicenter of the event is 9 km North along strike from the southern end of the first segment, coordinate (0,0) in Figure 1. All three segments extend from 1 km depth to 15 km depth. Rupture initiates at a depth of 7 km and then proceeds bilaterally at a constant velocity of 3 km/sec. When the rupture reaches the northern end of the first segment, it initiates on the second segment at a depth of 6 km. When it reaches the end of the second segment, it initiates on the third segment at a depth of 5 km. Rupture on the second and third segments proceeds unilaterally at a constant velocity of 3 km/sec from the initiation points at the southern ends. The total slip on the segments is taken from the work done by Kerry Sieh, which was presented at the 27 August 1992 SCEC meeting, on the surface breakage at Landers. Slip is constant with depth in this model. Slip on the first segment from the epicenter north is

3.5 m, from the epicenter south it tapers to 1 m. The second segment has a constant slip of 2 m. The third segment has a constant slip of 6 m along 22 km of strike, which tapers to 2 m at the northern end. The locations of the four TERRAscope stations relative to the fault are shown in Figure 1. The velocity structure is the crustal model for Southern California from Kanamori and Hadley (1975) with the addition of a low velocity surface layer described by Campillo and Archuleta (1992).

Higher frequency ground motion due to body waves is computed by the isochron method of Spudich and Frazer (1984). The high frequencies are generated by randomly perturbing the trigger times of points on the fault. In this case, the trigger times that are calculated from the constant rupture velocity of 3 km/sec are allowed to vary by +/- 0.3 sec. Attenuation in the form of a constant t* is applied to the seismograms in the frequency domain. Synthetic accelerations for the station PAS are shown along with the data in Figure 2. At PAS, a t* of 0.07 is applied to the synthetic motions. The East and North components of the synthetic are the top two traces, the East and North components of the data are the bottom two traces.

A comparison of the data and the synthetic records points out the areas where work needs to be continued. The duration of the strong shaking is longer in the data. The Landers earthquake generated a lot of surface waves, and these surface waves not modeled in the isochron method. The overall amplitudes of the synthetics are low compared to the data. I need to add low velocity material to the model to account for the site effect. Also, I am looking to obtain strong motion data from stations that are closer to the fault, since path effects may play a role at these TERRAscope stations. The final product of this work will be response spectra in the frequency range 1 - 10 Hz. For the higher frequencies, it is the response spectra that are of engineering interest.

References

Campillo, Michel and Ralph J. Archuleta, A Rupture Model for the 29 June 1992 M 7.4 Landers, California, Earthquake, submitted to *Nature* (1992).

Kanamori, H. and D. Hadley, *Pure and Appl. Geophys.*, **113**, 257 - 280 (1975).

Spudich, Paul and L. Neil Frazer, *Bull. Seism. Soc. Am.*, **74**, 2061 - 2082 (1984).

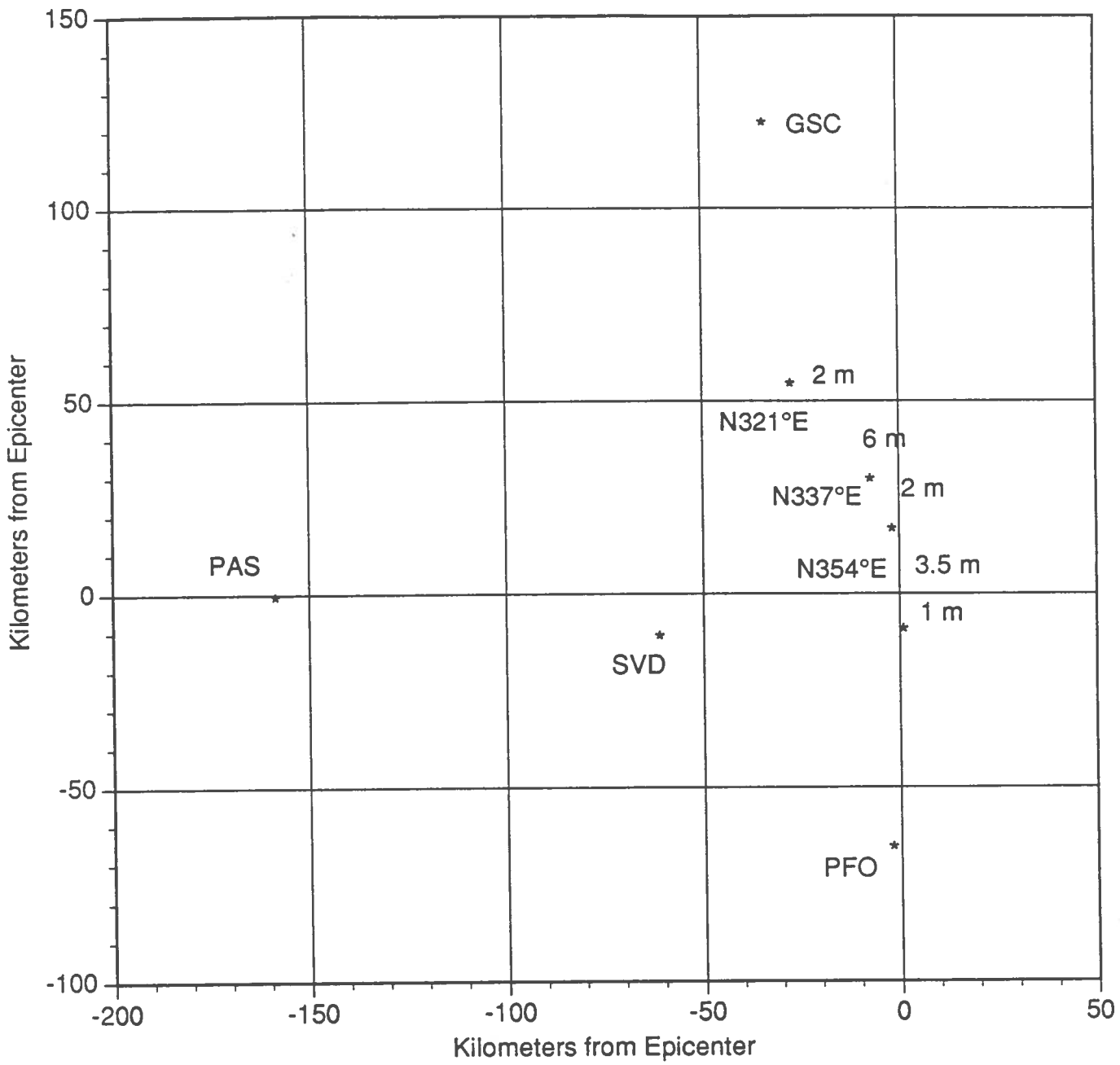

Figure 1. The three fault segments used to model the Landers event and the locations of the TERRAscope stations relative to the epicenter (0,0).

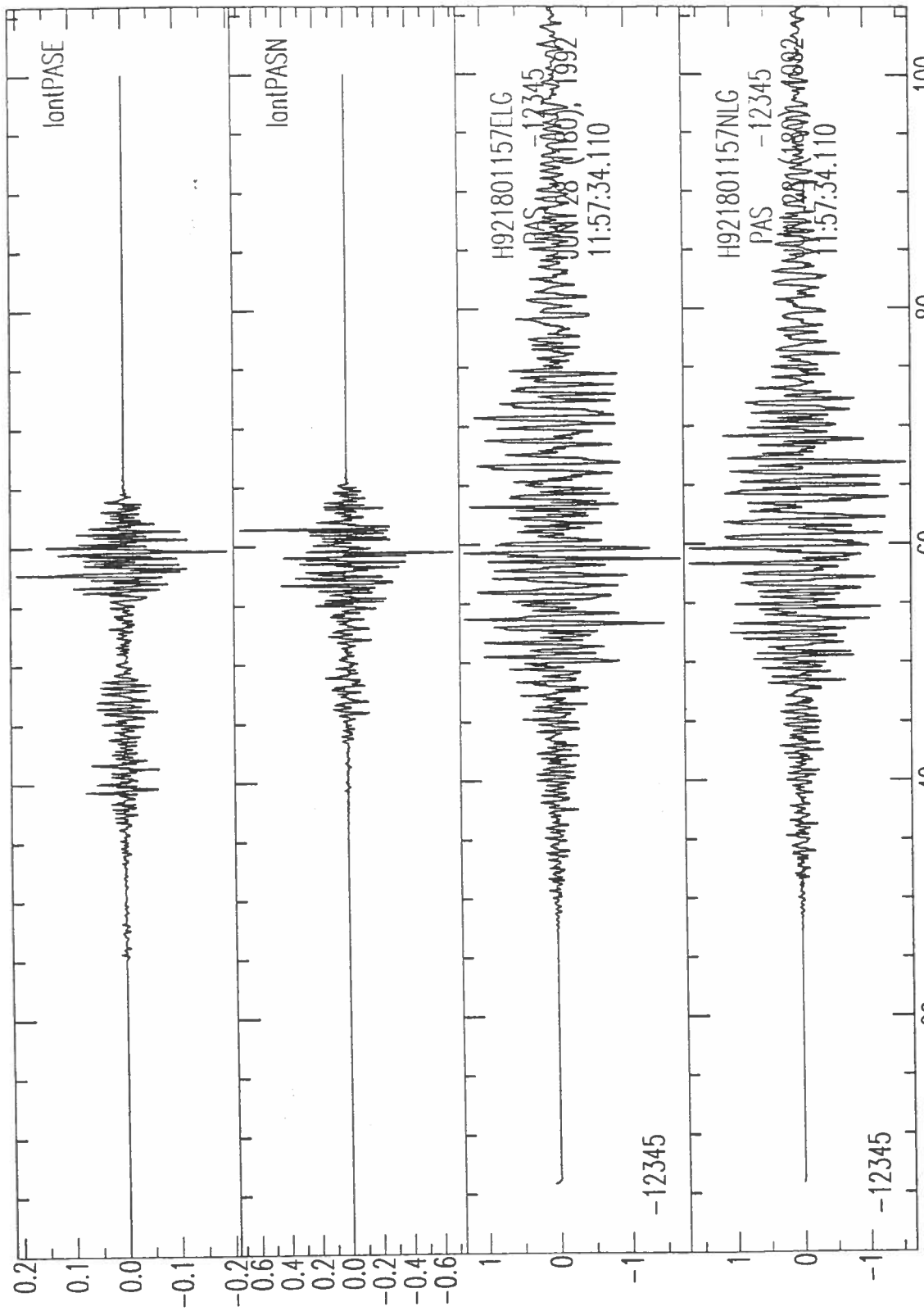

Figure 2. Synthetic and recorded accelerations from the 28 June 1992 Landers event at station PAS. The top two traces are the East and North components of the synthetic, the bottom two traces are the East and North components of the data.

A progress report on SCEC-funded research by M. Takeo

Abstract of paper titled "Simulation of long-period ground motions for the 1923 Kanto earthquake (M=8)" written by M. Takeo and H. Kanamori

In view of the recent increase of large structures such as high-rise buildings, oil tanks, suspension bridges and offshore drilling platforms, estimation of long-period strong ground motions from several seconds to twenty seconds is becoming increasingly important. Although it is relatively straightforward to compute long-period ground motions numerically for a given earthquake model, it is not possible to verify such simulations because no record of long-period ground motion in the epicentral area of a large earthquake (M>8) is presently available. In Los Angeles basin, we also have not experienced a large earthquake of magnitude greater than 8 which occurs just beneath or nearby Los Angeles. During the 1923 Kanto, Japan, earthquake (M_S=7.9 to 8.2,) which devastated Tokyo, Yokohama, and their environs, and caused more than 130,000 fatalities, three low-gain seismographs were in operation in Tokyo. Although these records do not contain complete information of the ground motion, they can still be used for verification purposes.

Another unique aspect of the Kanto earthquake is that it occurred beneath the Kanto plain, which is covered by thick soft sedimentary layers. The combination of a large earthquake and soft sediments is fairly common, e.g. Mexico, San Francisco, and Tangshan. Also, many major cities in the world are located in a sedimentary basin with high potential for a large earthquake (e.g. Los Angeles). Since sediments play a major role in excitation and propagation of long-period ground motion in the epicentral area of a large earthquake, it is important to understand their effects on ground motions.

Considering these aspects of the Kanto earthquake, we performed numerical simulations of long-period ground motions for this earthquake. The objective of this study is twofold: 1) to estimate the response spectrum for the 1923 Kanto earthquake; and 2) to investigate the effects of various source parameters on the ground motion. Although our simulations are for models of the 1923 Kanto earthquake, there is no reason to believe that the next large earthquake near Tokyo is a close duplicate of the 1923 Kanto earthquake. Many earthquake sequences along subduction zones demonstrate that earthquakes are very noncharacteristic from sequence to sequence. It is thus important to do a parameter sensitivity analysis so that we can assess the variability of estimated ground motions, and apply the results to a broader class of earthquakes than just a single design earthquake specifically for the 1923 event.

We used reflection-transmission matrices and the discrete wavenumber integration method to compute ground motions for fault models placed in layered structures. The Kanto earthquake was recorded in Tokyo with a Ewing seismograph and an Imamura seismograph. The Imamura strong-motion seismograph recorded the ground motions during the first 10 to 15 sec, but thereafter went off-scale. The Ewing seismograph recorded the ground motion almost on-scale on a turn table for about 2 min. The ground motions estimated by earlier investigators from these two seismograms differed significantly. This conflict can be reconciled if we assume that the solid friction of the Ewing seismograph was very high during shaking. We conclude that the ground motion of the Kanto earthquake had a very large long-period component with a velocity response spectrum of 120 cm/sec (5% damping) at a period of 13 sec. The velocity response spectrum at a period of 7.5 sec is estimated to be about 50 cm/sec.

Numerical simulations produced a wide range of ground motions and response spectra, even with a given fault geometry and seismic moment. The slip distribution and

the rupture direction significantly influence simulated ground motions. To further examine the effect of the soft surface layer and the slip distribution, we compared the response spectra for layered structures with and without a sedimentary soft surface layer. We varied the slip distribution on the fault plane, too. Figure 1 shows the velocity response spectra (5% damping) for a bilateral rupture mode using the structures with (left-side panel) and without the soft layer (right-side panel), respectively. Except in some extreme cases, the variation of response spectrum due to changes in slip distribution is about a factor of 4. We also estimate that the amplification factor of the horizontal components due to the soft layer is about 1.4 for the periods longer than 5 sec. The response spectra of the vertical component are, however, almost the same as those without the soft layer. For the ground motion with periods shorter than 5 sec, the amplification factor becomes as large as 2, because the reflection from the bottom of the sedimentary layer just beneath the station generates relatively large short-period waves. Other rupture modes also give a similar amplification factor for changing slip distribution and due to the soft layer. The response spectra vary by a factor of 2 for different rupture modes, except for a few special cases.

Large subevents in a shallow structure enhance the ground motion significantly, especially if the rupture propagation is toward the site. One of our extreme models, which has large slip of about 8 m in the shallow crust at the western end of the fault plane, could produce a large ground motion comparable to that estimated with the Ewing seismogram. Reducing the rise time or increasing the rupture propagation increases the spectral amplitude at periods shorter than 5 sec. We schematically show these effects in Figure 2.

The basin structure beneath Tokyo would increase the duration of ground motion significantly. Although increased duration does not significantly affect the response spectrum, it will play an important role in the nonlinear response of structures.

Although our simulations are made for models of the 1923 Kanto earthquake, the result of the parameter sensitivity analysis must be useful for assessing the variability of estimated ground motions to a broader class of earthquakes, for example "The Big One".

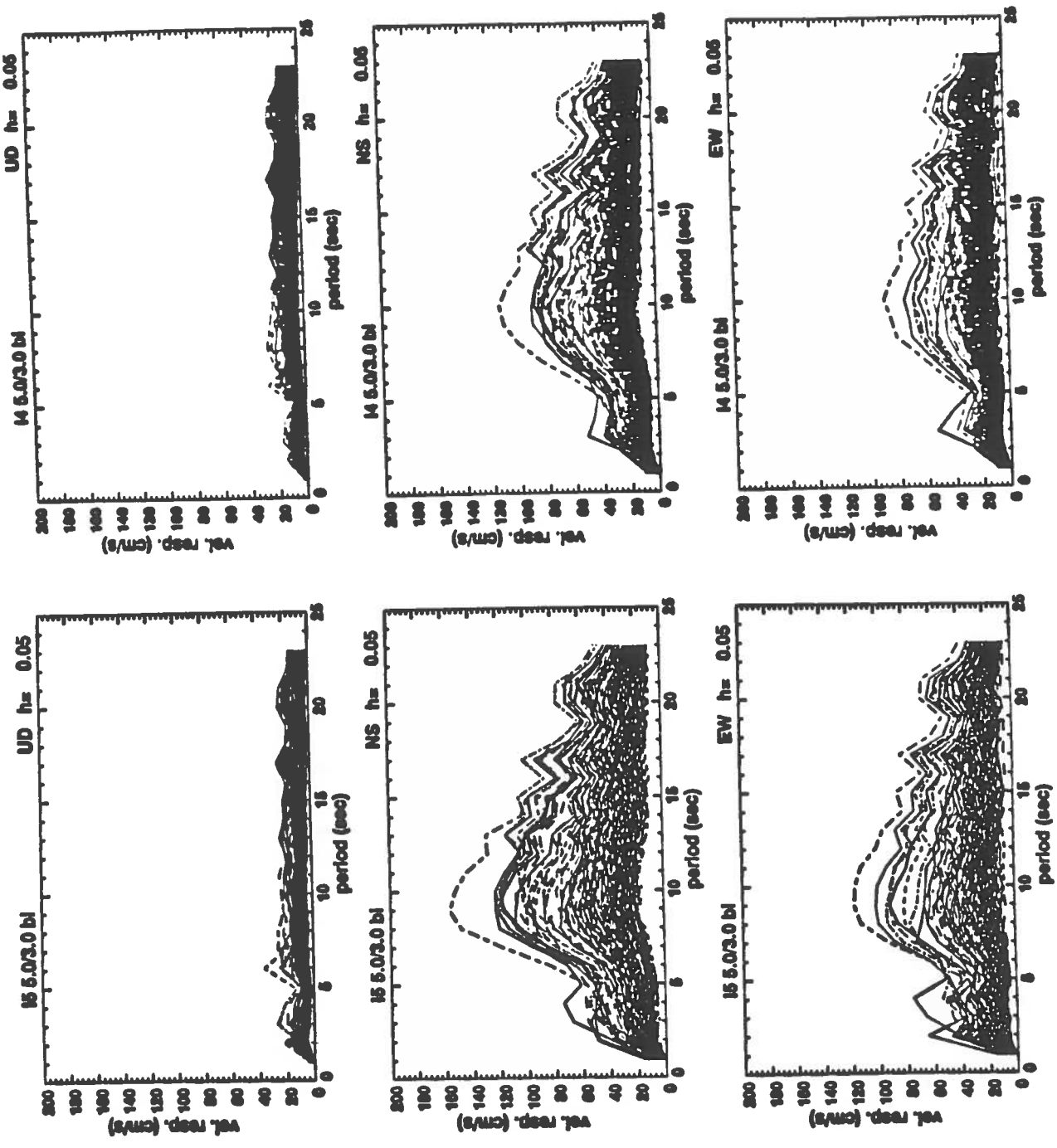

Fig. 1

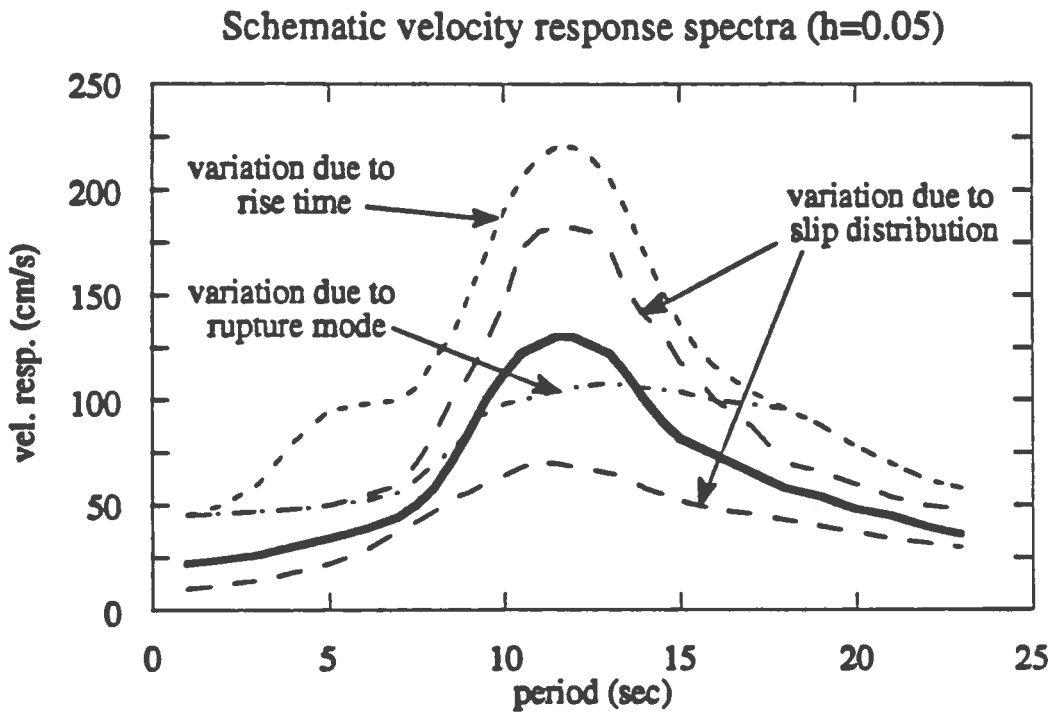
Schematic velocity response spectra (h=0.05)
vel. resp. (cm/s)
250
200
150
100
50
0
0
5
10
15
20
25
period (sec)
variation due to
rise time
variation due to
rupture mode
variation due to
slip distribution

Fig. 2

INTEGRATED ANALYSIS OF SITE EFFECTS

Principal Investigators : **John Vidale** and **Thorne Lay**
Graduate Student: **Ornella Bonamassa**

Institute of Tectonics and Earth Science Department
University of California, Santa Cruz

Working group: Group B, Strong Motion
Ralph Archuleta, Group Leader

1st Progress Report

15 September 1992

Proposal

We proposed an integrated study of site effects using strong motion, weak motion, and microtremor records. During the first part of the project we have focused on the analysis of dense array recordings of aftershocks, explosions, and microtremor in the Santa Cruz mountains. We have analyzed shear wave particle motions in order to investigate the presence of directional resonances. Resonances observed in weak motions and microtremor may prove useful in predicting characteristics of the strong motion at a particular site.

Introduction

In the last few years, we have examined the effects of lateral variation in basin structure, the effects of source radiation pattern, and the directional and amplitude resonances resulting from local geology. We hypothesized that lateral variations in low-velocity, near-surface layers may play an important role in both the frequencies at which a site resonates and the possible preferred directions of motion. The analysis of the shear wave particle motions of ten aftershocks of the Loma Prieta earthquake recorded by a 6-stations array on the Santa Cruz Mountains showed that the polarization direction was controlled by the site more than by the source.

This observation was further investigated on a data base of recordings of explosions set by the USGS and collected by a 20-stations small aperture array deployed in the same area previously studied. The array had an aperture of 45m by 60m and was laying along the side of a gently sloping hill. The analysis of the particle motion of the shear waves produced by the explosions showed that the direction of the polarization changes smoothly across the array, and it seems to be more consistent for the stations at the top side of the hill, than at the bottom. In general the polarization direction for some sites appeared to be influenced more by the site than by the location of the explosions. The observation that the polarization of shear waves is affected by the site and depends on frequency, while this is not evident for the first pulse, implies that anisotropy or similar phenomena cannot explain the data because they would act on the whole wave train. The observed site effect acts on the reverberations or scattered energy. We interpret the directional resonances as the result of some geological feature along the ray-path to the surface that is able to amplify the particle motion in selected frequency bands in particular directions compared to motions in other directions. This direction-dependent amplification alters the particle motion. The actual geological features that cause this amplification are not known: lateral gradients in near-surface shear wave velocity are likely to cause these resonances that change across short distances. Since the Loma Prieta data show that the preferred direction can change on a scale of 25 m, and that it remains constant through the shear wave onset and coda, these features must be very close to the receivers, probably within a few tens of meters. These observations, and the lack of detailed geological information about the area suggested to survey the region with the means of shallow refraction seismology.

Present project

Shallow refraction seismology in the Zayante region

We have deployed two orthogonal lines of geophones and used compressional and shear wave seismic sources to collect information about the fine scale structure of the area of interest (figure 1). We used the system designed by Willie Lee to record the signal produced by two different kind of seismic sources: a sledge hammer for compressional waves, and a device designed by Hsi-Ping Liu for the shear waves.

The system consists of a 64-channel converter, 21 2-Hz, 3-component L-22 geophones, a satellite receiver for the clock input, and a portable PC. The portable PC is fundamental for controlling the quality of the input and the functioning of the whole system. We deployed the 21 L-22 along a cross oriented North-South and East-West. Each sensor was buried at depths between 1 and 2 feet. The distance between receivers is 10 m. We chose 6 sites for the shear wave source at the middle and ends of the lines. We also used the sledge hammer at each sensor location.

Preliminary analysis

The air-powered, impulsive shear wave source and the hammer, used in the refraction profiling, produced clean, repeatable SH and P pulses. This allowed us to stack the signals in order to improve the signal-to-noise ratio. The PC-based 64 channel recording system allowed real-time data quality control, which resulted in no missing channels. A preliminary analysis shows that the crossing profiles reveal strongly varying, 3-D structures (see figure 2).

Future goals

We plan to see whether finite difference simulations with the true structure can explain and perhaps predict the incoherence of ground motion and the frequency-dependent preferred directions of motion observed, thus providing a new tool in earthquake hazard estimation.

Map of the 6-Station Array, Very Dense Array, and Shallow Refraction Seismology Lines in the Santa Cruz Mountains

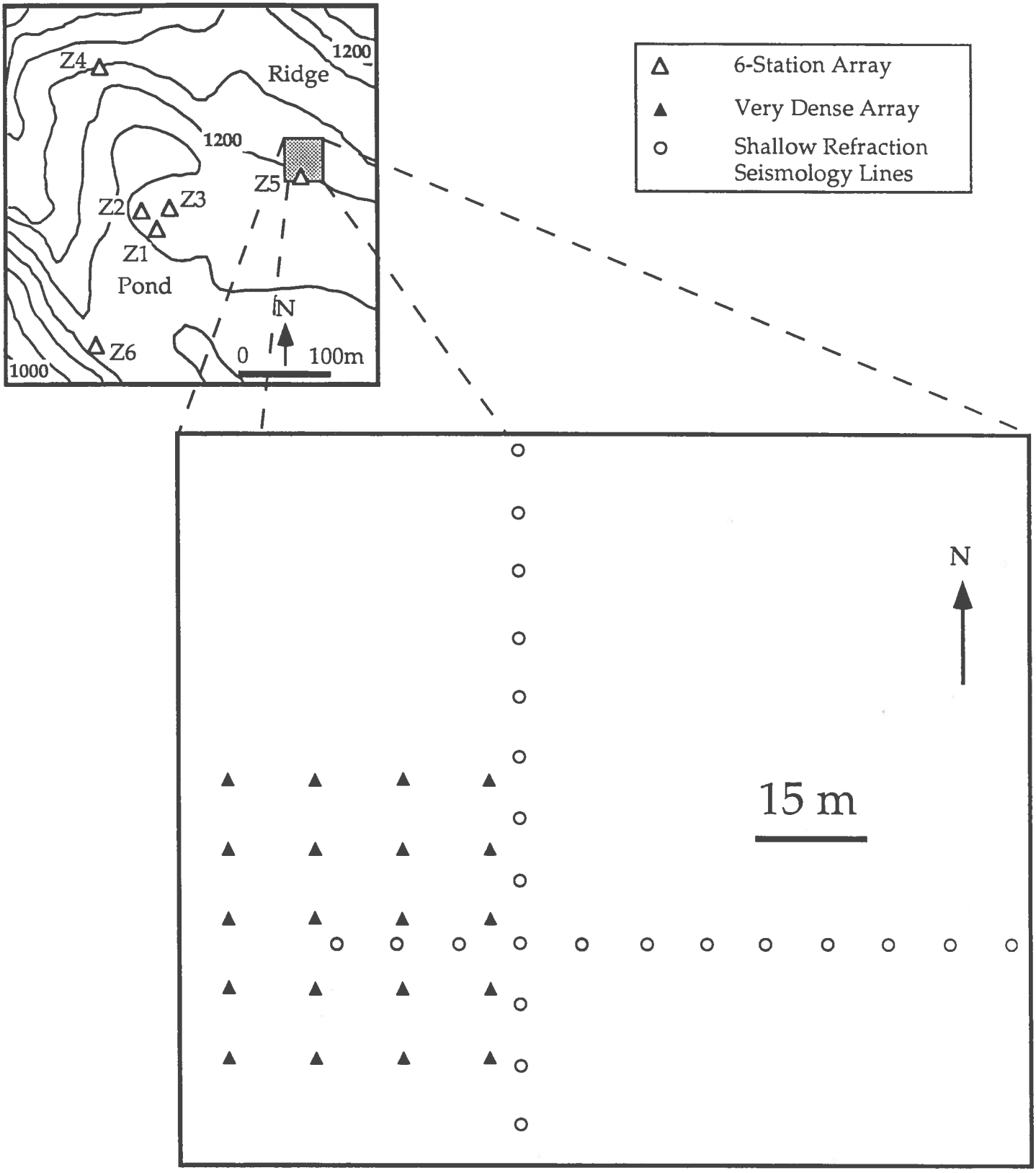

Fig.1 Map of the 6-station array, the very dense array, and the shallow refraction seismology lines deployed on the Santa Cruz Mountains.

a)

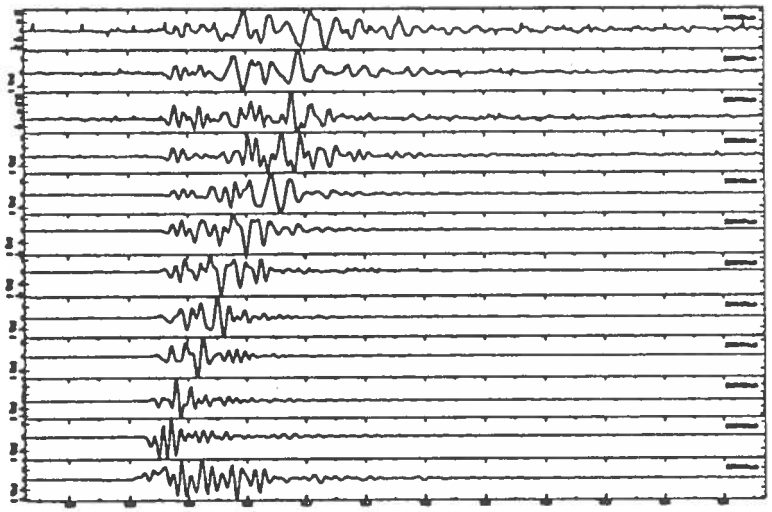

P-source, vertical component

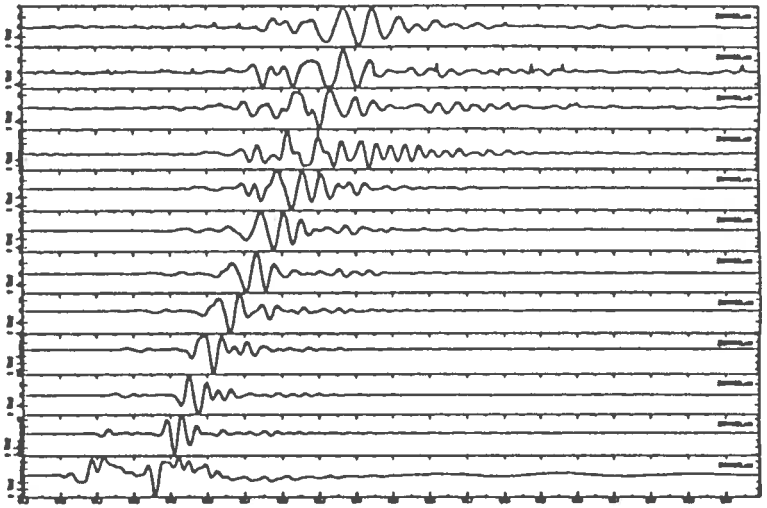

S-source, E-W component

b)

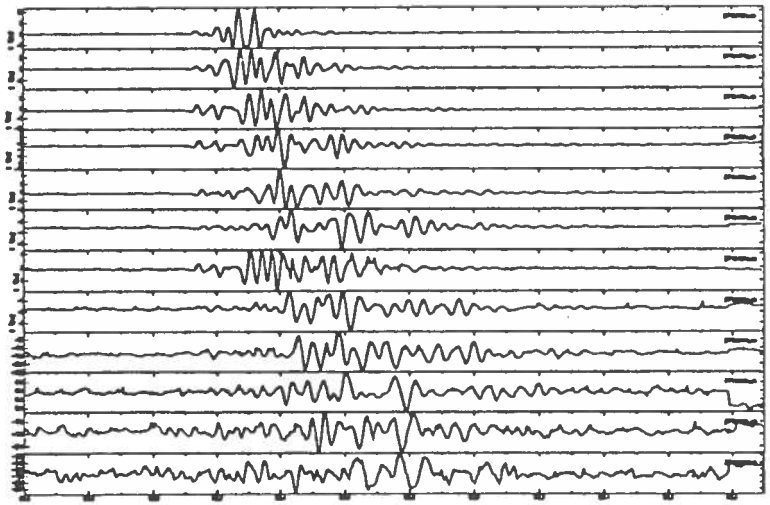

P-source, vertical component

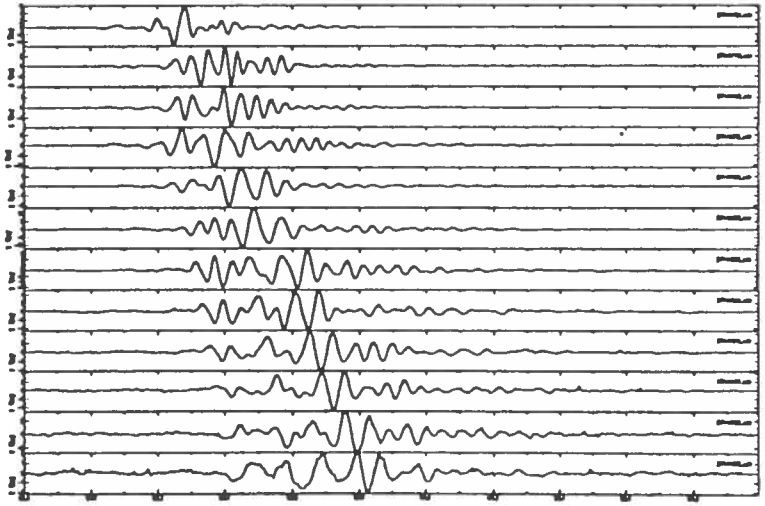

S-source, E-W component

Fig. 2 Profile of stacked signals recorded on the N-S line that lies along the gradient of the hill. a) The source is close to the bottom station. b) The source is close to the top station. Traces are normalized.

Group C: Earthquake Geology
Group Leader: Kerry Sieh

25 September 1992

Progress Report for Group C (Earthquake Geology)

Kerry Sieh

Because of the Landers earthquake this summer, the Earthquake Geology group has had two principal foci, rather than just one. A considerable percentage of our financial resources and hundreds of hours of our time were diverted to studying the Landers event during the summer months. Nevertheless, our group has made substantial progress toward our original goal -- evaluating the sources of potential large earthquakes in the Los Angeles Basin. In the paragraphs below, I summarize our progress in the Los Angeles region first, and our post-earthquake work second. Please refer to the reports of individual groups or investigators for more detail about specific projects, including illustrations.

Sources of large earthquakes in the LA Region

Northern region

Yeats, Huftile, Hummon and Tsutsumi at Oregon State University have made important refinements in their characterization of the geometry of the Wilshire Arch, through Hollywood. They are now able to demonstrate, from subsurface data, that the Wilshire Arch is a separate structure from the southeast plunging monocline beneath the Santa Monica fault. They also have estimates of the age of the deformed horizon they used to draw the structure contour map. They are about to begin creating structure contour maps of horizons beneath this first horizon, the base of Pleistocene marine sediment, so that they will be able, later, to create well-constrained fault-bend fold models of the blind faults that are creating these structures.

Dolan's and my work on the geomorphology of the Santa Monica fault, Hollywood fault and faults and folds atop the Wilshire Arch is also proceeding well. In our previous reporting period, we mapped in detail the surficial traces of the Hollywood and Santa Monica fault, but we had made no serious attempt to date the latest movements on these structures. In the past several months, we have identified additional scarps atop the Wilshire Arch, in and striking northwest from Downtown Los Angeles. The faults that have produced these scarps appear to have significant dextral components of slip. We have also identified folded surfaces atop the steep southern flank of the Wilshire Arch. Suppe's group at Princeton sees clear evidence for these structures, as well. These may form a continuous E-W belt of partitioned folding and dextral slip between the Newport-Inglewood and Whittier faults.

Our five-meter deep excavations across a prominent scarp of the Santa Monica fault revealed that the scarp represents monoclinally southward-dipping late Pleistocene alluvial sediments. Undeformed probable late Holocene sediments overlie the scarp. The scarp appears to be the limb of a monocline above a shallow blind thrust. Rockwell has assigned preliminary ages to soil horizons exposed in the excavations. Numerous, high-angle strike-slip faults break the late Pleistocene sediments and terminate within a soil of probable late Pleistocene or early Holocene age. Based upon these preliminary assignments, we believe that a shallowly buried reverse fault and associated

surficial strike-slip faults slipped last in the early Holocene. This suggests that earthquakes are produced by the Santa Monica no more frequently than early several thousand years, but that these events are large.

Western region

Suppe, Bischke and Shaw at Princeton University have developed new data on active structures related to the Newport-Inglewood fault. They interpret growth wedges on the western flank of the LA Basin to be the result of slip on a northeast-dipping blind thrust that may cut the northern half of the Newport-Inglewood fault and may be capable of an earthquake of at least M6.6. They have not yet estimated an average repeat time for this structure, and they suspect that it continues southeastward farther than the reflection lines currently available to them.

The Princeton group has also applied their fold theory to Signal Hill, an anticline along the Newport-Inglewood fault, in order to reassess the rate of dextral slip along that active fault. They calculate a rate of only 0.035 mm/yr, far lower than previous estimates.

At UC Santa Cruz, Ward and Valensise have completed a model of the deformation of the famous terraces of the Palos Verdes Peninsula, based upon the elevations and map-view patterns of the terraces. They can explain the pattern of terraces with oblique dextral/reverse slip on the Palos Verdes fault, if the fault has been moving at about 3 mm/yr. They estimate quake magnitudes and recurrence intervals from this model. The uniqueness of their model is not addressed in their summary.

Unfortunately Rockwell's attempts to find a suitable site for excavation of the Palos Verdes fault failed, due to urbanization of the fault trace.

Eastern region

Rockwell, Patterson and Herzberg, at CSU San Diego, have collected more data bearing on the size of past earthquakes of the Whittier fault, on the eastern flank of the LA Basin. Their recent 3D excavations confirm last-year's findings that the fault is, indeed, principally dextral, not reverse. The latest event appears to be associated with about 2 meters of dextral slip and probably occurred more than a few hundred years ago.

Investigations of faults of the Landers Earthquake

We have diverted a significant amount of our SCEC effort and money to Landers. Rubin and my grant to study the Sierra Madre fault zone was expended almost entirely on mapping the faults that produced the Landers earthquake. McGill, at CSU San Bernardino, spent the bulk of her grant on Landers field work as well. Finally, Lindvall's funds to study the paleoseismic history of the Sierra Madre fault were partially expended mapping these spectacular faults.

Our mapping team consisted of twelve geologists. The preliminary map of surficial faults that is available at this annual SCEC meeting has been compiled by Anne Lilje using ARC/INFO and our observations. A smaller version of the fault map appears in a manuscript that we and other SCEC scientists have submitted to Science. Our mapping of surficial slip has shown that six major faults produced the earthquake. This is a very unusual

occurrence in California and will influence substantially SCEC's probabilistic seismic-hazard mapping throughout southern California. This event clearly contradicts the convention wisdom that faults in California do not rupture together and that short faults produce small coseismic offsets and moderate earthquakes.

The slip patterns we have mapped will be important for estimating earthquake recurrence along these and other faults of the Mojave Shear Zone. McGill and Rubin's mapping of major fluctuations in dextral slip over very short distances have important implications for paleoseismic models of prehistoric earthquakes elsewhere in the State. Comparisons of coseismic slip patterns with total geological offsets will lead to interesting hypotheses about long-term patterns of large earthquakes along this complex fault zone. Furthermore, our mapping is providing important constraints for geodetic and seismological studies of the source of the earthquake. In addition, we wonder if the recent spate of moderate earthquakes in southern California, on small patches of major faults, will follow the pattern of the M5.2 Homestead Valley earthquake, near Landers. That is, will they prove to be harbingers of much larger events, with surficial slippage as great as that at depth.

A final observation we wish to mention is the extremely subdued nature of older fault scarps along the faults of the Landers earthquake. Lindvall and Rockwell have used most of the Lindvall SCEC grant to begin paleoseismic excavations across the Homestead Valley fault. Their preliminary estimation is that the fault had not produced a major slip event for more than about 10,000 years prior to the Landers earthquake. Thus it appears that, based upon current methodologies, the faults of the Landers earthquake had about one-fortieth the likelihood of rupture as did the nearby San Andreas fault. Should this influence our opinions about the value of the planned SCEC probabilistic hazard maps.

Rubin and I plan excavations across the Emerson fault in early November, to assess the timing of the most recent paleoseismic events along that fault, and our group has been discussing the possibility of a long-term collaboration, with SCEC funding, to assess the timing of past large events throughout the Mojave Shear Zone. This work would address fundamental questions about the mechanics of strain accumulation and relief and practical questions about the likelihood of ruptures of nearby Mojave faults in the next few years.

SCEC 1992 PROGRESS REPORT: PALEOSEISMOLOGY AND TECTONIC GEOMORPHOLOGY OF THE NORTHERN LOS ANGELES BASIN

James F. Dolan and Kerry Sieh, Seismology Lab 252-21, Caltech

During the past year we continued our studies of the seismic hazard potential of active structures in the northern Los Angeles Basin. Prior to initiation of this combined paleoseismologic and geomorphologic research program 15 months ago, little was known about the seismic hazard potential of this densely populated area. The location and structural style of the two major faults crossing the area, the Hollywood and Santa Monica Faults, were poorly known, and no information was available concerning the recency of activity on these structures; neither fault is zoned as active by the State of California. Furthermore, several other potentially seismogenic structures that we have subsequently identified were then completely unknown.

Tectonic Geomorphology: Identification of Potentially Seismogenic Structures

Our initial efforts to identify potentially active structures focused on a geomorphologic analysis of the area. These studies have resulted in a detailed map of the surficial traces of potentially active structures in the northern Los Angeles Basin (Figure 1). As we reported in last year's SCEC Progress Report, we first identified the most recently active surface traces of the Hollywood and Santa Monica faults. Although the youngest trace of the Hollywood fault revealed by our research largely coincides with that reported in previous studies, our analysis suggests that recent surface rupture on the Santa Monica fault has occurred along a series of en echelon scarps quite different from those shown on previous maps, most of which were based on ground water anomalies and surface projections of faults encountered in deep oil wells.

After completing our geomorphologic studies of the SMHFZ, we focused our attention on areas south and east of the Santa Monica Mountains. Data collected during 1992 reveal the existence of two previously unrecognized, WNW-trending topographic lineaments just west of downtown Los Angeles (Figure 1). We infer that these lineaments represent previously unrecognized faults based on the presence of laterally offset and tilted paleo-river channels, hanging valleys, consistently south-facing scarps, and a line of conical hills cored by Miocene strata that protrude above older alluvium southeast of Hollywood. We have tentatively named these features the MacArthur Park and Echo Park faults. The offset drainages and the WNW trend of these features suggests that they may represent RL strike-slip faults accommodating partitioned slip above the blind thrust fault responsible for the Wilshire Arch, recently identified by SCEC researchers at Oregon State University (Hummon and others, 1992). Thus far, no exposures of the faults have been identified, and no evidence concerning their recency of movement is available. Although we suspect that these faults may be relatively low slip-rate structures, they trend directly through the high-rise district of downtown Los Angeles. Consequently, paleoseismologic determination of the state of activity of these faults represents one of our goals for 1993 research.

In addition to the identification of the MacArthur and Echo Park faults, our geomorphologic studies reveal five major alluvial terraces between downtown Los Angeles and Beverly Hills, as well as numerous smaller alluvial and fluvial terraces. Differential stream incision and warping of these surfaces indicates that they have been folded into at least four WNW-trending anticlines (Figure 1). Like the MacArthur Park and Echo Park faults, these folds probably represent secondary structures developed in the hanging wall of the Wilshire Arch blind thrust.

Paleoseismology of the Santa Monica Fault System: Evidence of Probable Holocene Activity

Having largely completed our geomorphic studies of potentially active structures in the northwestern Los Angeles Basin, we began our paleoseismologic investigation of the Santa Monica fault during mid-1992. This research has been highly productive, and we feel confident that we can

demonstrate Holocene activity on the fault. During June, July and August we excavated two trenches across a prominent topographic scarp in West Los Angeles. These trenches exposed gently south-dipping alluvial sediments that are onlapped by flat-lying late Holocene strata. Analysis of surficial and buried soils by collaborating SCEC researcher Dr. Tom Rockwell of SDSU indicates that the south-dipping strata were probably deposited during late Pleistocene-early Holocene time. We interpret the south-dipping strata, which are cut by numerous steeply dipping faults and fractures, as the forelimb of an anticline developing above a shallow blind thrust. Many of the faults in the south-dipping sequence exhibit evidence of strike-slip offset, which suggests that they are secondary features accomodating partitioned transcurrent motion along a transpressional fault system. Locally the entire lower Holocene-Pleistocene sequence is intensely disrupted, with sediments tilted as much as 30^{o} to the north. It is unlikely that all deformation observed is attributable to a single early Holocene earthquake, suggesting the possibility of multiple Holocene events. However, the absence of evidence for latest Holocene activity in the flat-lying strata may indicate a recurrence interval measureable in terms of thousands, rather than hundreds, of years for the SMFS.

Having demonstrated Holocene activity, we now plan to refine our understanding of the seismic hazard potential of the Santa Monica fault system. Our planned approach is two-fold: (1) locate and excavate a trench site with a more continuous mid-Holocene sedimentary section in order to better refine the earthquake history of the secondary faults that we observed in the trench; and (2) initiate a seismic-reflection program in collaboration with Dr. Kaye Shedlock of the USGS using the mini-sosie unit. The seismic reflection data will constrain the location and nature of the shallow blind thrust, which probably represents the most significant seismic hazard associated with the Santa Monica fault system. These data will be integrated into balanced cross sections being constructed by Caltech graduate student Richmond Wolf and Kerry Sieh. Construction of such forward models is critical for understanding the dimensions of the potentially seismogenic portions of the blind thrust system beneath Santa Monica and West Los Angeles.

Figure 1. Map of potentially active structures in the northern Los Angeles Basin based on our tectonic geomorphologic analysis. Fault scarps shown in solid black. Freeways shown by dash-dot pattern.

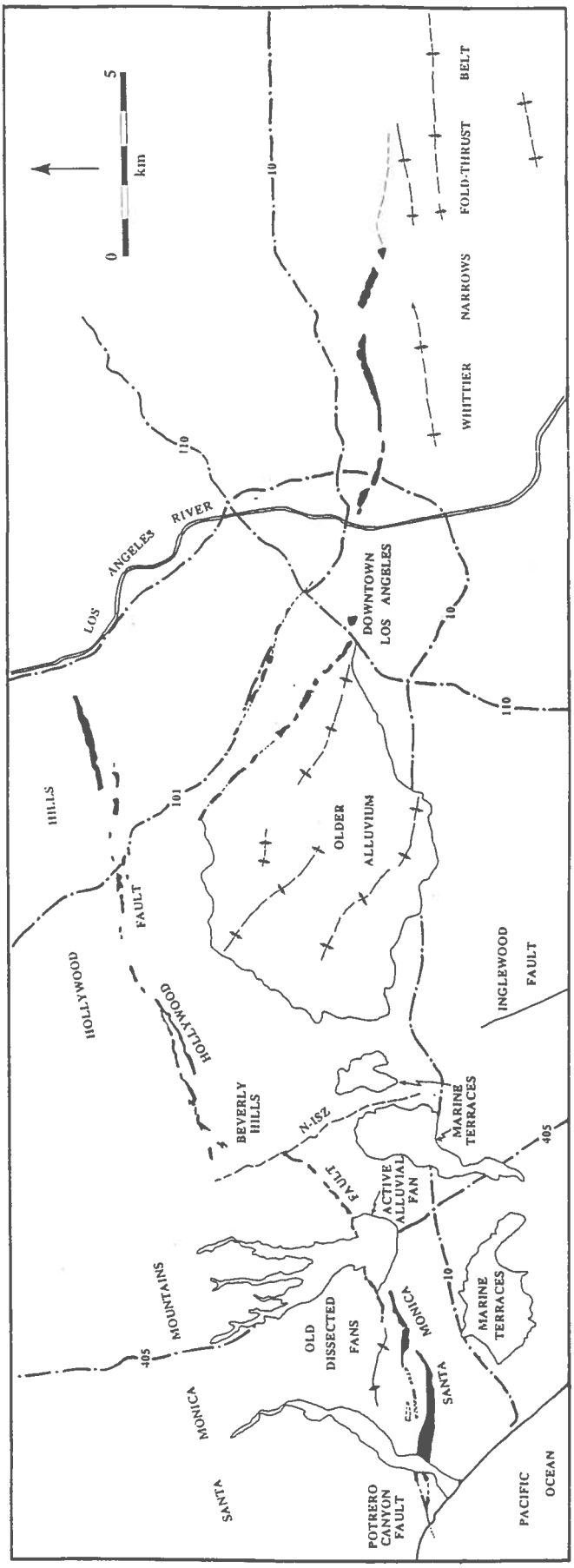
0
5
km
WHITTIER NARROWS FOLD-THRUST BELT
LOS ANGELES RIVER
DOWNTOWN LOS ANGELES
HOLLYWOOD HILLS
HOLLYWOOD FAULT
OLDER ALLUVIUM
INGLEWOOD FAULT
BEVERLY HILLS
N-ISZ FAULT
ACTIVE ALLUVIAL FAN
MARINE TERRACES
SANTA MONICA MOUNTAINS
OLD DISSECTED FANS
SANTA MONICA
MARINE TERRACES
POTRERO CANYON FAULT
PACIFIC OCEAN
10
101
110
405

Progress Report

PALEOSEISMIC STUDIES OF THE WHITTIER FAULT IN THE LOS ANGELES BASIN

P.I.: Eldon Gath
Leighton and Associates, Inc
1470 S. Valley Vista Dr., Suite 150
Diamond Bar, California 91765

INTRODUCTION

The Whittier fault is a northwest trending, right-lateral strike-slip fault channeling a minimum of 2.8 mm/yr of slip to the Los Angeles Basin. At the proposed study site, the fault is a positive flower structure with both north and south dipping reverse separation faults bounding an uplifted block of Puente Formation (see Figure 1). Both faults have similar geomorphic separations. The southern splay, within the study area, has been investigated and our results recently reported (Gath et al., 1992). The current investigation was intended to characterize the proportion of total slip that the northern splay is accommodating. The study site is located in the Olinda oil field on property owned by Santa Fe Energy Resources within the City of Brea.

FIELD INVESTIGATION

The intended trenching program was comprised of a series of trenches excavated perpendicular and parallel to the fault which would allow for a three dimensional exposure of the northern fault splay. The first trench (T-7) (trenching numbers continued from Gath et al., 1992) excavated, intersected the fault approximately 150 feet north of the southern strand. Unfortunately, water was impounded behind the fault, and was flowing into the trench along the fault at such a rate that only a brief examination of the fault contact was possible before conditions became too unsafe to remain in the trench. Within 24 hours approximately three feet of water had filled the trench and only a sketch from the surface was possible (Figure 2). The trench exposed a sand blow near the fault which had been injected into the channel deposits and overlying colluvium. Fragments of colluvium were entrained within the sand blow.

A second trench, T-8, was excavated 45 feet to the east of trench T-7. This trench exposed numerous layers of recent alluvium containing wood, paper, and plastic debris overlying channel deposits. Water also filled this trench covering the channel deposits and within minutes caused the east

wall to cave along the entire length of the trench. As in T-7, only a sketch of this trench was possible (Figure 2). Due to the rising water and the thickness of the recent alluvium it was not possible to excavate deep enough to expose the fault.

The placement of a subdrain system in the project area was explored as a method of lowering the ground water. The site could be allowed to drain for a few months and the trenches re-excavated when the water table had been lowered below the trench bottoms. This plan could not be completed because the draining water would interfere with hazardous waste cleanup efforts of Santa Fe Energy Resources south of the project area. We were also informed that due to health and safety concerns, our access to the project site would not be possible during the cleanup, which was to begin the first of September. The scheduled duration of the cleanup is approximately two years.

CONCLUSIONS

We were aware of the presence of ground water in the upper reaches of the channel sediments, and we postponed our investigation until as late in the fall as possible to allow the water levels to subside. Unfortunately, this was a very wet winter, and several of the storms occurred late in the spring. Our project budget did not include funds for active pumping of the ground water, and adverse site conditions prevented implementation of a passive drainage solution.

Although trenching conditions were not ideal and detailed logs were not possible, the presence and location of the northern splay of the Whittier fault in Olinda Creek was verified, and it clearly affects late Holocene colluvial soils. The presence of the liquefaction feature in trench T-7 also indicates strong seismic events, and that it may be possible to estimate a date of the latest seismic event in the area. Unfortunately, it appears that further research at this location will not be possible for at least two years, at which time single-family home construction is planned for the site. Therefore, we are intending to use the remainder of our award budget to investigate the compressional features south of the Whittier fault, which may be the surface expression slip partitioning within the Whittier fault zone.

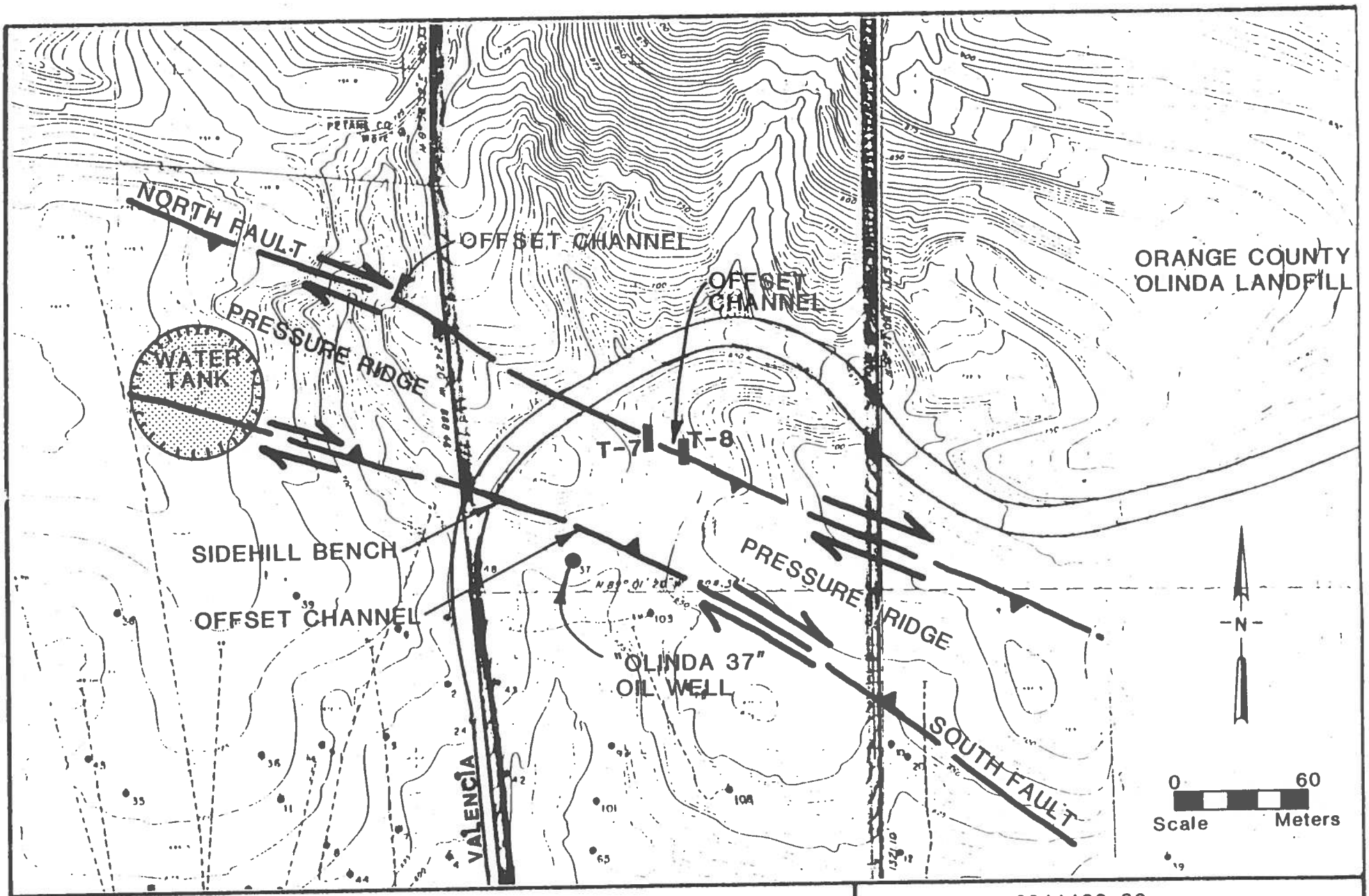

MAP OF TRENCHING LOCALITY WITHIN OLINDA CREEK

Project No.	2911138-02
Scale	As Shown
Engr./Geol.	EMG
Drafted By	lah
Date	9/18/92

Figure No. 1

C10

TRENCH T-7

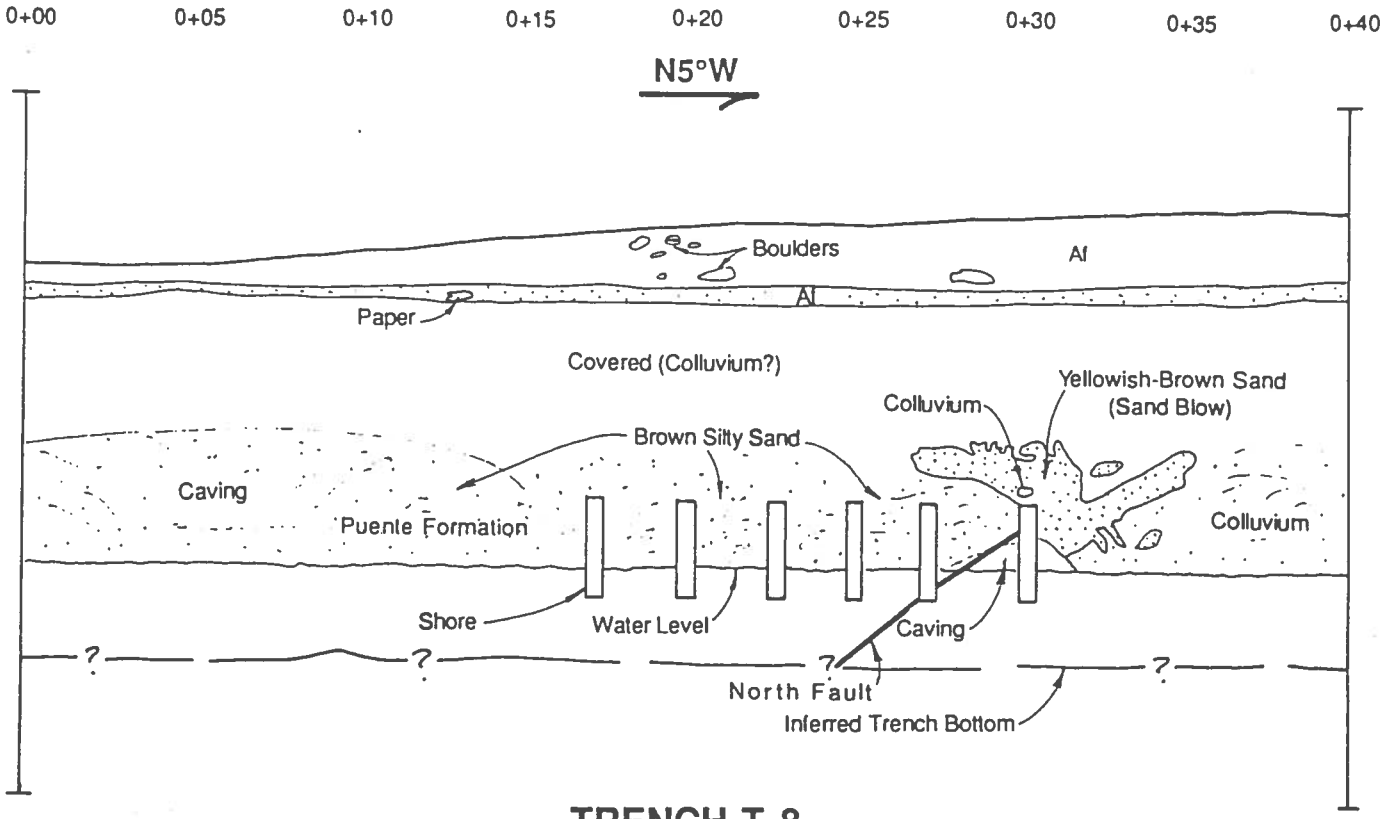

TRENCH T-8

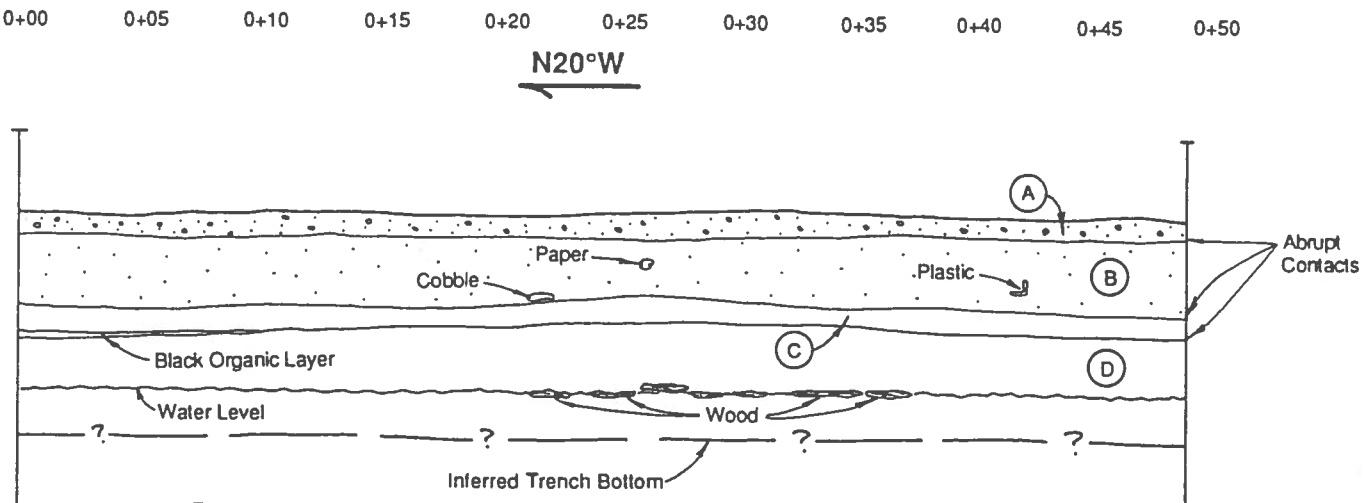

HISTORIC

A — Light brown to grayish white sand; scattered gravel; very loose and dry; scattered roots.

B — Reddish brown silty sand; damp, moderately dense; thinly bedded to laminated; scattered trash; occasional rootlet and pebble.

C — Dark olive gray silt; moderately stiff, moist; rootlets present; organic; thinly bedded.

D — Grayish brown silt; moderately stiff, moist to wet; organic; thinly bedded, minor amount of sand; rootlets present; abundant wood fragments "layered" along upper contact, like a road.

NOTE: ENTIRE EAST WALL HAS CAVED.

SKETCHES OF THE WEST WALL OF TRENCH T-7 AND THE EAST WALL OF TRENCH T-8

Project No.	2911138-02
Scale	Not To Scale
Engr./Geol.	EMG
Drafted By	lah
Date	9/18/92

Figure No. 2

The Mechanics of Fault-Bend Folding

1992 Annual Report of the Southern California Earthquake Center

Geoffrey C.P. King, Jian Lin, and Ross S. Stein

A significant hazard in the Los Angeles region is posed by the existence of blind thrust faults within the basin and associated with actively uplifting blocks such as the San Gabriel Mountains. We are currently pursuing two lines of inquiry to shed light on the nature and mechanical behavior of such faults. The first study probes the relation between coseismic fault slip on blind thrusts and shallow secondary faults (see *Lin, King and Stein*, this volume). The second study, discussed here, relates near-surface geological structure to the blind fault geometry by examining retrodeformable cross-sections in elastic/plastic media.

While the techniques to model faults that both reach the surface and which have simple geometries is well established, more complicated geometries have received less attention. Two approaches have been adopted. One is exemplified by the methods applied to the evolution of geological structures by Suppe and others (e.g. Suppe and Medwedeff 1990) while the second adopts concepts of the earthquake cycle to model geological structures (e.g. King, Stein & Rundle, JGR, 1988). The former has the advantage that, with modest computing power, it can produce balanced cross-sections that can mimic observed geological complexity (eg., the commerical Macintosh program FaultII). However, this is achieved by placing severe constraints on the rheological behavior of crustal rocks and their relation to the physical processes occurring in earthquakes is obscure. The earthquake cycle models, on the other hand, explicitly incorporate the earthquake process and can incorporate realistic rheologies but easily result in impossibly long computing times. The purpose of the project is to examine the middle ground between these two model categories which we will refer to as *"Geological"* and *"Seismological"* models.

Inherent in the *Geological* models is the concept that structures result from the interaction between faults (with bends and changes in slip amplitude) and rocks with closely spaced, friction-free bedding (or other horizontal surfaces). With these, and a constraint that volume is conserved, it is possible to set up analytic expressions to describe large deformation of complex structures. Examples of such models created by Fault II are

shown in the left column of the figure. These can be compared with a fault bend model with the same fault and ramp slip in a linear elastic, or linear ductile material (center column). The effect of using isotropic material is to cause the deformation to become diffuse with distance from the fault. Thus the upper figures for shallow faults are more similar to the Fault II models than the lower figures for deeper faults. Elastic/ductile models that incorporate bedding plane slip surfaces have been tested and example results are shown in the right column of the figure. Some features of the *Geological* models are reproduced; the deformation does not diminish rapidly with distance from the fault and places of maximum shear (dark shading) are located where large shear also occurs in the *Geological* models. Small changes in the separation of the slip surfaces and how they interact with the main faults can be very important. Future work will explore these questions further.

Another area for which only preliminary work has been carried out concerns the role of isostacy and the loading and unloading resulting from sedimentation and erosion. For example, erosion of the surface fold leads to futher uplift, while deposition into flanking basins futher depress these regions; the length scale of these isostatic adjustment depends on the flexural rigidity and density contrasts in the media. The necessary computer codes have been created and will be examined shortly.

G.C.P. King (Institut de Physique du Globe, Strasbourg 67084, France) and J. Lin (Woods Hole Oceanographic Institution, Woods Hole, MA 02543) are 1991/92 SCEC Visiting Fellows. R.S. Stein is at the U.S. Geological Survey, MS 977, Menlo Park, CA 94025

Comparison of Fault II Models with Elastic/Ductile Models with and without Bedding Plane Slip

(dark shading - high shear strain)

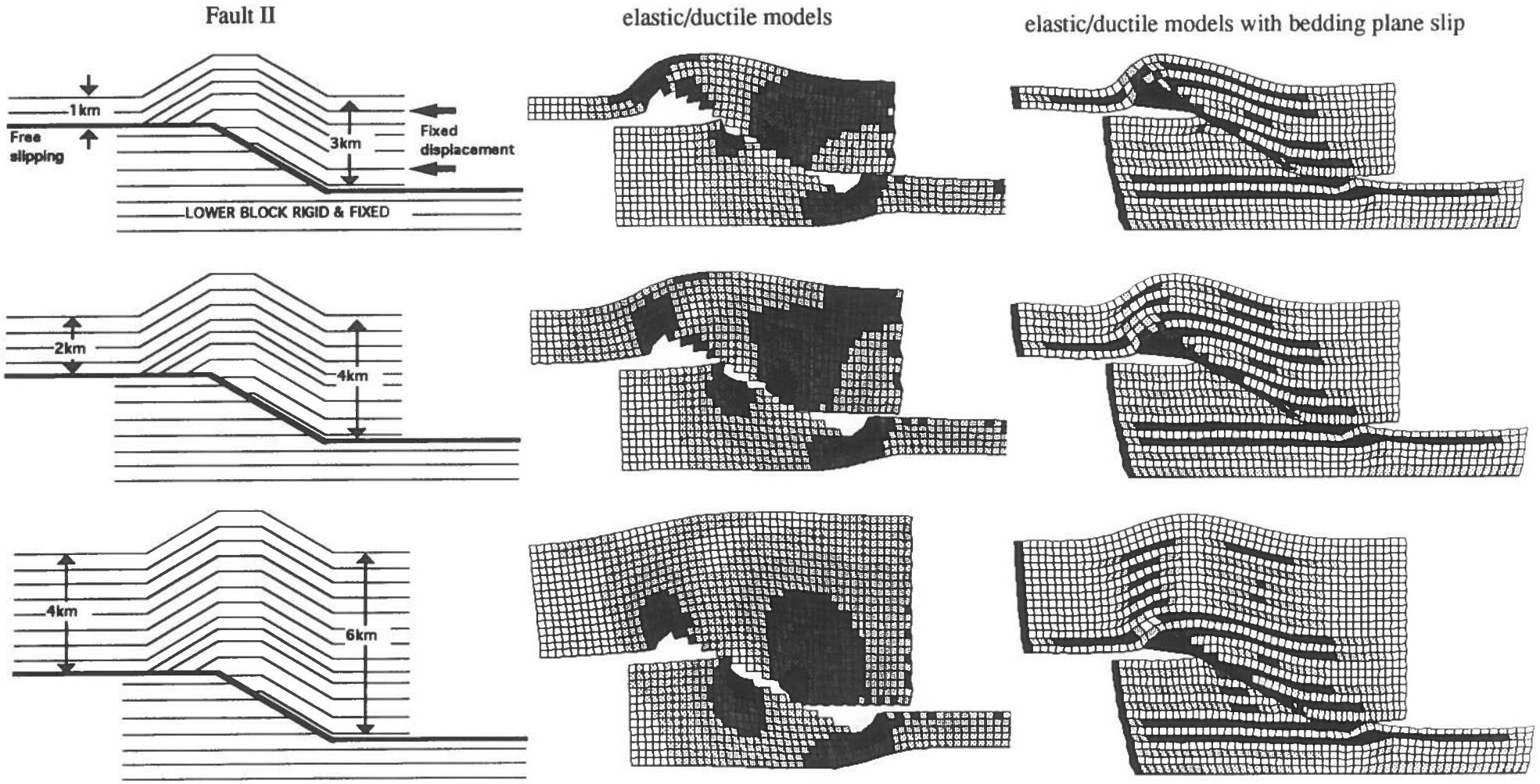

COSEISMIC STRESSING OF BLIND THRUST FAULTS BENEATH THE LOS ANGELES BASIN

Jian Lin, Ross S. Stein, and Geoffrey C. P. King

Geological and geodetic evidence has revealed a suite of active reverse and blind thrust faults that are accommodating ~ 8 mm/yr north-south contraction in the Los Angeles basin. The goal of our project is to understand the geometry, interactions, and slip rates of these faults and to assess their earthquake potential. We are currently pursuing two lines of inquiry. The first study probes the relation between coseismic slip on blind thrusts and formation of shallow secondary faults. The second study (see King, Stein, Lin report) relates near-surface geological structure to the blind fault geometry by examining retrodeformable cross sections in elastic/plastic media.

To probe the fundamental characteristics of blind thrust faults, we have constructed detailed coseismic stress models for each of the following recent thrust earthquakes in California: 1983 Coalinga, 1985 Kettleman Hills, 1987 Whittier Narrows, 1989 Loma Prieta, 1991 Sierra Madre, and 1992 Cape Mendocino. For each blind event, changes in failure stress are predicted for tectonic conditions of earthquake stress-drop, regional compressional stress, pore fluid pressure, and rock frictional strength (see Fig. 1). Results of numerical experiments are compared with aftershock spatial patterns and time sequences, geological structure inferred from seismic refraction where possible, and surface secondary faults where observed.

Results of these models reveal specific control of earthquake fault geometry in determining failure stress pattern of blind thrusts. We have found that when the depth of the fault (D) is less than its down-dip dimension (W), as in the case of Loma Prieta and Cape Mendocino earthquakes, the strain field is modified by proximity of the ground surface, with concentrated patches of high strains extending to the surface above the fault tip. If the rocks at this shallow depth are strong enough to store elastic strain and brittle enough to fail by faulting, then these strains will promote secondary fault failure. Our model predicts regions of enhanced ground surface failure that agree favorably with the observed secondary surface faults of the Loma Prieta earthquake. When the depth of the fault is comparable to or greater than its down-dip dimension, as in the case of Whittier Narrows, Coalinga and Sierra Madre earthquakes, coseismic changes in failure stresses favor growth of faults towards surface (see Fig. 1). In the case of Whittier Narrows earthquake, the dip of such upward fault growth is greater under stronger regional compressional stresses.

It is encouraging that our modeled zones of elevated stresses correspond to sites of high-angle reverse faults and shallow aftershocks observed in the cores of several active anticlines, including the Coalinga and Kettleman Hills folds. If a secondary fault forms in the zone of high shear strains in front of the fault tip, and slips freely to accommodate the strains produced by the blind fault tip, then the surface slip will be about 25% of the blind slip at depth.

The relationship between secondary surface faults and blind thrust at depth are critical to interpretation of the Santa Monica-Hollywood fault and other active reverse faults that mark the northern margin of the Los Angeles basin. The slip rate and geometry of the surface-cutting faults yield insights into the fault slip at depth, even if the surface faults are rootless and the thrust are blind. If, for example, the Santa Monica-Hollywood fault is rootless, then the rate of slip several kilometers below on an underlying blind fault may be four times greater than the slip rate on the surface fault.

We plan to examine the preferred orientations and geometries of the secondary faults, and to study the relationship between surface and blind-fault slip for the fault geometries along the northern margin of the Los Angeles basin. We will also investigate other near-surface strain concentration seen in these models, which may be associated with near-surface reverse faults with the opposite vergence.

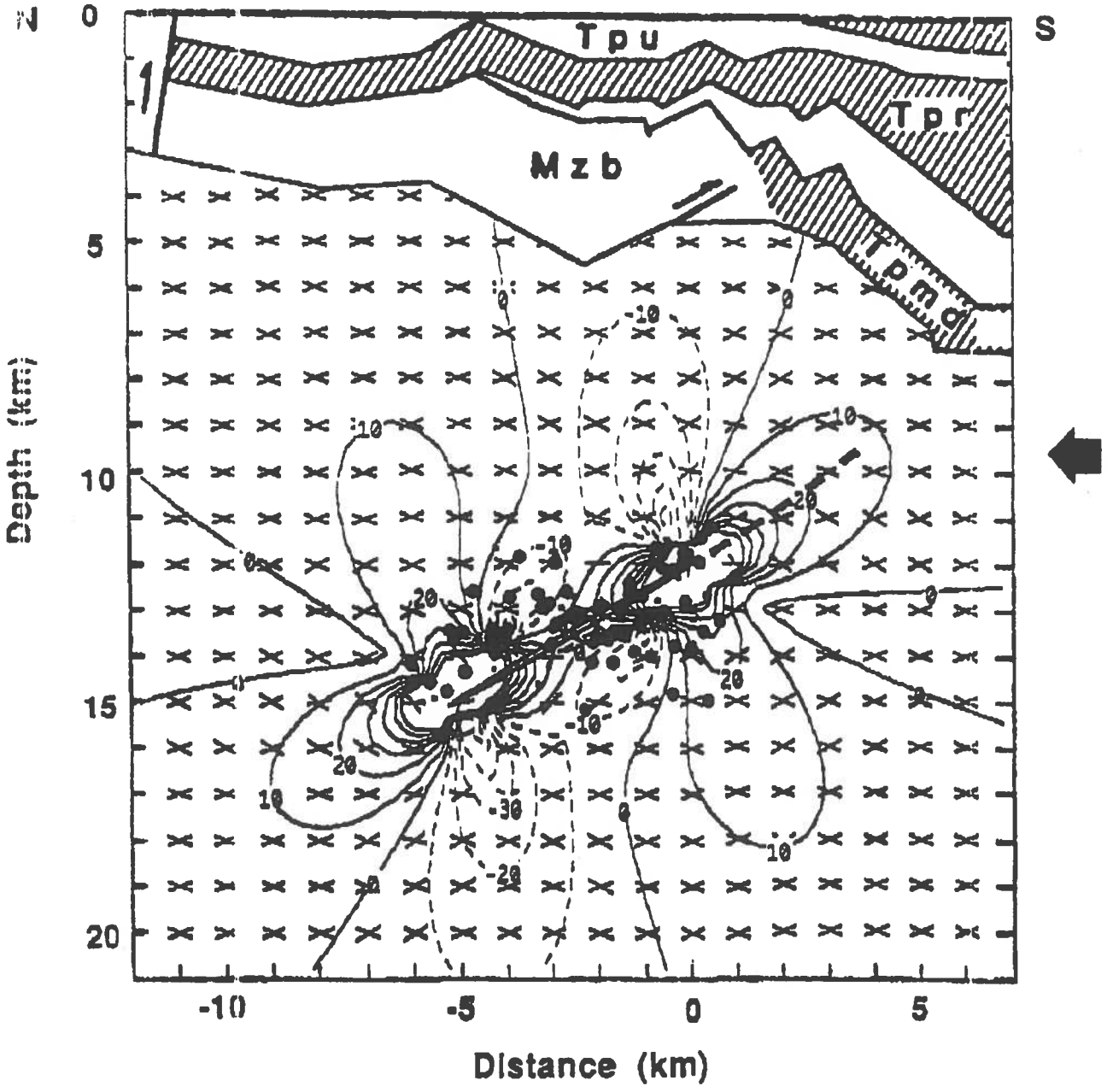

Fig. 1. Schematic geological cross section of the 1987 Whittier Narrows M5.9 epicenter (open circle) and aftershocks, together with predicted changes in Coulomb failure stress following the earthquake. Positive values correspond to elevated stresses. Using a boundary-element algorithm, we computed the Coulomb failure stress $\Delta\sigma_f=\Delta\sigma_s+\mu(\Delta\sigma_n-\Delta P)$, where $\Delta\sigma_s$, $\Delta\sigma_n$, and ΔP are the changes in static shear stress, normal stress, and pore fluid pressure, respectively. The optimum dip angles of secondary faults (crosses) are predicted considering both the regional stress σ_{far} (100 bars) and earthquake stress drop $\Delta\sigma_{fault}$ (60 bars). Note that changes in failure stress favor the upward growth (dashed) of Whittier Narrows fault segment (elongated ellipse). Downward growth is less favorable because of possible ductile flows at depth.

SCEC PROGRESS REPORT

Earthquake Geology of the Western Sierra Madre Fault Zone and Investigations of the Landers Earthquake Rupture

Scott Lindvall
Lindvall Richter Benuska Associates
825 Colorado Boulevard, Los Angeles, CA 90041

Preliminary air photo analysis and field reconnaissance was underway on the Sierra Madre fault when the M_w7.4 June 28, 1992 Landers earthquake struck southern California. This earthquake redirected my research efforts for this year. Following the earthquake, I spent several days in the field mapping surface ruptures and measuring displacements with Kerry Sieh and the group from Caltech.

Continuing the Landers research, Tom Rockwell and I are pursuing to study the past behavior of faults that ruptured in the earthquake. This work is currently being coordinated with similar efforts of Kerry Sieh and Charlie Rubin. Tom Rockwell and I have selected several trench sites on the Johnson Valley, Landers, Homestead Valley, and Camp Rock faults that have potential for determining the spatial and temporal pattern of past ruptures on this large zone of faults that ruptured in the M_w7.4 Landers event.

Three of these sites have been surveyed within the first few weeks of the earthquake. Multiple profiles were shot at each site with a Wild TC2000 to establish the vertical separation in this event as well as the total deformation of the old, degraded scarp that has been produced from past earthquakes. These profiles will allow a comparison of the slip in this event with that of the entire degraded scarp, as well as provide the initial measurements for future scarp degradation studies.

We have already placed 2 trenches across a subsidiary thrust fault at one of our sites on the Homestead Valley fault. The main dextral strand of the fault runs along the side of a hill in a compressional, left bend of the zone. The thrust fault, which produced vertical scarps about 50 cm in height at the base of the hill, had almost no lateral slip in this event. Trench 1 across this thrust fault exposed a sequence of Holocene sands and gravels that experienced 85 cm of dip slip in the Landers rupture (Figure 1).

Trench 2 exposed a much older sequence of alluvium that shows evidence for two rupture events which post-date a buried late Pleistocene paleo-surface (paleo-surface #1 in Figure 2). The age of this surface is estimated based on the soil characteristics of the B_t horizon developed in unit 5. The penultimate event is represented by a colluvial wedge of scarp debris (unit 4 in Figure 2) overlying the paleo-surface. These preliminary data suggest a long recurrence interval for this particular thrust splay of the Homestead Valley fault, which may only rupture in large, Landers-type earthquakes.

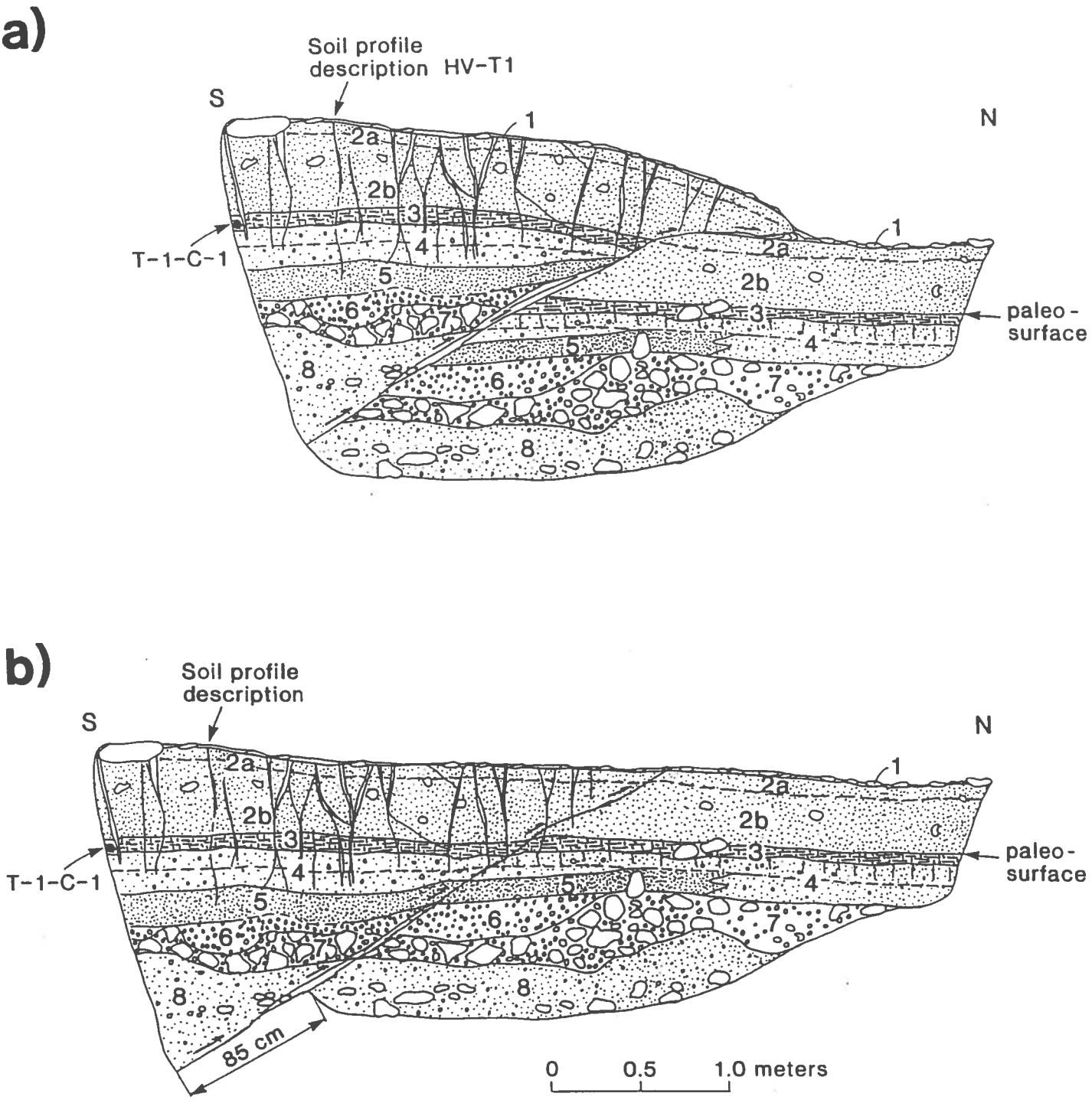

FIGURE 1. Trench 1 at the thrust site on the Homestead Valley fault showing **a)** log of west wall and **b)** a cut and splice reconstruction of 1992 slip. Logged by Tom Rockwell and Scott Lindvall.

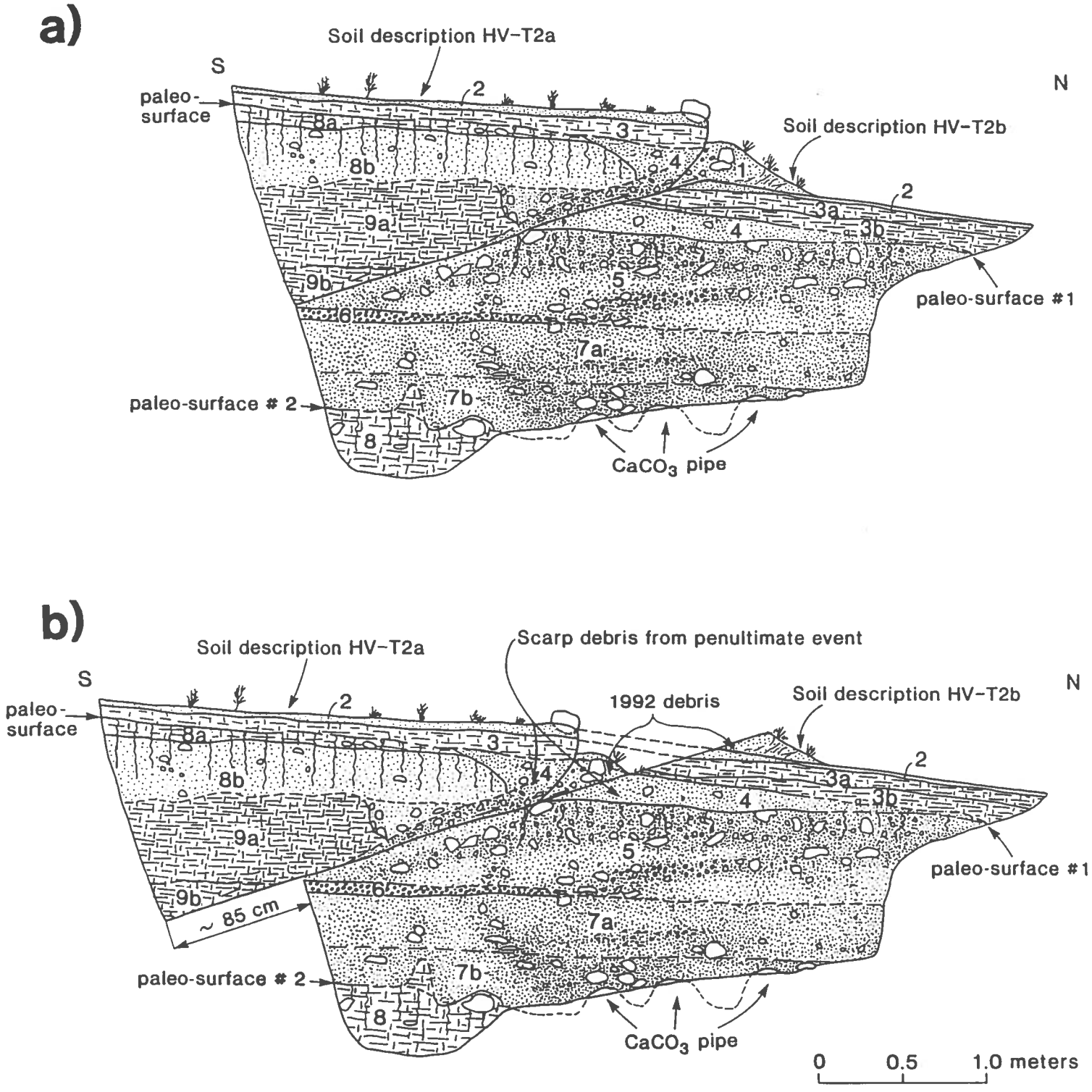

FIGURE 2. Trench 2 at the thrust site on the Homestead Valley fault showing **a)** log of west wall and **b)** a reconstruction of 1992 slip. The colluvial wedge (unit 4) overlying paleo-surface #1 represents scarp debris from the penultimate event. Logged by Tom Rockwell and Scott Lindvall.

Southern California Earthquake Center Progress Report
September 12, 1992
Sally F. McGill

1. Landers earthquake

This report presents the preliminary results of 3 weeks of field mapping of surficial ruptures on the southern half of the Emerson fault associated with the 28 June 1992 Landers earthquake. This work was done in collaboration with Dr. Charlie Rubin.

Along the 6-km-length of the Emerson fault shown in Figure 1, right-lateral displacement on the main rupture varies between about 1.5 and 6.7 meters (Figure 2). An 0.6-km length of the main trace did not break along discrete fractures, but rather was right-laterally and vertically warped. Vertical slip was up on the northeast side for most of the fault length studied, but a few areas exhibited southwest-side-up vertical slip (Figure 3). The average absolute vertical displacement was about 0.65 meters, and the maximum was 1.75 meters, northeast-side up.

Variations in right-lateral slip along strike occur at several distance scales (Figure 2). For example, for about 1.5 km southeast of Galway Lake road the right-lateral displacement averages about 4.2 meters. Between about 1.5 and 3.1 km southeast of that road, right-lateral slip averages about 2.7 meters. Between about 3.1 and 4.2 km slip averages about 4.0 meters and between 4.2 and 5.2 km slip drops to an average of 2.3 meters again. The northwestern one of the two areas with lower slip is located where slip begins to transfer to the Camp Rock fault, and the southeastern area of lower slip is located where slip is transferring from the Homestead Valley fault to the Emerson fault (Figure 1).

Variations in slip also occur over shorter distances. For example, about 2.2 km southeast of Galway Lake Road the right-lateral slip apparently changes from 1.5 m to 3.9 meters within about 100 meters along strike.

Figure 4 shows a histogram-like plot of the slip measurements. The two peaks at about 2 and 4 meters reflect the 1-2-km-scale variations in slip described above. Some portions of the fault exhibit close to 2 meters slip whereas others exhibit close to 4 meters of slip, with the transitions between these portions occurring over fairly short distances.

The bimodal nature of this plot has implications for the interpretation of offset geomorphic features along faults that have not ruptured historically. A similar bimodal plot representing measurements of offset geomorphic features along the Garlock fault in Pilot Knob Valley was interpreted to indicate that features making up the first peak had been offset in the most recent earthquake and that those contributing to the second peak had been offset in the past two events combined. However, Figure 4 shows that a bimodal histogram may be generated by features offset in a single earthquake. There is no way that the features offset about 4 meters, which make up the second peak in Figure 4, could have been offset in a previous event in addition to the 28 June earthquake. Many of them are motorcycle tracks that clearly were not present when the previous (prehistoric) earthquake occurred.

Significant displacement also occurred on secondary faults (Figure 1). Several northward-trending fractures each slipped 20-75 cm right-laterally. Two northeastward-trending faults slipped up to 50 cm left-laterally. Several westward- to northwestward-trending thrust faults, each with up to 25 cm throw, formed north of a convergent step-over in the main trace.

2. San Andreas fault

I have also viewed air photos of the San Andreas fault in San Bernardino and have visited a few potential paleoseismic sites, but have not yet selected one.

FIGURE CAPTIONS

Figure 1: Surficial ruptures on and near the Emerson fault associated with the 28 June 1992 Landers earthquake. Heavy dots show locations of slip measurements. Selected measurements are shown.

Figure 2: Right-lateral slip as a function of distance along main trace. Distance is measured southeastward from Galway Lake Road. Filled squares represent preferred values, short horizontal lines above and below each filled square indicate upper and lower bounds on the measurement. Measurements of features that do not cross the entire main trace, or whose correlations across the fault are less certain are not shown.

Figure 3: Vertical slip as a function of distance along the main trace.

Figure 4: Summation of Gaussian probability density functions for measured offsets along the southern Emerson fault. Each offset measurement is treated as a Gaussian probability density function with a mean at the preferred value of the measurement and with a standard deviation equal to one-quarter of the difference between upper and lower bounds of the measurement.

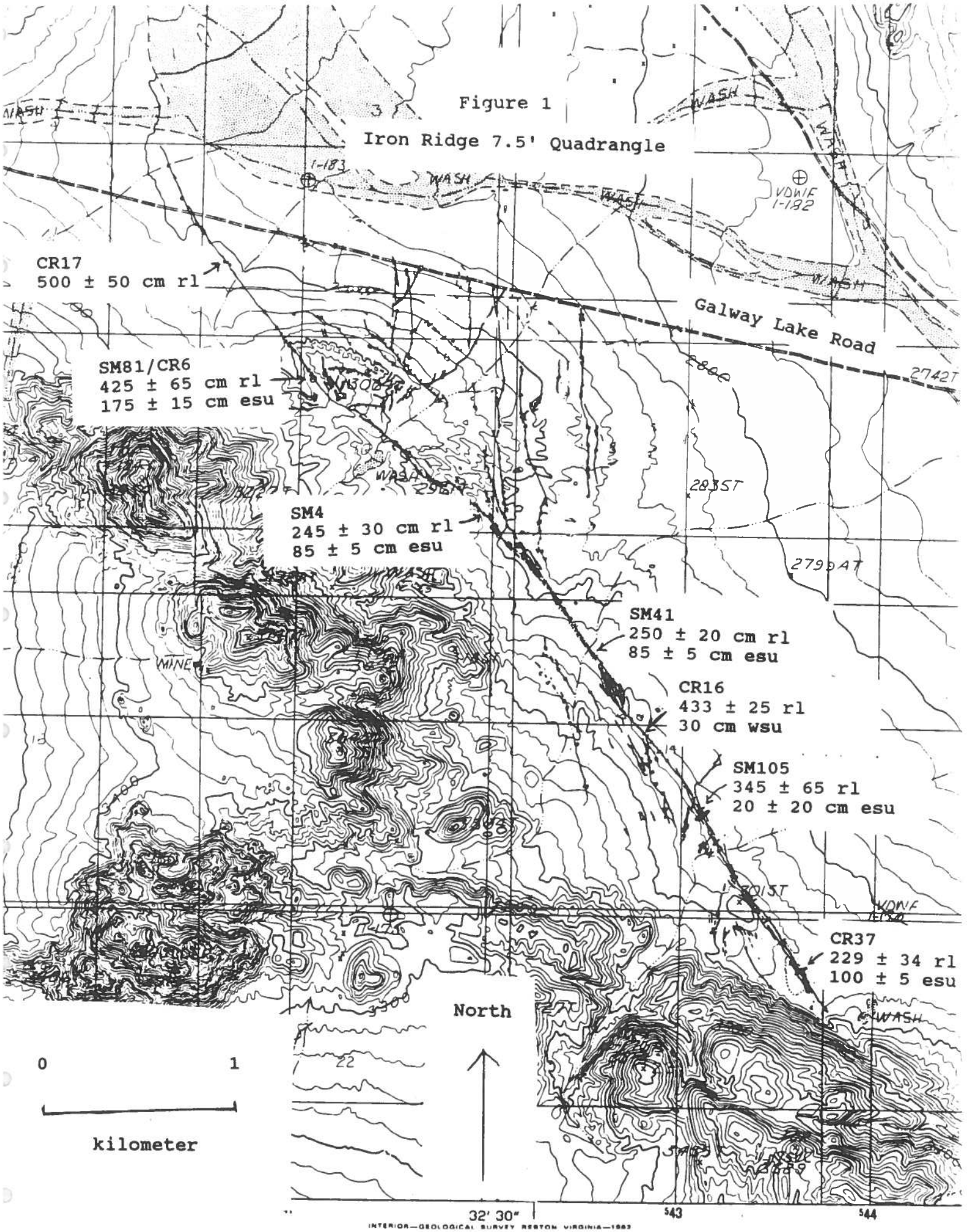
Figure 1
Iron Ridge 7.5' Quadrangle
CR17
500 ± 50 cm rl
SM81/CR6
425 ± 65 cm rl
175 ± 15 cm esu
SM4
245 ± 30 cm rl
85 ± 5 cm esu
SM41
250 ± 20 cm rl
85 ± 5 cm esu
CR16
433 ± 25 rl
30 cm wsu
SM105
345 ± 65 rl
20 ± 20 cm esu
CR37
229 ± 34 rl
100 ± 5 esu
Galway Lake Road
WASH
MINE
North
0
1
kilometer
32' 30"
543
544
INTERIOR—GEOLOGICAL SURVEY RESTON VIRGINIA—1982

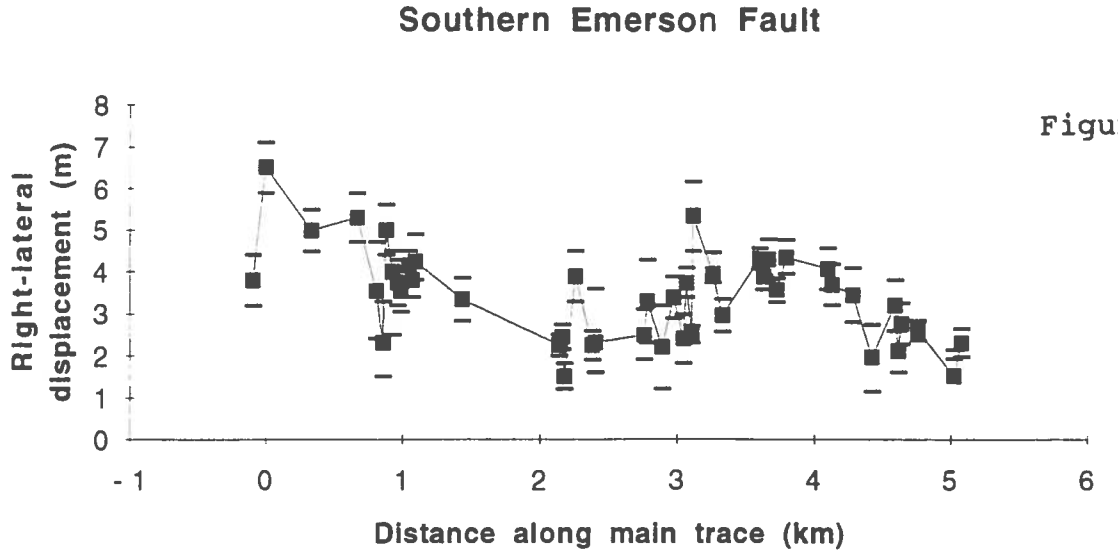

Figure 2

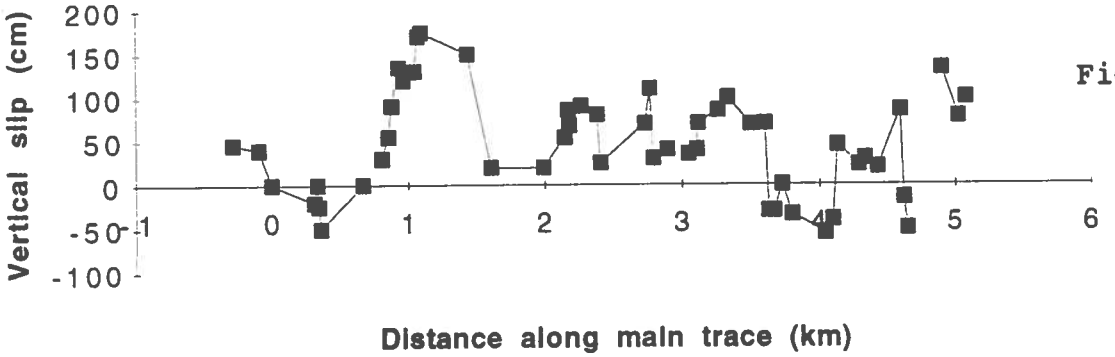

Figure 3

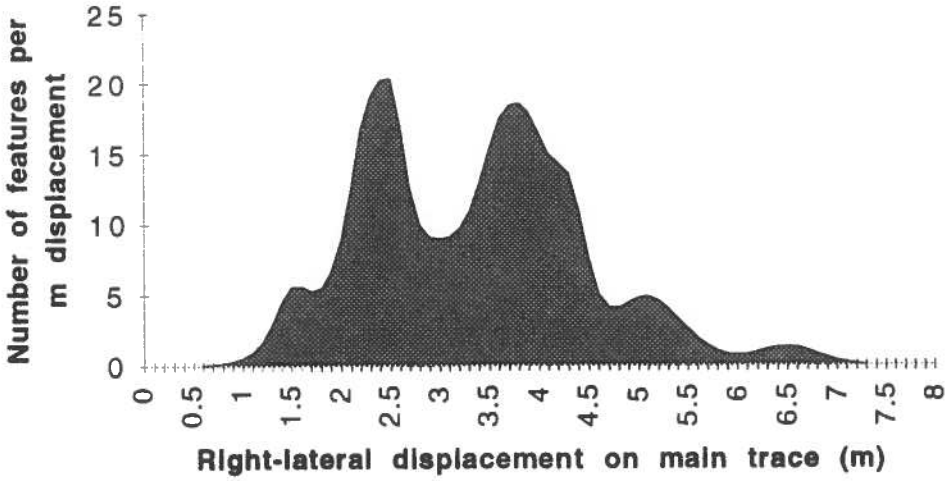

Figure 4

Davis and Namson Consulting Geologists
25600 Rye Canyon Road, Suite A
Valencia, California 91355
(805) 257-6870
FAX: (805) 257-6870

SCEC Progress Report, September 15, 1992

Davis and Namson are extending their previous studies of the Santa Monica Mountains anticlinorium and Elysian Park thrust system westward into offshore Santa Monica Bay. The main approach is the construction of retrodeformable cross sections that integrate high-quality, offshore, regional seismic reflection lines of Santa Monica Bay with surface and subsuface geology of the Santa Monica Mountains anticlinorium and ocean bottom geology (Figure 1). Over 780 miles of high-quality seismic reflection data have been loaned to us at no cost by a major oil company on a non-proprietary basis. Quaternary and Tertiary age control on structures will be provided by diatom and foram analyses from wells, seafloor samples and onshore outcrops.

To date we have concentrated on gathering well data from oil companies and the Mineral Management Service, surface mapping of the nearby Santa Monica Mountains from various sources including the Tom Dibblee Foundation, and ocean bottom mapping from various government and private sources. Our main efforts to date have been along seismic line 393-46-82 (Figure 1). Present SCEC funding will allow us to complete interpretation of the line and construct a retrodeformable cross section that will provide a first-order estimation of late Cenozoic shortening and thrust fault distribution.

In May 1992 we submitted a proposal to USGS-NEHRP to fund structural and seismotectonic interpretation along all of the seismic lines. Presently we do not know the status of that proposal.

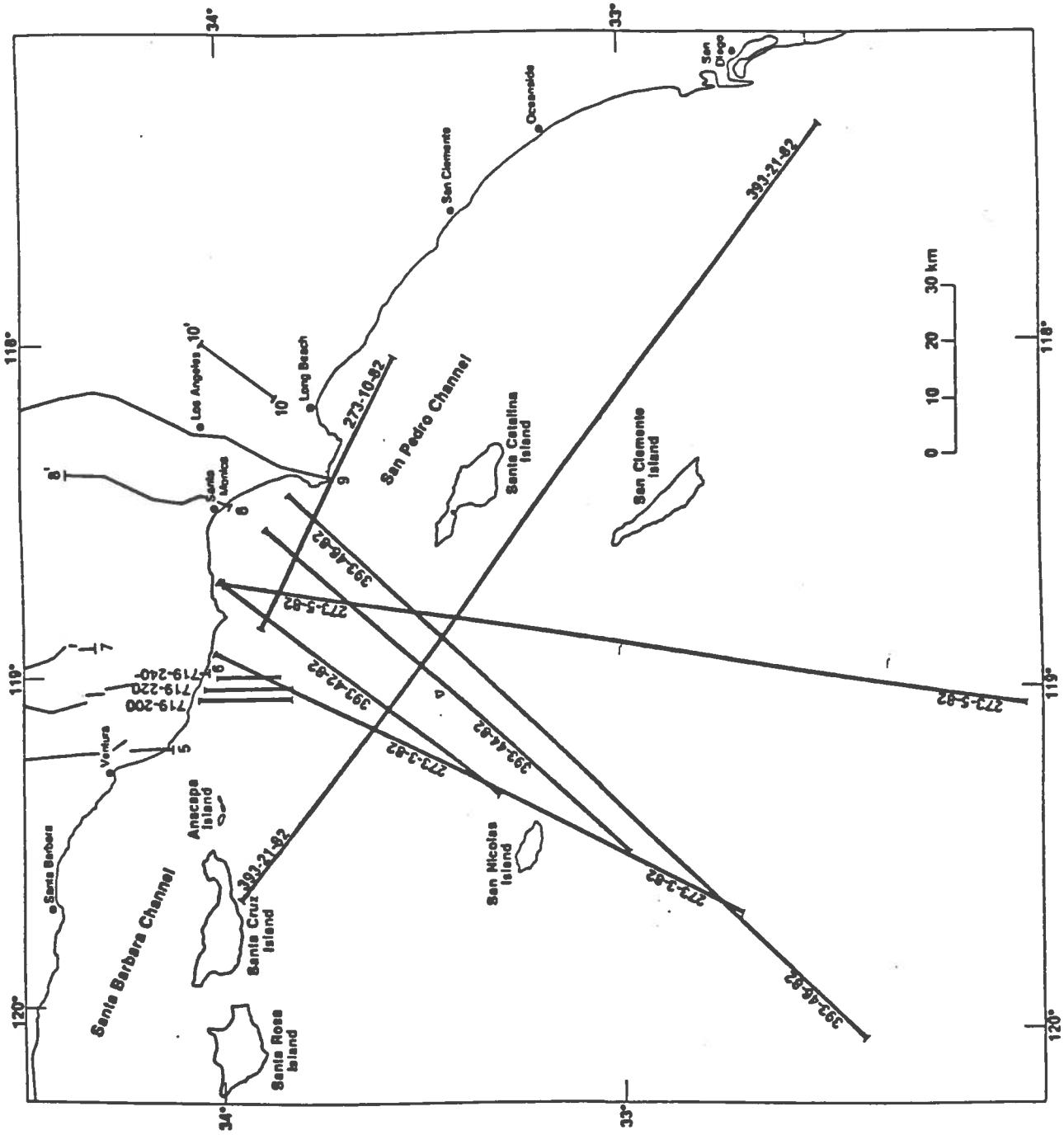

Figure 1 Geologic map of part of the western Transverse Ranges showing locations of previously completed cross sections and new proposed cross sections and seismic lines outlined in this proposal. The approximate locations of new seismic reflection lines and cross sections for this proposed study are shown

Paleoseismic study of active surface faults in the Los Angeles region

by

Thomas Rockwell, Aurie Patterson, and Maria Herzberg
Department of Geological Sciences
San Diego State University
San Diego, CA 92182

Paleoseismic investigations of active surface faults provide direct information on slip rates and the timing of past earthquakes. For many of the faults in the Los Angeles basin region, little information of this type is known. During 1992, work was focused in four areas: the Whittier fault in northeastern Orange County; the Palos Verdes fault in the Palos Verdes peninsula area; the Santa Monica fault (with Jim Dolan and Kerry Sieh); and faults associated with the Landers earthquake.

Over 20 trenches were excavated, logged and completed at one site along the Whittier fault, yielding information on the timing and slip for the last event. Much of the work was done by hand because of the size of the channels that were exposed. Five channels were recognized, with two being younger than the age of the last movement. Three channels that were affected by the fault are shown in figure 1.

Three strands of the fault cross the site, with apparently only the most easterly being active during the past 1-2 events. The oldest channel, indicated by triangles on Figure 1, is displaced about 11 m right-laterally and less than 50 cm vertically. No carbon was recovered from this channel so a slip rate can not be determined from this offset but it does indicate that the Holocene sense of slip has been nearly pure strike-slip.

The channel indicated by stars was traced into and across the fault and is offset 1.8-2.0 m. Several charcoal samples were recovered from this unit so its age will be known. Also of note, however, is that this channel appears to have "seen" the fault. The channel approaches the fault zone from the northeast and deflects along the fault within centimeters of it but does not cross it for several meters. This observation suggests that the channel may immediately post-date an earthquake and that a scarp was present at the time of channel formation.

Overlying the star channel, a younger channel indicated by dots in figure 1 appears not to be offset by the fault. The dot channel was originally interpreted in the cross-fault trenches to be part of the same nested channel sequence as the star channel, and there probably is very little time between their ages of formation. The fault appears to cut this channel deposit in at least one exposure but the displacement must be small. It should be pointed out, however, that one channel margin piercing point was removed during the excavation of our original trench in this canyon

whereas the other channel margin trends parallel to the fault for several meters and minor slip would be difficult to resolve. Nevertheless, projection of the southern channel margin into the fault over a distance of about 1 m from each side of the original trench suggests little or no lateral slip. This may represent displacement in a separate earthquake from the one that displaces the star channel. Alternatively, this channel may immediately postdate the earthquake that displaces the star channel and the minor displacement observed in the one trench exposure may be the result of afterslip.

Although ^{14}C will provide direct absolute age control on the ages of many of the stratigraphic units in this study and the time since the last earthquake, preliminary field observations suggest that it has been a considerable length of time since that event. In virtually all faults that I have trenched that have experienced rupture in the past several hundred years, the base of the A horizon as well as filled burrows of gophers or other animals are usually seen to be displaced. As time passes, subsequent activity by burrowing animals erases the evidence for very recent displacement. In the case of the active strand of the Whittier fault in this study, the fault could not be traced upward into the A soil horizon nor was it observed to displace filled animal burrows near the surface. This indicates that it has either been a substantial length of time since the last event or that the rate of bioturbation (soil mixing) is higher than in the other areas that I use for comparison.

The above data suggest that: 1) the sense of slip on the Whittier fault is nearly pure right-lateral; 2) the star channel is displaced by nearly 2 m of strike-slip whereas the dot channel is not noticably offset, suggesting displacement in a single event; and 3) it has been more than just a few hundred years since the last event based on the lack of expression of the fault in the overlying soil.

Studies continued on the Palos Verdes fault, with two shallow seismic surveys completed that provided information on the location of the main onshore fault traces. The main fault has been found to be virtually inaccessible for trenching due to either major historical surface disturbance or burial of the fault by development and other structures. Trenching across a secondary photolineament failed to expose a fault.

Due to the occurrence of the M7.4 Landers earthquake in June, some time has also been devoted to trenching along the surface rupture to resolve the timing of past events. This work is being conducted with Scott Lindvall, Charlie Rubin, and Kerry Sieh and his group, and is presented in the technical summary by Scott Lindvall.

Finally, I also collaborated with Kerry Sieh and his group (primarily Jim Dolan) on their study of the Santa Monica and Hollywood faults. We are using soils to quantify the ages of Holocene and Pleistocene alluvial deposits that are displaced by the faults, and trenching to study the paleoseismology.

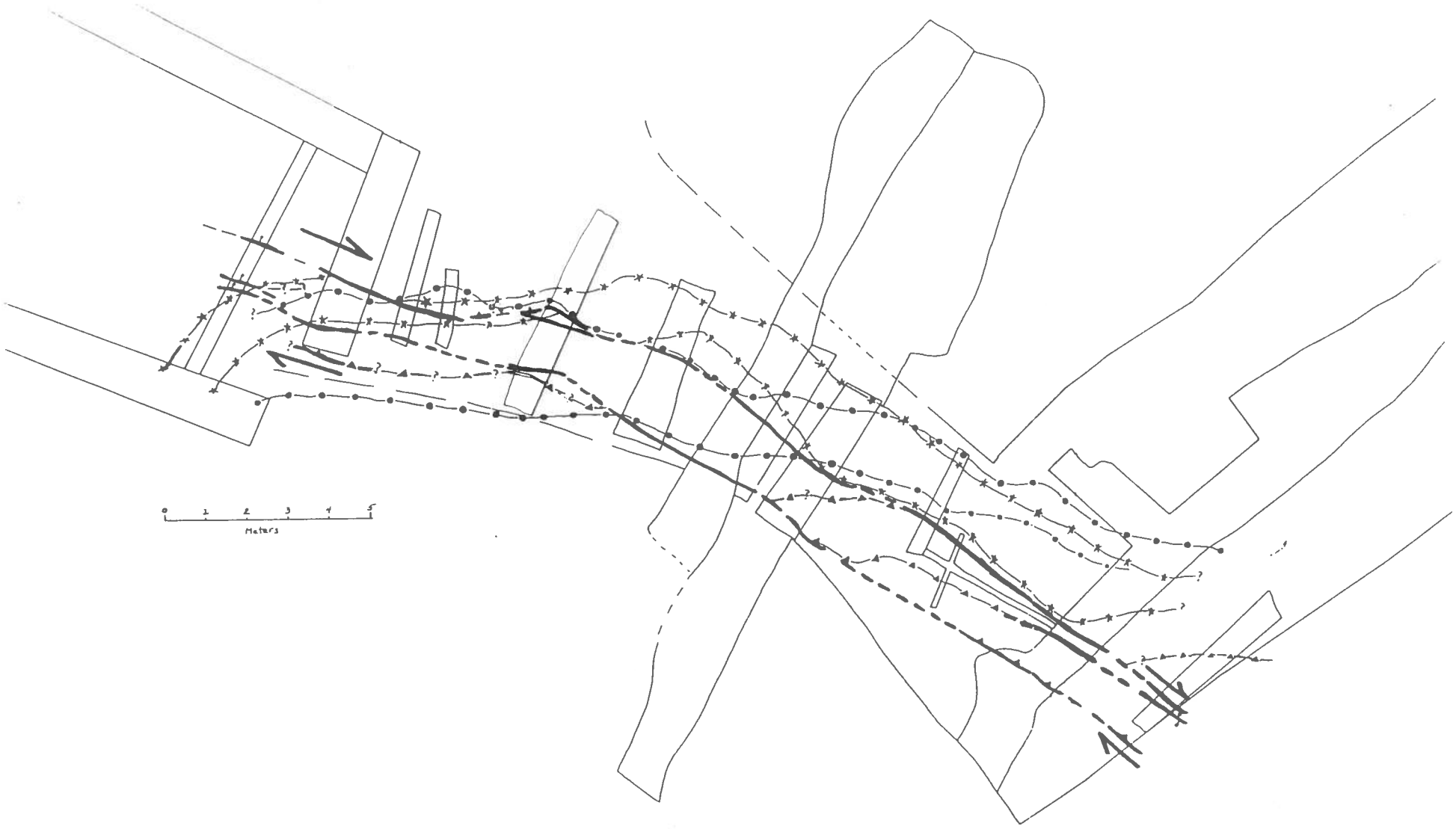

Figure 1. Map showing trench locations, traces of the Whittier fault, and displaced Holocene gravel-filled channels at the Olinda site, northeastern Orange County, California.

ACTIVE CRUSTAL SHORTENING ALONG THE SOUTHERN FLANK OF THE CENTRAL TRANSVERSE RANGES, CALIFORNIA

Charles Rubin. Department of Geology, Central Washington University, Ellensburg, Washington
and Kerry Sieh, Division of Geological and Planetary Sciences, Caltech, Pasadena, California

Over the past four months our efforts were divided into three main areas of research: (1) geological investigations on the June 28 Landers Earthquake, (2) geologic and paleoseismic earthquake studies along the Sierra Madre segment of the frontal fault system along the southern flank of the San Gabriel Mountains, and 3) integration of Geographic Information System (GIS) and Total Station surveying software.

The June 28 Landers Earthquake

1) Within a few hours of the June 28 Landers shock, with the Caltech group, we began to search for evidence of surface fault ruptures in both the Bear Bear area and north of the epicentral area in Landers. By the end of the second day, we had located most of the principal ruptures and had measured numerous surface offsets. Based on our initial two days of mapping, aerial photographs were taken on the third day, courtesy of the USGS. These 1:6,000 aerial photographs were used as the base for our detailed mapping of the faults.

The Landers earthquake was produced by rupture along five major faults. The length of the fault zone is about 70 kilometers, but the cumulative length of the major faults is nearly 100 kilometers. Spectacular surficial ruptures are present along a fairly wide zone that trends northward from the epicenter and bends northwestward. Observations indicate a predominance of right-lateral slip, with an average of about three meters and a maximum of 6.7 meters. Locally, vertical displacement exceeded 1.5 meters. Based on the measured surface offsets, the total geologic moment for the earthquake is about 10^{27} dyne/cm.

2) After the initial effort to map the 70 km length of the fault and to document offset markers, I began more detailed measurements of surface offsets and detailed geologic mapping (in collaboration with Sally McGill) at a scale of 1:6,000 along the central portion of the June 28th earthquake fault, where the maximum surface displacement was observed. All available offsets were measured and our work may represent the best documented study of slip distribution along an active strike-slip fault [Rubin, and McGill, in press]. In addition, preliminary geomorphic mapping along the central portion of the fault suggests that repeated large-scale surface faulting had occurred along the Emerson fault during the Quaternary time. Sally McGill and I will continue to study the variability in displacement vs. distance along the strike of the fault. These data will be compared with offset geomorphic features across faults in the region that have not ruptured historically. Based on the measured surface offsets, the total geologic moment for the earthquake on a 10 km part of the Emerson segment is about 2×10^{26} dyne/cm.

We have identified numerous sites for paleoseismic studies along this segment of the fault for future work. We hope to begin excavations in November, 1992. Our first trench will be sited near the right-lateral offset of ~6.7 m that we documented earlier. This site had the maximum displacement for the June 28 earthquake, and has the largest Twentieth Century strike-slip displacement measured in the Northern Hemisphere. We have permission from the District Manager of the Bureau of Land Management to excavate along this part of the fault. Documentation of the prehistoric earthquakes along the surface rupture of the Landers earthquake will allow us to make a more realistic assessment of the location, size, and timing of the next major earthquakes in the region.

Sierra Madre Segment

1) A geologic map of the Sierra Madre Fault has been completed (Figure 1). This map is a significant improvement over the Crook et al. [1987] map, since geomorphic features were used

extensively in our analysis. Topographic profiles have been constructed across active stream channels and alluvial fan surfaces. These profiles show abrupt steps that strongly suggest Quaternary deformation [Rubin and Sieh, in press]. In addition, we have compared the Sierra Madre segment with other active major reverse faults (Figure 2) in order to evaluate models of segmentation along the Sierra Madre fault and expected magnitude of potential earthquakes. Based on this reverse fault compilation, and using the lessons learned from the complicated surface rupture of the June 28 Landers Earthquake, it is clear that segmentation alone cannot be used to predict either the spatial distribution of the rupture or the size of an earthquake.

Based on the new map of the Sierra Madre segment and our comparison with other large reverse faults, we are beginning a manuscript on the earthquake potential along the southern flank of the San Gabriel Mountains that will be submitted to the Journal of Geophysical Research.

2) After excavating a trench in Duarte across one of the more promising sites along the frontal fault system no fault was found. It appears that the present-day landform in Duarte had been modified during the planting of the fruit groves during the early part of this century. Because the trench bottom was in crystalline upper plate rocks, the thrust fault must be located to the south of our excavations, where cultural modifications of topography obstruct our studies. We have identified a few other promising excavation sites along the Sierra Madre segment. We intend to pursue SCEC 1993 funding for these paleoseismic studies. By excavating new trenches at various locations along the fault trace, we hope to date prehistoric earthquakes and thereby determine the average recurrence interval and slip rate for the frontal fault system.

Integration of Geographic Information System and Total Station Surveying

In collaboration with Anne Lilje at Caltech, we have completed preliminary software that will link survey data from the Wild Total Station with ARC/INFO, using a SUN workstation. The software is not platform specific, therefore, Total Station survey data can potentially be downloaded directly to a SUN workstation, an IBM compatible PC, or a Macintosh. We have extensively modified the TOPOS surveying program as the basis for this new software package.

References

Buwalda,J. P., and P. St-Amand, Geological effects of the Arvin-Tehachapi earthquake, 1952, Calif. Dept. Nat. Res., Div. Mines Bull. 171, 41-56, 1955.

Crook, R. Jr.,. C. R. Allen, B. Kamb, C. M. Payne, and R. J. Proctor, Quaternary geology and seismic hazard of the Sierra Madre and associated faults, western San Gabriel Mountains, edited by D. M. Morton and R. F. Yerkes, U. S. Surv. Prof. Pap. 1339, 27-64, 1987.

Kamb, B., L .T. Silver, M. J. Abrams, B. A. Carter, T. H. Jordan, J. B. Minster, Pattern of faulting and nature of fault movement in the San Fernando earthquake, The San Fernando, California, earthquake of February 9, 1971, U.S.G.S. Professional Paper 733, 41-54, 1971.

Landers Earthquake Response Team, Near-Field observations of the June 28, 1992 Landers Earthquake, California, to be submitted to Science.

Matsuda, T., H. Yamazaki, T. Nakata, and T. Imaizumi, The surface faults associated with the Rikuu Earthquake of 1896, Bull. Earthq. Res. Inst., 55, 795-855, 1980.

Philip, H., and M. Meghraoui, Structural analysis and interpretation of the surface deformation of the El Asnam earthquake of October 10, 1980, Tectonics, 2, 17-49, 1983.

Rubin, C. M., and K. E. Sieh, Active crustal shortening along the southern margin of the central Transverse Ranges, Association of Engineering Geologists Annual Meeting, in press.

Rubin, C. M., and K. E. Sieh, Active thrust faulting along the southern margin of the central Transverse Ranges, Los Angeles, California, Eos, Transactions of the American Geophysical Union, in press.

Rubin, C. M., and S. F. McGill, The June 28, 1992 Landers earthquake: Slip distribution and variability along a portion of the Emerson Fault, Eos, Transactions of the American Geophysical Union, in press.

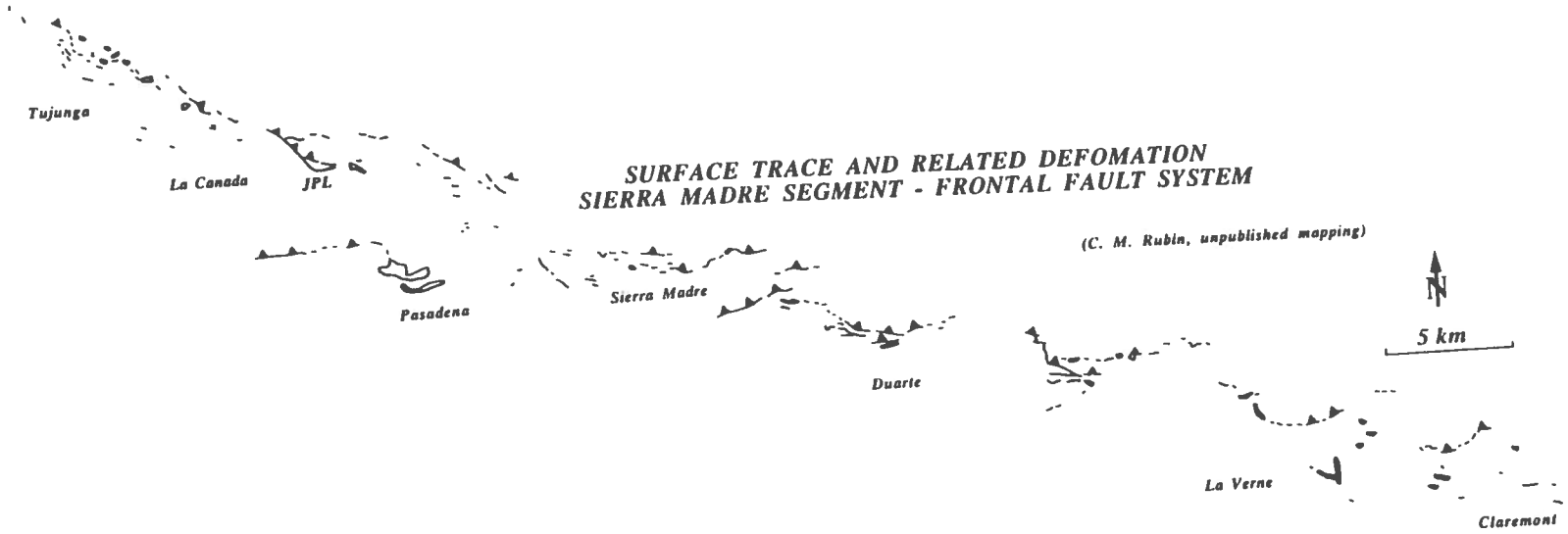

Figure 1. Surface trace of the Sierra Madre segment and adjancent deformed alluvial fan surfaces [Crook et al., 1987; C. M. Rubin, unpublished mapping].

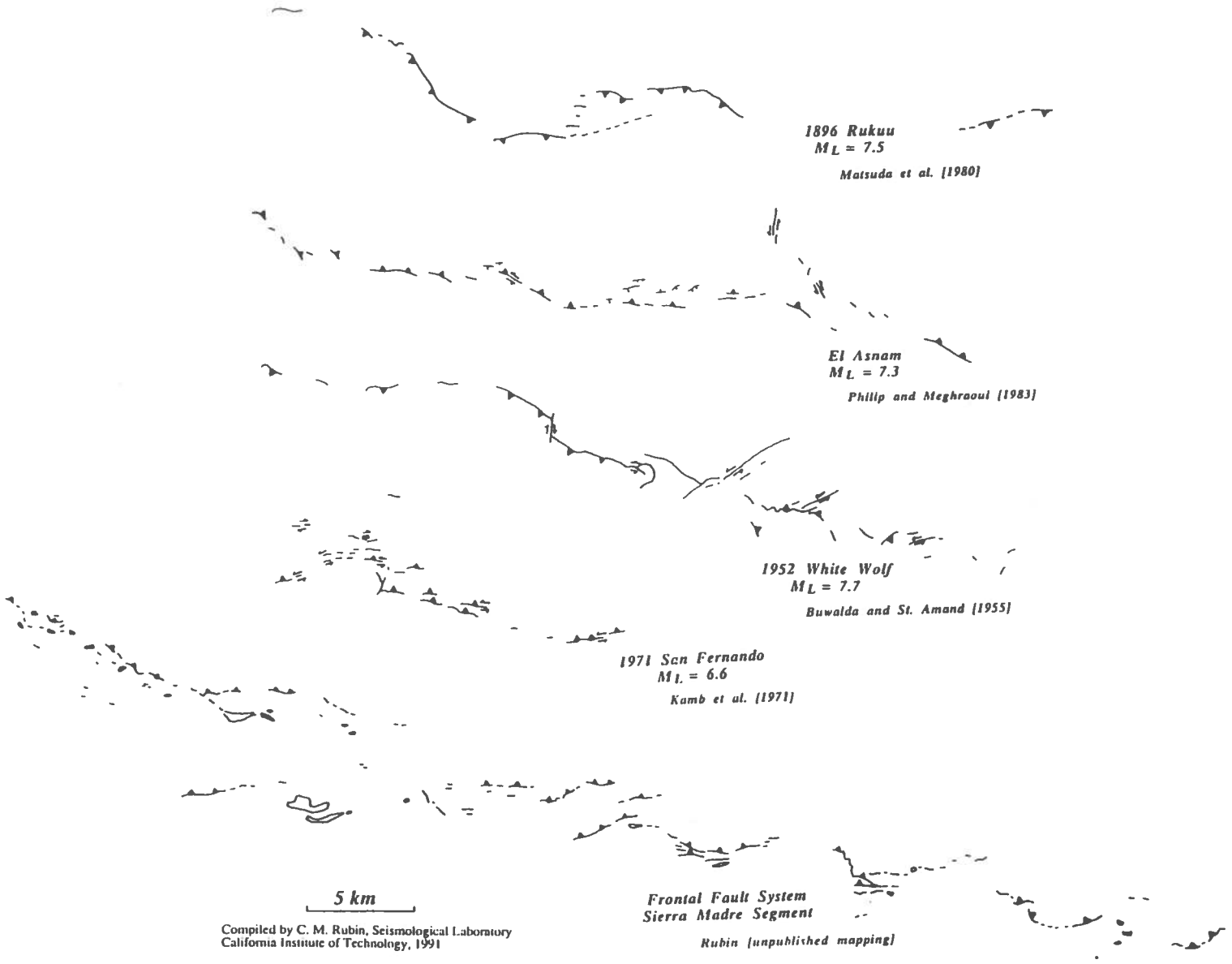

Figure 2. Comparison of the Sierra Madre fault with other active reverse faults.

Development of Software for Paleoseismic Studies

Kerry Sieh and Anne Lilje
Seismological Laboratory
California Institute of Technology

Introduction

During the past six months our group has been aggressively developing and employing ARC/INFO to use as a tool for solving problems in paleoseismology and neotectonics. A brief overview of progress on our current projects follows.

Tmap: Software for making topographic and trench maps from Total Station Surveys

We are nearing completion of development for a software package called Tmap. Briefly, Tmap facilitates creation of topographic and trench-wall maps from data collected with modern electronic surveying equipment. By October we expect to have a version of the software that will allow easy data collection with the Wild TC2000 electronic surveying instrument and processing with MS-DOS, UNIX, or Macintosh computer. The reason for producing the software is three-fold. First, existing software available for processing and manipulating digital survey data is almost exclusively intended for surveying/civil engineering uses. Simple tasks, such as forcing these packages to produce trench maps, is unnecessarily tedious and time consuming. Additionally, existing software packages are slow and poorly documented. Tmap will provide a well documented standard package for those geologists in SCEC who will be using electronic surveying equipment in their paleoseismic and neotectonic work. The Tmap package should be available for MS-DOS and UNIX by the end of October 1992.

DSM's (Digital Surface Models) of the Los Angeles Basin

Detailed U.S.G.S. topographic maps created in the 1920's are proving to be very useful for interpreting the activity of active reverse faults in the northern Los Angeles region. We have been constructing three-dimensional surface models from these topographic maps called Digital Surface Models (DSM's). These models are stored as ARC/INFO TIN structures and are created through a relatively simple, but tedious process.

In order to create these maps one must first obtain mylar "topography only" prints of the quadrangle from the U.S.G.S.. However, in this case, since the maps are out of print we had to have these quadrangles drafted at Caltech. The next step has been to scan these maps at 700 dpl. The result is a faithful digital reproduction of the 1:24,000 quad. Next, any errors in the original map, or those introduced in the scanning process are corrected. The resulting raster file is then vectorized and each topographic line is assigned its' proper elevation. These 1:24,000 scale surface models can be used in conjunction with our groups geomorphic mapping.

The DSM's of the old topo maps are now being used for compilation of geologic/ geomorphic maps, the production of cross-sections and topographic profiles, as well as with a slip analysis application being developed by our group. The set of DSM's will be available by the end of October 1992.

General Geological Mapping and DSM's of the San Andreas Fault in the San Gorgonio Pass Region

The geometry and kinematics of the San Andreas fault in the region of San Gorgonio Pass is poorly understood. We have been mapping in the Cabazon Whitewater area of the Pass. Two DSM's have been created for the area, one on the Whitewater 1:24,000 quadrangle and one of the Cabazon 1:24,000 quadrangle (Figure 1). Onto this DSM we will be adding structural, geomorphic, and lithologic information.

Work Associated with the Landers Earthquake

An ARC/INFO database of the Landers Surface Rupture

Our group has been creating a map of the Landers surface ruptures which contains information about horizontal and vertical slip at hundreds of sites. The creation of this database has given us the opportunity to simultaneously examine large-scale and small-scale structures quickly and efficiently (Figures 2a and 2b). Figure 3 is a graph of dextral skip plotted as a function of latitude. Further study of the Landers event, especially the integration of geological, seismological and geodetic databases, will be made easier through the use of this database.

Digital Surface models (DSM's) of topography along the Lander's Surface Rupture

The Landers earthquake rupture offers a spectacular opportunity to compare tectonic landforms with coseismic ruptures. The 90 ft. resolution of Digital Elevation Models (DEM's) available from the U.S.G.S. is not sufficient for these comparisons. As a result, we have begun to create a set of Digital Surface Models for the Landers, Melville Lake, Emerson Lake, and Iron Ridge 1:24,000 scale U.S.G.S. topographic maps. These 4 quadrangles and an application to perform slope analysis on these areas will be available within the next few months.

Figure 1: Example of DSM (Digital Surface Model) of the Whitewater Quadrangle. Each contour interval is tagged with an elevation and archived in an ARC/INFO Database.

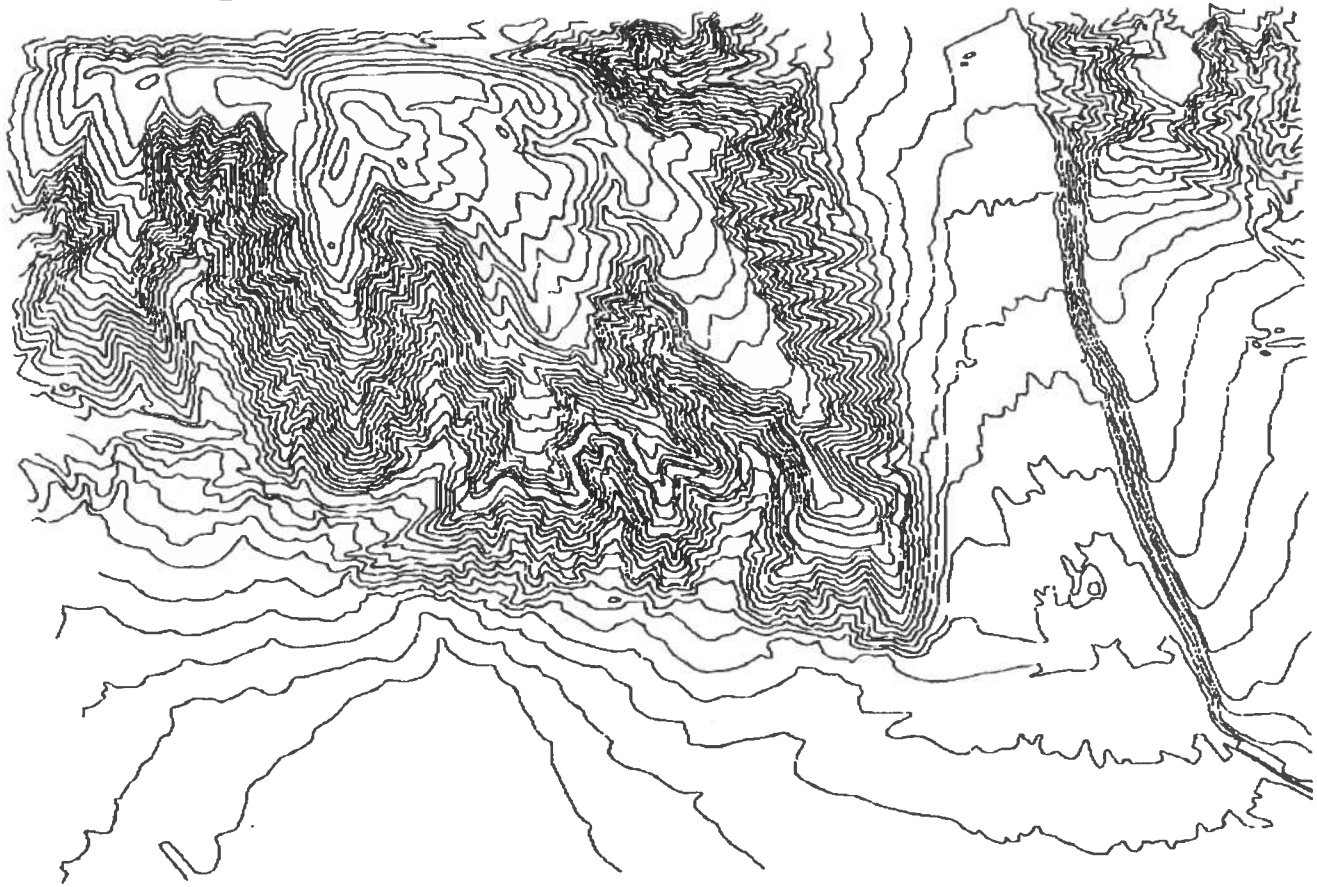

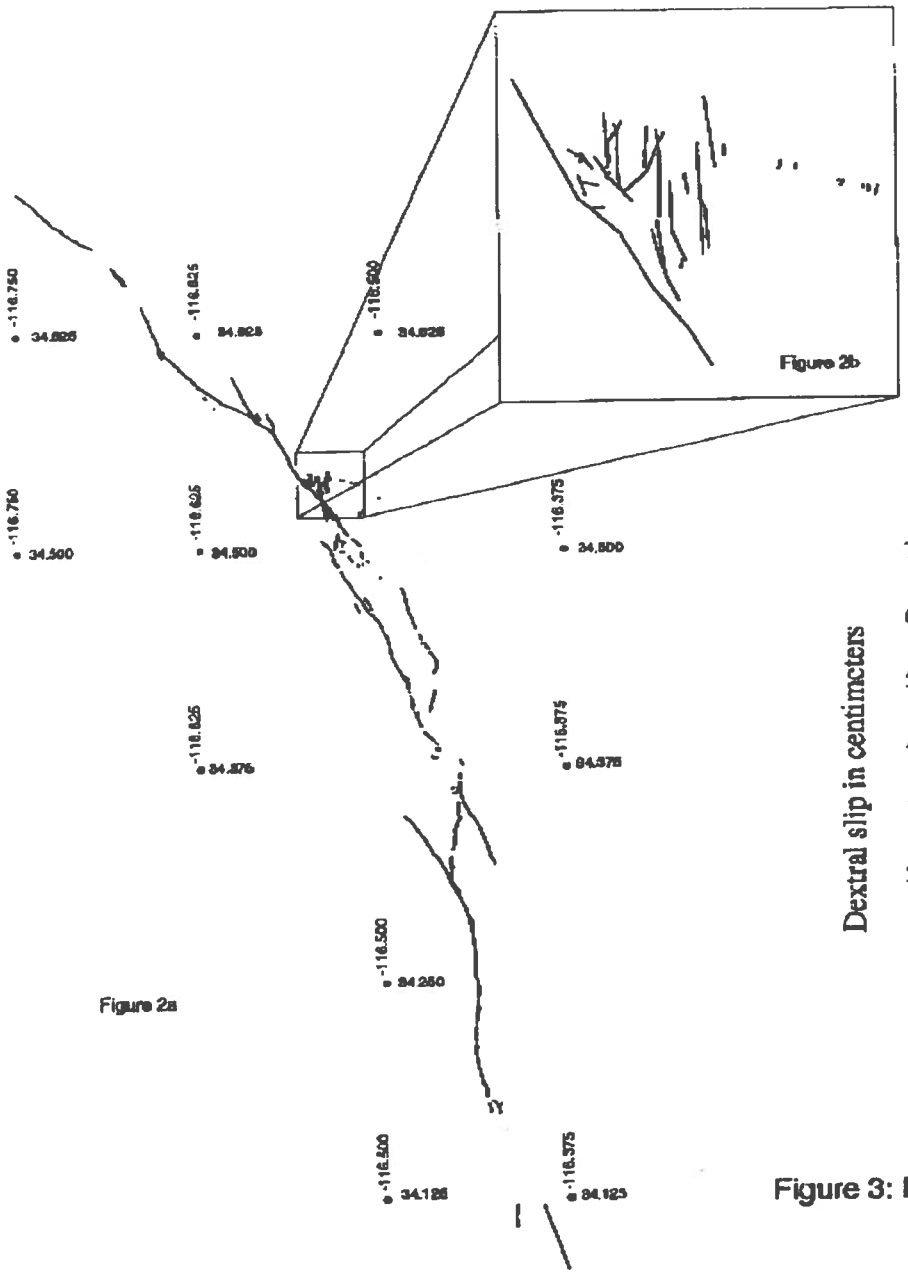

Figure 2: a) Landers Surface Rupture ARC/INFO Database as of August 1, 1992.
b) Enlargement of detail

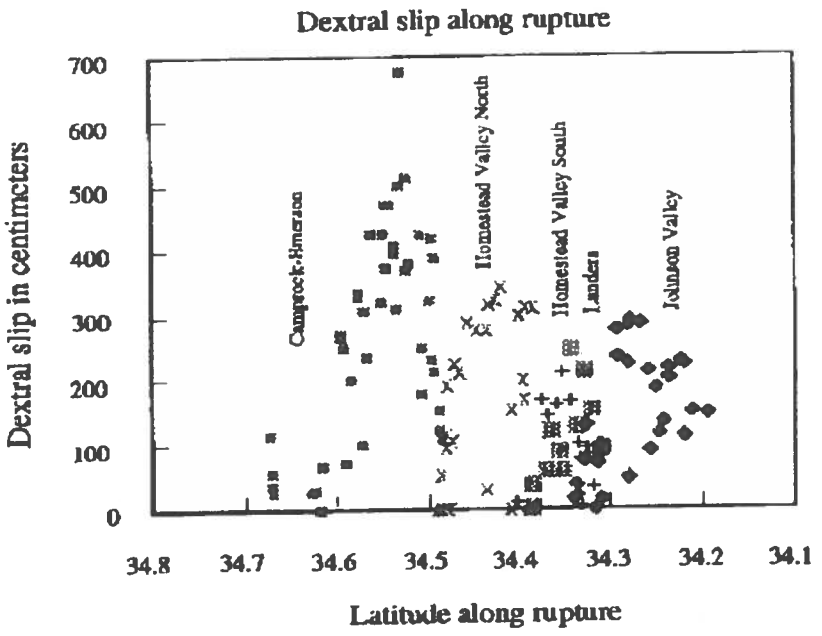

Figure 3: Dextral Slip as a function of latitude for the Landers surface rupture.

REGIONAL MAP-VIEW AND CROSS-SECTIONAL DETERMINATION OF FAULT GEOMETRY AND SLIP FOR BLIND THRUSTS IN POPULATED AREAS OF SOUTHERN CALIFORNIA

JOHN SUPPE, RICHARD E. BISCHKE, AND JOHN H. SHAW
Dept. of Geological and Geophysical Sciences
Princeton University, Princeton, NJ, 08544

Section 1: Active Blind Thrust Faults in the Central Los Angeles Basin

We apply new methods to identify and map active fault systems in the Los Angeles basin, CA, using over 70 high-resolution seismic reflection profiles and well logs obtained from industry. The seismic reflection profiles image a number of narrowing-upward kink-bands or growth triangles (Suppe et al. 1992) that form along bends in underlying faults (fig. 1). The distance between axial surfaces that bound kink-bands (fold limbs) records the dip-slip fault motion (fig. 2). Therefore, maps of axial surfaces that bound kink bands, constructed through grids of high-resolutions seismic reflection profiles, highlight changes in fold and causative thrust fault geometry along strike and record lateral fault-slip distribution. Ends and offsets of kink bands in map view highlight fault terminations and lateral changes in thrust fault geometry that may limit the area that ruptures in individual earthquakes. The area of fault ramp segments identified on axial surface maps can therefore be used through empirical relationships between rupture area and magnitude (Kanamori and Anderson, 1975) to estimate the size of potentially damaging earthquakes on these fault segments.

The most prominent kink band in the central Los Angeles basin trends northwest-southeast for over 25 km along the Compton-Los Alamitos trend (fig. 3, ***A***). This trend has previously been interpreted as a near-vertical strike-slip fault; however, we contend that continuous and coherent seismic reflectors across the trend preclude high-angle faulting. We suggest that the previously mapped fault is an active axial surface that marks a ramp from a deep decollement that shallows to the southwest. The axial surface map (fig. 3) indicates that this ramp in the *Compton thrust* terminates to the northwest and may continue to the southeast beyond the limits of our seismic coverage. Our preliminary investigations suggest that the thrust ramp lies beneath the Newport-Inglewood trend and flattens to a decollement below the Wilmington-Belmont Offshore oil field. Seismic rupture of this fault ramp (minimum area = 400 km^2) could generate a Ms ≈ 6.6 earthquake beneath this populated region of greater Los Angeles.

Other prominent kink bands that we have identified lie toward the northeast border of the central Los Angeles basin (fig. 3). Kink-band ***B*** (fig. 3), which also trends northwest-southeast in the basin, may pose an earthquake hazard similar to that along the Compton trend. In continuing investigations we plan to:

- finalize and disseminate our axial surface map with potential earthquake magnitude predictions to SCEC scientists through the centers Arc/Info database;
- determine long-term fault slip rates and potential earthquake recurrence intervals for these faults by analysis of syntectonic (growth) strata;
- generate and refine balanced cross sections and three-dimensional models of active faulting and folding in the central Los Angeles basin. These sections will incorporate existing catalogues of seismicity and may provide a structural framework for continuing geodynamic surveys and geologic investigations. These sections and models will contribute toward the lithospheric transect proposed along the *SCEC* trend (fig. 3).

Suppe, J., Chou, G.T. and Hook, S.C., 1992, Rates of folding and faulting determined from growth strata, in *Thrust Tectonics*, K.R. McKlay ed., Unwin Hyaman, Publisher, pp. 105-121.

Kanamori, H., and Anderson, D.L., 1975, Theoretical basis of some empirical relations in seismology, Bulletin of the Seismological Society of America, vol. 65, no. 5, p. 1073 -1095.

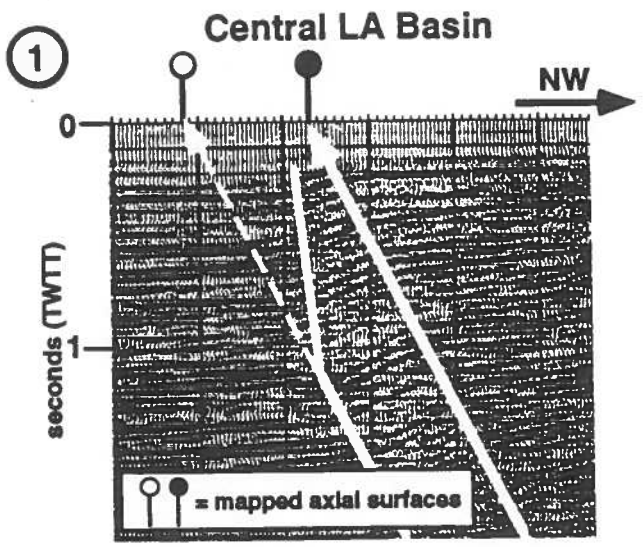

Figure 1: A high-resolution seismic reflection profile images an active narrowing-upward kink-band, or growth triangle, in the central LA basin. These folds form by slip on underlying blind thrust faults (Suppe et al., 1992).

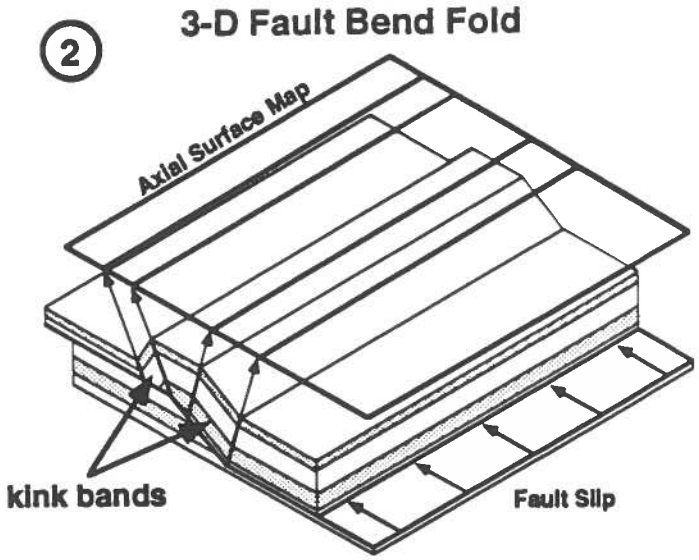

Figure 2: Kink bands, bounded by axial surfaces, grow above bends in underlying thrust faults. Axial surfaces are mapped by projecting their locations in section to a horizontal datum. Map patterns reflect the geometry of underlying thrust fault segments.

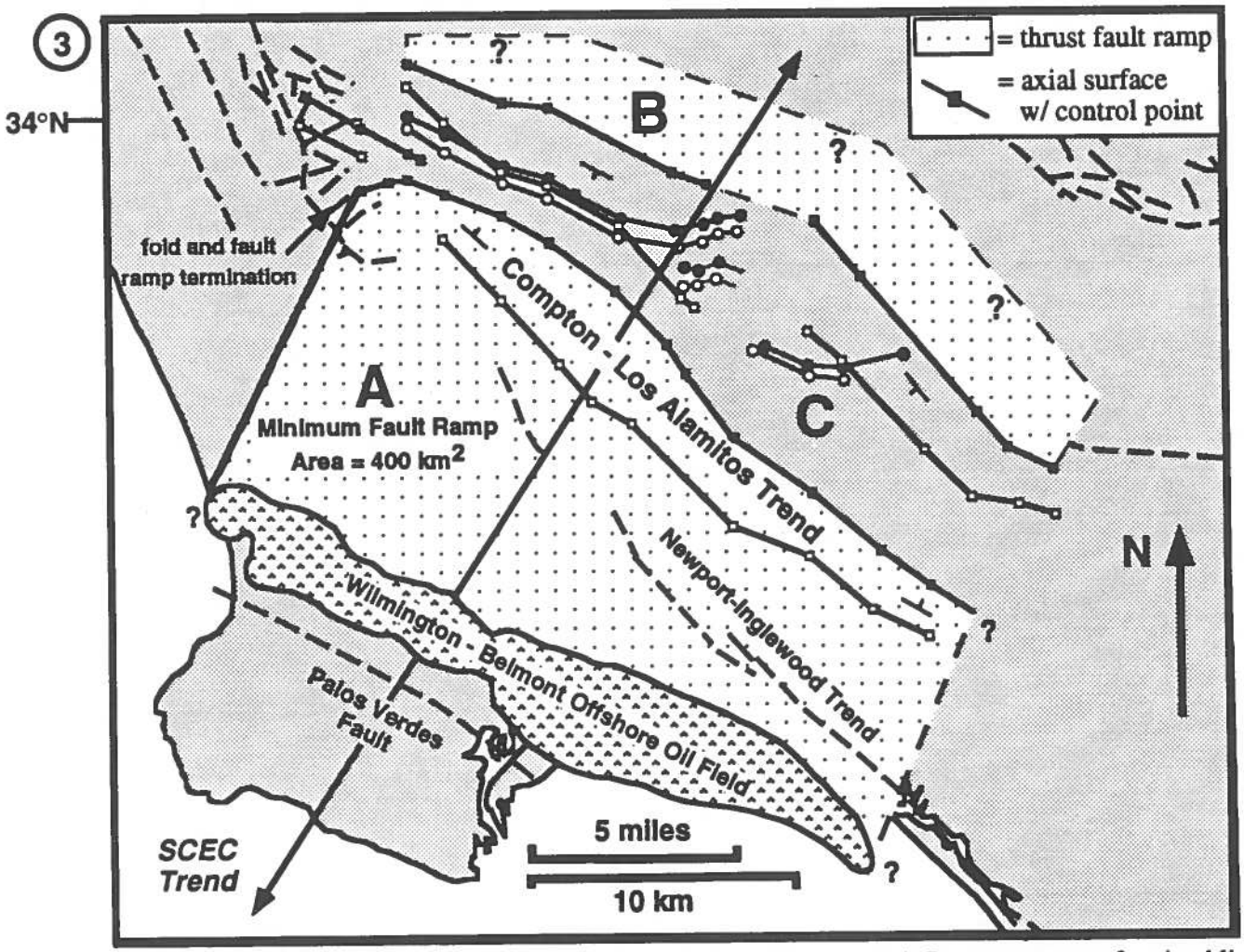

Figure 3: An axial surface map through the central Los Angeles basin defines segments of active blind thrust faults that may rupture in damaging earthquakes. A kink-band along the Compton-Los Alamitos trend overlies one such fault ramp (A), that is capable of generating a Ms ≈ 6.6 earthquake.

Section 2: The Signal Hill Restraining Bend; Long Beach Anticline, Newport-Inglewood Trend, California

In the absence of piercing point evidence, it is difficult to document the amount of lateral motion on strike-slip faults (Harding, 1990; Stone, 1991). Shaw et al. (in press) have shown that in some cases piercing point (or line) evidence exists in the compressional restraining bends (Crowell, 1974), that connect major offsets in strike-slip fault systems. If the fault geometry and the displacement direction in the restraining bend can be determined, it is possible to derive both horizontal and vertical slip components based on offset horizons (Fig. 1). Combined with absolute age estimates of syntectonic horizons, long-term strike-slip and dip-slip rates can be determined.

At the Long Beach oil field the Cherry Hill and Northeast Flank faults system forms a left-stepping restraining bend along the right-lateral Newport-Inglewood trend. Strike-slip motion on the faults causes thrusting along a connecting fault ramp that uplifts the Signal Hill promontory (fig. 1). The orientation of the thrust fault that connects these strike-slip faults is known from subsurface mapping, and the slip direction is inferred to be parallel to the line of intersection of the strike-slip and reverse fault segments (Shaw et al., in press). Lower Pliocene beds are offset a vertical distance of 245 meters and a horizontal distance of 170 meters across the thrust fault (Taylor, 1973).

We apply a new method of analyzing subsurface data to determine fault slip rates beneath the Signal Hill pressure ridge. The method is based on the distance that beds are vertically separated during faulting (Fig. 2). Vertical separation (***VS***) is equal to the missing section as determined from bore hole or seismic data (Tearpock and Bischke, 1991). If missing section or fault cut measurements are available from subsurface data or well-constrained cross-sections, then ***VS*** versus depth curves can be constructed. Provided that the absolute ages of horizons are known and the fault is subject to a single period of deformation, then these curves describe the history of fault motion.

VS versus depth curves constructed from well-constrained cross-sections of the Long Beach Anticline (Taylor, 1973), show that the Cherry Hill fault above 3000 m is a growth reverse fault, and that the Northeast Flank fault, within the restraining bend, formed in the lower Pliocene (Fig. 3). As the timing of the uplift and the direction of fault motion is known beneath Signal Hill, it is possible to determine slip rates on the Cherry Hill-Northeast Flank Fault system. The horizontal and vertical slip rates within this restraining bend are 0.035 and 0.050 mm/yr. respectively, which is lower than previous estimates. Geomorphic evidence (Bryant, 1988) suggests that the Cherry Hill fault may die out directly to the southeast of Signal Hill. However, if additional strike-slip motion on the Cherry Hill fault bypasses Signal Hill to the southwest, then our estimates of strike-slip are a minimum for the Newport-Inglewood trend.

Bryant, W. A., 1988, Recently active traces of the Newport-Inglewood Fault zone, Los Angeles and Orange Counties, Ca., California Dept. of Mines and Geol. Open File Report, 88-14, 15 p.

Crowell, J. C., 1974, Origin of late Cenozoic basins in southern California, in Tectonics and Sedimentation, W. R. Dickinson, ed., SEPM Special Pub., no. 22, p. 190-204.

Harding, T. P., 1990, Identification of wrench faults using subsurface structural data; criteria and pitfalls; AAPG Bulletin v. 74, p. 1590-1609.

Shaw, J.H., Bischke, R.E., and Suppe, J., (in press), Relationships between faulting and folding in the Loma Prieta epicentral zone; Strike-slip fault-bend folding, in *The Loma Prieta, California, Earthquake of October 17, 1989*, U.S.G.S. Prof. Paper.

Stone, D. S., 1991, Identification of wrench faults using subsurface structural data; criteria and pitfalls; AAPG Bulletin, v. 75, p. 1784-1785.

Taylor, J. C., 1973, Recent developments at Signal Hill Long Beach Oil Field: Pacific Sections AAPG, SEPM, and Society of Exploration Geophysicists, Guidebook, Trip 1, p. 16-25.

Tearpock, D., and R. E. Bischke, 1991, Applied subsurface geological mapping, Prentice-Hall, N. J., 648 p.

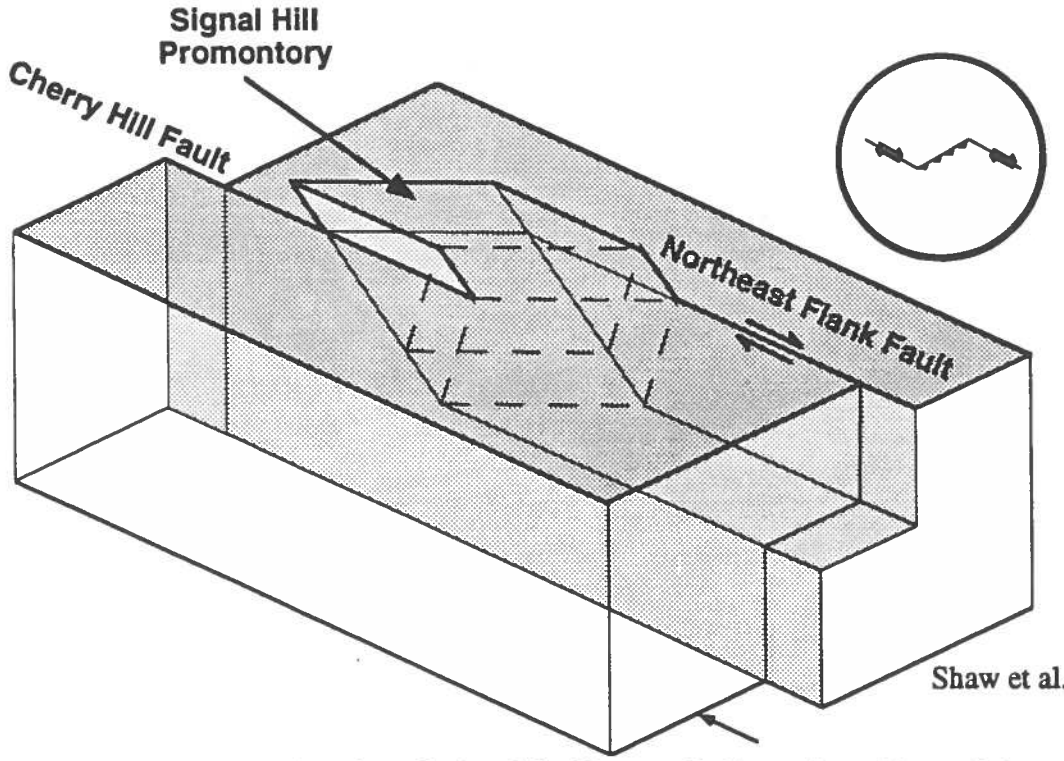

Figure 1: Right-lateral motion along faults of the Newport-Inglewood trend into a left-stepping restraining bend causes thrusting and uplift of the Signal Hill Promontory. Vertical separation of horizons across the Cherry Hill fault and subsurface fault geometry are used to infer horizontal and vertical slip rates along this section of the Newport-Inglewood trend.

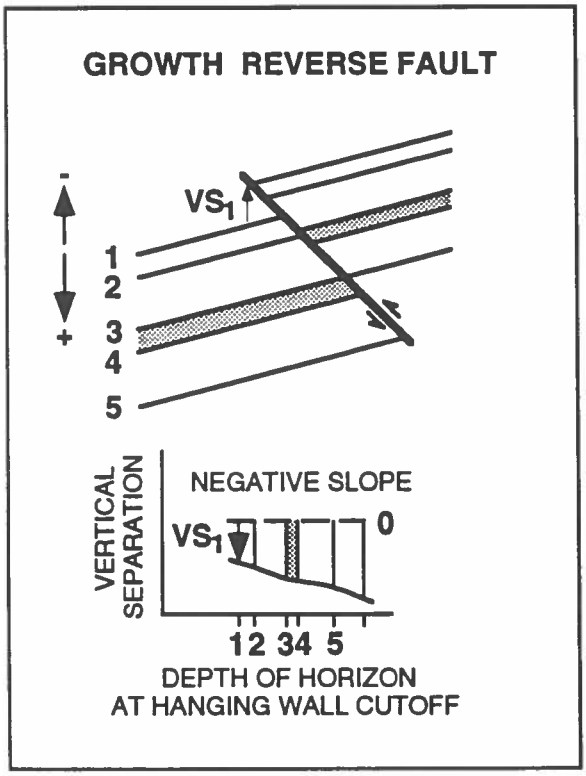

Figure 2: Vertical Separation (*VS*) or missing section is plotted against the depth of each displaced horizon at the stucturally higher position. The plot defines the type and timing of faulting.

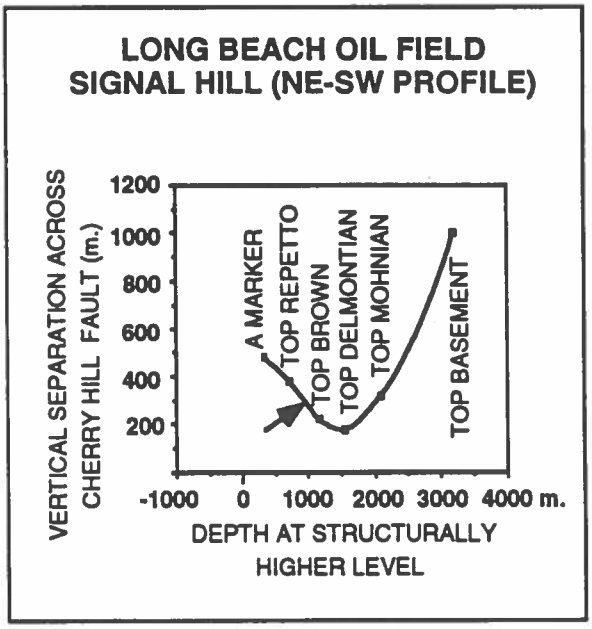

Figure 3: *VS* versus depth plot across the Cherry Hill Fault, Newport-Inglewood Trend, Ca. The Cherry Hill fault above Top Delmontian (Plio-Miocene boundary) is an upward dying growth reverse fault. Reverse motion in the restraining bend is a result of strike-slip on the Northeast Flank fault.

SOUTHERN CALIFORNIA EARTHQUAKE CENTER

1. **Name of PI:** Steven N. Ward
2. **Institution:** University of California, Santa Cruz
3. **Title of Project:** Dislocation models of the Palos Verdes Terraces

Progress Report for 1992

Space geodesy tells us that ≈8 mm/y of roughly North-South motion is being accommodated between Palos Verdes and the base of the Transverse Ranges. The goal of this project is to employ geological and geomorphological data to isolate the fraction of this motion on some of the faults closest to the coast. Marine terraces are particularly useful in this regard because they supply both an age and a geodetic datum to pace tectonic deformation.

Due to the presence at UC Santa Cruz of Dr. Gianluca Valensise, a SCEC visiting scientist, significant progress was accomplished in 1992. We abstract our results below:

Uplift of the Palos Verdes peninsula has long been ascribed to slip on a northwest-trending, southwest-dipping blind reverse fault. Unfortunately, the Palos Verdes fault has no obvious surface displacement and little background seismicity to substantiate its dimension, orientation or slip rate. We have found however, that many blind thrusts can be quantified by proper interpretation of their associated deformation even if the faults are hidden and seismically quiet. We have investigated the style and slip rate of the Palos Verdes fault by analyzing the geometry of the 13 marine terraces which encircle the peninsula in a bathtub ring configuration (Figure 1). In view of the uncertainties in terrace correlation and dating, we first concentrated on those aspects of fault geometry and tectonic style which can be deduced from the location and elevation of the scattered terrace remnants *independent* of their age and mutual correlation. An analysis of 211 uncorrelated terrace elevations constrained a Geological Fault Model which strikes N128.5° E, dips 67° and has a length and width of 19 and 7 km respectively. The upper southern corner of the GFM locates ≃5 km off the Long Beach Harbor at 6 km depth. Initiated in an ocean 854 m deep, 9,106 m of oblique, right lateral slip with a rake angle of 142.3° would raise an oblong anticline to an elevation ≃400 m above sea level (Figure 2) in a mannor similar to that observed. If Terrace 5 was carved during the 330 ka highstand, then the average slip rate of the Palos Verdes fault is 3.03 to 3.68 mm/yr. If the rate was constant through time, the inception of the fault would have occurred 2.4-3.0 ma. Earthquake recurrence intervals were determined under the assumption that seismicity follows a Gutenberg-Richter relationship up to some maximum magnitude M_{max}. Based on stress drop arguments, we propose that $M_{max} \approx 6\frac{3}{4}$ is the largest credible event on the Palos Verdes fault. Estimated repeat times for $M_W \geq 5$ and $M_W \geq 6$ earthquakes fall between 33-59 years and 330-590 years (Figure 3). With repeat times of about 1,400 years, earthquakes of magnitude greater than $6\frac{1}{2}$ should be infrequent.

Ward, S.N. and G. Valensise, Bathtub Rings from a Buried Thrust Fault: The Palos Verdes Terraces, *Science*, (in preparation).

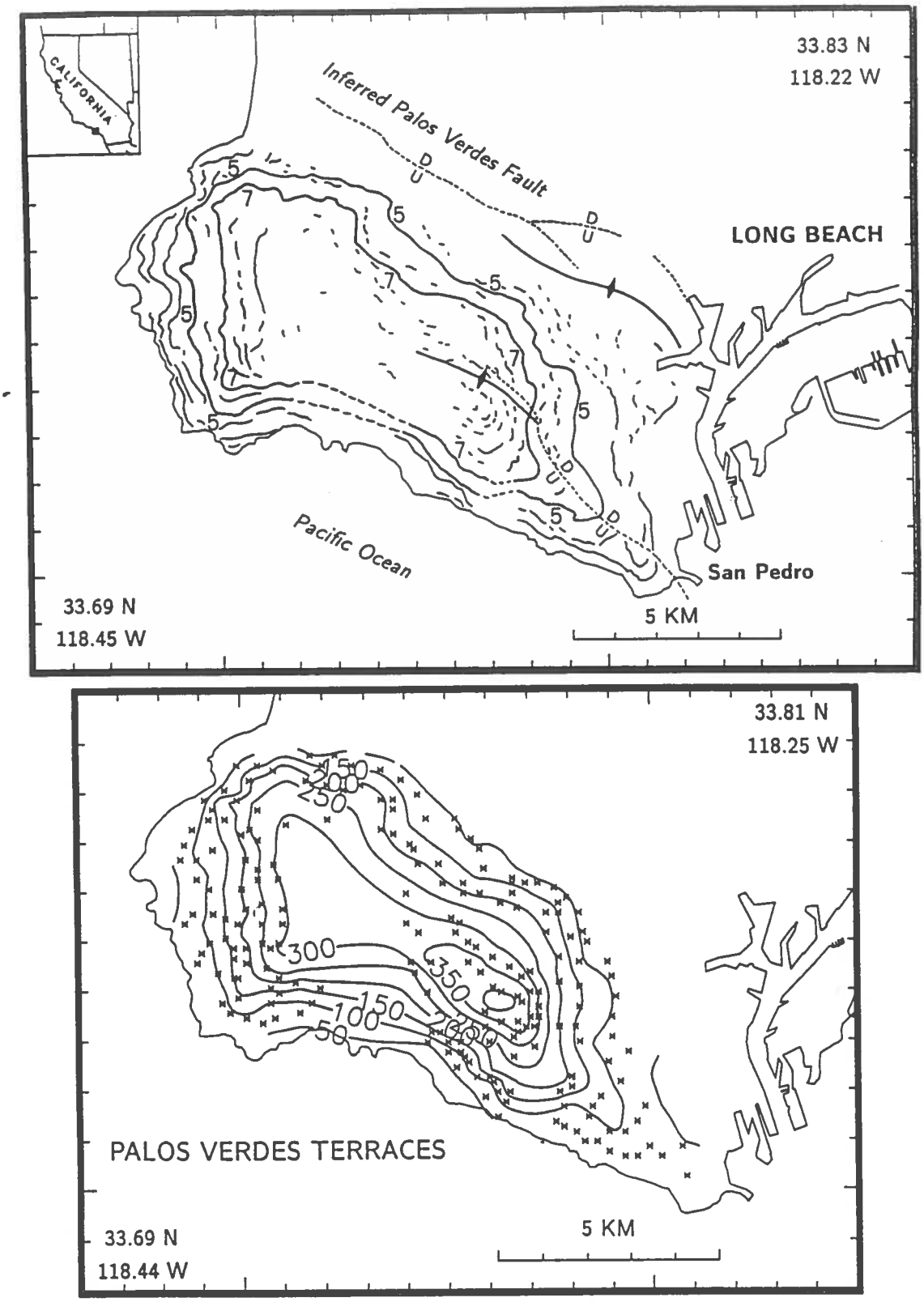

Figure 1. Top. Short line segments show the location of terrace remnants in the Palos Verdes Hills. Longer curves marked 5 and 7 show a possible correlation for Terrace 5 and 7 as first defined by *Woodring et al.* [1946]. The correlation was later substantially revised by *Lajoie*, who also tabulated the elevation of most of the terrace remnants shown in the map. *Bottom.* Elevation contours of the inner edge of 211 remnants of Terrace 4, 5, 6, 7, 9, 10, 12, 13 (data from *Woodring et al.* [1946], and *Lajoie* [personal communication, 1991]). Our premise is that the source of tectonic uplift is slip on a buried Palos Verdes Fault. Our goal is to use these terrace elevations as geodetic control to contrain the style and slip rate of the fault.

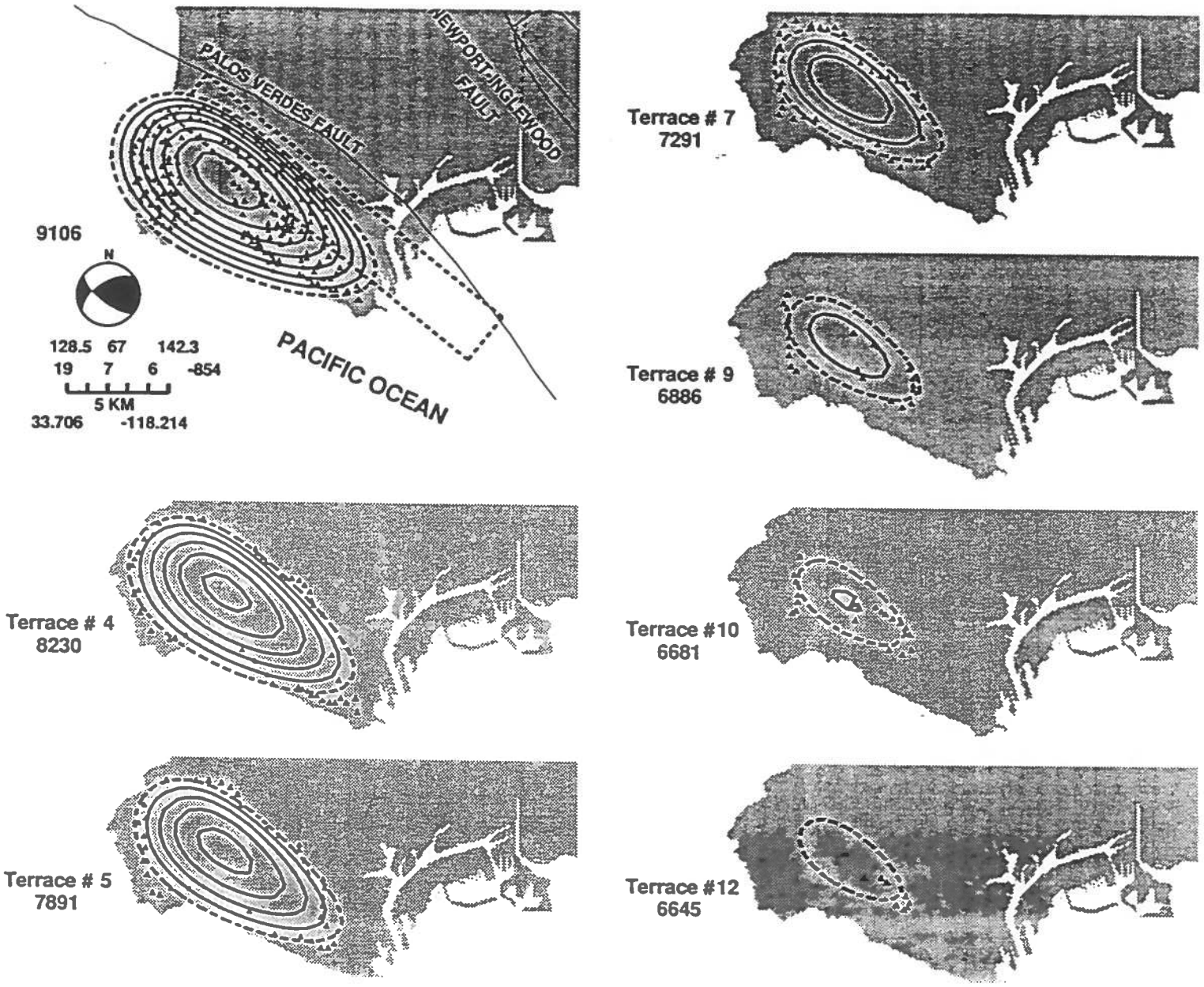

Figure 2. Map showing the predicted elevation of the Palos Verdes Hills today (***upper left***) and at the time of formation of Terrace 4, 5, 7, 9, 10, and 12. The contour interval is 50 meters. The dashed contour is sea level and marks the position of the shoreline at the creation of the given terrace. The expanding "bath tub ring" character of the terraces is reproduced quite well. Small triangles locate 211 uncorrelated terrace remnants used for the inversion. The focal parameters of the Palos Verdes Geological Fault Model are given in the upper left. Due to the significant right lateral component of motion in the focal mechanism, the anticline is offset by 6-8 km relative to the middle of the fault's projection. Also notice that the currently exposed portion of the Palos Verdes anticline is $\simeq$25% shorter than the fault that is responsible for its growth. Misfit between the observed terrace inner edge locations and the zero contour by $\pm$0.5 Km results mostly from lateral variations in the depth of carving of each individual wave-cut platform. Note that Terrace 12 is represented only by a few fragments clustered toward the southeastern corner of the low ($\leq$ 50 m) island predicted to exist at its formation. The northwestern portion of this terrace may have been lost to erosion, or else the clustering may reflect a slight change in the style of faulting after its cutting.

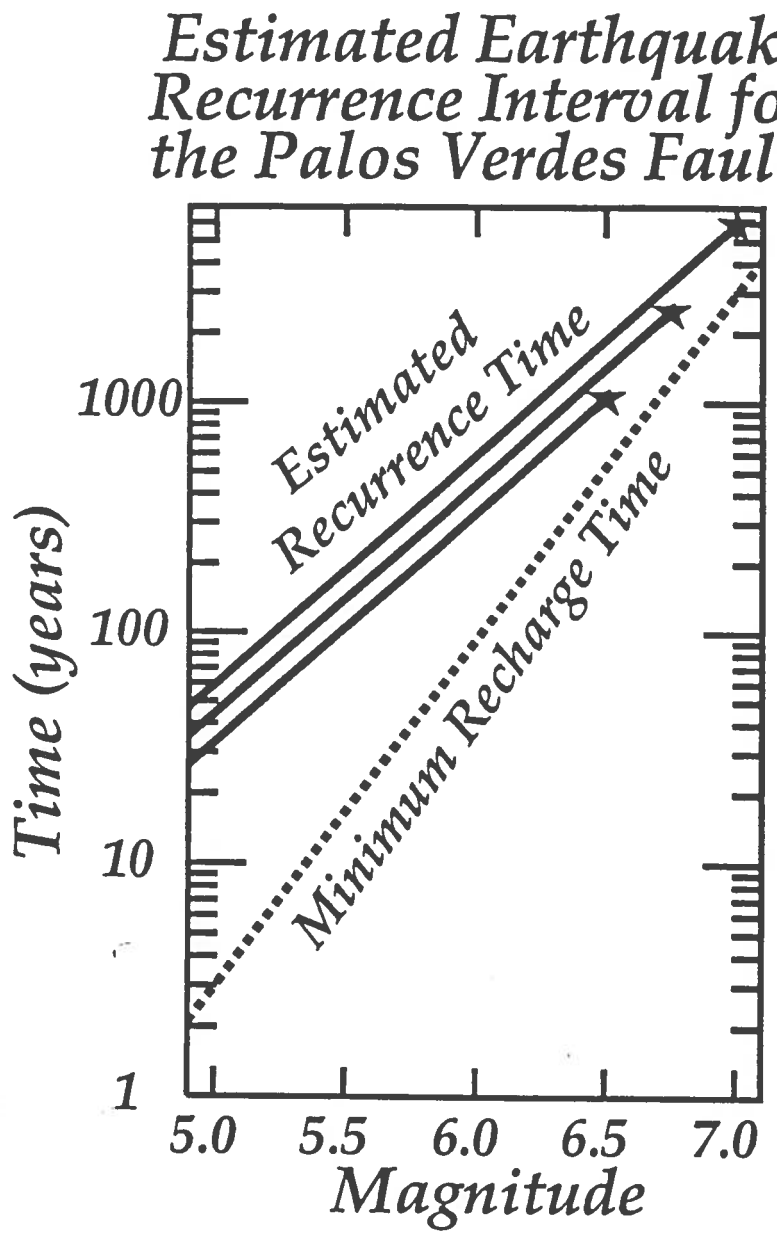

Figure 3. Plot of the minimum recharge time (*dashed*) and estimated recurrence times (*solid*) for earthquakes of magnitude M_w on the Palos Verdes fault. The minimum recharge time is the interval required for the entire fault to recharge the moment lost in an event of magnitude M_w. The recharge time is a minimum estimate of the earthquake recurrence interval since it does not take into consideration the moment lost to other earthquakes which are likely to occur during recharge. The estimated recurrence times, which assume that intervening seismicity follows a Gutenberg-Richter relation up to some maximum magnitude M_{max}, are longer. We propose that the middle curve which fixes M_{max} at $6\frac{3}{4}$ is the most reasonable. Thus the Palos Verdes fault should not be very active; magnitude 5 and greater and 6 and greater earthquakes should not recur more often than every 44 and 440 years, respectively.

Subsurface Geology of Northern Los Angeles Fold-and-Thrust Belt and the Eastern Ventura Basin

Robert S. Yeats, Department of Geosciences, 104 Wilkinson Hall, Oregon State University, Corvallis, OR 97331-5506, (503-737-1226)

Investigations. A structure-contour map of the base of the Pleistocene gravels has been revised to incorporate additional water-well, oil-industry biostratigraphic, and Metro Rail boring data. Other structure-contour maps on the top Repettian Stage, the Miocene-Pliocene contact, the upper Puente-middle Puente Formation contact (within the upper Miocene), and the Santa Monica fault strands are under construction. Several detailed cross sections are under construction (by Tsutsumi west of the Newport-Inglewood fault zone [NIFZ] and by Hummon and Schneider east of the NIFZ) in preparation to balance cross sections across the northern Los Angeles basin. The well base map, 3 panels at a scale of 1:6,000, is nearly complete.

Cheryl Hummon is concentrating on deformation of Pleistocene strata. This work is being published in a special volume of the Association of Engineering Geologists (Hummon et al., 1992a) and has been submitted to Geology (Hummon et al., 1992b).

Yeats et al. (1992) have finished a paper on the details and timing of structures in the east Ventura basin. This paper has been accepted by the American Association of Petroleum Geologists. A companion paper (Huftile et al., in prep.) balances cross sections to determine the convergence rate across the basin. A paper on the convergence rates across the central Ventura basin (Huftile and Yeats, 1992) has been submitted to the Journal of Geophysical Research.

Results. The base of the Pleistocene gravels is the youngest horizon that can be contoured extensively over the entire area, and its age is critical to determining rates of deformation. Ponti (1989) found that the base of the Pleistocene San Pedro Formation in the subsurface of the southwest Los Angeles basin is considerably older than it is at the type locality in San Pedro. Our best estimate now, prior to obtaining direct dates, is that the base of the gravels was deposited between 800-1,600 ka. Our revised map of the base of the Pleistocene gravels is shown in Figure 1. The Wilshire arch, Hollywood basin, and Los Angeles trough all terminate westward against the NIFZ. However, the structure previously mapped as the Wilshire arch to the west of the NIFZ is now recognized as a monocline, with a steep south-facing flexure which is expressed as a set of young fault scarps (Dolan and Sieh, 1991). The boundary between the Wilshire arch and Hollywood basin is in part marked by the North Salt Lake fault shown in Figures 1 and 2, which is parallel to the Hollywood fault to the north. The steep south flank of the Wilshire arch is underlain by two en-echelon fault-propagation folds, the Las Cienegas anticline and the East Beverly Hills anticline. Figure 2 is an unbalanced cross section. Note that the North Salt Lake fault has normal separation. The inset shows that there is no thinning of the Puente, Repetto, or middle-lower Pico formations across the Wilshire arch, implying that the Wilshire arch did not begin to form until after the deposition of the middle Pico Formation.

For several years, convergence rates across the Ventura basin were based on the assumption that active high-angle reverse faults (Oak Ridge, Red Mountain, San Cayetano) flatten to horizontal at the brittle-plastic transition, a décollement at the base

of the seismic zone. However, Bryant and Jones (1992) found earthquakes at 20-30 km depth beneath the Ventura basin. The deep keel on the base of the seismogenic zone implied by these earthquakes is difficult to reconcile with the décollement model. The Moho is also depressed 7-10 km indicating crustal thickening. 2.7 years of GPS data suggest convergence of 7 mm/y (Donnellan, 1991; Donnellan et al., 1992), about a third of the rate based on the décollement model. If the reverse faults do not flatten at the base of brittle crust but instead continue into the lower crust as ductile shear zones, horizontal shortening would be based on the fault slip rates times the cosine of the fault dip, resulting in a convergence rate closer to that based on GPS. The keel at the base of the seismic zone would be explained by downward displacement of the central Ventura basin between opposing reverse faults, a process dominant in the basin for the past several million years (Yeats and Huftile, 1992).

References cited.

Bryant, A. S., and Jones, L. M., 1992, Anomalously deep crustal earthquakes in the Ventura basin, southern California: Jour. Geophys. Res., v. 97, p. 437-447.

Dolan, J. F., and Sieh, K. E., 1991, Structural style and geomorphology of the Santa Monica-Hollywood fault system: Constraints on kinematics of recent fault movement: EOS, Trans. Am. Geophys. Union, v. 72, p. 319-320.

Donnellan, A., 1991, A geodetic study of crustal deformation in the Ventura basin region, southern California: unpub. Ph. D. dissertation, California Inst. Tech., Pasadena, California, 220 p.

Donnellan, A., Hager, B. H., and King, R. W., preprint, Rapid north-south shortening of the Ventura basin, southern California:

Huftile, G. J., and Yeats, R. S., 1992, Convergence rates across a displacement transfer zone in the western Transverse Ranges near Ventura, California: submitted to Jour. Geophys. Res.

Huftile, G. J., Yeats, R. S., and Huafu, L., 1992, Convergence rates across the east Ventura basin: in prep.

Hummon, C., Schneider, C. L., Yeats, R. S., and Huftile, G. J., 1992a, Active tectonics of the northern Los Angeles basin: An analysis of subsurface data: Assoc. Eng. Geol. Proc., in press.

Hummon, C., Schneider, C. L., Yeats, R. S., and Huftile, G. J., 1992b, The Wilshire arch: Active tectonics of the Los Angeles basin, California: submitted to Geology.

Ponti, D. J., 1989, Aminostratigraphy and chronostratigraphy of Pleistocene marine sediments, southwestern Los Angeles basin, California: unpub. Ph. D. dissertation: Univ. Colorado, boulder, Colorado, 409 p.

Yeats, R. S., Huftile, G. J., and Stitt, L. T., 1992, Late Cenozoic tectonics of the east Ventura basin, Transverse Ranges, California: accepted by the Am. Assoc. Petrol. Geol.

Yeats, R. S., and Huftile, G. J., 1992, Alternate model for convergence across the Ventura basin, California: submitted to EOS, Trans. of Am. Geophys. Union.

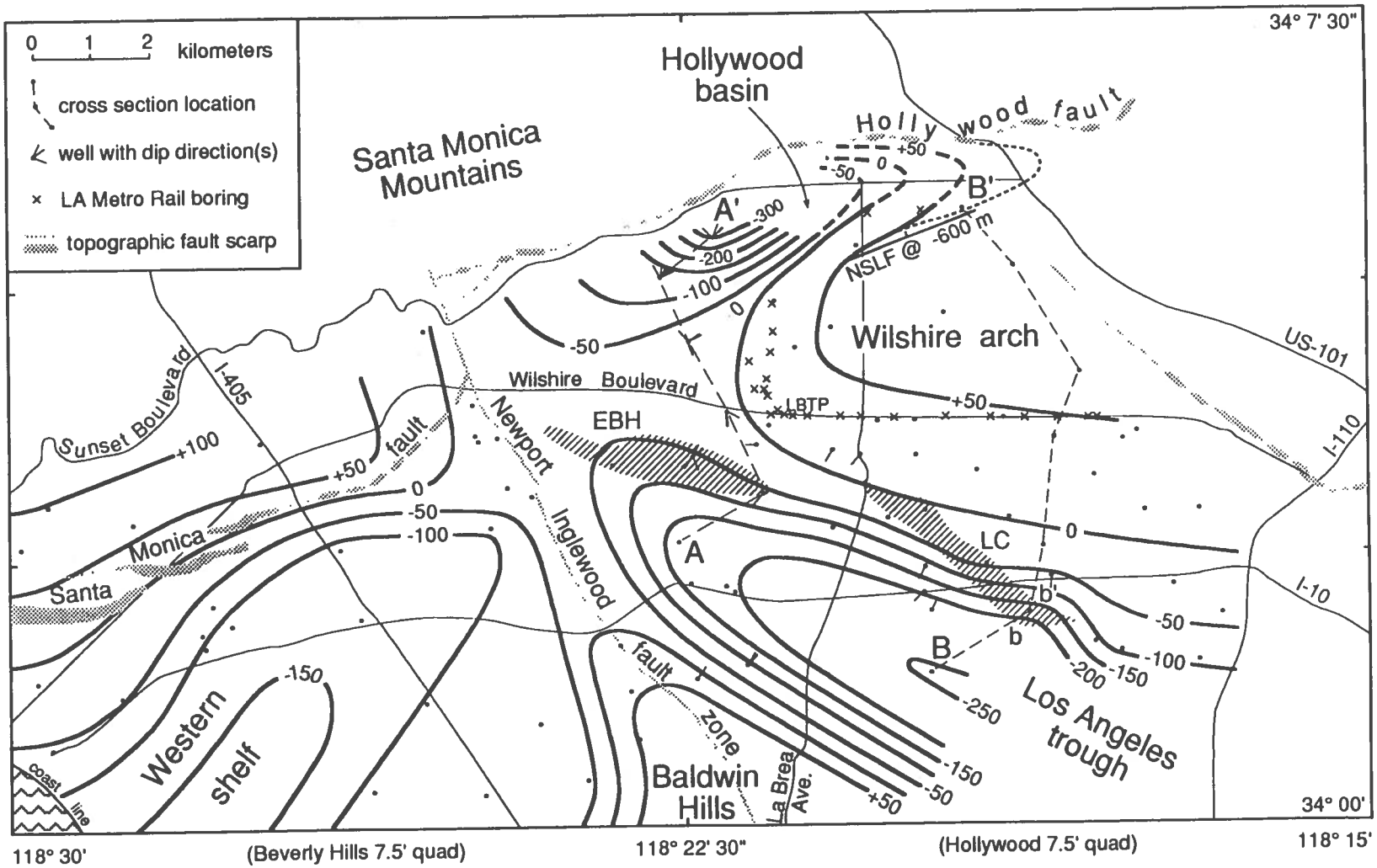

Figure 1. Structure contours on the base of the Pleistocene marine gravels, based primarily on e-log correlation of oil wells. Dashed contours at eastern end of Hollywood basin are estimated form groundwater studies. The +50 m structure contour on the Wilshire arch is the approximate edge of the marine Pleistocene gravels, which are not present over the highest part of the Wilshire arch. In the Hollywood basin, the same contact is indicated by a dotted line. Diagonal-lined areas show the extent of the East Beverly Hills (EBH) and Las Cienegas (LC) SW-vergent anticlines. Stippled areas are topographic fault scarps from Dolan and Sieh (1991). NSLF is the North Salt Lake fault at the -600 m structure contour. LBTP indicates the location of the La Brea tar pits. Cross section location for Figure 2 (A-A') is shown.

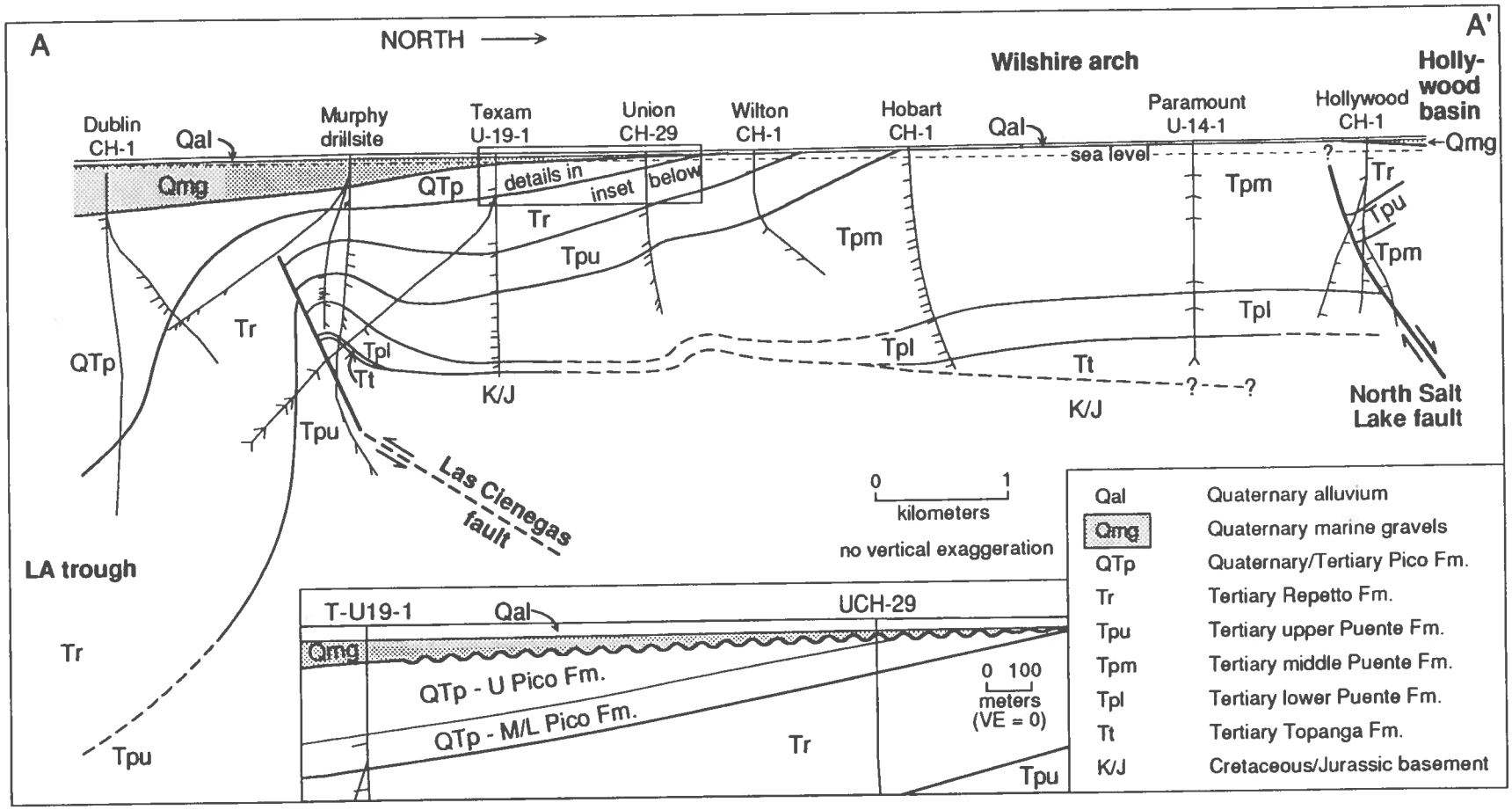

Figure 2. Cross section (not balanced) across the Wilsire arch and Las Cienegas fault (location shown on Figure 1). Formation dips on wells are from dipmeter data (single tick marks) and core dips (double dip symbol). The inset shows details of the unconfomable contact between the Quaternary marine gravels (Qmg) and the underlying Pico Formation (QTp), showing that uplift on the Wilshire arch began after deposition of the M/L Pico Formation.

Group D: Subsurface Imaging of Seismogenic Zones

Group Leader: Rob Clayton

*Project combined with project of Okaya and Henyey above.

SUMMARY REPORT: SUBSURFACE IMAGING (GROUP D)

Report compiled by R. Clayton

The goal of Group D is to produce three-dimensional maps of the structure, velocity, and attenuation in the subsurface. The products are necessary for tectonic modelling, seismicity studies and strong motion simulation.

Velocity Models

Three studies were funded to determine lateral velocity variation in southern California. On a large scale, Paul Davis is using teleseismic phase times and waveforms to make maps of the long-wavelength variations in velocity in the upper mantle beneath southern California. Thus far, data from 12 events have been collected and analyzed. Dapeng Zhao, a SCEC visitor at Caltech, has used P-wave travel time data to produce a 3D map of crustal velocities. The results agree with the main structural features. A paper has been submitted to GRL.

On a more local scale, Egill Hauksson has inverted P-wave travel times for structure in the Los Angeles Basin. The results show remarkable agreement with the geologic cross-sections produced by Tom Wright. A paper on this was presented at the SSA-92 conference. Dapeng Zhao has also produced a fine-scale model for the Landers area that improves epicenter locations. It will be presented at the Fall-AGU-92.

Reflection/Refraction Profiling

Okaya and Henyey at USC, in collaboration with Shedlock (USGS/Denver) and Rockwell (SDSU) have run a shallow high-resolution seismic profile over the Palos Verdes fault. Preliminary results indicate that the fault is not a single strand, but rather a series of en-echelen segments.

Efforts are continuing to obtain the release of oil industry data in the Los Angeles Basin for use by SCEC researchers. Bob Yeats and John Suppe are pursuing this with Chevron and Texaco.

Plans are also proceeding with a refraction profile through the Los Angeles Basin. A line that approximately follows the San Gabriel River and runs from the Mojave Desert to the Pacific Ocean was scouted this summer and appears to be feasible. Gary Fuis and Rufus Catchings have submitted a proposal to the USGS internal program to do the San Gabriel Mtn. portion. Current plans call for the SCEC participants to enhance and piggy-back on this experiment.

Attenuation Studies

Jin, Mayeda, Adams, and Aki of USC continue their work on measuring the frequency dependence of Q. So far the data from the TERRAscope stations ISA and SUD have been processed.

Fault Zone Studies

Li and Teng of USC have recorded fault zone trapped waves along the San Jacinto fault near Anza. The results suggest that the fault zone is a narrow (~200m) low velocity zone extending to 14 km.

Mapping of Scattering and Intrinsic *Q* in Southern California using TERRAscope and Regional Network Data

Anshu Jin, Kevin Mayeda, David Adams, and Keiiti Aki

Department of Geological Sciences, University of Southern California
Los Angeles, CA 90089-0740

Attenuation of S-waves measured by Q^{-1} consists of contributions from scattering and absorption, namely, $Q^{-1} = Q_s^{-1} + Q_i^{-1}$, $Q_s^{-1}=k^{-1}\eta_s$ and $Q_i^{-1}=k^{-1}\eta_i$, where k is the wavenumber and η_s and η_i are the scattering and intrinsic attenuation coefficients, respectively. Hoshiba et al., (1991) have developed a method, called " multiple lapse time analysis", considering energy for three consecutive time windows as a function of hypocentral distance to estimate the seismic albedo, $B_0=\eta_s/(\eta_s+\eta_i)$, and the total attenuation coefficient L_e^{-1}. Where $L_e=1/(\eta_s+\eta_i)$ is the extinction distance over which the primary S-wave energy is decreased by e^{-1}. Figure 1 shows the shapes of the three time window energy as a function of source-receiver distance. They are calculated by Monte-Carlo simulations using homogeneously distributed scatterers in a full-space with uniform intrinsic attenuation under the assumption of isotropic multiple scattering for various B_0 and L_e (Hoshiba et al., 1991).

To obtain both the scattering and intrinsic Q^{-1} as a function of frequency , for each TERRAscope seismic station, we selected earthquakes within 60 km. Then calculated, for each seismogram, the squared amplitude spectrum, $|F(\omega)|^2$ for three time windows: 0 to 15 seconds , 15 to 30 seconds, and 30 to 45 seconds measured from the onset of the S-wave arrival. We eliminated the effect of ambient noise by taking a noise sample of the length of 25 s prior to the P-wave arrival and subtracted the noise energy from the $|F(\omega)|^2$ in each time window. Data with signal power less than twice the noise was discarded. At a lapse time of about 40 seconds the coda energy is almost spatially homogeneous for earthquakes of different magnitudes and within the selected range of hypocentral distances. To normalize the observed energy for different magnitude earthquakes we chose a coda reference sample at 45 ± 2.5 seconds and calculated the squared amplitude spectrum, $|F_{coda}(\omega)|^2$. The spectrum for each time window and the coda reference are averaged over three components of the seismograms for every earthquake. Then the normalized energy observed at hypocentral distance r, $E(\omega \mid r)$, is given by $E(\omega \mid r) = \dfrac{|F(\omega)|^2}{|F_{coda}(\omega)|^2}$. As an example Figure 2 shows the normalized energy, corrected for geometrical spreading by $4\pi r^2$, as a function of hypocentral distance for station SVD and ISA at frequency of 1.5 Hz.

We have finished the data processing for station SVD and ISA for four frequency bands centered at 0.75, 1.5, 3.0, and 6.0 Hz. We plan to combine 'vbb' data with 'vsp' and 'lg' data to extend the frequency band to 24 Hz high and 0.05 Hz low. We are going to complete data processing for six TERRAscope stations and calculate the best fit theoretical simulation of Q_s^{-1} and Q_i^{-1}. Then, we'll compare the results for different

stations and different regions, such as central California, Japan, and Hawaii, to study the spatial variation of B_0 (if there is any).

Reference

Hoshiba, M, H. Sato, and M. Fehler, Numerical basis of the Separation of scattering and intrinsic absorption from full seismogram envelope, --a Monte-Carlo simulation of multiple isotropic scattering, Meteorology and Geophysics, 42, 65-91,1991.

Figure captions

Figure 1. Energy for three time windows (0-15s, 15-30s,and 30-45s) as a function of hypocentral distance r (km) for different pairs of L_e and B_0 predicted by Monte-Carlo simulations. Here the scatterers are homogeneously distributed in a full-space with uniform absorption under the assumption of isotropic multiple scattering. (Following Hoshiba et al., 1991.)

Figure 2. Plots of normalized energy corrected for geometrical spreading, $4\pi r^2$, as a function of hypocenteral distance r (km), for frequency 1.5 Hz, measured at station SVD (top) and ISA (bottom). Where E_1, E_2, and E_3 represent energy measurements for time windows of 0-15, 15-30, and 30-45 second, respectively.

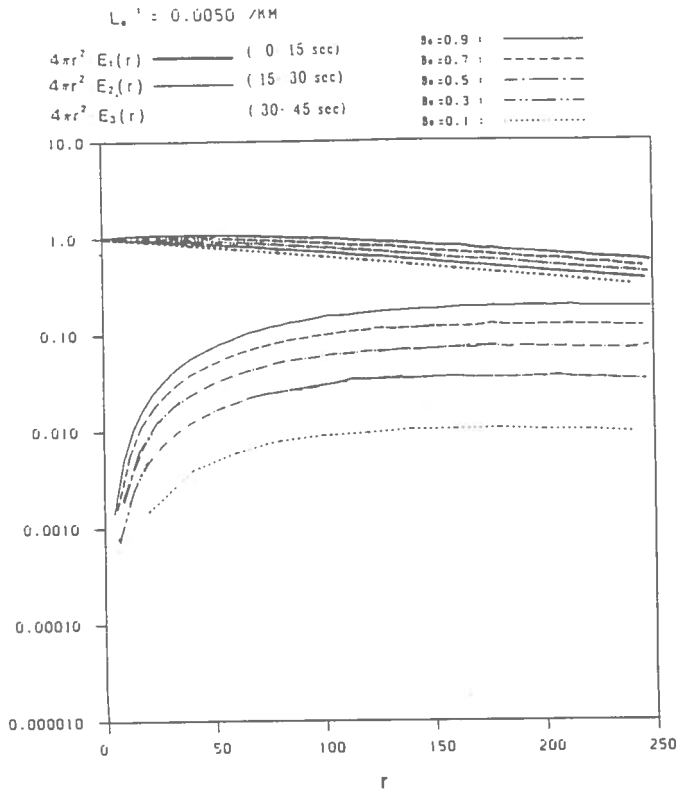
L_e^{-1} = 0.0050 /KM
$4\pi r^2 E_1(r)$ (0- 15 sec)
$4\pi r^2 E_2(r)$ (15- 30 sec)
$4\pi r^2 E_3(r)$ (30- 45 sec)
B_e=0.9
B_e=0.7
B_e=0.5
B_e=0.3
B_e=0.1
10.0
1.0
0.10
0.010
0.0010
0.00010
0.000010
0
50
100
150
200
250
r

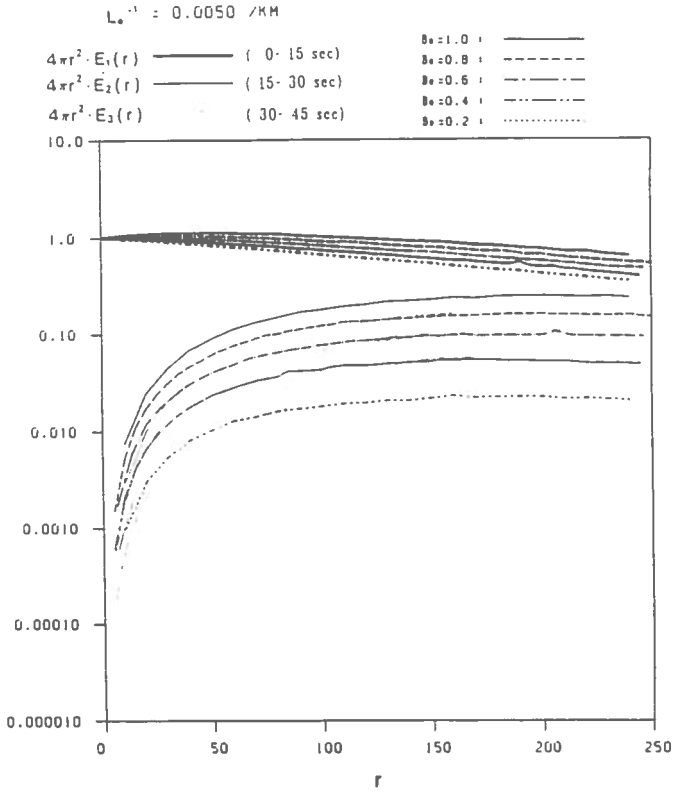
L_e^{-1} = 0.0050 /KM
$4\pi r^2 \cdot E_1(r)$ (0- 15 sec)
$4\pi r^2 \cdot E_2(r)$ (15- 30 sec)
$4\pi r^2 \cdot E_3(r)$ (30- 45 sec)
B_e=1.0
B_e=0.8
B_e=0.6
B_e=0.4
B_e=0.2
10.0
1.0
0.10
0.010
0.0010
0.00010
0.000010
0
50
100
150
200
250
r

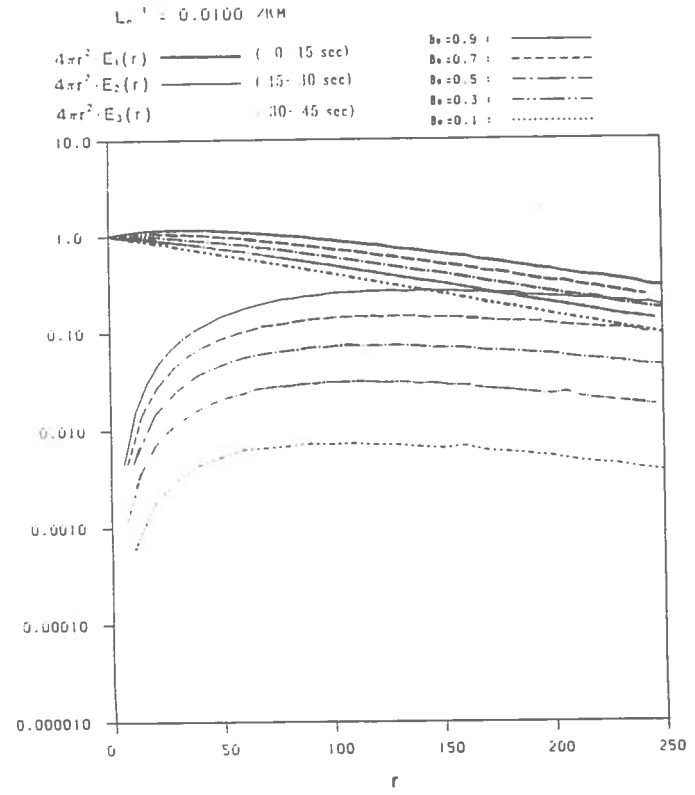
L_e^{-1} = 0.0100 /KM
$4\pi r^2 \cdot E_1(r)$ (0- 15 sec)
$4\pi r^2 \cdot E_2(r)$ (15- 30 sec)
$4\pi r^2 \cdot E_3(r)$ (30- 45 sec)
B_e=0.9
B_e=0.7
B_e=0.5
B_e=0.3
B_e=0.1
10.0
1.0
0.10
0.010
0.0010
0.00010
0.000010
0
50
100
150
200
250
r

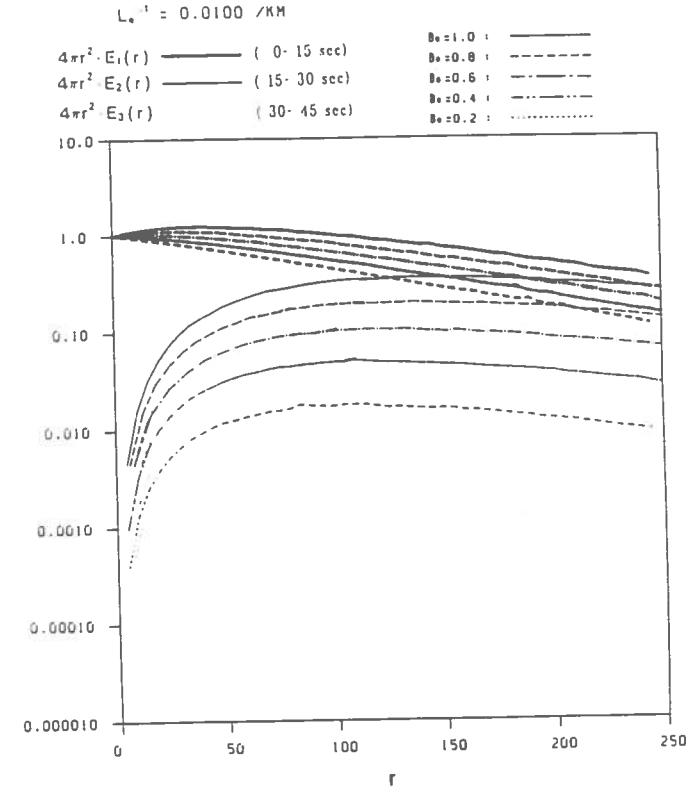
L_e^{-1} = 0.0100 /KM
$4\pi r^2 \cdot E_1(r)$ (0- 15 sec)
$4\pi r^2 \cdot E_2(r)$ (15- 30 sec)
$4\pi r^2 \cdot E_3(r)$ (30- 45 sec)
B_e=1.0
B_e=0.8
B_e=0.6
B_e=0.4
B_e=0.2
10.0
1.0
0.10
0.010
0.0010
0.00010
0.000010
0
50
100
150
200
250
r

Figure 1

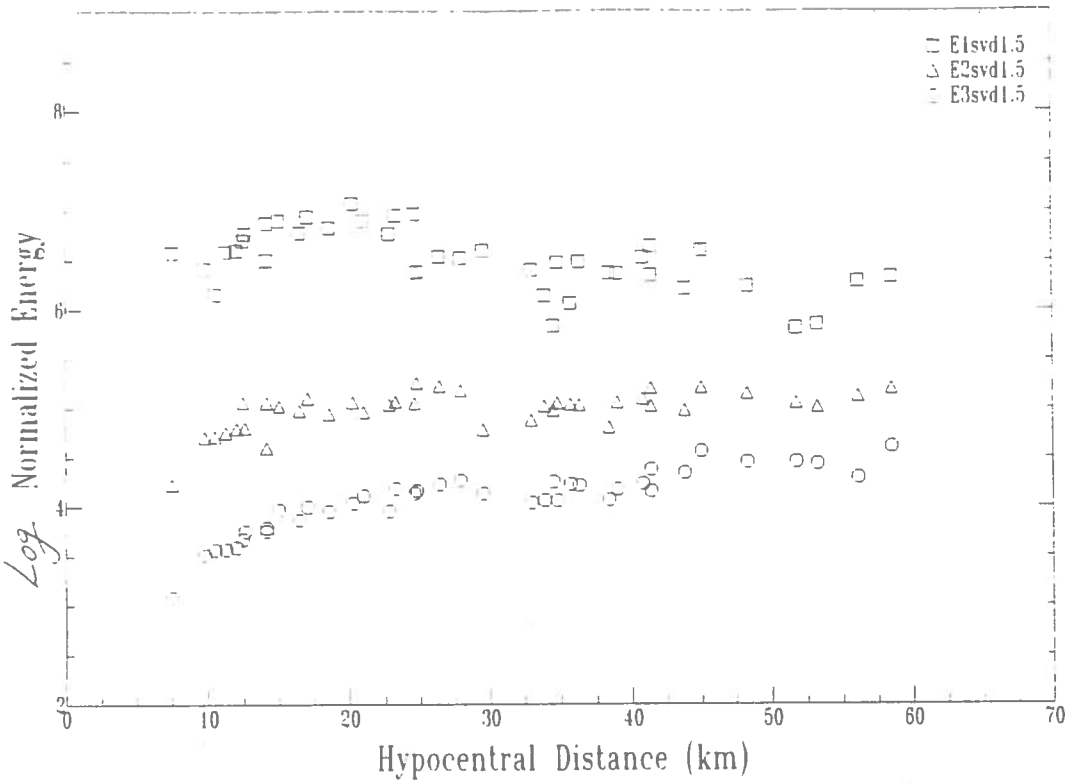
E1svd1.5
E2svd1.5
E3svd1.5
Log Normalized Energy
Hypocentral Distance (km)

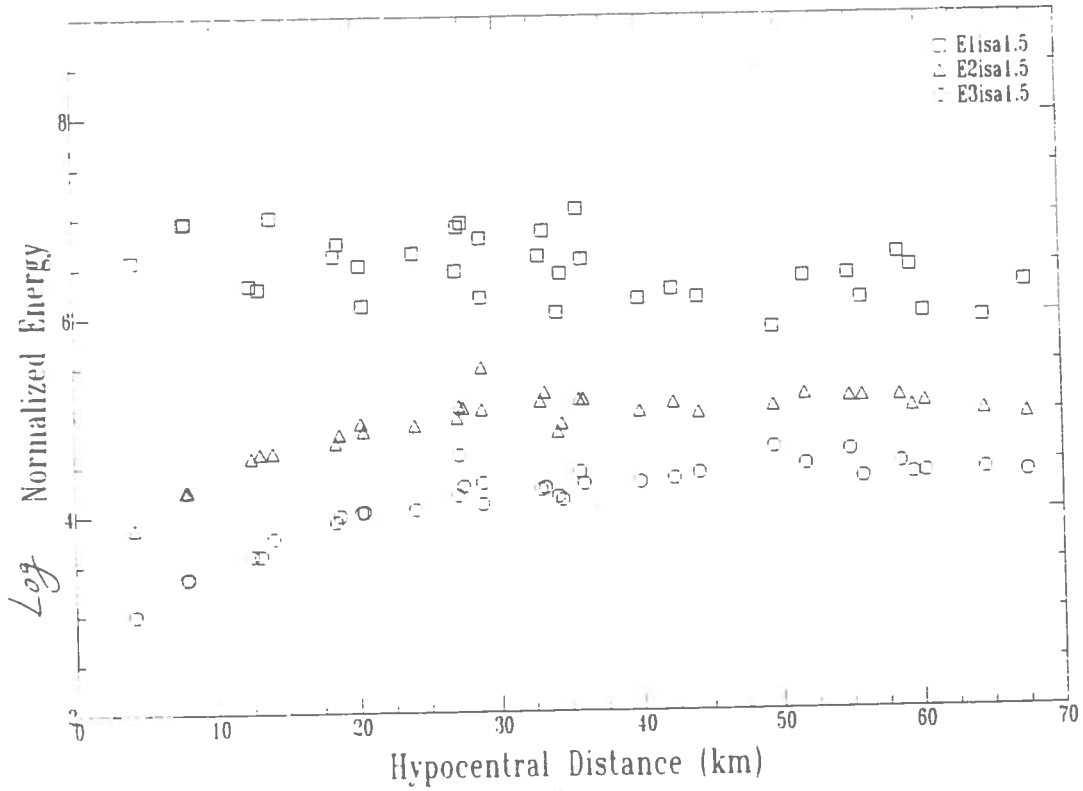
E1isa1.5
E2isa1.5
E3isa1.5
Log Normalized Energy
Hypocentral Distance (km)

Figure 2

A SCEC Project: Progress Report, 24 Sept. 1992

PIs: Robert Clayton and Egill Hauksson
Institution: California Institute of Technology
Title: Velocity and Structure Models for Southern California and the Los Angeles Basin Region

INVESTIGATIONS

The purpose of this project is to determine a three-dimensional velocity model of the Los Angeles basin. This model, in turn, will be correlated with geological data and used to determine more accurate hypocenters and focal mechanisms.

RESULTS

Preliminary results of our work were presented at the 1992 SSA meeting (Hauksson, 1992). Arrival time data from 530 earthquakes and two blasts have been inverted for the P-wave velocity structure of the Los Angeles basin. An initial one-dimensional velocity model was specified at 648 nodes forming a sparse grid with 21 km horizontal spacing between grid points at depths of 1, 4, 8, 12, and 16 km. The velocity model from the sparse grid was interpolated and used as input for an inversion for a second set of 2048 grid nodes with 6 km horizontal spacing. Both grids are rectangular and centered on the basin proper. The velocities at most of the nodes of the dense grid are well resolved except to the northwest where the resolution is below average.

Because the starting model is one-dimensional the final three-dimensional model can be correlated with the local geologic structures. Preliminary results of the inversion show high velocities in the crystalline rocks beneath the Santa Monica mountains and to the southeast. The flanks of the basin, where thrust faulting and folding is observed, can be recognized in the three-dimensional velocity structure and are characterized by intermediate velocities. The lowest velocities reflect the shape of the basin and form a gently dipping zone extending from Palos Verdes to the center of the basin. The more steeply dipping northeast flank of the basin can also be seen where the northeast trending velocity model cross section is compared to the north-northwest trending geologic cross section from Davis et al. [1989]. In the deepest part of the central basin low velocities extend down to 8-10 km depth. Some shallow basement velocity contrast exists across the Palos Verdes and the Newport-

Inglewood faults. The most prominent low velocity zone associated with thrust faulting exists adjacent to the Sierra Madre fault zone.

Wright (1991) provided an excellent summary of the geology of the Los Angeles basin. Figure 1, from Wright (1991), is an index map that shows major structural features and the location of geologic cross section A through F. We have made similar cross sections through our preliminary three-dimensional model and made an overlay with the geologic cross sections from Wright (1991). Figure 2 is an overlay of our velocity model and geologic cross sections A, B, C, and D Wright (1991) Figure 8. Figure 3 is an overlay of our velocity model and geologic cross sections E, F, and G from Wright (1991) Figure 8 continued. These overlays show remarkable agreement between the geology and the preliminary velocity model. The bottom of the basin is clearly reflected by velocities of 6 km/s or higher. The near-surface sediments correspond to low velocities of 3.0 km/s or less. The west flank of the basin is clearly defined by higher velocities at shallower depth than beneath the center of the basin. The east flank of the basin that consists of metamorphic rocks has lower velocities than the west flank and hence is not as well defined as the west flank.

The next step is to use the final three-dimensional model to improve hypocenters and focal mechanisms. Results from such inversions for the greater Los Angeles basin combined with results from our focal mechanisms studies, will provide a more comprehensive picture of the geological structure and seismotectonics of the Los Angeles basin than available before.

Figure Captions

Figure 1. From Wright (1991). An index map that shows major structural features and the location of cross section A through F. We have made similar cross sections through our three-dimensional model and made an overlay with the geologic cross sections from Wright (1991).

Figure 2. Overlay of our preliminary 3-D velocity model and geologic cross sections A, B, C, and D from Wright (1991) Figure 8.

Figure 3. Overlay of our preliminary 3-D velocity model and geologic cross sections E, F, and G from Wright (1991) Figure 8 continued.

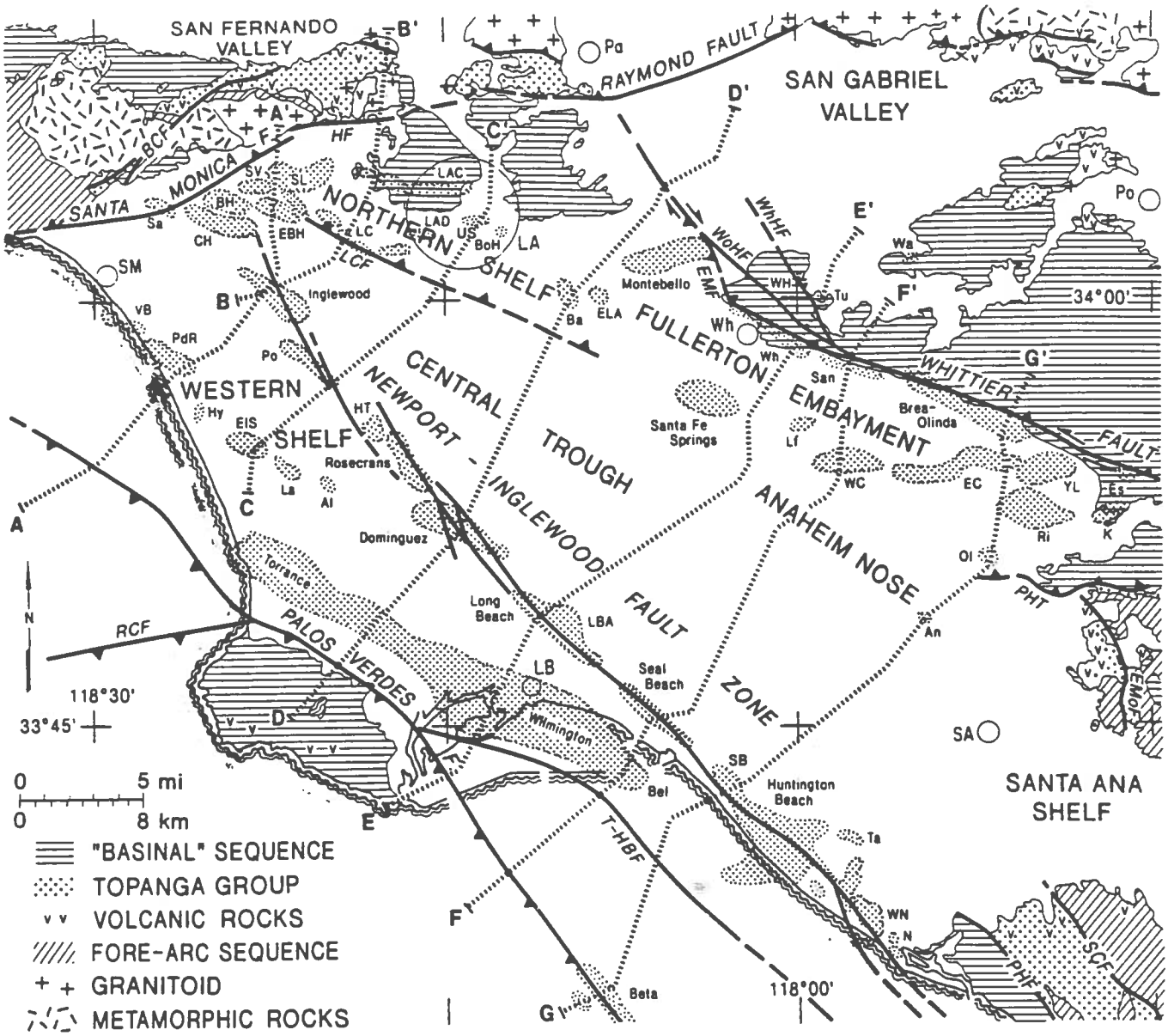
SAN FERNANDO VALLEY
SAN GABRIEL VALLEY
RAYMOND FAULT
SANTA MONICA
NORTHERN SHELF
CENTRAL TROUGH
NEWPORT - INGLEWOOD FAULT ZONE
ANAHEIM NOSE
FULLERTON
WHITTIER FAULT
EMBAYMENT
WESTERN SHELF
PALOS VERDES
SANTA ANA SHELF
Inglewood
Montebello
Santa Fe Springs
Brea-Olinda
Rosecrans
Dominguez
Torrance
Long Beach
Seal Beach
Wilmington
Huntington Beach
34°00'
118°30'
33°45'
118°00'
0 5 mi
0 8 km
"BASINAL" SEQUENCE
TOPANGA GROUP
VOLCANIC ROCKS
FORE-ARC SEQUENCE
GRANITOID
METAMORPHIC ROCKS

Figure 1

LOS ANGELES BASIN

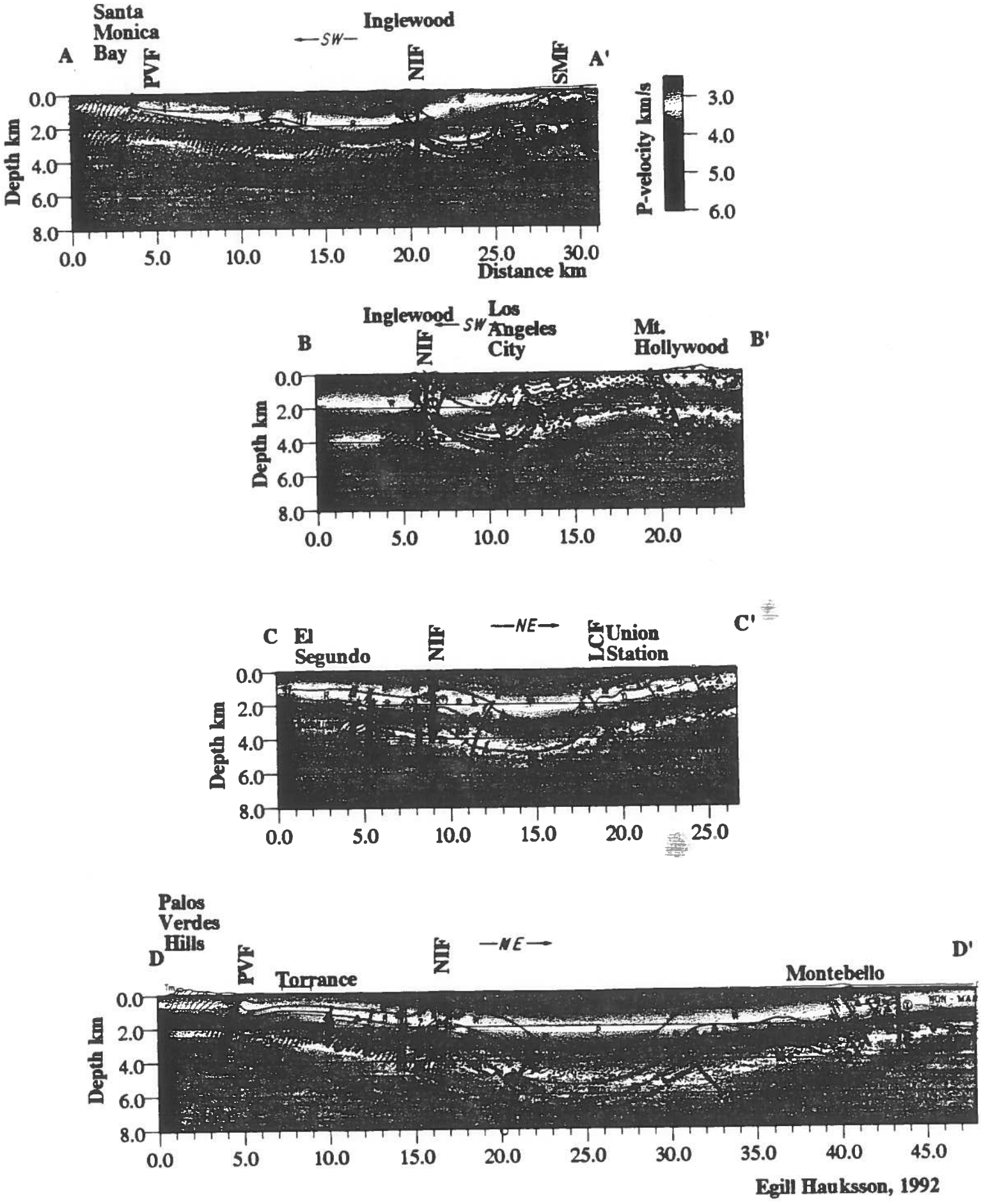

Figure 2

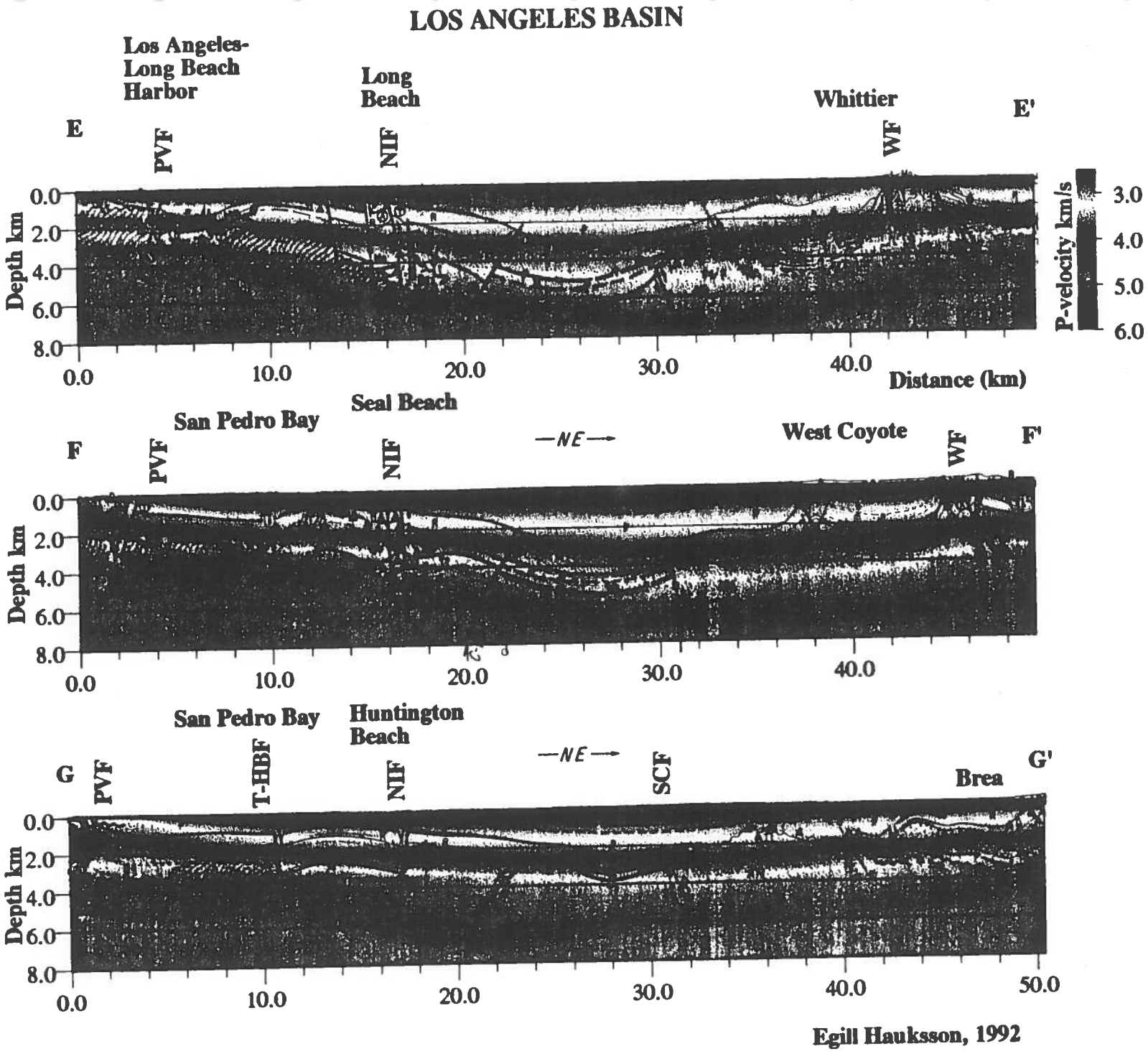
LOS ANGELES BASIN
Los Angeles-
Long Beach
Harbor
Long
Beach
Whittier
E
E'
PVF
NIF
WF
Depth km
0.0
2.0
4.0
6.0
8.0
P-velocity km/s
3.0
4.0
5.0
6.0
0.0
10.0
20.0
30.0
40.0
Distance (km)
Seal Beach
San Pedro Bay
F
F'
—NE—
West Coyote
San Pedro Bay
Huntington
Beach
G
G'
T-HBF
SCF
Brea
50.0
Egill Hauksson, 1992

Figure 3

Analysis and Inversion of Teleseisms

Paul M. Davis, UCLA

The objective is to use teleseismic phase times and waveforms to image lateral variation in southern California. With the assistance of Jim Mori (USGS) UCLA graduate student Herbert Rendon has acquired data from, and analyzed 17 well-recorded teleseisms at the more than 200 sites of the southern California network. Semblance analysis has been used to stack waveforms to form a beam. A least squares technique which maximizes cross-correlation between nearby stations has been used to correct for local statics. Sixteen hundred first arrival travel time residuals have been calculated. Travel time anomalies associated with the transverse ranges can be seen in the residuals, as has been seen by others (Hadley and Kanamori, 1977; Raikes, 1980; Humphreys and Clayton, 1990). We have stripped off effects of the crust using the crustal model of Sung (1989), Sung and Jackson (1992, BSSA) which is based on arrival times of Pg and Pn waves. Slowness in the crust, upper mantle and variation in depth to Moho were expressed in terms of spatial harmonic expansions. Also station time terms were obtained in their analysis. We have used this model to calculate times of teleseismic rays between the Moho and surface including station terms. We then strip off crustal effects from teleseismic residuals and use the Aki et al., 1977 block inversion scheme to find lateral variation in the upper mantle. Figure 1 shows crustal and mantle velocity variations for the data set without crustal stripping, i.e., the standard approach. Figure 2 shows corresponding velocity variation in the mantle after crustal stripping. Figure 2a shows ray paths in the crust from local earthquakes, used by Sung and Jackson to determine their crustal model. These figures are preliminary, being based on data for 17 earthquakes recorded from the southern Californian network. We are in the process of expanding the data set to many times this size. However the programs for the analysis scheme are written.

Our search for coherent scatterers in the teleseismic coda has continued by examining the cross-correlation between individual stations and the average waveform found from the semblance beam stack. When high noise stations are excluded, it is anticipated that degraded correlation will occur where scattered radiation is greatest. At this stage in our analysis two regions stand out, the Mojave and the Sierras. The next step will involve a systematic search for scatterers using the method of Hedlin et al., (1991) who detected body - Rayleigh scattering SW and E of the NORESS array. We propose to search for body-body scattering also, guided by the results of the velocity studies.

We have also continued our theoretical work on calculating teleseismic synthetic seismograms generated by scattering from upper mantle and crustal heterogeneities. We have extended uniform asymptotic methods to handle the deep shadow, illuminated zone and penumbra zone for cylindrical hard and soft scatterers (Rendon and Davis, BSSA 1992). We have nearly completed the inclusion problem and will use the Geometric Theory of Diffraction to generalize the approach to bodies of arbitrary, but smooth, curvature. Part

of this work involves comparison with waveforms generated by finite differences. The objective is to generate simple methods to model forward scatterers in the teleseismic wave field from southern California in order to interpret associated coda variations.

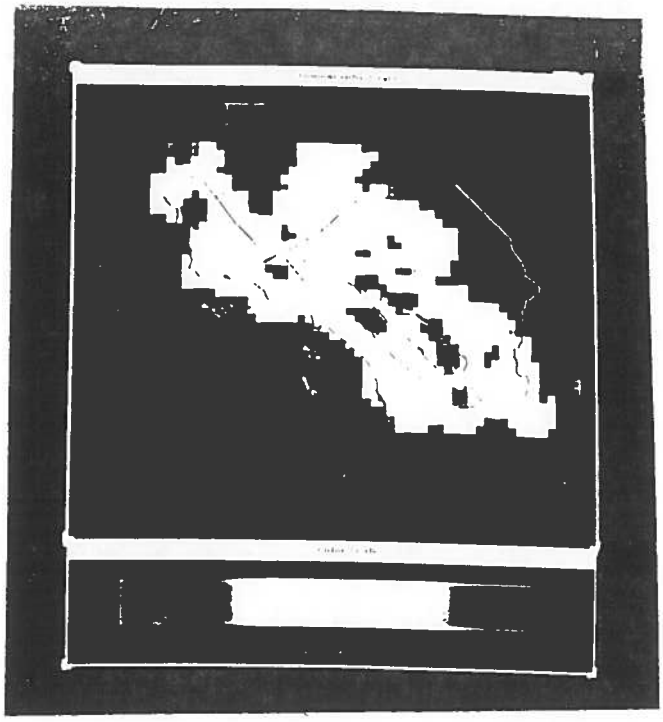

Crustal Layer 0-40 km

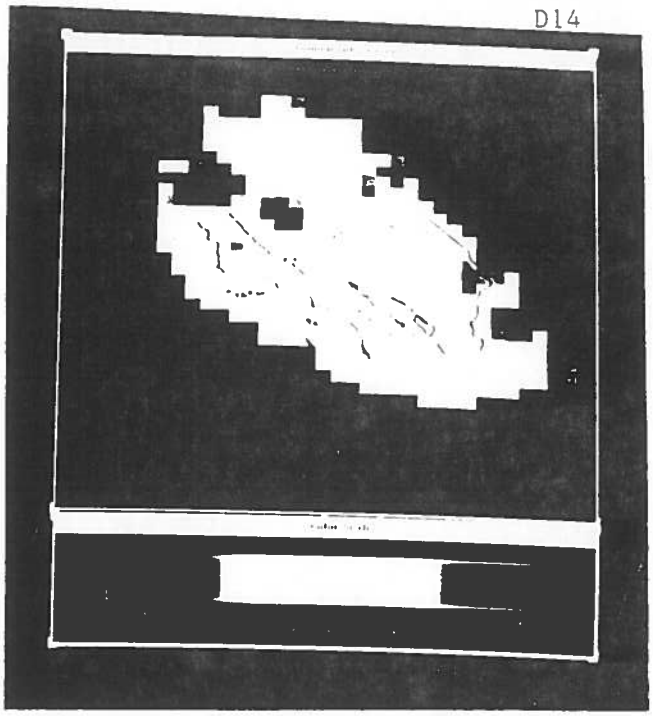

40-100 km

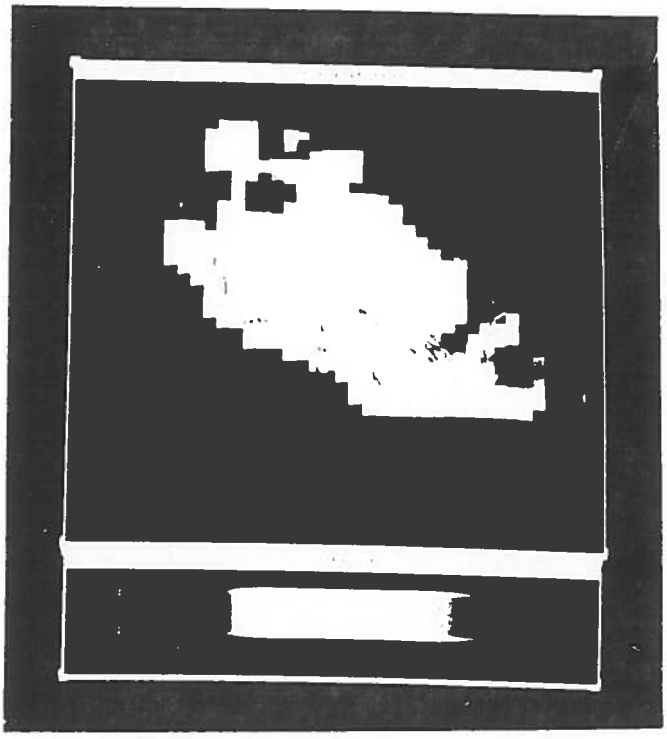

100-160 km

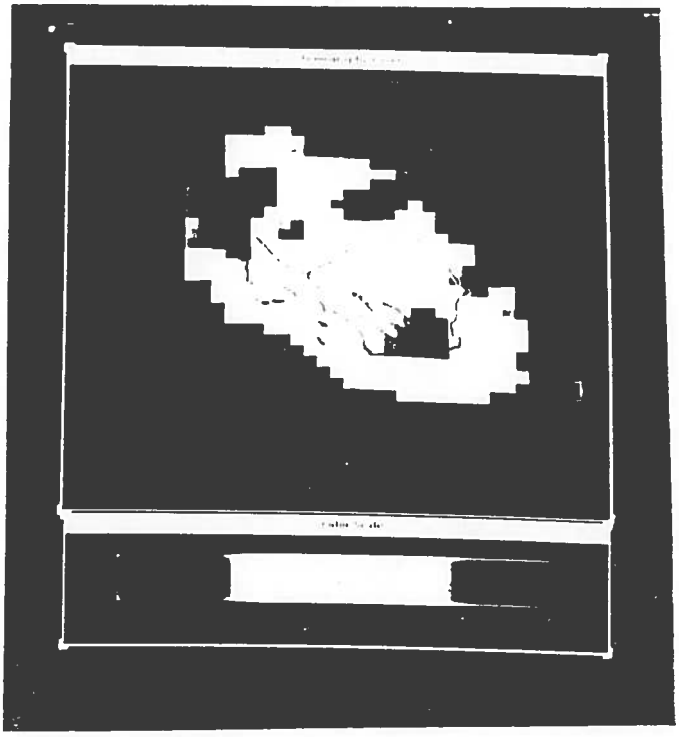

160-220 km

Figure 1 ACH inversion without crustal stripping

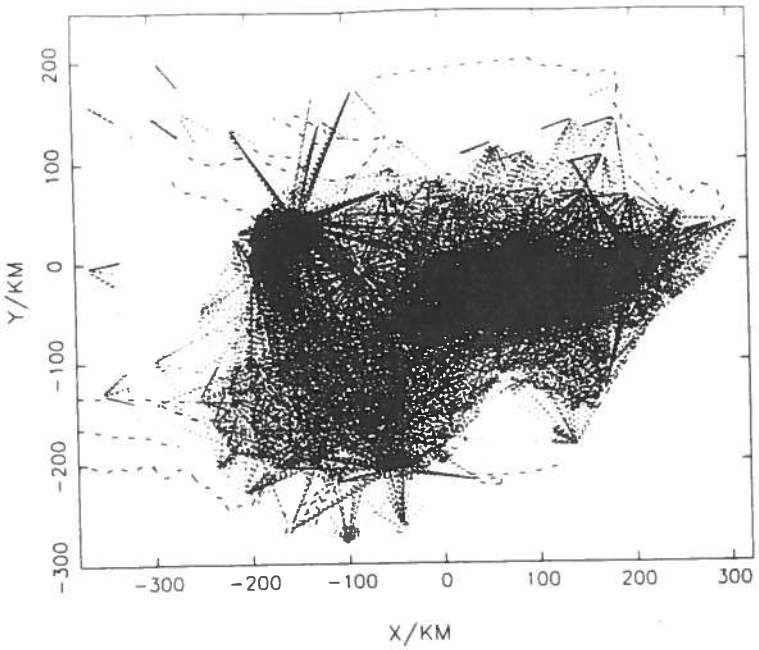

Sung-Jackson Crust from Pn and Pg

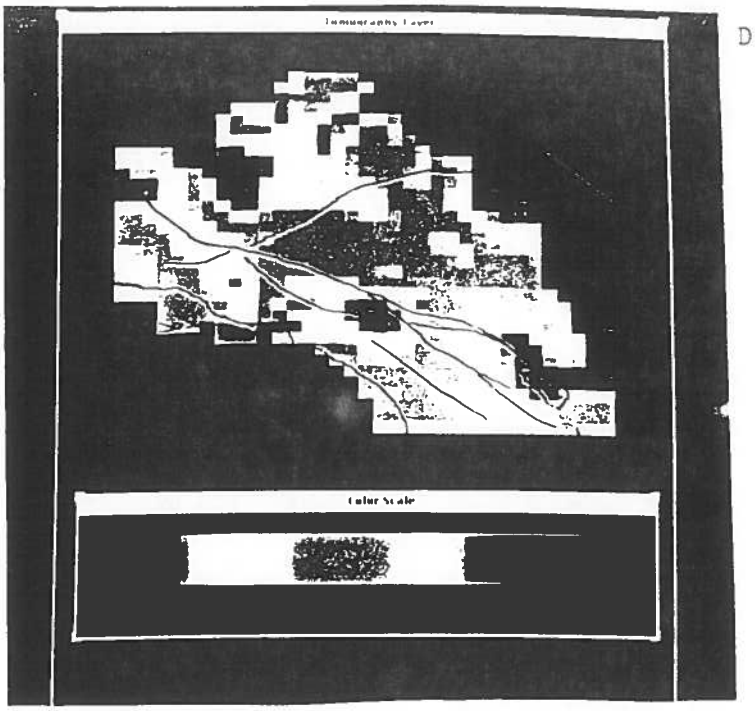

40-100 km

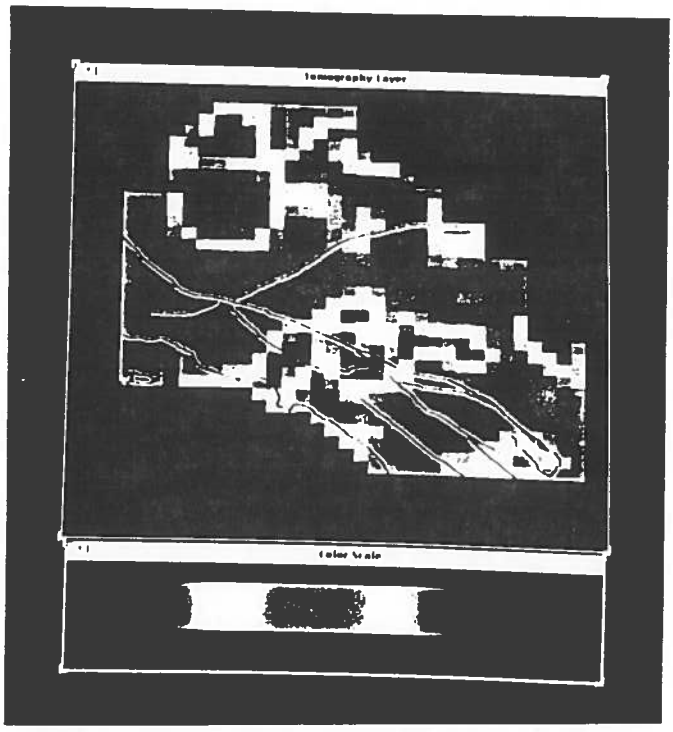

100-160 km

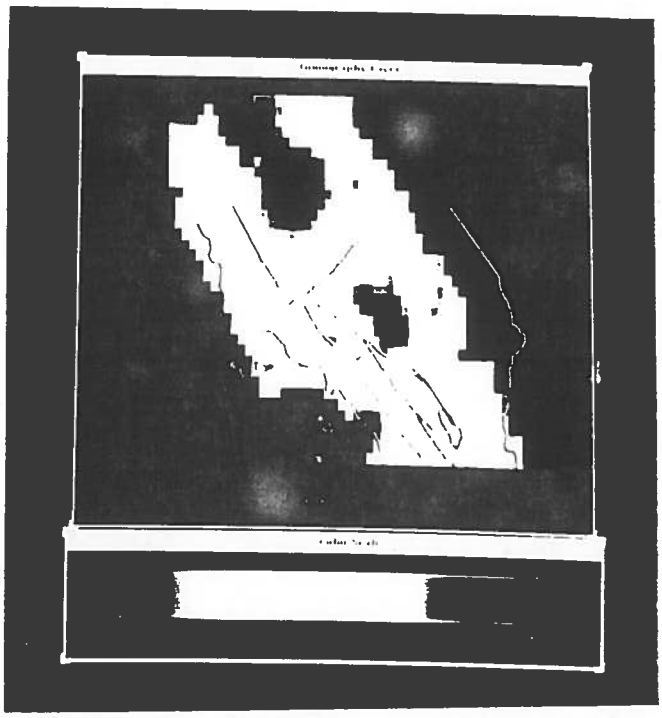

160-220 km

Figure 2 ACH inversion after crustal stripping

Seismic Trapped Waves along the San Jacinto Fault at Anza

Yong-Gang Li and Ta-Liang Teng
University of Southern California

We used five portable instruments (REFTEKs) along the San Jacinto fault (SJF) at Anza to record earthquakes for further evidence for trapped waves in southern California. Five recorders with ten L22 2 Hz 3-component sensors were deployed along and across the fault trace at Anza seismic gap from December, 1991 to April, 1992 (Figure 1). We observed clear fault zone trapped waves excited by some earthquakes occurring within the fault zone at depths between 6 km and 14 km, and with epicenters of 5-15 km away from recording stations. Figure 2 illustrates fault zone trapped waves recorded by one sensor located on the fault trace for a M2.0 earthquake (marked by A in Figure 1) occurring at the depth of 13.7 km and 15 km southeast of the station. This event is located by USGS/UCSD Anza seismic network with its epicenter on the surface trace of the SJF. Fault zone trapped waves follows S-waves and are characteristic of large amplitude, long period and dispersion in a narrow frequency band between 2 Hz and 6 Hz. They clearly appear on the horizontal component of seismograms, with the shear motion parallel to the fault plane. But, no such type of wavetrains were recorded by sensors deployed with large offsets (several hundred meters) outside the fault trace for the same event (bottom panel, Figure 2). The observation of fault zone trapped waves at Anza suggests that a low velocity zone (LVZ) may exist along the Anza segment of the SJF. This fault LVZ is narrow (maybe a couple of hundred meters wide) and extends to the depth of ~14 km.

Based on portable instrument recordings of fault zone trapped waves on the SJF at Anza, we informally examined the USGS/UCSD Anza seismic network data for confirmation of our preliminary observation. We found that the network station SND, which is located with the offset of ~200 m from the SJF, also recorded fault-zone trapped waves excited by earthquakes occurring within the fault zone. Figure 3 (upper panel) shows large amplitude dispersive wavetrains recorded by station SND for the same event in the previous example. But, no significant trapped waves were recorded by other network stations with large offsets from the fault zone (bottom panel, Figure 3). The preliminary observations of fault zone trapped waves on the SJF at Anza encourage us to systematically examine the existing catalog of Anza seismic network (it starts operating since 1982) for further evidence of trapped waves.

We believe that there is much to be learned from an observation program keyed to finding and interpreting fault zone trapped waves recorded at Anza. They will address to: (1) Where is the locked segment along the SJF ? (2) What is the spatial dimension of the fault LVZ (fault gouge) at Anza seismic gap ? (3) Which earthquakes occurred on or very close to the fault plane ? If the fault gouge is thought of a potential rupture plane of a main shock, the nucleation process of the main shock may be studied from the location pattern of seismic events occurring in the immediate vicinity of the fault gouge. The high resolution location of seismic events around the fault zone may be obtained from systematic observation of fault zone trapped waves.

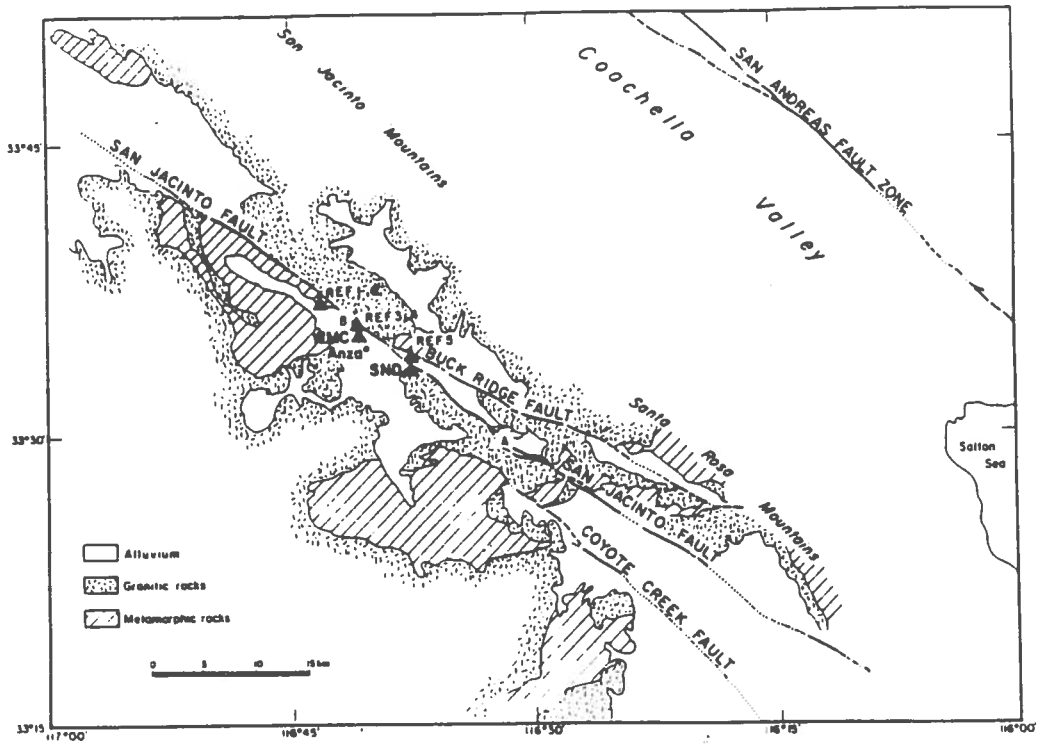

Fig. 1 Location map of portable instruments (REFTEKs) deployed on the San Jacinto fault at Anza. Stations are denoted by REF1-5 for REFTEC stations. SND and WMC are two network stations.

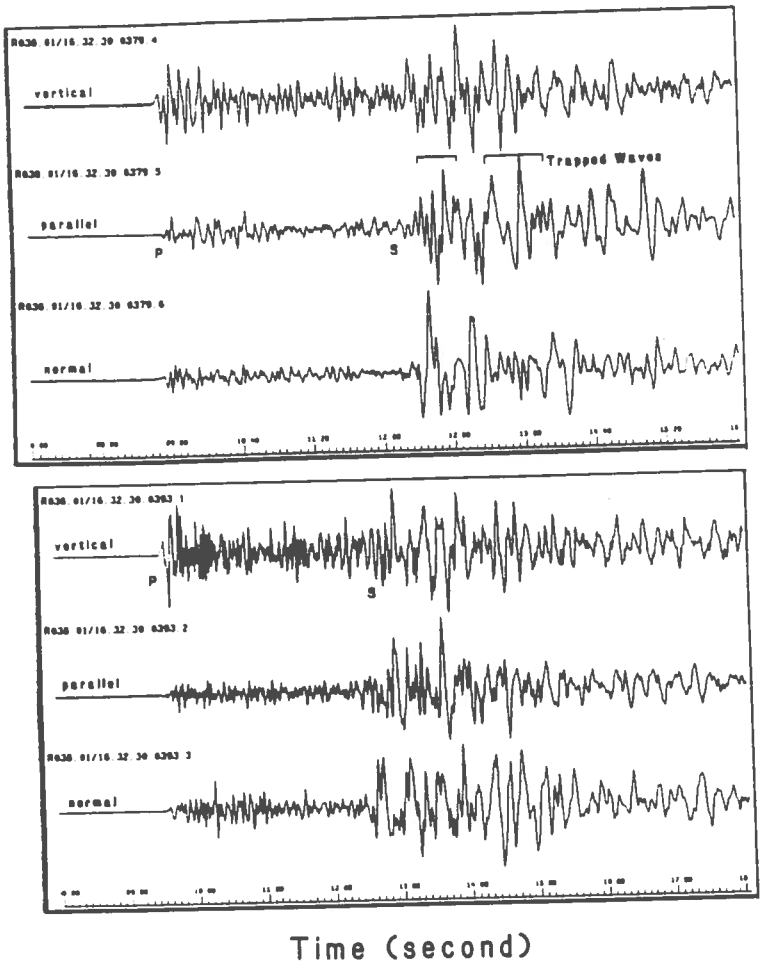

Fig. 2 Three-components of seismograms recorded by REFTEK station 3 located on the San Jacinto fault at Anza (Top) and by station 2 located outside the fault zone (Bottom) for an earthquake occurring within the fault zone (event A in Fig. 1). Three components are the vertical, parallel to the fault plane, normal to the fault plane. Fault zone trapped waves are recorded by the station on the fault zone.

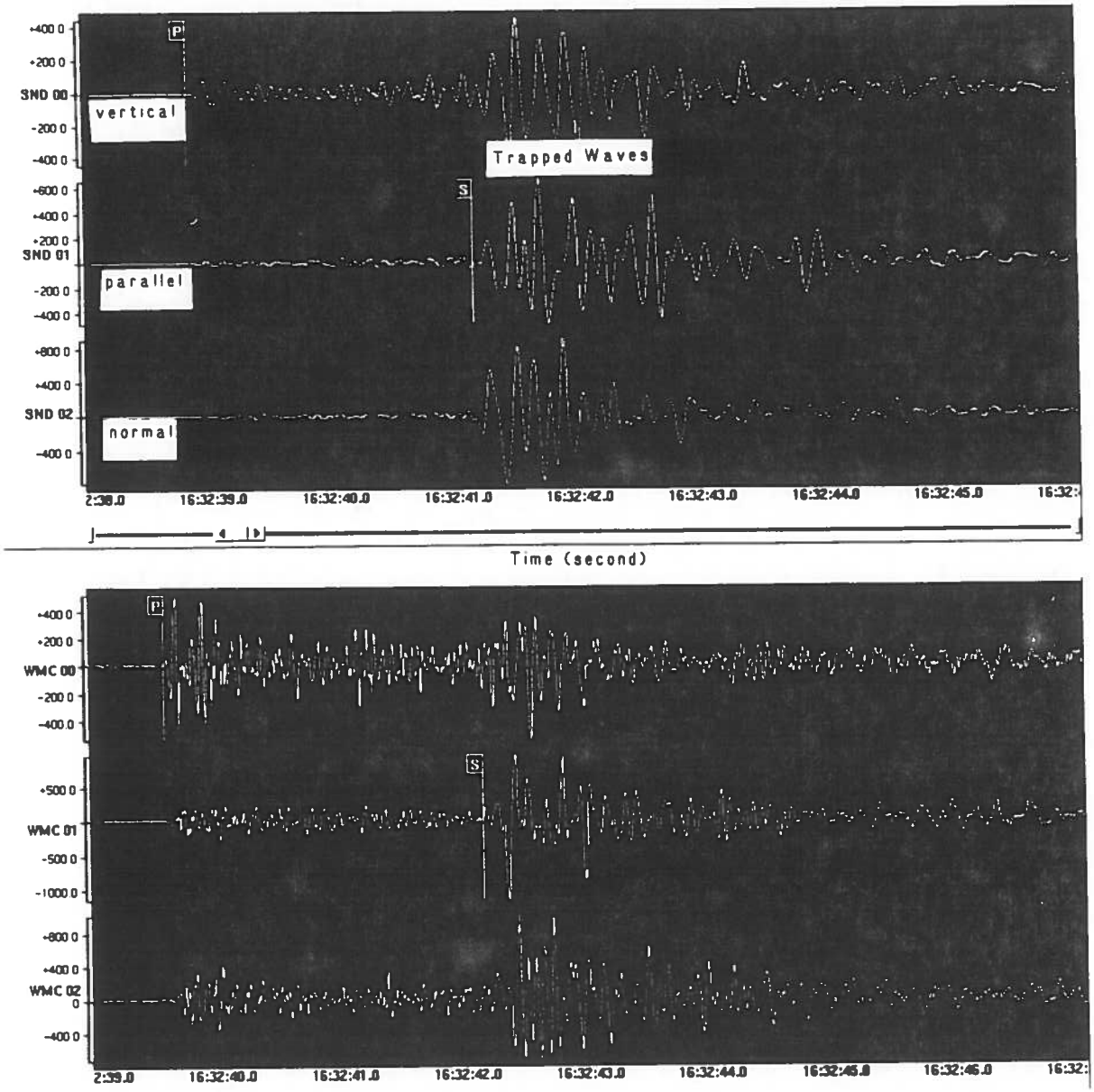

Fig. 3 Three-components of seismograms recorded by USGS/UCSD network stations SND (Top) and WMC (Bottom) for the same event in Fig.2. Fault zone trapped waves are recorded by station SND close to the fault zone but no significant trapped waves are recorded by station WMC that locates 1 km away from the fault zone.

Structural Geometries of the Los Angeles Basin: Seismic Reflection Studies of Basin and Fault Structures

David Okaya
Tom Henyey
Univ. Southern California

Working Group D: Seismic Imaging
Progress Report - SCEC FY93

Seismic reflection studies of the Los Angeles basin focussed on the following activities during FY92:

*high resolution seismic profiling of the Palos Verdes fault on the Palos Verdes Peninsula (collaboration w/ Kaye Shedlock, USGS/Denver and Tom Rockwell, SDSU).

*initiation of program to reprocess/interpret Chevron industry data (collaboration w/ Bob Yeats, OSU).

*initial dialogues to establish both a database of seismic reflection profiles within the Los Angeles basin and working groups to analyze these data.

Seismic profiling of the Palos Verdes fault on the Palos Verdes Peninsula

The Palos Verdes fault in western Los Angeles is one of several major L.A. faults of which very little is known about its past seismic history and its potential for possibly destructive activity. Some proprietary offshore information exist to locate the fault within Long Beach Harbor and to indicate that it is currently active; but similar information is not available onshore. Little knowledge currently exists to precisely locate the fault onshore or to indicate the expected size or frequency of earthquakes along this fault zone. The Palos Verdes fault trend takes a bend to the west as it comes onshore onto Palos Verdes peninsula from Long Beach Harbor (Figure 1); the involvement of a single fault bend or a series of en-echelon faults to accomodate this bend is not known.

A collaborative program was begin in FY93 to provide subsurface images of the Palos Verdes fault on the eastern portion of Palos Verdes peninsula. The primary objectives of these high-resolution seismic reflection profiles were (A) to identify the location of the Palos Verdes fault as it comes onshore from Long Beach Harbor, (B) to identify if a series of aerophotographic lineaments are en-echelon steps of the fault further inland at the town of Lomita, and (C) to determine the 3-D subsurface geometries of these faults in order to determine the amounts of dip-slip or thrust components of movement.

Acquisition of the seismic profiles was conducted by the USGS/Denver Mini-Sosie crew under the direction of Kaye Shedlock. P.I.'s Okaya and Henyey were responsible for site selection, permitting with several city and county agencies as well as with private landholders, and assisting in the actual data acquisition (parameter selection and roll-along). USC and SDSU also provided additional field personnel. The funds to cover the field program were provided jointly by the USGS and the P.I.'s with additional support provided by SDSU.

Two CDP profiles were located roughly perpendicular to the trend of the Palos Verdes fault, the first on Palos Verdes Drive East (Rolling Hills Estates) - Oak Street (Lomita) (line 1 in Figure 2) and the second on Gaffey Street (San Pedro) - L.A. Harbor Park (line 3 in Figure 2; line 2 was permitted but not collected). Field acquisition parameters included a 24-channel off-end array using 25-feet receiver spacings. Source spacing was 25 feet. Early portions of the profiles were collected using 50-feet receiver spacings in order to examine the effects of longer offsets to image steep dips and sub-sediment reflections. One sec of travel-time was recorded by the Mini-Sosie system. Processing of the profiles was conducted at the USGS/Denver.

The southern portion of the Gaffey Street profile is shown in Figure 3. Data quality is moderate to high. Abrupt lateral changes in reflection character ('X') across the profile indicate the presence of major fault strands interpreted to be related to the Palos Verdes fault; the fault in the

eastern Palos Verdes peninsula is not a single fault but a series of en-echelon fault strands. These strands acommodate the western bend in the Palos Verdes fault. The locations of the fault strands in the seismic profiles correlate with aerophotograhic lineaments.

Interpretation of these profiles will be completed by the end of the current funding period. A collaborative (USGS-USC-SDSU) manuscript is anticipated to be completed by this time. P.I. Okaya will continue his interactions with Rockwell on the subsurface imaging of trenched faults in the L.A. basin region and is investigating additional imaging techniques to provide lateral coverage extending from paleoseismologic trench sites.

Seismic profiling of the Los Angeles basin using Industry Profiles

The LA basin has historically been subjected to active hydrocarbon exploration by Industry. An extensive body of knowledge and data has been accumulated over the years by these petroleum companies. With the recent downturn in domestic exploration/production, these companies have begun to withdraw from the LA basin. The P.I.'s are currently funded to establish cooperative interactions with industry to tap this vast body of information and to begin preliminary analysis of data from the LA basin. The primary application of these data is three-fold: first, to establish a regional structural framework of the LA basin for the master model; second, to make the data available for SCEC researchers, assisting in data processing and/or analysis as needed; and, third, to provide an advance image of acquisition targets and conditions in the LA basin in preparation for the LA basin seismic experiment.

An extensive set of seismic and geologic data exists within industry. The state of industry exploration/production are such that now is an opportune moment to ask oil companies for the donated use of their data. For example, preliminary discussions with Chevron have resulted in their offer to allow us access to most of their entire LA basin data set. These data, in the form of seismic reflection profiles and subsurface well data, are thus available for structural/tectonic analysis. For the cost of tape duplication, seismic data in digital form can be obtained for reprocessing. Vibroseis profiles can be recorrelated to extract full crustal images via reprocessing.

Through the efforts of the OSU group led by Bob Yeats, an initial set of seismic profiles has been requested from Chevron for interpretation and reprocessing. In collaboration, the P.I.'s will use their funds to cover the data copying charges (few to several $K as requested by Chevron) and will reprocess the profiles at USC. Careful processing will be applied to the shallow portions of the profiles as requested by the OSU group. In addition, the Vibroseis profiles will be automatically extend-correlated in order to identify the presence of middle and lower crustal reflections.

The establishment of data exchange agreements with other companies for seismic data in digital form is still under way. Rather than centralize all communciations with companies, the P.I.'s are working with those SCEC researchers who have already established industry contacts. During this past year companies have been preoccupied with internal rearrangements which have been widespread throughout industry and have had less time/resources to devote to academic data requests. However, we anticipate receiving additional seismic profiles in the basin which meet the three-fold application criteria stated above.

During the past year, the P.I.'s have upgraded their seismic reflection data processing facilities (without the use of SCEC funds). The USC seismology computational network has 10 Sun workstations and related peripherals. Seismic data processing is primarily conducted on a SUN 4/390 and a dedicated SparcStation 2 accessing 2 Gbytes disk storage, three tape drives, two exabyte cartridge drives, and a 36" Versatec plotter. One tape drive is capable of demultiplexing seismic field tapes. Seismic software includes SierraSeis batch processing with IRIS-SEIS extensions, Sierra ISX interactive processing, and a number of external self-developed applications. We anticipate purchase of the ProMax processing system to allow for even more interactive processing capability.

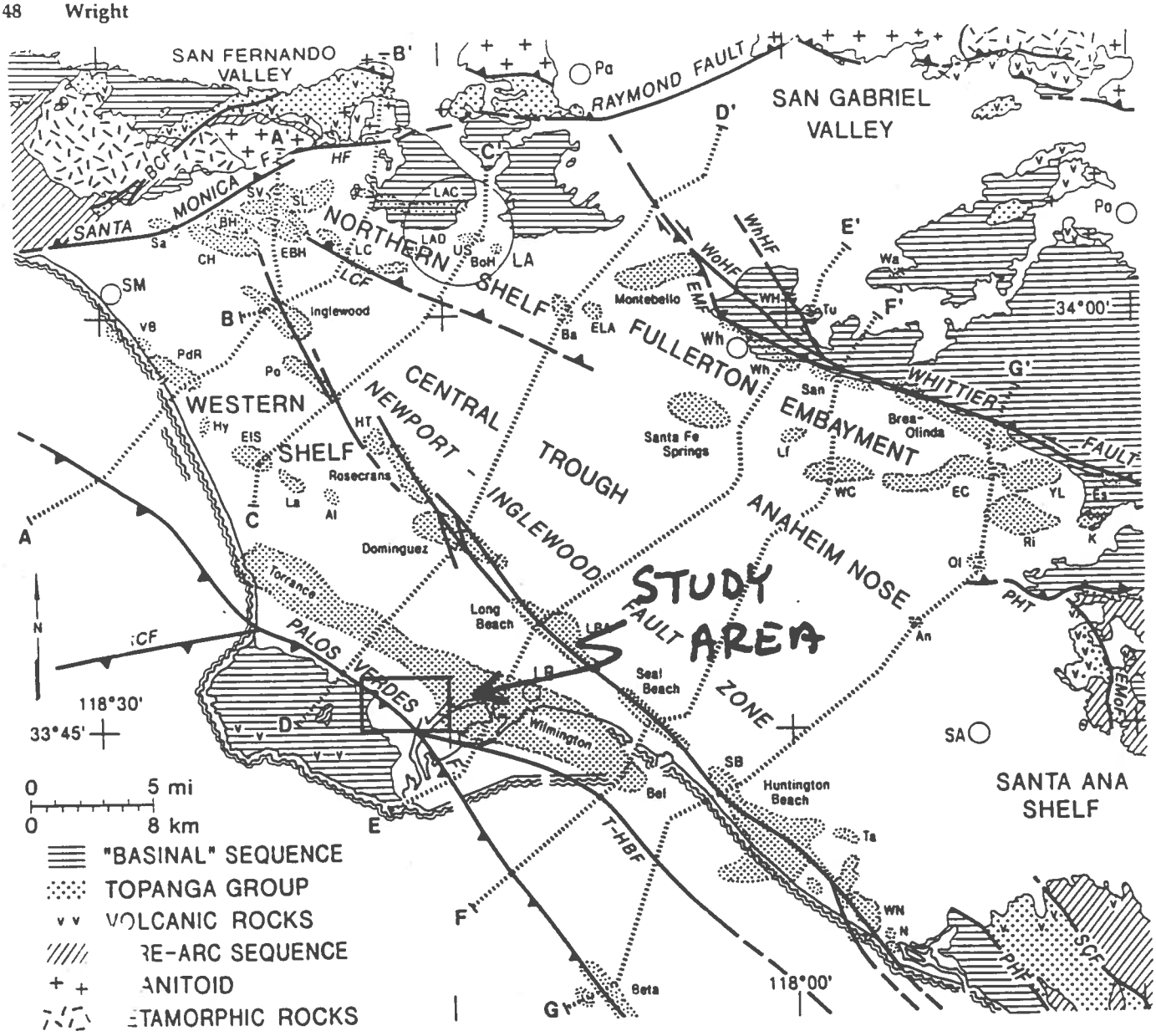

A)

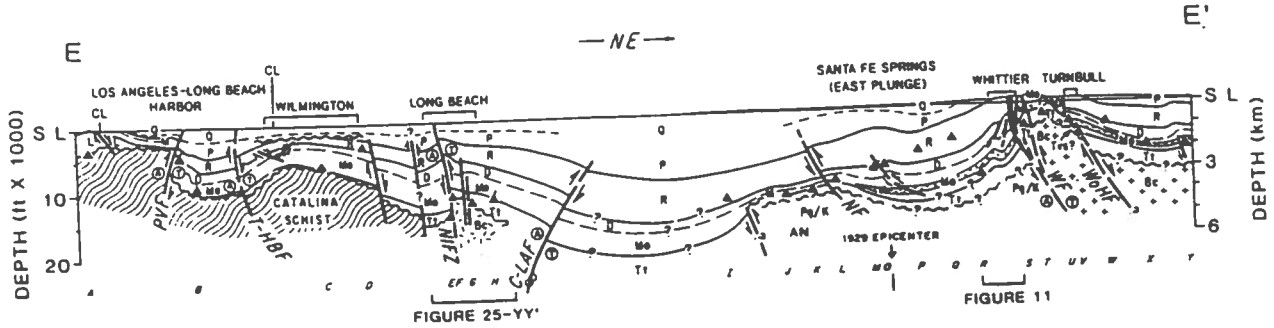

FIGURE 25-YY'

FIGURE 11

B)

From Wright (1991) 'Structural Geology and Tectonic Evolution of the Los Angeles Basin California'

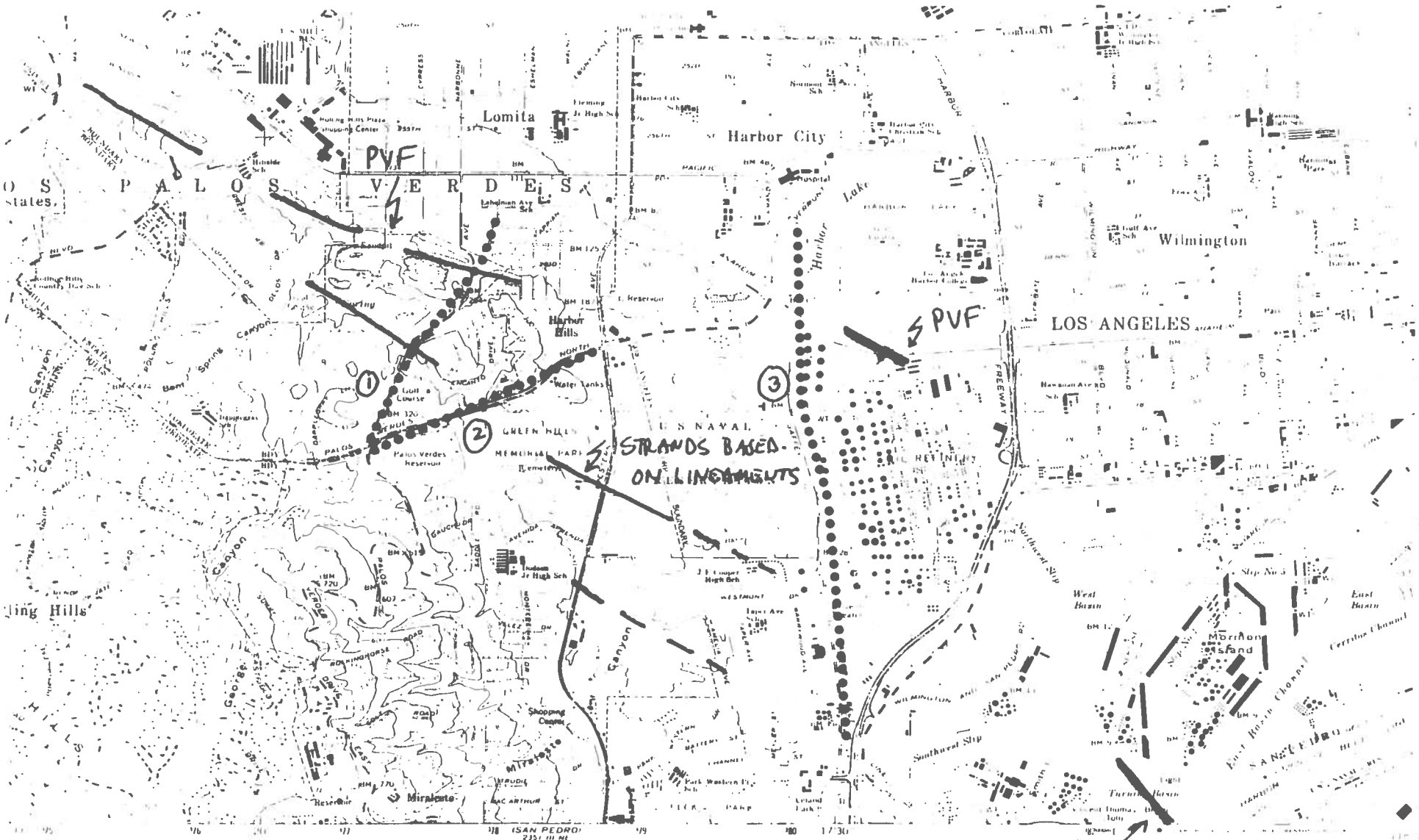

SCALE 1:24000

CONTOUR INTERVAL 20 FEET

DOTTED LINES REPRESENT 5-FOOT CONTOURS

NATIONAL GEODETIC VERTICAL DATUM OF 1929

DEPTH CURVES AND SOUNDINGS IN FEET. DATUM IS MEAN LOWER LOW WATER

THE RELATIONSHIP BETWEEN THE TWO DATUMS IS VARIABLE

SHORELINE SHOWN REPRESENTS THE APPROXIMATE LINE OF MEAN HIGH WATER

THE MEAN RANGE OF TIDE IS APPROXIMATELY 4 FEET

THIS MAP COMPLIES WITH NATIONAL MAP ACCURACY STANDARDS

FOR SALE BY U S GEOLOGICAL SURVEY DENVER COLORADO 80225 OR RESTON VIRGINIA 22092

A FOLDER DESCRIBING TOPOGRAPHIC MAPS AND SYMBOLS IS AVAILABLE ON REQUEST

ROAD CLASSIFICATION

Heavy duty ——— Light duty

Medium duty — — — Unimproved dirt

TORRANCE, CALIF.

1964

D22

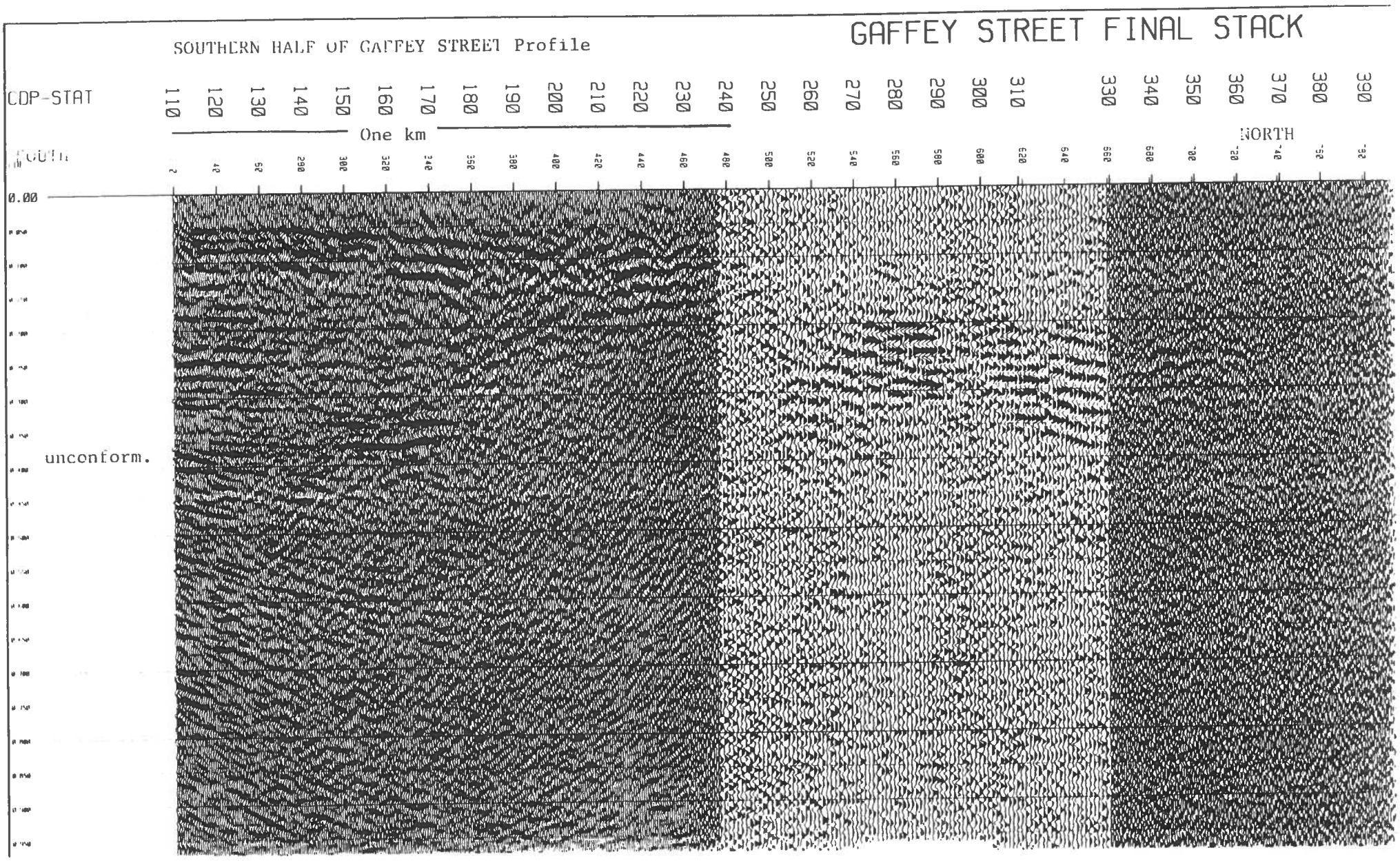
GAFFEY STREET FINAL STACK
SOUTHERN HALF OF GAFFEY STREET Profile
CDP-STAT
110 120 130 140 150 160 170 180 190 200 210 220 230 240 250 260 270 280 290 300 310 330 340 350 360 370 380 390
One km
NORTH
0.00
unconform.
abrupt changes:
X
X
X

D23

A PROGRESS REPORT ON SCEC-FUNDED RESEARCH

DAPENG ZHAO
Seismological Laboratory, California Institute of Technology

I have been supported by SCEC since May 25, 1992. During the past three months I have made the following two researches.

1. Tomographic Imaging of the Crust and Uppermost Mantle of Southern California

Three-dimensional seismic velocity structure of southern California has been investigated by several researchers by inverting local earthquake arrival times [Ergas and Jackson, 1981; Hearn and Clayton, 1986a,b; Sung and Jackson, 1992]. However, the previous studies did not determine the depth variation of tomographic image in the crust, which prevents us from discussing in detail the tectonics of southern California, e.g., the depth extent of the major sedimentary basins, batholiths and large fault zones in the crust.

In the present study, I have determined a detailed P-wave tomographic image of the crust and uppermost mantle by using 131,372 P-wave arrival times from 6,437 local and regional earthquakes recorded by the Caltech-USGS Southern California Seismic Network in the past twelve years (see Figures 1a and 1b). The tomography method of Zhao et al.[1992] is used. The obtained image (see Figure 2) has a spatial resolution of 25 km in horizontal direction and 8-11 km in depth direction. The tomographic image is found to correlate well with the major surface geological features. For the structure close to the surface, sedimentary basins such as the Los Angeles Basin, Ventura Basin and Santa Maria Basin are well imaged as low velocities, while batholiths such as the Peninsular Ranges and San Gabriel Mountains are imaged as high velocities. At deeper crust, the velocity is low beneath the Mojave Desert, Coso volcanic area and Salton Trough, while

it is high beneath the Great Valley, Continental Borderland and the major basins. A high velocity layer exists at the mid-crust beneath the Salton Trough, in good agreement with a previous study using explosion sources and gravity data [Fuis et al.,1982]. For the uppermost mantle, the velocity is low beneath southeastern Sierra Nevada and the Quaternary volcanic areas, while it is high beneath the Mojave Desert and along the Pacific coast. The present result cast a new light on the complex structure and tectonics of southern California.

This study has been submitted for publication [Zhao and Kanamori, 1992a].

2. Landers Earthquake Sequence: Relationship Between Earthquake Occurrence And Structural Heterogeneities

The June 28, 1992, Ms 7.4 Landers Earthquake occurred in the southern Mojave Desert, California, and ruptured a fault approximately 60-70 km in length. Thousands of aftershocks of the earthquake have been recorded by the Caltech-USGS Southern California Seismic Network (SCSN). To investigate the relationship between complexities in the crustal structure and variations in seismicity, I performed a joint inversion for 3-D velocity structure and hypocentral locations using 145,098 P-wave arrival times from 3,740 Landers Earthquake aftershocks and 1,148 other events recorded by 60 permanent and temporary SCSN stations. Grid nodes set in the study area have a spacing of 5 km in horizontal direction and 5-8 km in depth direction.

A detailed P-wave image is determined and hypocentral locations are improved with the 3-D velocity model. Large velocity variations amounting to 6% are found in the aftershock regions. Most of the aftershocks occurred in normal or relatively high velocity

(high-V) areas. Swarms of the aftershocks are separated by low velocity (low-V) zones, which may be too weak in strength to generate earthquakes. Most aftershocks have focal depths shallower than 15 km, but some occurred at the depths of 15-25 km; most of them are located in high-V areas. Below the Black Mountain volcano a prominent low-V zone exists continuously from the surface to the uppermost mantle. Earthquakes occurred in normal or high-V areas surrounding the low-V zone below the volcano. These results suggest that earthquake occurrence is closely related to the in situ structural heterogeneities.

This study will be presented at the 1992 Fall AGU meeting in San Francisco [Zhao and Kanamori, 1992b].

References

Ergas,R.A., D.D.Jackson, Spatial variations of seismic velocities in southern California, *Bull. Seism. Soc. Am.*, *71*, 671-689, 1981.

Fuis,G.S., W.D.Mooney, J.H.Healy, J.A.McMechan, and W.J.Lutter, Crustal structure of the Imperial Valley Region, *U.S. Geol. Surv. Profess. Pap.*, *1254*, 25-49, 1982.

Hearn,T.M., and R.W.Clayton, Lateral velocity variations in southern California I. Results for the upper crust from Pg waves, *Bull. Seism. Soc. Am.*, *76*, 495-509, 1986a.

Hearn,T.M., and R.W.Clayton, Lateral velocity variations in southern California II. Results for the lower crust from Pn waves, *Bull. Seism. Soc. Am.*, *76*, 511-520, 1986b.

Sung, L.Y., and D.D.Jackson, Crustal and uppermost mantle structure under southern California, *Bull. Seism. Soc. Am.*, *82*, 934-961, 1992.

Zhao,D., A.Hasegawa, and S.Horiuchi, Tomographic imaging of P and S wave velocity structure beneath northeastern Japan, *in press, J. Geophys. Res.*, 1992.

Zhao,D., and H.Kanamori, P-wave image of the crust and uppermost mantle in southern California, *submitted to Geophys. Res. Lett.*, 1992a.

Zhao,D., and H.Kanamori, Landers earthquake sequence: Joint inversion for 3-D velocity structure and hypocentral locations, *submitted to AGU for presentation at the 1992 Fall AGU Meeting in San Francisco*, 1992b.

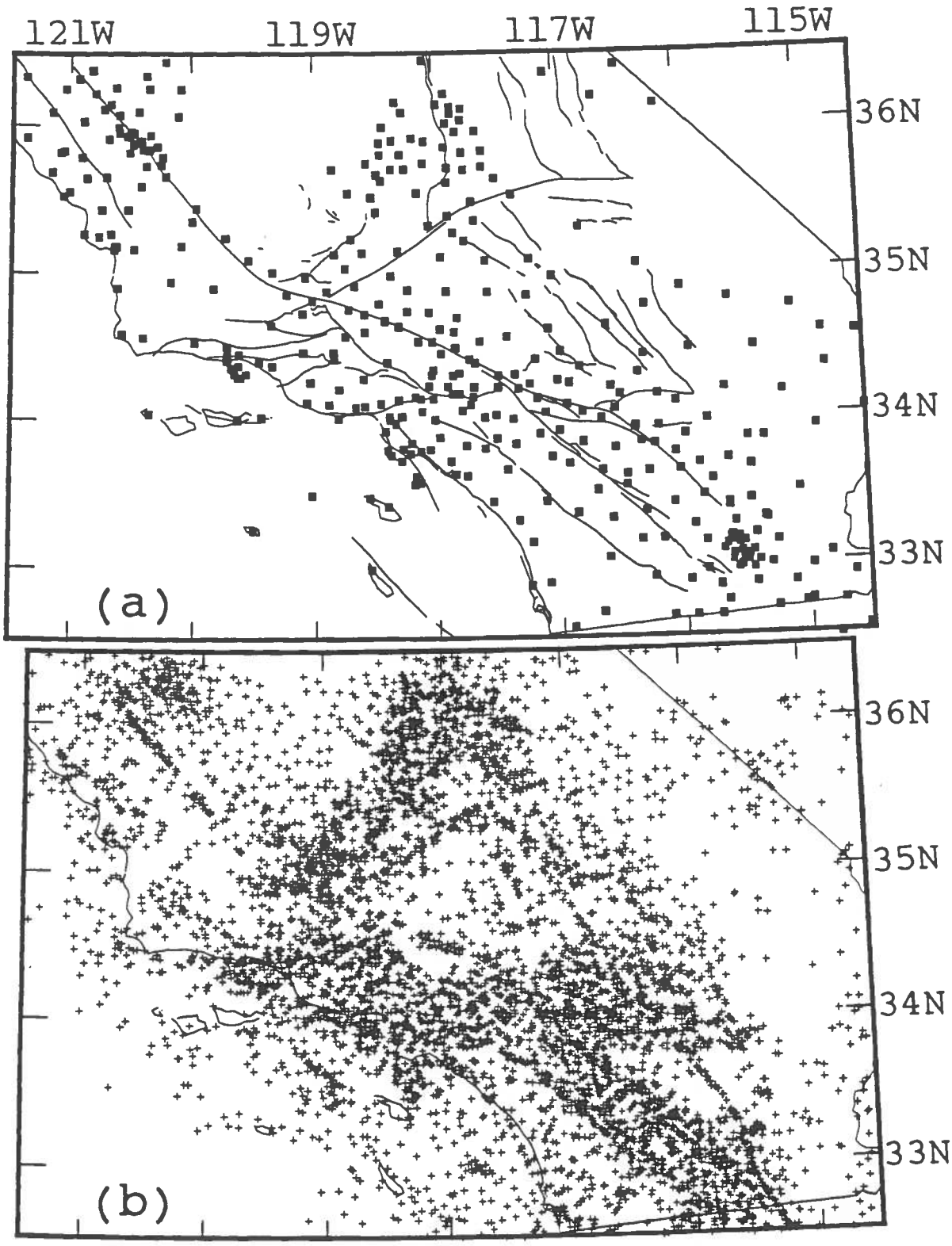

Fig.1 (a) Locations of the 293 stations of the Caltech-USGS Southern California Seismic Network as of 1992, which are used in this study.
(b) Epicentral locations of the 6,437 earthquakes used in this study.

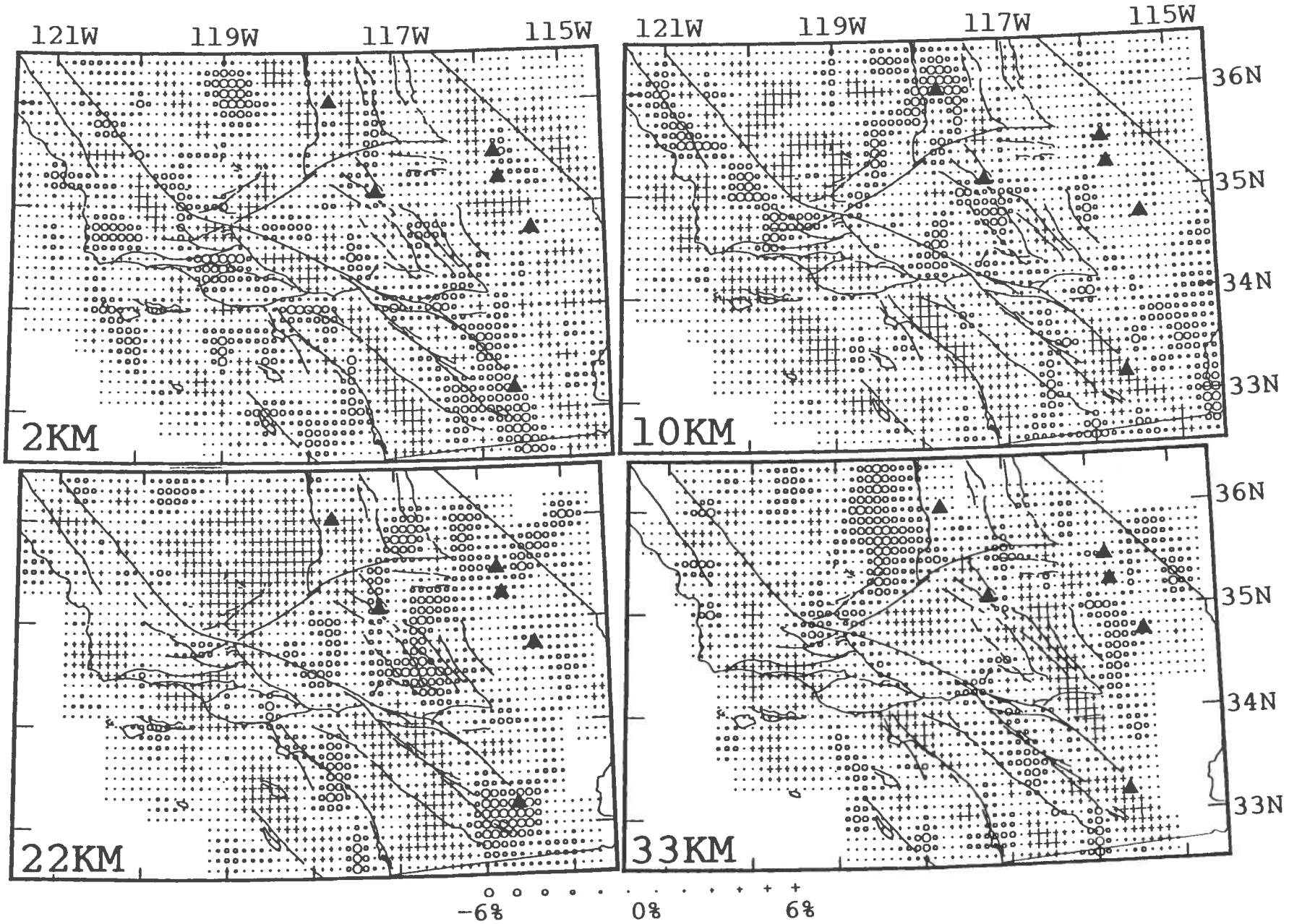

Fig.2 Fractional P-wave velocity perturbations (in %) at each grid-mesh layer. The depth of each layer is shown at the lower-left corner of the map. Cross and circle symbols denote high and low velocities, respectively. The perturbation scale is shown below the figure.

Group E: Crustal Deformation

Group Leader: Dave Jackson

* This Progress Report under Group C.

SOUTHERN CALIFORNIA EARTHQUAKE CENTER

Group E, Geodesy

Progress Report Sep 30, 1992

David D. Jackson
Department of Earth & Space Sciences
UCLA

GPS data collection: Before the Landers earthquake, our priorities were the Los Angeles Basin, the Gorman "Big Bend" area, and the intersection of the San Andreas and San Jacinto Faults. The Landers earthquake occurred within the what we consider the SAF-SJF intersection area, so our priorities became reordered somewhat. The Landers earthquake caused significant displacements throughout southern California, with cm level motions occurring at over 200 km from the event, and large time-dependent, postseismic displacements occurring at up to 50 km from the earthquake. This event will force a review of our strategy, because data before the earthquake can no longer be combined with data after the earthquake to determine velocities, unless there are enough additional data to determine the coseismic and postseismic contribution..

The Los Angeles Basin work is on schedule. UCLA, Caltech, and several county agencies cooperated to observe most of the relevant GPS monuments in the greater Los Angeles area in early 1992 before the earthquake. UCLA has resurveyed about a dozen sites since the earthquake. Caltrans, the several counties, and Los Angeles City are actively resurveying in the LA basin, and SCEC will archive and process the data. We are now beginning the Gorman "Big-Bend" project, and we will survey about 50 sites in the SAF-SJF region before 1993 begins.

The data collection effort is described more completely in the Geodesy Infrastructure report. Figure 1 shows the sites that will have been measured by GPS by the beginning of 1993.

Permanent GPS array in southern California: Through cooperation between UCSD, UCLA, Caltech, MIT, JPL, NGS, and Riverside County, we now have permanent GPS installations at Scripps, Pinon Flat, JPL, Vandenberg, and Goldstone. Palos Verdes, Gorman, Lake Mathews, and Yucaipa should be operational by the end of the year.

Interpretation: MIT, Scripps, and UCLA have been developed and improved GPS analysis and interpretation software, now used at all three places. MIT and UCLA have both produced maps of crustal deformation velocity, included in their individual reports. These maps include a substantial amount of common data, although there are different emphases and different assumptions in the processing. The maps are in good agreement, although there are some differences on the order of 5 mm/yr yet to be resolved. The new results clearly confirm the offshore displacement and convergence in the Los Angeles

Basin, Santa Barbara Channel, and Ventura basin that we tentatively reported before. Also, many intermediate sized faults can now be resolved by the data now. Richard Snay of NGS is working with us on a detailed comparison of our model predictions with the results of his model based largely on triangulation data. This comparison could reveal weaknesses in either model, and perhaps indicate evidence for changes in strain rate over the last century.

GPS, VLBI, and trilateration data have been fit to a regional dislocation model at UCLA. This approach allows geodetically observed displacements to be mapped onto geological faults, for comparison with geological data. The comparison is quite satisfactory, and there is promise that the geologic slip rate data developed by the SCEC Geology group can be integrated with these geodetic results to produce a detailed, "master model" fault slip map for use in seismic hazard calculations.

Interpretation and Modeling Theory: Hadley Johnson of UCSD has developed a constrained inversion approach to dislocation modeling. He divides a fault zone into patches, sets a limit on the allowable dislocation slip on any patch, then finds the range of total moment compatible with the data. Using GPS data for the Landers Earthquake, he determined a range of 0.8 to 1.4 x 10^{20} Nt m, consistent with the seismologically determined value.

Lin, Stein, and King, of Woods Hole, USGS Menlo Park, and Strasbourg, respectively, have investigated the relationship between stress and displacement on faults. In one study, they used a detailed computational model for the mechanics of a layered, faulted, and folded medium with realistic rheologies to compare with the results of the much simpler "retrodeformable cross-section" model. There was generally good agreement for simple models, but the more detailed calculations show that the model results are very sensitive to assumptions about rheology and separation of slip surfaces. In another study they computed stress increments on nearby faults caused by several blind thrusting earthquakes in California. Shallow faulting tends to favor secondary faulting, while deeper faulting favors upward propagation of the initial fault..

Figure caption: Sites for which SCEC will have archived high quality GPS data by the beginning of 1993.

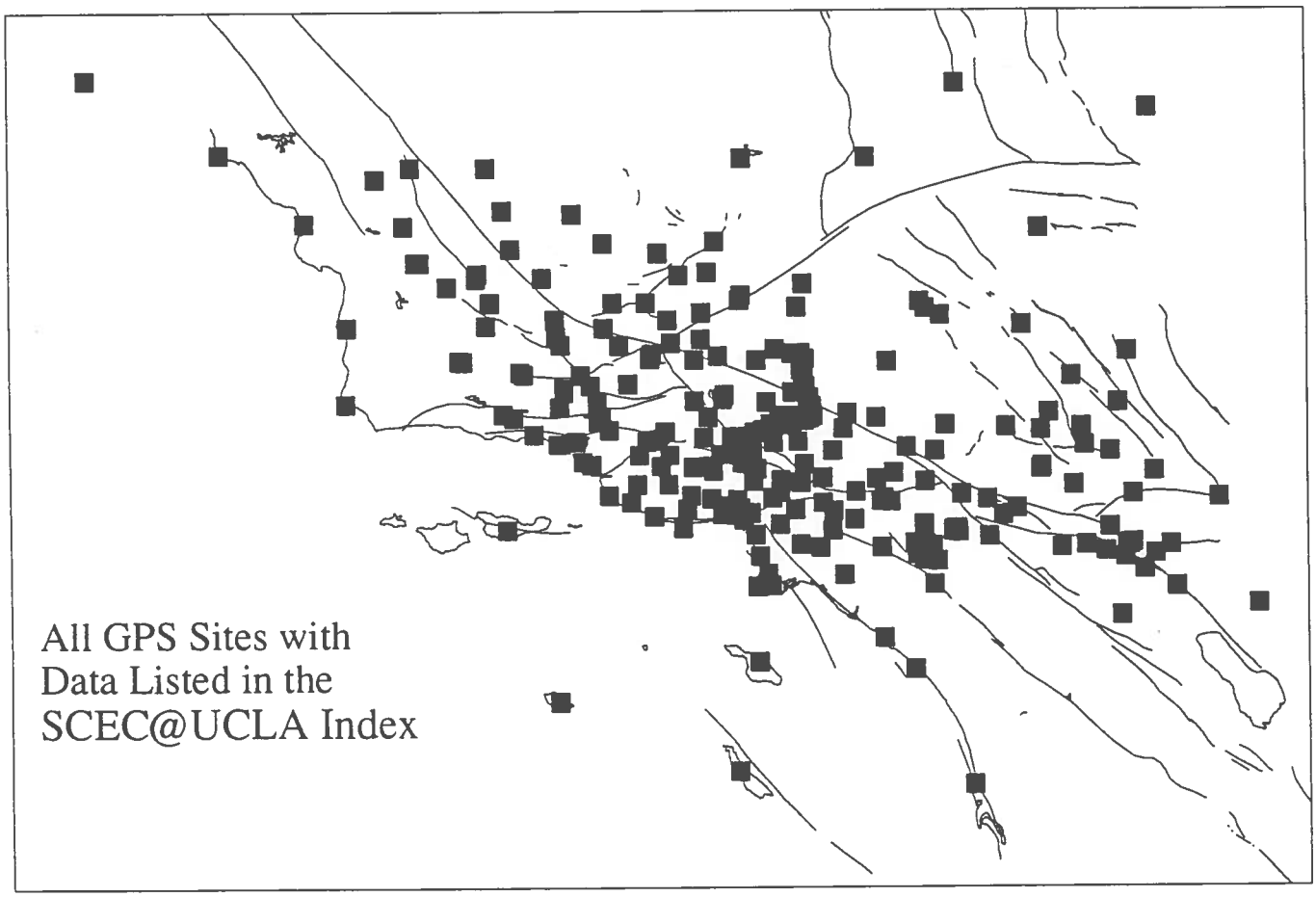
All GPS Sites with
Data Listed in the
SCEC@UCLA Index

PROJECT REPORT: **Inversion Methods for Spatially Variable Fault Slip**
PROJECT PERIOD: February 1, 1992 — January 31, 1993
SUBMISSION DATE: September 24, 1992

PRINCIPAL INVESTIGATOR: Duncan Carr Agnew, Professor, Geophysics - (619) 534-2590
ASSOCIATE INVESTIGATOR: Hadley Johnson, Graduate Student - (619) 534-2019
Institute of Geophysics and Planetary Physics
Scripps Institution of Oceanography, MC 0225
University of California, San Diego
La Jolla CA 92093-0225

We have been investigating how, in collecting geodetic data, we can best learn about fault behavior. Geodetic measurements made before and after a large earthquake can be used to estimate subsurface slip if one assumes a model of how the earth responds to slip on a buried fault plane. We have developed a technique based on this principle, but whose final product is an estimate of the size, or moment, of the earthquake, instead of an estimate of the slip distribution. We have used this new technique to estimate the geodetic moment release of the Landers earthquake.

To begin with, we divide the fault plane into small (1×1 km) patches from the surface to a depth of 15 km and follow the length of the surface rupture (83 km long). Using elastic dislocation theory, we compute the Green's function for uniform slip on each of these patches. If $\hat{s}$ is the vector of slip on the patches, and d is the vector of measured displacements at a set of geodetic stations, the Green's function is the matrix A which gives $d = A\hat{s} + \varepsilon$, where ε is the discrepancy between the measured displacements and those predicted from the slip model.

Our problem is then to invert for the slip model $\hat{s}$ which minimizes the misfit between the measured displacements d and the predicted displacements $\hat{d}$, given the additional constraints that all elements of $\hat{s}$ be positive (right-lateral slip only), and that the sum of the individual elements of $\hat{s}$ (related to the moment release of the earthquake) be constrained to some pre-set level. We use a non-negative least squares technique to solve for this best-fitting slip model. By varying the constraint on moment we can map the limits over which the problem has a statistically acceptable solution based on the error estimates in the measured data. When the moment constraint is too small, the inversion routine cannot place enough slip on the fault patches to adequately reproduce the measured data, while when the moment constraint is too large, the routine is unable to "hide" the excess slip without misfitting the data.

We obtained GPS-measured displacements for the Landers earthquake from the United States Geological Survey in Menlo Park and the Southern California Earthquake Center in Los Angeles, at 11 points around the fault. The accompanying plot shows the results of the inversions with this data. Each of the curves represents the minimum misfit slip model as a function of the moment constraint for different upper bounds on the individual elements of the slip model (i.e. the elements of the slip model are constrained to lie between zero and this upper limit). As this upper bound is reduced from 1,000 meters to 10 meters, and finally to 5 meters, we see that the resulting 90% confidence limits on the moment release converge until eventually the curve for a 5 meter upper bound never dips below the 90% level. Depending on which upper bound we accept (based on our geological prejudices) we end up with a different bound on the moment. Certainly the 1,000 meter limit is absurdly conservative and the 5 meter limit too small (especially since 6+ meter surface offsets have been measured in several places along the rupture zone). If we take the 10 meter upper bound as a reasonable compromise the resulting 90% bound on the geodetic moment is about 0.8×10^{20} to 1.4×10^{20} N-m.

We believe this technique for using geodetic measurements to place quantifiable constraints on the moment release of an earthquake is a valuable addition to the many seismic techniques. As more data are processed and included in this inversion scheme we expect to be able to place significantly tighter bounds on the moment release of the Landers earthquake.

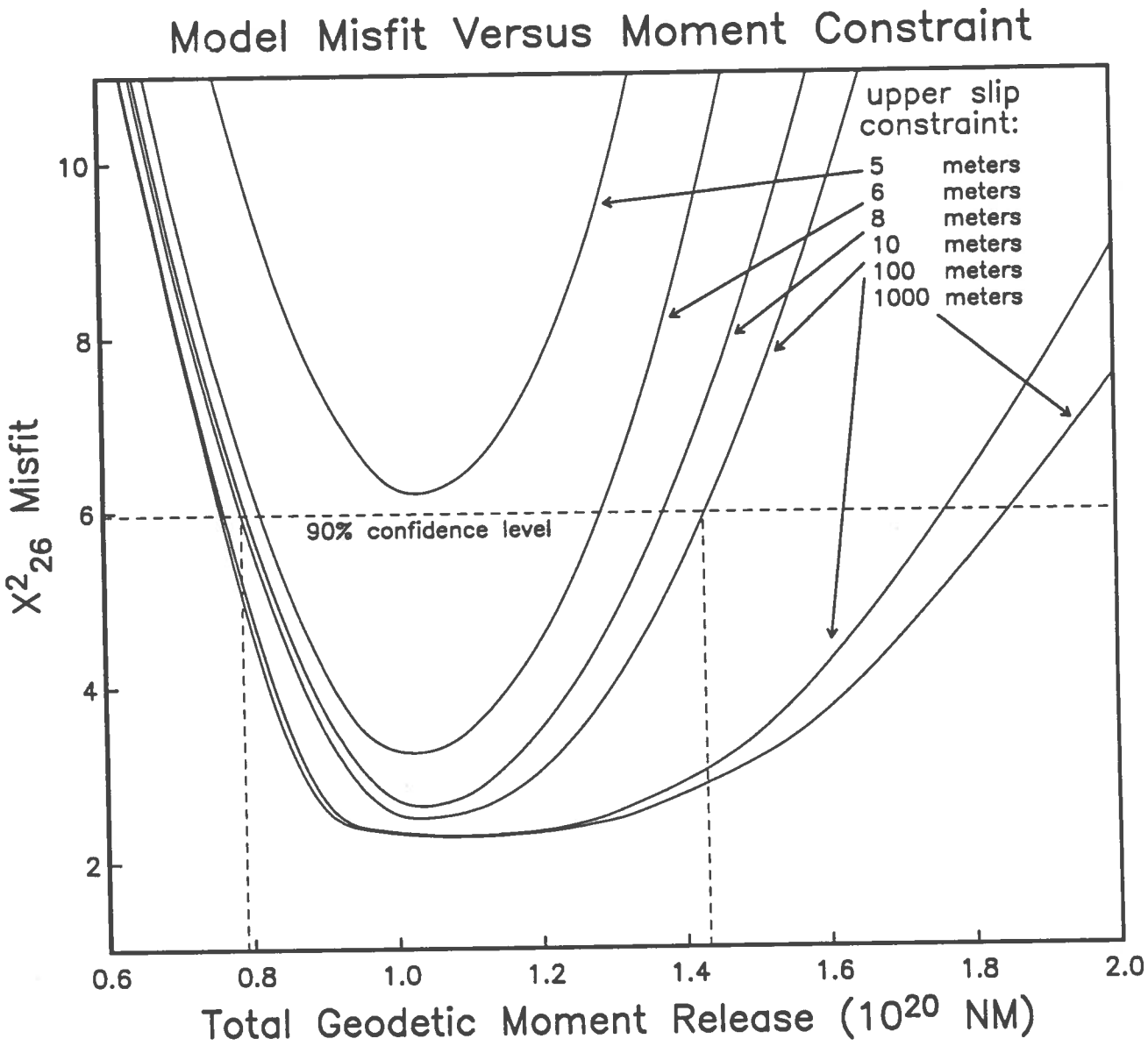

Fig 1. Non-negative least squares model-misfit as a function of the geodetic moment release for the Landers earthquake. Each curve presents the results for a different upper bound placed on the individual elements of the best-fitting slip model. The horizontal dashed line represents the 90% confidence level for a χ^2 function with 26 degrees of freedom (there are 26 GPS-measured offsets in the inversion). If we take the 90% limits for an upper bound slip limit of 10 meters, the resulting bound on the moment release for the earthquake is 0.8×10^{20} to 1.4×10^{20} N-m.

Progress Report to SCEC

Velocity Field in Southern California from GPS, VLBI, and Conventional Geodetic Data

B. H. Hager, PI; T. A. Herring and R. E. Reilinger, co-I's
Massachusetts Institute of Technology, Cambridge, MA 02139
September 17, 1992

We proposed two projects directly related to SCEC goals: 1) to produce a map of the velocity field in southern California using all available GPS, VLBI, and conventional data in the region, and 2) to interpret this velocity field using both "traditional" dislocation models of creep at depth on faults and more "realistic" models that include viscous relaxation in the intracrustal asthenosphere. Most of our effort to date has been directed at task 1).

The velocity field from space geodesy is estimated using Herring's Globk software, which uses a Kalman filter to combine station-position covariance matrices and estimates to form a single rigorous solution for positions and velocities. The covariance matrices are included in "H-file" format, a format which is now standard output from the GAMIT GPS processing package. Figure 1 shows our latest estimate of the velocity field in southern California from combined GPS and VLBI measurements. (The VLBI data were collected by NASA and NGS during the time span of the Crustal Dynamics Project. Most of the GPS data were collected by Caltech, MIT, UCLA and UCSD investigators under NSF, NASA, AFOSR, and USGS sponsorship. These data include observations from field campaigns between 1986 and 1991, as well as more recent PGGA data.) Of note are the rapid convergence across the LA and Ventura basins, as well as the significant deformation between the mainland and the Channel Islands. For the LA basin, the combination of VLBI and GPS solutions decreases the uncertainty in the velocity between JPL1 and PVER by more than a factor of two.

In collaboration with UCSD, we have made revisions to the GAMIT software, with a new release in beta test, and general release, including to SCEC, due within a month. Once SCEC runs their GPS data through this software update, we will be able to add the SCEC GPS data to our global analysis, greatly increasing the spatial coverage of our velocity map and reducing the errors on important baselines such as that across the LA basin.

Danan Dong, the student supported by this grant, has improved his FONDA software for combining conventional and space geodetic survey data. FONDA now provides H-file output for conventional data, allowing conventional, as well as space-geodetic data to be analyzed using Globk. The software has been extensively tested using synthetic data. We are in the process of collecting trilateration and triangulation data for California.

Finally, we have collaborated with a number of others at Scripps and Livermore in the analysis of the coseismic displacement at PGGA sites caused by the Landers earthquake sequence. A manuscript entitled "Detection of Coseismic Deformation in Southern California using Continuous Global Positioning System Measurements" has been submitted to *Nature*. Figure 2, from that paper, shows the observed displacements at the PGGA sites. These displacements are consistent with a moment of 0.9×10^{20} N-m, $\pm$ 10%.

Fig. 1: Combined GPS and VLBI velocities

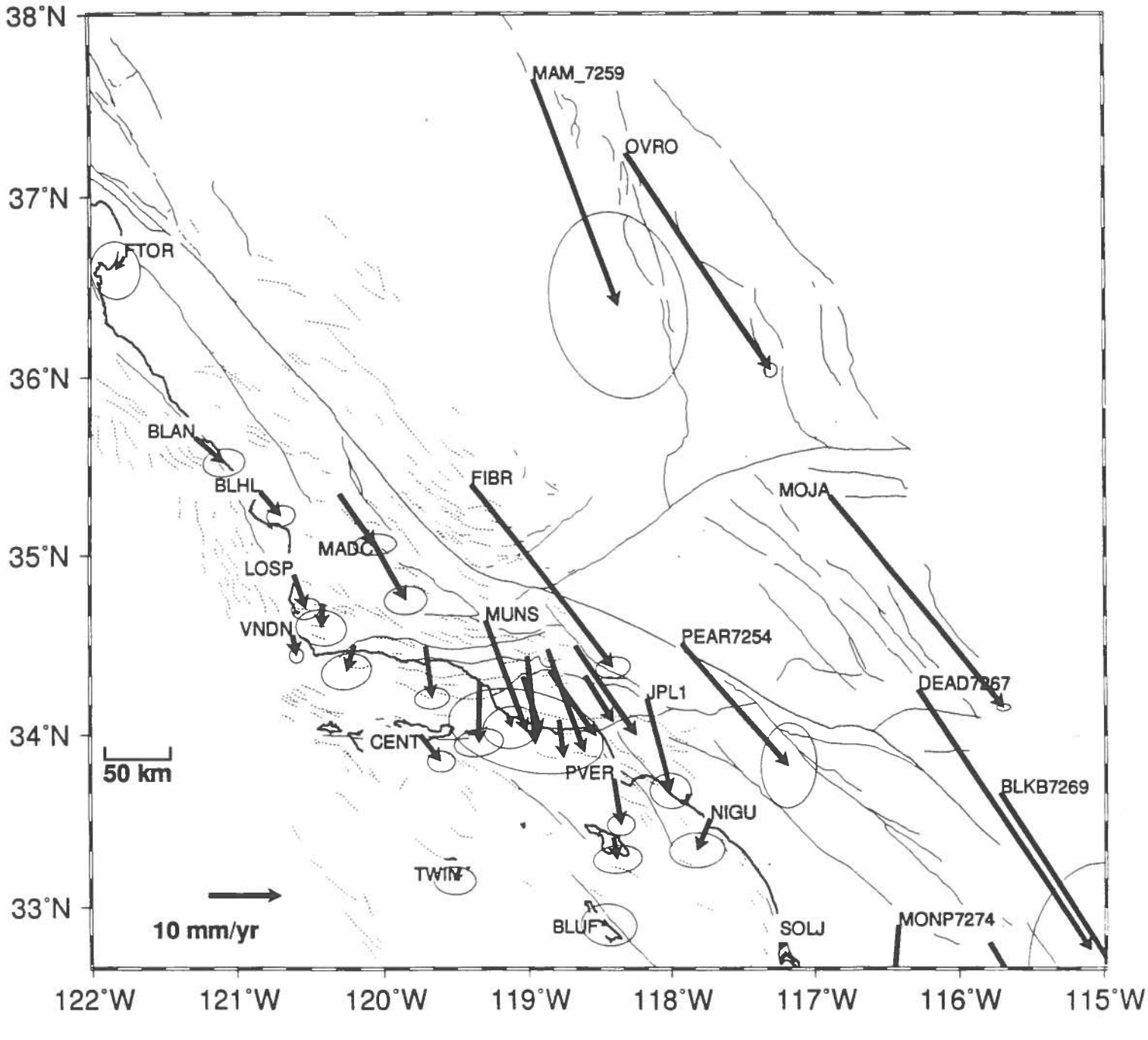

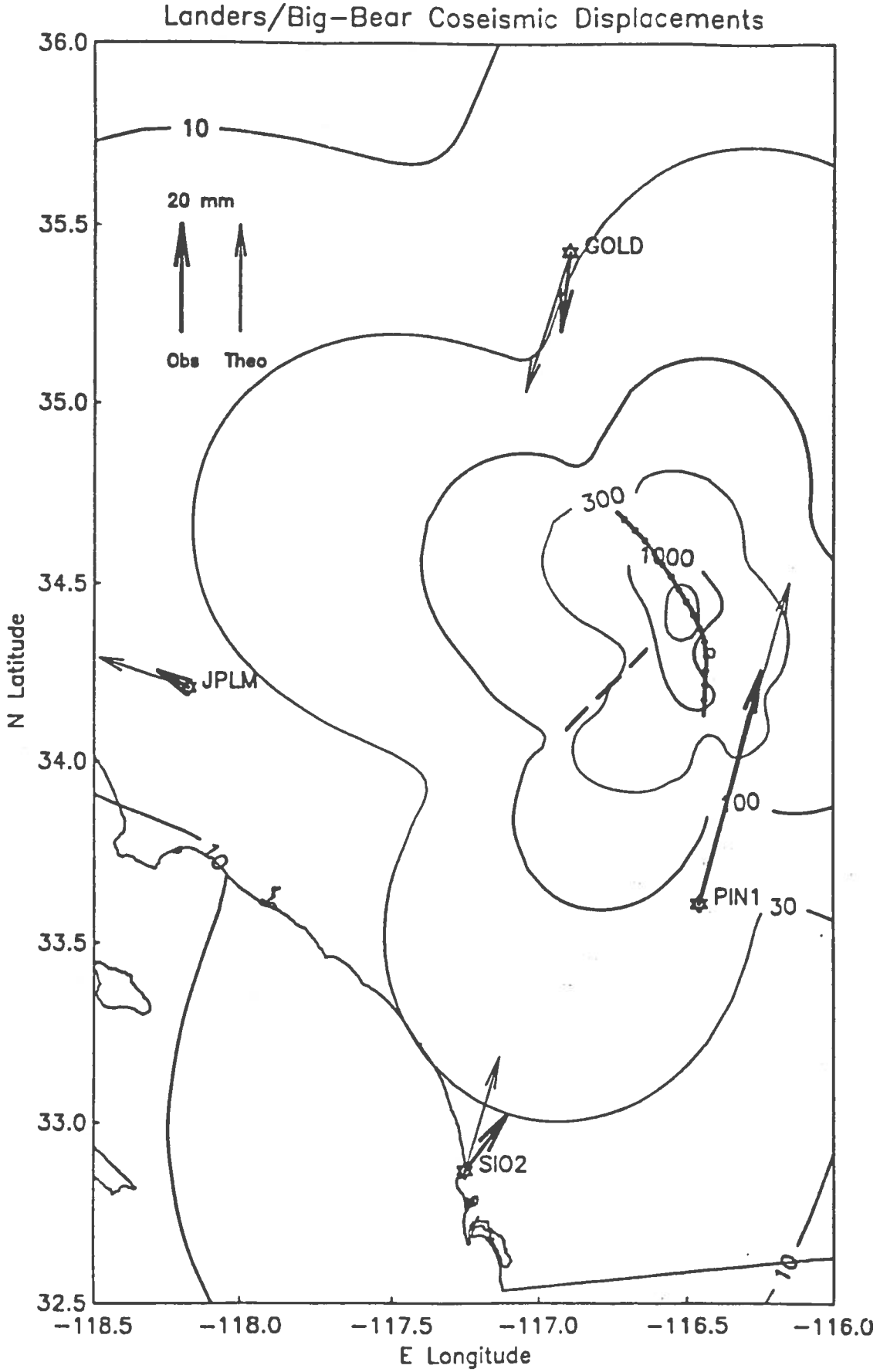
Landers/Big–Bear Coseismic Displacements
20 mm
Obs
Theo
GOLD
JPLM
PIN1
SIO2
10
300
1000
100
30
36.0
35.5
35.0
34.5
34.0
33.5
33.0
32.5
N Latitude
−118.5
−118.0
−117.5
−117.0
−116.5
−116.0
E Longitude

Figure 2.

Southern California Earthquake Center

Geodetic Modeling

Progress Report Sep 30, 1992

David D. Jackson
Department of Earth & Space Sciences
UCLA

Velocity Map: We have combined processed GPS data with VLBI data for sites in southern California to estimate the horizontal velocity of about 50 survey markers in southern California. We cooperated extensively with MIT, sharing data files and results. Figure 1 shows the result of calculations to date, expressed as velocities relative to Palos Verdes. All of the observations used were made before the Landers earthquake. We find about 45 mm/yr relative velocity across the entire study area (San Nicolas Island relative to Mojave), in good agreement with the NUVEL-1 plate estimate of 48 mm/yr. Of this displacement, 7 mm/yr occurs offshore southwest of Palos Verdes, and 11 mm/yr occurs within the Mojave desert, more than25 km northeast of the San Andreas fault. We find compression of 8 mm/yr within the Los Angeles Basin (between Palos Verdes and JPL) 5 mm/yr compression across the Santa Barbara Channel, and approximately 10 mm/yr compression across the Ventura basin.

We have used these data, along with USGS trilateration data and selected triangulation data to construct a dislocation model for southern California.We estimate horizontal translation velocity and rotation rate for about 20 crustal blocks, and slip rate for about 200 fault segments. The model is in good agreement with geological estimates for foult slip rates. We are working with Richard Snay of NGS to make a detailed comparison between our model and that developed by Snay from a mix of data including older triangulation data. There are some substantial differences between the two models, which might reflect temporal differences in strain rate.

Landers post-seismic deformation: Following the Landers earthquake, we put most of our effort into monitoring coseismic and post-seismic displacements from this event. The post-seismic displacements are especially interesting, as they are larger than seen in other recent earthquakes. Figure 2 shows a map of observed sites, and Figure 3 shows baseline measurements between a few of the sites. Estimated velocities exceed 1 mm/day at stations 7000, 7001, PAXU, and CABA, relative to PIN1 at Pinon Flat Observatory.

Figures: (1) Velocity map; small box marks the site location, ellipse is approximate 2σ region based on formal errors. (2) Map of sites near Landers earthquake, showing estimated postseismic velocity during month of July 1992. (3) Some baseline data for a few sites near the Landers earthquake.

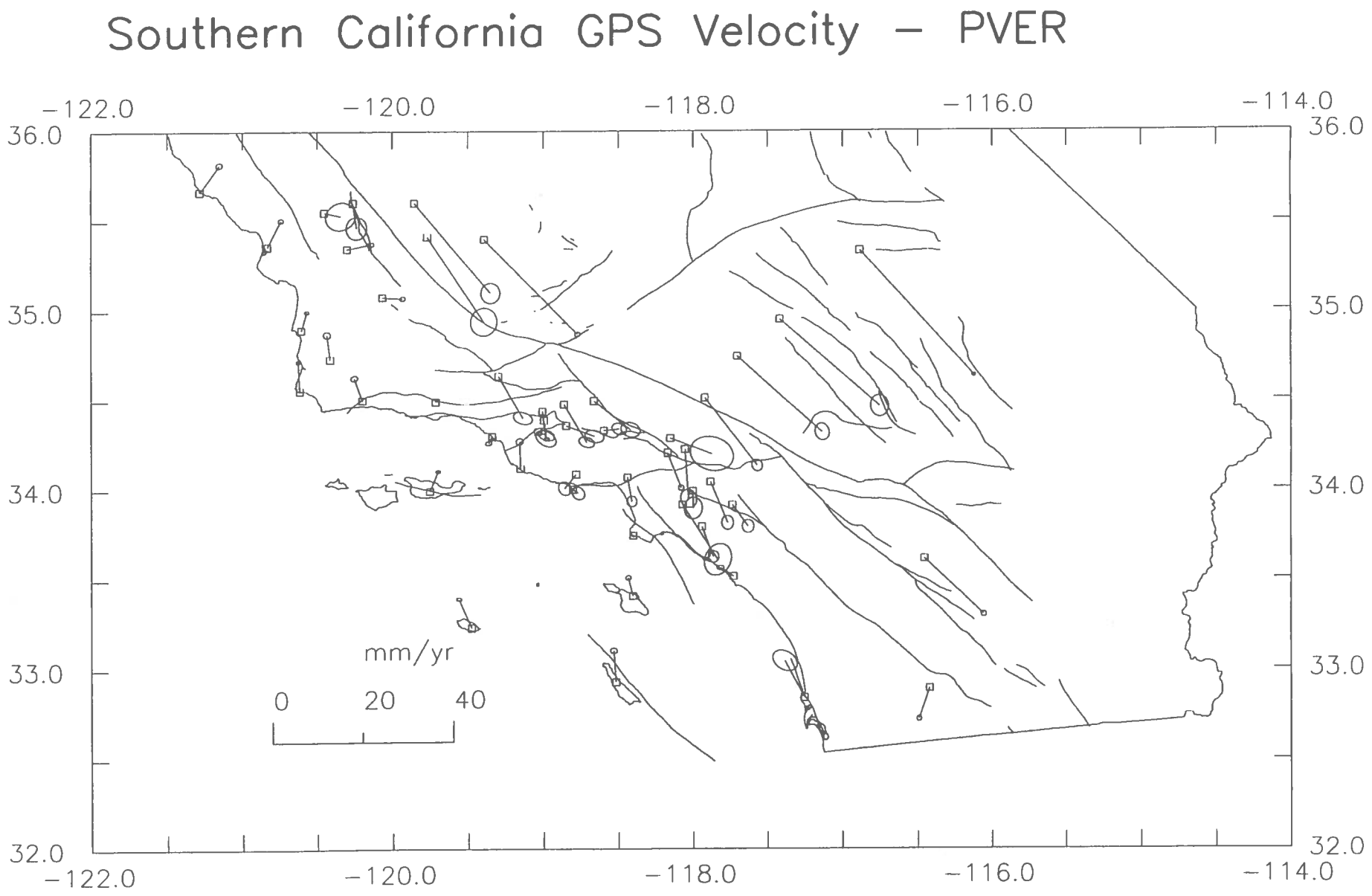
Southern California GPS Velocity – PVER
−122.0
−120.0
−118.0
−116.0
−114.0
36.0
35.0
34.0
33.0
32.0
mm/yr
0
20
40

Figure 1 E11

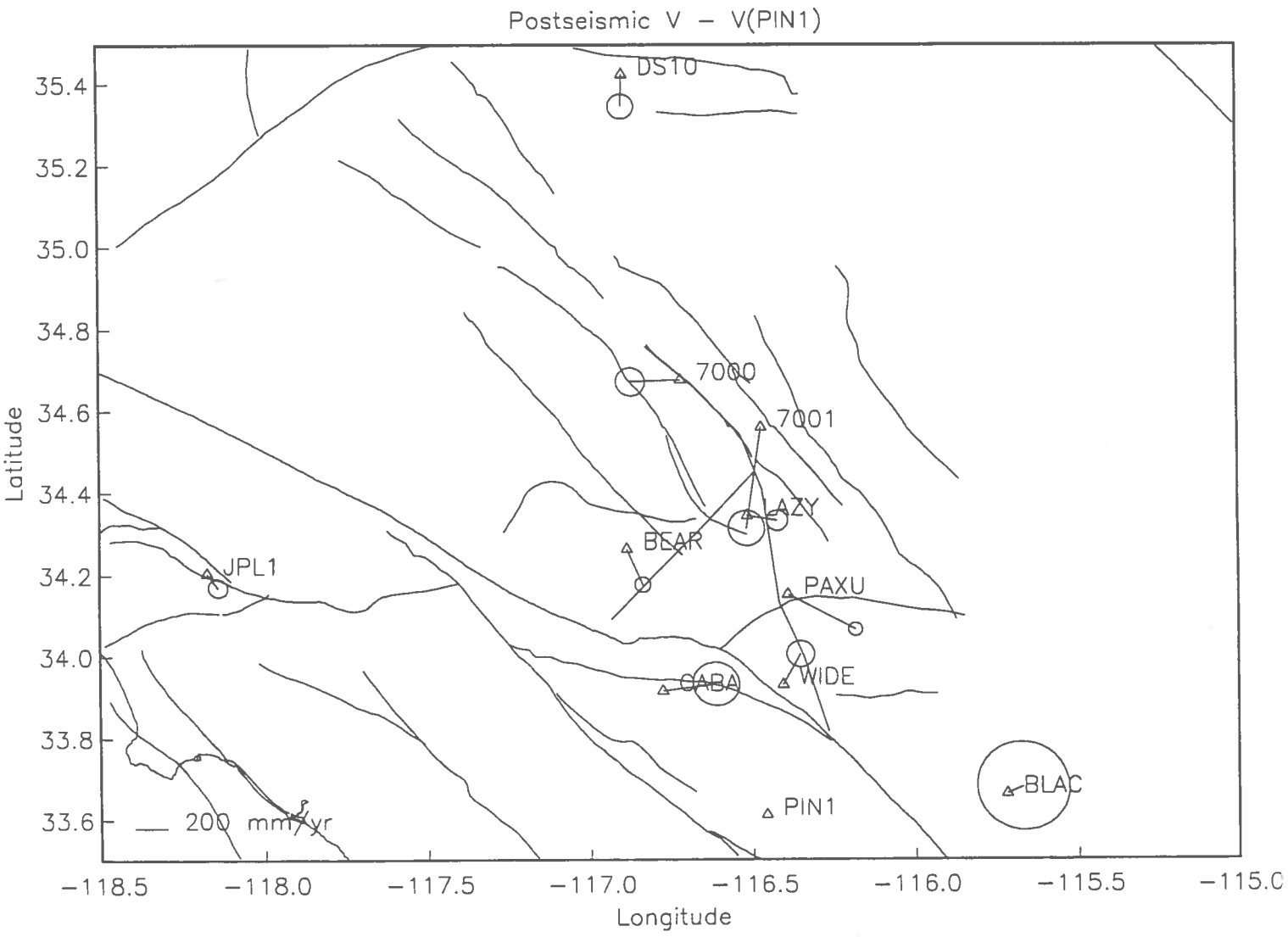
Postseismic V – V(PIN1)
DS10
7000
7001
LAZY
BEAR
JPL1
PAXU
WIDE
CABA
BLAC
PIN1
200 mm/yr
35.4
35.2
35.0
34.8
34.6
34.4
34.2
34.0
33.8
33.6
Latitude
−118.5
−118.0
−117.5
−117.0
−116.5
−116.0
−115.5
−115.0
Longitude

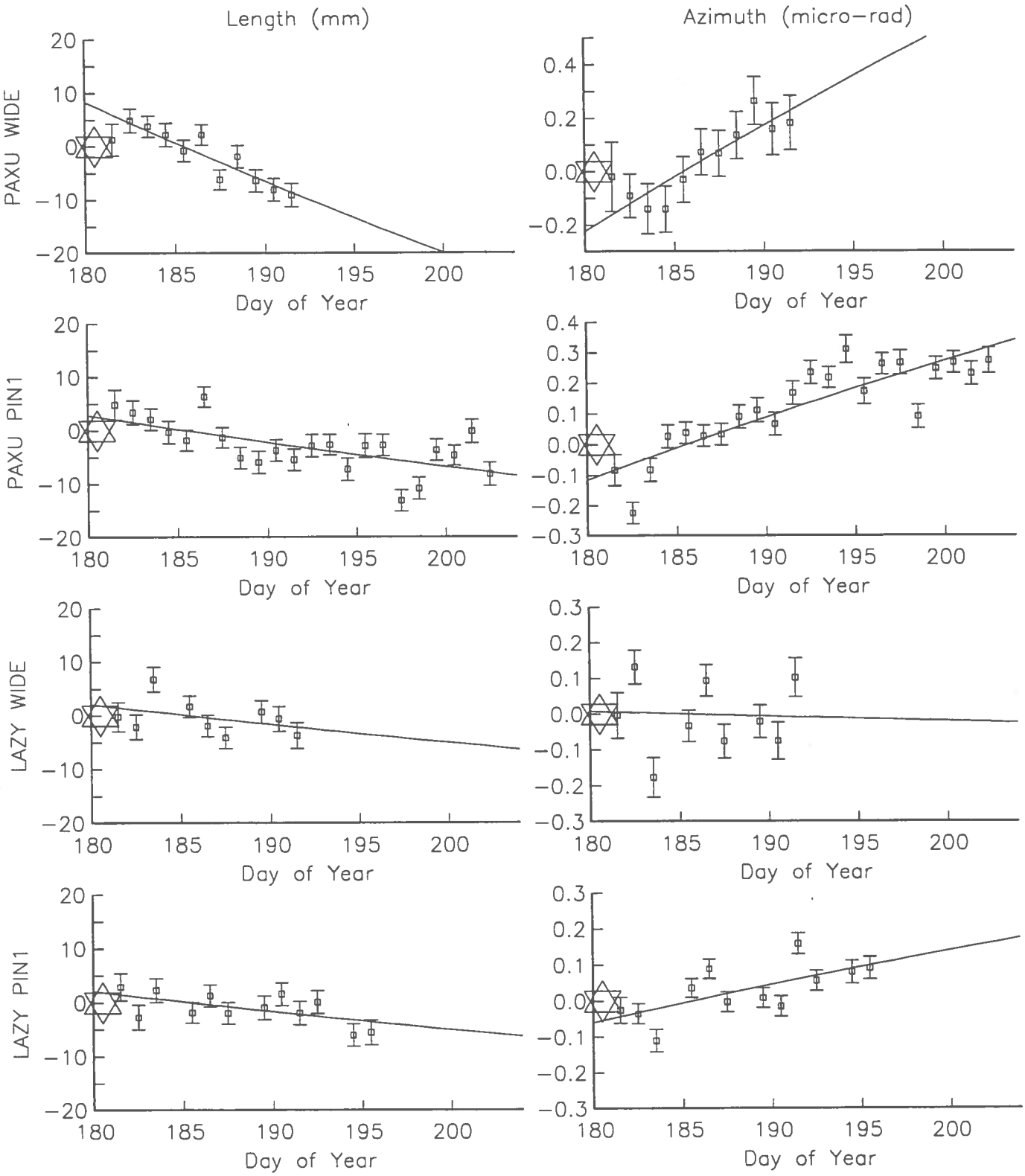
Length (mm)
Azimuth (micro-rad)
PAXU WIDE
PAXU PIN1
LAZY WIDE
LAZY PIN1
Day of Year
180
185
190
195
200

Extremal Bounds on Earthquake Moment from Geodetic Data: Application to the Landers Earthquake

Hadley O. Johnson

Institute of Geophysics and Planetary Physics, Scripps Institution of Oceanography, University of California, San Diego

Geodetic measurements made before and after a large earthquake can be used to estimate subsurface slip if one assumes a model of how the earth responds to slip on a buried fault plane. We have developed a technique based on this principle, but whose final product is an estimate of the size, or moment, of the earthquake, instead of an estimate of the slip distribution. We have used this new technique to estimate the geodetic moment release of the Landers earthquake.

To begin with, we divide the fault plane into small (1x1 km) patches from the surface to a depth of 15 km and follow the length of the surface rupture (83 km long). Using elastic dislocation theory, we compute the Green's function for uniform slip on each of these patches. If $\S$ is the vector of slip on the patches, and d is the vector of measurement displacements at a set of geodetic stations, the Green's function is the matrix A which gives $d = A\S + \varepsilon$, where ε is the discrepancy between the measured displacements and those predicted from the slip model.

Our problem is then to invert for the slip model $\S$ which minimizes the misfit between the measured displacements d and the predicted displacements $\hat{d}$, given the additional constraints that all elements of $\S$ be positive (right-lateral slip only), and that the sum of the individual elements of $\S$ (related to the moment release of the earthquake) be constrained to some pre-set level. We use a non-negative least squares technique to solve for this best-fitting slip model. By varying the constraint on moment we can map the limits over which the problem has a statistically acceptable solution based on the error estimates in the measured data. When the moment constraint is too small, the inversion routine cannot place enough slip on the fault patches to adequately reproduce the measured data, while when the moment constraint is too large, the routine is unable to "hide" the excess slip without misfitting the data.

We obtained GPS-measured displacements for the Landers earthquake from the United Stated Geological Survey in Menlo Park and the Southern California Earthquake Center in Los Angeles, at 11 points around the fault. The accompanying plot shows the results of the inversions with this data. Each of the curves represents the minimum misfit slip model as a function of the moment constraint for different upper bounds on the individual elements of the slip model (i.e. the elements of the slip model are constrained to lie between zero and this upper limit). As this upper bound is reduced from 1,000 meters to 10 meters, and finally to 5 meters, we see that the resulting 90% confidence limits on the moment release converge until eventually the curve for a 5 meter upper bound never dips below the 90% level. Depending on which upper bound we accept based on our geological prejudices) we end up with a different bound on the moment. Certainly the 1,000 meter limit is extremely conservative and the 5 meter limit too small (especially since 6+ meter surface offsets have been measured in several places along the rupture zone). If we take the 10 meter upper bound as a reasonable compromise the resulting 90% bound on the geodetic moment is about 0.8×10^{20} to 1.4×10^{20} NM.

We believe this technique for using geodetic measurements to place quantifiable constraints on the moment release of an earthquake is a valuable addition to the many

seismic techniques. As more data are processed and included in this inversion scheme we expect to be able to place significantly tighter bounds on the moment release of the Landers earthquake.

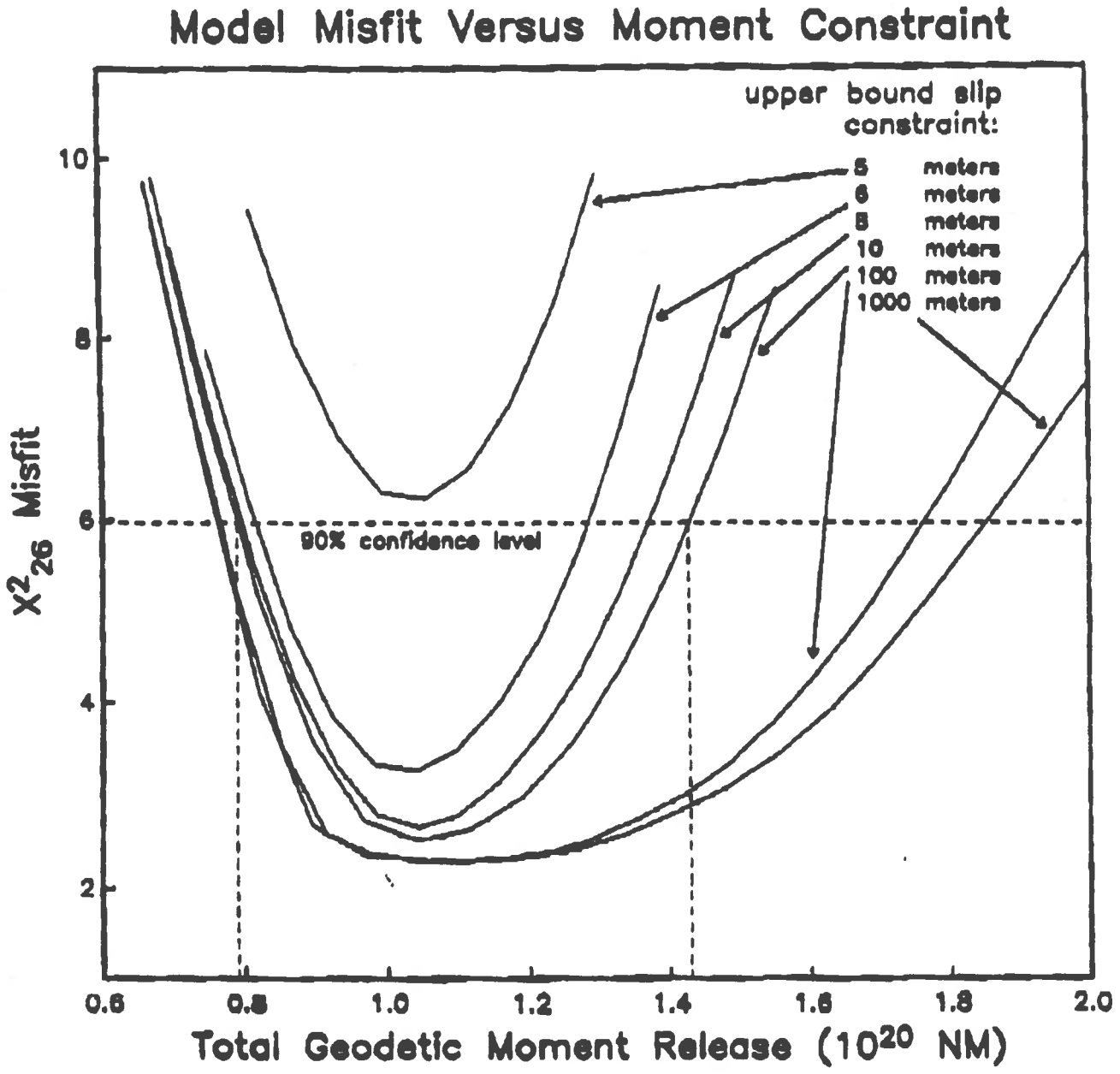

Fig. 1. Non-negative least squares model-misfit as a function of the geodetic moment release for the Landers earthquake. Each curve presents the results for a different upper bound placed on the individual elements of the best-fitting slip model. The horizontal dashed line represents the 90% confidence level for a χ^2 function with 26 degrees of freedom (there are 26 GPS-measured offsets in the inversion). If we take the 90% limits for an upper bound slip llimit of 10 meters, the resulting bound on the moment release for the earthquake is 0.8×10^{20} to 1.4×10^{20} NM.

Accuracy of the TDP-H91-CA Model for Predicting Horizontal Crustal Velocities in California

Richard A. Snay
National Geodetic Survey
Coast and Geodetic Survey
National Ocean Service, NOAA
Rockville, Maryland 20852

In 1991 the National Geodetic Survey adopted the TDP-H91-CA model for predicting how horizontal positional coordinates change as a function of time in California. This model had been derived from geodetic data spanning over a century. Secular velocities predicted by the model have been compared with independently derived velocities to assess the model's accuracy. A comparison with velocities derived from electronic distance measurements (EDM) collected under the auspices of USGS's Crustal Strain Project indicates that discrepancy vectors for the relative velocity between any two USGS sites less than 50 km apart have an rms magnitude of 2.2 mm/yr. A comparison with velocities derived from VLBI measurements collected under NASA's Crustal Dynamics Project reveals that the discrepancy vectors at 19 sites have an rms magnitude of 4.1 mm/yr. Here velocities are expressed relative to a fixed North American plate. The largest of these discrepancy vectors occurs at Mammoth Lakes (magnitude = 12.9 mm/yr). A comparison with velocities derived by the Southern California Earthquake Center using GPS data from various sources reveals that the discrepancy vectors at 32 sites have an rms magnitude of 9.6 mm/yr. Here velocities are expressed relative to the VLBI site known as MOJAVE (35.3°N, 116.9°W). The three largest of these discrepancy vectors occur in the Channel Islands (magnitudes = 18.8, 16.2, and 16.1 mm/yr). Whereas the aforementioned EDM and VLBI data had been used to produce the model, the GPS data were not. Hence the GPS velocities provide the most discriminating indicator of accuracy among these three sets of test velocities. Formal standard errors for the magnitudes of these GPS velocities are mostly less than 2 mm/yr.

Working Group E - Geodesy

Los Angeles Region GPS Studies: Inter-County '92 Support

Principal Investigators: Kerry E. Sieh and Kenneth W. Hudnut[1]
Institution: Seismological Laboratory, Caltech
[1]now at U.S.G.S., Pasadena Office

SCEC partially supported the Inter-County 1992 GPS survey planning, operation, and field logistics and expenses. This survey accomplished the repeated measurement of 70 GPS stations across southern California that were surveyed in February and March of 1991, and the addition of 3 new stations (2 of which are at potential continuous-tracking sites). Twenty of the Inter-County stations that surround the Los Angeles Basin were also surveyed by GPS initially in March 1990 by Caltech, assisted by the City and County of Los Angeles.

The map below shows stations that were surveyed by Caltech in the 1991 & 1992 GPS surveys - the 1992 work was accomplished with partial support from SCEC. The network forms an important part of the network that the SCEC Geodesy Group monitors to determine velocity-field maps. Data from the 1992 survey, as well as from Caltech's 1990 and 1991 surveys, are important for SCEC's efforts to produce detailed velocity maps.

1991 & 1992 Inter-County GPS Surveys

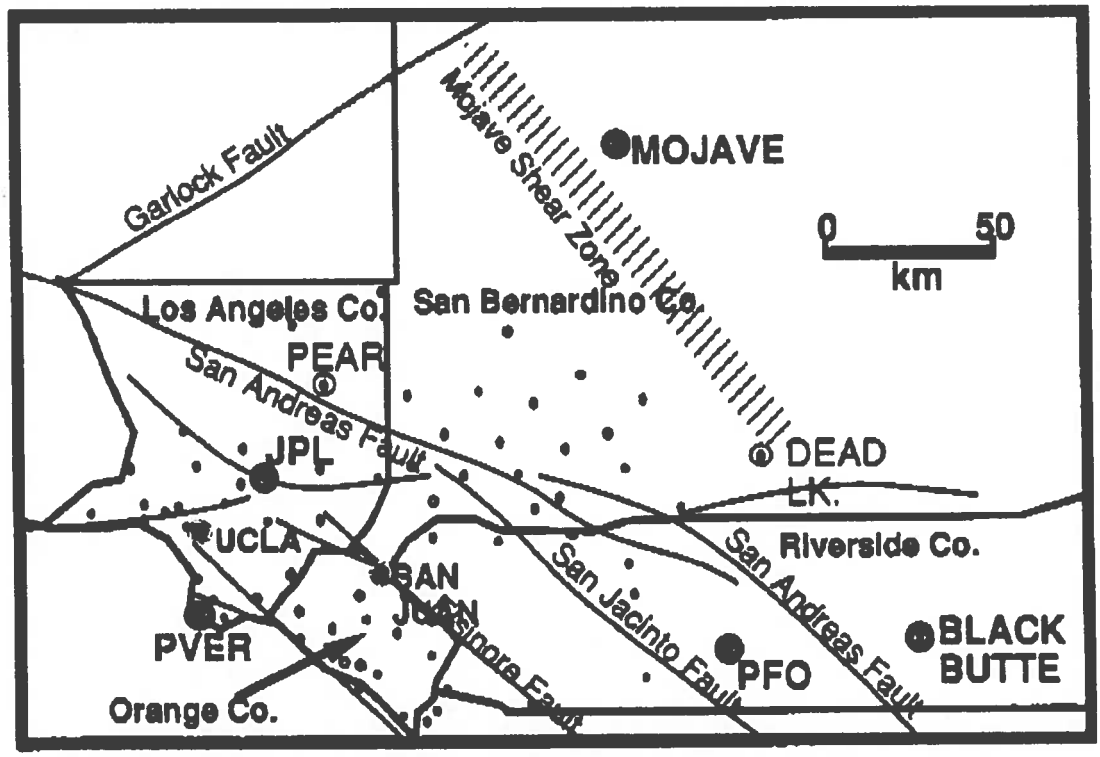

In light of the increased M>4.5 seismicity in the region, the resurvey in 1992 was particularly important. In retrospect, it also provided us with an unprecedented set of high-accuracy, regional GPS data shortly prior to the Joshua Tree - Landers - Big Bear earthquake sequence. As has been already seen, the nearfield coseismic GPS data are fit well by elastic dislocation models that are based on the seismological and geological

source information. However, more distant stations have observed displacements up to a factor of ~2 less than the elastic model predicts (e.g., Bock *et al.*, manuscript submitted). A layered crustal model was proposed by Bock *et al.* to account for these observations, and there is potential to attempt still other models to determine how this interesting phenomenon may be explained. We are trying to acheive a complete resurvey of the Inter-County network in early 1993 in order to determine the regional extent of this pattern and use this in modeling crustal structure, as well for better determining the source of the Landers sequence.

The Inter-County survey was performed from April 13 through April 24, 1992. A total of 27 field receivers were operated for nine days over a two-week interval to complete the survey. The attached tabulation of the final observation schedule provides details of the survey and monuments used. We had good weather and few logistical problems in this years' survey, in contrast with the 1991 Inter-County survey, during which inclement weather caused major problems on 3 days of that survey. The only minor failure to obtain data was due to an equipment problem on one field unit, that was corrected after 3 days. During the survey, the tracking stations in the California PGGA operated well, as did the global fiducial tracking network. The 1992 Inter-County survey benefited greatly from having a much better global and regional tracking than had the 1990 Los Angeles GPS survey or the 1991 Inter-County survey.

By July 1992, we had completed the transfer of all data collected in the field to the SCEC GPS facility at UCLA for analysis and archiving. At the present time, most of the data have already been converted to the RINEX ascii format. Once this task is completed, processing will be carried out by Caltech and UCLA-SCEC using the GAMIT software.

Matching support for field work was made available from the County and City agencies totalling approximately $120,000 for the 1992 Inter-County survey. Other NEHRP support for the 1992 Inter-County survey was from the USGS external grants program, for a Caltech grant entitled "Earthquake Geodesy in Southern California." Because of the matching support from the County and City agencies, this Inter-County 1992 data set was obtained for a relatively low price per station-day of data. For the survey, a total of 240 receiver station-days (6 hours each) of data were collected at a rate per station-day of $166.67 in SCEC-paid dollars. In contrast, the SCEC Geodesy Group negotiated a subcontract/cooperative survey agreement with the National Geodetic Survey at a cost to SCEC of $500.00 per station-day of data. So, the Inter-County 1992 data are three times less expensive to the SCEC than the data from the subcontract with NGS for the Gorman network. That NGS subcontract does, however, include some work items that were not supported by the Inter-County SCEC grant, so this large discrepancy in rate is not an entirely fair comparison. For instance, that subcontract with NGS does involve setting a few more new monuments, and field data processing and archiving through the NGS 'bluebooking' procedure will be performed.

Inter-County GPS Survey: April 13 - 24, 1992

Observation Schedule

Julian Day: in UTC	104 (4/13)	105 (4/14)	106 (4/15)	107 (4/16)	108 (4/17)	••	111 (4/20)	112 (4/21)	113 (4/22)	114 (4/23)
Start Time:										
UTC	18:50	18:50	18:50	18:50	18:50		18:50	18:50	18:50	18:50
Local	*11:50 am*	*11:50*	*11:50*	*11:50*	*11:50*		*11:50*	*11:50*	*11:50*	*11:50*
End Time:										
Local	*5:50 pm*	*5:50*	*5:50*	*5:50*	*5:50*		*5:50*	*5:50*	*5:50*	*5:50*

All sessions planned at 6 hours long (6:00)

Party	SITE - NAMES Station I.D. #									Unit #	Type	Operator
1) SCEC 1	BE 102 0102	ECHO echo	USC usc1	BE 102 0102	ECHO echo	USC usc1	ECHO 0102	BE 102 echo	USC usc1	SIO 1	Trimble	
2) SCEC 2	PV Aries 1000	PV Aries 1000	PV Aries 1000	PV Aries 1000	PV Aries 1000	PV Aries 1000	PV Aries 1000	PV Aries 1000	PV Aries 1000	SIO 2	Trimble	Auto
3) SCEC 3	PEAR 5001	PEAR 5001	PEAR 5001	PEAR 5001	PEAR 5001	PEAR 5001	PEAR 5001	PEAR 5001	PEAR 5001	SIO 3	Trimble	Auto
4) LA City 1	CHAT 0330	NIKE 0260	DMI 0250	CHAT 0330	NIKE 0260	DMI 0250	CHAT 0330	NIKE 0260	DMI 0250	CIT 1	Trimble	Garay
5) LA City 2	WORK 0140	MAND 0255	TUNA 0210	WORK 0140	MAND 0255	TUNA 0210	WORK 0140	MAND 0255	TUNA 0210	CIT 2	Trimble	Bawayan
6) LA City 3	MAYO 0370	CULV 0701	VDGO 0310	MAYO 0370	CULV 0701	VDGO 0310	MAYO 0370	CULV 0701	VDGO 0310	MIT 1	Trimble	Garcia
7) LA Co. 1	CAHA 0280	JEFF 0160	SPHI 0040	CAHA 0280	JEFF 0160	SPHI 0040	CAHA 0280	JEFF 0160	SPHI 0040	SIO 4	Trimble	Quezada
8) LA Co. 2	CALA 0240	OATM* 0385	DAWS 0060	CALA 0240	OATM* 0385	DAWS 0060	CALA 0240	OATM* 0385	DAWS 0060	SIO 5	Trimble	Anderson
9) LA Co. 3	PACO 0350	VERN 5007	IRMI 5008	PACO 0350	VERN 5007	IRMI 5008	PACO 0350	IRMI 5008	VERN 5007	LA Co. 1	Trimble	
10) LA Co. 4	LANO 0705	SAUG 5002	BUTTE 5003	LANO 0705	SAUG 5002	BUTTE 5003	LANO 0705	MOND 5009	MOND 5009	LA Co. 2	Trimble	Peer
11) LA Co. 5	PVOO 0010	SATI 5004	HOLL 5005	PVOO 0010	SATI 5004	HOLL 5005	PVOO 0010	SATI 5004	HOLL 5005	LA Co. 3	Trimble	
12) LA Co. 6	VENI 5006	WBCH 0090	CAST 0230	VENI 5006	WBCH 0090	CAST 0230	VENI 5006	WBCH 0090	SAUG 5002	LA Co. 4	Trimble	Howard

13) San B. 1	CHAP 6011	CRAF 6004	POINT 6007	CHAP 6011	CRAF 6004	POINT 6007	CHAP 6011	CRAF 6004	POINT 6007	MIT 2	Trimble	Lamb
14) San B. 2	BEAR 6002	NORCO*** 6005	MILL 6008	BEAR 6002	NORCO*** 6005	MILL 6008	BEAR 6002	NORCO*** 6005	MILL 6008	MIT 3	Trimble	Simon
15) San B. 3	BALD 6003	HIGH 6006	JUNI 6017	BALD 6003	HIGH 6006	JUNI 6017	BALD 6003	HIGH 6006	JUNI 6017	MIT 4	Trimble	Amori
16) Riv Co. 1	DEAD 6001	SANO 0047	ROSA 0065	DEAD 6001	SANO 0047	ROSA 0065	DEAD 6001	SANO 0047	ROSA 0065	Riv. Co. 1	Ashtec	
17) Riv. Co. 2	MATH math	CHER 0051	ANZA 0054	MATH math	CHER 0051	ANZA 0054	MATH math	CHER 0051	ANZA 0054	Riv. Co. 2	Ashtec	
18) Riv. Co. 3	GARN 0078	CABA 0052	INDO 0053	GARN 0078	CABA 0052	INDO 0053	GARN 0078	CABA 0052	INDO 0053	Riv. Co. 3	Ashtec	
19) Riv Co. 4	BLAC 0110	BLAC 0110	BLAC 0110	BLAC 0110	BLAC 0110	BLAC 0110	BLAC 0110	BLAC 0110	BLAC 0110	MIT 5	Trimble	J. Dodrill
20) Orange 1	BREA 0048	LANW A.3 0045	SANTI 0061	BREA 0048	LANW A.3 0045	SANTI 0061	BREA 0048	LANW A.3 0045	SANTI 0061	Or. Co. 1	Ashtec	
21) Orange 2	YORBA 0051	3R.75.71 0056	CHIQ 0058	YORBA 0051	3R.75.71 0056	CHIQ 0058	YORBA 0051	3R.75.71 0056	CHIQ 0058	Or. Co. 2	Ashtec	
22) Orange 3	NIGU 0310	BEE	BELA 0060	NIGU 0310	BEE	BELA 0060	NIGU 0310	BEE	BELA 0060	Or. Co. 3	Ashtec	
23) Orange 4	FLOOD 0044	LEMON 0039	DANA 0055	FLOOD 0044	LEMON 0039	DANA 0055	FLOOD 0044	LEMON 0039	DANA 0055	Or. Co. 4	Ashtec	
24) Orange 5	FIFTH 0018	S.JOAQ 0050	TALE 2 0059	FIFTH 0018	S.JOAQ 0050	TALE 2 0059	FIFTH 0018	S.JOAQ 0050	TALE 2 0059	Or. Co. 5	Ashtec	
25) Orange 6	CHICA 0085	KITE 9008	ONOF 0301	CHICA 0085	KITE 9008	ONOF 0301	CHICA 0085	KITE 9008	ONOF 0301	Or. Co. 6	Ashtec	
26) Orange 7	WOOD ----	----	----	WOOD ----	VICK ----	SEAL ----	WOOD ----	VICK ----	SEAL ----	Or. Co. 7	Ashtec	
27) Orange 8	*bad rec'r	San Juan 0054	San Juan 0054	San Juan 0054	San Juan 0054	San Juan 0054	San Juan 0054	San Juan 0054	San Juan 0054	Or. Co. 8	Ashtec	

PGGA stations at JPL, Pinon Flat, and Scripps will be operating continuously, as will the CIGNET station at Mojave

Group F: Regional Seismicity

Group Leader: Egill Hauksson

SUMMARY REPORT: REGIONAL SEISMICITY (GROUP F)

Report assembled by Egill Hauksson from contributions by PIs.; 24 September 1992

The major goals of Group F are: (1) an improved understanding of earthquake occurrence; (2) determining the relationship between source processes and patterns of damaging ground motions from earthquakes and (3) providing rapid information following a major earthquake in southern California.

Real-time Seismology

Progress is being made in developing new techniques for analyzing broad-band data from TERRAscope and IRIS World-Wide stations. Helmberger et al. report successful inversion of whole broad-band waveforms including surface waves. Taking a different approach Lay et al. have chosen to work only with long-period seismograms and focus on deriving source parameters from waveforms with periods of 50 sec and longer. A more applied approach is being taken by Hauksson and Kanamori who are assembling a software analysis system needed to automatically analyze the TERRAscope data real-time. The 1992 Landers earthquake sequence provided a challenging environment that tested all our present real-time systems to their limit and sometimes beyond.

Sundry Research Projects

Jin, Mayeda, and Aki are studying earthquake scaling in southern California using TERRAscope data. Their goal is to document any departures from self-similarities of the earthquake scaling law. Crustal anisotropy of the Los Angeles basin continues to be target of study for Li and Teng. Abercrombie and Leary have analyzed data from the Cajon Pass borehole and produced source scaling lawns extending over 6 magnitude units. Seeber has continued his studies of earthquake focal mechanisms in southern California. Kanamori and Hauksson continued to record teleseisms under extreme noise conditions in the Los Angeles basin. They plan to use these data to map the long period response of the basin.

Landers Earthquakes

Earthquake data from the 1992 Landers sequence were recorded by the Southern California Seismographic Network, TERRAscope, SCEC portable instruments, and IRIS World-Wide stations. Fifteen REFTEK instruments were deployed in the Landers area as a joint project of the SCEC institutions. Vernon, Nicholson, Magistrale, Li, and Hauksson were all involved in the effort of successfully running this project. Li and Teng extended the field deployment by deploying several instruments for fault zone studies.

Numerous SCEC seismologists have been involved in analyzing data from the Landers earthquake sequence. Hauksson and others have been studying the distribution of aftershocks, focal mechanisms, and stress patterns. Several independent tomographic studies are underway. Zhao of SCEC/Caltech, Eberhart-Phillips of USGS, Nicholson and coworkers of UCSB are doing tomographic inversions using arrival time data from SCSN and eventually portable SCEC instruments. Thio and Kanamori of Caltech, and Lay of UCSC have studied teleseismic data to determine the source properties. Helmberger and Wald are using strong-motion, TERRAscope, and IRIS World-Wide data to map the slip distribution during the mainshock rupture. Abercrombie and Mori have studied data obtained from the Cajon Pass borehole and shown that the Landers earthquake started as small earthquake and within a few seconds grew into a M7.5 event. The slow start is also confirmed by TERRAscope data. Stein, King and Lin and other stress modeling groups have shown how the stress field around the San Andreas fault changed as a result of the M7.5 earthquake. Most of these studies are ongoing and will be reported on in detail at the fall AGU.

EARTHQUAKE SOURCE PARAMETERS, SCALING AND NUCLEATION FROM DEEP BOREHOLE RECORDING

RACHEL ABERCROMBIE
(Visiting SCEC Scientist)

Annual Report to SCEC September 1992

My SCEC funded research, in collaboration with P. Leary, has fallen into two main sections, both utilizing seismic data recorded at a depth of 2500 m down the Cajon Pass borehole, 4 km from the San Andreas fault in southern California. Earthquakes recorded within 30 km of the borehole cover the approximate magnitude range -2 to 4, and have stress drops in the range 10 to 1000 bars. We see no evidence of a breakdown in constant stress drop scaling and conclude that earthquakes are self similar over the size range 1 to 10^5 m. The 28 June Landers earthquake was also well recorded downhole. Investigation of the emergent onset of this event as recorded at the borehole, and at two other local stations reveals the first onset to be of similar amplitude to a 4 - 5 M_L event, and that the large fault slip started within 2 km of the hypocenter despite being delayed by about 3 seconds.

Small Earthquake Source Parameters and Earthquake Scaling

A triaxial seismometer was installed at a depth of 2500 m in the Cajon Pass borehole, southern California, by P. Leary in August 1991. Several hundred small (< 4 M_L) local earthquakes occurring within the San Andreas fault zone have been recorded (Figure 1). Seismograms recorded at this depth contain the high frequencies (above about 20 Hz) needed to observe small earthquake sources which are lost to surface stations in the severely attenuating near-surface. At 2500 m depth the seismic noise is below the amplifier sensitivity allowing a large dynamic range for recording, and a wider than average spectral bandwidth of clear signal (2 to 200 Hz). These favorable conditions enable us to determine perhaps the first reliable source parameters for such small tectonic earthquakes, and evaluate claims made by recent surface studies that constant stress drop scaling, long accepted for larger events, breaks down at an earthquake size of a few hundred meters. We are also able to calculate intrinsic attenuation in the upper crust and investigate scattering in the absence of surface waves.

Whole path Q_S for earthquakes within about 40 km of the borehole is at least 1000, and Q_P is about twice that value. Comparison of the seismograms of an earthquake recorded both down hole and at the wellhead show $Q_S \sim 25$ in the upper 2500 m of the crust, and $Q_P \sim 50$ (Figure 2).

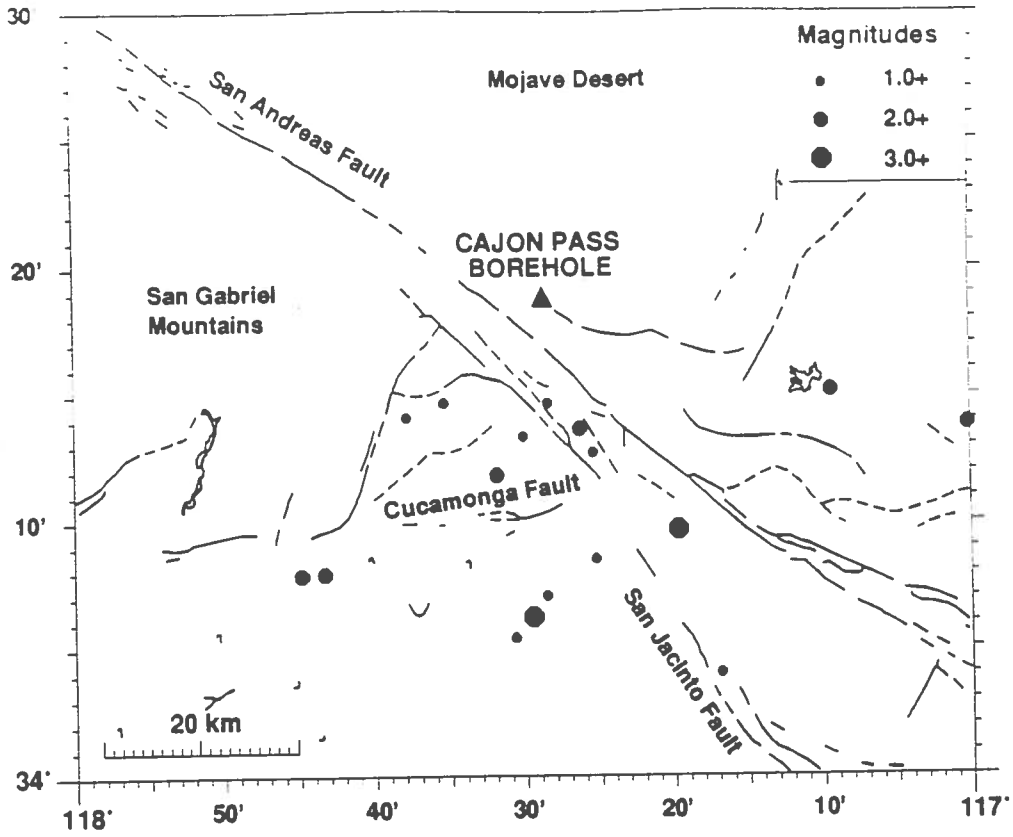

Figure 1 Location map showing the Cajon Pass borehole and major fault zones. The plotted epicenters are representative of the events recorded to date, large enough to be located by the Southern California Seismographic Network.

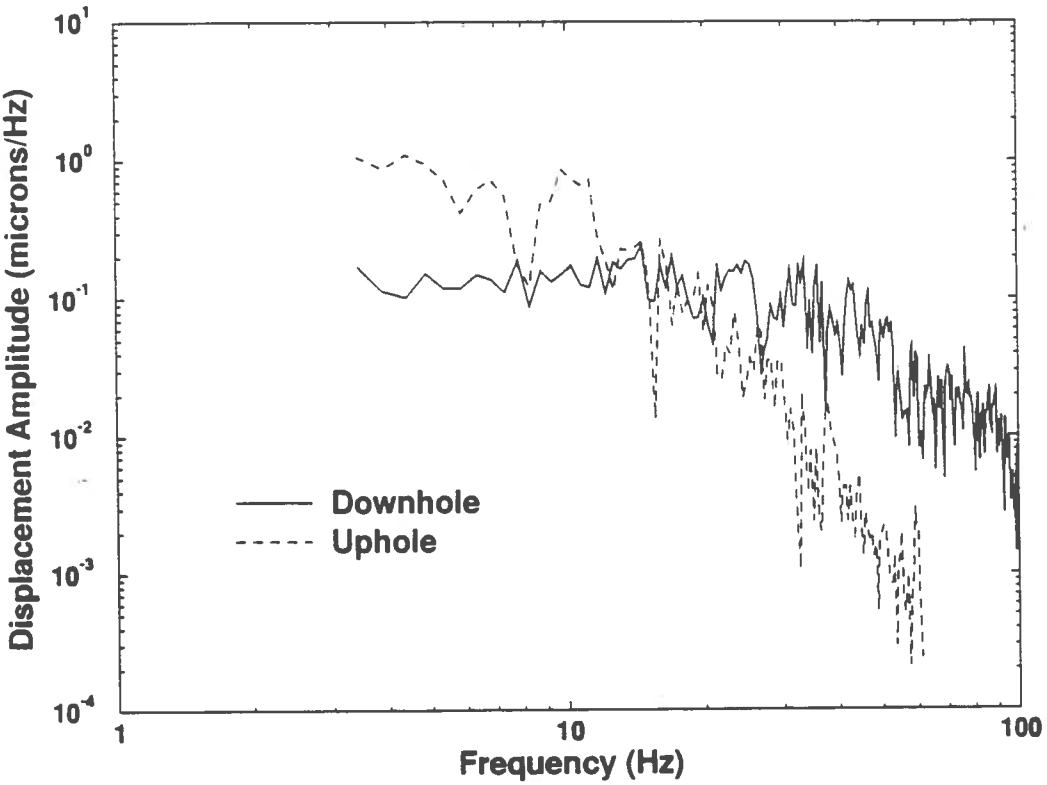

Figure 2 The effect of the near surface on seismic waves: *S* wave spectra of a nearby event. The low frequencies (< 10 Hz) are amplified by about 7 and the high frequencies are significantly attenuated, greatly distorting the surface spectrum.

Spectral analysis of 40 small ($< 3\ M_L$) earthquakes occurring within 30 km of the borehole was used to determine the source parameters seismic moment and source radius, and to estimate the stress drop. Corner frequencies are in the range 10 to 80 Hz and stress drops in the range 10 to 1000 bars. Figure 3 shows these 40 earthquakes together with 800 other events from a range of previous studies. It is clear that there is no breakdown in stress drop scaling at about magnitude 4 (~ 100 m), and that earthquakes are self similar with stress drops in the range 1 to 1000 bars over the magnitude range -2 to 8.We suggest, therefore, that reports of minimum earthquake source dimension of a few hundred meters are more likely due to loss of high frequencies to surface stations by near surface attenuation, and bias in bandlimited catalogs than to properties of the seismic crust. We also note (in Figure 3) that stress drops of tectonic earthquakes recorded at Cajon Pass are significantly higher than those of hydrofracture events of the same size (0.1 to 1 bar).

Work is continuing to increase the number of analyzed earthquakes, and also confirm the spectral results with a time domain analysis. In collaboration with Jim Brune I am investigating the ratio of P to S wave energy at high frequencies to determine if there is evidence of earthquake sources having a normal component of motion.

The Nucleation and Propagation of the Landers earthquake, 28 June 1992

The 28 June Landers earthquake ($7.5\ M_S$) was recorded clearly at the Cajon Pass borehole station, remaining on scale throughout on the "low gain" component. We calculate that the waves traveling to the borehole station at 95 km experience only as much intrinsic attenuation as to a surface station at 10 km. The Landers earthquake had a very emergent onset and, in collaboration with Jim Mori (USGS), I have studied the first few seconds before the arrival of the large amplitudes in detail to investigate how this event nucleated and grew.

To discover if it is possible to distinguish the onset from an ordinary small earthquake we compare it with nearby foreshocks and aftershocks of varying size. The amplitude of the onset is similar to that of a magnitude 4 to 5 earthquake.

We observe that at 3 stations at a range of azimuths the time delay between the initial onset and the first large amplitude arrivals varies by only 0.5 seconds. This implies that the rupture front had moved less than 2 km from the initial hypocenter within the first 3 seconds, quite different from conventional models in which it would typically have travelled about 10 km.

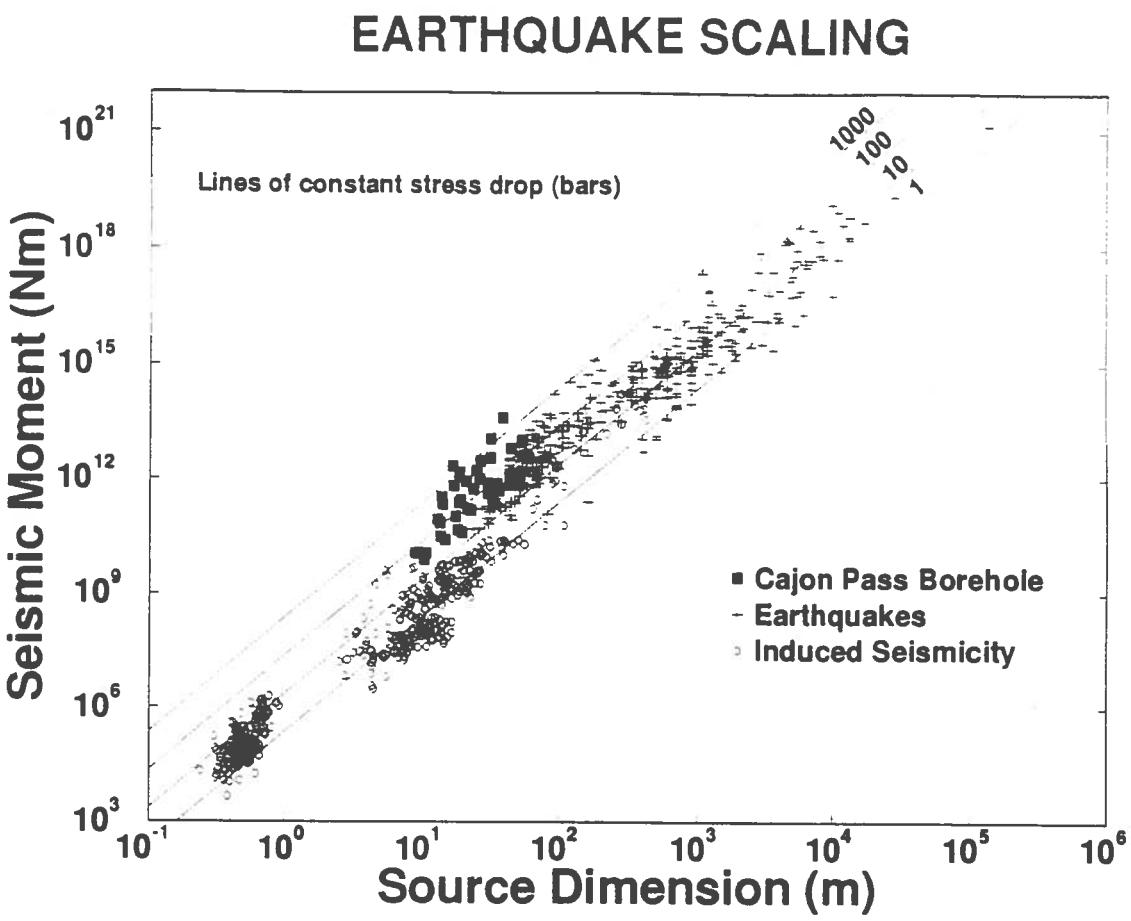

Figure 3 Earthquakes recorded at Cajon Pass set in context. For details of the other studies of tectonic and induced seismicity see Abercrombie & Leary (1992).

Publications

Abercrombie, R. & P. Leary (1992). Source parameters of small earthquakes recorded at 2.5 km in the Cajon Pass borehole, southern California: implications for earthquake scaling, *Geophys. Res. Letts., submitted.*

Abercrombie, R. (1992). Regional bias in estimates of earthquake M_S due to surface wave path effects. *Bull. Seism. Soc. Am., submitted.*

Acknowledgements

Recording of the downhole data was accomplished between March July 1992 using a SCEC RefTek loaned by Leon Teng. Recording restarted in September and is continuing using a RefTek loaned by Paul Davis (UCLA).

Study of Earthquake Scaling by the use of TERRAscope Data of Southern California

Anshu Jin, Kevin Mayeda and Keiiti Aki

University of Southern California

The motivation for studying earthquake scaling in southern California comes from the "Scale-dependence in earthquake phenomena" revealed by studies of the correlation between coda Q^{-1} and seismicity (Jin and Aki, 1989, 1992), and the magnitude dependence of precursory seismicity patterns (e.g. Taylor et al., 1992). The study we proposed is to check for departures from self-similarity of the earthquake source scaling law. Since the Joshua Tree-Landers-Big Bear earthquakes occurred while we were testing the method, we decided to concentrate on the determination of spectral ratio of the aftershocks of these earthquakes using TERRAscope data. We will then compare the observations with the predictions by the ω-squared model.

We have tested about 10 pairs of Landers' aftershocks with different δM (magnitude difference) and $\delta\Delta$ (hypocentral distance between two earthquakes of a pair). We found the following constrains on the data for establishing the scaling law observationally.

(1) Since the magnitude error is about 0.1- 0.3 for aftershocks, the magnitude difference between two earthquakes of a pair should not be smaller then 0.5. Also because we use the same time window for two events of a pair for the spectral ratio, both seismograms should have the same S/N level and so δM should not be larger than 1.

(2) We calculated S-wave and coda spectral ratios for each pair, and found that both ratios are almost identical as long as $\delta\Delta<0.01\Delta$, where Δ is hypocentral distance of the station. As an example, figure 1a and 1b show the spectral ratio of S-wave and coda wave for a earthquake pair with magnitude 4.3 and 3.3, and $\delta\Delta$=0.94 km. Station GSC is located at NNE of the epicenter with hypocenter distance about 101 km. The spectral ratios of coda and S-waves are very similar demonstrating that the spectral ratio method works well for eliminating the path, site, and source radiation pattern effects. However, at station SVD the shape of the spectral ratio for coda and S waves are significantly different, and may be attributed to the source radiation pattern effect not being eliminated in the S-wave spectrum when $\delta\Delta$ is comparable with Δ.

According to Jin and Aki (1989, 1992) the characteristic magnitude in Southern California may be in the range 3 to 3.5, therefore we need the magnitude range of aftershocks to be about 1 to 5 for the source scaling study. We have had some difficulties to acquire sufficient high quality data:

(1) The coda part of the seismograms of the earlier, larger aftershocks are often contaminated by smaller ones. So far we have found only one M>4.5 aftershock which seems to be good enough. So, we have to wait for more contaminated larger aftershocks.

(2) Caltech's "/pub/gopher/RTP" does not usually offer the seismograms of earthquakes with M<2.3. We may have to use the Caltech-USGS network data for M< 2.4 earthquakes.

(3) Another problem is that most TERRAscope seismometers have high frequency cut-off at 10 Hz. Now we are trying to combine 'VSP' data with 'vbb' data to extend the analysis to the high frequency side of the spectra.

References

Jin, A., and K. Aki, Spatial and temporal correlation between coda Q^{-1} and seismicity and its physical mechanism, JGR, 94, 14041-14059, 1989.

Jin, A., and K. Aki, Temporal correlation between coda Q-1 and seismicity , --Evidence for a structural unit in the brittle-ductile transition zone--, submitted to JGR, 1992.

Taylor, D.W.A., J.A. Snoke, I.S. Sack, and T. Takanami, Seismic quiescence before the Urakawa-Oki earthquake, BSSA, 81, 1255-1271, 1991.

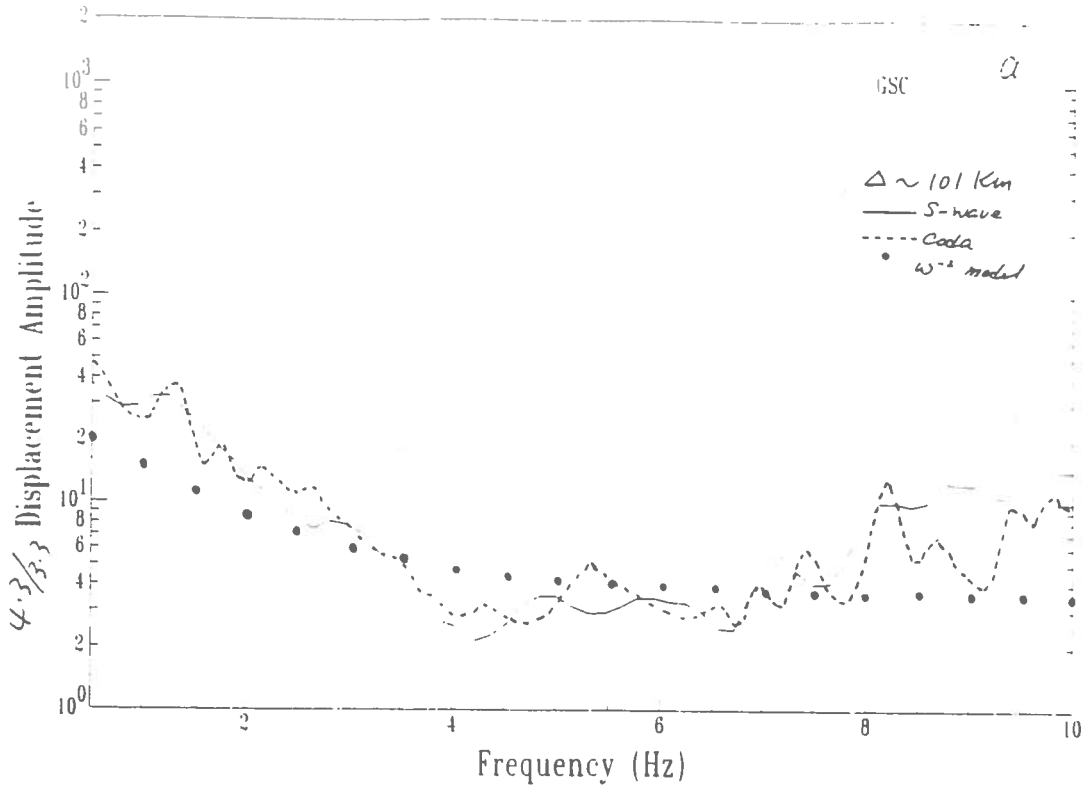
a
GSC
Δ ~ 101 Km
S-wave
Coda
ω⁻² model
4.3/3.3 Displacement Amplitude
Frequency (Hz)

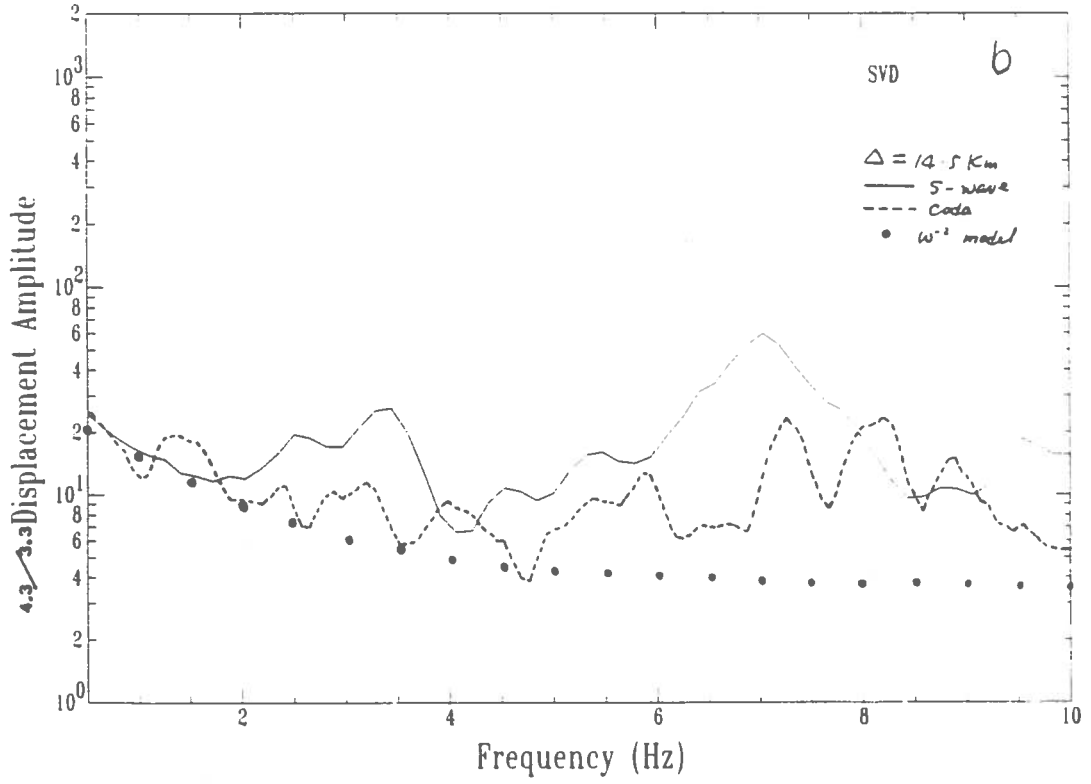
b
SVD
Δ = 14.5 Km
S-wave
Coda
ω⁻² model
4.3/3.3 Displacement Amplitude
Frequency (Hz)

Figure 1

A SCEC Project: Progress Report, 24 Sept. 1992

PIs: Egill Hauksson
Institution: California Institute of Technology
Title: Recording and Studies of the Joshua Tree Earthquake Sequence 1992

INVESTIGATIONS

To collect data from Joshua Tree aftershocks using four IRIS/RAMP REFTEKs and two Caltech REFTEKs. The goal of deploying these instruments was to collect onscale high-quality waveforms of aftershocks in the near-field.

RESULTS

The M_L 6.1 Joshua Tree earthquake of 23 April 1992 04:50 GMT occurred at 33°N 57.7', 116°W 19.2' about 8 km northeast of the southern San Andreas fault and about 20 km south of the Pinto Mt fault. It occurred at a depth of 12 to 13 km. The earthquake was preceded by a distinct foreshock sequence that included a M_L 4.6 event at 02:25. The mainshock was followed by over 6,000 aftershocks recorded by the regional network and an 11-element portable network deployed by the Southern California Earthquake Center. No surface rupture for the sequence has yet been found. The seismic moment is estimated at 2×10^{25} dyne-cm [*H. Kanamori,* 1992]. From directivity effects, the mainshock ruptured unilaterally to the north along a fault about 15 km long. P-wave polarities indicate right-slip initiated on a fault striking N14°W, dipping 80°W, with a rake of 175°. Well located aftershocks dip east at about 85°. A large number of aftershocks occurred off the mainshock rupture plane on adjacent secondary structures, similar in many ways to the cross-shaped or 'winged-shaped' pattern of events following the 1979 M_L 5.5 Homestead Valley earthquake. Many of these off-fault earthquakes occurred on structures either sub-parallel to the mainshock plane or on secondary left-lateral faults that strike at high angles. Most of the off-fault seismicity was shallow (< 8 km deep), while most of the events on the main fault plane extended to depths of 13 km. Aftershocks continued to migrate to the north and south following the mainshock, and ultimately extended from the southern San Andreas fault near the Indio Hills to the Pinto Mt fault. The northern 15 km part of the aftershock zone had a strike more nearly N10°E. The 1992 Joshua Tree sequence occurred in the area of the 1940 M5.4 Covington Flats earthquake—part of the

premonitory activity leading up to the 1948 M6.5 Desert Hot Springs event. The 1992 sequence was part of an accelerated moment-release rate that began in 1985–86 and which lead up to the M7.5 Landers event that initiated north of the Pinto Mt fault. The Landers earthquake caused continued aftershock activity along the fault that caused the Joshua Tree mainshock. Seismicity on nearly all the secondary structures active during the Joshua Tree sequence, however ceased in the hours prior to the M 7.5 Landers event, and has not yet resumed.

REFRENCES

Nicholson, C. and E. Hauksson. The April 1992 M_w 6.2 Joshua Tree Earthquake Sequence: Seismotectonic Analysis and Implications, submitted to the AGU Fall meeting,1992.

A SCEC Project: Progress Report, 24 Sept. 1992

PIs Egill Hauksson and Hiroo Kanamori
Institution: California Institute of Technology
Title: Towards, Real-time, Routine Broad-band Seismology

INVESTIGATIONS

The goal of this project is to establish rapid data analysis methods for data from the TERRAscope broad-band seismic network.

RESULTS

We report the following accomplishments:

1) We have implemented a new version of the GOPHER dialup software for TERRAscope with the help of Steve Malone. This new version allows the retrieval of 80 sps data and strong motion data for bigger events. The older version only allowed the retrieval of 20 sps data. The new GOPHER also allows more than one workstation to dialup the stations. Currently two workstations do the dialing and data retrieval. We have also almost completed the development of a computer program for magnitude determination using TERRAscope data. We plan to add this program to the GOPHER process to determine magnitudes automatically.

2) Workshop on real-time seismology was held at Caltech on 26 June 1992. Ten speakers (see enclosed agenda) gave talks about ongoing work in real-time seismology in southern and northern California. Two of the most promising efforts in real-time seismology are the development of new analysis methods for the broad-band data and real-time transmission of parametric data to users via radio-pager systems.

3) This project has provided half-time salary for Steve Bryant to develop real-time software for the SCSN and TERRAscope. Since 22 April we have redirected his efforts to help with managing data flow, software maintenance, and installation of new hardware. This has proven to be necessary to make information available rapidly, for instance, to OES and CEPEC.

4) We also have an ongoing effort that consists of analyzing data from the Landers earthquake sequence. (See also enclosed preprint; SCEC publication number 11).

Publications

Hauksson, E., K. Hutton, and L. M. Jones, Preliminary report on the 1992 Landers earthquake in southern California, to appear in Guidebook to the Landers earthquake 28 June 1992, *Edited by* D. Ebersold and G. Rasmussen, *published by* Southern California Section of the Association of Engineering Geologists, October 1992.

Hauksson, E., K. Hutton, H. Kanamori, S. Bryant, H. Qian, K. Douglass, L. M. Jones, D. Eberhart-Phillips, J. Mori, and T. Heaton, Overview of the 1992 (M_w6.2,7.4,6.3) Landers Earthquake Sequence in San Bernardino County, California, submitted to AGU Fall meeting, 1992.

Kanamori, H., H. K. Thio, D. Dreger, E. Hauksson, and T. Heaton, Initial investigation of the Landers California, earthquake of 28 June 1992 using TERRAscope, *submitted to Geophys. Res. Letters.*

Nicholson, C. and E. Hauksson, The April 1992 M_w 6.2 Joshua Tree Earthquake Sequence: Seismotectonic Analysis and Implications, submitted to the AGU Fall meeting,1992.

Hauksson, E., K. Hutton, K. Douglass, and L. Jones, Earthquake Atlas for Southern California, 1978 1990, submitted to: Engineering Geology of southern California, 1991.

Kanamori, H ,E. Hauksson, and T. Heaton, Experiment Toward Realtime Seismology Using TERRAscope ---1991 Sierra Madre Earthquake----, (abstract) AGU meeting 1991

INTEROFFICE MEMORANDUM

CALIFORNIA INSTITUTE OF TECHNOLOGY

SEISMOLOGICAL LABORATORY 252-21

DATE: 8 June. 1992

TO: SCEC members
FROM: Egill Hauksson
SUBJECT: **SCEC seminar at Caltech on real-time seismology 25 June 1992**
PLACE: SALVATORI ROOM, 3rd floor south Mudd

SCHEDULE 2nd Version

1:00	E. Hauksson	Introduction
1:15	H. Kanamori	TERRAscope: real-time applications
1:35	H K Thio	Mechanisms from surface waves
1:45	T. Lay	Real-time inversion of very long period signals
2:05	K. Mayeda & K. Aki	Source parameters from coda waves
2:20	D. Helmberger	Source retrieval from regional seismograms
2:40	W. Ellsworth	Real-time seismology in northern California
3:00		Discussion
3:10	*BREAK*	
3:30	M. Pasyanos	Real-time seismology at UC Berkeley
3:45	F. Vernon	Real-time seismology at Anza and other arrays
4:00	D. Given	Hypocenter/magnitude determination: Pickle
4:15	T. Heaton	CUBE/ Issues for the future
4:30-5:00		Discussion

Rapid Source Retrieval

Don Helmberger, Laura Jones and Douglas Dreger
California Institute of Technology
Pasadena, California 91125

Objective:

We continue to make progress in inverting three-component TERRAscope data to obtain rapid source information for local and regional earthquakes. Presently source parameters for a given event are obtained by inverting the long–period bodywave portions of the data, since surface waves display the greatest variation and are more difficult to match synthetically. Long–period body waves at regional distances are composed of P_{nl} and S_n waves that are relatively insensitive to lateral heterogeneity, but sensitive to source orientation. Several recent studies of moderately sized southern California earthquakes suggest that a relatively simple flat–layered model explains many features of the observed waveforms. This model, however, often requires alteration before it may be successfully employed in regions where the crustal structure differs or is more complex. The recent Joshua Tree-Landers-Big Bear earthquake sequence has provided us with the opportunity to develop path-specific Green's functions using aftershock data and to begin refining and extending our inversion methods. Given the development of path-specific Green's functions, we now begin inverting the entire broadband waveform rather than restricting ourselves to the long-period body-wave portion. In addition, we have been using a previously computed catalog of stored Green's functions to study the distributed slip and directivity of selected local earthquakes. Since the Landers sequence has provided us with such a wealth of broadband data, the focus of this report will be on the Landers earthquake only. We split our results into two sections, to be discussed separately: (1) The Landers Mainshock, and constraints on source directivity and slip distribution from TERRAscope acceleration, velocity and displacement records, and (2) broadband modeling of aftershocks from the Landers-Big Bear-Joshua Tree sequence, development of path-specific Green's functions using aftershock data, and inversion of aftershock data to obtain source mechanisms.

Results:

The Mainshock Source Process. The June 28, 1992 Landers earthquake (M_w=7.3) was located approximately 160 km east of Pasadena, and was recorded by all six TERRAscope stations. Figure 1A shows the location of the epicenter (star) relative to the stations used in our analysis. Also plotted on this map is the trend of observed surface offsets (bold line) [Kerry Sieh, personal communication]. Note that the stations cover 180° around the fault, and are located at tangential component maxima relative to the observed surface rupture orientation.

The motions due to the earthquake were large enough to clip the VBB channels at all of the stations, however they were recorded by co-located FBA-23 instrumentation. Initial observations of the amplitude and duration at each of the stations indicated that the event had a strong component of northward directivity during the rupture. The method that we employed was a deterministic forward modeling approach in which the mainshock rupture is approximated by summing the response due to a series of point-sources on a plane, themselves triggered by a passing rupture front. A number of models were tested including uniform slip on both straight and bent faults. The observed surface slip shows that the fault has a rather substantial bend (Figure 1A). Our modeling indicates that this bend in the fault is present at depth and is required in modeling the data. Teleseismic body waves also show this to be the case [Kanamori et al., 1992]. The best–fitting model to date is shown as dashed lines on Figure 1A, where the rupture begins at the hypocenter (star) and ruptures unilaterally northward, with a substantial change in strike 20 km north of

the epicenter. We found that uniform slip on these two planes did not explain the data and that tapering the slip on the edges improved the fit. Figure 1B compares the fit to the displacement waveforms recorded at GSC, SVD, PAS and PFO. For GSC and PFO the east-west component is shown, effectively the tangential direction. For SVD and PAS the north-south direction, also effectively the tangential direction is shown. The synthetics are aligned in absolute travel–time and are plotted on the same amplitude scale as the data. Generally, there is a good level of fit with the displacement waveforms. The azimuthal variation in amplitude appears to be well modeled in this bandwidth, and the double pulse features of both SVD and PAS are explained with the bent fault plane, double sub-event model (tapered slip). The observed surface slip also indicates that there were two regions that underwent the most slip with little or no slip in between. Figure 1C compares the north-south component displacement, velocity and acceleration data recorded at PAS with the synthetics for the bent fault, tapered slip model. The agreement with the velocity data is remarkable. Clearly, the displacement and velocity records are dominated by the two large sub-events. There is evidence of the relatively long-periods excited by the two sub-events in the acceleration data, but there is also clearly additional complexity that is not explained. One of the interesting features of this comparison is that the amplitudes are well matched both at long-periods (displacment) and short-periods (acceleration). This may just be fortuitous at PAS since the accelerations are over-predicted at GSC and under-predicted at SVD. A continuing research effort will focus on explaining both the long–period and the short–period observations with a single source model.

Broadband Modeling of Aftershocks. We have constructed a profile of 20 aftershocks from the Joshua Tree, Landers and Big Bear events. A map of the source area is shown in figure 2A; the aftershock locations are indicated by filled and open stars. These small events possess preliminary magnitudes of between 3.5 and 4.8, and maximum source depths of 15 kilometers. Most have strike-slip or oblique-slip source mechanisms. This sequence, which also includes the M_w=4.3 Joshua Tree foreshock forms a rough profile which follows, aproximately, the trend of the June 28, 1992 Landers rupture (shown in bold line on Figure 2A, [K. Sieh, personal communication]). The events in our profile range southward 14 to 160 km epicentral distance from the GSC TERRAscope station, and produced high signal–to–noise, three component broadband waveforms which were recorded on the entire TERRAscope array. This provided the opportunity for careful structural studies of several important source–reciever paths, including the path northward across the Mojave from Joshua Tree to Goldstone station (GSC). For brevity's sake we consider only 7 of the 20 events in the Mojave profile; with source–receiver distances of 38 to 156 km. Locations for the aftershocks used are indicated by the filled stars in Figure 2A. Waveforms for these events are shown in bold line in Figures 2B–2D, along with synthetics from the Mojave model. The model is listed in Table 1. Records at these distances are dominated by the effects of the crust, and in this case suggest a layered model both thinner than the standard southern California model [Hadley and Kanamori, 1978] and slower for both P and S velocities. The Mojave model suggested by this study has a crustal thickness of only 25 km, as compared with the 35 km suggested by the southern California model. In addition, the lower crust is 4% slower for P waves and 5% slower for S waves.

Path–dependent Green's functions were developed for the various source–receiver paths connecting the Landers–Joshua Tree source region to the TERRAscope stations ISA, PAS, PFO and SVD (see Figure 2A). Improved fits of synthetics to data have enabled us to begin performing source inversions using the entire waveform. This provides potentially greater accuracy in the determination of source depth and mechanism, and may be used to resolve details of the Landers rupture, in particular the shallow dislocation history. Future work will include continued refining of path–specific models, and eventual application of the resulting Green's functions to the assessment of older events recorded at historic broadband stations such as Pasadena (PAS).

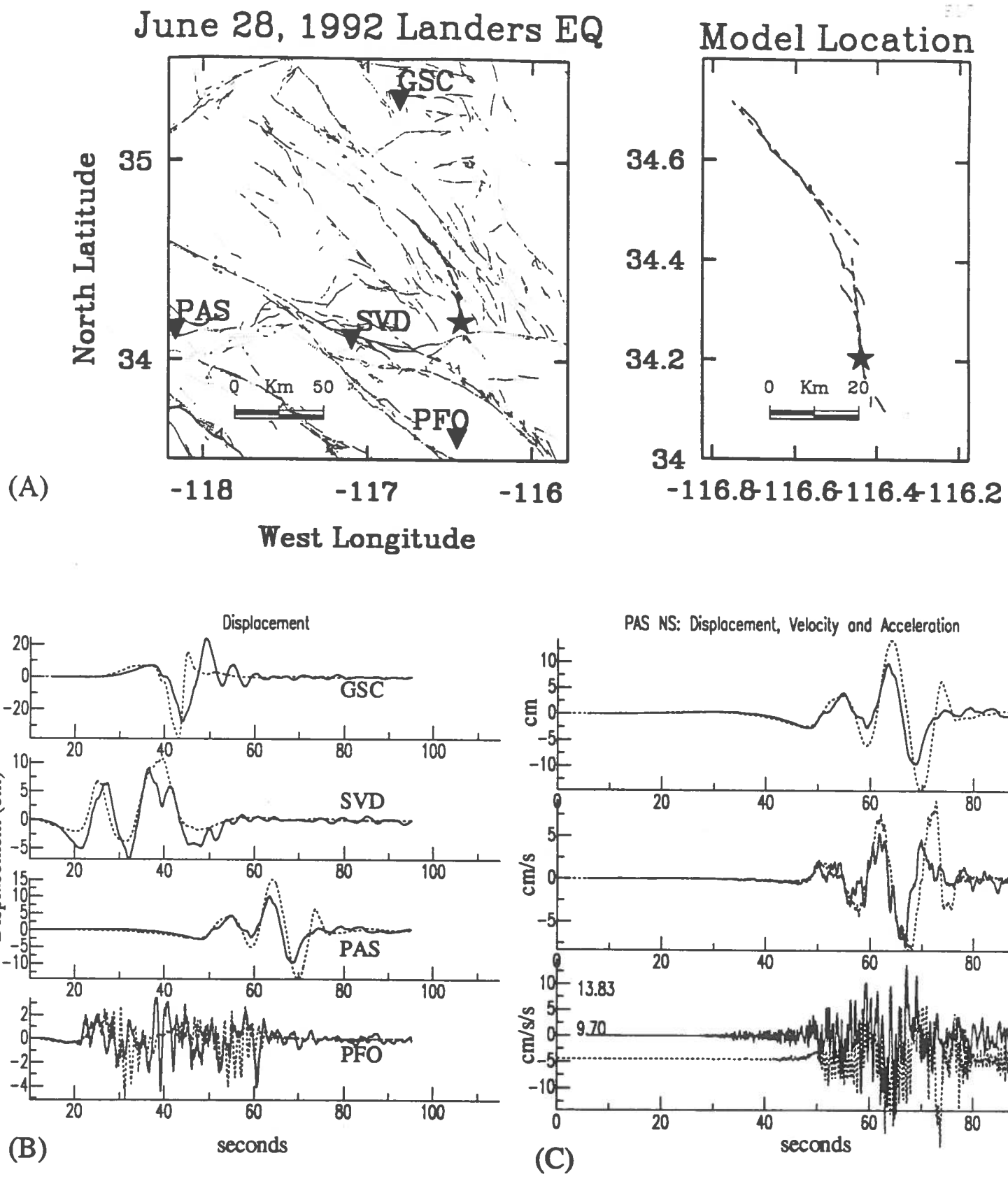
June 28, 1992 Landers EQ
Model Location
GSC
PAS
SVD
PFO
0 Km 50
0 Km 20
North Latitude
35
34
34.6
34.4
34.2
-118
-117
-116
-116.8
-116.6
-116.4
-116.2
West Longitude
(A)
Displacement
Displacement (cm)
seconds
(B)
PAS NS: Displacement, Velocity and Acceleration
cm
cm/s
cm/s/s
13.83
9.70
seconds
(C)

TABLE 1. Mojave Model

P	*S*	*Rho*	depth
5.00	2.60	2.40	2.5
5.50	3.45	2.40	5.5
6.30	3.60	2.67	16.0
6.45	3.68	2.80	25.0
7.65	4.30	3.40	30.0
7.85	4.40	3.42	half space

Figure 2:
The Landers Source location is shown in Figure 2A. Locations of the aftershocks used in finding the Mojave model are shown as open and filled stars. The filled stars indicate the locations of aftershocks shown in this report. Panels 2B—2D show the radial (R), tangential (T) and vertical (V) components of the displacements recorded at TERRAscope station GSC (boldface). Below each displacement record is an appropriate synthetic from the Mojave model. Source mechanisms from our inversions or from Hong Kie Thio [personal communication] are included.

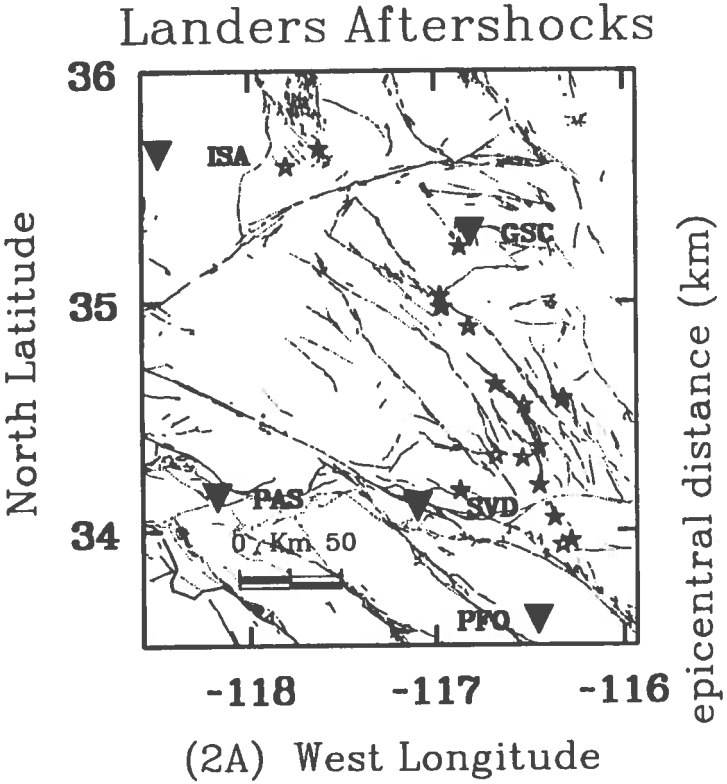

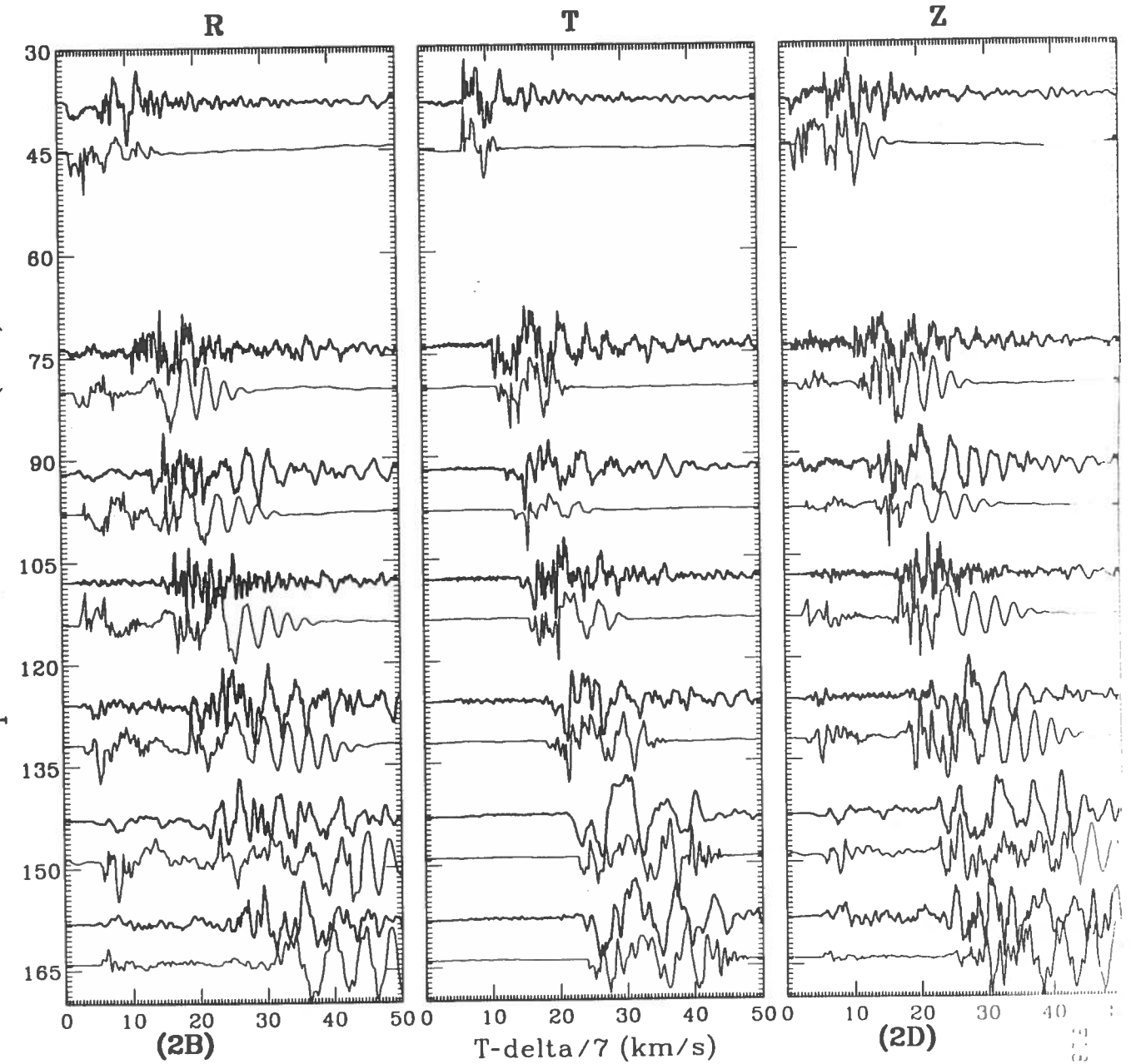

Figure 2A-2D

A SCEC Project: Progress Report, 24 Sept. 1992

PIs Egill Hauksson and Hiroo Kanamori
Institution: California Institute of Technology
Title: Investigation of Site Response of the Los Angeles Basin Using Portable Broadband Seismographs

INVESTIGATIONS

The purpose of this project is to investigate long-period (1 to 10 sec) site response in the Los Angeles basin. Understanding what sensors are suitable for this project and the seismic noise levels in the urban environment has become an important part of this project.

RESULTS

At the start of this project we deployed two REFTEK instruments at the Pasadena Station (PAS) from March to July 1991 to compare and calibrate several different sensors to the Streckeisen STS-1. The sensors being tested were: 1) two 3-component Guralp CMG-4 broad-band seismometers; 2) a 3-component broad-band Ranger; and 3) a single component FBA with velocity output; and 4) 3-component short-period Ranger.

The results of the test showed that the Guralp CMG-4 were not sensitive enough for monitoring teleseismic events to obtain the response of the Los Angeles basin. Subsequently, the Guralp CMG-4 seismometers were returned to the factory and were replaced by Guralp CMG-3ESP seismometers in late December 1991. The CMG-3ESP is a much more sensitive instrument, although it will not record strong ground motions on scale. This problem with the sensors has caused some delays in the field work initially proposed.

As a part of this contract, RAMP aftershock studies, and site studies for TERRAscope we have deployed REFTEK instruments at the following sites:

REFTEK	SITE	DATES
SCEC1	Imperial Highway	08/05/91-06/29/92
SCEC2	USC Campus	01/16/92-06/29/92
CIT1	USC Campus	01/16/92-04/22/92
CIT2	Rancho Palos Verdes	01/20/92-04/22/92
CIT1	Joshua Tree	04/23/92-05/28/92
CIT2	Joshua Tree	04/23/92-05/28/92

CIT1	Long Valley	06/13/92 06/28/92
CIT2	Long Valley	06/13/92 06/28/92
CIT1	Landers	06/29/92 09/25/92
CIT2	Landers	06/29/92 09/25/92
SCEC1	Landers	06/29/92 08/10/92
SCEC2	Landers	06/29/92 08/10/92

Two of the REFTEKs belong to Caltech and two belong to SCEC. The two SCEC instruments have been returned to SCEC as of August 1992.

The data collected so far are: 1) several teleseisms recorded in the Los Angeles basin and by TERRAscope stations; 2) unique recording of the Landers mainshock in Long Valley, which is being used to study the onset of triggered seismicity in the region; 3) several thousand Joshua Tree aftershocks; 4) several thousand Landers aftershocks. We plan to use the data for studies of long period site response, determining crustal receiver functions, and using arrival times of local earthquakes for 3-D velocity inversions.

The teleseisms from the Los Angeles basin are being analyzed to determine spectral ratios and receiver functions (see enclosed Figures 1 and 2).

PUBLICATIONS

Hauksson, E., H. Qian, and H. Kanamori, Investigation of Site Response of the Los Angeles Basin Using Broadband Waveforms, (Abstract) presented at Berkeley January, 1992.

Figure Captions

Figure 1. Teleseism from Japan recorded by TERRAscope and REFTEKs. The two USC records are from the USC Guralp CMG-4 and the Caltech Guralp 3-ESP. This record shows that the CMG-4 instruments performs adequately for recording deep teleseisms.

Figure 2. Teleseism from the Aleutians. The LPC record in from Lone Pine Canyon on the San Andreas fault.

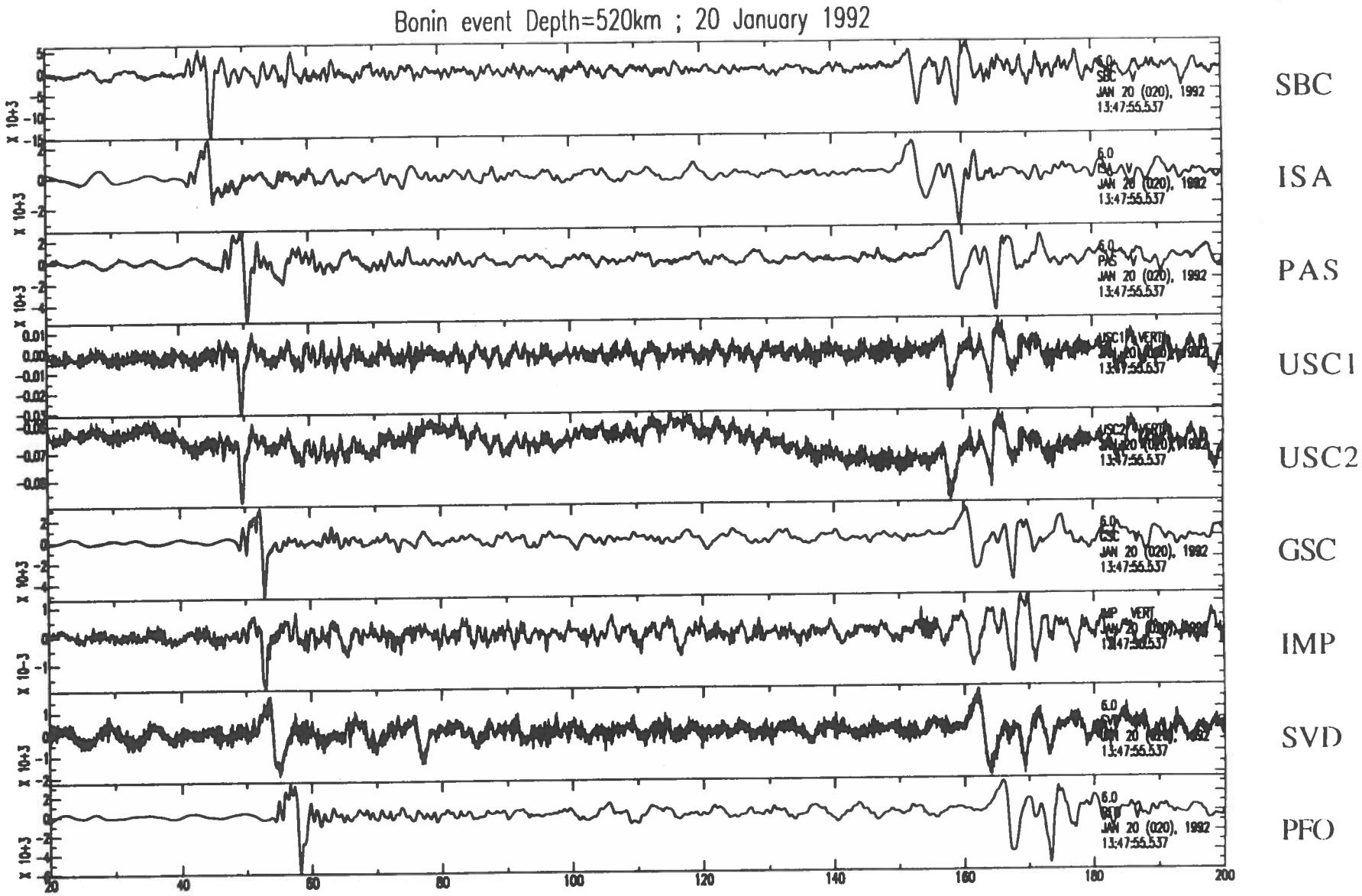
Bonin event Depth=520km ; 20 January 1992
SBC
ISA
PAS
USC1
USC2
GSC
IMP
SVD
PFO
X 10+3
X 10-3
20
40
60
80
100
120
140
160
180
200

Figure 1

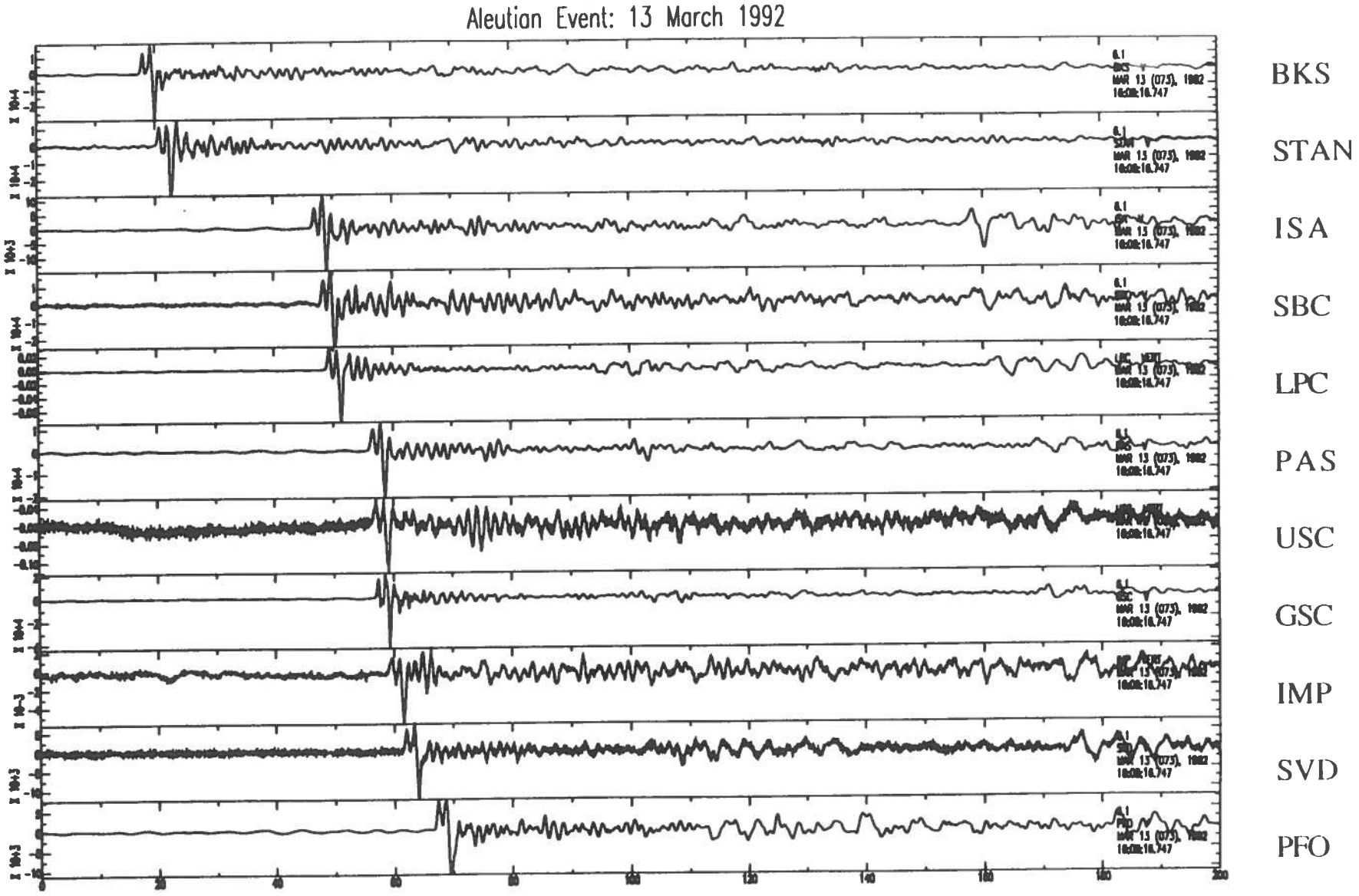
Aleutian Event: 13 March 1992
BKS
STAN
ISA
SBC
LPC
PAS
USC
GSC
IMP
SVD
PFO

Figure 2

PI Thorne Lay

Institution University of California, Santa Cruz

Title: Continued Research on Rapid Determination of Regional Earthquake Fault Parameters

Research Program: This project is directed at rapid determination of regional earthquake fault parameters using data from TERRASCOPE and other regional distance very broadband array stations in the Western U.S.. One objective is to establish a routine procedure for determining the focal mechanism and moment of regional events larger than magnitude 5.0, within one half hour or so of the event. Following the 1992 Landers earthquake, for which the focal mechanism was soon available, we also began to address the issue of rapid determination of the actual fault plane, by analyzing rupture finiteness.

Results: We have established a very successful procedure for rapidly analyzing the source moment tensor for large regional events by using the long-period signals contained in regional seismograms. Our process involves a waveform inversion of the lowpass (or bandpass) filtered seismograms, which isolates signal energy with periods longer than 50 s. This energy is primarily fundamental mode Rayleigh and Love wave energy, but we do not attempt a spectral isolation of the fundamental modes because very short propagation paths are involved, and there is overlap with the overtone signals. Instead, we use a CMT inversion procedure (developed by H. Kawakatsu), to invert the signals using normal modes for a homogeneous earth structure (currently PREM is used). At the short distances involved the waves have little dispersion, and a homogeneous model is very successful in matching the waveforms for periods longer than 50 s, as long as the inversion allows for a temporal and spatial shift of the source centroid to project out any effects of phase mismatch. While eventually a regionally specific earth model could be introduced, either with or without lateral variations, we expect that this will have only very minor effects on the source inversions, given comparisons between results using the PREM and 1066B models.

The 'Regional CMT' inversion procedure works quite well with as few as 3 stations, if they have good azimuthal distribution, on-scale long-period energy with good signal to noise levels, and distances from 100-1000 km. Such data sets are routinely available now in near real-time due to the Caltech gopher system, which collects the TERRASCOPE data, along with the IRIS gopher system which also retrieves the IRIS broadband signals. Since the TERRASCOPE system is activated by local triggers, the CMT inversion could be performed as soon as 10 minute duration signals are available, which is much sooner than the data are available through the NEIS QED system which drives the IRIS gopher. Thus, dial-up access of the regional stations linked to the Caltech gopher can retrieve a suitable set of seismograms for regional events located by the regional network. We have not yet automated an interface between this data retrieval and the inversion code, but that could be undertaken if desired.

Our work so far under this year's contract has involved testing of the algorithm, and application to the many recent California, Nevada and Utah events with magnitudes larger than 5.0. Examples of the focal mechanisms that we have retrieved for these events are shown in Figure 1, with comparisons to Harvard rapid CMT inversions, short-period surface wave inversions at Caltech, and first-motions from regional short-period network data. We have very consistent solutions for the source moment tensor, although using the PREM model does tend to give 30-50% larger moments for the larger events than model 1066B. The mechanisms were typically determined with only 3 or 4 stations, and more stations can routinely be used now as additional rapidly retrieved data comes on-line. We

find that using a homogeneous model is in fact successful down to periods of 50 s, but clearly regionalized velocity models would be needed to push to shorter periods, but that is best done by spectral methods rather than the normal-mode summation underlying the CMT procedure. We are currently preparing two papers describing the development and application of the Regional CMT procedure, with the next phase being to work on the real-time aspect.

In addition to rapidly determining the focal mechanism, it is important for large events to assess which nodal plane is the actual fault plane. Rupture directivity is the key to establishing the finiteness of the event, and the degree of directivity is highly variable from event to event. Since directivity is a 'second order' feature of the radiation (meaning that a point source moment tensor is the 'first order' source characteristic), it is difficult to rapidly analyze source finiteness in most cases. Some exceptions have been provided by the April Joshua Tree event as well as the Landers event, both of which have had TERRASCOPE stations located in both directions along strike, enabling clear directivity effects to be seen in the raw data (in the form of azimuthal variations in the body wave and surface wave pulses). On the day of the Landers event we set out to develop a general method to analyze the regional and teleseismic data to quickly determine the source directivity. This was motivated by the fact that the TERRASCOPE STS-1 recordings had clipped, and there were delays in recovering the strong motion records which subsequently exhibited clear directivity. In addition, for many events the station coverage will not allow a trivial recognition of the fault plane (for example the 1992 Cape Mendocino event).

Our strategy for quickly determining finiteness is based on the well-established 'Empirical Green's Function' procedure, common in the analysis of small earthquakes. This involves the deconvolution of the mainshock recordings by recordings at the same station from a much smaller event with the same mechanism and source location. Of course, this involves some degree of approximation, as no small event will serve as a perfect Green's function for the entire rupture of a large event. Given the rapidly determined mechanism for the Landers event, and recognizing its similarity to the nearby April Joshua Tree event, we used the latter event as an Empirical Green's Function, and deconvolved the entire wavetrain of regional and teleseismic surface waves (dominated by the fundamental mode energy near the Airy phase) at stations retrieved by the IRIS gopher. The deconvolutions revealed two subevents in the mainshock with centroids separated by about 30 km, with a very clear northward directivity. This uniquely identified the rupture plane as well as a 22° rotation of the strike of the second (northerly) subevent (this was done before any other determination was possible, other than by flying over the surface break). Deconvolution of the body waves using the same procedure also works well, and confirms the results of the rapid surface wave deconvolutions, but the signals tend to be less stable due to limitations of the Green's function. Figure 2 shows a plot of the finite source model found for the Landers event, which was basically obtained the day of the event (delayed only by having to think up and implement the deconvolution procedure). We have subsequently applied this approach to several other large events with suitable smaller events and have successfully identified the fault plane for the 1992 Cape Mendocino event, as well as large events in 1991 in the Gorda Plate. A JGR paper describing these applications is in preparation.

Publications

Ammon, C. J., A. A. Velasco, and T. Lay (1992). Rapid estimation of rupture directivity: application to the 1992 Landers (Ms=7.4) and Cape Mendocino (Ms=7.2) California earthquakes, Geophys. Res. Lett., submitted July 13, 1992.

LANDERS earthquake 06/28/92

Regional CMT: 50<T<200s
$\phi = 344^\circ$
$\delta = 90^\circ$
$\lambda = -136^\circ$
$M_0 = 1.6\ 10^{27}$dyn.cm

Regional CMT: 80<T<200s
$\phi = 345^\circ$
$\delta = 53^\circ$
$\lambda = -168^\circ$
$M_0 = 1.6\ 10^{27}$dyn.cm

Regional CMT: 111<T<200s
$\phi = 339^\circ$
$\delta = 77^\circ$
$\lambda = -160^\circ$
$M_0 = 1.7\ 10^{27}$dyn.cm

HARVARD CMT:
$\phi = 341^\circ$
$\delta = 84^\circ$
$\lambda = 167^\circ$
$M_0 = 1.9\ 10^{27}$dyn.cm

CALTECH:
$\phi = 340^\circ$
$\delta = 74^\circ$
$\lambda = -176^\circ$
$M_0 = 1.1\ 10^{27}$dyn.cm

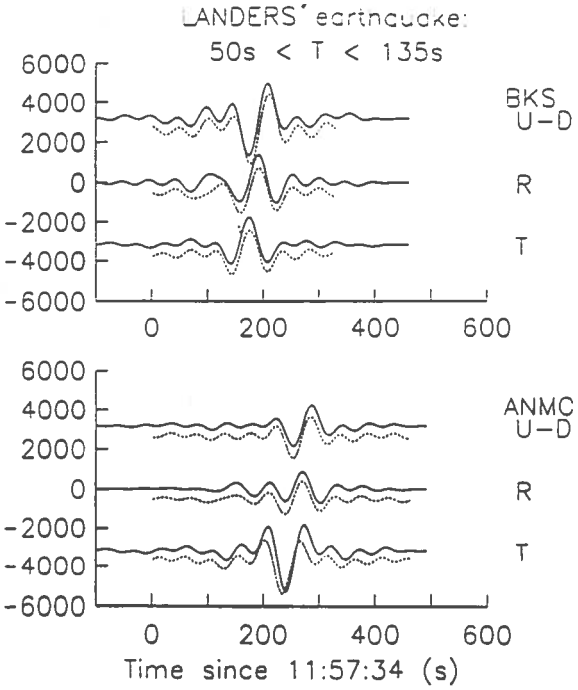

Joshua Tree earthquake 04/23/92

Regional CMT: 80<T<200s
$\phi = 351^\circ$
$\delta = 90^\circ$
$\lambda = -178^\circ$
$M_0 = 3.2\ 10^{25}$dyn.cm

Regional CMT: 50<T<200s
$\phi = 356^\circ$
$\delta = 69^\circ$
$\lambda = -163^\circ$
$M_0 = 3.0\ 10^{25}$dyn.cm

HARVARD CMT:
$\phi = 352^\circ$
$\delta = 81^\circ$
$\lambda = 177^\circ$
$M_0 = 2.2\ 10^{25}$dyn.cm

CALTECH:
$\phi = 83^\circ$
$\delta = 78^\circ$
$\lambda = 366^\circ$
$M_0 = 1.9\ 10^{25}$dyn.cm

Big Bear earthquake 06/28/92

Regional CMT: 111<T<200s
$\phi = 230^\circ$
$\delta = 99^\circ$
$\lambda = -17^\circ$
$M_0 = 1.1\ 10^{26}$dyn.cm

Regional CMT: 80<T<200s
$\phi = 227^\circ$
$\delta = 82^\circ$
$\lambda = -17^\circ$
$M_0 = 1.1\ 10^{26}$dyn.cm

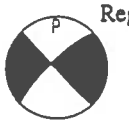

Regional CMT: 50<T<135s
$\phi = 227^\circ$
$\delta = 78^\circ$
$\lambda = 2^\circ$
$M_0 = 9.2\ 10^{25}$dyn.cm

HARVARD CMT:
$\phi = 237^\circ$
$\delta = 86^\circ$
$\lambda = -20^\circ$
$M_0 = 5.2\ 10^{25}$dyn.cm

LANDERS aftershock 07/11/92

Regional CMT inversion
$\phi = 28^\circ$
$\delta = 86^\circ$
$\lambda = 26^\circ$
$M_0 = 8.0\ 10^{23}$dyn.cm ($M_w = 5.2$)

Short-Period Surface Wave Inversion
Kanamori (Pers. Comm.)
$\phi = 35^\circ$
$\delta = 82^\circ$
$\lambda = 37^\circ$
$M_0 = 7.6\ 10^{23}$dyn.cm ($M_w = 5.2$)

Hauksson (Pers. Comm.)
$\phi = 20^\circ$
$\delta = 80^\circ$
$\lambda = 0^\circ$

Near California-Nevada Border 06/29/92

Regional CMT: 80<T<200s
$\phi = 3^\circ$
$\delta = 68^\circ$
$\lambda = -110^\circ$
$M_0 = 5.9\ 10^{24}$dyn.cm ($M_w = 5.8$)

Regional CMT: 50<T<135s
$\phi = 217^\circ$
$\delta = 40^\circ$
$\lambda = -70^\circ$
$M_0 = 5.8\ 10^{24}$dyn.cm ($M_w = 5.8$)

HARVARD CMT:
$\phi = 212^\circ$
$\delta = 55^\circ$
$\lambda = -106^\circ$
$M_0 = 5.8\ 10^{24}$dyn.cm ($M_w = 5.8$)

Fig. 1 Lay

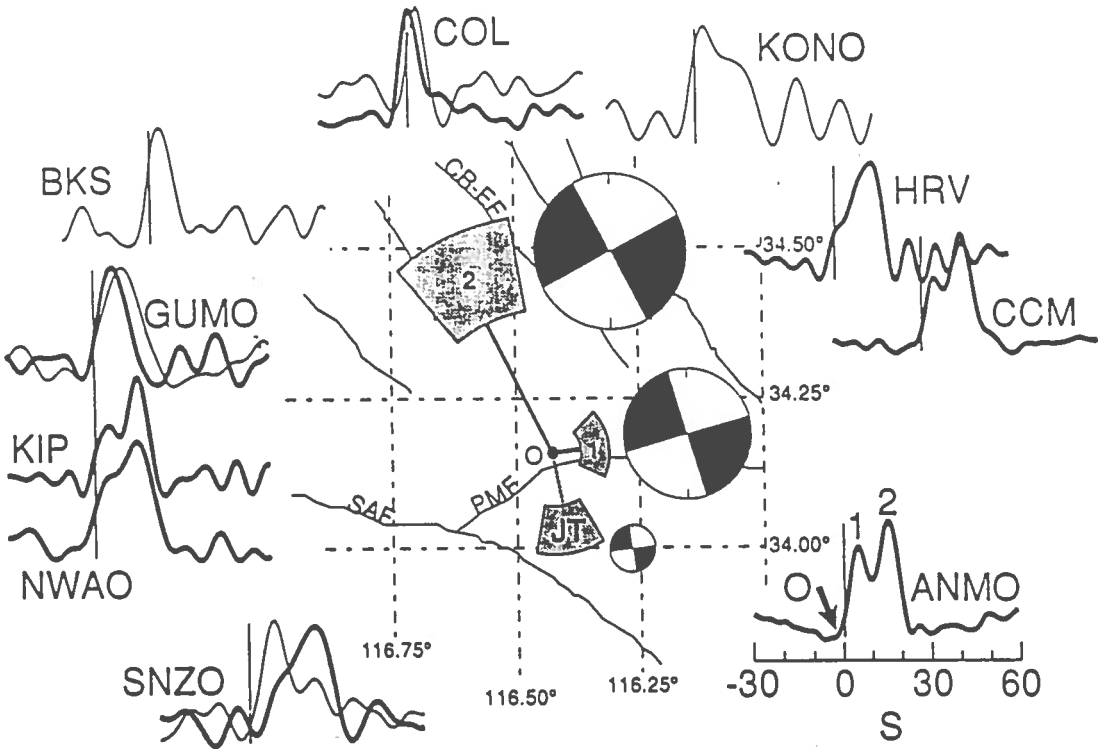

P Wave Source Time Functions

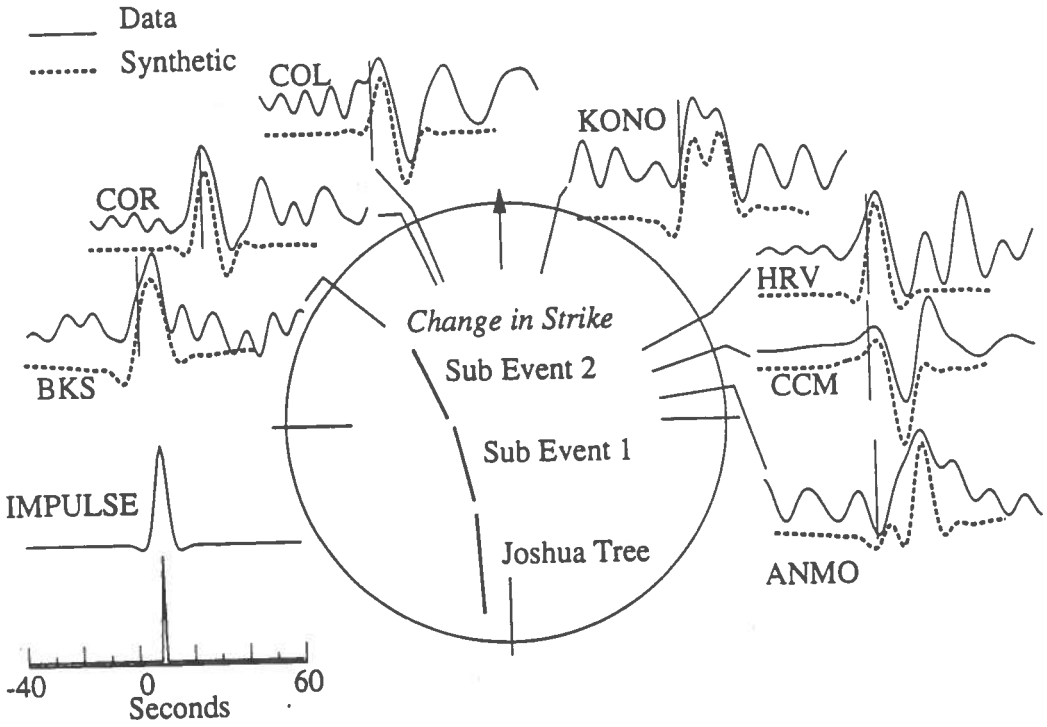

Fig. 2 Lay

Investigation of Crustal Anisotropy and Stress Regimes in the Los Angeles Basin based on Shear-Wave Splitting Observations

Yong-Gang Li and Ta-liang Teng
University of Southern California

Recently, we have systematically examined 3-component seismograms recorded by the USC Los Angeles basin seismic network (LABSNET) and portable instruments (SCEC REFTEKs) for evidence of shear-wave splitting at the crustal depth beneath the Los Angeles basin. The data are taken from eleven three-component network stations and three mobile REFTEK stations in the Los Angeles basin area (Figure 1).

We observed 20-120 ms traveltime difference between the two split shear waves for earthquakes occurring in the crystalline basement at the depths of 6-18 km beneath the Los Angeles basin. We interpret the observed shear-wave splitting to be caused by stress-induced crustal anisotropy. We suggest that the seismic anisotropy is mainly the result of microcracks aligned in the direction of maximum principal stress at the crustal depth. Fig. 2 shows 100 ms shear-wave splitting for a deep earthquake occurring at the depth of 18 km with epicenter 10 km east of station SCS in the northern Los Angeles basin. The polarization direction of the fast shear wave is determined to be N-S by horizontal particle motion diagrams and aspect ratio diagrams, consistent with the regional N-S compressional tectonics in the Los Angeles basin. Assuming vertical microcracks being aligned with crack planes in the N-S direction, we determined that the crack density in the seismogenic zone beneath the Los Angeles basin is 0.04 using ray tracing for crack-induced anisotropic media to fit arrival times in this case (lower left, Fig. 2). Phase velocities of the two split shear waves in this example are determined to be 3.32 km/sec and 3.24 km/sec, respectively, as solutions of the eigenvalue problem for wave propagation in the cracked medium (lower right, Fig. 2). Figure 3 shows the further evidence for shear-wave splitting from three M2.5-3.0 earthquakes occurring on April 2, May 26 1991 and August 30, 1992, respectively, at the same focal depth (~12 km) and with the same epicenter location (~5 km) from the recording station in the northwestern Los Angeles basin. We observed repeated 60 ms traveltime difference between the two split shear waves for these three earthquakes. The smaller time difference in this case is due to the shorter travel distance than that in the above example.

Figure 4 summarizes our observations of shear-wave splitting at seven three-component stations in the Los Angeles basin. The average polarization direction of fast shear waves is N-S$\pm$15^{o}, indicating the N-S direction of the regional maximum principal stress at depth in this area. The average crack density in the basement beneath the central Los Angeles basin is 0.04, but the crack density is found to be 0.06 around the north part of the Newport-Inglewood fault where the seismicity is high. We also found an anomaly of shear-wave splitting at station GFP that is located on the Santa Monica Mountains. The complicated polarization pattern of shear-waves suggests that crustal microcracks and/or geological macrocracks may be aligned with crack planes in the sub-horizontal, corresponding to the vertical direction of the least principal stress in this currently thrusting region.

Based on analyses of shear-wave splitting data in the Los Angeles basin, we did not find significant temporal variation of shear-wave splitting before and after the M5.5 Upland earthquake (on Feb. 28, 1990), M5.8 Sierra Madre earthquake (on June 28, 1991), and Joshua-Landers-Big Bear earthquake sequence (on April 22 and June 28, 1992, respectively). It may be because our stations used for shear-wave splitting observation are too far away from source areas of these three earthquakes that occurred about 60 km, 40 km and 120 km away from our recording stations, respectively. We suggest that dilatancy might occur in the rock before a major earthquake only within a small distance range

(maybe several kilometers for M~6 earthquakes and several tens of kilometers for M7-8 earthquakes) around the source region.

The present SCEC-funding scientific program, "shear-wave splitting observation and its implication of stress regimes in the Los Angeles basin", is on-going in this fiscal year. We still need to use portable instruments for data collection in gaps between network stations in the basin area. Finally, we plan to produce two distribution maps resulting from the shear-wave splitting data recorded at 15-20 three-component stations in the Los Angeles basin area by the end of this fiscal year: They are the distribution map of polarization directions of shear waves that indicates directions of the maximum principal stress in the basin area, and the distribution map of crack densities that may infer the degree of crustal fracturing and the level of the stress in the basin area.

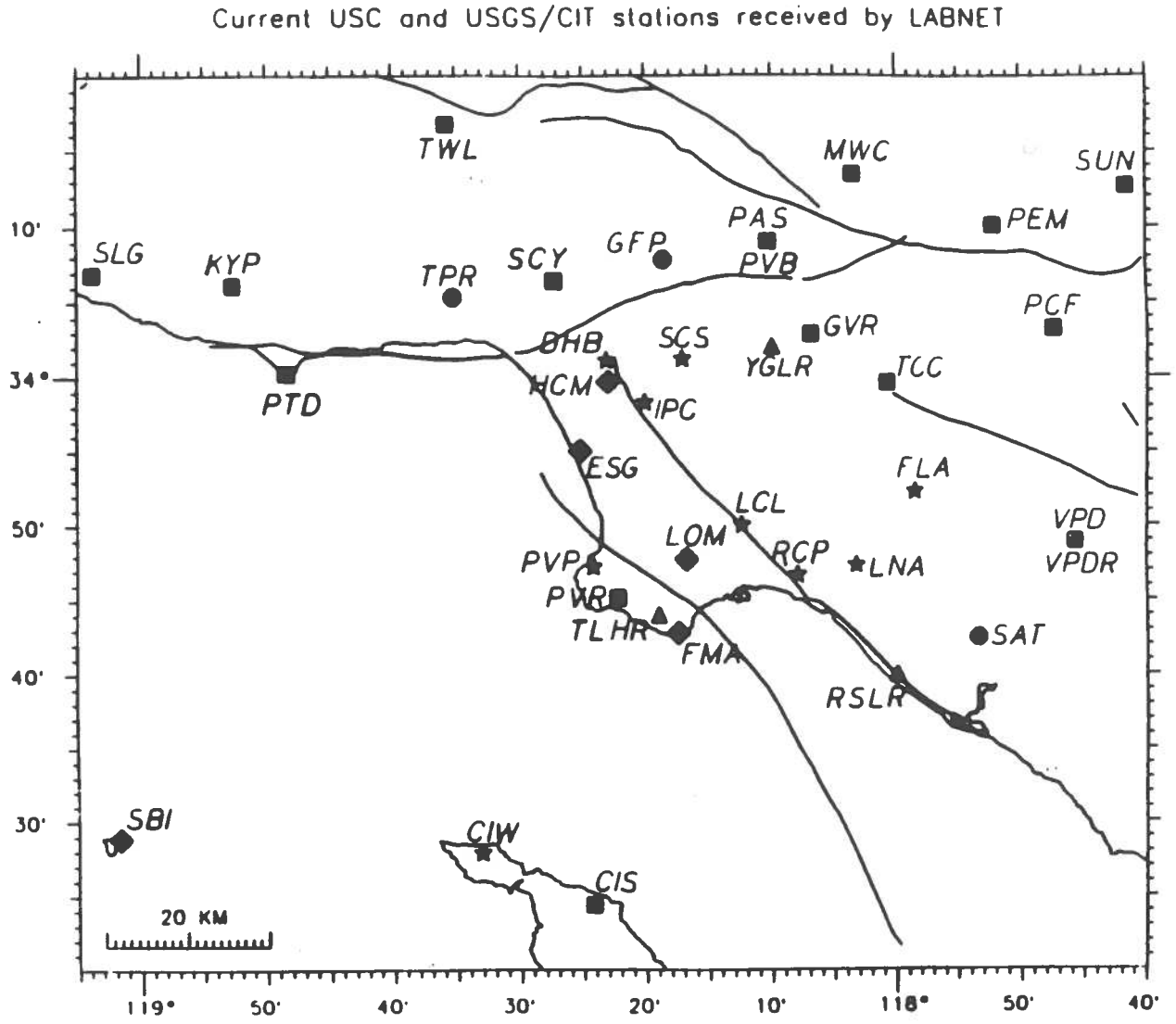

Fig. 1 Map of station locations of the USC seismic network in the Los Angeles basin. Solid stars and circles denote 3-component network stations currently used for shear-wave splitting observation. Solid triangles denote REFTEK stations. Solid squares denote the USGS/CIT stations.

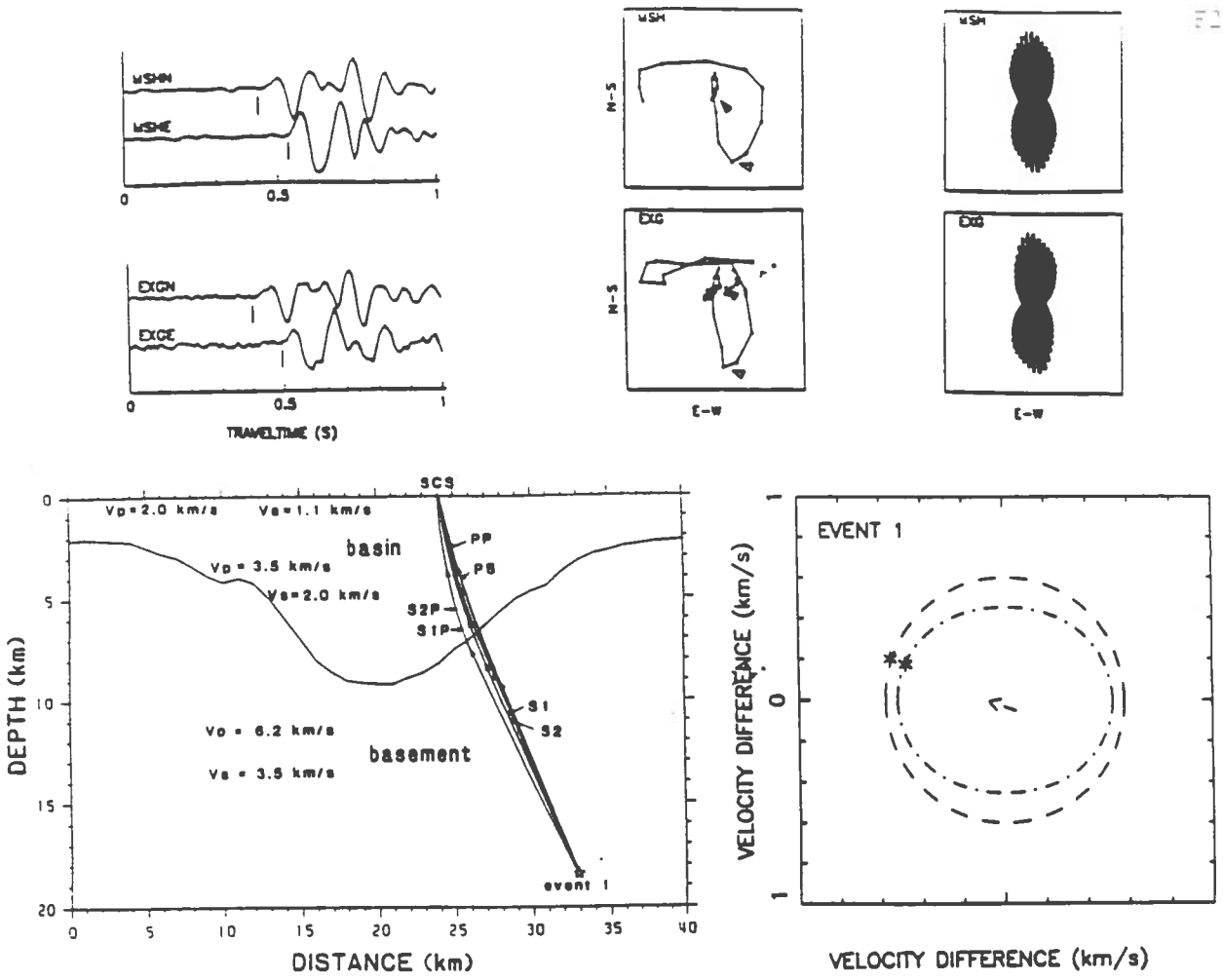

Fig. 2 Upper Left: Horizontal components of seismograms for a M2.3 event occurring at the depth of 18 km in the Los Angeles basin.
Upper Mid: The corresponding polarization diagrams. Onsets of the fast and slow shear waves are denoted by filled triangles and open triangles, respectively. The interval time between dots is 10 ms.
Upper Right: Aspect ratio diagrams.The maximum aspect ratio represented by a longest bar in the aspect ratio diagram indicates the direction of the maximum principal stress. The aspect ratio is defined as the ratio of the total projections of particle displacements onto a pair of orthogonal axes in a time window between the two split shear wave arrivals. The maximum aspect ratio determines the linear particle motion direction for the fast shear wave.
Lower Left: Ray tracing diagram for this event. P and S velocities are given for the sedimentary basin and crystalline basement, respectively. SCS - the station located in the USC campus. P - the P transmitted wave, PS - the P-to-S converted wave, S_1P - the S_1-to-P converted wave, S_2P - the S_2-to-P converted wave, S_1 - the fast S wave, S_2 - the slow S wave.
Lower Right: Synthetic phase velocity differences between the fast (dashed line) and slow (solid line) shear waves traveling in the basement (containing N-S aligned microcracks with the crack density of 0.04) versus azimuth angles from 0° to 360°, corresponding to the incidence angle at station SCS determined by ray tracing. The ordinate is in N-S while the abscissa is in E-W. The arrow points the phase propagation direction. The observed velocity difference between the two split shear waves for this event are denoted by a pair of asterisks.

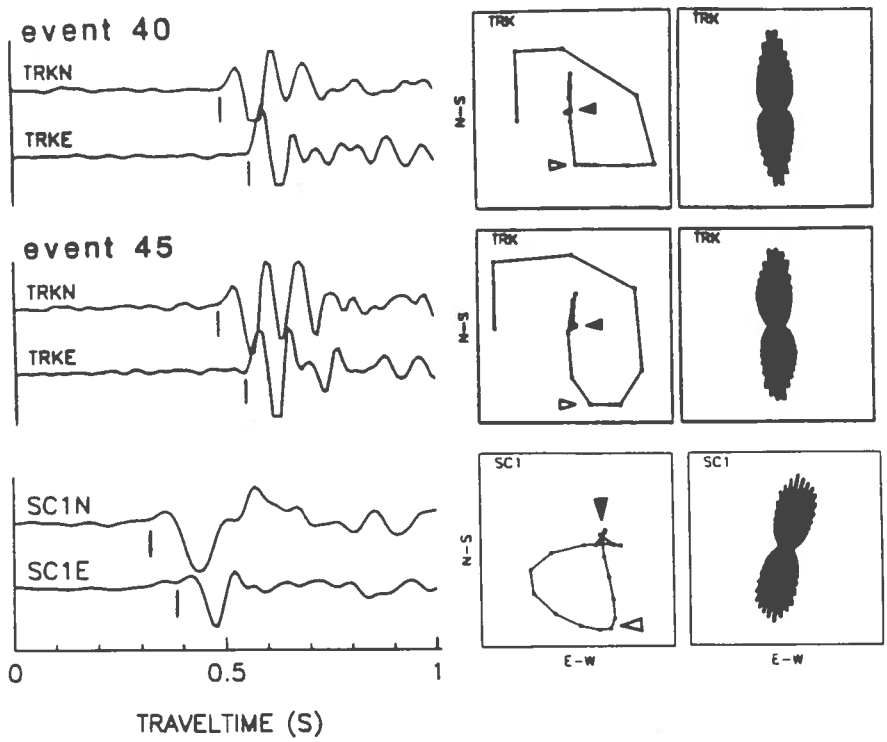

Fig. 3 Shear-wave splitting observed for three earthquakes occurring at the depth of ~12 km in the Los Angeles basin. The figure notation is the same as in Fig.2.

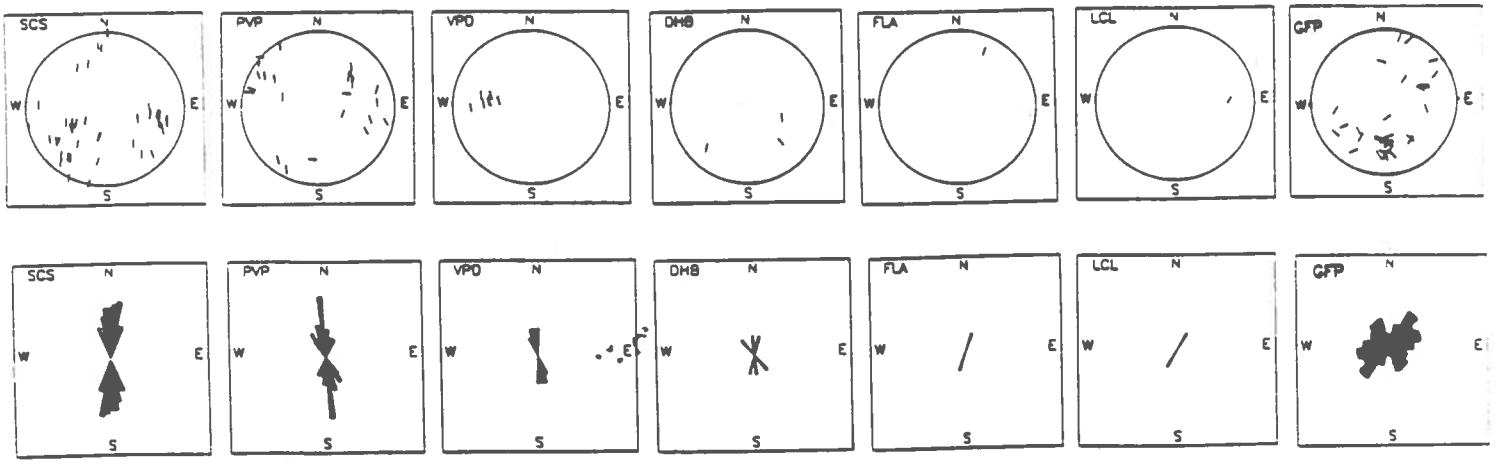

Fig. 4 Upper panels: Polarizations of the fast shear waves in seven shear-wave windows in the Los Angeles basin are plotted in equal-area projections of a lower hemisphere of directions out of 45°.
Lower Panels: Equal-area rose diagrams of the distributions of polarization directions of leading shear wave arrivals from events used in upper panels. The center of each panel corresponds to the station location.

Seismic Trapped Waves and Attenuation Along the Fault Zone of the Landers Earthquakes

Yong-Gang Li and Keiiti Aki

We used a mobile array of five REFTEKs with seven L4-C 1 Hz 3-component geophones and three FBA broad-band sensors to record aftershocks at eleven sites along the fault zone of the June 28, 1992 M7.4 Landers earthquake (Figure 1) for seismological study of fault zone details. At each site, seven geophones were deployed across and along the fault zone in an array with maximum offset $\pm$ 1 km from the fault trace (Figure 2). From mid July to mid August, we recorded more than 2000 aftershocks along a 45 km segment of the fault zone. We found large amplitude long period wavetrains with slight dispersion following S-waves on seismograms recorded by geophones located on or close to the fault trace for aftershocks occurring within the fault zone. Such wavetrains were not recorded by geophones located with large offsets from the fault trace for those same aftershocks. We interpret these wavetrains as fault zone trapped waves. As the fault zone low velocity layer (break-down zone, fault gouge ?) sandwiched between high velocity basement rocks forms a wave-guide, seismic energy may be trapped in this wave-guide when excited by earthquakes occurring within it. Because the excitation and recording of fault zone trapped waves is strictly dependent on locations both of seismic source and receiver relative to the fault zone wave-guide, we may obtained a high-resolution structural image of fault zone based on observation of fault zone trapped waves. The result may serve as a link between in-site fault zone dynamics studies and earthquake source studies.

Figure 3 shows clear evidence for fault zone trapped modes for two M2.0 aftershocks occurring at the depth of 6 km and 1.5 km south of the geophone array at recording site 8. Because P-motions registered by six geophones deployed on both sides of the fault trace show opposite directions, we believe that these two events occurred on the fault plane which transacts the geophone array. Large amplitude dispersive (between 2 Hz and 6 Hz) wavetrains following S-waves are recorded by geophones located close to the fault trace but not recorded by the two geophones located 1 km away from the fault trace. To confirm our observation of fault zone trapped waves, we used Coda waves to normalize seismograms recorded within and outside of the fault zone removing site and source effects from the surface recordings. The spectral ratio of the S-wave to Coda wave for each recording station is shown in Figure 3. We found that the maximum spectral ratio in a narrow frequency band with the central frequency of 3.5 Hz is registered by the station located closest to the fault zone, and the ratio decreases as the distance increases from the fault trace. We also found that seismic waves with high frequencies (>10 Hz) are attenuated rapidly within the fault zone but are not attenuated much outside the fault zone. These amplitude patterns of fault zone trapped waves strongly suggest the existence of fault zone low velocity wave-guide.

Based on our preliminary analysis of observed fault zone trapped waves, we found that the fault low velocity zone (LVZ) is well developed on the ~20 km long segment of the fault zone around the epicenter of main shock. The width of fault LVZ at Landers segment is estimated to be ~300 m; it is characteristic of low shear velocity (1.5-2.0 km/s) and low Q (~10) as comparison with flanking basement rocks with Vs~3.0 km/s. This fault LVZ may extend from the surface to depth at least 12 km in the rupture zone. The width of the fault LVZ is found to vary along the fault zone, being wider in the south segment around the main rupture region and narrower in the north segment along the pre-existing faults. We also found that the LVZ diminishes or becomes very narrow at the segment of the fault zone, 20 km north of the main shock epicenter, where the direction of the fault trace changes from sub-S-N to sub-E-W. These preliminary results from observations of fault zone trapped waves may be compared with results from geological and strong motion studies.

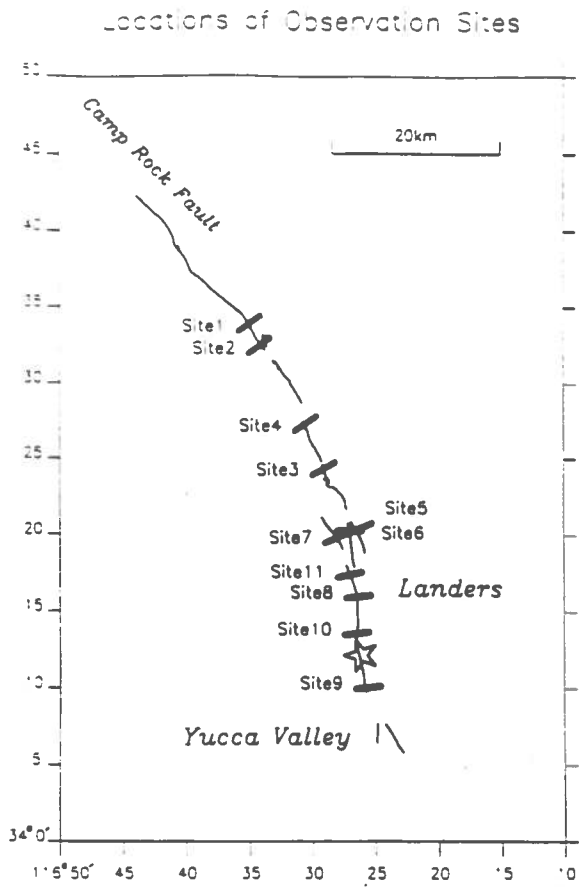

Fig. 1 The map of the fault zone surface trace of Landers earthquakes and locations of recording sites. The mobile REFTEK array is denoted by a solid bar at each site.

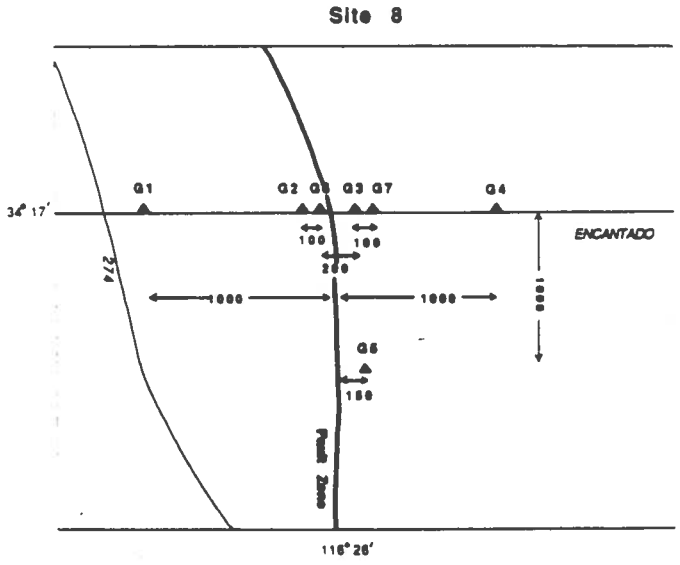

Fig. 2 The deployment layout of REFTEK array at recording site 8. Seven 1 Hz 3-component geophones are denoted by G1-7, respectively. The unit of the station space is meter.

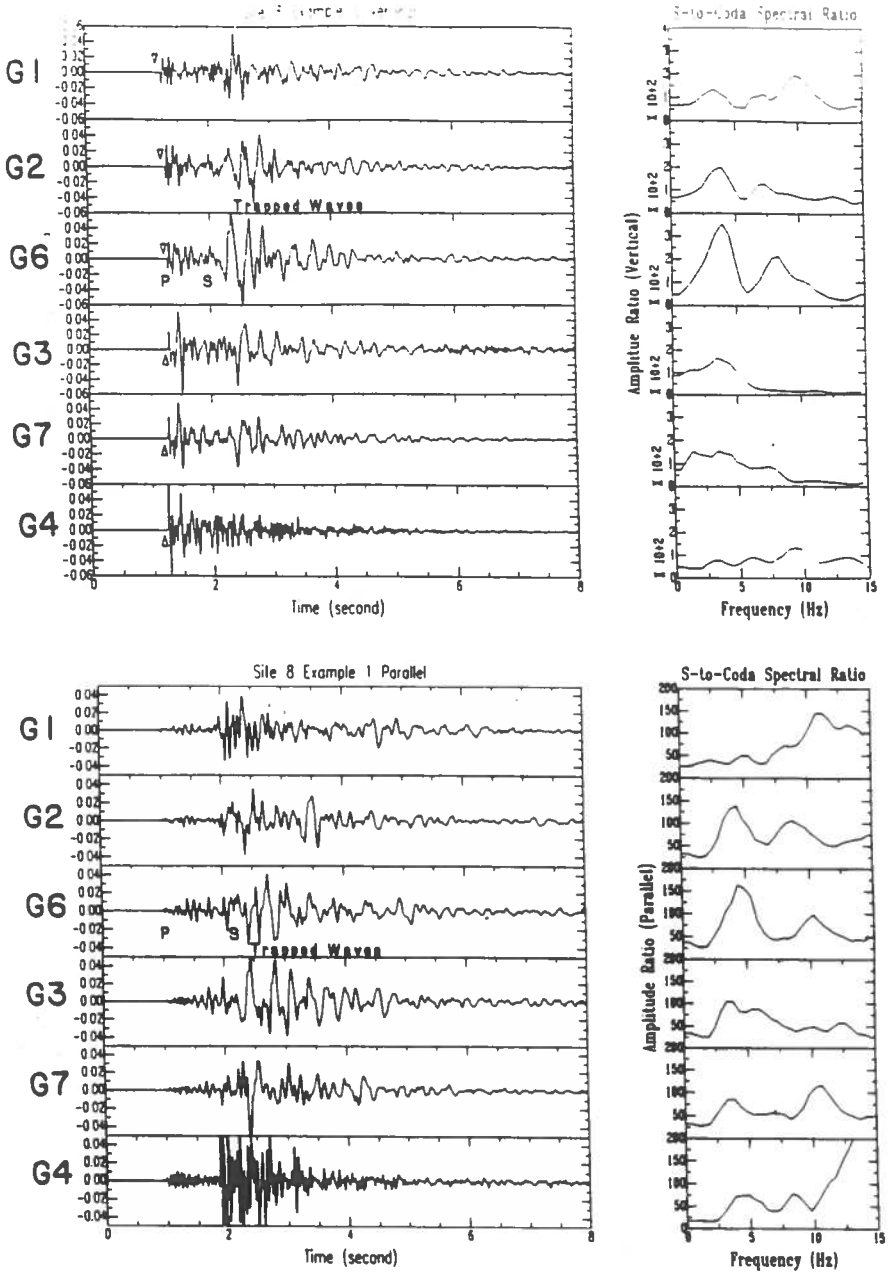

Fig. 3 Upper Left: Vertical components of seismograms recorded by six geophones deployed in a line across the fault trace at site 8 for a aftershock (R212:09:33) occurring within the fault zone. Open arrows point the directions of P-motions registered by the six sensors. Fault zone trapped waves clearly appear on seismograms from geophones G2, G6 and G3 which are close to the fault trace.
Right: Amplitude spectral ratioes of S-waves to Coda waves corresponding to seismograms in left panels. The maximum ratio is registered by G3 which is closest to the fault trace.
Lower Left: Horizontal components of seismograms (parallel to the fault plane) recorded by six geophones deployed in a line across the fault trace at site 8 for a aftershock (R212:19:36) occurring within the fault zone. Fault zone trapped waves clearly appear on seismograms from the two geophones G6 and G3 which are closest to the fault trace.
Right: Amplitude spectral ratioes of S-waves to Coda waves corresponding to seismograms in left panels. The maximum ratio is again registered by G3 which is closest to the fault trace.

SCEC ANNUAL PROGRESS REPORT: FY1992

SCEC SCIENTIST: Craig Nicholson, Institute for Crustal Studies, University of California at Santa Barbara, CA 93106-1100

1. The April 1992 M_L 6.1 Joshua Tree Earthquake Sequence: Seismotectonic Analysis and Implications

C. NICHOLSON (Institute for Crustal Studies, University of California at Santa Barbara, CA 93106), AND
E. HAUKSSON (Seismological Laboratory 252-21, California Institute of Technology, Pasadena, CA 91125)

The M_L 6.1 Joshua Tree earthquake of 23 April 1992 04:50 GMT occurred at 33°N 57.7', 116°W 19.2' about 8 km northeast of the southern San Andreas fault and about 20 km south of the Pinto Mt fault. It occurred at a depth of 12 to 13 km. The earthquake was preceded by a foreshock sequence that included a M_L 4.6 event at 02:25. The mainshock was followed by over 6,000 aftershocks recorded by the Southern California Seismic Network and an 11-element portable network deployed by the Southern California Earthquake Center (Figure 1). No surface rupture for the sequence has yet been found. The seismic moment is estimated at 2×10^{25} dyne-cm [*Kanamori*, 1992]. From the distribution of aftershocks and directivity effects, the mainshock ruptured unilaterally to the north along a fault about 15 km long. The focal mechanism indicated right-slip on a plane striking N14°W, dipping 80°W, with a rake of 175°. A large number of aftershocks occurred off the mainshock rupture plane on adjacent secondary structures, similar to the cross-shaped or 'winged-shaped' pattern of events following the 1979 M_L 5.5 Homestead Valley earthquake. Many of these off-fault earthquakes occurred on structures either sub-parallel to the mainshock plane or on secondary left-lateral faults that strike at high angles. Aftershocks continued to migrate to the north and south following the mainshock, and ultimately extended from the southern San Andreas fault near the Indio Hills to the Pinto Mt fault. The northern 15-km section of the aftershock zone had a strike more nearly N10°E. The 1992 Joshua Tree sequence occurred in the area of the 1940 M_L 5.3 Covington Flats earthquake—part of the premonitory activity leading up to the 1948 M_w 6.2 Desert Hot Springs event. The 1992 sequence was part of an accelerated moment-release rate that began in 1985–86 and which culminated in the M_S 7.5 Landers event that initiated north of the Pinto Mt fault. The Landers earthquake caused continued aftershock activity along the fault responsible for the Joshua Tree mainshock. Seismicity on nearly all the secondary structures active during the Joshua Tree sequence, however, ceased in the hours prior to the M_S 7.5 Landers event, and has not yet resumed.

2. SCEC Portable Instrument Deployment for the 1992 Landers - Big Bear Earthquake Sequence

F. VERNON AND A. EDELMAN (Scripps Institute of Oceanography, University of California, La Jolla, CA 92093),
C. NICHOLSON AND A. MARTIN (Institute for Crustal Studies, University of California at Santa Barbara, CA 93106-1100),
E. HAUKSSON AND D. JOHNSON (Seismological Laboratory 252-21, California Institute of Technology, Pasadena, CA 91125), AND
Y.-G. LI AND M. ROBERTSON (Department of Geological Sciences, University of Southern California, Los Angeles, CA 90089-0740)
S. DAY AND H. MAGISTRALE (Department of Geological Sciences, San Diego State University, San Diego, CA 92182)

A collaborative investigation of the June 1992 M7.5 Landers and M6.5 Big Bear earthquakes was undertaken by several groups associated with the Southern California Earthquake Center (SCEC), including Caltech, UC Santa Barbara, USC, UC San Diego, SDSU, IRIS/Passcal and the USGS. The M7.5 Landers earthquake occurred at 04:58 PDT about 10 km north of Yucca Valley along the southern extension of the Johnson Valley fault. Aftershocks extended from the Camp Rock fault at

34°N40', 116°W40' south to 33°N50', 116°W18'near the southern San Andreas fault—a distance of nearly 100 km (Figure 1). The M6.5 Big Bear earthquake occurred at 08:04 PDT about 35 km west of the Landers epicenter in the San Bernardino Mountains. The Big Bear aftershocks extend over an area about 30 km long, extending roughly NE between the San Andreas fault at Yucaipa to the Helendale fault. Four portable instruments were installed and operating within 12 hours, two in the San Bernardino Mountains near Big Bear, and the other two in the epicentral region of the Landers earthquake. By Tuesday, June 30, another 13 portable instruments were installed and operating (Figure 1). These instruments supplemented the regional network of permanent stations operated by Caltech/USGS, accelerometers operated by the USGS and CDMG, and temporary instruments deployed following the April M6.1 Joshua Tree earthquake and still in operation at the time of the June mainshocks. The portable equipment consists mostly of Reftek digital recorders using L-22 velocity and FBA acceleration sensors. Two sites employ Guralp broadband instruments, 3 sites use outputs from very broadband STS-2's, and 3 sites use digital SSR-1's. These instruments supplement 5 USGS GEOS instruments operating at the time of the Landers and Big Bear mainshocks. The SCEC data are 250 sps; several sites exhibit significant high-frequency (above 100 Hz) signal. Over 8 Gbytes have been collected; approximaely 8,000 events are recorded by 2 or more stations.

3. 3-D Tomographic Velocity Inversion of the 1992 Landers–Big Bear–Joshua Tree Sequence, Southern California

C. NICHOLSON (Institute for Crustal Studies, University of California at Santa Barbara, CA 93106-1100; craig@quake.ucsb.edu), AND
J.M. LEES (Department of Geology and Geophysics, Yale University, New Haven, CT 06511-8130; lees@lamb.geology.yale.edu)

The extensive seismicity associated with the 1992 Southern California earthquake sequence provides a high quality dataset for a detailed tomographic inversion of P-wave arrival times. The dataset, augmented by the 1986 North Palm Springs sequence, consists of 7009 events with more than 10 P-wave arrivals from the permanent Caltech/USGS network, providing 76,306 raypaths for inversion. The events were relocated relative to a standard 1D model used in previous inversions at North Palm Springs; station corrections were determined iteratively by manual inspection and relocation. The target area consisted of a 104×104×32 km^3 volume divided into 52×52×10 rectilinear blocks. Laplacian regularization was applied and the residual RMS misfit was reduced by ~30%. Preliminary results indicate a low-velocity anomaly that parallels the Landers rupture and dips to the west to 12-km depth. A high-velocity anomaly is present along the San Andreas fault between 5-12 km depth (Figure 2, Layers 5 & 6); such high-velocity anomalies are often sites of rupture nucleation.

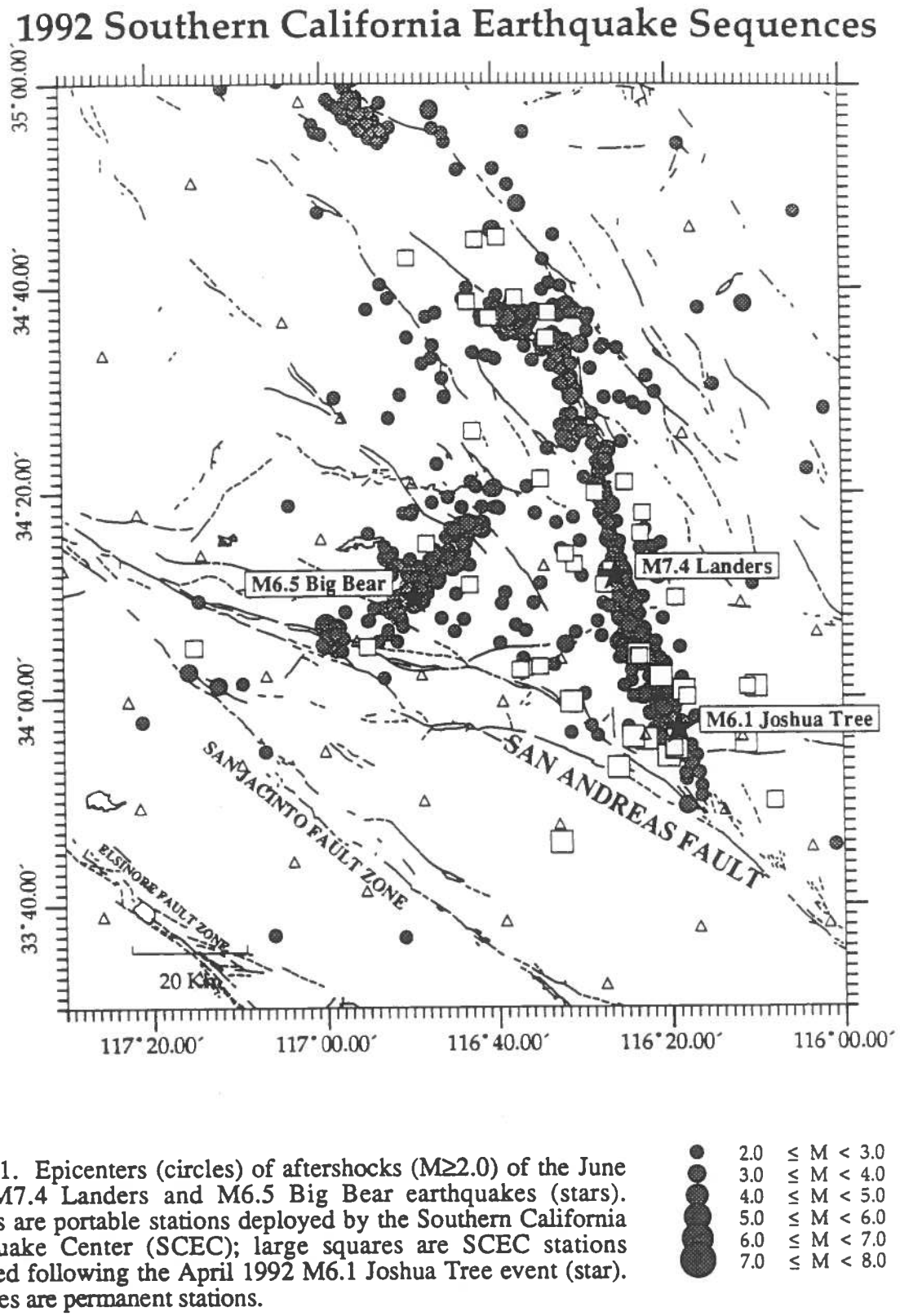

Figure 1. Epicenters (circles) of aftershocks (M≥2.0) of the June 1992 M7.4 Landers and M6.5 Big Bear earthquakes (stars). Squares are portable stations deployed by the Southern California Earthquake Center (SCEC); large squares are SCEC stations deployed following the April 1992 M6.1 Joshua Tree event (star). Triangles are permanent stations.

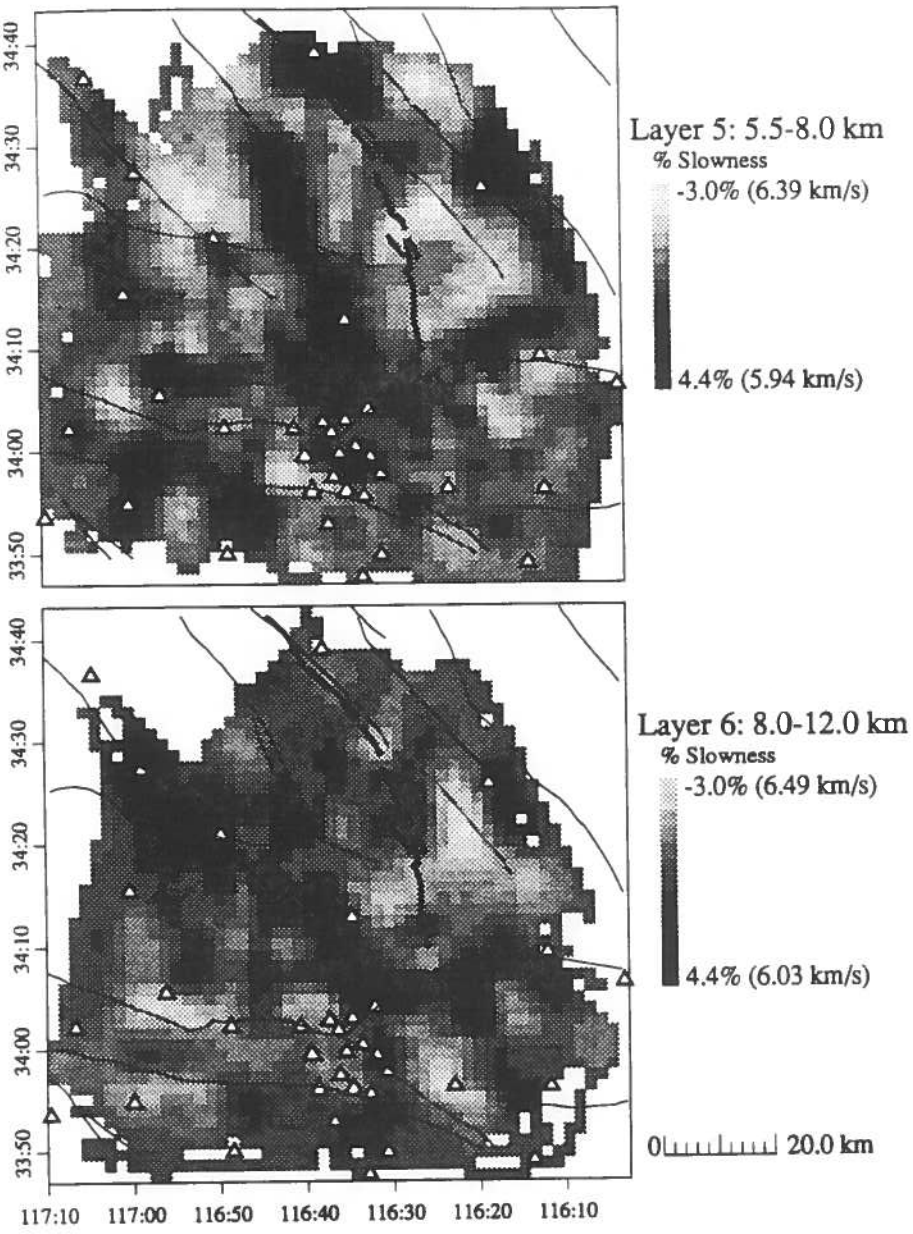

Figure 2. P-wave velocity perturbations (in %slowness) relative to a 1-D model. High slowness (low velocity) is black; low slowness (high velocity) is light grey. Heavy black line is the mapped surface rupture of the M7.5 Landers earthquake; light lines are faults from Jennings et al. [1975]. Open triangles are stations. Notice the high-velocity anomalies along the San Andreas fault through San Gorgonio Pass (Layer 6), and the prominant low-velocity anomaly that parallels the Landers rupture, but offset to the west and dipping west (Layer 5 and 6).

Fault Kinematics from Earthquakes in Southern California

L. Seeber and John G. Armbuster, Lamont-Doherty Geological Observatory

The main purpose of this project is to use the abundant earthquake data accumulated over the last decade by the Caltech-USGS network to map active faults and to study their interactions. Accomplishments so far include: 1) A set of relocated earthquakes and about 10,000 focal mechanisms over an area covering most of southern California; 2) A technique for tectonic analysis using a high-density field of focal mechanisms; 3) A structural model for the area from the Landers sequence to the northern San Jacinto fault zone; and 4) Concepts about fault interaction and the role of pre-existing faults in fault development derived from a comparison of the San Andreas fault zone along constricting bends at Loma Prieta and at San Gorgonio Pass.

We have generated a file of relocated hypocenters and quality-selected focal mechanisms in a single procedure for an area covering most of southern California (32.5N-35.5N; 114.5W-120.0W). We adopted a joint relocation technique based on location-dependent station-correction applied to a field of 10 distinct 1-dimensional velocity structures with smooth transitions between them. About 20,000 quality-selected hypocenters were obtained. Relatively accuracy is good, but systematic errors may be larger. Focal mechanisms were obtained with a grid-search scheme. After quality selection designed to optimize resolution and based on various parameters, we have obtained about 10,000 well-constrained focal mechanisms for southern California (1980-1990). Correlation between seismically defined and mapped faults provides constraints on systematic location errors.

The San Andreas fault (SAF) zone in the San Bernardino Mountains-San Gorgonio pass area is characterized by a particularly complex pattern of secondary faults, high uplift rates and unusually deep seismicity. This complex structure is centered at a major constricting left-stepping bend of the SAF. This bend is centered at the "T" junction between the SAF and the Pinto Mountain fault (PMF), a regional latitudinal left-lateral fault that terminates towards the west against the SAF. This fault was apparently not cut by either the Joshua Tree or the Landers rupture. Many features of the seismicity as well as surface structure suggest that the left bend in the master fault may reflect left slip on the PMF. Patterns of rupture along the SAF are thought to be profoundly affected by the constricting bend. If this bend is the result of the long-term interaction between the SAF and the PMF, then space-time rupture patterns on these faults may also be interdependent. Pre-1991 earthquake data delineate many active structures than can be grouped in three distinct zones bounded by the three branches of the "T" intersection. The San Bernardino Mountain zone, in the northwestern quadrant of the intersection, is characterized by a network of either northwest right-lateral or northeast left-lateral strike-slip faults. One of the later faults is recognized as the source of the 1992 Big Bear Lake earthquake. Thrusts dominate surface structure, and are also illuminated by the seismicity. This zone is interpreted as a southern extension of the Mojave block covered by north-verging thrust sheets which originate along the SAF and reflect space problems resulting from the bend. The Joshua Tree zone, in the southeast quadrant of the intersection, is also characterized by transcurrent faults, but the inferred direction of maximum horizontal compression is rotated clockwise relative to the San Bernardino area and secondary faults tend to be normal rather than thrusts. Finally, an east-west zone of abnormally deep and diffuse seismicity with a wide range of focal mechanisms characterizes the southwest side of the SAF. This zone is sharply defined in space and abuts the SAF at the intersection with the PMF, but it cannot, generally, be resolved into distinct faults. This seismic source may reflect diffuse deformation accommodating left shear along the westward extrapolation of the PMF and accounting for the bend on the SAF.

Change in Failure Stress on the San Andreas and Surrounding Faults Caused by the 1992 M=7.4 Landers Earthquake

Ross S. Stein, Geoffrey C.P. King, and Jian Lin

The Landers earthquake brought the San Andreas fault significantly closer to failure near San Bernardino, a site that has not sustained a large earthquake since 1812. Stress also increased on the San Jacinto Fault near San Bernardino and on the San Andreas fault southeast of Palm Springs. Unless creep or moderate shocks relieve these stress changes, the next great earthquake on the southern San Andreas is likely to be hastened by a decade. In contrast, stress on the San Andreas north of Los Angeles dropped, potentially retarding the next great earthquake there by several years.

In our SCEC investigation, we show that several small shocks which occurred near the Landers event during the preceding 17 years increased stress along much of the eventual Landers rupture path. Similarly, we argue that the Landers earthquake and its aftershocks have changed the stress along the San Andreas fault system. We use an elastic-halfspace boundary element model to simulate the immediate static response of the crust to the earthquakes. Earthquakes are represented by cuts extending from the ground surface to 12.5 km depth using published seismic moments; stress is sampled at a depth of 6.25 km. To assess the long-term response after the lower crust has fully relaxed, we use an elastic plane-stress boundary element model, in which the seismogenic zone is treated as a 12.5-km-thick plate. In practice, the halfspace yields a lower bound on the stress changes, and the plate model furnishes an upper bound.

To gauge the change in proximity to failure of faults in the earth's crust, we calculate the Coulomb failure stress change, $\Delta\sigma_f$, acting on vertical planes in the crust. Here $\Delta\sigma_f = \Delta\tau_s + \mu(\Delta\sigma_n - \Delta P)$, where $\Delta\tau_s$ is the static shear stress change (positive in the direction of the regional τ_s) and $\Delta\sigma_n$ is the normal stress change (positive tensile), μ is the static coefficient of friction, and ΔP is the pore pressure change. For plausible fault zone rheologies $\Delta\sigma_f$ may reduce to $\Delta\tau_s + \mu'(\Delta\sigma_n)$, where $\mu' = \mu(1-B)$ and B is Skempton's coefficient, which can range between 0-1 [*Rice*, 1992]. Thus ΔP acts to cancel $\Delta\sigma_n$, and low μ' may be the product of laboratory values of μ (0.75) and high pore fluid pressure ($B \rightarrow 1$). We examined $\mu' = 0.0$-0.75; the figures illustrate $\mu' = 0.4$. We assign a regional principal compressive stress of 100 bars aligned N7°E. This is the orientation of the measured principal strain contraction there [*Lisowski et al.*, 1991; *Sauber et al.*, 1986]. It is also the orientation derived from stress inversion of small shocks along the nearest 50-150 km of the San Andreas fault [*Jones*, 1988; *Williams et al*, 1990].

The change in Coulomb failure stress caused by the 1975 Galway Lake, 1979 Homestead Valley, 1986 North Palm Springs and 1992 Joshua Tree earthquakes is shown in Fig. 1a. The shocks caused a ~1 bar increase in the proximity to failure of the Landers fault at the future epicenter. Equally important, the failure stress along most of the future Landers rupture rose about 1 bar. For comparison, the Landers earthquake stress drop was ~85 bars. *Stein & Lisowski* [1983] showed that aftershocks of the 1979 Homestead Valley earthquake occurred where the Coulomb failure stress increased by as little as

---

G.C.P. King (Institut de Physique du Globe, Strasbourg 67084, France) and J. Lin (Woods Hole Oceanographic Institution, Woods Hole, MA 02543) are 1991/92 SCEC Visiting Fellows. R.S. Stein is at the U.S. Geological Survey, MS 977, Menlo Park, CA 94025.

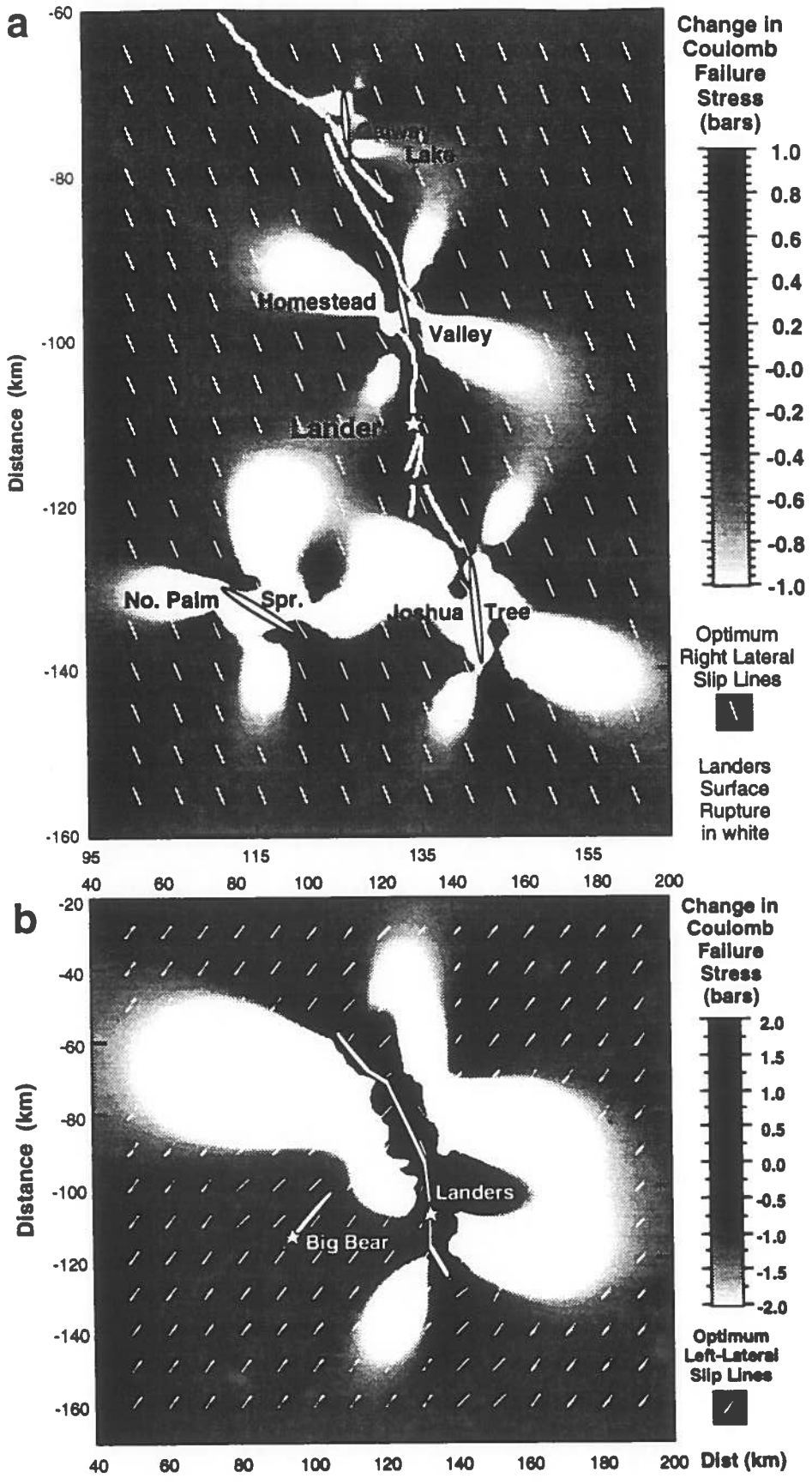

Fig. 1. (a) Failure stress changes (for μ = 0.4) caused by the four *ML*≥5.2 shocks within 50 km of the Landers earthquake occurring during 17 yr before the right lateral Landers rupture. Note that the Landers surface rupture tends to lie within the zone of elevated failure stress change. (b) Failure stress changes (μ=0.4) preceding the left-lateral Big Bear aftershock of the Landers earthquake. The stress change at the Big Bear epicenter is 3.0 bars. The Landers rupture is divided into 11 slip segments based on preliminary fault mapping and seismic data from *Rubin et al*, *Ponti et al*, *Ekström et al*, and *Thio et al* (written communication). Both models are carried out for 12.5 km-deep faults embedded in an elastic halfspace with Poisson's ratio of 0.25 and Young's modulus of 8.8E11 dyne-cm-2. For all figures, 80 km E. dist. = 117°W long.; -20 km N. dist. = 35°N lat.

0.3 bar, and that the Landers fault crept about 10 cm near the future epicenter during 2 years following the Homestead earthquake. Thus some parts of the Landers fault were apparently near failure 12 years ago. Two months before the Landers rupture, the Joshua Tree earthquake further increased the stress.

The same process of stress transfer can be observed with the apparent triggering of the Big Bear earthquake 3 hr 26 min after the Landers shock. The Landers rupture increased the proximity to failure at the Big Bear epicenter by 3 bars (Fig. 1b). The rupture plane of the Big Bear shock is optimally aligned for failure, lies in the largest lobe of enhanced Coulomb failure stress resulting from the Landers event, and terminates where the failure stress change becomes negative. Smaller aftershocks during the 25 days after the main shock occur in regions where the failure stress increased by 0.1 bar or more, and aftershocks rarely occur where the failure stresses dropped more than 0.3 bars (Fig. 2). Within the four largest lobes of enhanced failure stress, aftershocks extend SW to the San Andreas and San Jacinto faults near Yucaipa, SE of the Landers fault to the San Andreas toward Indio, and NE to the Pisgah fault. Northwest of the Landers rupture, the Camp Rock, Lenwood, Blackwater and eastern Garlock faults, have been loaded; Landers aftershocks are found on or near these faults. Aftershocks are absent where the San Andreas fault is closest to the Landers rupture, between Yucaipa and Indio, where predicted stress changes are negative. Near Indio the San Andreas was loaded by the Landers, Imperial Valley, Elmore Ranch, and Superstition Hills events. Despite this, few aftershocks are found along this segment.

San Andreas segmentation inferred by the [*Work. Group on CA. EQ Probabilities*, 1988] accord roughly to changes in the failure stress imposed by the Landers event. In Fig. 3a the failure stress is resolved on the San Andreas fault, rather than illustrating the maximum stress independent of orientation, as shown in Fig. 2. The immediate, post-Landers stress change is positive in the central Coachella Valley segment, negative at the segment boundary near Desert Hot Springs, and is greatest in the San Bernardino Mountain segment (site of a M_L=4.4 aftershock 37 min before the Big Bear shock). All of the Mojave segment is negative (Fig. 3a). The failure stress change on the northern San Jacinto fault SE of San Bernardino, which though farther from Landers is more favorably oriented than the San Andreas, is 1 bar. The stress change resolved on the San Andreas is more positive for high μ, since tension normal to the fault increases.

We calculate the response of the San Andreas to the stress changes shown in Fig. 3a by letting the fault slip freely to relieve shear stress imposed by the surrounding earthquakes (Fig. 3b). The immediate response is slip of 15 cm near Yucaipa (equivalent to a **M**=6.2 event if it occurred seismically), and 5 cm NW of Indio (equivalent to **M**=5.9). In contrast, a load comparable to a **M**=6.1 event is removed from the Mojave segment, and a **M**=6.0 load is removed at Desert Hot Springs, taking these fault strands farther from failure. Thus two moderate events are needed simply to relieve the immediate stresses added by the Landers earthquake. After relaxation of the viscous substrate, the stress change on the San Andreas and surrounding faults doubles (Fig. 3a, thick curve), and the slip required to relieve the stress will also rise (Fig. 3b, light fields). So far neither creep nor moderate earthquakes have occurred on the San Andreas fault since the Landers earthquake. If these events do not take place, the probability of great earthquakes on the San Andreas must rise as well.

A moderate event on the southern San Andreas fault could cascade into a great earthquake. All or part of the San Bernardino Mountain segment last ruptured no later than 1812 [*Jacoby et al.*, 1988]; given its 24±3 mm/yr slip rate [*Weldon and Sieh*, 1985], a ≥4.3-m slip deficit has since accumulated, which could yield a M≥7.5 event. The Coachella Valley segment last ruptured in 1680, has a prehistoric repeat time of ≥235 yrs [*Lindh*, 1988], and has accumulated a ≥6 m deficit (M≥7.5). The San Bernardino Valley segment of the San Jacinto fault may have last ruptured in 1890; it has a slip rate of 8±3 mm/yr [*Working Group on California Earthquake Probabilities*, 1988], and thus has a slip deficit of ≥0.8 m (M≥6.8).

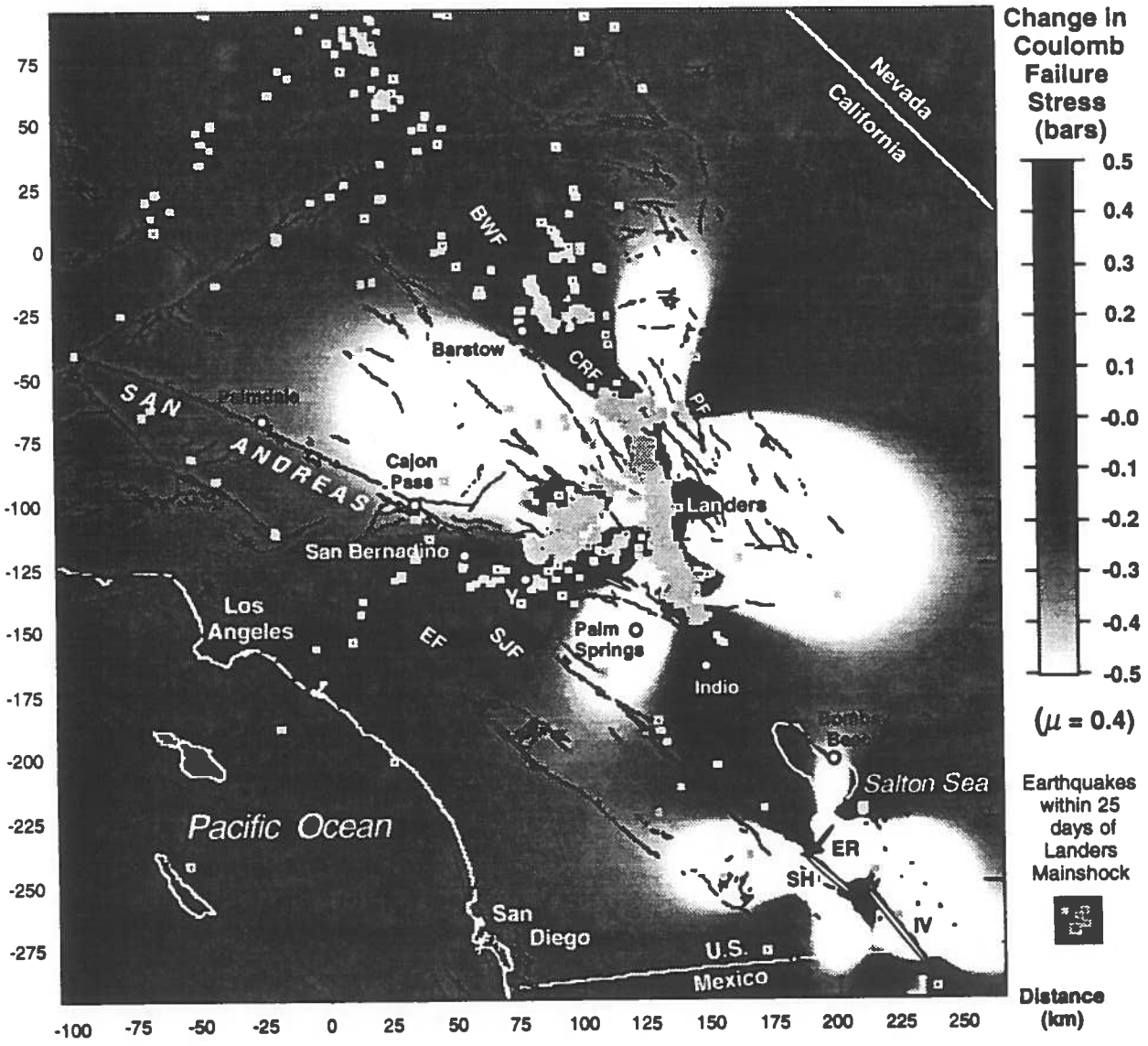

Fig. 2. Coulomb failure stress changes caused by M≥6 earthquakes in southeastern California during 1979-1992. *ML*≥1 earthquakes are from Caltech-USGS RTP network (rms≤0.4 s, ≥7 arrivals). Stress changes caused by the Imperial Valley (IV), Elmore Ranch (ER) and Superstition Hills (SH) earthquakes are included. Stress has risen in the Coachella Valley (Bombay Beach to north of Indio) and the San Bernardino Mountains (North of Palm Springs to Cajon Pass). The western Mojave Desert (Cajon Pass to west edge of map) has been unloaded. Y=Yucaipa. Other faults are Elsinore (EF), San Jacinto (SJF), Garlock (GF), Camp Rock (CRF), Pisgah (PF), Lenwood (LF), and Blackwater (BF).

The correspondence between seismicity and the Coulomb failure stress changes produced by the Landers and earlier events suggests that regions of predicted increase are candidates for future major events. The probability of a great earthquake on the southern San Andreas is already high; it was estimated to be 60% by the year 2018 [*Working Group on California Earthquake Probabilities*, 1988]. We estimate the change in occurrence time of great earthquakes on the San Andreas by dividing the immediate slip required to relieve the applied shear stress shown in Fig. 3b by the ~24±3 mm/yr San Andreas slip rate. This yields an advance in the time of the next San Bernardino Mountain and Coachella Valley earthquakes by 6 and 2 years, respectively, and a delay in the next Mojave shock by 2 years.

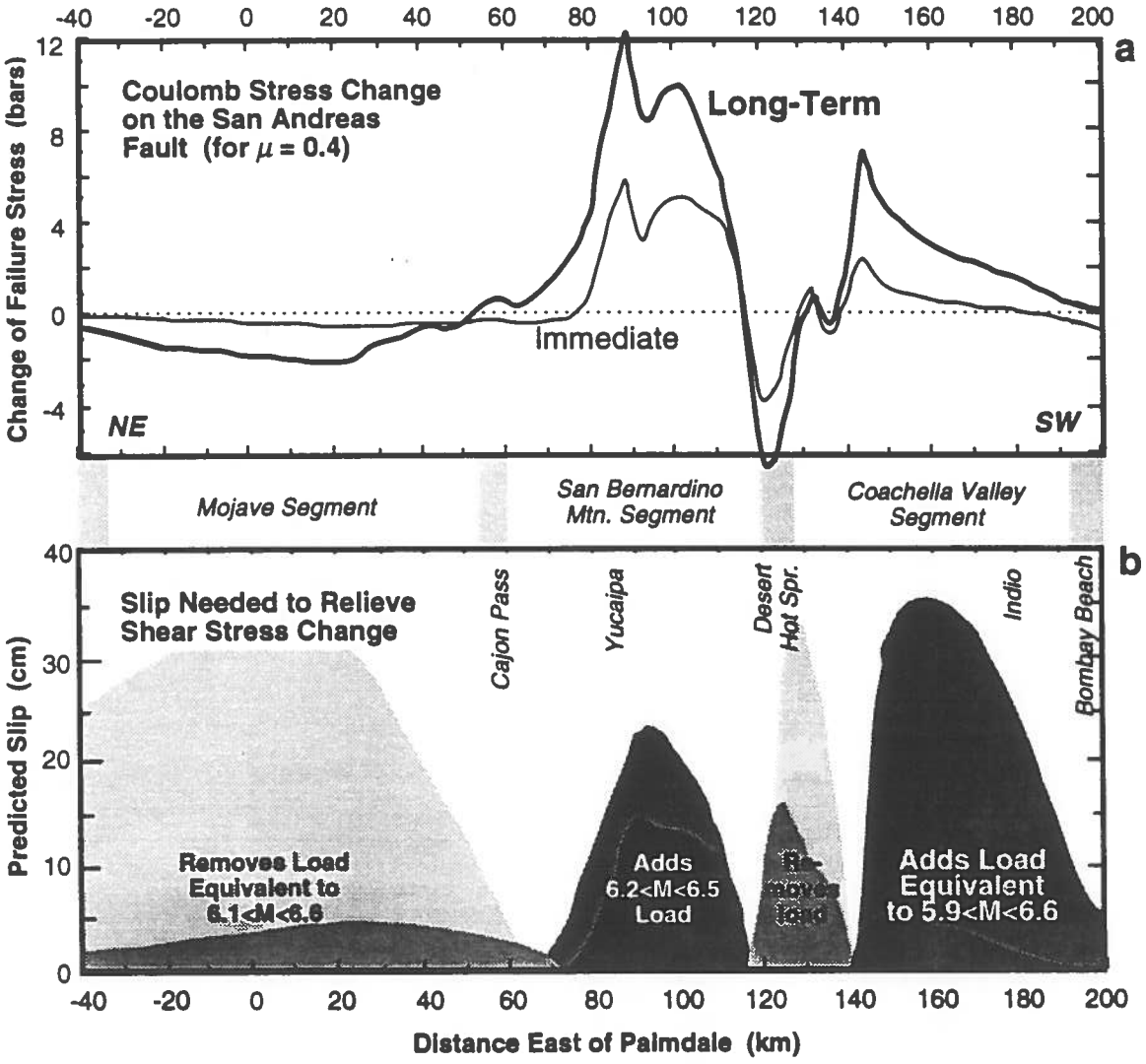

Fig. 3. (a) Change in the Coulomb failure stress resolved on the San Andreas fault caused by M≥6 earthquakes in southeastern California since 1979. Model fault is vertical and passes between the two San Andreas surface strands east of Yucaipa. (b) Corresponding slip distribution along the San Andreas fault needed to relieve shear stress imposed by M≥6 earthquakes since 1979. Immediate changes (larger displacements shown by darker stiples) are calculated in an elastic halfspace, and so the base of the fault restrains displacement. Long-term changes are calculated in an elastic plate, with upper and lower surfaces stress-free. Long-term changes probably correspond to 10-100 yr after the earthquake.

SCEC Portable Instrument Deployment for the 1992 Landers - Big Bear Earthquake Sequence

F. VERNON AND A. EDELMAN (Scripps Institute of Oceanography, University of California, La Jolla, CA 92093),
C. NICHOLSON AND A. MARTIN (Institute for Crustal Studies, University of California at Santa Barbara, CA 93106-1100),
E. HAUKSSON AND D. JOHNSON (Seismological Laboratory 252-21, California Institute of Technology, Pasadena, CA 91125),
Y.-G. LI AND M. ROBERTSON (Department of Geological Sciences, University of Southern California, Los Angeles, CA 90089-0740),
S. DAY AND H. MAGISTRALE (Department of Geological Sciences, San Diego State University, San Diego, CA 92182)

A collaborative investigation of the June 1992 M7.5 Landers and M6.5 Big Bear earthquakes was undertaken by several groups associated with the Southern California Earthquake Center (SCEC), including Caltech, UC Santa Barbara, USC, UC San Diego, SDSU, IRIS/Passcal and the USGS. The M7.5 Landers earthquake occurred at 04:58 PDT about 10 km north of Yucca Valley along the southern extension of the Johnson Valley fault. Aftershocks extended from the Camp Rock fault at 34°N40', 116°W40' south to 33°N50', 116°W18' near the southern San Andreas fault—a distance of nearly 100 km. The M6.5 Big Bear earth-quake occurred at 08:04 PDT about 35 km west of the Landers epicenter in the San Bernardino Mountains. The Big Bear aftershocks extend over an area about 30 km long, extending roughly NE between the San Andreas fault at Yucaipa to the Helendale fault. Four portable instruments were installed and operating within 12 hours, two in the San Bernardino Mountains near Big Bear, and the other two in the epicentral region of the Landers earthquake. By Tuesday, June 30, another 13 portable instruments were installed and operating. These instruments supplemented the regional network of permanent stations operated by Caltech/USGS, accelerometers operated by the USGS and CDMG, and temporary instruments deployed following the April M6.1 Joshua Tree earthquake and still in operation at the time of the June mainshocks. The portable equipment consists mostly of Reftek digital recorders using L-22 velocity and FBA acceleration sensors. Two sites employ Guralp broadband instruments, 3 sites use outputs from very broadband STS-2's, and 3 sites use digital SSR-1's. These instruments supplement 5 USGS GEOS instruments operating at the time of the Landers and Big Bear mainshocks. The SCEC data are 250 sps; several sites exhibit significant high-frequency (> 100 Hz) signal. Over 8 Gbytes have been collected; approximaely 8,000 events are recorded by 2 or more stations.

Group G: Physics of Earthquake Sources

Group Leader: Leon Knopoff

* This Progress Report under Group A.

Summary Report for Group G - Earthquake Physics

Leon Knopoff - Group Leader

I. Phenomenology

The seismicity of Southern California is a target for constructing physical models of the occurrence of earthquakes in the region. The seismicity of Southern California has the usual well-substantiated statistical attributes: 1) the Gutenberg-Richter frequency of occurrence law, 2) the Omori law for the decay of aftershocks, 3) the Kagan-Knopoff inverse power law for the distribution of epicenters in space. The fault map of Southern California gives additional constraints on the modeling process. Other presumed correlations are reported occasionally, but we found in the time period 1933-1992 that it is difficult to give them statistical significance, they may be fluctuations due to unique local structures. New contributions to the seismicity of Southern California are:

1. Keilis-Borok and Levshina have found that there is a large increase in seismicity with intermediate magnitudes, before all but one of the earthquakes with $M \geq 6.4$, since the time that the catalog was given in 0.1 magnitude intervals. Each strong earthquake with $M \geq 6.4$ is preceded by a burst of earthquakes above a certain threshold with magnitudes in the range $4.8 \leq M \leq 6.4$ in a two year window; the peak does not disappear in more than 1 year before each strong earthquake. If the lower threshold is lowered to 4.6, the correlation is substantially weakened. The precursor earthquakes are widespread in two-dimensions over all of the region, and are not local with respect to the later strong earthquake. Some latitude of the values of the parameters can be allowed.

If the magnitude threshold for a strong earthquake is lowered to 6.0, all earthquakes in this category in Southern and Northern California and in the Cape Mendicino area are preceded by a significant increase in numbers of earthquakes in the range between $4.2 \leq M \leq 5.9$ in an area of radius 1^{o}. If it is hypothesized that the precursory peak in intermediate magnitude seismicity occurs in a region where time and space windows scale with the future great earthquake, then the one failure (see above), which was the Landers earthquake, is "predicted" as well by the same algorithm. Thus all earthquakes in Southern California with magnitudes $M \geq 6.0$ are preceded by a suitably scaled burst of precursory activity.

2. Kagan has studied whether the recent proposal by Pacheco et al. that there is a kink in the frequency of occurrence law that corresponds to earthquakes with down-dip fracture dimensions near that of the thickness of the seismogenic zone, and finds that this proposal cannot be substantiated statistically. The numbers, especially of small strike-slip earthquakes with moments less than the kink value are too small in the

Harvard CMT catalog to confirm or deny this proposal. The same argument applies for large earthquakes in subduction zones with magnitudes greater that the kink value. Kagan also finds a statistically significantly larger mean normal stress and a larger shear stress (in precursory earthquakes) before large earthquakes than after them.

3. Scholz is studying the geometry of growth of tensile cracks in previously unfractured, but initially flawed, thin glass plates.

II. Physics of Fault Zones

Most models of seismicity make an a priori assumption regarding the nature of the bonds that restrain slip in the fault zones. These bonds must ultimately weaken and break under sufficiently large stress, whether quasistatically or dynamically derived. Increasingly we have been concerned that a simplistic (parametric) picture of the rheological and geometrical nature of the fault zone, especially that it is a simple fracture surface, is not adequate for our needs. In particular we must recognize that the fault zone is a region of finite width, filled with gouge fragments derived from the ongoing fault process. We need to know more about how a finite layer of gouge deforms under stress and how it fails under stress.

1. Scott has been performing laboratory deformation experiments on natural gouge. During deformation in bulk, the shear strain in a sample will localize to a single shear band inclined at about 30^{o} to the axis of compression with a steady state coefficient of friction of about 0.45. During continued deformation, this layer becomes thinner with lower coefficients of friction corresponding to larger rates of thinning. But deformation experiments on thin samples show that the coefficient of friction is around 0.75, a value consistent with a theory that takes into account the development of shear bands oblique to the layer. The two results appear to be a property of the mode of the experiments. A hypothesis is proposed that the smaller value is preferred as a long-term property while the latter is a transient.

2. Sammis has done experiments to measure the relevance of rate- and state-dependent laws of creep, if a layer of gouge is introduced between two rigid rock surfaces. He finds the same qualitative behavior as in the rock-on-rock experiments. He proposes that any differences can be accommodated by a critical slip strain in the layer, rather than a critical slip displacement, so that a wider "crack" zone should be more stable, as is presumed to be in the creeping section of the San Andreas fault, than in "locked" or brittle fracture zones that support large earthquakes.

III. Modeling of Seismicity

Recent efforts at modeling by this group still show significant divergence of opinion of the appropriate physics of the rupture process, with consequent significant divergence of the output among the end products. This is a process that is undergoing continuing refinement that will ultimately yield an appropriate vehicle for the study of Southern California seismicity. I believe that the "final model" or models, will contain aspects of all three of these systems. The differences are outlined in the following table:

Rice	Shaw	Knopoff
quasistatic	dynamic	dynamic
3-D	1-D	1-D
precursory creep (rate-state)	creep + brittle fracture	brittle fracture
homogeneous	homogeneous	inhomogeneous friction
slip events only	no elastic wave radiation	elastic wave radiation
fast "fracture" drop	velocity weakening	instantaneous decrease in friction

1. Rice considers the growth of cracks under a viscous slip condition at the edges. The slip condition is the rate-state-dependent model with a critical displacement criterion for fracture. Because of the latter the cracks cannot grow elastically and hence remain viscous slip events. The cracks are inbedded in a 3-D infinite elastic medium. For a purely homogeneous system, no (chaotic) complexity of slip events evolves, but rather they develop into a series of periodic individual events. To develop a broad spectrum of slip sizes, inhomogeneity in the fault region must be invoked.

2. Shaw considers a 1-D dynamical crack model without a radiative seismic energy loss. Hence, there are no seismic waves, but the elastic fractures simulate earthquakes slip events. The dissipation is in the velocity-dependent friction. When viscosity is added to the fracture criterion, making it viscoelastic, foreshocks and aftershocks are developed as supplements to the usual (dynamical chaos) complex history of independent events. There is no long term localization because of the homogeneity of the system. The statistical identification of intermediate-term precursors is being made through a clustering algorithm.

3. Knopoff considers a 1-D dynamical crack model with seismic radiation effects, which have a strong influence on damping fracture growth. The system has a velocity-independent sliding friction. The breaking or critical fracture strength is strongly heterogeneous, which induces localization approximating the characteristic earthquake model, with an overlay of chaotic features. It has been observed that quasistatic models

must derive accurately the state of stress on the fracture surface after rupture to approximate the results from dynamical models; assumption that the final stress is the sliding friction is a poor one, because of failure to take into account dynamical overshoot due to healing.

In an application to the patterns of seismicity of multiple interacting fault strands in Southern California, a study has been made of the pattern on two fault strands each with spatial inhomogeneity of fracture strength. (A good example of parallelism in Southern California is the interaction between the San Jacinto and San Andreas faults in the southern part of the region.) In general the strand with the greater strength is "locked" and most of the seismicity appears on the weaker. The "interesting" dynamics appears at the regions of crossover in strength. Here the seismicity undergoes frequent and erratic shifts from one strand to the other often over very long periods of time. At this time it is difficult to evaluate the potential that a strong earthquake on one strand trigger a strong earthquake on the other, without knowing a very long sequential history of seismicity of (many) strong earthquakes on both.

Kagan, Y. Y., (UCLA): SCEC 1992 annual summary report.

During the period from March 1, 1992, to September 24, 1992 I have conducted research in two fields: (1) Physics of earthquake source, and (2) Master model.

(1) I have reviewed (with L. Knopoff, see paper [6] below) statistical tests used to prove the nonlinearity of the magnitude-frequency law, in particular the suggestion that the b-value of small earthquakes differs from that of large events (Pacheco, Scholz, and Sykes, *Nature*, **355**, 71, 1992). For this purpose we analyze the scalar seismic moment data listed in the Harvard catalog. The statistical analysis shows no significant b-value crossover in the magnitude interval 6.0–7.5, which is most often invoked as the place where an earthquake rupture should modify its character from two-dimensional to one-dimensional and hence, it is expected, that the b-value should change. Actually our simulations show that the quantity of available data is now insufficient to resolve this problem, even if such b-value change exists. It will require significant time of additional observation to prove the existence of b-value variation in the magnitude interval.

I have also started the study of statistical relations between the incremental stress caused by prior earthquakes and the occurrence of future events. There are two reasons to investigate such relations: (a) to study the fracture criteria for earthquakes, and (b) to predict earthquakes based on the analysis of stress patterns. Initially, I analyze statistically the Harvard catalog of seismic moment tensor solutions. Since detailed geometry of earthquake faults is not known in most seismogenic regions, I determine stress invariants or principal stresses (Jaeger and Cook, 1979). In Fig. 1, I show the distribution of the first invariant (I_1) and of the square root of the second deviatoric invariant ($\sqrt{-J_2}$) of the incremental stress. These distributions are calculated for two cases: for earthquakes preceding a reference event and for those following the event. We can compare how two factors influence the stress: the geometry of the seismogenic zone and static incremental stresses which influence the occurrence of future earthquakes. It is clear from the plot that the deviatoric stress before an event is larger than the stress caused in the neighborhood of the centroid by earthquakes that follow. Hopefully this feature may be used for earthquake forecasting.

(2) I have reviewed statistical tests used to prove the characteristic earthquake hypothesis [5]. Several distributions of earthquake size (seismic moment-frequency relations) are described. Based on the results of other researchers as well as my own tests, I show that the evidence of the characteristic earthquake hypothesis can be explained either by statistical bias, or statistical artifact. Since other distributions of earthquake size provide a simpler explanation for available information, the hypothesis cannot be regarded as proven.

D. Jackson and I extrapolate recent seismicity and focal mechanisms to predict local and global earthquake probabilities [7]. We map probabilities of centroid position and of focal mechanism orientation for future earthquakes. Earthquake focal mechanisms are used to obtain expected hazard maps, to forecast mechanisms for future earthquakes, and to calculate possible random variations of the forecast mechanism. We base our forecast on temporal clustering of large earthquakes (Kagan and Jackson, *GJI*, **104**, 117, 1991) and on correlations of seismic moment tensor solutions [4]. Seismicity levels undergo random variations thus we can extrapolate the earthquake occurrence only for a time

comparable to the length of the catalog (about 15 years for the best catalogs of focal mechanisms). We use temporal and spatial smoothing with exponents $\theta = -0.5$ and $\delta = -1.0$, respectively. We can update seismic hazard maps as soon as moment tensor solutions are available, usually a few hours after a significant earthquake. We illustrate the results with a seismicity forecast in the neighborhood of the Landers earthquake of 1992. For this prediction we use the Harvard catalog of seismic moment solutions. For latitude and longitude limits $33.5 - 35.5°N$, $115.5 - 117.5°W$, for the period starting 1/1/1977 we obtain the following Poisson probabilities for an earthquake with $M \geq 7$: period end 1/1/1985 - $2.4 \cdot 10^{-10}$eq·day^{-1}km^{-2}, period end 1/1/1992 - $3.5 \cdot 10^{-10}$eq·day^{-1}km^{-2}, period end 7/1/1992 - $5.8 \cdot 10^{-10}$eq·day^{-1}km^{-2}. The increase of these probabilities is caused by a general seismic activation in recent years in Southern California (*cf.* Jones, Hauksson, and Kanamori, *EOS*, **72**, 320, 1991), and by the occurrence of the Joshua-Tree–Landers–Big-Bear sequence of earthquakes. If we use the clustering model, the probabilities increase significantly: for example, on 7/1/1992 for $\theta = -0.2$ the next day probability is 2.1 times higher than the Poisson, for $\theta = -0.5$ the probability is 8.9 times higher than the Poisson. We show the hazard map calculated for 1/1/1992 using $\theta = -0.5$ (Fig. 2). The circle's area is proportional to the probability of an earthquake, and the predicted focal mechanism is displayed in a standard format. The map predicts the focal mechanisms of Joshua-Tree–Landers earthquakes.

Published or prepared papers:

1. Kagan, Y. Y., 1992. Seismicity: Turbulence of solids, *Nonlinear Sci. Today*, **2**, 1-13, (SCEC publication number 3).
2. Kagan, Y. Y., 1992. On geometry of earthquake fault system, *Phys. Earth Planet. Interiors (PEPI)*, **71**, 15-35.
3. Molchan, G. M., and Y. Y. Kagan, 1992. Earthquake prediction and its optimization, *J. Geophys. Res.*, **97**, 4823-4838, (SCEC publication number 4).
4. Kagan, Y. Y., 1992. Correlations of earthquake focal mechanisms, *Geophys. J. Int.*, **110**, 305-320.
5. Kagan, Y. Y., 1992. Statistics of characteristic earthquakes, *Bull. Seismol. Soc. Amer.*, accepted, (SCEC publication number 5).
6. Knopoff, L., and Y. Y. Kagan, 1992. Earthquake size distribution, manuscript, in preparation.
7. Kagan, Y. Y., and D. D. Jackson, 1992. Forecasting focal mechanisms, manuscript, in preparation.

Invited talks during this period:

1. Seismological Society of America, 1992 annual meeting at Santa Fe, April 14-16 (Section 'Fault Dynamics'). Talk title: ***Fractal Geometry of Earthquake Faulting.***
2. 12th International Symposium on Forecasting, Wellington, New Zealand, August 7-10, 1992. Talk title: ***Fractal Geometry and Earthquake Prediction.***
3. Workshop on Modelling earthquake probabilities and characteristic earthquakes, Wellington, New Zealand, August 11, 1992. Talk title: ***Seismic gaps and characteristic earthquakes.***

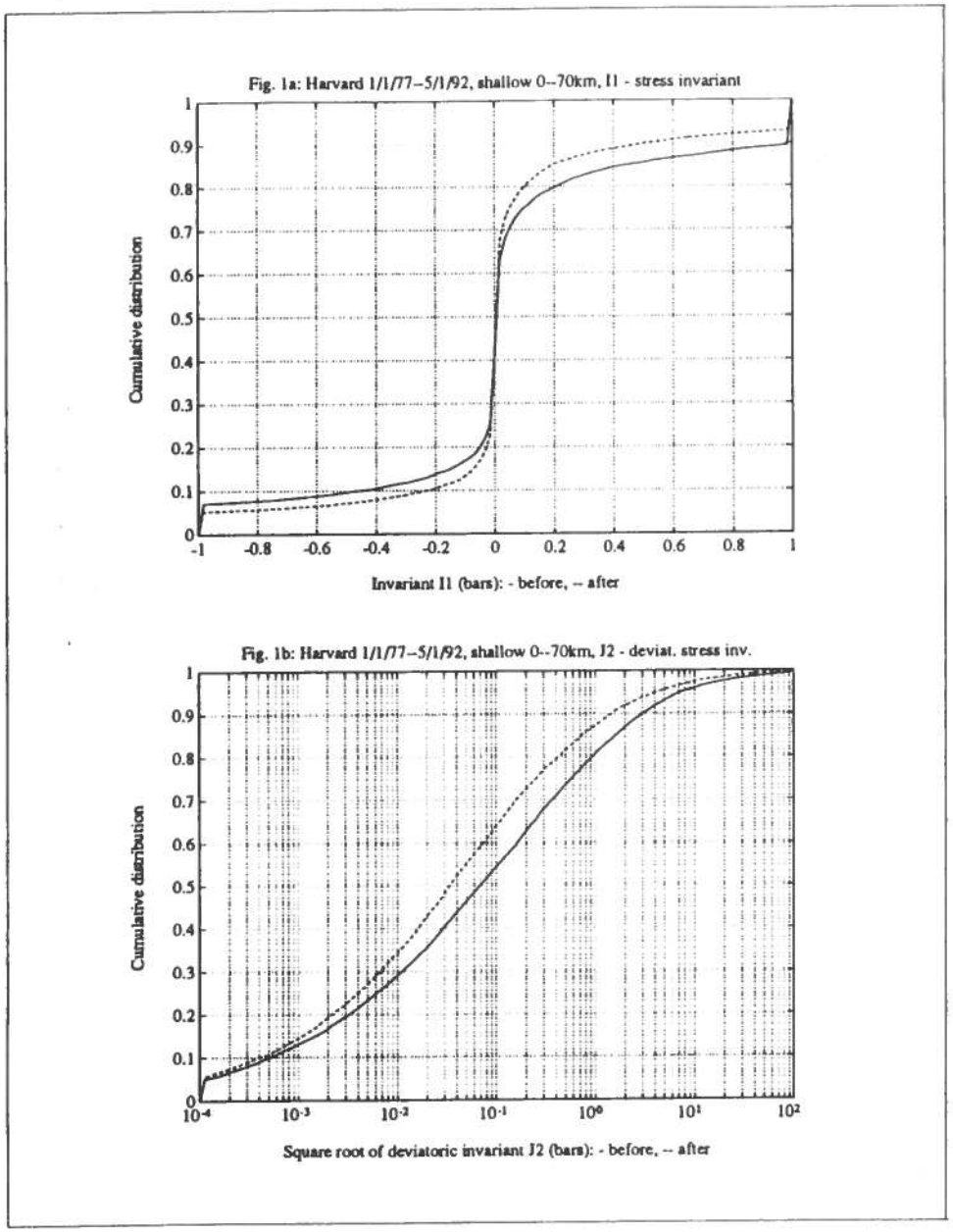

Fig. 1. Distribution of incremental stress invariants. We calculate the incremental stress caused by earthquakes in the Harvard catalog at a centroid point of any event. Two stress distributions are compared, that of preceding earthquakes (solid lines) and of following events (broken lines). The distributions for both invariants exhibit higher incremental stress levels for earthquakes before the reference event. The difference between these distributions indicates the possibility of using the incremental stresses caused by earthquakes for forecasting future seismicity.
(a) The first invariant (I_1) of the stress tensor (corresponds to the sum of principal stresses, or to the mean normal stress; see Jaeger and Cook, 1979, p. 23).
(b) The second deviatoric invariant (J_2), $\sqrt{-J_2}$ is equal to the mean shear stress (see Jaeger and Cook, 1979, p. 33).

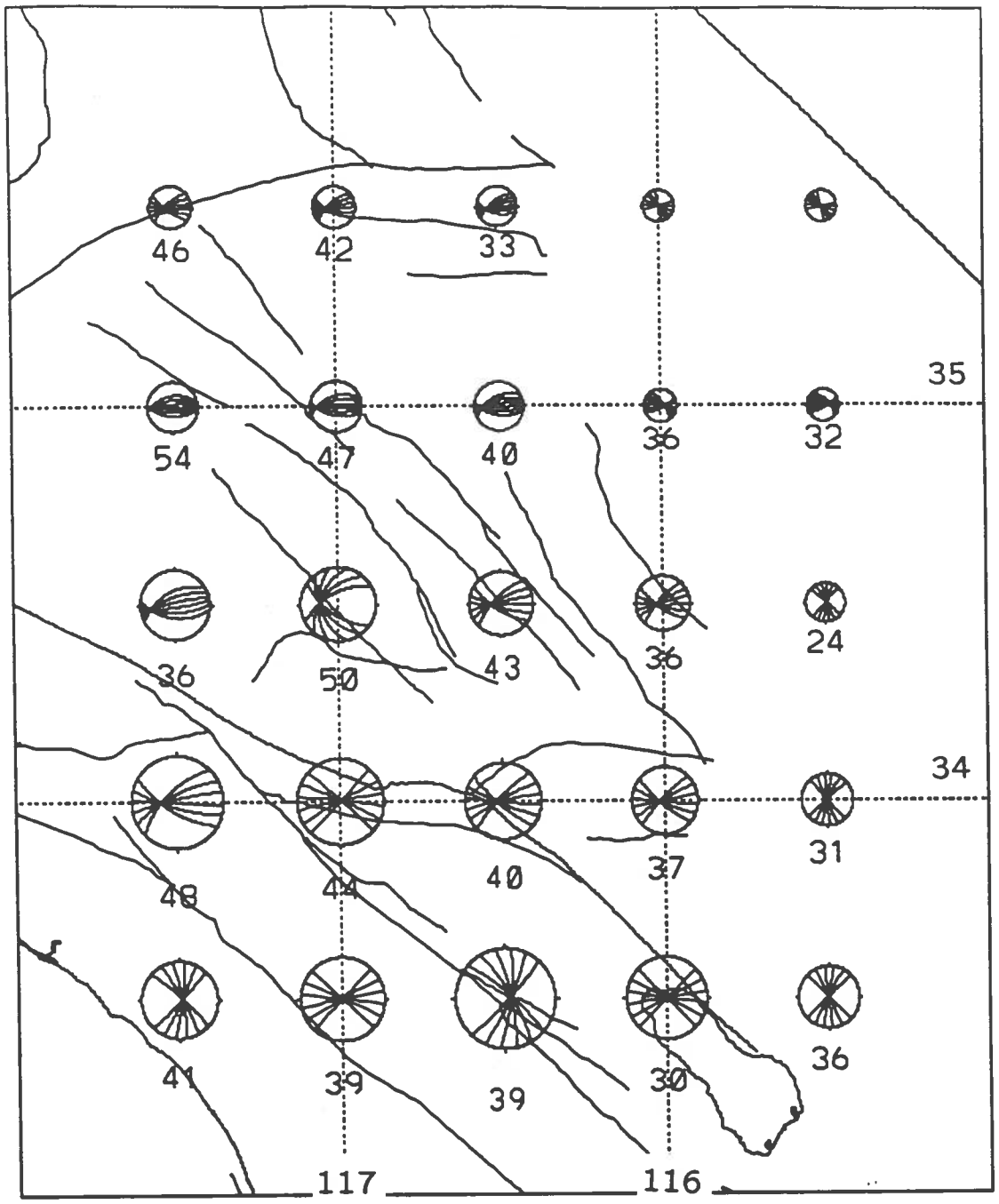

Fig. 2. Long-term forecast diagrams of earthquake focal mechanisms in Southern California; Harvard catalog for 1977-1991 is used. The area of diagrams of earthquake focal mechanisms corresponds to the probability of earthquake occurrence. The numbers below the diagrams of earthquake focal mechanisms correspond to a standard deviation of a weighted 3-D rotation angle. As focal mechanisms surrounding a point usually have various orientations, we first calculate the average seismic moment tensor, and then compute the rotation of earthquake focal mechanisms with regard to the average double-couple source. Therefore the angle standard deviation shows the degree of tectonic complexity and can be used to assess the efficiency of risk prediction.

V.Keilis - Borok, T.Levshina

Abstract of the progress report to SCEC, 9/15/92.

PREMONITORY ACTIVATION IN THE CALIFORNIAN FAULTS' SYSTEM: AREAS INVOLVED; SCALING AND SIMILARITY; HYPOTHETICAL PREDICTION ALGORITHM.

We have outlined the areas, which were involved in premonitory activation of seismicity prior to 31 strong earthquake in California, with magnitudes from 6 to 7.7.

Within each area the other relevant fields can now be jointly analysed and, with luck, the faults' dynamics leading to a strong earthquake can be reconstructed. We have found the scaling and level of averaging suitable for such analysis.

This activation took place in the intermediate-term time scale, 3 to 10 years. It was defined on the basis of the previous studies of premonitory seismicity patterns [1] by a modified algorithm, which may be of independent interest for prediction and/or modeling.

Preliminary findings

1.**Definitions**.Premonitory activation (PA) before a strong earthquake of magnitude M is expressed by the increase of the number n(t) of the main shocks in the magnitude range ($M - \Delta \leq m < M$), in the sliding time-window $(t - \tau, t)$ and in the area of characteristic linear dimension $D(M)$. Here m is the magnitude of the main shock. PA is defined by condition that $n(t)$ exceeds a certain percentile N.

PA is revealed at least in the range of space - time - magnitude windows which are shown in Table 1. These values were estimated by analysis of the earthquake catalogs CIT and NEIC. The common value $\Delta = 1.8 \pm 0.2$ may be assumed. We see, that PA is a stable phenomenon revealed in a wide range of windows. This is supported by the fact that the wide set of premonitory seismicity patterns worldwide is defined in similar windows [1], except that PA is defined here for larger magnitudes. Particularly important are the large values of $D(M)$: as in [1] the area of activation before each strong earthquake is much larger than its source.

2.**The areas of PA** are defined before 15 out of 17 strongest ($m \geq 6.0$) main shocks in Southern California, 1935 - 1992, and before all 9 such main shocks in the Coast Ranges and the Mendocino area 1965-1992. For the Southern California this score does not include 5 earthquakes with M between 6.0 and 6.3, for which PA could be not established: 3 of them are in the areas of low seismicity, one is too close to the beginning of the catalog and one was the second in a pair of the main shocks.

The examples of premonitory activation are shown in the figs 1,2.

3. **Magnitude-area trade-off.** An activation in a certain magnitude range $(M - \Delta, M)$ sometimes spreads over much larger distances than $D(M)$. This reflects the approach of an earthquake in the higher magnitude range.

4. **The time scale.** The apparent increase of τ with M is unusual for premonitory patterns: in the previous studies the time scale was found to be independent of M [1] , with few possible exceptions (for patterns "sigma" and "B"). However, the window $\tau = 5$ years is suitable for all strong earthquakes considered.

5.**Geometry of premonitory activation.** We juxtaposed the earthquakes, which formed each particular PA, with the major faults. The examples are shown in the figs 3,4. We see that an area of PA is indeed much larger, than the source of a subsequent strong earthquake. Moreover PA may not include this source. For example, before the Kern County and San Fernando earthquakes PA took place around San Jacinto fault and on the offshore faults system that includes the San Nicholas and Hosgri faults together with their extensions.

It is interesting, that PA most often starts with activation of these offshore faults.

Hypothetical prediction algorithm.

1. To establish the possibility to verify these findings on the future seismicity, we formulated them as a prediction algorithm. It declares an alarm (a "TIP") for one year, starting from the beginning of PA; the alarm terminates one vear after the end of PA or after a strong earthquake, whichever comes first. The complete definition of the algorithm will be given in the whole report.

This algorithm is close to algorithms CN and M8 [1] sharing with them the basic perceptions and many essential features.

It is more convenient for determination of geometry of premonitory activation; however CN and M8 use a wide set of premonitory phenomena.

The retrospective score of successes and failures is summarized in table 2. It does not include the earthquakes with magnitude 6.0 - 6.3, for which the magnitude-area trade-off has to be used; we need more data to incorporate it in the algorithm. The very high stability of the diagnosis of premonitory activation is shown in fig 5.

2. **Why did we fail to predict the Landers earthquake** by essentially the same algorithm, formulated in the previous progress report? This is because the scaling was not introduced: the same windows (τ = 2years, $m \geq 4.8$, D = 600km) were assumed for all M considered from 6.4 to 7.7. For the strongest earthquake the larger time window (5 to 10 years) and higher magnitudes range ($m \geq 5.4$) are more suitable for detection of PA (as suggested by L.Knopoff for premonitory activation before Loma Prieta earthquake). Forward monitoring will show, how justified is this scaling.

The "product".

As of now it consist of

(i) Identification of earthquakes which formed premonitory activation before 31 strong earthquake.

(ii) Determination of scaling and of the level of averaging which are suitable for reconstruction of the intermediate-term premonitory phenomena.

(ii) Algorithm for diagnosis of premonitory activation.

The opened possibilities.

(i) Reconstruction of dynamics of different fields within the areas outlined. Most relevant seem slow movements, source mechanisms and geometry of aftershocks' zones.

(ii) Reproduction of these fields on numerical models of Californian seismicity.

(iii) Forward monitoring of PA. As a prediction, it has better be done by the other algorithms too. In particular, incorporation of smaller earthquakes, $m \geq 2.5$, will allow to test "Mendocino scenario", which allows to increase territorial accuracy of prediction by factor 5 to 10. T. Levshina has already started monitoring for prediction of strong aftershocks.

Further problems opened:

(i) To explore the limits of similarity. They have to be tested for the other territories and for extended magnitude range.

(ii) To integrate the scaling and similarity relations into a hopefully analytical measure of premonitory activation.

(ii) To outline the comprehensive intermediate-term scenario of the approach of a strong earthquake.

(iii) To incorporate the other relevant fields in a prediction algorithm.

References

1.V.I.Keilis-Borok (editor). "Intermediate-Term Earthquakes Prediction: Models, Algorithms, Worldwide Tests". PEPI, Special Issue, Vol.61 Nos. 1-2, May 1990.

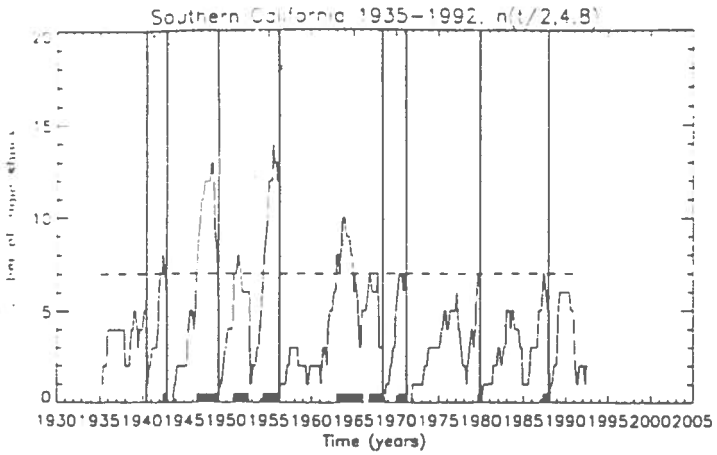

_ – number of main shocks n(t/s,m) with m ≥4.8 within s=2 years sliding window; I– moment of occurrence of strong earthquake.; --- – threshold for diagnosis of alarms; * – alarms.

Fig. 1

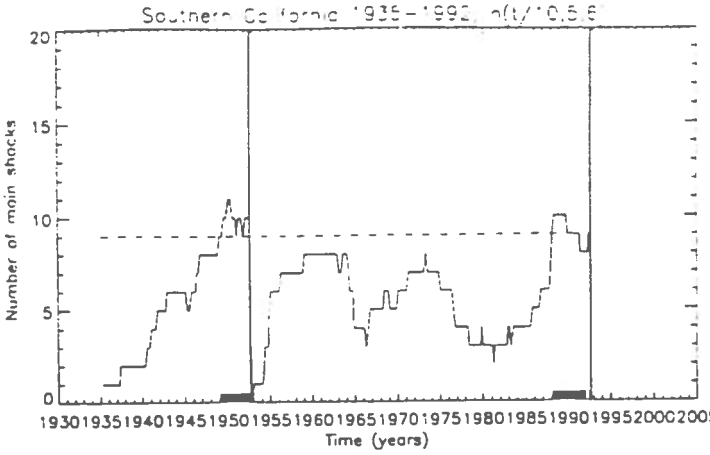

_ – number of main shocks n(t/s,m) with m ≥5.6 within s=10 years sliding window; I– moment of occurrence of strong earthquake; --- – threshold for diagnosis of alarms; * – alarms.

Fig. 2

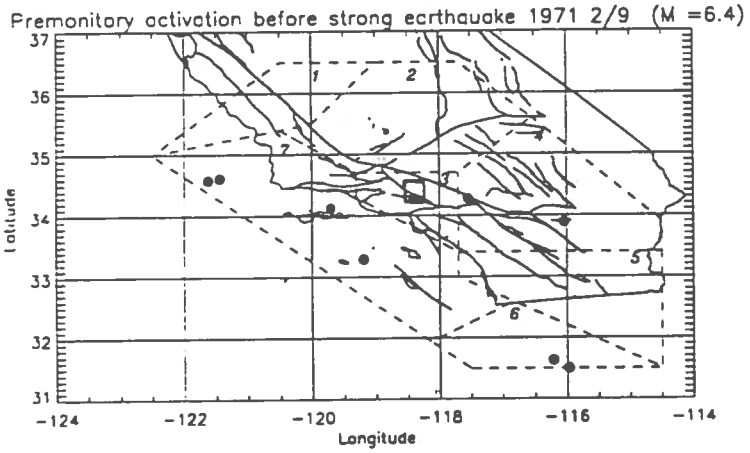

□ – strong earthquake with magnitude M≥6.4; • – main shocks with magnitude ≥4.8; – – faults; - - – coastline; --- – regions.

Fig.3

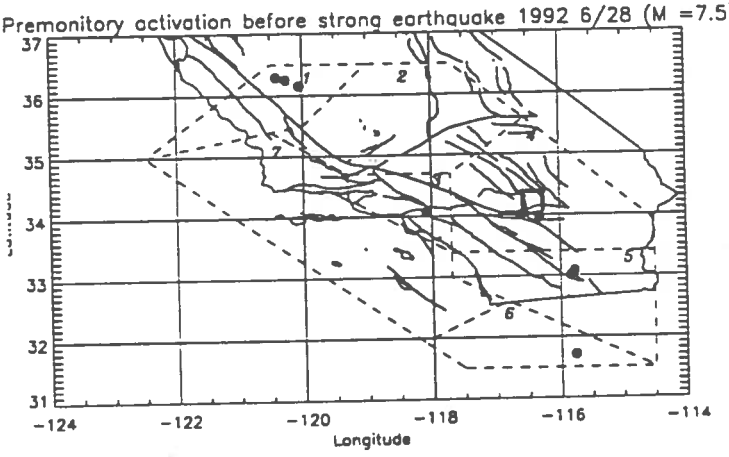

□ – strong earthquake with magnitude M≥7.5; • – main shocks with magnitude ≥5.6 – – faults; - - – coastline; --- – regions.

Fig.4

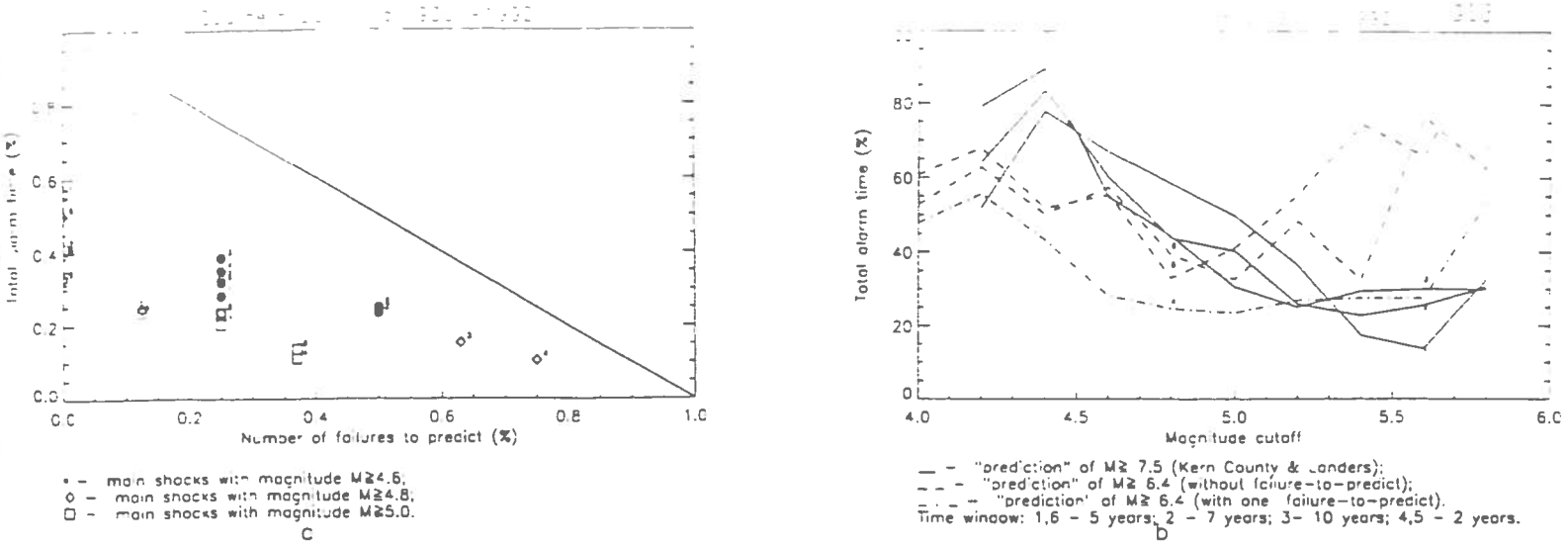

Fig 5. Stability of the diagnosis of premonitory activation.

Table 1

M	$m \geq$	τ, *years*	D
6.0 - 6.3	4 - 4.4 (4.0)	2 - 5	200-300
6.4 - 6.9	4.6 - 5.0 (4.8)	2 - 5	500-600
~~7.0 - 7.4~~	5.0 - 5.4 (5.2)	5 -10	500-600+
~~6.0 - 6.3~~ 7.5 - 7.7	5.4 - 5.8 (5.6)	5 -10	600-800

Table 2

Region	Strong main shocks "predicted"	not "predicted"	Duration of alarms total (%)	per a strong shock (years)
Southern California				
1935 Jan -1992 Jul				
$M \geq 7.5$	2	-	14	4
$M \geq 6.4$	7	1	25	2
Mendocino				
1965 Jan-1992 Jan				
$M \geq 7.0$	2	-	27	4
$M \geq 6.4$	3	-	36	3
Coast Ranges				
1965 Jan-1992 Jan				
$M \geq 7.0$	1	-	14	4

SIMULATION OF EARTHQUAKE DYNAMICS

UCLA Modeling Group:

L. Knopoff, M.S. Abinante, P.M. Jogi, J.A. Landoni, X.X. Ni

We report the following observations based on numerical simulations:

LONG-TERM SEISMICITY

1. A model that yields the Gutenberg-Richter magnitude-frequency law is not validated because of it.

2. Seismic wave radiation is an important mechanism for damping dynamical fracture growth, and models of seismicity must take radiation into account accurately. We must simulate seismicity through the use of dynamical models that include radiation effects or quasistatic models that simulate them well. Models that do not account for *elastic* growth and healing of fractures, i.e. on which the stress drops are not calculated dynamically, are not satisfactory for simulation of long histories of seismicity.

3. Barriers are probably associated with geometrical irregularities in fault structure and are a potent mechanism for stopping fractures. No barrier, however strong, can remain forever unbroken and the fracture of the strongest barriers causes the greatest earthquakes. The characteristic earthquake model follows from the barrier model. Because of localization by barriers, small earthquakes occur in their "own" region of space; the flow of small earthquakes in this region can be interrupted by large earthquakes that originate outside the region. Large earthquakes *originate* in regions of large strength; in these regions, there are few (if any) small earthquakes. Localized seismicity in regions characterized by inhomogeneities due to irregular geometry of faulting, may show instabilities in the form of nonstationarity, episodicity, sudden shifts in periodicity, etc.

4. One-dimensional models are inappropriate to simulate small earthquakes.

5. Long fault ruptures develop from a moving rupture "patch" having linear dimensions of the order of the thickness of the seismogenic zone.

6. We have begun a study of the seismicity on several interactive faults, with a view toward ultimately finding the potential of a large earthquake on one fault strand to trigger a second on another fault strand. Consider a modification of the Burridge-Knopoff model to two periodic fault strands (Fig. 1a), each having inhomogeneous frictions. The strands are coupled so that an event on one *reduces* the stress on the other. Figs. 1b and 1c show the time-evolution of seismicity on each chain as a function of position along the chain. These are *dynamical* models that take seismic radiation effects into account. In general the strand that has the lower breaking strength at a common coordinate will be the strand that displays most of the seismicity, the other strand being locally "dormant". Much of the "interesting" interplay between the two strands occurs at the cross-over points where the two have approximately equal frictions. Among a rich phenomenology, we note

the sequence of strong earthquakes characterized by long, relatively infrequent fractures on chain 1 near coordinate 200: this pattern of regularity dissipates in a sequence of ever weakening earthquakes, and disappears altogether around time 250. The sequence on chain 2, extending from coordinates 240 to 70, essentially stops near time 260, and the activity switches to chain 1 from this time forward, for the same coordinates. The sequence of small and intermediate events from coordinates 90 to 120 on chain 2, is suddenly interrupted from times 190 to 210 by a brief migrating sequence of the smallest events on chain 1 in the same coordinate interval; activity on chain 2 at this time is a negative image of that on chain 1. Other features testify to the complexity of even such a simple system. We conclude that it would be difficult to assess the potential for one large earthquake to trigger another on an adjacent fault, if the long-term history of seismicity on both is unknown.

7. We are not as pessimistic as before concerning the inability of quasistatic models to imitate results from models with dynamics. Fig. 2a shows a space-time simulation of *quasistatic* ruptures in a Burridge-Knopoff model with inhomogeneous frictions (shown at the right), where the forces on the particles after rupture are *assumed* to have the values of the dynamical friction. Fig. 2b shows the results for the same model with *dynamics* that takes *radiation* into account. We have now generated a set of *quasistatic* simulations for the same distribution of physical properties and derive Fig. 2c through a modification of the assumptions for the final state of stress on each fracturing element. The improvement encourages us to think that we may be able ultimately to bypass the dynamics. Simple assumptions about the final state of stress on a fracture, are inadequate to do a good job of simulating the chaotic dynamics of dynamical models.

INTERMEDIATE-TERM CLUSTERING

1. Intermediate-term precursory clustering such as quiescence, foreshocks, and increased activity of intermediate-magnitude earthquakes cannot be simulated by purely elastic block-spring systems. (Nonlinear) viscosity of the fault bonds and three-dimensional geometry of faulting must be incorporated into the models. The same viscous mechanism that regulates precursory clustering can regulate aftershocks as well.

2. Fluids play an important role in generating intermediate term precursors, through their action in regulating stress corrosion, variable healing rates, slip weakening, etc.

3. To simulate the widespread geometry of precursory intermediate-magnitude clustering observed for Southern California seismicity, we require that the models involve, not only two-dimensionality of individual faults, but also that we consider a 2-D network (and possibly a 3-D) network of faults. Precursory intermediate magnitude clustering is initiated through stress corrosion on buried faults at the base of the seismogenic zone. Intermediate-term activity is switched off by a large earthquake. Self-similarity as a determinant of scale may be present.

4. To simulate precursory clustering of seismicity, the slip conditions must involve viscoelastic rheologies rather than purely viscous rheologies. A critical slip distance criterion for a purely viscous rheology, is inappropriate to simulate radiative fractures.

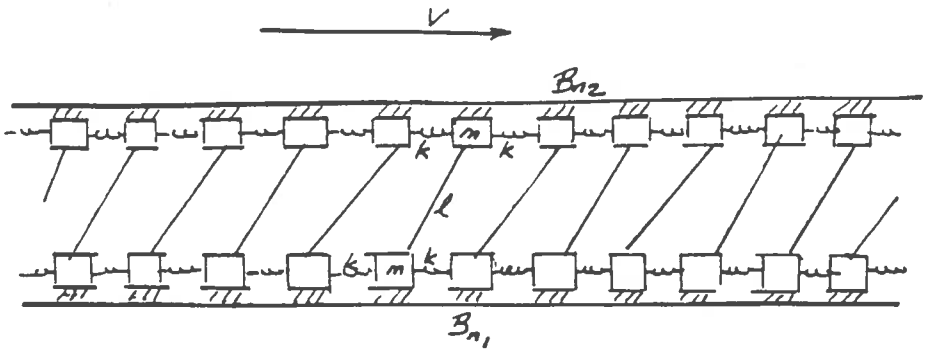
V
B_{n2}
k
m
k
l
k
m
k
B_{n1}

Fig. 1a

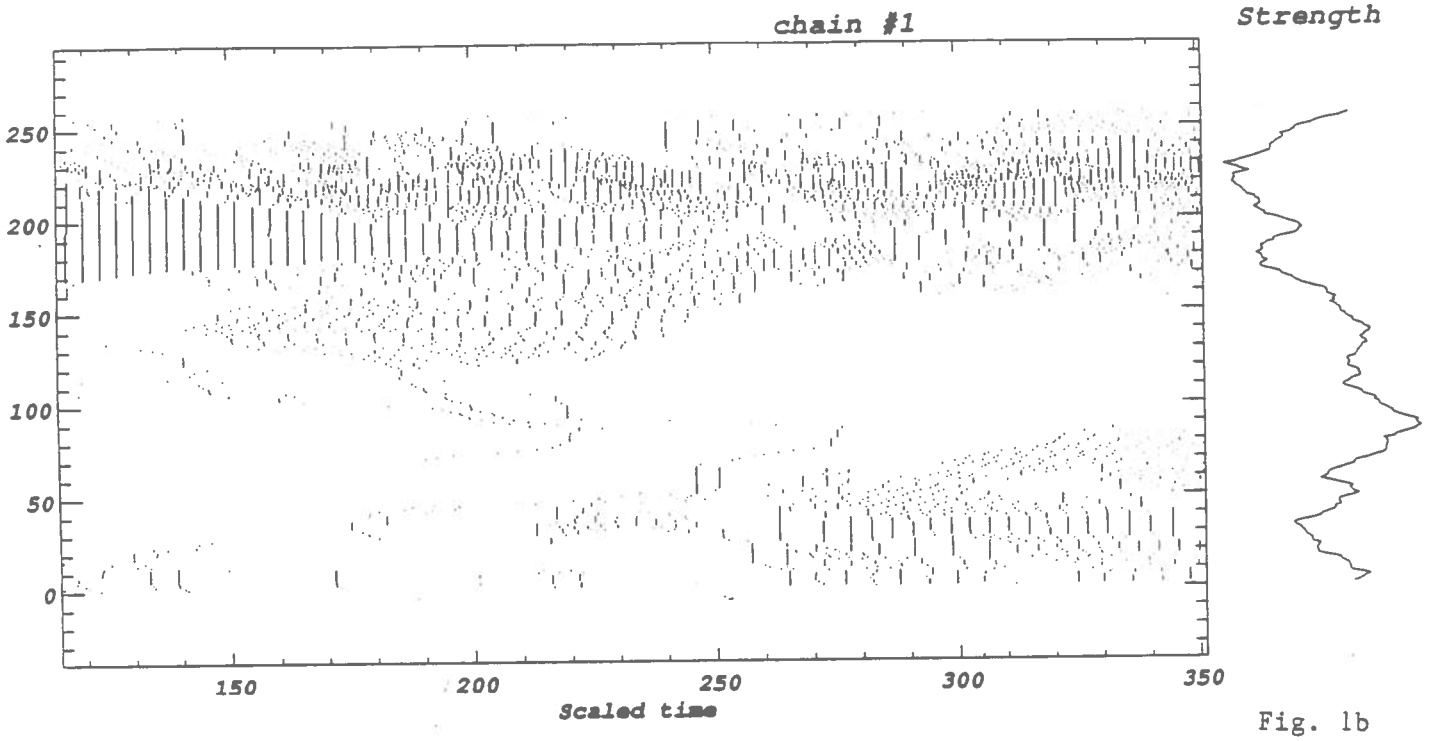
chain #1
Strength
250
200
150
100
50
0
150
200
250
300
350
Scaled time

Fig. 1b

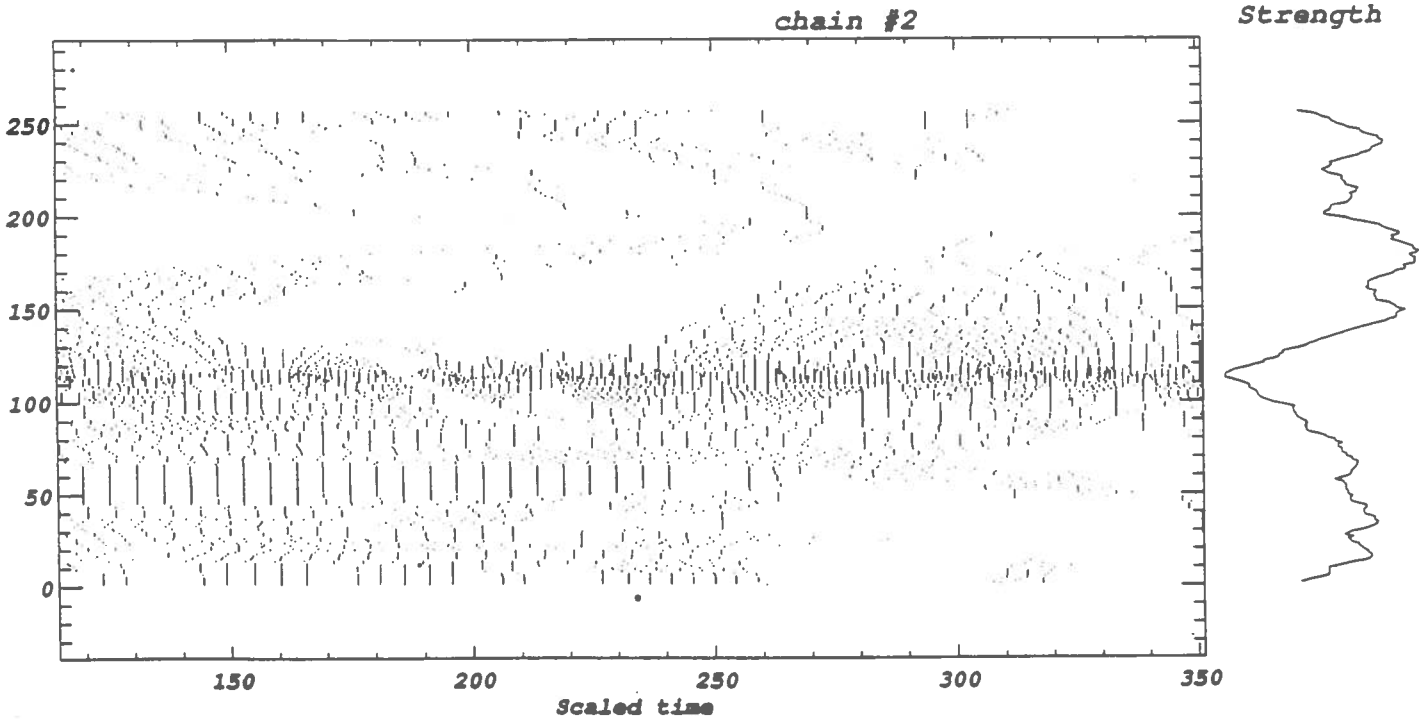
chain #2
Strength
250
200
150
100
50
0
150
200
250
300
350
Scaled time

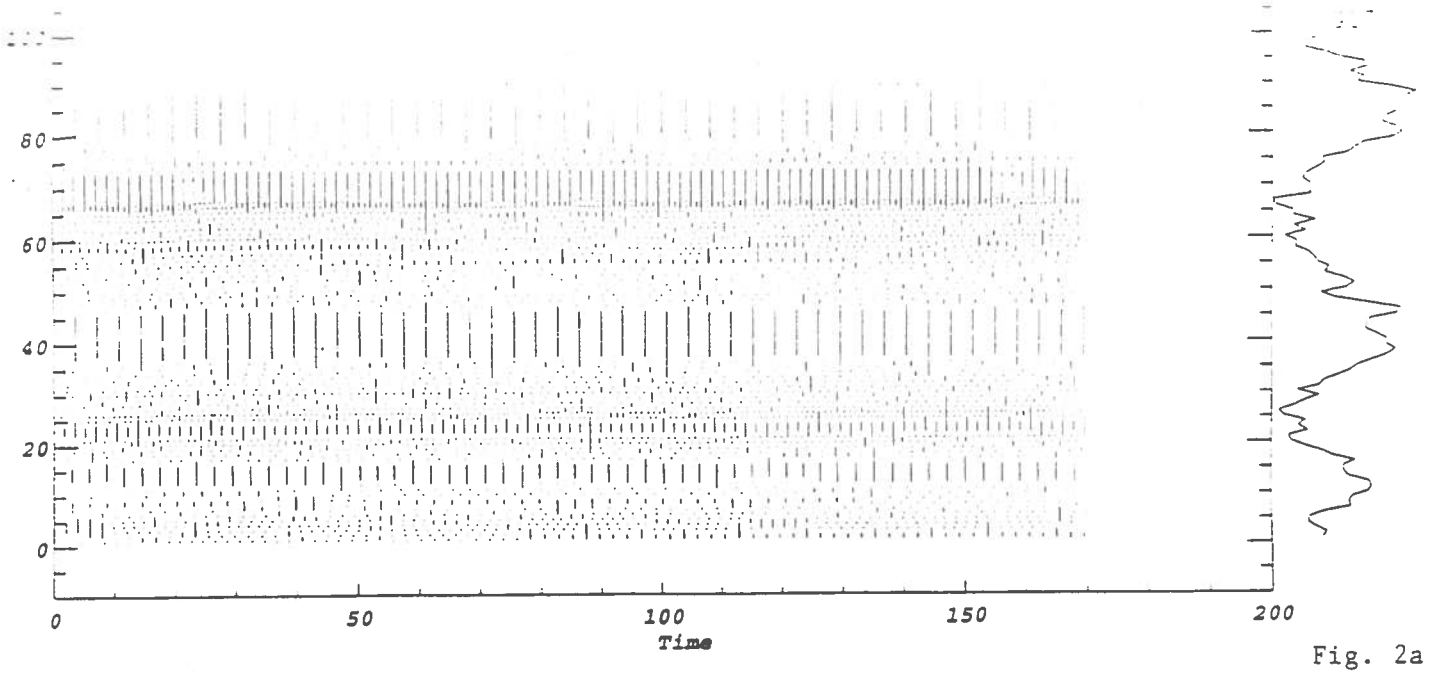

Fig. 2a

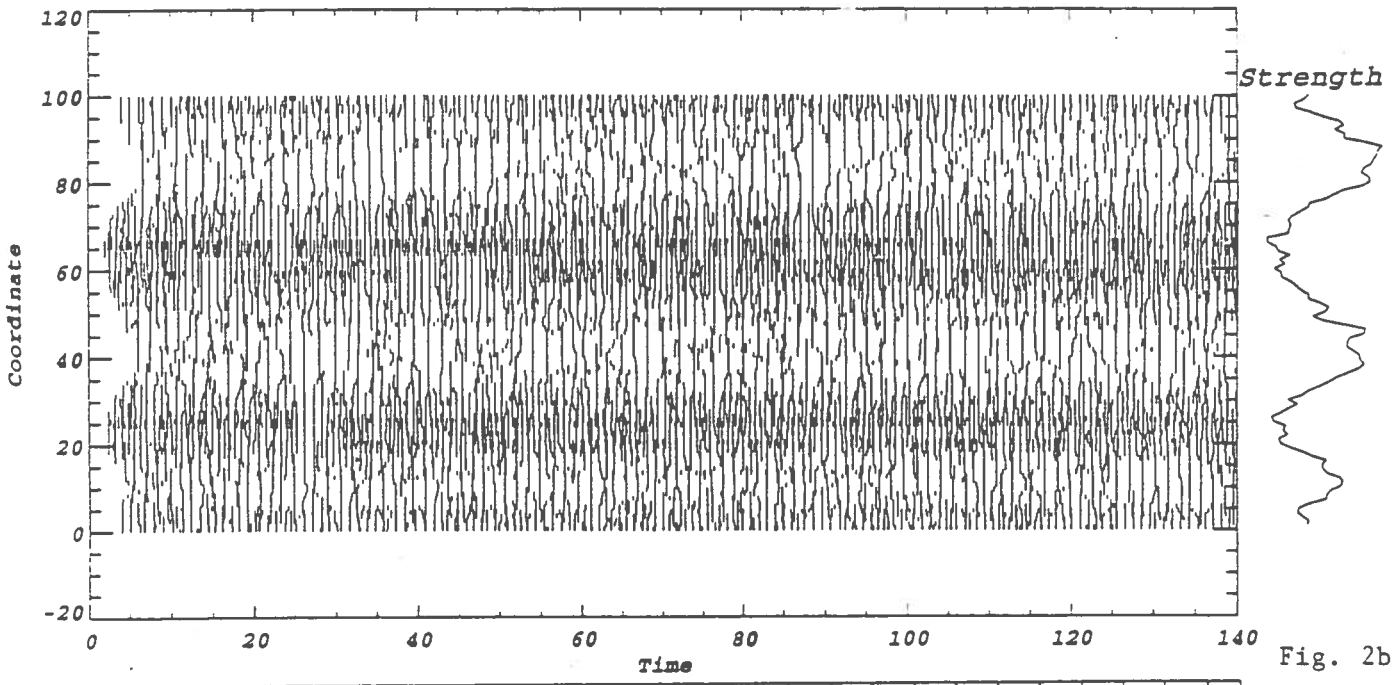

Fig. 2b

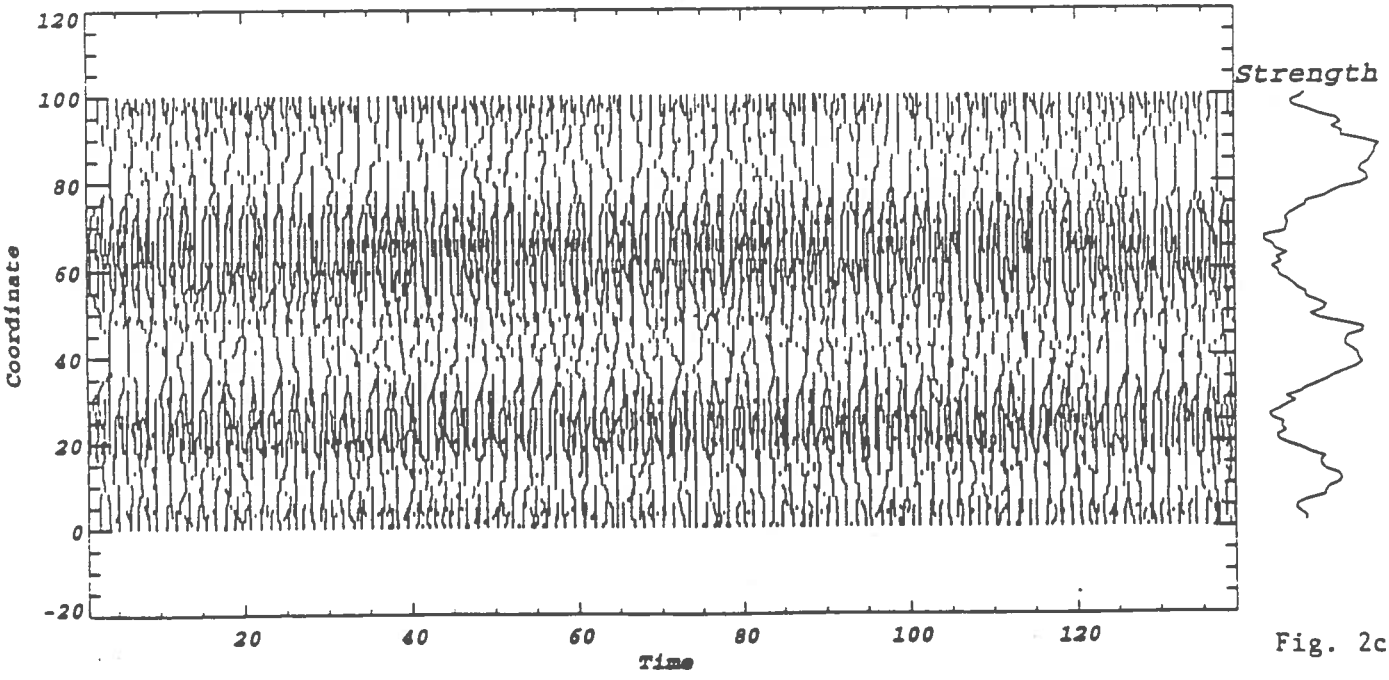

Fig. 2c

RELATING FAULT STABILITY TO FAULT-ZONE STRUCTURE USING A DAMAGE MECHANICS MODEL

Charles G. Sammis
Department of Geological Sciences
University of Southern California
Los Angeles, CA 90089-0740

Progress Report to the
Southern California Earthquake Center

15 September, 1992.

Earthquakes have traditionally been associated with frictional instabilities on preexisting faults. To a first approximation, frictional instabilities may be divided into dynamic instabilities and mechanical instabilities. Dynamic instabilities develop once the fault surfaces are moving and, as recently proposed by Brune and co-workers, may involve modes of vibration or waves which relieve normal stress on the fault. Mechanical instabilities develop if the initial displacement on a fault weakens the fault faster than that same displacement reduces the driving stress. The nucleation of earthquakes may be thus controlled by mechanical instabilities, while continued propagation may depend on dynamic instabilities.

Mechanical instabilities are commonly modeled using the Bowden-Tabor asperity model in which two sliding surfaces contact at a number of asperities. Asperities grow in strength with time, but their lifetime is limited by their size and the sliding velocity. A sudden increase in sliding velocity produces an instantaneous strengthening of the existing asperities "a" due to the increase in strength associated with the higher loading rate. However, as sliding proceeds at the higher velocity, the average asperity lifetime decreases which results in a decrease in asperity strength by an amount "b" over a characteristic sliding distance D_c which, in the Bowden-Tabor model is interpreted as the sliding distance required to completely change the population of asperities to ones having the new shorter lifetime. If b > a, then the material velocity weakens and, depending on the unloading rate of the fault, a stick-slip instability is possible. Stability is determined by comparing the apparent stiffness of the fault-zone: $(b-a)\,\sigma_n / D_c$ with the elastic stiffness of the fault walls which, for a circular dislocation patch of radius r may be approximated as: $7\pi G/24r$ where G is the shear modulus of the wall rock.

Because fault zones generally contain a layer of crushed rock between the wall rocks, the direct application of the Bowden-Tabor model is problematical in terms of the identification of asperities and characteristic displacements. Experimental studies of friction in which a layer of crushed rock is introduced

between the sliding rock surfaces have observed the same rate- and state-dependent phenomenology. Step changes in velocity still produce a signal which can be parameterized using a, b, and D_c as discussed above, but the values of all three parameters are significantly larger than those observed in rock-on-rock experiments. Figures 1 and 2 show the comparison between a and b parameters measured on a layer between rough rock surfaces and those for an identical layer deformed between smooth surfaces. For the case of smooth surfaces, the parameters are comparable to those measured in rock-on-rock experiments, and do not evolve significantly with displacement. For rough surfaces, the parameters are approximately twice as large and evolve with displacement. In particular, the b parameter increases which produces a transition from velocity strengthening to velocity weakening. We interpret the larger values of both "a" and "b" observed for rough surfaces as being due to a velocity dependent dilatancy commonly observed in granular layers and show that the observed dilatancy produces instantaneous and evolutionary signals indistinguishable from those produced by the asperity model. The large increase in "b" and slight decrease in "a" which produce the transition to velocity weakening for rough surfaces are produced by a transition from fracturing particles which has no lifetime effect to slip between particles which does. This work will be presented at the Fall AGU meeting.

The significance of the above observations is as follows: if the rate and state parameters in a fault zone depend on dilatancy, then they may not depend directly on fault displacement, but on strain within the fault-zone. This result is predicted by both soil mechanics and damage mechanics models for the strength of a crushed rock layer. The stiffness of the wall rock still depends on the displacement as discussed above, but the stiffness of the fault-zone now depends on strain=displacement/width. The immediate result is that wider fault zones should be more stable in the sense that a larger sliding patch is required to nucleate an instability. There are indeed hints that the creeping segment of the San Andreas fault has a wider crush zone than locked portions, and that small characteristic quasi-stable creep events also occur in these regions.

A more quantitative stability analysis of a finite-width fault-zone requires either a calculation of the post-peak rheology using the damage mechanics model, or an analysis of dilatant behavior and localization in the soil model. As detailed in David Scott's report, we have been making significant progress on the latter approach.

Figure 1 Rate and state "a" and "b" parameters for 3mm thick synthetic granite gouge layers deformed between rough and smooth granite surfaces.

"a" - PARAMETER

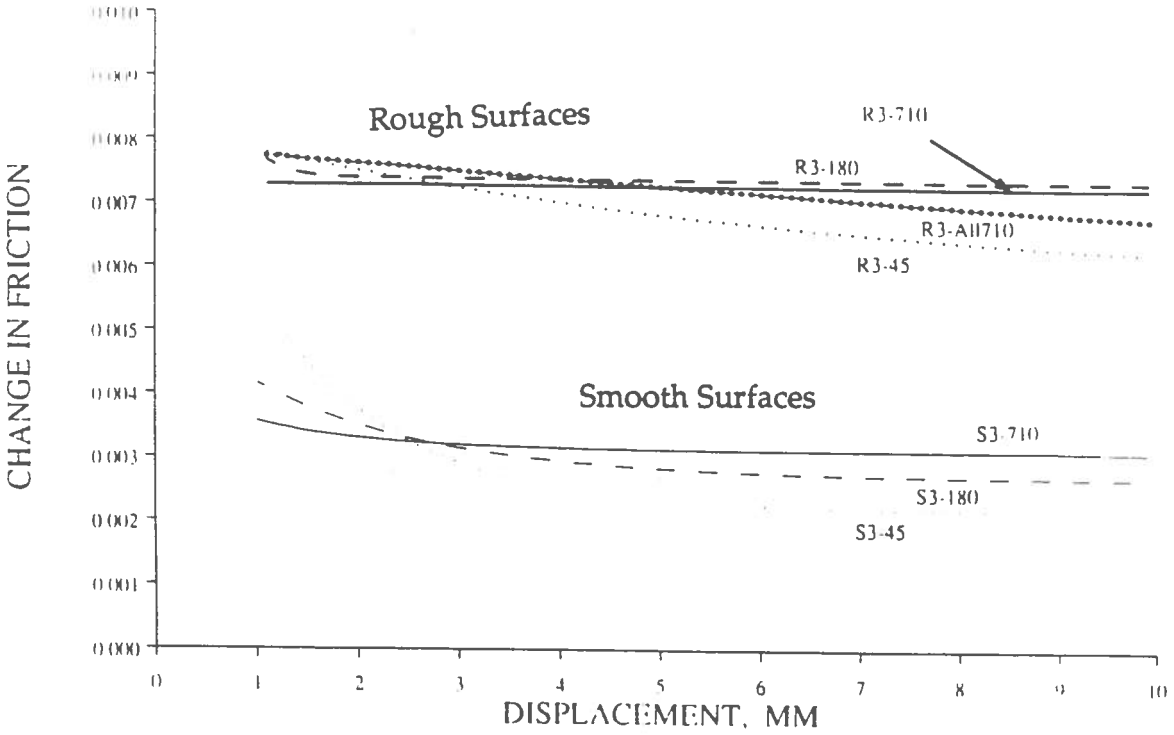

"b" - PARAMETER

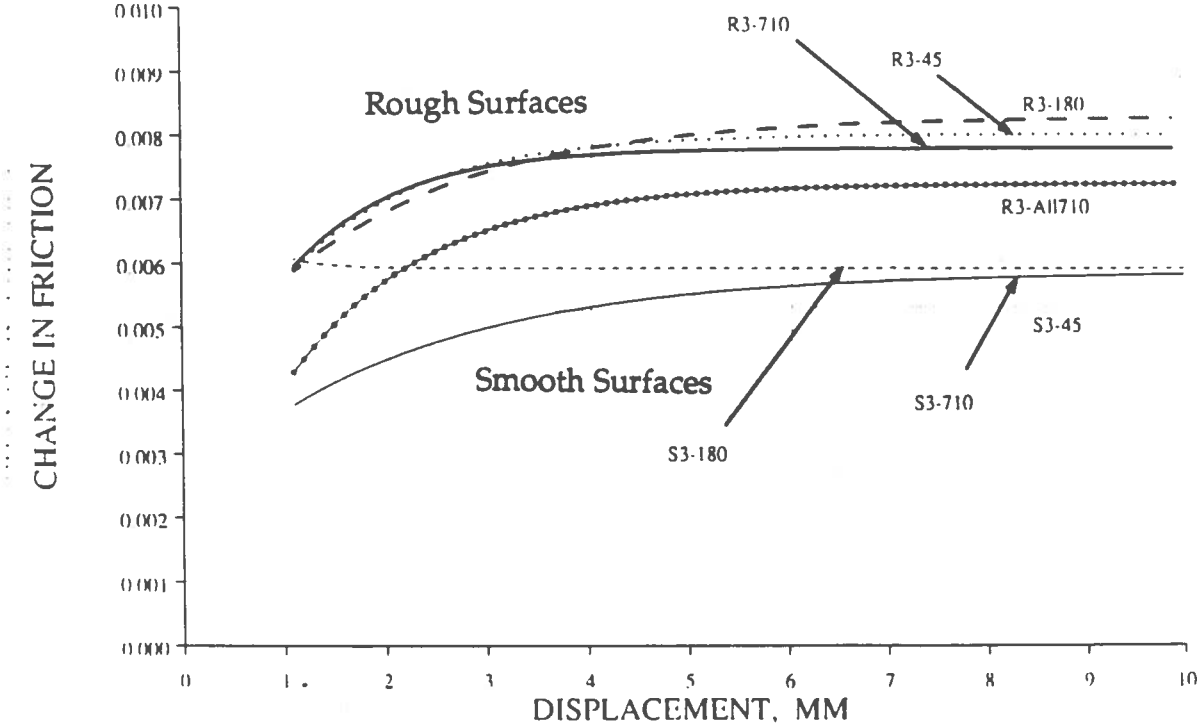

"Application of Models of Dynamical Systems to Seismicity, Earthquake Patterns and Predictions"

SCEC Progress Report

C. H. Scholz

1. Numerical spring-block earthquake models.

Work we reported on last year demonstrated several problems with these models as realistic models of earthquakes: 1) they produce incorrect scaling, which we believe is due to the lack of long-range forces. This also produces problems in the continuum limit; 2) The region of interesting SOC behavior seems to be parameter sensitive.

We have not found adequate ways to avoid these problems, and since several others groups are pursuing these models as well, we have suspended work on them for the present.

2. Study of physical model of dynamic crack arrays.

Natural fields of cracks, such as joints and faults, have properties, such as power law size distributions, that cannot be derived by considering the growth of an individual crack. To study this behavior we are investigating the growth of array of cracks generated in a thin glass plate bonded to a thick sheet of poly carbonate. The plate is sand blasted to provide an initial flaw distribution, and then submitted to a bending stress.

The cracking process is videotaped using the lighting reflected from crack walls. A Macintosh is then used to capture selected frames and digitize them as gray-scale images. Image data are exported to a Sun workstation for enhancement producing a binary image of the crack positions for analysis.

The analysis focuses on two components. On one hand, the geometry of the entire array (distribution of the crack size as well as spatial arrangement) and the influence of flaws on the geometry are studied. On the other hand, evolution of this array over time is examined with respect to loading history (internal stresses and applied bending). This involves both qualitative measurements such as local speed of crack propagation as well as the quantitative methods used for the geometrical analysis. This work will be presented at the Fall 1992 AGU meeting.

3. Scaling laws for faults.

We have continued developing a growth model for faults based on an elastic-plastic fracture mechanics model (Dugdale-Barenblatt). This model predicts linear scaling between fault slip and length, and current work involves modeling the brittle process zone at the fault tip. This work will be presented at the October meeting of the GSA in Cincinnati.

Progress Report on SCEC-Funded Research: The Mechanics of Granular Fault Gouge

David. R. Scott
SCEC Visitor
U.S.C.

September 1992

1 Introduction

Fault gouge is granular material found ubiquitously in the plane of major faults, formed by fragmentation of the surrouding rocks. An understanding of its mechanical behavior is essential in developing a deterministic understanding of earthquake nucleation and slip. The work described below investigates the constitutive behavior of gouge, attempting to relate micromechanical processes to the continuum rheology. Progress in this investigation will allow us to explore the effect of gouge on the behavior of seismogenic faults on the geological scale.

My original intention as a SCEC visitor was to work on the role of fluids in earthquake mechanics, but I have become convinced that it is at present more important to improve our understanding of the solid mechanics of gouge. As this work progresses, I will be able to incorporate the effects of fluids into the mechanics; this applies in particular to the numerical modeling described in Section 3.

2 Experimental Studies

2.1 Triaxial testing of natural fault gouge

In collaboration with David Lockner and Charlie Sammis, I am performing triaxial tests on samples of natural fault gouge from the Lopez fault in the San Gabriel fault zone. This locality was used in studies of grain size distribution in gouge by Biegel, Sammis and others. The fractal distribution that they identified has been related convincingly to the the micromechanical process of grain fragmentation during development of the gouge. The present tests, building on the grain size work, attempt to characterise the mechanical behavior of this mature fractal gouge.

A technique for coring and jacketing cylindrical samples of gouge was developed, and these samples were taken to the USGS, Menlo Park for testing in collaboration with Lockner. An initial week of testing in June 1992 produced some intriuging and novel observations. During testing, the strain in the cylindrical samples localises to a single shear band inclined at about 30° to the axis of compression. After one or two millimeters of displacement, the coefficient of friction of this shear band reaches a constant residual value of about 0.45, significantly lower than the friction previously measured for a quartz-rich gouge. This observation wil be discussed further in Section 2.3.

A key procedural detail is the use of constant mean stress during the axial compression of the sample (this means that the radial confining pressure must be reduced as the axial stress increases). This procedure suppresses the large volumetric effects that are characteristic of an uncemented, granular material, and exposes the shear rheology more clearly.

Next week I am returning to Menlo Park to perform some further tests. We plan to explore further the observed low friction of shear bands in gouge, and also to investigate the behavior of gouge under cyclic loading, as occurs in active fault zones.

2.2 Interpretation of double-shear tests on granular fault gouge

In collaboration with Chris Marone and Sammis, I am examinating the frictional behavior of granular layers in double shear tests. These tests were designed to investigate the rate-dependence of friction, but they show large variations in friction which cannot be ascribed to the more subtle rate-dependent effects. We have established that these variations are directly related to the rate at which the layer thins during the test; samples with a large rate of thinning have anomalously low friction.

I have developed a theory for this phenomenom, extending an idea proposed by Byerlee and Savage in a recent preprint; the theory agrees well with a number of data points from recent tests performed by Marone. In the theory, the strain in a granular layer is accommodated on shear bands that are oblique to the layer. The alignment of the shear bands is determined by the orientation of principal stresses, not by the sample geometry. The coefficient of friction of the individual bands is larger than that displayed by the layer as a whole. The real success of the theory is in demonstrating that a constant coefficient of friction for the shear bands (around 0.75) is consistent with the observed variations in friction for the layer as a whole.

We are preparing a paper describing these results.

2.3 Peak and residual strengths of shear bands in gouge

The previous two sections report contradictory results. In the triaxial tests we measure residual shear band friction of around 0.45, whereas the layer tests indicate a shear band friction of 0.75. My interpretation of this contradiction is that the friction of a shear band evolves, with displacement, from a peak down to a significantly lower residual level. The residual level is observed in the triaxial tests. In the layer tests, however, individual shear bands cannot accommodate very much displacement because they are oblique to the walls of the layer: the population of shear bands must keep changing. Each shear band operates at its peak strength because it cannot evolve down to the residual level before the band is abandoned.

This idea will be the subject of my presentation at the Fall AGU meeting, co-authored with Sammis, Lockner and Marone. I anticipate following up with a paper after we have performed more triaxial tests.

3 Numerical Modeling

At the microscopic level, the mechanics of fault gouge must involve at least three processes: intergranular slip, grain rotation, and grain fragmentation. Some understanding the interaction between the first two has been developed in the soil mechanics, by using a numerical technique called the distinct (or discrete) element method. In this method, a granular material is simulated by an assemblage of elastic discs with frictional contacts. The assemblage is maintained close to static equilibrium by dynamic relaxation, meaning that small inertial and viscous forces are added to the dominant elastic forces.

I have been collaborating with J.-P. Bardet (Civil Engineering, USC) in modifying this method for use in simulating fault gouge. This method will be invaluable in the interpretation of experimental results. I am applying the method to simulations of the triaxial and layer tests on gouge described in Section 2, attempting to inform our speculation about the micromechanical processes at work. Once we have some confidence that the correct microscopic processes are being modeled, the method will allows us to explore the behavior of fault gouge under conditions not accessible in the laboratory. Our present and planned modifications are described below.

3.1 Fractal grain size distribution

Fault gouge features a large range in grain sizes. This size distribution introduces a wide spectrum frequencies that must be carefully monitored to ensure that the time step and damping used in the dynamic relaxation algorithm produce both stability and optimal convergence to equilibrium. I have designed and implemented the necessary improvements to an adaptive dynamic relaxation algorithm developed by Bardet and Proubet, to allow the simulation of an arbitrary grain size distribution. In practice, two-dimensional systems with several thousand grains and a factor of ten variation in grain size should be practicable on a serial machine. We are preparing a paper describing the improved algorithm.

3.2 Grain fragmentation

In collaboration with Sammis, we plan to implement a simple simulation of grain fragmentation, by replacing highly stressed grains with a number of smaller grains. The direction this modification takes will depend on the results of the initial implementation, but the basic goal is to see how inelastic strain is distributed between fragmentation, fricitional slip and grain rotation.

3.3 Pore fluids and true dynamic simulations

The dynamics part of the present method is algorithmic; it provides a recipe for reaching static equilibrium from states close to equilibrium. It would, however, be simple to extend the method to simulate true dynamical deformation. Pore fluids are important in the dynamic regime because the rapid deformation gives rise to variations in pore fluid pressure in a fluid-saturated material (e.g. during soil liquefaction). This means that the effects of pore pressures on the solids grains, and the percolation of fluid through the solid framework, must be added to the numerical model. I have planned an approach to making these modifications, treating the fluid in a quasi-continuum fashion within the discrete solid assemblage. These modifications will permit us to explore the behavior of fault gouge during earthquake slip, a regime that is presently out of the range of laboratory techniques.

1992 SCEC Progress Report SCEC for Bruce E. Shaw

My main work this last year was focussed on two projects: developing intermediate term forecasting algorithms of large events with model seismicity catalogues, and formulating a general theory of time dependent response in self-driven runaway failure– a theory which seems to explain aftershocks. Below, some results from these projects are discussed.

A group of us at UC Santa Barbara have been working to develop intermediate term forecasting algorithms, using catalogues of events generated by theoretical models. The idea in using model catalogues is to take advantage of the unlimited clean data sets that can be generated to develop and improve forecasting algorithms, and examine possible limitations of these algorithms. My work so far has been concerned with developing the model to produce the catalogues, and setting up the forecasting algorithm using individual measures of the small event activity. The model I developed to generate the catalogue is a modification of the one dimensional Burridge-Knopoff model, modified to include long range interactions which produce foreshocks and aftershocks– something missing in the simplest model. The model produces a power law distribution of small events, and a different distribution of large events. The algorithm uses different measures of the small event activity to turn on a warning signal of a coming large event [see, *e.g.*, Kelis-Borok, *et. al.*]. It then keeps track of how long the warning signal is on, and when a large event occurs, whether the warning signal was on or off. Clearly, there is a tradeoff between the goals of having the warning signal be off for the maximum amount of time, and having the large events occur when the signal is on. The use of a quality function which expresses this tradeoff is therefore needed to quantify how well the algorithm is doing. This tradeoff can be expressed by defining a quality function $Q = pw^{\beta}$ where p is the fraction of a large events that occurred when the warning was on, w is the fraction of time that the warning was off, and β is a parameter set by public policy decisions. If one were more concerned about having the warning on for a minimal amount of time, then β would be set larger, while if the concern were to have more events happen when the warning was on, then β would be set smaller. Maximizing Q is the forecasting goal. Having defined a Q function, different measures and catalogues can be quantitatively

compared and algorithm parameters can be set to maximize Q. An example of the kinds of measurements I have made is shown in Figure 1. There, the value of Q is measured from a given catalogue for algorithms using different individual measures of activation. Each curve corresponds to a different measure with the threshold value of when the warning signal is turned on increasing along the curve as p decreases. From the figure, we can see that there is an optimal setting of the threshold on each curve where Q is maximized, and that different measures do better than others. The measures shown, in descending order of maximum Q, are: number of events, fraction of area that has ruptured in some event, number of medium sized events, number of aftershocks of small events, number of aftershocks of small events per small event, and change in number of events. The next step in the project is to begin combining the different measures. There are a number of interesting questions that arise in this context, such as how best to combine them, how independent each of the measures is, and how much better can a combination do than the measures do separately.

The second project involves a study of the process that gives the time delays associated with foreshocks and aftershocks. I have found a very general mathematical formulation of a class of failure processes which produces the generalized Omori law, which I believe to be applicable to earthquakes. I am currently writing up this work. The results, omitting the details, can be summarized as follows. For a system which undergoes self-driven failure, meaning that once some quantity reaches a threshold an event occurs, and the rate of approach to the threshold depends on the quantity, the response of quickly loading the system is a power law decay in time of the rate of events. For a dynamics where the time to failure decreases rapidly as the threshold is approached, the exponent of the decay has a value close to 1. In the case of earthquakes, unstable rupture is believed to initiate with large exponents [Das and Scholz, J. Geo. Res., 1981; Sornette, Vanneste, and Knopoff, Phys. Rev. A, 1992], giving an exponent close to 1 for aftershocks, as is typically observed. I am currently working on a number of aspects and implications of this theory.

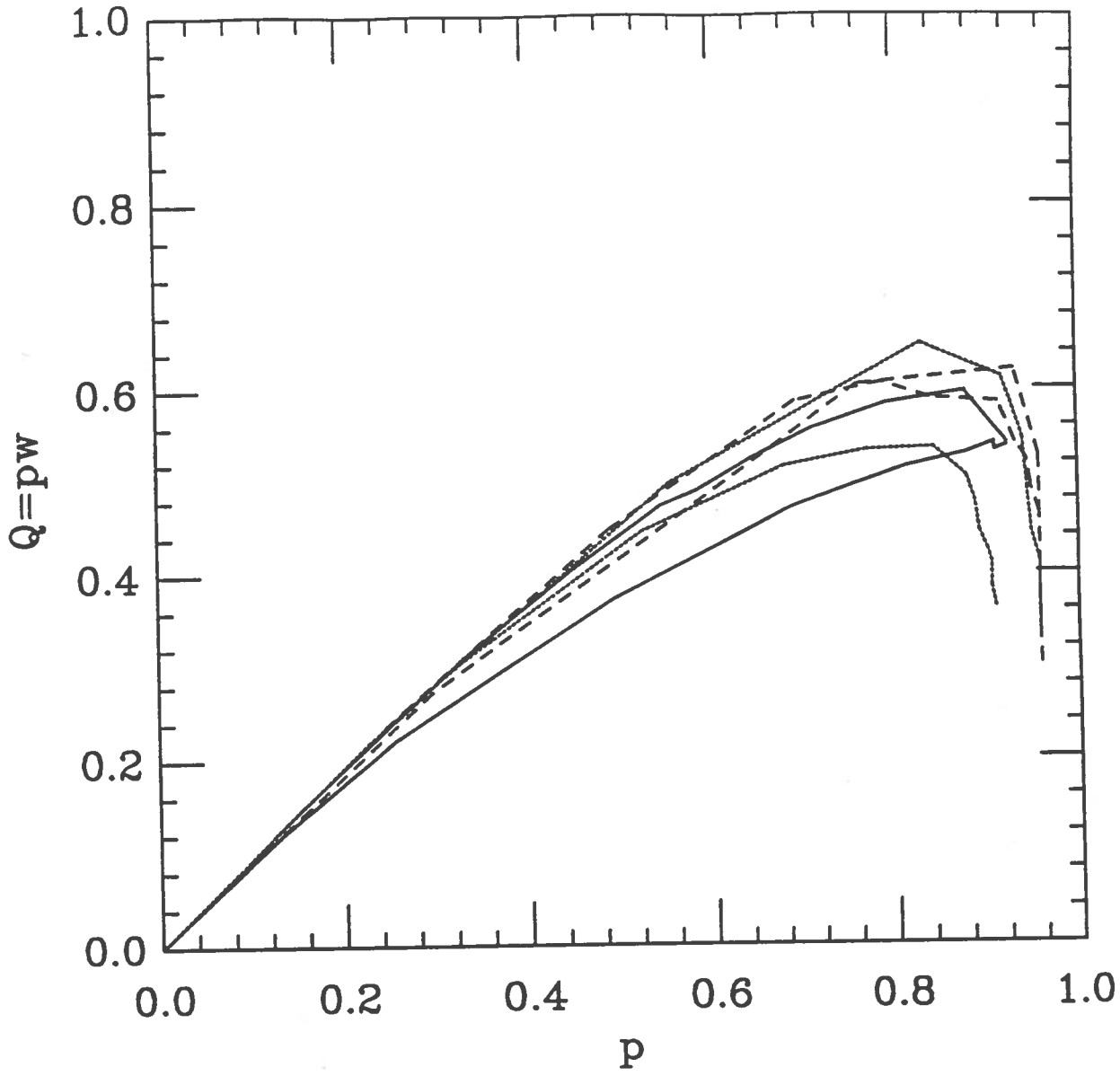

Figure 1. The quality of forecasting large events in a model catalogue. Different measures of the small event activity preceding large events are used to determine whether a warning signal of a coming large event is turned on or off. Each curve represents a different measure, with the threshold of the measure varying along the curve. The quantities plotted are the quality function Q defined by $Q = pw$, where p is the fraction of large events that occurred when the warning signal was on, and w is the fraction of time the warning signal was off. See text for more explanation of the figure.

GROUP H
THE CHARACTERISTICS OF EARTHQUAKE GROUND MOTIONS FOR SEISMIC DESIGN

A research project between the Southern California Earthquake Center and

- **California Department of Transportation**
- **City of Los Angeles Department of Public Works**
- **Los Angeles County Department of Public Works**

Group Leader: Geoff Martin

Formal confirmation of the contract award was received by SCEC on May 21, 1992. The contract start date is backdated to April 15, 1992. However, due to the above time lag and subsequent University administrative procedures to set task funding vehicles in place, progress on research tasks to date has been limited. In particular, Caltech tasks (H-2 and H-6) were not formally funded until September.

The following tasks form part of Year 1 funding.

TASK: H-1 CHARACTERISTICS OF EARTHQUAKE RESPONSE SPECTRA IN SOUTHERN CALIFORNIA

CO PI'S: LEE, TRIFUNAC, TODOROVSKA

The purpose of this task is to develop improved empirical equations for estimation of smooth elastic response spectra, for use in seismic design in Southern California. The emphasis will be placed on developing and justifying the spectral shapes which relate to the physical characteristics of the source (near field, far field), attenuation, and local site (geological and soil) effects.

To date the effort in this task has focused on the following:

- Development, analysis and interpretation of spectral shapes at low, intermediate and high frequencies, in terms of the source parameters (stress drop, source dimensions, dislocation amplitudes, seismic moment, magnitude, etc.). The purpose of this analysis is to provide constraints and guidelines on the functional form of the empirical equations for scaling response spectra and to indicate which additional scaling parameters may have to be added to the data, before we start the regression analyses.

- We started digitization and pre-processing of data for Whittier, Malibu, Upland and Sierra Madre earthquakes.

- Fieldwork to gather data from Landers and Big Bear earthquakes of June 1992.

TASK: H-2

CHARACTERIZATION OF POTENTIAL EARTHQUAKE SOURCES IN THE LOS ANGELES BASIN

Kerry Sieh and James F. Dolan
Seismological Laboratory, 252-21, Caltech, Pasadena, CA 91125

During the past year, we have used C^3 funds to support study of potentially seismogenic structures in the Los Angeles Basin. Our research thus far has two principal foci: (1) a geomorphologic analysis of the northern and western Los Angeles Basin designed to assess the exact location, kinematics, and structural style of all potentially active structures; and (2) paleoseismologic analysis of the Santa Monica Fault designed to determine the earthquake history and seismic hazard potential of this poorly understood fault. Highlights of our studies include: (1) delineation of two previously unrecognized, NW-trending strike-slip faults that cut through downtown Los Angeles. These faults, along with several potentially active anticlines that we have identified just west of downtown, probably represent surface manifestations of the buried thrust fault responsible for the Wilshire Arch, a major anticline recently identified by SCEC researchers at Oregon State University. These structures, along with the buried thrust fault responsible for the Whittier Narrows earthquake, may represent a mechanically continuous blind thrust system that extends for more than 40 km beneath Los Angeles; and (2) identification of probable Holocene activity on the Santa Monica Fault, which was previously thought to be inactive. Preliminary age control based on soil analysis by Tom Rockwell of San Diego State University suggests that the Santa Monica Fault last ruptured at least several thousand years ago. This implies that earthquakes on the fault system are infrequent, but large. For a more complete review of our geomorphologic and paleoseismologic results during the past year, please refer to our SCEC progress report for Working Group C.

During the next few months, we will integrate our results, together with those of other researchers, into a synthesis of potentially active structures in the Los Angeles basin. This report, which will represent our final product, will center around a map of all potentially seismogenic faults with the basin. The accompanying report will contain all information currently available on these structures, including recency of activity, probable recurrence intervals, slip rates, and kinematics of fault movement. We have already prepared a map of potentially seismogenic structures for the northern half of the basin. Analysis of these data will allow us to provide our best estimates of the future behavior of structures in the Los Angeles basin. This synthesis of potential earthquake sources in the Los Angeles area will provide one of the most important basic building blocks for construction of the SCEC master model.

TASK: H-3

Progress Report for the Southern California Earthquake Center

Effects of Local Site Characteristics on Ground Accelerations

by B.H. Chin, K. Aki and G.R. Martin

University of Southern California

Recently, we carried out a complete study in the Central California on the effects of source, propagation path and local site conditions on strong ground motion from the Loma Prieta earthquake of 1989. We found a pervasive non-linear site effects at sediment sites in the epicentral area by the simultaneous consideration of the above three effects. The first seismological detection of this non-linear site effect is within the range expected by geotechnical engineers. We then approached this problem using geotechnical methods, and found that the analysis of records obtained at Treasure Island during the Loma Prieta earthquake did not require a non-linear model. The record at the stiff-soil site station Gilroy #2 is analyzed by a 1-D non-linear method, using the record at Gilroy #1 which underlain by weathered sandstone as an input motion. The synthesized records show good agreement with the observed during the Loma Prieta earthquake in both time histories and response spectral shape. We found, however, that the input motions at Gilroy #2 during the 1979 Coyote Lake earthquake and 1984 Morgan Hill earthquake are at a lower level (PGA$<$ 0.38 g) at which the linear prediction is valid. The temporal and spatial distribution of nonlinearity at Gilroy #2 during Loma Prieta earthquake was examined through the hysteresis loops developed at different depths of the soil column as shown in Figure 1. During strong shaking, the nonlinear behavior became obvious at the soft silty-clay layer (between 21 to 40 m) where the maximum strain reaching up to 0.4 %. The whole soil response returned to the linear range in the later part of motion.

The weak-motion amplification factor for the region of Los Angeles basin is shown to be greater than most of Southern California. The preliminary result shows that the amplification factor in this area decreases with increasing frequency, the range is about 2 to 4 in natural logarithm for 1.5 and 3.0 Hz, about 2 to 3 for 6.0 Hz and about 1 to 2 for 12 Hz. We will examine these factors more thoroughly as soon as the digital portable instruments become available. Figure 2 shows the strong-motion accelerographs operated by USC, USGS and CDMG, the USC network and the USGS-CALTECH stations in the Los Angeles basin. The number beside the accelerograph indicates the averaged horizontal PGA in percentage of g during the 1987 Whittier-Narrows earthquake. We plan to make a detailed study of source, path and site effects as well as one dimensional linear and non-linear site response analysis at these strong motion sites.

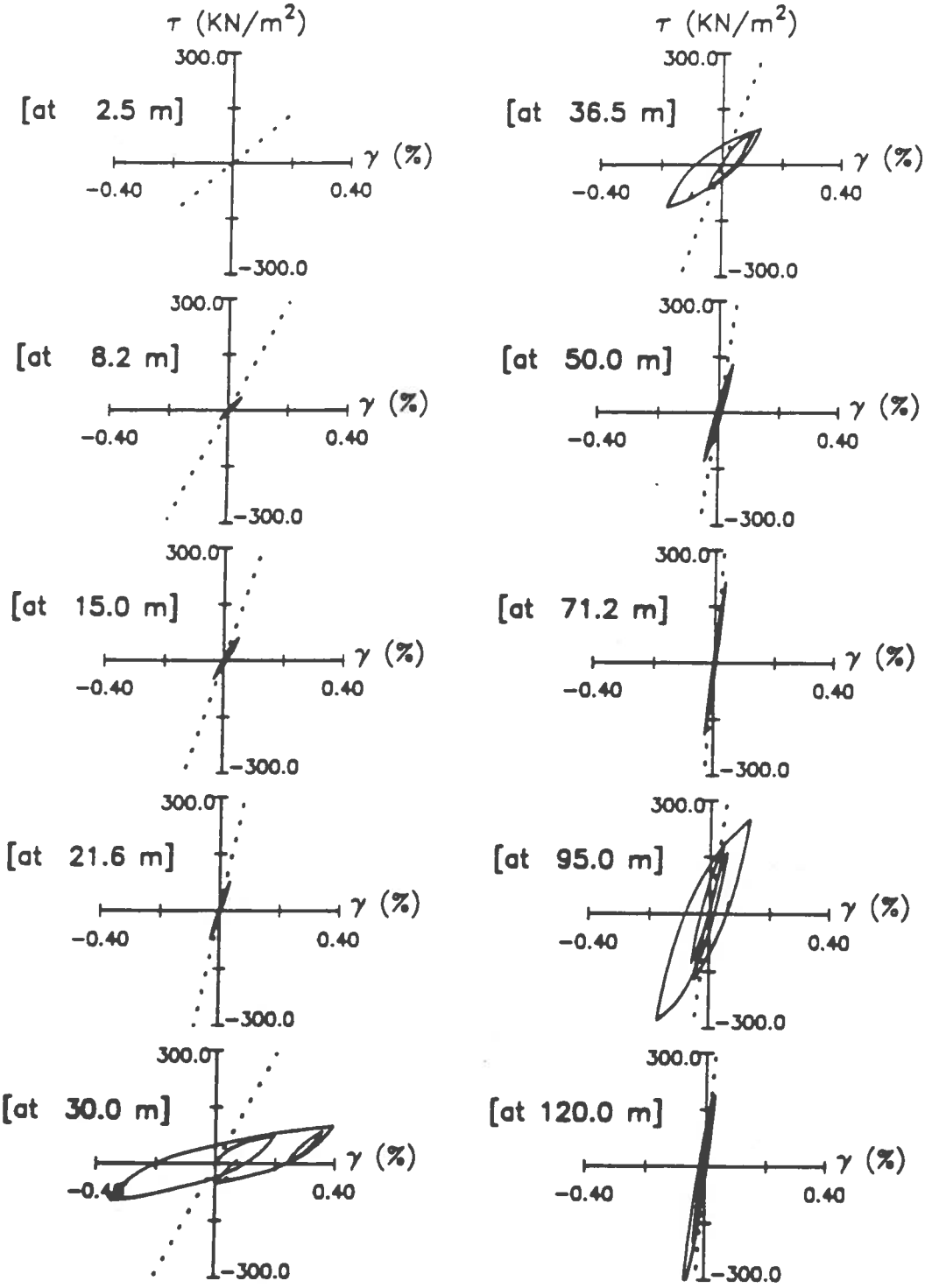
τ (KN/m²)
300.0
[at 2.5 m]
γ (%)
-0.40
0.40
-300.0
[at 8.2 m]
[at 15.0 m]
[at 21.6 m]
[at 30.0 m]
[at 36.5 m]
[at 50.0 m]
[at 71.2 m]
[at 95.0 m]
[at 120.0 m]

Figure 1

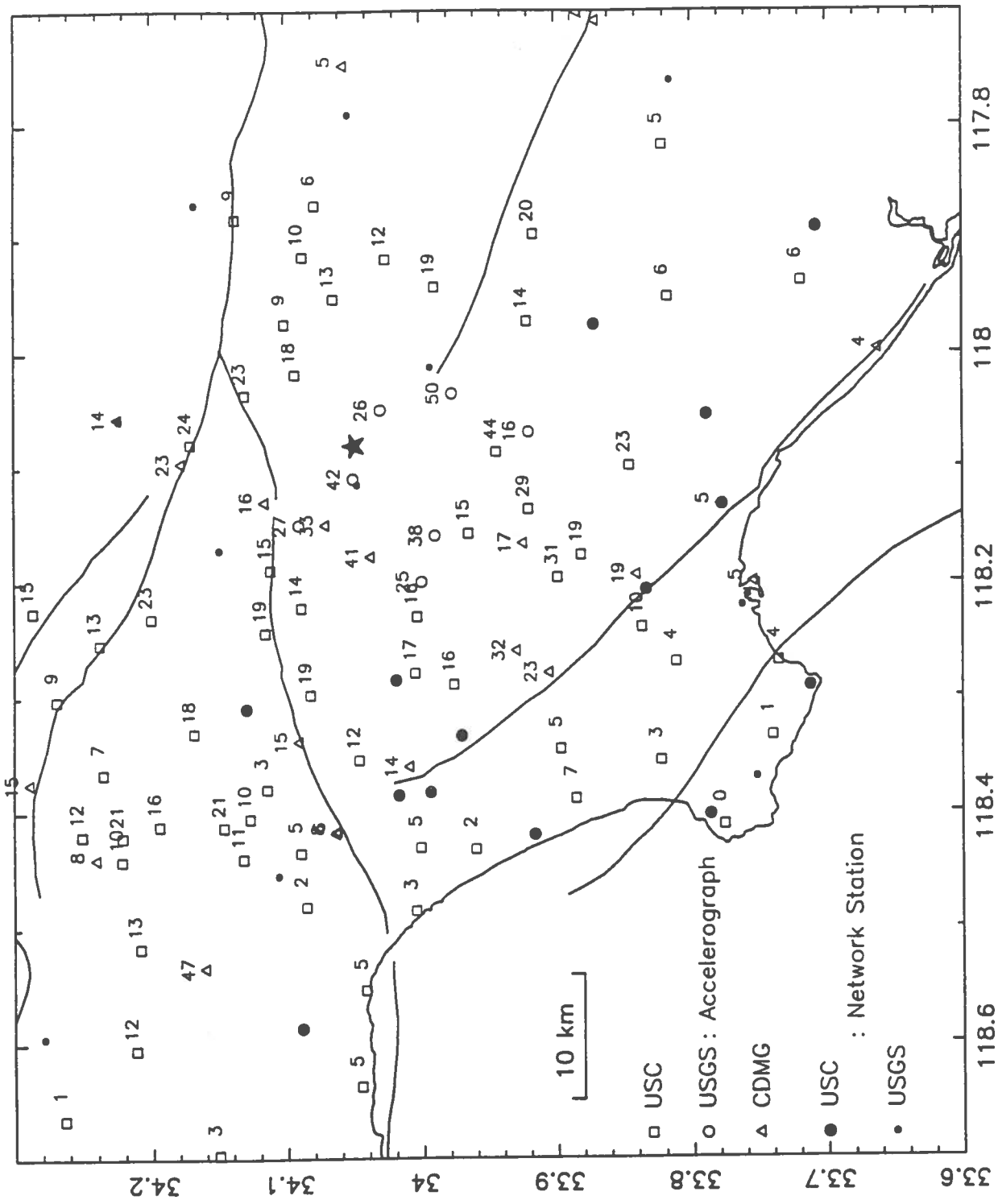
Los Angeles Basin Seismic Network
34.2
34.1
34
33.9
33.8
33.7
33.6
118.6
118.4
118.2
118
117.8
10 km
USC
USGS : Accelerograph
CDMG
USC
: Network Station
USGS

Figure 2

TASK: H-4 DURATION OF STRONG MOTION SHAKING IN SOUTHERN CALIFORNIA

CO PI'S: TRIFUNAC, LEE, TODOROVSKA

We will develop new regression equations describing duration of strong ground motion in terms of seismic energy available to excite the structures. The physical characterization of strong motion pulses, their amplitudes, number, frequency content, etc., will be analyzed to describe the nature of the bursts of energy exciting the structures. Between the pulses "quiet" portions of strong motion, and the strong motion coda, will be investigated to provide continuity and to understand the physical nature of strong motion relative to the weaker coda waves in seismological studies. Two- and three-dimensional geometry of sedimentary basins (depth, width, length) relative to the station-source geometry will also be considered in describing the duration of strong motion.

To date the work on this task has progressed well and has focused on the following:

- Generation of band-pass filtered data to describe the frequency dependent characteristics of strong motion duration.

- Studies of the physical nature of the observed duration to formulate a basis for selecting the regression equations. In this we are using the old uniformly processed strong motion data while we prepare for the analysis of the large database for Southern California, now under preparation in Task H-1.

Research Project:	"Geotechnical Site Data Base for Southern California," Component of "The Research Program on the Characteristics of Earthquake Ground Motions for Seismic Design," managed by Professor G.R. Martin
Funding Agency:	Southern California Earthquake Center - funded by Caltrans, County of L.A. and City of L.A.
Principal Investigator:	Mladen (Mike) Vucetic, Civil Engineering Department, University of California, Los Angeles
Period of Performance:	First year: 04/15/92 - 04/14/93 (3 year project)

PROGRESS REPORT
September 15, 1992

Research Objective

Past earthquakes have shown that damage patterns may be associated with local soil and geologic conditions. In order to study the potential for such damage in Southern California, a systematic analysis and mapping of all available geotechnical and local geological data will be performed. The systematically collected and cataloged geotechnical data will ultimately form a data file in the planned SCEC geographic information system, i.e., GIS system.

Technical Progress

To systematically catalog a reasonable number of relevant data, the key parameters and factors governing the following geotechnical earthquake engineering phenomena were reviewed: (1) amplification and attenuation of seismic motion through soil deposits, (2) cyclic strength degradation of cohesive soils, (3) liquefaction of saturated cohesionless soils, and (4) settlement or subsidence of cohesionless soils due to densification during seismic shaking. The review of these parameters encompassed their significance, frequency of their utilization in different design procedures, availability from standard geotechnical investigations, and their role in the state-of-the-art trends in the field of geotechnical earthquake engineering. The review resulted in a list of more than 20 relevant parameters or factors, covering soil classification properties, soil stress-strain-strength-pore water pressure characteristics, site specific properties (geometry, stratification and geology), parameters obtained by field testing, and seismic loading characteristics. From the above list, three groups with different numbers of the most relevant parameters are preliminary identified. These are:

Parameter	10 most	7 most	5 most
Mass density of soil, ρ_s	•	•	•
Mass density of base rock, ρ_b	•		
G_{max} or V_s of soil	•	•	•
G_{max} or V_s of base rock	•		
Shear strength, S_u or τ_f and friction angle, ϕ	•	•	
Plasticity index, *PI*	•	•	•
Stratification and groundwater table, g.w.t.	•	•	•
SPT blow count, *N*	•	•	•
CPT resistance, q_c	•		
Content of fines (silt content)	•	•	

Depending on the desired scope of the future GIS, and the availability of listed parameters from the information and data bases that will be compiled in the second phase of this years effort, the final number and list of the parameters will be decided upon. These selected parameters will be used to develop different maps comprising the planned GIS, such as sketched in Fig. 1. In addition to such maps, a capability of generating geotechnical soil profiles (2-dimensional or 3-dimensional) will be a part of GIS, employing the Techbase Geotechnical Software Package. In this way, as a routine operation of GIS many of the above listed parameters will be displayed directly on the soil profiles, as shown in Fig. 1.

Besides defining and refining the list of the parameters for the final data base, progress was made in identifying major sources of the data. The companies and individuals who can potentially contribute the information have been contacted, and the data are being collected and organized. Currently, the data collection is focussed on the geological and geotechnical properties at the strong ground motion stations, maintained by USGS and CDMG (for USGS stations, see Fig. 2).

Organizational Progress

The research team consisting of the Principal Investigator, one Ph.D. student (for whom this project will be the main component of his Ph.D. study) and one M.S. student, was established. Acquisition of the software for generating geotechnical soil profiles (Techbase) and a 486 PC computer with all necessary components is in progress.

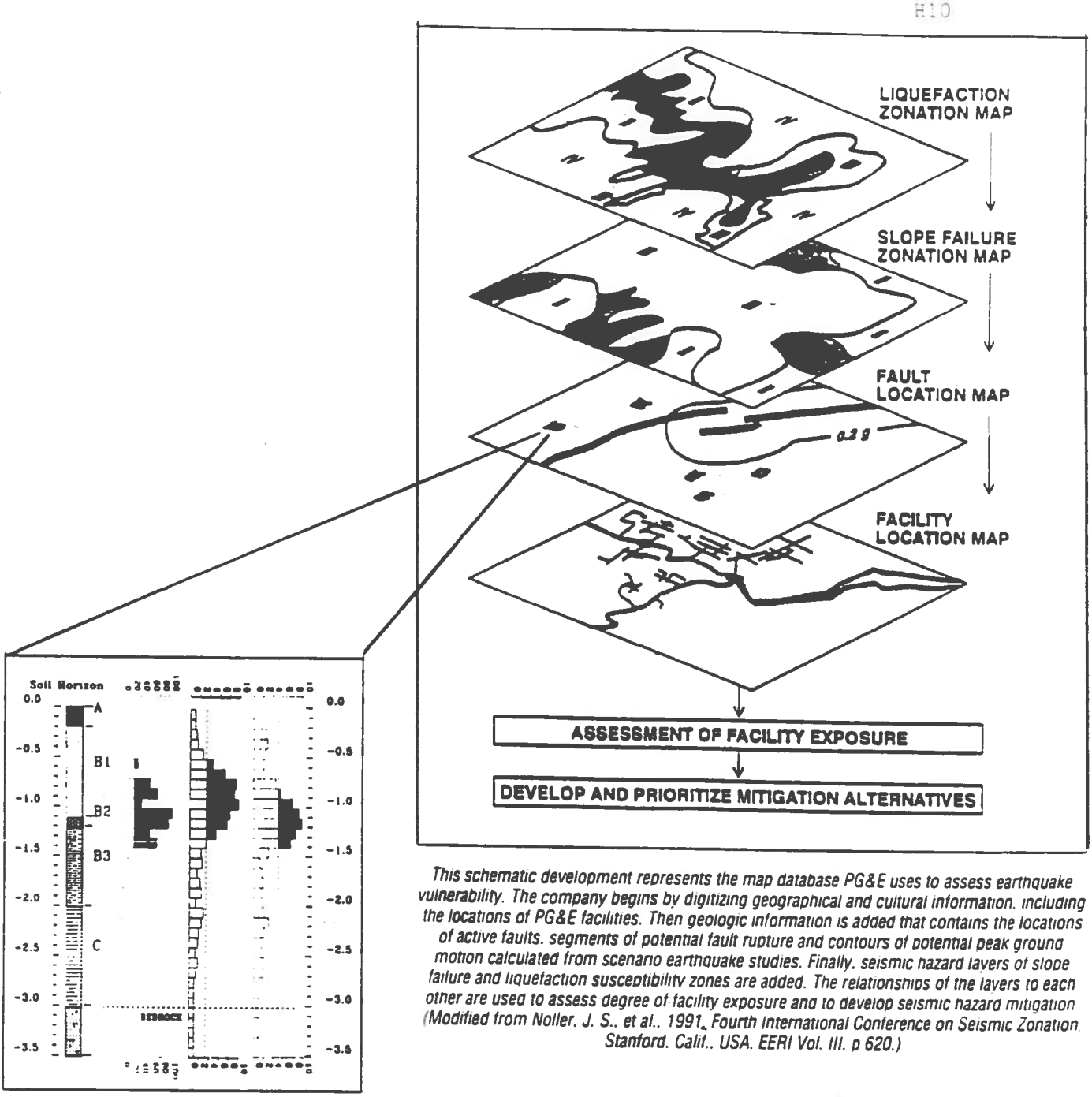

This schematic development represents the map database PG&E uses to assess earthquake vulnerability. The company begins by digitizing geographical and cultural information, including the locations of PG&E facilities. Then geologic information is added that contains the locations of active faults, segments of potential fault rupture and contours of potential peak ground motion calculated from scenario earthquake studies. Finally, seismic hazard layers of slope failure and liquefaction susceptibility zones are added. The relationships of the layers to each other are used to assess degree of facility exposure and to develop seismic hazard mitigation (Modified from Noller, J. S., et al., 1991, Fourth International Conference on Seismic Zonation, Stanford, Calif., USA, EERI Vol. III, p 620.)

BORING LOG DATABASE

All types of boring information can be stored and plotted on downhole logs and cross sections. These data might include inclinometer, piezometer, and geophysical logs, as well as core-derived information, laboratory test, and chemical analysis data.

Fig. 1 Sketch of planned combination of GIS and geotechnical soil profile output.

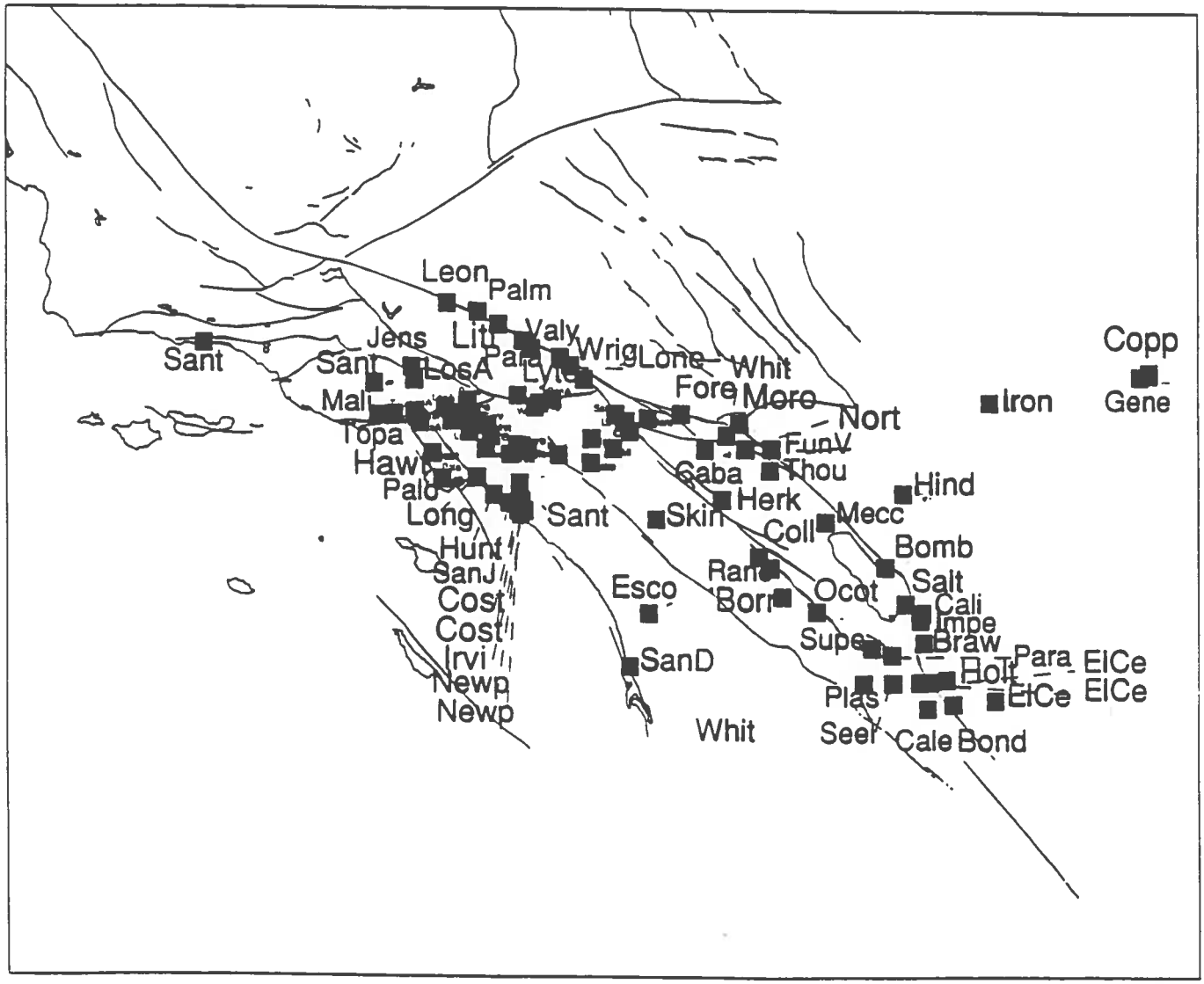

Fig. 2 Distribution of strong ground motion instrument locations encompassed by USGS, currently under investigation.

TASK: H-6 EVALUATION OF BRIDGE DAMAGE IN RECENT EARTHQUAKES

CO PI's: JOHN HALL AND RON SCOTT (CALTECH)

Progress Report

The purpose of this research project is to learn as much as possible from recent foreign earthquakes about the earthquake performance of bridges. The damage incurred to bridges in the magnitude 7.8 Luzon, Philippines earthquake (July 1990) and the magnitude 7.5 Costa Rica earthquake (April 1991) is known to have been extensive and a major part of the effort is being devoted to these two events.

Specific bridges have been identified both in the Philippines and Costa Rica for study and correspondence has been initiated to gather information, including construction techniques, soil and foundation conditions, damage descriptions and ground motion. Some of these case histories will be selected for evaluation in more detail and this process will include site visits. The study should provide a significant database to aid in the development of performance criteria for the seismic retrofit of existing bridges.